

University of Alberta

**Modified Nazarov Reactions and Ring Expansion Chemistry: Useful
Methodologies for the Construction of Carbocyclic and Heterocyclic Compounds.**

by

Tina Nicola Grant



A thesis submitted to the Faculty of Graduate Studies and Research
in partial fulfillment of the requirements for the degree of

Doctor of Philosophy

Department of Chemistry

Edmonton, Alberta

Spring 2008



Library and
Archives Canada

Bibliothèque et
Archives Canada

Published Heritage
Branch

Direction du
Patrimoine de l'édition

395 Wellington Street
Ottawa ON K1A 0N4
Canada

395, rue Wellington
Ottawa ON K1A 0N4
Canada

Your file *Votre référence*
ISBN: 978-0-494-45439-8
Our file *Notre référence*
ISBN: 978-0-494-45439-8

NOTICE:

The author has granted a non-exclusive license allowing Library and Archives Canada to reproduce, publish, archive, preserve, conserve, communicate to the public by telecommunication or on the Internet, loan, distribute and sell theses worldwide, for commercial or non-commercial purposes, in microform, paper, electronic and/or any other formats.

The author retains copyright ownership and moral rights in this thesis. Neither the thesis nor substantial extracts from it may be printed or otherwise reproduced without the author's permission.

AVIS:

L'auteur a accordé une licence non exclusive permettant à la Bibliothèque et Archives Canada de reproduire, publier, archiver, sauvegarder, conserver, transmettre au public par télécommunication ou par l'Internet, prêter, distribuer et vendre des thèses partout dans le monde, à des fins commerciales ou autres, sur support microforme, papier, électronique et/ou autres formats.

L'auteur conserve la propriété du droit d'auteur et des droits moraux qui protègent cette thèse. Ni la thèse ni des extraits substantiels de celle-ci ne doivent être imprimés ou autrement reproduits sans son autorisation.

In compliance with the Canadian Privacy Act some supporting forms may have been removed from this thesis.

Conformément à la loi canadienne sur la protection de la vie privée, quelques formulaires secondaires ont été enlevés de cette thèse.

While these forms may be included in the document page count, their removal does not represent any loss of content from the thesis.

Bien que ces formulaires aient inclus dans la pagination, il n'y aura aucun contenu manquant.


Canada

Abstract

The design and development of new chemical transformations is an important area of organic chemistry. Many synthetic chemists are compelled to explore novel methodologies to improve upon or successfully complete an elegant total synthesis. As an example, the Nazarov reaction has been used extensively in strategies towards the synthesis of numerous natural products. The reaction provides a direct route to functionalized five-membered carbocycles through the Lewis or protic acid-mediated 4π electrocyclization of cross-conjugated dienones. The Nazarov reaction has garnered a great deal of attention in recent years with the advent of very useful asymmetric and catalytic variants, as well as “interrupted” Nazarov reactions.

Recent advances in Nazarov cyclization chemistry will be reviewed (chapter one) prior to the introduction of *gem*-dihalocyclopropanes as innovative substrates for the Nazarov reaction. In chapter two, preparation of the requisite 1,1-dihalo-2-(silyloxy)-2-vinylcyclopropanes will be outlined and their reactivity towards treatment with silver tetrafluoroborate will be described. It was found that these conditions induced sequential disrotatory ring opening and 4π electrocyclization (Nazarov cyclization) to furnish α -chlorocyclopentenone products. This strategy was also used in our preliminary investigation into a general approach towards imino Nazarov reactions.

During our examination of the scope of this reaction, a surprising “interrupted” Nazarov variant was observed. A *gem*-dichlorocyclopropane substrate bearing a tethered phenyl ring was able to participate in an intramolecular trapping process wherein the unsubstituted phenyl moiety captured the intermediate cyclic oxyallyl cation, affording a

benzohydrindenone product. Further investigation revealed that electron-poor, neutral, and electron-rich aromatic rings were compatible with this reaction sequence, providing a number of benzohydrindenone products in moderate to good yields. In chapter three, the results of this investigation are described and a new mode of arene trapping is also presented.

In chapter four, the development of a two-step ring expansion sequence for the synthesis of functionalized heterocycles is reported. Ring expansion was found to proceed as a result of *tert*-butyl propiolate addition into simple and readily available lactones or lactams, providing conjugated ynones that could undergo cyclization in the presence of pyridinium acetate. This methodology provides a straightforward route to the construction of six- and seven-membered oxygen- and nitrogen-containing heterocycles.

For Mum and Daddio

Acknowledgements

Sometimes I wonder where I might be if I hadn't gone into grad school, and other times I'm just thankful for the people I've met and the experiences I've gained along the way...

To the Boss...

Thanks for everything. You have given all of us the freedom to explore our own ideas and learn from our mistakes. Thank you for your patience, guidance, and for having a good sense of humor. I can't imagine that too many supervisors would put up with our crazy antics!

To the West Group...

It's been a great pleasure working with all of you, past and present! To the Gypsies, keep on rockin' and don't forget your side-projects! I expect you will have those natural products done in a week or so! To my lab-mates (Craig & Liya): *Don't stop, believin'!* And don't stop enjoying your work...even though it's hard to see the light sometimes, trust me when I say it *is* there!

To all of my friends...

You have been so supportive of me and have kept me from going crazy. From martinis to keg parties, hockey games to Folk Fest, and chemistry to karaoke, I don't know what I would have done without you! Just remember: all work and no play makes for a very unhappy grad school experience! **H**: thanks for being there for me wherever and whenever I needed you...If it weren't for you I wouldn't have anyone to play with,

and that TRULY would be a sad state of affairs! I don't think I've ever laughed so hard as I have over the past few years, and I owe a lot of that to you...I'm sorry I couldn't fit *rocket launcher* into this thesis, maybe next time around!

To my family...

I've moved so far away, but it doesn't seem like you're too far from here. Thank you for all of your support. You have always been there for me and always thought that I would amount to something...I hope that I have made you proud! I appreciate the late night phone calls and the long-distance guitar lessons, and I'm dedicating this thesis to you...even if you have no particular love of chemistry!

To Chris...

You have put up with a lot of garbage from me over the years...long hours in the lab and lots of crazy mood swings...

Thanks for your encouragement and for making me laugh.

Thank you for keeping me grounded.

Table of Contents

Chapter 1

1	The Nazarov Cyclization.....	1
1.1	The Traditional Nazarov Reaction.....	1
1.1.1	Introduction.....	2
1.1.2	Asymmetric Nazarov Reactions.....	6
1.1.3	Catalytic Nazarov Reactions.....	12
1.1.4	Non-traditional Substrates for Nazarov Cyclization.....	18
1.2	The Interrupted Nazarov Reaction.....	21
1.2.1	Intramolecular Trapping.....	22
1.2.2	Intermolecular Trapping.....	28
1.3	Recent Examples in Total Synthesis.....	34
1.3.1	Roseophilin.....	35
1.3.2	Cephalotaxine.....	36
1.3.3	Merrilactone A.....	37
1.4	New Directions in the Nazarov Cyclization.....	39
1.5	References.....	40

Chapter 2

2	<i>gem</i> -Dichlorocyclopropanes as Novel Substrates for the Nazarov Cyclization.....	46
2.1	The Chemistry of <i>gem</i> -Dihalocyclopropanes.....	46
2.1.1	Dihalocarbenes.....	47
2.1.2	Preparation of <i>gem</i> -Dichlorocyclopropanes.....	47
2.1.3	Cationic Ring Opening of <i>gem</i> -Dichlorocyclopropanes.....	50

2.1.4	Cationic Ring Opening of <i>gem</i> -Dichlorocyclopropanes in Synthesis....	51
2.2	<i>gem</i> -Dichlorocyclopropanes and the Nazarov Cyclization.....	56
2.2.1	Introduction.....	56
2.2.2	Results & Discussion.....	59
2.2.3	Conclusions.....	75
2.3	A General Approach to the Imino Nazarov Reaction.....	77
2.3.1	Preliminary Results & Discussion.....	79
2.4	Future Directions.....	83
2.5	Experimental.....	85
2.5.1	General Information.....	85
2.5.2	Characterization.....	85
2.6	References.....	114

Chapter 3

3	Interrupted Nazarov Reactions Using <i>gem</i> -Dichlorocyclopropanes.....	118
3.1	Introduction.....	118
3.2	<i>gem</i> -Dichlorocyclopropanes as Substrates for Interrupted Nazarov Reactions.....	119
3.2.1	Traditional Arene Trapping.....	120
3.2.2	Novel Mode of Arene Trapping.....	132
3.2.3	Conclusions.....	139
3.3	Future Directions.....	141
3.4	Experimental.....	143
3.4.1	General Information.....	143

3.4.2	Characterization.....	144
3.5	References.....	181

Chapter 4

4	Synthesis of Functionalized Oxo- and Azacycles: A Pyridinium Acetate-Catalyzed Ring Expansion Sequence.....	182
4.1	Synthesis of Functionalized Heterocycles.....	182
4.1.1	Recent Contributions to Heterocycle Synthesis.....	183
4.2	A New Ring Expansion Sequence.....	191
4.2.1	<i>tert</i> -Butyl Propiolate Addition.....	192
4.2.2	Ring Expansion.....	196
4.2.3	Conclusions.....	206
4.3	Future Directions.....	207
4.4	Experimental.....	208
4.5.1	General Information.....	208
4.5.2	Characterization.....	209
4.5	References.....	231

Appendices

Appendix I.....	235
Appendix II.....	271
Appendix III.....	290
Appendix IV.....	320
Appendix V.....	343

List of Tables

Chapter 2

<i>Table 2.1.</i> Preliminary results using <i>gem</i> -dichlorocyclopropane 38a	61
<i>Table 2.2.</i> Dichlorocyclopropanation of 2-triisopropylsilyloxydienes.....	66
<i>Table 2.3.</i> Optimization for sequential ring opening/Nazarov cyclization reaction.....	68
<i>Table 2.4.</i> AgBF ₄ -mediated rearrangement of <i>gem</i> -dichlorocyclopropanes 38	71
<i>Table 2.5.</i> Comparison of reaction conditions for the Ag(I)-mediated Nazarov reaction.....	73
<i>Table 2.6.</i> Reactivity of aminodichlorocyclopropane 65	81

Chapter 3

<i>Table 3.1.</i> <i>gem</i> -Dichlorocyclopropanation of 2-silyloxydienes 7	123
<i>Table 3.2.</i> Ag(I)-Mediated interrupted Nazarov reactions.....	127

Chapter 4

<i>Table 4.1.</i> ^t Bu-propiolate addition to lactones/lactams.....	193
<i>Table 4.2.</i> Pyridinium acetate-catalyzed ring expansion.....	199
<i>Table 4.3.</i> Ring expansion of nitrogen-substrates 35	203

List of Figures

Chapter 1

<i>Figure 1.1.</i> The Nazarov cyclization.....	1
<i>Figure 1.2.</i> Possible conformations of divinyl ketones.....	3
<i>Figure 1.3.</i> Conrotatory ring closure of the pentadienyl cation.....	3
<i>Figure 1.4.</i> Helical conformation of 9 leading to stereoselectivity.....	7
<i>Figure 1.5.</i> Chiral transition state leading to selective protonation of the dienolate.....	11
<i>Figure 1.6.</i> Polarization of divinyl ketones.....	12
<i>Figure 1.7.</i> The “interrupted” Nazarov reaction.....	22

Chapter 2

<i>Figure 2.1.</i> Preparation of <i>gem</i> -dihalocyclopropanes.....	46
<i>Figure 2.2.</i> Mechanism of carbene generation.....	48
<i>Figure 2.3.</i> The Makosza method: phase transfer catalysis.....	49
<i>Figure 2.4.</i> Cationic ring opening of <i>gem</i> -dihalocyclopropanes.....	50
<i>Figure 2.5.</i> Stereoelectronic factors affecting cationic ring opening.....	50
<i>Figure 2.6.</i> Concept behind the use of <i>gem</i> -dihalocyclopropanes in the Nazarov reaction.....	56
<i>Figure 2.7.</i> The formation of products due to treatment of 38a with AgBF ₄	62
<i>Figure 2.8.</i> nOe enhancement illustrating the <i>Z</i> -geometry of the enol ether.....	63
<i>Figure 2.9.</i> Overcyclopropanation of cyclic 2-triisopropylsilyloxydienes 37f and 37g	67
<i>Figure 2.10.</i> The relative stabilities of cyclic and acyclic cationic species.....	78
<i>Figure 2.11.</i> Proposed strategy for a general imino Nazarov methodology.....	79
<i>Figure 2.12.</i> Potential chiral amine substrates for use in an asymmetric Nazarov reaction.....	83
<i>Figure 2.13.</i> Novel modes of trapping in interrupted Nazarov reactions.....	84

Chapter 3

<i>Figure 3.1.</i> The proposed reactive oxyallyl cationic intermediate.....	119
<i>Figure 3.2.</i> Isolated spin systems observed in the ^1H NMR spectrum.....	136
<i>Figure 3.3.</i> Representative <i>Galbulimima belgraveana</i> alkaloids.....	139
<i>Figure 3.4.</i> Participation of monochlorocyclopropanes in Nazarov processes.	142

Chapter 4

<i>Figure 4.1.</i> Examples of natural products containing saturated heterocyclic motifs.....	182
<i>Figure 4.2.</i> Examples of heterocycles generated from the organocatalytic process.....	190
<i>Figure 4.3.</i> Evidence for the formation of 3-oxooxepan-2-ylidene 43a	198
<i>Figure 4.4.</i> Characteristic HMBC correlations for azacen-4-one 47h	204
<i>Figure 4.5.</i> Comparison of ^1H NMR data for <i>E/Z</i> -isomers of 46h	205

List of Schemes

Chapter 1

<i>Scheme 1.1.</i> The mechanism of the Nazarov cyclization.....	2
<i>Scheme 1.2.</i> A silicon-directed Nazarov cyclization.....	4
<i>Scheme 1.3.</i> Fluorine-directed elimination in the Nazarov cyclization.....	5
<i>Scheme 1.4.</i> Pridgen's asymmetric Nazarov cyclization utilizing chiral auxiliaries.....	6
<i>Scheme 1.5.</i> D-glucose-derived chiral auxiliary for cyclopentannelation.....	8
<i>Scheme 1.6.</i> The effect of D-glucose-derived chiral auxiliaries on cyclopentannelation.....	9
<i>Scheme 1.7.</i> Aggarwal and Belfield's asymmetric Nazarov reaction.....	10
<i>Scheme 1.8.</i> Enantioselective Nazarov reactions due to asymmetric proton transfer.....	11
<i>Scheme 1.9.</i> Examples of Cu(OTf) ₂ -catalyzed Nazarov cyclizations.....	12
<i>Scheme 1.10.</i> Sc(OTf) ₃ -Catalyzed Nazarov cyclizations of heteroaromatic vinyl ketones.....	13
<i>Scheme 1.11.</i> Mechanistic proposal for generation of 25 and 26	14
<i>Scheme 1.12.</i> Co-ordination of dicationic Ir(III) complex to dienone substrates.....	15
<i>Scheme 1.13.</i> An organocatalytic enantioselective Nazarov cyclization.....	16
<i>Scheme 1.14.</i> Rautenstrauch rearrangement of enynyl acetates.....	18
<i>Scheme 1.15.</i> The gold-catalyzed Rautenstrauch rearrangement mechanism.....	19
<i>Scheme 1.16.</i> The mechanism of cyclopentenone formation from hexatrienes 35	20
<i>Scheme 1.17.</i> Direct Nazarov cyclization from Fischer carbene complexes.....	20
<i>Scheme 1.18.</i> de Lera's Nazarov-type cyclization of (2 <i>Z</i>)-vinylallene acetals.....	21
<i>Scheme 1.19.</i> Trapping of the oxyallyl cation with a tethered olefin.....	23
<i>Scheme 1.20.</i> Cascade polycyclization of aryltrienones.....	24
<i>Scheme 1.21.</i> Benzohydrindenone formation from aryl dienones.....	25
<i>Scheme 1.22.</i> Electron-rich versus electron-poor arene trapping.....	26
<i>Scheme 1.23.</i> Intramolecular azide trapping of the cationic Nazarov intermediate.....	27

<i>Scheme 1.24.</i> Formation of trapping products from dienones with tethered azides.....	27
<i>Scheme 1.25.</i> The reductive Nazarov cyclization.....	28
<i>Scheme 1.26.</i> An interrupted Nazarov reaction terminated with ionic reduction.....	29
<i>Scheme 1.27.</i> Intermolecular trapping of the Nazarov intermediate with allylsilanes.....	30
<i>Scheme 1.28.</i> Intermolecular diene trapping to furnish cyclooctene carbocycles.....	31
<i>Scheme 1.29.</i> Mild amine trapping in the interrupted Nazarov reaction.....	32
<i>Scheme 1.30.</i> An asymmetric interrupted Nazarov reaction.....	32
<i>Scheme 1.31.</i> Intermolecular azide trapping to furnish dihydropyridones.....	33
<i>Scheme 1.32.</i> Tius' retrosynthesis of roseophilin.....	35
<i>Scheme 1.33.</i> The key asymmetric Nazarov cyclization in the synthesis of roseophilin.....	36
<i>Scheme 1.34.</i> A Nazarov-type cyclization in the synthesis of Cephalotaxine.....	37
<i>Scheme 1.35.</i> Retrosynthesis of (±)-merrilactone A.....	38
<i>Scheme 1.36.</i> The key Nazarov reaction in Frontier's approach to merrilactone A.....	38

Chapter 2

<i>Scheme 2.1.</i> Stereochemical retention in dihalocyclopropanation.....	47
<i>Scheme 2.2.</i> Towards the synthesis of phenanthroquinolizidine alkaloids.....	52
<i>Scheme 2.3.</i> Intermolecular trapping of the allyl cation by indole nucleophiles.....	53
<i>Scheme 2.4.</i> Synthetic strategy for the assembly of gibberellin frameworks.....	54
<i>Scheme 2.5.</i> Paquette's sequential ring opening/ 8π electrocyclization process.....	57
<i>Scheme 2.6.</i> Methodology for the synthesis of substituted aromatic rings.....	58
<i>Scheme 2.7.</i> The synthesis of 1,1-dihalo-2-(silyloxy)-2-vinylcyclopropanes.....	59
<i>Scheme 2.8.</i> Preparation of 2-triisopropylsilyloxydienes 37b and 37c	63
<i>Scheme 2.9.</i> Preparation of 2-triisopropylsilyloxydienes 37d and 37e	64
<i>Scheme 2.10.</i> Preparation of 2-triisopropylsilyloxydienes 37f-h	64

<i>Scheme 2.11.</i> Preparation of 2-triisopropylsilyloxydienes 37i	65
<i>Scheme 2.12.</i> Attempts to cyclopropanate silyl enol ether 37c	66
<i>Scheme 2.13.</i> Chloride-assisted termination of the pentadienyl cation XII	69
<i>Scheme 2.14.</i> Effect of silyl substituents on sequential ring opening/ Nazarov cyclization.....	70
<i>Scheme 2.15.</i> Mechanism for the formation of dione enol 54h	71
<i>Scheme 2.16.</i> Equilibration experiment: conversion of 49e(cis) to 49e(trans)	72
<i>Scheme 2.17.</i> Anomalous reactivity of <i>gem</i> -dichlorocyclopropane 38b	73
<i>Scheme 2.18.</i> Treatment of chlorodienones with AgBF ₄	74
<i>Scheme 2.19.</i> A surprising interrupted Nazarov variant.....	75
<i>Scheme 2.20.</i> Tius' imino Nazarov cyclization.....	77
<i>Scheme 2.21.</i> Preparation of <i>gem</i> -dichlorocyclopropane 65	79
<i>Scheme 2.22.</i> Mechanistic proposal for the formation of cyclopentenone 66	82

Chapter 3

<i>Scheme 3.1.</i> An "interrupted" Nazarov reaction using <i>gem</i> -dichlorocyclopropanes.....	118
<i>Scheme 3.2.</i> Synthesis of 2-silyloxydienes 7b-f	120
<i>Scheme 3.3.</i> The preparation of 2-silyloxydiene 7g	121
<i>Scheme 3.4.</i> The preparation of 2-silyloxydiene 7h	122
<i>Scheme 3.5.</i> The preparation of 2-silyloxydiene 7i	122
<i>Scheme 3.6.</i> Treatment of <i>gem</i> -dichlorocyclopropanes 1b and 1c with AgBF ₄ in CH ₂ Cl ₂	124
<i>Scheme 3.7.</i> Conversion of vinyl dihalocyclopropanes to dienones in refluxing MeCN.....	125
<i>Scheme 3.8.</i> Comparison of original reaction conditions with AgBF ₄ in refluxing MeCN.....	126
<i>Scheme 3.9.</i> The effect of α -substitution on the interrupted Nazarov variant.....	128
<i>Scheme 3.10.</i> Proposed mechanism for arene-trapping.....	130
<i>Scheme 3.11.</i> Harmata's use of α -chlorocyclopentanones in [4+3] cycloadditions.....	131

<i>Scheme 3.12.</i> Attempted intermolecular trapping of the second oxyallyl cation.....	132
<i>Scheme 3.13.</i> Preparation of <i>gem</i> -dichlorocyclopropanes 29a and 29b	133
<i>Scheme 3.14.</i> Conversion of substrate 28a to benzohydrindenone products.....	134
<i>Scheme 3.15.</i> The unexpected formation of bridged bicycle 32b	135
<i>Scheme 3.16.</i> Preparation of silyl enol ethers 28c-e	137
<i>Scheme 3.17.</i> The formation of bridged bicyclic products 32	138
<i>Scheme 3.18.</i> <i>E/Z</i> -Isomerization of dienones in the reductive Nazarov cyclization.....	138

Chapter 4

<i>Scheme 4.1.</i> Two-step olefination/RCM strategy for benzo-fused heterocycle synthesis.....	183
<i>Scheme 4.2.</i> Formation of benzoazepine 9 from amide 7	184
<i>Scheme 4.3.</i> Key step in the synthesis of (+)- <i>trans</i> - 195A	185
<i>Scheme 4.4.</i> Palladium-catalyzed construction of cyclic aryl ethers.....	186
<i>Scheme 4.5.</i> The two-step assembly of a nitrogen-containing heterocycle from dioxin 15	186
<i>Scheme 4.6.</i> Aziridination using bromoallene substrates.....	187
<i>Scheme 4.7.</i> The synthesis of medium-sized heterocycles from bromoallene substrates.....	188
<i>Scheme 4.8.</i> Three-step protocol for the formation of eight-membered oxacycles.....	189
<i>Scheme 4.9.</i> Mechanism for organocatalytic preparation of sulfur heterocycles.....	189
<i>Scheme 4.10.</i> Proposed strategy for the iterative assembly of polyether motifs.....	191
<i>Scheme 4.11.</i> Outline of two-step ring expansion methodology.....	192
<i>Scheme 4.12.</i> Formation of cyclic enyne side-product 39h	195
<i>Scheme 4.13.</i> Possible formation of lactam enolates during <i>tert</i> -butyl propiolate addition.....	196
<i>Scheme 4.14.</i> Schreiber's ring expansion reaction.....	197
<i>Scheme 4.15.</i> Proposed mechanism.....	200
<i>Scheme 4.16.</i> Treatment of <i>N</i> -Boc substrate 36d to pyridinium acetate.....	201

<i>Scheme 4.17.</i> Mechanism for the formation of bicycle 45d	202
<i>Scheme 4.18.</i> Hydrogenation of 3-oxo-1-tosylazepan-2-ylidenes 46f _(E/Z)	203
<i>Scheme 4.19.</i> Re-subjection of a mixture of <i>E/Z</i> -isomers to pyridinium acetate.....	205
<i>Scheme 4.20.</i> Possible strategy towards the synthesis of the core of rhoedine.....	207

Standard List of Abbreviations

Ac	acetyl
Ar	aryl
app	apparent (spectral)
aq	aqueous
BAR ^f	tetrakis(3,5-bis(trifluoromethyl)phenyl)borate
Bn	benzyl
Boc	<i>tert</i> -butyloxycarbonyl
br	broad (spectral)
ⁱ Bu	isobutyl
ⁿ Bu	butyl
^t Bu	<i>tert</i> -butyl
°C	degrees Celsius
calcd	calculated
Cbz	benzyloxycarbonyl
CPME	cyclopentyl methyl ether
d	day(s); doublet (spectral)
dd	doublet-of-doublets (spectral)
DBU	1,8-diazabicyclo[5.4.0]undec-7-ene
DIB	<i>ortho</i> -diiodobenzene
DIBALH	diisobutylaluminum hydride
DIPA	diisopropyl amine
DMAP	4-dimethylaminopyridine

DMP	Dess-Martin periodinane
DMS	dimethyl sulfide
DMSO	dimethyl sulfoxide
dppe	1,2-bis(triphenylphosphino)ethane
dr	diastereomeric ratio
ee	enantiomeric excess
EI	electron impact (mass spectrometry)
equiv	equivalents
ESI	electrospray ionization (mass spectrometry)
Et	ethyl
g	gram(s)
h	hour(s)
HFIP	hexafluoroisopropanol
HRMS	high resolution mass spectrum
Hz	hertz
IR	infrared
<i>J</i>	coupling constant (spectral)
LDA	lithium diisopropylamide
M	moles per liter
m	multiplet (spectral)
Me	methyl
MeCN	acetonitrile
MHz	megahertz

min	minute(s)
mol	mole(s)
MOM	methoxymethyl
mmol	millimole(s)
m.p.	melting point
Ms	mesyl; methanesulfonyl
MS	molecular sieves
m/z	mass to charge ratio (mass spectrometry)
NMO	<i>N</i> -methylmorpholine- <i>N</i> -oxide
NMR	nuclear magnetic resonance
Ns	nosyl; 2-nitrophenylsulfonyl
Nu	nucleophile
Ph	phenyl
ppm	parts per million (spectral)
pyr	pyridine
pyr•AcOH	pyridinium acetate
q	quartet (spectral)
R _f	retention factor (chromatography)
r.t.	room temperature
s	singlet (spectral); second(s)
t	triplet (spectral)
TBAB	tetrabutylammonium bromide
TBDMS	<i>tert</i> -butyldimethylsilyl

TEA	triethylamine
TEBA	triethylbenzylammonium chloride
TES	triethylsilyl
TFE	trifluoroethanol
TIPS	triisopropylsilyl
Tf	trifluoromethanesulfonyl
THF	tetrahydrofuran
TLC	thin layer chromatography
TMS	trimethylsilyl
TPAP	tetra- <i>n</i> -propylammonium perruthenate
Ts	tosyl; <i>p</i> -toluenesulfonyl

Chapter 1

The Nazarov Cyclization

1.1 The Traditional Nazarov Reaction

The Nazarov cyclization is an electrocyclic process that typically transforms a cross-conjugated dienone, **1**, into a cyclopentenone product, **2**, by means of conrotatory ring closure (*Figure 1.1*). Since its initial discovery in 1941,¹ the Nazarov reaction has been keenly investigated and important advances have been made to expand both the scope and utility of this process. This electrocyclicization has found general use in the synthesis of functionalized 5-membered carbocycles, a structural motif that is prevalent

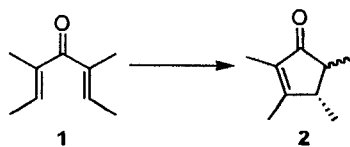
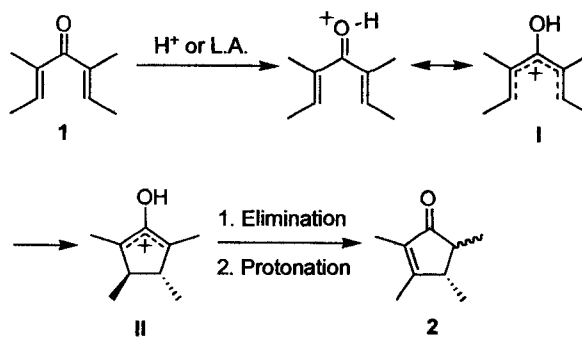


Figure 1.1. The Nazarov cyclization.

in numerous natural product skeletons. This chapter will focus on introducing the traditional Nazarov cyclization as well as related developments in the areas of asymmetric induction and catalysis. The “interrupted” Nazarov reaction will also be addressed, and the utility of these processes examined in the context of total synthesis.

1.1.1 Introduction

The traditional Nazarov reaction² involves the 4π -electron cyclization of a pentadienyl cation generated from a divinyl ketone, **1**. The mechanism of this reaction involves initial activation of the ketone carbonyl by at least one equivalent of strong protic or Lewis acid (*Scheme 1.1*). This activation generates an intermediate pentadienyl cation, **I**, that can undergo cyclization to produce a cyclic oxyallyl cationic species, **II**. Elimination and subsequent tautomerization of the resultant enol ether then leads to the cyclopentenone product, **2**.



Scheme 1.1. The mechanism of the Nazarov cyclization.

Efficient cyclization of divinyl ketones occurs when the substrates are predisposed to occupy the *s-trans/s-trans* arrangement (*Figure 1.2*). Substitution at the α -position of the divinyl ketones helps to populate the *s-trans/s-trans* configuration, since

α -substitution presents unfavorable steric interactions in the *s-cis/s-cis* arrangement. It has been demonstrated that α -substitution improves the efficiency and yields of traditional Nazarov cyclizations.³

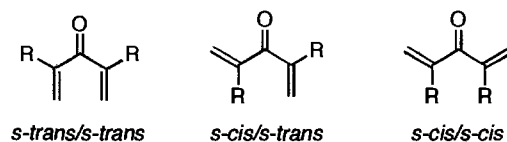


Figure 1.2. Possible conformations of divinyl ketones.

The electrocyclization process itself abides by rules defined by Woodward and Hoffmann⁴ with respect to the conservation of orbital symmetry in pericyclic reactions. As a result, ring closure of the cationic pentadienyl species proceeds in a conrotatory fashion (Figure 1.3). The conrotation can occur in a “clockwise” or “counterclockwise” manner to generate a mixture of two oxyallyl cationic species. Should the cyclization preferentially occur to generate *one* of the oxyallyl intermediates, the reaction is said to

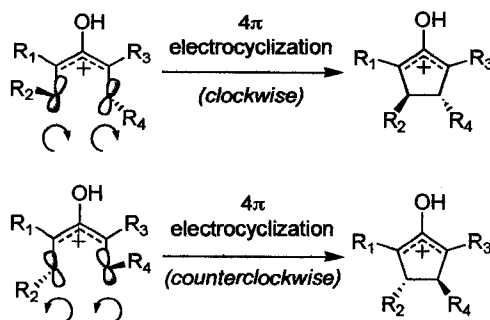
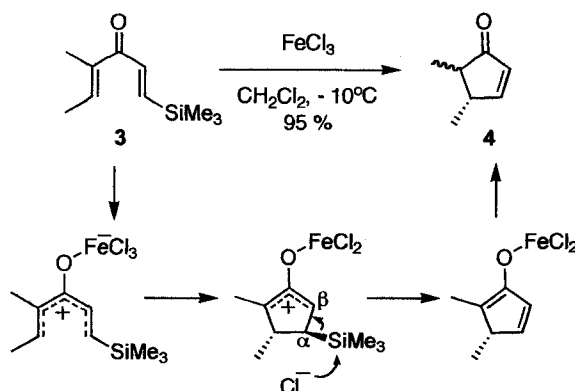


Figure 1.3. Conrotatory ring closure of the pentadienyl cation.

have occurred in a torquoselective manner. Torquoselectivity⁵ describes the preference for electrocyclization to proceed in one direction over another and is a difficult process to control in the Nazarov reaction. Torquoselective cyclization has been the main focus of many groups who work in the area of asymmetric Nazarov methodologies (see *Section*

1.1.2). Typically, the Nazarov cyclization is terminated by an eliminative pathway that results in the destruction of potential stereogenic centers established during ring closure. In some instances, the eliminative pathway can be avoided and the stereochemistry retained when competing rearrangement or trapping pathways are available (see *Section 1.2*).

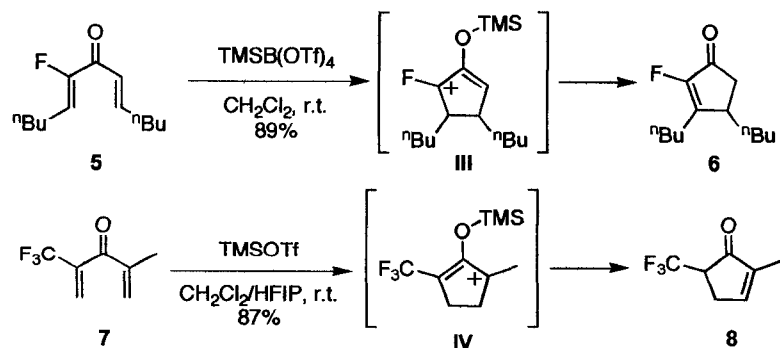
Although it can be difficult to control the regioselectivity of the terminal elimination process, typically elimination proceeds to generate the product with the more highly substituted, electron rich double bond, which corresponds to the more thermodynamically stable product; however, this Zaitsev selectivity may not always provide the desired products. In such cases, regioselectivity can be controlled if the substrate is predisposed to selectively stabilize one side of the 2-oxidocyclopentenyl cation, **II** (*Scheme 1.1*). Denmark's pioneering work on the silicon-directed Nazarov cyclization⁶ illustrated that careful placement of an electrofugal heteroatom (*i.e.* silicon, tin) could provide regioselective elimination to prepare the desired, often less thermodynamically stable cyclopentenone products (*Scheme 1.2*). The trimethylsilyl



Scheme 1.2. A silicon-directed Nazarov cyclization.

substituent on divinyl ketone **3** aids in stabilization of the cyclic oxyallyl cation through overlap of *d*-orbitals on silicon with the vacant *p*-orbital that is closest to the silicon atom (at the β -position to Si). This stabilization predisposes the cyclized intermediate to chloride-assisted desilylation, generating the observed elimination product **4** as the sole product in 95% yield (*cis:trans*, 59:41).

Another example of regioselectivity in the eliminative step of the Nazarov cyclization can be attributed to the strategic placement of fluorine or trifluoromethyl groups on the divinyl ketone substrate. Ichikawa⁷ presented examples of fluorine stabilization due to donation from a filled *p*-orbital on fluorine to an empty *p*-orbital on the adjacent carbon of the cyclic oxyallyl intermediate **III** (Scheme 1.3). The resulting polarization of the allyl group, with greater charge density on the fluorine-substituted carbon, led to preferential deprotonation to provide the fluorine-substituted double bond in cyclopentenone product **6**. A related example illustrates the complementary use of a trifluoromethyl group on divinyl ketone **7** as a destabilizing functionality on the cyclic oxyallyl **IV**. The electron-withdrawing nature of the trifluoromethyl group led to elimination on the opposing side of the fluorinated substituent.

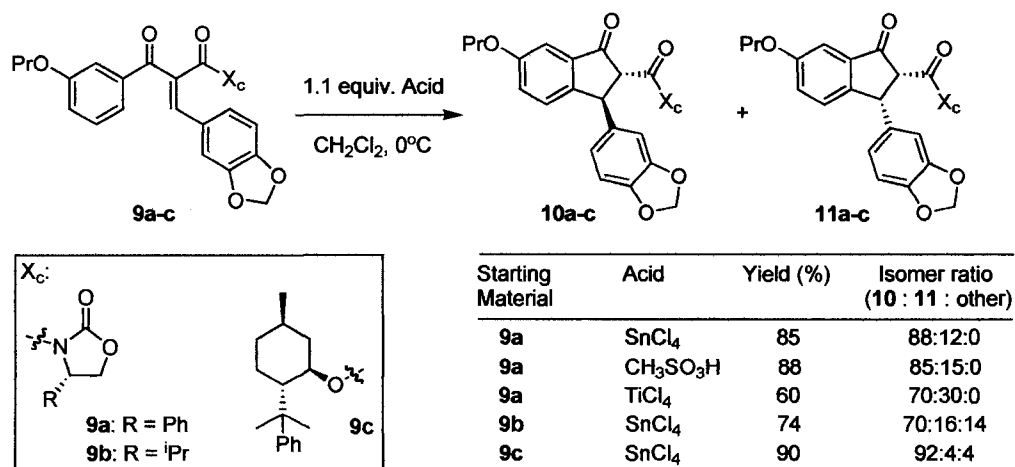


Scheme 1.3. Fluorine-directed elimination in the Nazarov cyclization.

A great deal of work has been done to improve various aspects of the Nazarov reaction. Insights into the mechanism as well as the effect of different electron-withdrawing and releasing groups on the cyclization process have led to advancements in regiocontrol of the final elimination step. These same insights have been examined in order to influence torquoselectivity, leading to asymmetric Nazarov variants.

1.1.2 Asymmetric Nazarov Reactions

Although remote stereogenic centers and restrictive carbon frameworks have been shown to influence the torquoselectivity of the cyclization process,⁸ the first successful asymmetric Nazarov cyclization of dienone substrates was not realized until 1999 by Pridgen and co-workers.⁹ In this work, the most efficient examples employed an Evans' oxazolidinone chiral auxiliary in conjunction with either protic or Lewis acid to impart stereoselective cyclization of the pentadienyl cation generated from **9** (*Scheme 1.4*). The chiral indanone products **10** and **11** were obtained as a result of 1,5-asymmetric induction



Scheme 1.4. Pridgen's asymmetric Nazarov cyclization utilizing chiral auxiliaries.

across the intermediate pentadienyl cation. Initially, the authors believed that bidentate metal-carbonyl complexation was responsible for the observed stereoselectivity; however, the observation that protic acids as well as chiral auxiliaries without carbonyl functionality (**9c**) could generate similar results led the authors to a different explanation for the apparent stereoselectivity. The revised proposal invoked formation of a specific helical conformation (*Figure 1.4*) in the pentadienyl cationic intermediate. This highly ordered structure would be conferred to the substrates due to steric demands imparted by the chiral auxiliary, leading to selective formation of one stereoisomer over the other. Computational methods were used to analyze potential conformations of **9** in order to provide support for the proposed stereochemical induction. Flynn and co-workers have also investigated the use of oxazolidinones as chiral auxiliaries in the Nazarov cyclization with similar results.¹⁰

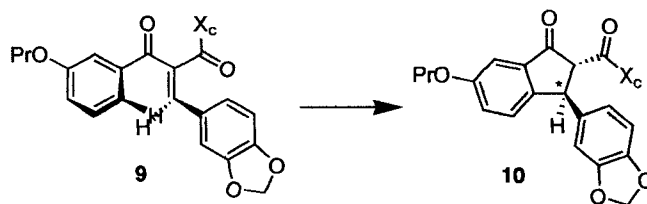
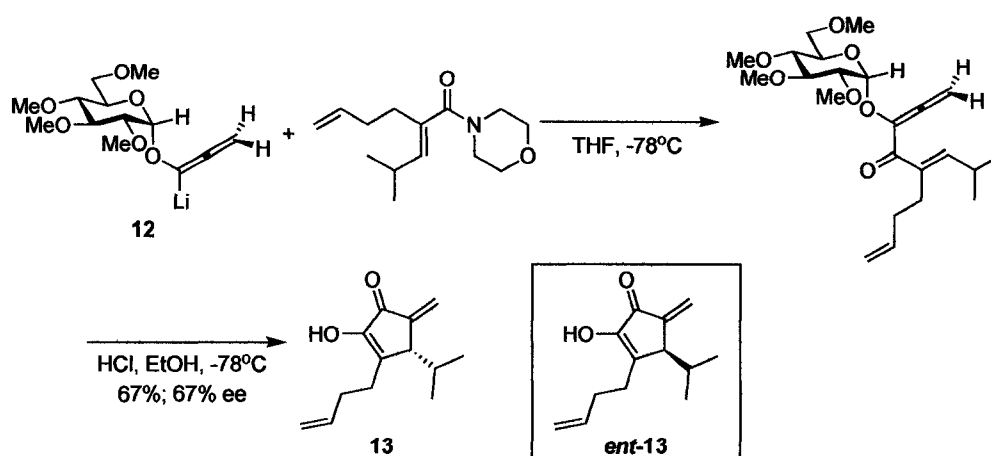


Figure 1.4. Helical conformation of **9** leading to stereoselectivity.

Another example of asymmetric induction utilizing chiral auxiliaries is the enantioselective cyclopentannulation reaction of α -allenyl ketones presented by Tius in 2000 (*Scheme 1.5*).¹¹ In Tius' initial publication, a readily available α -D-glucose-derived auxiliary was appended to the allenyl lithium reagent, **12**, used to synthesize α -allenyl ketones. When exposed to acidic work-up conditions (HCl, EtOH, -78°C) the allenyllithium addition product underwent immediate cyclopentannulation to provide **13** in 67% yield and 67% ee. Advantageous loss of the glucose moiety during the

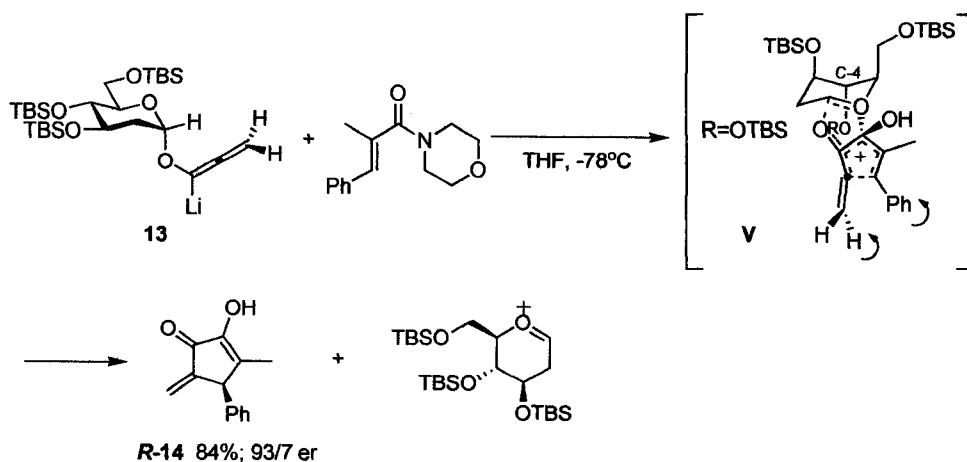
cyclization reaction is illustrative of a traceless auxiliary: additional chemical transformations are not needed to remove the chiral component at a later stage in any synthetic strategy. An additional benefit of using this strategy is that both enantiomers of **13** can be easily accessed through use of either the α - or β -glucose derivative as the chiral



Scheme 1.5. D-glucose-derived chiral auxiliary for cyclopentannulation.

auxiliary. In the latter case, *ent*-**13** was obtained in 71% and 82% ee when the reaction mixture was treated to an acidic work-up of HCl and hexafluoroisopropanol (HFIP) at 0°C. Since this initial work, Tius and co-workers have developed more effective chiral auxiliaries¹² that both circumvent some of the problems arising from scale-up of the previously outlined reactions and provide better enantioselectivities. Development of the improved chiral auxiliaries arose from a comprehensive examination of substitution on the original D-glucose-derived allenyllithium reagents,^{12c} which provided a greater understanding of how these auxiliaries were affecting the torquoselectivity of the cyclization process. The proposed transition state (**V**, *Scheme 1.6*) involves electron donation to the pentadienyl cation from the oxygen in the pyranose ring, which induces a conformational change in the auxiliary. The new conformation places the C-4 OTBS

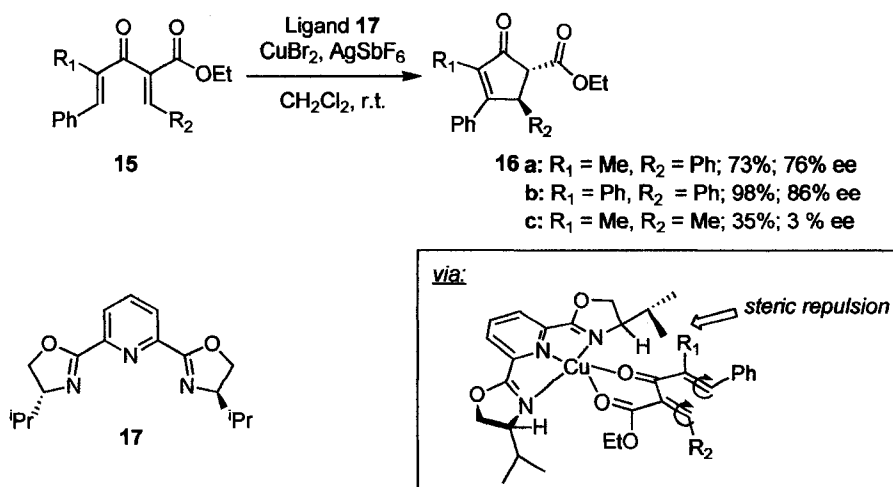
substituent in an axial position, close enough to block the back face of the pentadienyl cation. The steric interaction between the bulky OTBS group at C-4 and the substrate forces counterclockwise rotation in the cyclization step resulting in **R-14** in 84% yield in a 93:7 enantiomeric ratio.



Scheme 1.6. The effect of D-glucose-derived chiral auxiliaries on cyclopentannulation.

The most notable problem associated with the use of chiral auxiliaries for asymmetric induction is that the auxiliary needs to be removed in subsequent steps. Although Tius' traceless auxiliaries are an attractive solution to this problem, the methodology has only been proven in the realm of cyclopentannulation reactions of allenyl vinyl ketones and not with traditional Nazarov substrates. In an effort to find alternative solutions to the problem of asymmetric Nazarov cyclizations, many research groups have turned to the use of chiral Lewis acids. The first successful methodology was reported in 2003 when Aggarwal and Belfield disclosed an asymmetric Nazarov reaction promoted by 1 equivalent of a Cu(II)-pybox or Cu(II)-box complex (*Scheme 1.7*).¹³ Efforts to reduce the catalyst loading resulted in lower yields despite attempts to improve the catalyst turnover using molecular sieves and other additives. This

methodology relies on the presence of an α -ester or α -amide functionality that can participate in bidentate co-ordination to the Lewis acid. Although the Lewis acid complex with ligand **17** provided the best results for cyclization of substrates **15** - with

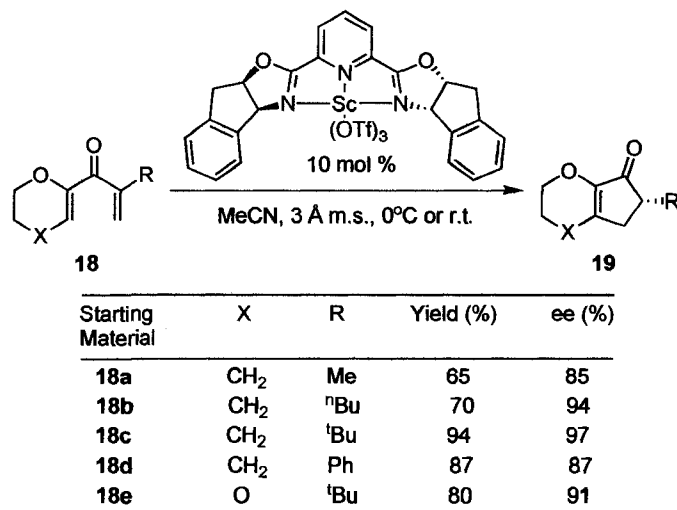


Scheme 1.7. Aggarwal and Belfield's asymmetric Nazarov reaction.

α -ester substitution – it was not reactive towards the analogous amide substrates. Further optimization was therefore required in order to determine the most suitable Cu(II) complex for different substrates. Also, it was observed that bulky substituents at R_1 and R_2 were necessary for good catalyst turnover and high enantioselectivities. This is undoubtedly due to an increase in steric repulsion between the substrate and the isopropyl groups on the Cu(II)-complex when R_1 and R_2 are of significant size (*Scheme 1.7*).

The first example of enantioselective Nazarov reactions involving catalytic loading of the Lewis acid complex was reported by Trauner in 2004.¹⁴ The methodology utilized a chiral Sc(III)-pybox complex (10-20 mol %) to transform 2-alkoxy-1,4-pentadien-3-ones **18** into cyclopentenones **19** in good yields and with high

enantioselectivities (*Scheme 1.8*). Strategic placement of oxygen at the α -position on the divinyl ketone substrates not only increased reactivity towards cyclization, but also



Scheme 1.8. Enantioselective Nazarov reactions due to asymmetric proton transfer.

helped to stabilize the cyclic oxyallyl intermediate thereby promoting regioselective deprotonation to install the ring-fusing alkene. Presumably, the transition state for these reactions occurs through bidentate coordination of the Lewis acid to both carbonyl and heterocyclic oxygen atoms in the substrate. The tight transition state (*Figure 1.5*) is also believed to influence facial selectivity in the terminal protonation step of the Nazarov reaction, resulting in particularly high enantioselectivities when R is a bulky substituent.

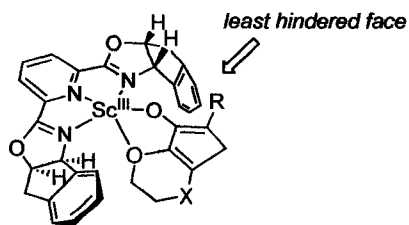


Figure 1.5. Chiral transition state leading to selective protonation of the dienolate.

1.1.3 Catalytic Nazarov Reactions

Typically, the Nazarov cyclization is initiated using at least one equivalent of strong protic or Lewis acid. Although there had been early indication that the reaction could be performed with low catalyst loading^{6b,15} the first examples of general and mild Lewis acid catalysis did not appear in the literature until 2003. Frontier and co-workers¹⁶ accomplished successful catalysis using 2 mol% Cu(OTf)₂ on substrates that were polarized towards cyclization of a “nucleophilic” double bond onto an “electrophilic” double bond (*Figure 1.6*). This polarization facilitated cyclization more readily than with

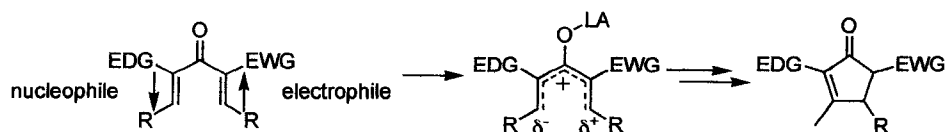
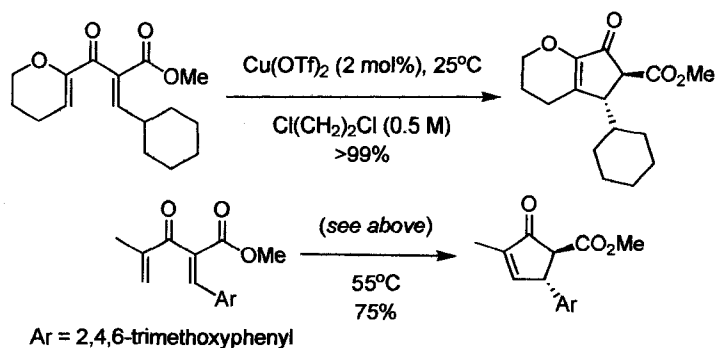


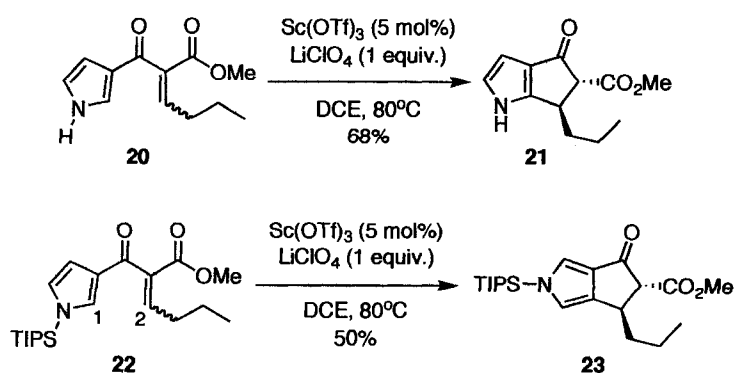
Figure 1.6. Polarization of divinyl ketones.

simple, alkyl-substituted divinyl ketones, which undoubtedly contributed to the success of the catalytic reaction. It was found that treatment of the polarized substrates with catalytic Cu(OTf)₂ led to generation of the cyclopentenone products in good yields and in relatively short reaction times (*Scheme 1.9*). The products were generally obtained as



Scheme 1.9. Examples of Cu(OTf)₂-catalyzed Nazarov cyclizations.

single regioisomers, with elimination having occurred on the opposite side to the ester functionality. This result is in accordance with the earlier discussion wherein electron-withdrawing substituents on the 2-oxidocyclopentenyl cation destabilize the positive charge, resulting in regioselective elimination on the opposing side of the oxyallyl cation. The *trans*-relationship between α - and β -substituents of the vinyl “electrophile” was assigned based on the assumption that the thermodynamic product would be obtained under these reaction conditions. More recently, the same research group has uncovered that a $\text{Sc}(\text{OTf})_3/\text{LiClO}_4$ system can be used to perform analogous catalytic Nazarov cyclizations on relatively unreactive heteroaromatic vinyl ketones (*Scheme 1.10*).¹⁷ These reactions might also be thought of as *intramolecular vinylogous Friedel-Crafts acylations*. Interestingly, the authors discovered that these reactions proceeded smoothly

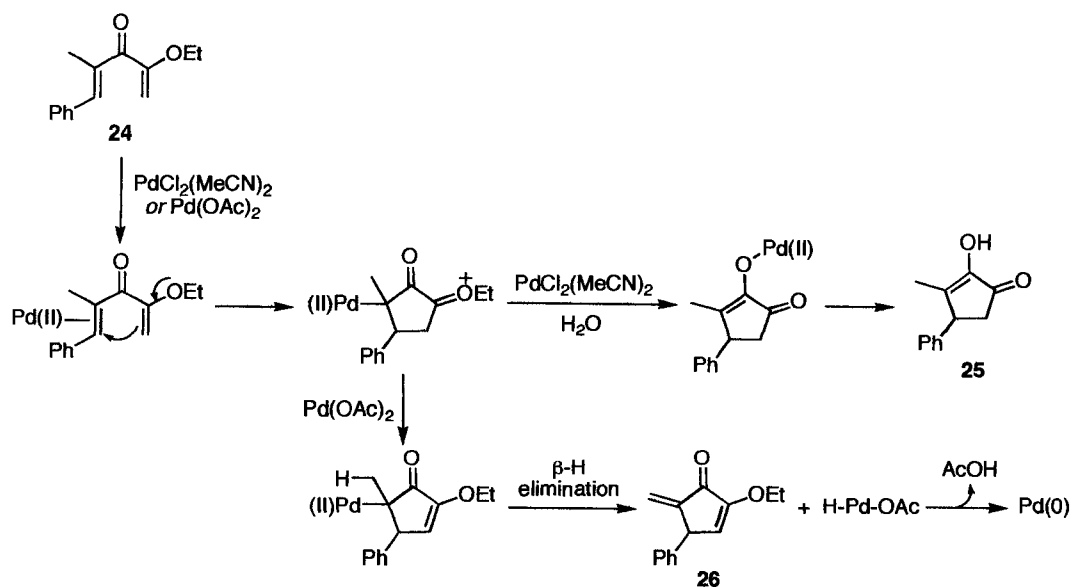


Scheme 1.10. $\text{Sc}(\text{OTf})_3$ -Catalyzed Nazarov cyclizations of heteroaromatic vinyl ketones.

to furnish the desired compounds (such as **21**), in moderate to excellent yields without protection of the pyrrole or indole functional groups; however, when a bulky protecting group was placed on pyrrole substrate **22**, a Friedel-Crafts reaction occurred to provide **23** in 50% yield and none of the desired Nazarov product was observed. The formation

of **23** was attributed to unfavourable steric interactions that would predominate when the sp^2 carbons, C-1 and C-2, approach to participate in a typical Nazarov cyclization.

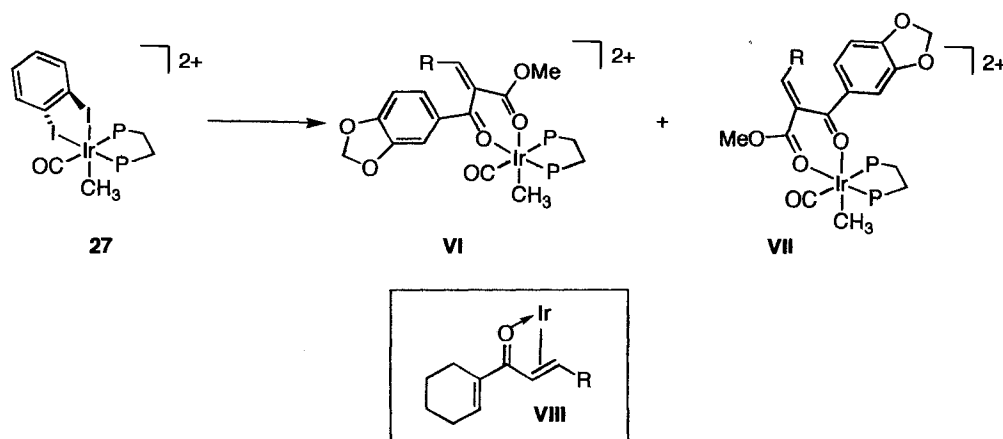
During an investigation into asymmetric variants of the Nazarov reaction, Tius and co-workers¹⁸ discovered a Pd(II)-catalyzed Nazarov-type cyclization. Although the mechanism of these reactions is not believed to proceed through an obvious pentadienyl cation, it is worth discussing this methodology in the context of the development of catalytic Nazarov variants. Tius and co-workers observed that Pd(II) could be used to catalyze the cyclization of dienone **24** to generate cyclopentenone **25** or dienone **26** selectively, depending on the catalyst used (*Scheme 1.11*). A number of examples were provided, which illustrated the broad scope of the reaction, and the yields were moderate to excellent when $\text{PdCl}_2(\text{MeCN})_2$ (1-10 mol %) was used to generate the cyclopentenone products. However, the yields were lower when the $\text{Pd}(\text{OAc})_2$ -catalyzed transformations were examined and higher catalyst loadings (20 mol %) were necessary. It was also



Scheme 1.11. Mechanistic proposal for generation of **25** and **26**.

determined that only divinyl ketones with α -oxygenation were suitable substrates for this methodology. On the basis of their observations, the mechanism was postulated to involve initial activation of the electron-poor olefin by the catalyst as opposed to the traditional carbonyl-activation seen in Nazarov cyclizations. Cyclization therefore occurs as a result of electron-rich olefin attack onto the Pd(II)-olefin complex, and thereafter the mechanism is highly dependant on the choice of catalyst. Due to the propensity for palladium hydride species to undergo reductive elimination to irreversibly generate Pd(0), the reactions utilizing Pd(OAc)₂ were performed in the presence of an oxidant to regenerate the active catalyst.

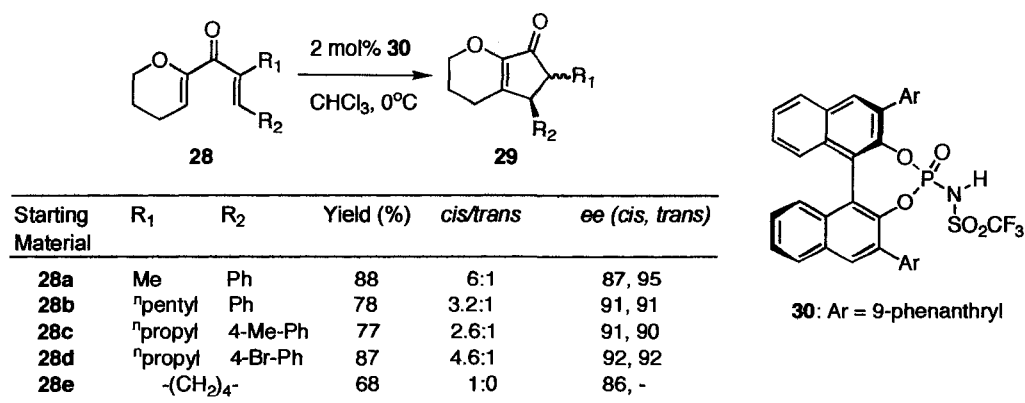
In recent years, a number of Lewis acid catalysts have been developed to induce Nazarov cyclization of various dienone substrates.^{14a,19} One of the most interesting of these examples is the dicationic Ir(III) complex [IrMe(CO)(dppe)(DIB)](BAR^f)₂ (**27**) developed by Eisenberg, Frontier, and co-workers (*Scheme 1.12*).²⁰ The iridium complex has been found to efficiently catalyze Nazarov cyclization of many aryl vinyl and divinyl ketones, generating the corresponding cyclopentenone products in high yields and



Scheme 1.12. Coordination of dicationic Ir(III) complex to dienone substrates.

short reaction times. Using ^{31}P NMR spectroscopy, it has been determined that the substrate is activated through bidentate coordination to the catalyst, **VI** or **VII**, after preliminary dissociation of the *o*-diiodobenzene (DIB) ligand. This complexation holds the substrate in the *s-trans/s-trans* conformation that is necessary for Nazarov cyclization to occur. The mechanism for this process involves dissociation of the DIB ligand, revealing two free coordination sites on the Ir(III) center. In the absence of α -carbonyl substitution - or some alternate coordinating heteroatom - on the divinyl ketone, Ir(III) will coordinate with the carbonyl and one of the conjugated olefins, **VIII**, thereby impeding the cyclization process. This is the major limiting factor associated with the use of this highly reactive catalyst, because not all substrates can meet the requirements for catalysis.

Very recently a catalytic asymmetric Nazarov reaction has been disclosed which utilizes chiral Brønsted acids to both initiate the cyclization process and generate a chiral environment to influence the torquoselectivity of the reaction.²¹ This work presents the first organocatalytic electrocyclization reaction, providing the desired cyclopentenone



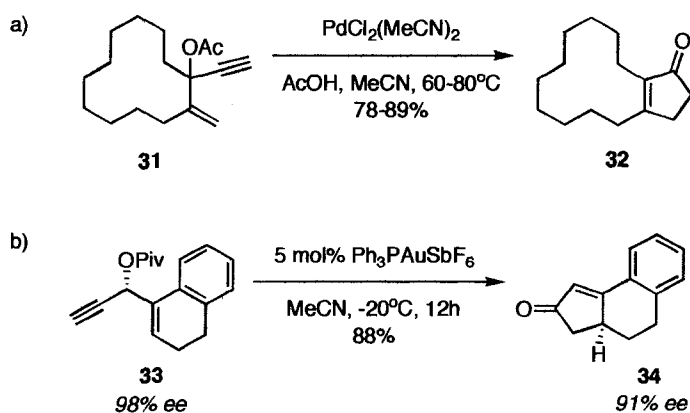
Scheme 1.13. An organocatalytic enantioselective Nazarov cyclization.

products **29** in good yields and with high enantioselectivities (*Scheme 1.13*). Once again, substrates with α -oxygenation, **28**, were used to ensure regioselective elimination during termination of the reaction, but a number of examples were presented to demonstrate the toleration of both aromatic and alkyl substitution on the opposing vinyl moiety. The authors propose that Brønsted acid **30** activates the divinyl ketone through protonation to generate a tight ion pair involving the protonated substrate and chiral phosphoramidate anion. This tight transition state is believed to force selective conrotation in the electrocyclization step. The authors also suggest that protonation of the intermediate enol species occurs stereoselectively as a result of proton transfer from the Brønsted acid to furnish the *cis*-cyclopentenones as the major products. Upon treatment with basic alumina, the *cis*-products could be isomerized to the *trans*-cyclopentenones without loss of enantiomeric purity. Since the *trans* stereochemistry is typically observed as a result of the previously outlined methodologies, this approach provides a complementary route to *cis*-isomers.

A great deal of work has been done in an effort to approach some of the major drawbacks associated with the traditional Nazarov cyclization. Recent developments in catalysis and asymmetric cyclization have made the Nazarov reaction much more attractive for use in total synthesis, since harsh reaction conditions and full equivalents of catalyst are no longer essential to the electrocyclization process. However, there is still room for improvement in these areas as most of the catalysts that have been developed require bidentate coordination to the divinyl ketones, limiting the number of substrates that can be used with these methodologies.

1.1.4 Non-traditional Substrates for Nazarov Cyclization

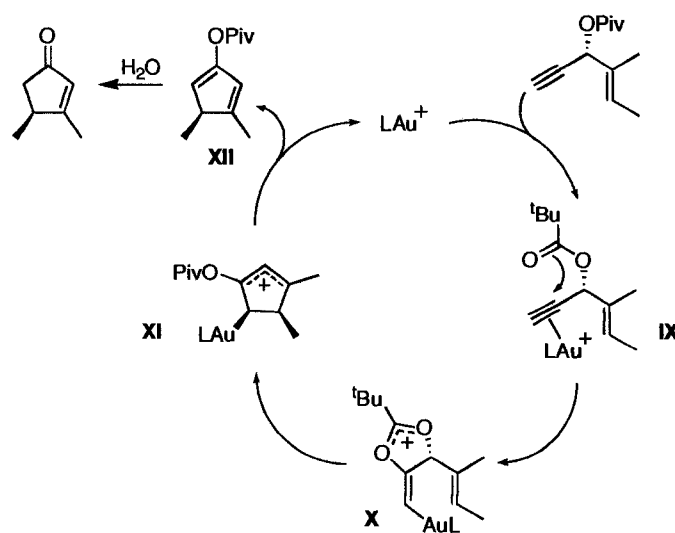
Thus far, discussion of the Nazarov cyclization has focused on the activation of divinyl ketones to provide cyclopentenone products. However, there have been many examples in the literature wherein pentadienyl cationic species were accessed without the need for divinyl ketone activation. For example, the transient generation of pentadienyl cations is often observed in transition metal-catalyzed transformations of enynyl acetates. This reaction, known as the Rautenstrauch²² rearrangement (*Scheme 1.14*), is a classic



Scheme 1.14. Rautenstrauch rearrangement of enynyl acetates.

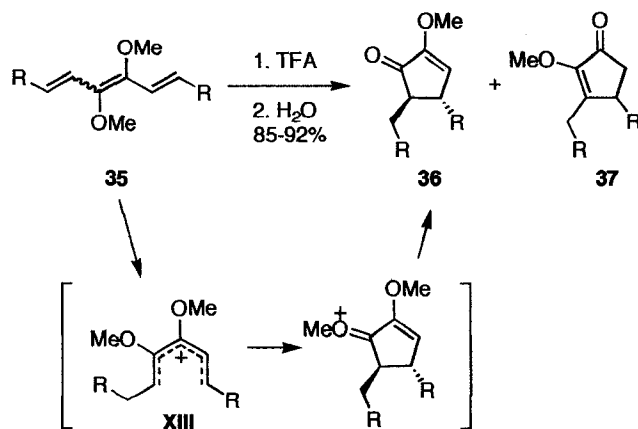
example of cyclopentenone synthesis as a result of non-traditional Nazarov cyclization. Treatment of enynyl acetates **31** with 0.025-0.1 equivalents of $\text{PdCl}_2(\text{MeCN})_2$ in the presence of acetic acid, led to the generation of **32** in 78-89% yield (*Scheme 1.14*, Equation a). With the recent explosion of gold catalysis, the Rautenstrauch reaction has received renewed attention²³ and substrates such as **33** have been found to undergo effective transformation to **34** with high retention of enantiomeric purity^{23a} (*Scheme 1.14*, Equation b). The mechanisms for both the palladium and gold-catalyzed reactions are believed to proceed through similar intermediates; however, only the gold-catalyzed

process will be discussed at this time (*Scheme 1.15*). Activation of the alkyne moiety with cationic Au(I) induces attack by the ester functionality onto the internal alkyne carbon (**IX**). The result of this attack is a pentadienyl cationic species, **X**, which can undergo conrotatory Nazarov cyclization to form the oxyallyl cation **XI**. Subsequent elimination of the cationic Au(I) complex releases diene **XII**, and upon hydrolysis the cyclopentenone product is revealed.



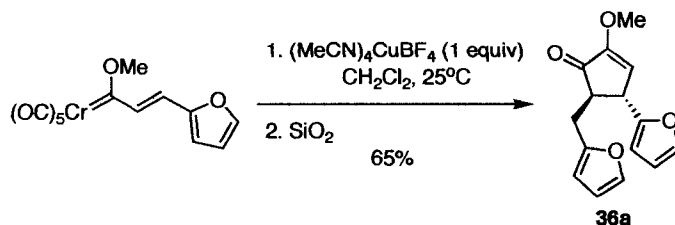
Scheme 1.15. The gold-catalyzed Rautenstrauch rearrangement mechanism.

Another example of Nazarov-type cyclization from non-traditional substrates can be found in Barluenga's 2004 publication discussing the synthesis of dimethoxyhexatrienes **35** through the copper-catalyzed dimerization of chromium Fischer carbene complexes.²⁴ Upon treatment with trifluoroacetic acid, hexatrienes **35** (*Scheme 1.16*) were found to undergo protonation to form the pentadienyl cations **XIII**, which then underwent electrocyclic ring closure to furnish a 1:1 mixture of cyclopentenones **36** and **37** in 85-92% yield. Interestingly, it was found that some of the Fischer carbene



Scheme 1.16. The mechanism of cyclopentenone formation from hexatrienes **35**.

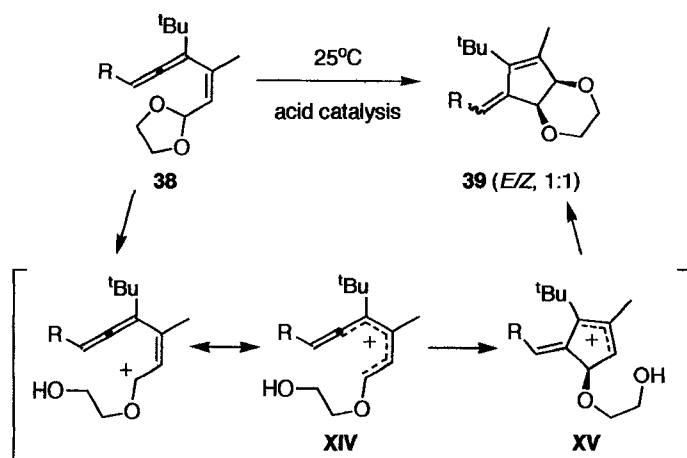
starting materials could be induced to proceed directly to the cyclopentenone products upon treatment with 1 equivalent of $(\text{MeCN})_4\text{CuBF}_4$ and direct transfer of the crude material to a silica gel column for purification (*Scheme 1.17*). Due to the nature of these dimethoxyhexatriene substrates and the reaction mechanism, both stereocenters that are established during Nazarov cyclization are retained in the cyclopentenone products **36**.



Scheme 1.17. Direct Nazarov cyclization from Fischer carbene complexes.

One final example of non-traditional substrates participating in the Nazarov cyclization can be observed in de Lera's use of (*Z*)-vinylallene acetals **38** to synthesize alkylidenecyclopentenones **39** under acid catalysis (*Scheme 1.18*).²⁵ A number of mild acidic conditions (*i.e.* $\text{FeCl}_3 \cdot \text{SiO}_2$, CHCl_3 ; *p*- TsOH , acetone/ H_2O ; LiClO_4 , Et_2O , 25°C) were examined in an attempt to deprotect the acetal in **38**; however, the same mixture of

E- and *Z*-isomers of **39** was obtained in almost quantitative yield regardless of catalyst used. The authors propose that the products are formed as a result of acetal protonation to generate the pentadienyl cation **XIV**, which undergoes Nazarov cyclization to furnish cyclic allyl cation **XV**. The pendant alcohol moiety then acts to intercept the carbocation



Scheme 1.18. de Lera's Nazarov-type cyclization of (2*Z*)-vinylallene acetals.

from the same face to generate *cis*-fused bicyclic products. Although the authors were not expecting these results, this work demonstrates an intriguing Nazarov-type process and presents an early example of a pendant nucleophile trapping out a cyclic allyl cation in an “interrupted” Nazarov reaction.

1.2 The Interrupted Nazarov Reaction

One of the major drawbacks associated with the Nazarov cyclization that has yet to be discussed is the loss of intermediate stereogenic centers arising from standard termination pathways. The “interrupted” Nazarov reaction allows for the preservation of stereochemistry established during the electrocyclization by using internal or external

nucleophiles as traps for the 2-oxidocyclopentenyl cation (*Figure 1.7*). Essentially, the cationic intermediates that are generated during Nazarov cyclization can be used to initiate domino or cascade processes.²⁶ Trapping of the oxyallyl cation can lead to the synthesis of highly functionalized, complex products in a stereocontrolled fashion.

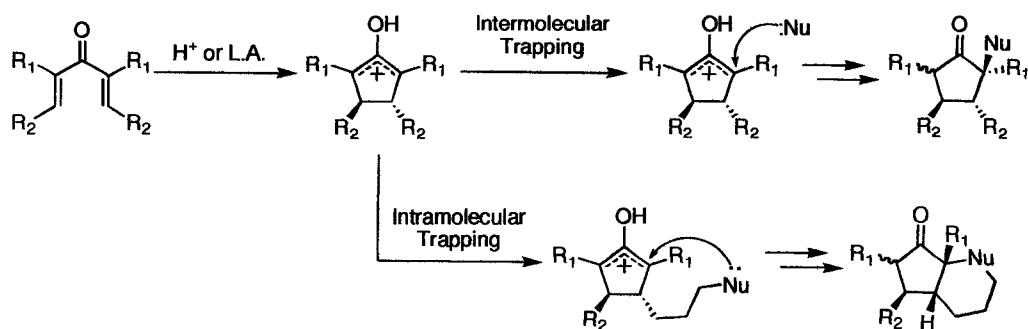
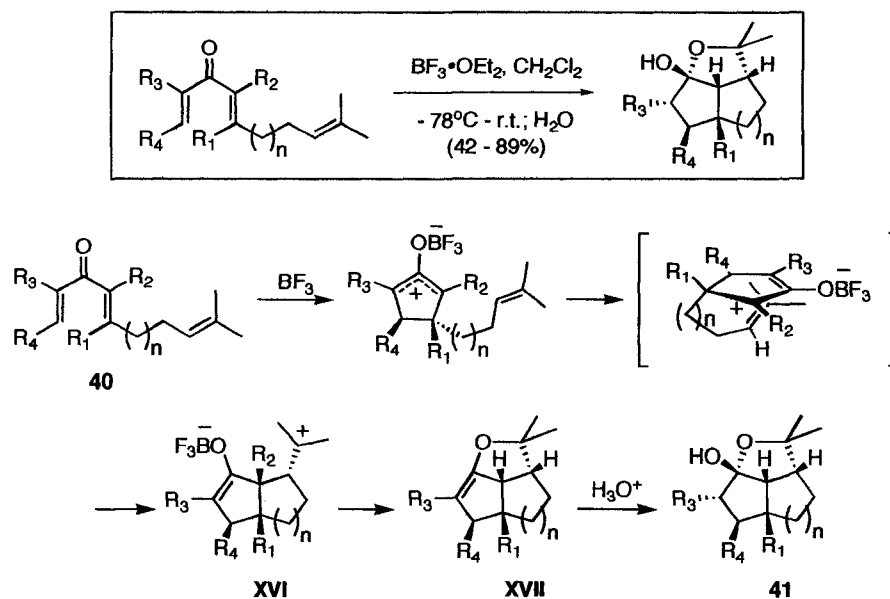


Figure 1.7. The “interrupted” Nazarov reaction.

1.2.1 Intramolecular Trapping

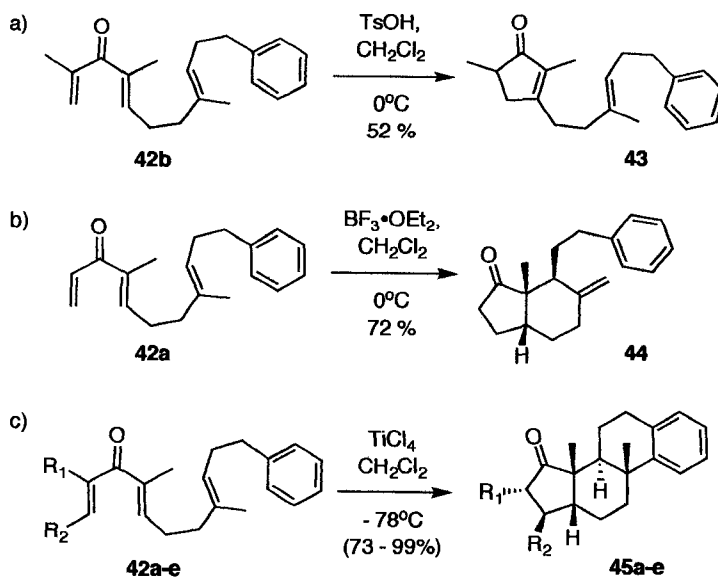
The earliest examples of “interrupted” Nazarov reactions were observed in the disrotatory photochemical cyclizations of pyran-4-ones appended with tethered nucleophiles.²⁷ The success of these photochemical transformations encouraged West and co-workers to develop an analogous process for the thermal, Lewis acid-mediated Nazarov reaction. In 1998,²⁸ a diastereoselective cycloisomerization was presented in which acyclic dienone precursors **40** underwent efficient Nazarov cyclization and were subsequently trapped by a tethered olefin (*Scheme 1.19*). This sequence generated complex, polycyclic products **41** from simple starting materials due to the formation of two new carbon-carbon bonds and multiple stereogenic centers. Also, the stereochemistry that was established during the initial electrocyclization influenced the formation of subsequent stereogenic centers, furnishing single diastereomers as products.



Scheme 1.19. Trapping of the oxyallyl cation with a tethered olefin.

The mechanism for this reaction sequence proceeds through the traditional Lewis acid activation and electrocyclization pathway to furnish a 2-oxocyclopentenyl cation. Subsequent 5-*exo* cationic cyclization onto the remote olefin generates an intermediate cationic species **XVI**, which leads to carbon-oxygen bond formation (**XVII**) as a result of the close proximity between the enolate oxygen and newly formed tertiary carbocation. Aqueous work-up conditions led to selective protonation of the enol ether moiety with subsequent trapping of the oxocarbenium by water to generate the observed hemiketal product **41**. Yields for these transformations were good to excellent, with two exceptions: when $n = 2$, analogous 6-*exo* cyclization did not proceed as efficiently as the 5-*exo* process, providing products in diminished yields and as mixtures of diastereomers, and when there was no substitution at one/both of the α -positions on the divinyl ketone only a complex mixture of unidentified products was observed.

Intramolecular trapping of the cationic Nazarov intermediate has been demonstrated using differentially substituted olefins²⁹ as well as dienes,³⁰ allowing access to a variety of fused and bridged polycyclic skeletons. One of the most impressive of these processes involves an olefin polycyclization that is terminated by trapping with a pendent arene moiety (*Scheme 1.20*).³¹ In this work, the Nazarov cyclization was



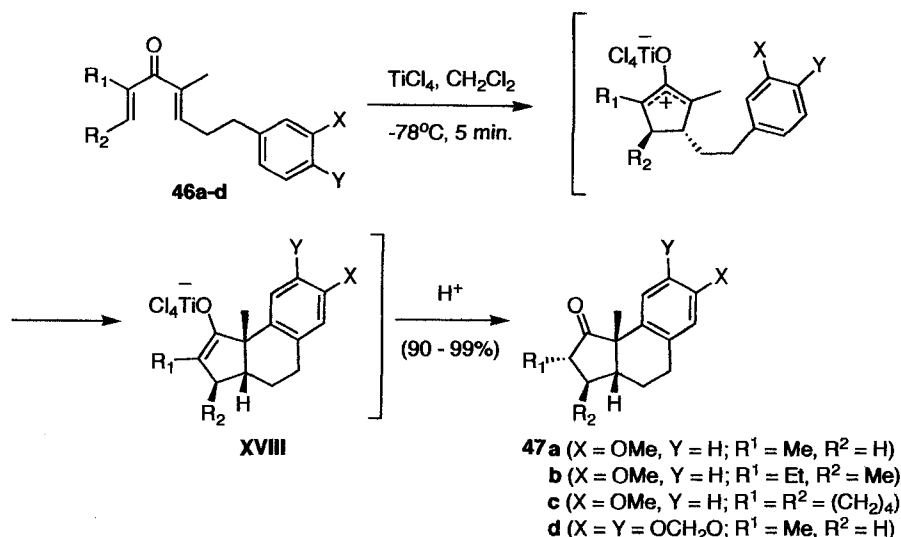
Starting Material	R ₁	R ₂	Yield (%)
42a	H	H	-
42b	Me	H	99
42c	Me	Et	73
42d		-(CH ₂) ₄ -	98
42e		-(CH ₂) ₅ -	74

Scheme 1.20. Cascade polycyclization of aryltrienones.

initiated by activation with TiCl_4 , since protic acid and $\text{BF}_3 \cdot \text{OEt}_2$ provided **43** and **44**, in 52% and 72% yields respectively, as a result of premature termination of the cascade process. Only TiCl_4 furnished a cationic species capable of promoting the desired polycyclization. Subsequently, multiple bond-forming steps and the establishment of numerous stereogenic centers proceeded to provide tetra- or pentacyclic products **45** in

good to excellent yields and in a diastereoselective manner. Since aryltrienone **42a** did not participate in the desired cascade pathway, the major limitation of this methodology appears to be the requirement for α -substitution on the starting materials.

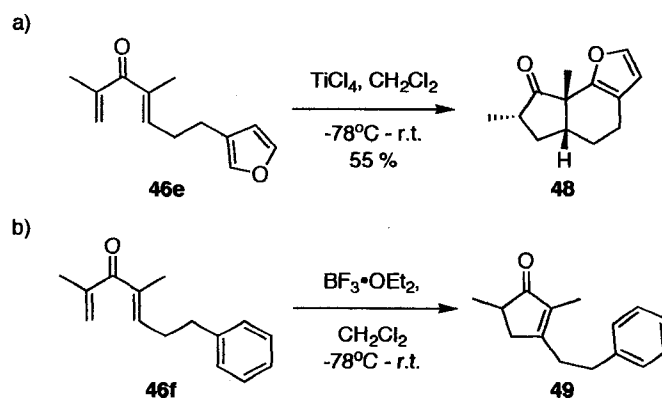
An analogous trapping methodology was developed in 2001³² wherein tethered arene moieties were used to trap the cyclic oxyallyl intermediate directly, furnishing benzohydrindenones **47** from the respective dienones **46** in excellent yields (*Scheme 1.21*). Once again, this trapping process proceeded in a diastereoselective fashion with electrophilic aromatic substitution occurring at the least hindered position (*para* to X) to generate *cis* ring-fused products. Also, protonation of the penultimate enolate occurred



Scheme 1.21. Benzohydrindenone formation from aryl dienones.

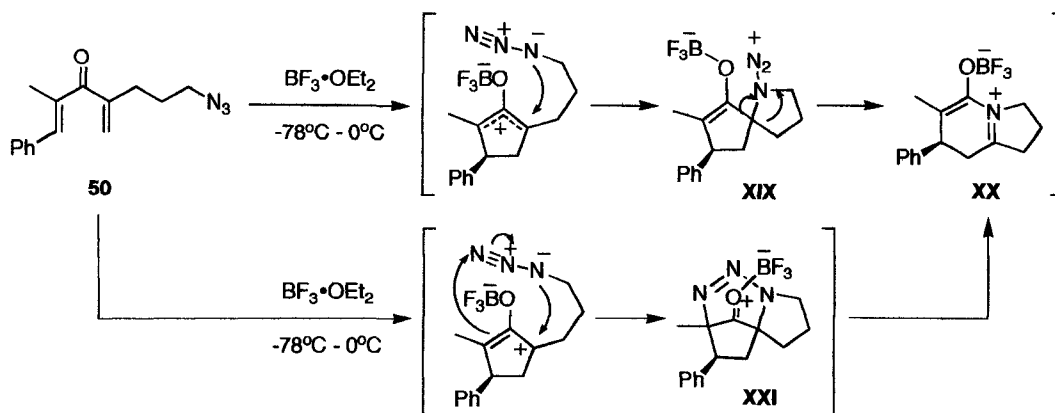
selectively from the least hindered, convex face of the polycyclic intermediate **XVIII**. Notably, a pendent furan could participate in the trapping process to provide the furylhydrindenone **48** in 55% yield upon raising the reaction temperature to room temperature (*Scheme 1.22*, Equation a). The lower yield was attributed to

oligomerization and decomposition processes that may have become prevalent upon raising the temperature of the cyclization reaction. An obvious limitation to this methodology is that an electron-rich arene unit is required to trap the cationic Nazarov intermediate. Dienone **46f** did not react cleanly under the influence of TiCl_4 , providing a complex mixture of products, whereas the same substrate only provided the simple cyclopentenone **49** when subjected to $\text{BF}_3 \cdot \text{OEt}_2$ (Scheme 1.22, Equation b).



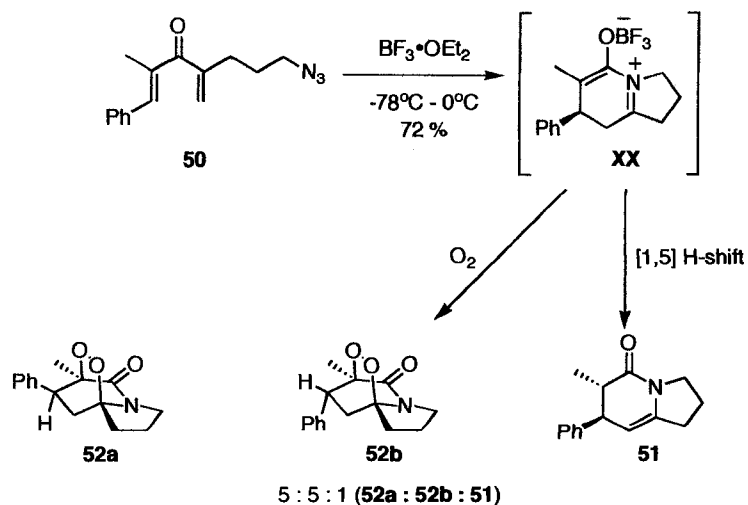
Scheme 1.22. Electron-rich versus electron-poor arene trapping.

Thus far, the discussion of intramolecular interrupted Nazarov reactions has focused on the formation of carbon-carbon bonds as a result of trapping the 2-oxidocyclopentenyl cation with tethered π -systems. Recently there has been some success utilizing oxygen-³³ and nitrogen-based³⁴ nucleophiles in a similar fashion to synthesize heterocyclic structures in a single operation. One example of these processes is the participation of tethered azides in an interrupted Nazarov/Schmidt rearrangement sequence to generate peroxy-bridged indolizidinones **52**.³⁴ Although the mechanism is not completely understood, there is literature precedent that suggests initial trapping of the cyclic oxyallyl cation by the internal azide nitrogen,³⁵ which results in a zwitterionic



Scheme 1.23. Intramolecular azide trapping of the cationic Nazarov intermediate.

species (**XIX**) that can rearrange to a 1,4-dipole (**XX**) with concomitant loss of N_2 (*Scheme 1.23*). Alternatively, the 1,4-dipole might be generated as the result of Lewis acid-mediated decomposition of a [3+3] cycloaddition product (**XXI**).³⁶ The 1,4-dipole can subsequently proceed down a [1,5]-hydrogen shift pathway to generate dihydropyridone **51**, or undergo oxidation in the presence of ambient oxygen to furnish the peroxy-bridged compounds **52a** and **52b** (*Scheme 1.24*). As an added feature, it was

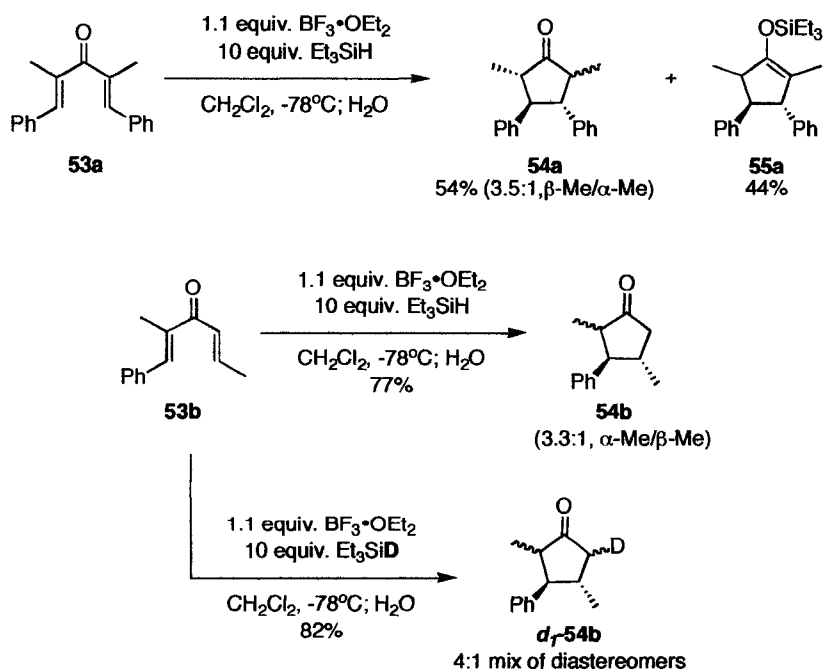


Scheme 1.24. Formation of trapping products from dienones with tethered azides.

found that formation of the peroxy compounds could be suppressed upon rigorous exclusion of oxygen from the reaction flask, providing **51** in 70% yield. Interestingly, when the analogous intermolecular trapping process was examined, none of the peroxy-bridged products were observed (see *Section 1.2.2*).

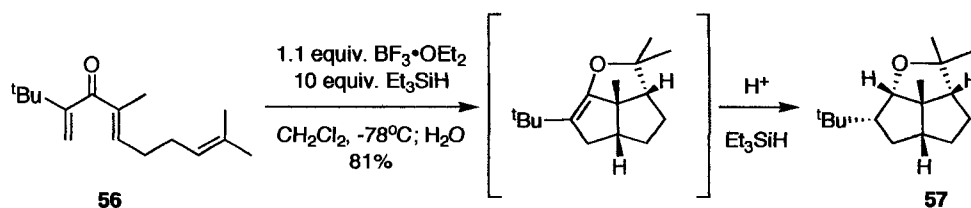
1.2.2 Intermolecular Trapping

Not long after the first examples of intramolecular interrupted Nazarov processes had been disclosed, intermolecular variants were developed. These intermolecular trapping reactions provided an alternate route towards carbocyclic ring construction that also retained stereochemical information established during the initial conrotatory electrocyclicization. The reductive Nazarov cyclization^{15a,37} utilizes a Lewis acid-tolerant hydride source to trap the cationic oxyallyl intermediate, providing a direct route to cyclopentanones **54** from divinyl ketone precursors **53** (*Scheme 1.25*). It was found that



Scheme 1.25. The reductive Nazarov cyclization.

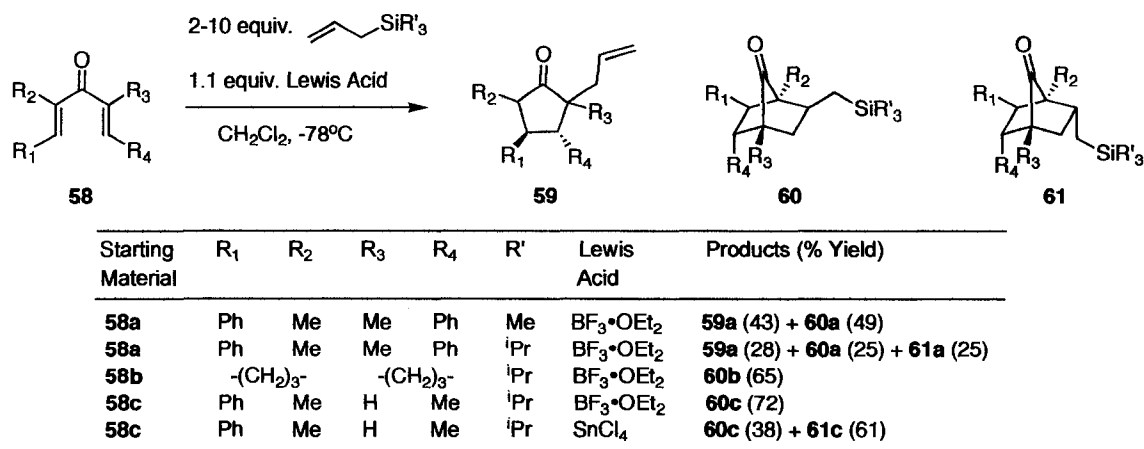
treatment of **53a** with 1.1 equivalents of Lewis acid in the presence of 2-10 equivalents of triethylsilane resulted in a mixture of cyclopentanones **54a** and silyl enol ethers **55a**. When an acidic aqueous work-up was carried out, hydrolysis of the silyl enol ethers occurred to furnish the cyclopentanones as the sole products in excellent yields. The reductive Nazarov cyclization was one of the first examples wherein less than 1 equivalent of Lewis acid could be used to catalyze the cyclization; however, in these cases the yields were reduced. A number of interesting observations were made during this study including the observation that hydride delivery was regioselective for the less substituted side of the oxyallyl cation. This was confirmed by treatment of non-symmetrical dienone **53b** with deuterated triethylsilane, which provided *d*₁-**54b** in 82% yield. Also, the conversion of **56** to **57** illustrated that intermolecular trapping could be used in conjunction with intramolecular processes to generate new carbon frameworks in a single operation (*Scheme 1.26*).



Scheme 1.26. An interrupted Nazarov reaction terminated with ionic reduction.

In an attempt to synthesize 2-allylcyclopentanones **59** using nucleophilic allylsilanes to trap the cationic Nazarov intermediate, West and co-workers discovered that allylation was, in fact, the minor product of such reactions.³⁸ Instead, the bicyclo[2.2.1]heptanones **60** and/or **61** were generated in moderate yields due to formal [3+2] addition of the oxyallyl cation to the olefin of the allylsilane (*Scheme 1.27*). When

the bulky allyltriisopropylsilane was used, the desilylation process leading to **59** was suppressed, providing increased yields of the bicyclo[2.2.1]heptanone products.

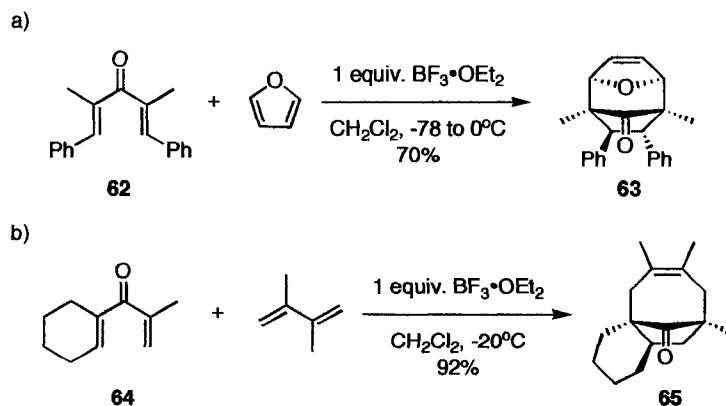


Scheme 1.27. Intermolecular trapping of the Nazarov intermediate with allylsilanes.

Regioselectivity in these reactions followed the same principles observed in the reductive Nazarov reaction, with attack of the allylsilane occurring from the least hindered side of the oxyallyl cation; however, the *exo/endo* stereochemistry appeared to be very dependent on the choice of Lewis acid. For example, treatment of dienone **58c** with BF₃•OEt₂ in the presence of allyltriisopropylsilane led to exclusive formation of the *exo* product **60c** in 72% yield, but SnCl₄-catalysis generated a mixture of *exo* and *endo* products in 38% and 61% yields respectively.

The success of intramolecular trapping of the cationic Nazarov intermediate with tethered dienes³⁰ prompted West and co-workers to develop an analogous intermolecular approach to the synthesis of cyclooctanoids using various dienes to trap the 2-oxidocyclopentenyl cation in a [4+3] fashion (*Scheme 1.28*).³⁹ Optimal conditions for this domino process were observed when dienones were treated with 1 equivalent of

$\text{BF}_3 \cdot \text{OEt}_2$ in the presence of 2 equivalents of the desired diene at -20°C . Under these relatively mild conditions it was found that furan (Equation a), cyclopentadiene, isoprene, and 2,3-dimethylbutadiene (Equation b) could all be used to capture the intermediate

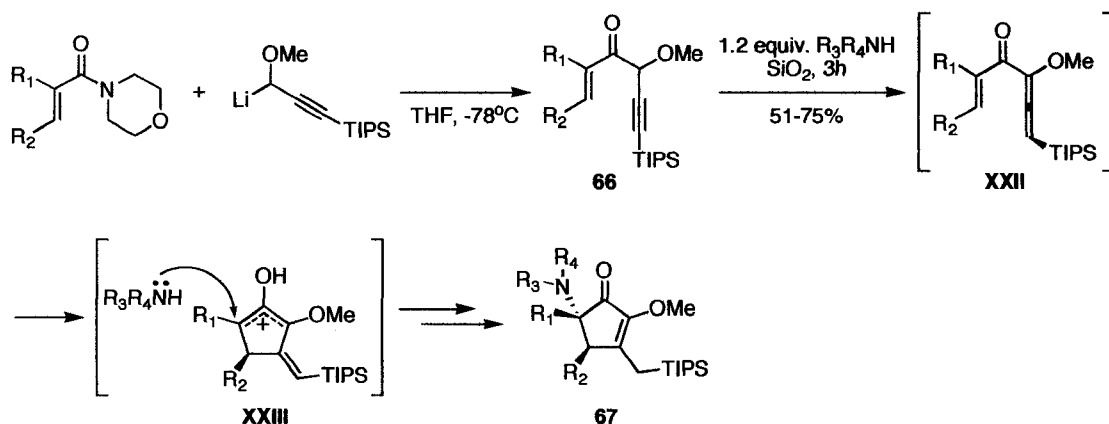


Scheme 1.28. Intermolecular diene trapping to furnish cyclooctene carbocycles.

oxyallyl cation, providing the corresponding eight-membered rings, **63** or **65**, in good to excellent yields and with generally high diastereofacial selectivity due to approach of the diene from the least hindered face of the cationic Nazarov intermediate. This methodology complements the intramolecular process and provides access to highly functionalized cyclooctenoid skeletons in a single operation starting from simple dienone and diene precursors.

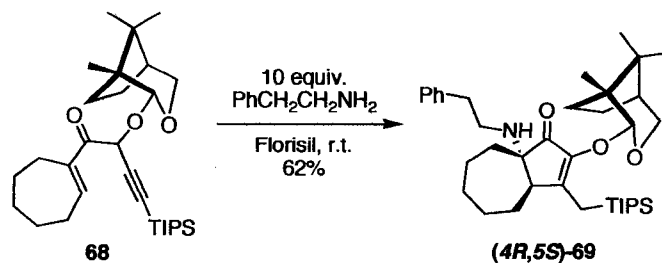
Very recently, there have been successful reports of heteroatom-based nucleophiles participating in intermolecular interrupted Nazarov reactions.⁴⁰ Of particular interest is the amine trapping of 2-oxidocyclopentenyl cations generated *in situ* from the exposure of ketones **66** to dry silica gel (*Scheme 1.29*).^{40b} The cyclization process undoubtedly proceeds through an allenyl vinyl ketone **XXII**, which cyclizes spontaneously to generate the cyclic oxyallyl cation **XXIII**. Although this cationic

intermediate could proceed through a number of terminative pathways, it is long-lived enough to allow nucleophilic trapping by primary or secondary amines, furnishing aminocyclopentenones **67** in good yields. As observed in previous studies, approach of the nucleophile occurs from the least hindered face of the oxyallyl intermediate, with



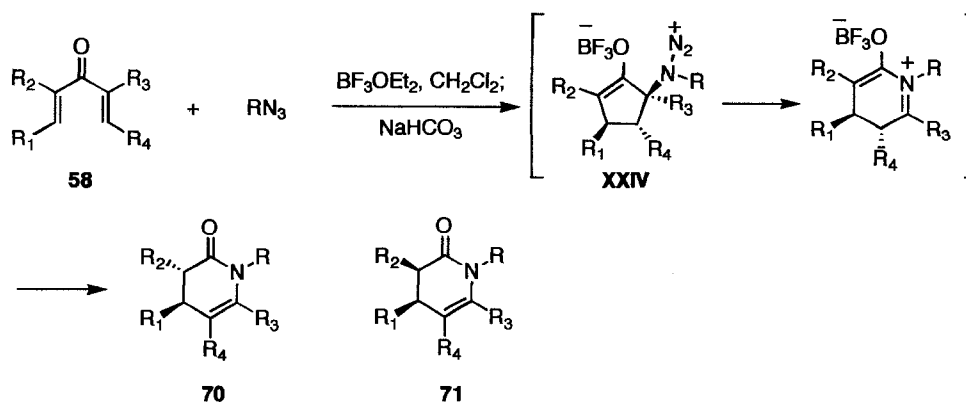
Scheme 1.29. Mild amine trapping in the interrupted Nazarov reaction.

regioselective attack on the opposite side to the methoxy substituent. These stereochemical aspects were exploited in the development of the first asymmetric interrupted Nazarov reaction,^{40c} wherein a camphor-derived auxiliary replaced the methoxy substituent to generate chiral ketones (**68**, *Scheme 1.30*). The participation of these chiral auxiliaries in the previously outlined reaction led to diastereomerically pure aminocyclopentenones in good yields.



Scheme 1.30. An asymmetric interrupted Nazarov reaction.

Another example of trapping the cyclic oxyallyl intermediate with nitrogen-based nucleophiles is observed in the domino Nazarov cyclization/azide-trapping/Schmidt rearrangement sequence that is under investigation in the West laboratories.⁴¹ A similar intramolecular process has previously been discussed wherein the Nazarov intermediate was trapped by tethered azides (see *Section 1.2.1*); however the starting materials for these intramolecular reactions were prepared over a lengthy synthetic sequence. During an investigation into the intermolecular process, it was found that simple dienones **58** underwent efficient azide trapping to generate a zwitterionic intermediate **XXIV**, which subsequently rearranged through a Schmidt-like process, furnishing a 1,4-dipolar intermediate (Scheme 1.31). A [1,5]-hydride shift might then be responsible for generation of the major *trans*-dihydropyridone adducts **70** in moderate to good yields. In some instances, the *cis*-isomers **71** were also observed as a result of competing proton-



Starting Material	R ₁	R ₂	R ₃	R ₄	R	Products (% Yield; Ratio)
58a	Ph	Me	Me	Ph	PhCH ₂	70a + 71a (82; 2:1)
58b	Ph	Me	Me	H	PhCH ₂	70b (75)
58c	Ph	Me	H	H	PhCH ₂	70c (62)
58c	Ph	Me	H	H	PhCH=CHCH ₂	70d (43)

Scheme 1.31. Intermolecular azide trapping to furnish dihydropyridones.

transfer processes. This methodology presents the first examples of extreme skeletal reorganization of the dienone precursor following interception of the cationic Nazarov intermediate by tethered or free organic azides.

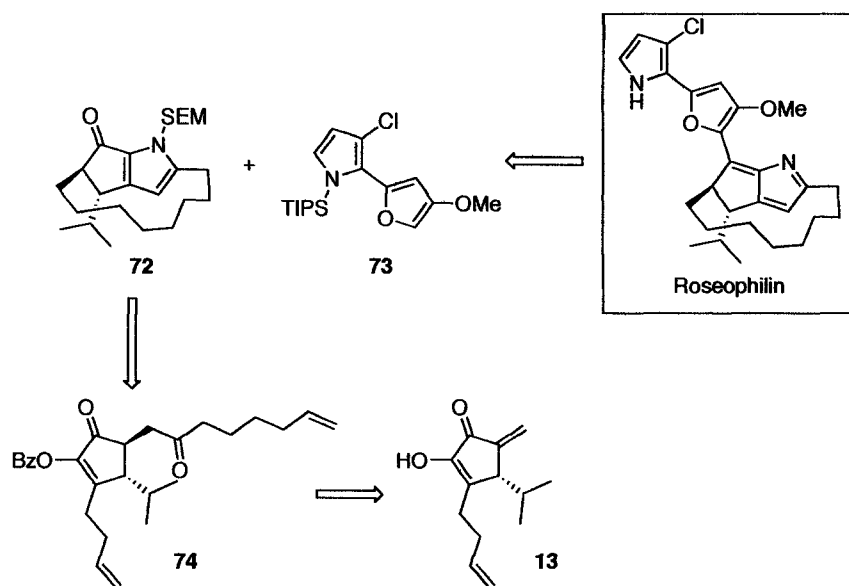
Development of the interrupted Nazarov reaction has allowed access to a broad array of highly functionalized carbocyclic and heterocyclic skeletons in a single operation starting from readily available dienone substrates. Due to the establishment of two stereogenic centers in the initial conrotatory electrocyclization, these transformations generally occur in a highly stereoselective manner with the internal or external nucleophile approaching from the less hindered face of the 2-oxidocyclopentenyl cation. Although this review has focused on trapping of the oxyallyl cationic intermediate, there have also been reports wherein the penultimate enolate formed during the Nazarov reaction has been used to trap various electrophiles.⁴² It is clear that a number of avenues remain open for investigation in this area and that new modes of trapping might be available for discovery.

1.3 Recent Examples in Total Synthesis

The Nazarov reaction has been used as the strategic step in a number of approaches towards the synthesis of different natural products. Selected examples demonstrating original use of the Nazarov reaction will be presented herein to illustrate the usefulness of this electrocyclization process in organic synthesis.

1.3.1. Roseophilin

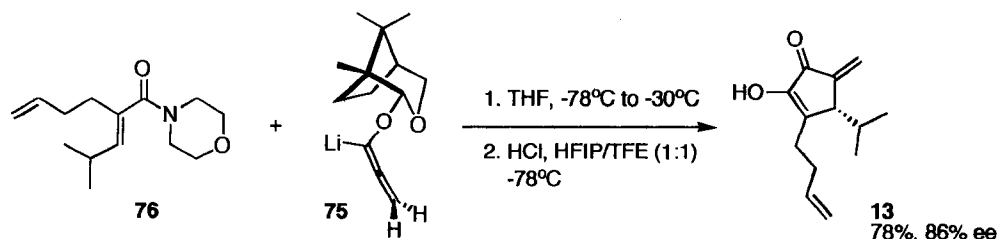
In 2001, Tius and Harrington reported the first asymmetric total synthesis of the potent antitumor alkaloid roseophilin. Their synthetic strategy utilized an asymmetric Nazarov cyclization to establish the correct stereochemistry of the isopropyl moiety on the azafulvene core (*Scheme 1.32*).⁴³ In this approach, roseophilin was synthesized from coupling ketopyrrole **72** with the pyrrolylfuran **73**, followed by deprotection of the SEM



Scheme 1.32. Tius' retrosynthesis of roseophilin.

protecting group to initiate "aromatization" to the desired azafulvene. Ketopyrrole **72** was synthesized as a result of ring closing metathesis performed on diene **74**, with subsequent Knorr condensation to establish the pyrrole functionality. Diene **74** was obtained through elaboration of cyclopentenone **13**, which was constructed in an asymmetric cyclopentannelation reaction. The key step was realized through the addition of the camphor-derived allenyllithium reagent **75** to morpholine amide **76**. Acidic work-up led to direct generation of the desired product **13** in 78% yield and with 86% ee

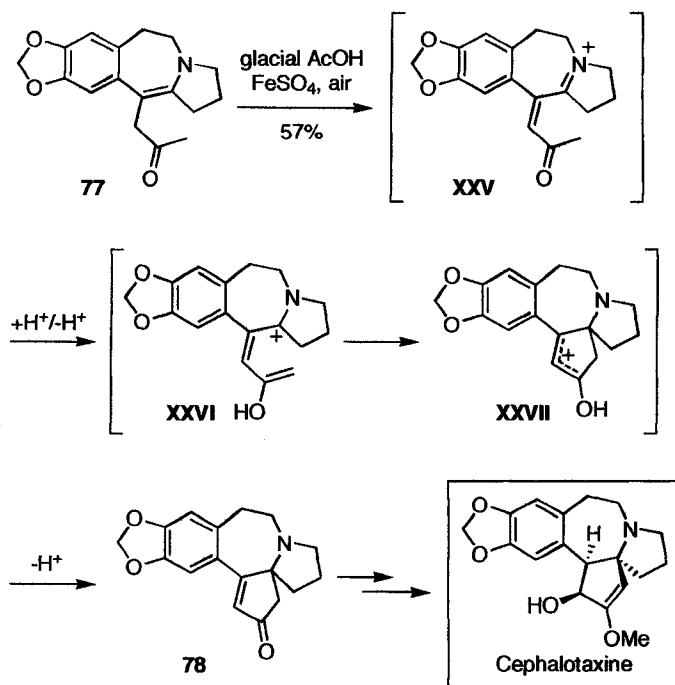
(Scheme 1.33). Use of this chiral auxiliary resulted in the formation of **13** in increased yields and with higher enantioselectivities compared to earlier studies wherein glucose-based auxiliaries were used.^{11,12}



Scheme 1.33. The key asymmetric Nazarov cyclization in the synthesis of roseophilin.

1.3.2. Cephalotaxine

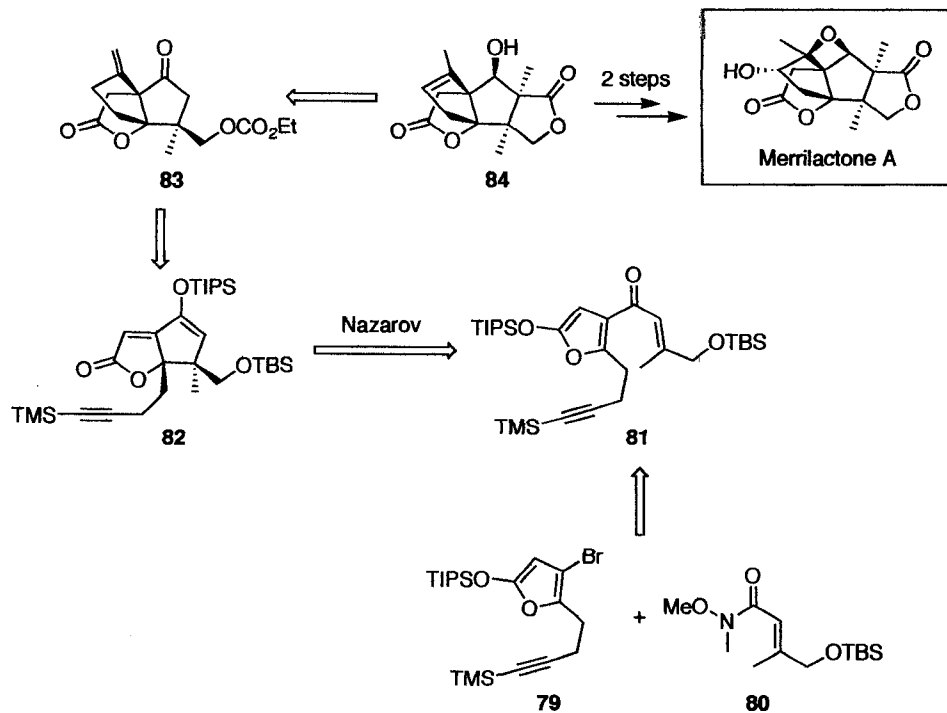
Cephalotaxine is a structurally intriguing antileukemia alkaloid that contains a benzazepine motif and a pentacyclic core. When Li and Wang⁴⁴ undertook the total synthesis of racemic cephalotaxine, they uncovered an unusual Nazarov-type cyclization (Scheme 1.34). When the advanced intermediate **77** was treated with glacial acetic acid and 1 equivalent of FeSO₄ in open air, the spirocyclic product **78** was obtained in 57% yield. The authors propose that the reaction is initiated by an acid-catalyzed autoxidation, which generates the conjugated imine species **XXV**. Tautomerization of the methyl ketone furnishes a pentadienyl cationic species (**XXVI**) that can undergo conrotatory electrocyclization to the cyclic oxyallyl cation **XXVII**. Finally, loss of a proton would afford the cyclopentenone product **78**. Although this reaction did not provide the most efficient route to the final target, it presents an interesting variant of the Nazarov reaction that may be useful in other synthetic strategies.



Scheme 1.34. A Nazarov-type cyclization in the synthesis of Cephalotaxine.

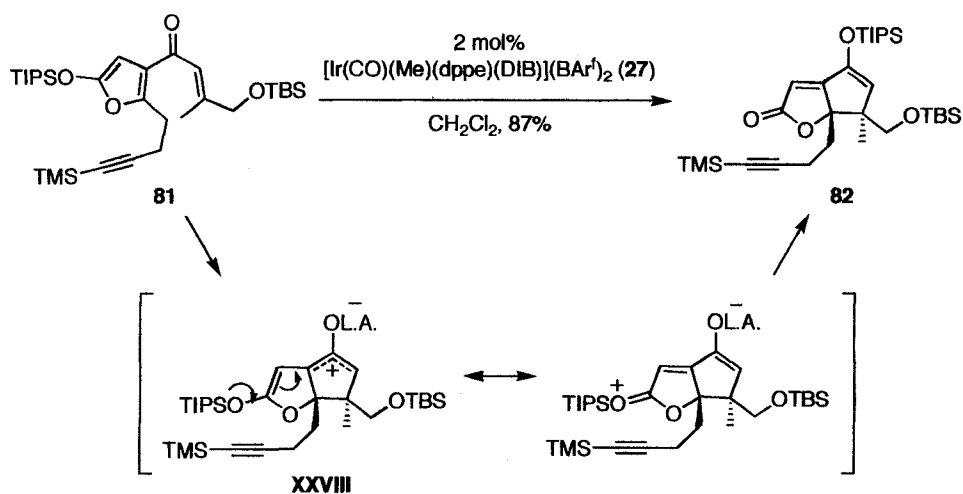
1.3.3. Merrilactone A

Very recently Frontier and co-workers have completed a total synthesis of (\pm)-merrilactone A.⁴⁵ The synthetic strategy involved coupling of silyloxyfuran **79** with Weinreb amide **80** to form a highly substituted furyl vinyl ketone substrate **81** (*Scheme 1.35*). This ketone was then used in the key Nazarov cyclization to provide lactone **82**. Radical cyclization of the 1,6-enyne and manipulation of the protecting groups furnished tricycle **83**, which could be elaborated to the tetracycle **84**. It has previously been established that **84** can be transformed to merrilactone A in two steps.⁴⁶ The key step in this synthesis involved use of the previously discussed $[\text{IrMe}(\text{CO})(\text{dppe})(\text{DIB})](\text{BAR}^f)_2$ catalyst (**27**) to catalyze Nazarov cyclization of substrate



Scheme 1.35. Retrosynthesis of (±)-merrilactone A.

81 (*Scheme 1.36*). Treatment of **81** with 2 mol% catalyst induced conrotatory cyclization to furnish the cyclic oxyallyl cation **XXVIII**. Dissociation of the Lewis acid and subsequent silyl transfer, resulted in generation of the product in 87% yield. This



Scheme 1.36. The key Nazarov reaction in Frontier's approach to merrilactone A.

reaction presents the first example of Nazarov cyclization on silyloxyfuran substrates and is used in this synthesis to establish the relative stereochemistry of two important quaternary stereogenic centers present in merrilactone A.

1.4 New Directions in the Nazarov Cyclization

The Nazarov cyclization is a convenient way to synthesize carbocyclic structures that are prevalent in many classes of natural products. With recent advances in the areas of catalytic and stereoselective variants, as well as the advent of many “interrupted” Nazarov cascade processes, the Nazarov cyclization continues to be a prominent area of research in the development of new methodologies for use in total synthesis. We hoped to expand the scope of this reaction even further by revealing alternate methods for the generation of Nazarov-type pentadienyl cations that may permit novel trapping pathways or improved functional group compatibility. Most importantly, new trapping sequences might provide simplified routes to the assembly of complex polycyclic intermediates that could be used towards the synthesis of natural products. To this end, we envisioned using non-traditional Nazarov substrates, namely *gem*-dichlorocyclopropane compounds, to access the cationic intermediates observed during Nazarov cyclization. The unique chemistry of *gem*-dichlorocyclopropanes and the development of our novel Nazarov-type reaction will be disclosed in the following chapters.

1.5 References

1. Nazarov, I. N.; Zaretskaya, I. I. *Izv. Akad. Nauk. SSSR, Ser. Khim.* **1941**, 211-224.
2. For recent reviews on the Nazarov reaction: a) Denmark, S. E. *In Comprehensive organic synthesis. Vol. 5. Edited by Trost, B. M. and Fleming, I.* Pergamon, Oxford. 1991. pp. 751-784; b) Habermas, K. L.; Denmark, S. E.; Jones, T. K. *Org. React.* **1994**, *45*, 1-158; c) Tius, M. A. *Eur. J. Org. Chem.* **2005**, 2193–2206; d) Pellisier, H. *Tetrahedron* **2005**, *61*, 6479-6517; e) Frontier, A. J.; Collison, C. *Tetrahedron* **2005**, *61*, 7577-7606.
3. a) Denmark, S. E.; Habermas, K. L.; Hite, G. A. *Helv. Chim. Acta*, **1988**, *71*, 168-194; b) Tius, M. A. *Acc. Chem. Res.* **2003**, *36*, 284-290.
4. Woodward, R. B.; Hoffmann, R. *Conservation of Orbital Symmetry*; Academic Press: New York; 1970.
5. Jefford, C. W.; Bernardinelli, G.; Wang, Y.; Spellmeyer, D. C.; Buda, A.; Houk, K. N. *J. Am. Chem. Soc.* **1992**, *114*, 1157-1165.
6. a) Denmark, S. E.; Jones, T. K. *J. Am. Chem. Soc.* **1982**, *104*, 2642-2645; b) Jones, T. K.; Denmark, S. E. *Helv. Chim. Acta.* **1983**, *66*, 2377-2396; c) Jones, T. K.; Denmark, S. E. *Helv. Chim. Acta.* **1983**, *66*, 2397-2411.
7. Ichikawa, J. *Pure Appl. Chem.* **2000**, *72*, 1685-1689.

8. a) Denmark, S. E.; Wallace, M. A.; Walker, C. B., Jr. *J. Org. Chem.* **1990**, *55*, 5543-5545; b) Hu, H.; Smith, D.; Cramer, R. E.; Tius, M. A. *J. Am. Chem. Soc.* **1999**, *121*, 9895-9896; c) Prandi, C.; Ferrali, A.; Guarna, A.; Venturello, P.; Occhiato, E.G. *J. Org. Chem.* **2004**, *69*, 7705-7709; d) Prandi, C.; Deagostino, A.; Venturello, P.; Occhiato, E. G. *Org. Lett.* **2005**, *7*, 4345-4348; e) Occhiato, E. G.; Prandi, C.; Ferrali, A.; Guarna, A. *J. Org. Chem.* **2005**, *70*, 4542-4545; f) Mazzola, R. D., Jr.; White, T. D.; Vollmer-Snarr, H.R.; West, F. G. *Org. Lett.* **2005**, *7*, 2799-2801.
9. Pridgen, L. N.; Huang, K.; Shilcrat, S.; Tickner-Eldridge, A.; DeBrosse, C.; Haltwanger, R. C. *Synlett* **1999**, 1612-1614.
10. Kerr, D. J.; Metje, C.; Flynn, B. L. *Chem. Commun.* **2003**, 1380-1381.
11. Harrington, P. E.; Tius, M. A. *Org. Lett.* **2000**, *2*, 2447-2450.
12. a) Harrington, P. E.; Murai, T.; Chu, C.; Tius, M. A. *J. Am. Chem. Soc.* **2002**, *124*, 10091-10100; b) Delos Santos, D. B.; Banaag, A. R.; Tius, M. A. *Org. Lett.* **2006**, *8*, 2579-2582; c) Banaag, A. R.; Tius, M. A. *J. Am. Chem. Soc.* **2007**, *129*, 5328-5329.
13. Aggarwal, V. K.; Belfield, A. J. *Org. Lett.* **2003**, *5*, 5075-5078.
14. a) Liang, G.; Gradl, S. N.; Trauner, D. *Org. Lett.* **2004**, *5*, 4931-4934; b) Liang, G.; Trauner, D. *J. Am. Chem. Soc.* **2004**, *126*, 9544-9545.

15. a) Giese, S.; West, F. G. *Tetrahedron* **2000**, *56*, 10221-10228; b) Wang, Y.; Schill, B. D.; Arif, A. M.; West, F. G. *Org. Lett.* **2003**, *5*, 2747-2750.
16. He, W.; Sun, X.; Frontier, A. J. *J. Am. Chem. Soc.* **2003**, *125*, 14278-14279.
17. Malona, J. A.; Colbourne, J. M.; Frontier, A. J. *Org. Lett.* **2006**, *8*, 5661-5664.
18. Bee, C.; Leclerc, E.; Tius, M. A. *Org. Lett.* **2003**, *5*, 4927-4930.
19. Larini, P.; Guarna, A.; Occhiato, E. G. *Org. Lett.* **2006**, *8*, 781-784.
20. a) Janka, M.; He, W.; Frontier, A. J.; Eisenberg, R. *J. Am. Chem. Soc.* **2004**, *126*, 6864-6865; b) Janka, M.; He, W.; Frontier, A. J.; Flaschenriem, C.; Eisenberg, R. *Tetrahedron* **2005**, *61*, 6193-6206; c) He, W.; Huang, J.; Sun, X.; Frontier, A. J. *J. Am. Chem. Soc.* **2007**, *129*, 498-499.
21. Reuping, M.; Jeawsuwan, W.; Antonchick, A. P.; Nachtsheim, B. J. *Angew. Chem. Int. Ed.* **2007**, *46*, 2097-2100.
22. Rautenstrauch, V. *J. Org. Chem.* **1984**, *49*, 950-952.
23. a) Shi, X.; Gorin, D. J.; Toste, F. D. *J. Am. Chem. Soc.* **2005**, *127*, 5802-5803; b) Zhang, L.; Wang, S. *J. Am. Chem. Soc.* **2006**, *128*, 1442-1443; c) Faza, O. N.; López, C. S.; Álvarez, R.; de Lera, A. R. *J. Am. Chem. Soc.* **2006**, *128*, 2434-2437.

24. Barluenga, J.; Barrio, P.; Vicente, R.; López, L. A.; Tomás, M. *J. Organomet. Chem.* **2004**, *689*, 3793-3799.
25. de Lera, A. R.; Rey, J. G.; Hrovat, D.; Iglesias, B.; López, S. *Tetrahedron Lett.* **1997**, *38*, 7425-7428.
26. For recent reviews see: a) Tietze, L. F. *Chem. Rev.* **1996**, *96*, 115-136; b) Poli, G.; Gimabastiani, G.; Heumann, A. *Tetrahedron* **2000**, *56*, 5959-5989; c) Tietze, L.F.; Modi, A. *Med. Res. Rev.* **2000**, *20*, 304-322; d) Padwa, A. *Pure Appl. Chem.* **2003**, *75*, 47-62; e) Nicolaou, K.C.; Montagnon, T.; Snyder, S.A. *Chem. Commun.* **2003**, 551-564; f) Tietze, L. F.; Brasche, G.; Gericke, K. M. *Domino Reactions in Organic Synthesis*, Wiley-VCH: New York; 2006.
27. a) West, F. G.; Fisher, P. V.; Arif, A. M. *J. Am. Chem. Soc.* **1993**, *115*, 1595-1597; b) West, F. G.; Willoughby, D. W. *J. Org. Chem.* **1993**, *58*, 3796-3797.
28. Bender, J. A.; Blize, A. E.; Browder, C. C.; Giese, S.; West, F. G. *J. Org. Chem.* **1998**, *63*, 2430-2431.
29. a) Browder, C. C.; West, F. G. *Synlett* **1999**, 1363-1366; b) Giese, S.; Mazzola, R. D., Jr.; Amann, C. M.; Arif, A. M.; West, F. G. *Angew. Chem., Int. Ed.* **2005**, *44*, 6545-6549.
30. Wang, Y.; Arif, A. M.; West, F. G. *J. Am. Chem. Soc.* **1999**, *121*, 876-877.
31. Bender, J. A.; Arif, A. M.; West, F. G. *J. Am. Chem. Soc.* **1999**, *121*, 7443-7444.

32. a) Browder, C. C.; Marmsäter, F. P.; West, F. G. *Org. Lett.* **2001**, *3*, 3033-3035;
b) Browder, C. C.; Marmsäter, F. P.; West, F. G. *Can. J. Chem.* **2004**, *82*, 375-385.
33. Nair, V.; Bindu, S.; Sreekumar, V.; Chiaroni, A. *Org. Lett.* **2002**, *4*, 2821-2823.
34. Rostami, A.; Wang, Y.; McDonald, R.; West, F. G. *Org. Lett.* **2007**, *9*, 703-706.
35. a) Bräse, S.; Gil, C.; Knepper, K.; Zimmermann, V. *Angew. Chem., Int. Ed.* **2005**, *44*, 5188-5240; b) Lang, S.; Murphy, J. A. *Chem. Soc. Rev.* **2006**, *35*, 146-156.
36. Aubé, J.; Desai, P. *Org. Lett.* **2000**, *2*, 1657-1659.
37. Giese, S.; West, F. G. *Tetrahedron Lett.* **1998**, *39*, 8393-8396.
38. Giese, S.; Kastrup, L.; Stiens, D.; West, F. G. *Angew. Chem., Int. Ed.* **2000**, *39*, 1970-1973.
39. a) Wang, Y.; Schill, B. D.; Arif, A. M.; West, F. G. *Org. Lett.* **2003**, *5*, 2747-2750; b) Yungai, A.; West, F. G. *Tetrahedron Lett.* **2004**, *45*, 5445-5448.
40. a) White, T. D.; West, F. G. *Tetrahedron Lett.* **2005**, *46*, 5629-5632; b) Dhoro, F.; Tius, M. A. *J. Am. Chem. Soc.* **2005**, *127*, 12472-12473; c) Kristensen, T. E.; Stockmann, V.; Yap, G. P. A.; Tius, M. A. *J. Am. Chem. Soc.* **2007**, *129*, 7256-7257.
41. Song, D.; Rostami, A.; West, F. G. *J. Am. Chem. Soc.* **2007**, *129*, 12019-12022.

42. a) Janka, M.; He, W.; Haedicke, I. E.; Fronczek, F. R.; Frontier, A. J.; Eisenberg, R. *J. Am. Chem. Soc.* **2006**, *128*, 5312-5313; b) Nie, J.; Zhu, H.-W.; Cui, H.-F.; Hua, M.-Q.; Ma, J.-A. *Org. Lett.* **2007**, *9*, 3053-3056.
43. Harrington, P. E.; Tius, M. A. *J. Am. Chem. Soc.* **2001**, *123*, 8509-8514.
44. Li, W.-D. Z.; Wang, Y.-Q. *Org. Lett.* **2003**, *5*, 2931-2934.
45. He, W.; Huang, J.; Sun, X.; Frontier, A. J. *J. Am. Chem. Soc.* **2007**, *129*, 498-499.
46. Birman, V. B.; Danishefsky, S. J. *J. Am. Chem. Soc.* **2002**, *124*, 2080-2081.

Chapter 2

gem-Dichlorocyclopropanes as Novel Substrates for the Nazarov Cyclization

2.1 The Chemistry of *gem*-Dihalocyclopropanes

gem-Dihalocyclopropanes **1** (Figure 2.1) are useful substrates in organic synthetic chemistry due to their ease of preparation and unique modes of reactivity.¹ The *gem*-dihalocyclopropane moiety can provide access to numerous hydrocarbon structures including simple or substituted cyclopropanes, dienes, allenes, and cyclopentenenes. This chapter will introduce the distinctive chemical reactivity of *gem*-dihalocyclopropane compounds and present the use of these compounds in a new approach to the Nazarov reaction.

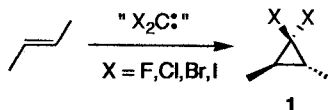
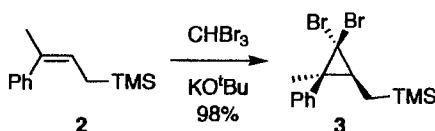


Figure 2.1. Preparation of *gem*-dihalocyclopropanes.

2.1.1 Dihalocarbenes

The synthesis of *gem*-dihalocyclopropane compounds is accomplished by addition of a dihalocarbene species to an olefin (Figure 2.1). Dihalocarbenes are sp^2 -hybridized singlet carbenes that have empty p -orbitals capable of accepting electron donation from full orbitals on the adjacent halogen atoms. The electronic configuration of dihalocarbenes implies that they react through a concerted cyclopropanation mechanism as opposed to a radical pathway during the addition to olefin compounds. Evidence to support this mechanistic proposal can be found in the retention of relative stereochemistry observed as a result of cyclopropanation onto substrates such as alkene **2** (Scheme 2.1).² Dihalocarbenes are also electrophilic carbene species that selectively react with electron-rich over electron-poor olefins. Dihalocyclopropanation onto electron-poor alkenes can be achieved in the absence of other olefins; however, the cycloaddition proceeds slowly and generally results in the formation of side-products due to competing C-H and/or X-H insertion reactions.



Scheme 2.1. Stereochemical retention in dihalocyclopropanation.

2.1.2 Preparation of *gem*-Dichlorocyclopropanes

Although there are examples of *gem*-difluoro-, *gem*-dichloro-, *gem*-dibromo-, *gem*-diiodo-, and mixed dihalocyclopropanes, this discussion will focus on the preparation of the dichloro species. In many cases the same preparative techniques can

be used to synthesize the other *gem*-dihalocyclopropane compounds. In the earliest example of *gem*-dichlorocyclopropane synthesis, it was shown that treatment of CHCl_3 with ${}^t\text{BuOK}$ under anhydrous conditions could generate a carbene capable of reacting with numerous alkene compounds.³ The mechanism of carbene generation is believed to proceed through initial deprotonation of the haloform to provide a trihalomethylcarbanion species **I**, the lifetime of which is quite short due to facile α -elimination to furnish dichlorocarbene **II** (Figure 2.2). In the presence of an olefin, the carbene reacts quickly to provide a *gem*-dichlorocyclopropane product in moderate yields. Although this traditional set of conditions is still used to prepare *gem*-dichlorocyclopropane

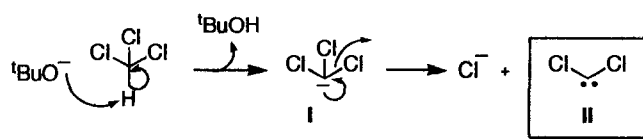


Figure 2.2. Mechanism of carbene generation.

compounds, significant improvements have been made that allow access to these products in increased yields and with better selectivity. At present, the most commonly used approaches to carbene generation include the previously outlined procedure as well as treatment of ethyl trichloroacetate with alkoxide,^{1b} and thermal decomposition of either sodium trichloroacetate or trichloromethyl(phenyl)mercury reagents.⁴ Despite the development of new methodologies,⁵ the most general and reliable method for the preparation of *gem*-dichlorocyclopropane compounds is a phase transfer catalysis procedure designed by Makosza in 1969.⁶

Phase transfer catalysis utilizes a lipophilic salt complex to catalyze a reaction by acting as a shuttle between the aqueous and organic layers in a biphasic reaction mixture.

In a dichlorocyclopropanation reaction the organic phase is CHCl_3 , the aqueous phase is 50 % NaOH solution, and the lipophilic salt is most commonly a quaternary ammonium salt such as benzyltriethylammonium chloride (TEBA) or tetrabutylammonium bromide (TBAB). Under these reaction conditions, deprotonation of CHCl_3 occurs at the interface of the two phases and subsequent anion exchange with the ammonium salt occurs to form a lipophilic ion pair (Figure 2.3). The bulky ammonium cation shuttles

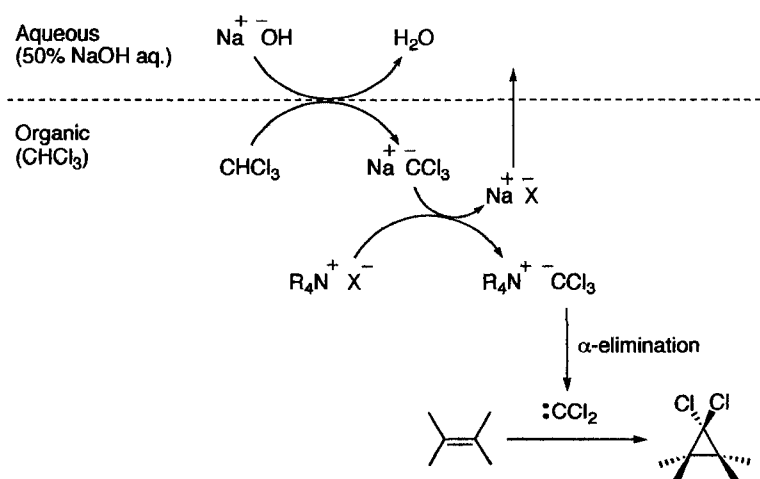


Figure 2.3. The Makosza method: phase transfer catalysis.

the trichlorocarbanion species into the organic layer where it undergoes α -elimination and addition of the resultant carbene to an available olefin. This procedure, coined the Makosza method, generally furnishes *gem*-dichlorocyclopropanes in high yields due to the mild reaction conditions and the suppression of carbene consumption by water or hydroxide.

2.1.3 Cationic Ring Opening of *gem*-Dichlorocyclopropanes

gem-Dichlorocyclopropanes are useful substrates for a variety of different reactions including partial reduction to furnish monohalocyclopropanes and complete reduction to simple cyclopropanes, as well as substitution and elimination reactions to provide cyclopropene compounds. In all of these cases, the integrity of the three-membered ring is preserved as a result of careful manipulation of the halogen substituents. One of the most interesting aspects of *gem*-dihalocyclopropane chemistry is

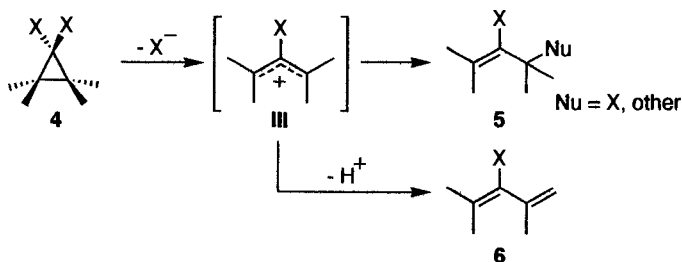


Figure 2.4. Cationic ring opening of *gem*-dihalocyclopropanes.

the fact that they undergo facile cationic ring opening to provide an allyl cation III, which can lead to subsequent elimination or nucleophilic trapping products^{7,8} (6 and 5, Figure 2.4). The ring opening process occurs in a disrotatory fashion with concomitant loss of a halide anion, and the direction of disrotation is strongly influenced by stereoelectronic factors.⁹ Orbitals that are involved in the breaking of the C-C α -bond

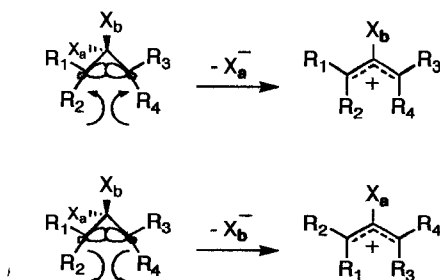


Figure 2.5. Stereoelectronic factors affecting cationic ring opening.

must rotate in a direction that assists halide departure by overlapping with the σ^* -orbital of the dissociating halogen (*Figure 2.5*). This stereoelectronic effect implies that chemoselective removal of one of the halogens would result in the formation of one allyl cation over the other. Exploitation of this aspect of ring opening could be valuable for the development of asymmetric transformations.

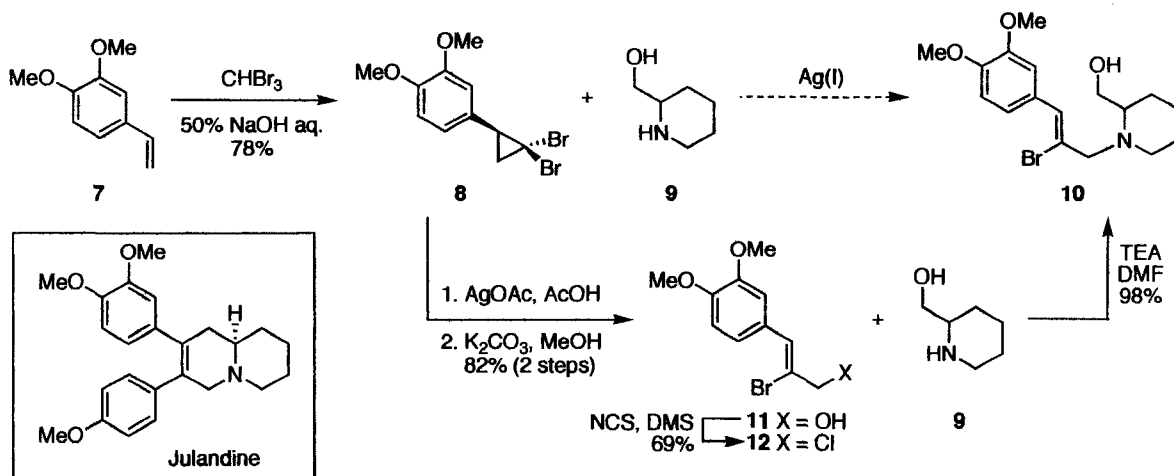
The cationic ring opening of *gem*-dihalocyclopropanes can be induced under strictly thermal conditions or in the presence of a Lewis acid.¹⁰ The most common Lewis acids used in these reactions are Ag(I) salts. The silver-mediated reactions can be carried out at low temperatures and have the additional benefit of sequestering halide anions liberated in the ring opening process, effectively removing free halide species from the reaction mixture.

2.1.4 Cationic Ring Opening of *gem*-Dichlorocyclopropanes in Synthesis

gem-Dihalocyclopropanes and their derived allyl cations have been used in different approaches towards the synthesis of natural products. Recent literature examples will be discussed in an effort to illustrate the utility of these compounds in organic synthesis.

In 2004 Banwell and Sydnese¹¹ disclosed their efforts towards the total synthesis of plant-derived phenanthroquinolizidine alkaloids such as julandine.¹² Their initial strategy involved the intermolecular trapping of an allylic cation species with 2-piperidinemethanol **7** (*Scheme 2.2*). The desired *gem*-dibromocyclopropane precursor **8** was derived from dibromocarbene addition to the respective olefin (**7**) in 78% yield under

standard Makosza conditions. When ring opening of **8** was induced using a variety of Ag(I) salts, the desired intermolecular trapping product **10** was not observed. Instead, the cationic species was efficiently trapped by solvent or the anion coordinated to Ag(I).

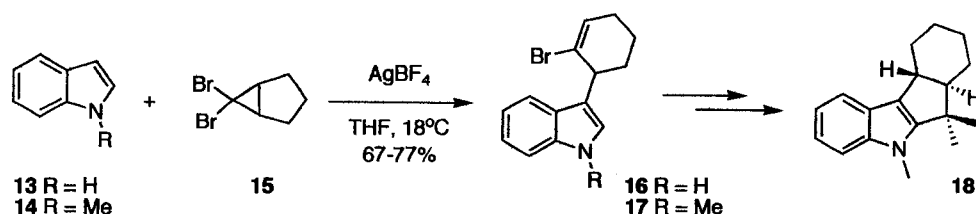


Scheme 2.2. Towards the synthesis of phenanthroquinolizidine alkaloids.

The authors decided to approach the synthesis of **10** in a different manner, inducing ring opening of the *gem*-dibromocyclopropane with AgOAc in the presence of AcOH to afford an allylic acetate. The allylic acetate was smoothly converted to the allylic alcohol **11**, with a yield of 81% over the two steps. Subsequently, allylic alcohol **11** was treated with N-chlorosuccinimide (NCS) in dimethylsulfide (DMS) to afford allyl chloride **12**, which was then coupled with 2-piperidinemethanol **9** to provide the desired product **10** in 98% yield. Although the planned intermolecular trapping process was unsuccessful, *gem*-dibromocyclopropane **8** was a useful synthetic intermediate, allowing access to a vinyl bromide substrate that participated in Suzuki-Miyaura cross-coupling reactions later in the synthetic scheme.

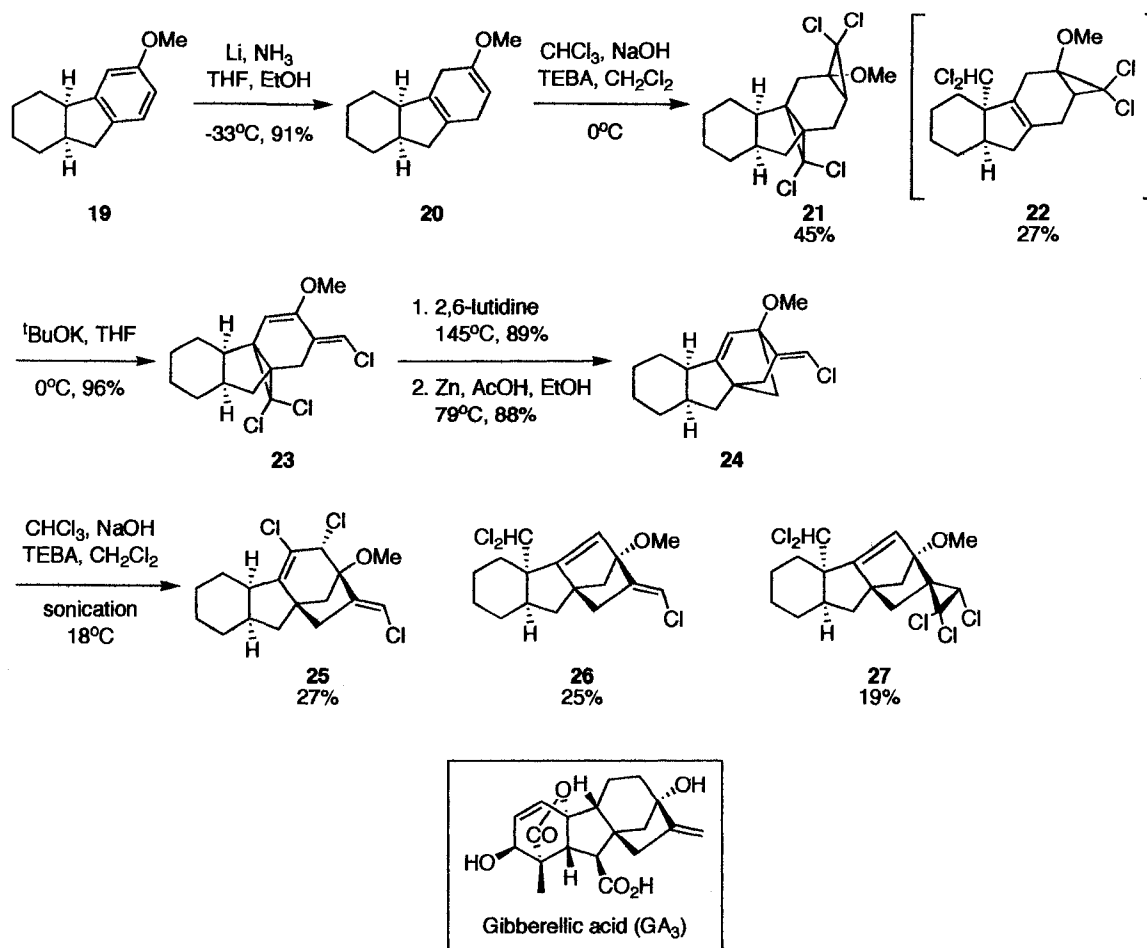
The intermolecular trapping of allyl cations generated from ring opening of *gem*-dihalocyclopropanes has recently been utilized in the synthesis of hapalindole and

fischerindole alkaloid frameworks (*Scheme 2.3*).¹³ It was found that indoles **13** and **14** could capture the allyl cation generated from treatment of *gem*-dibromocyclopropane **15** with AgBF₄ in THF, providing the tricyclic products **16** and **17** in 67 to 77% yields. The trapping products could be carried on to afford tetracycle **18** (or its *cis* ring-fused isomer) in 4 steps. This strategy allows for the rapid construction of complex, polycyclic skeletons from simple starting materials and in good yields.



Scheme 2.3. Intermolecular trapping of the allyl cation by indole nucleophiles.

One final example of the use of *gem*-dihalocyclopropanes in synthesis can be found in the recent assembly of complex polycyclic intermediates used in the construction of gibberellin frameworks (*Scheme 2.4*).¹⁴ In this work, Banwell and co-workers assembled the tetracycle **25** in 6 steps from the readily available precursor **19**. Birch reduction of **19** proceeded smoothly to provide the methyl enol ether **20**, which underwent dichlorocyclopropanation to provide **21** as the major product in 45% yield. The major side-product of this reaction (**22**) was generated as the result of initial dichlorocyclopropanation from the opposite face of the enol double bond followed by C-H insertion at a ring fusion position instead of a second cyclopropanation reaction. Subsequently, treatment of **21** with ^tBuOK in THF induced an intriguing rearrangement process that provided diene **23** in excellent yield. Exposure of **23** to 2,6-lutidine at high temperature resulted in a vinylcyclopropane rearrangement¹⁵ to furnish the norbornene



Scheme 2.4. Synthetic strategy for the assembly of gibberellin frameworks.

framework observed in **24** and, after dehalogenation, the final dichlorocyclopropanation reaction and subsequent ring-opening was performed to provide **25** as the major product in a mixture of three cyclopropanated and/or C-H insertion products (**26** and **27**). Although the final step in this sequence was not selective for generation of the desired compound (**25**), this strategy presents a very short synthesis of structurally complex intermediates that can be further elaborated to gibberellins and their analogues.

gem-Dihalocyclopropanes are interesting functional groups that can be used to generate complex structures from simple, readily available starting materials. The ease with which *gem*-dihalocyclopropanes can be synthesized makes them attractive intermediates for total synthesis, and the unique reactivity associated with these compounds reveals great potential for the development of new methodologies.

2.2 *gem*-Dichlorocyclopropanes and the Nazarov Cyclization

One of the main research focuses in the West laboratories has been the development of new methodologies involving the Nazarov cyclization. In keeping with this objective, the unique cationic ring opening reaction of *gem*-dihalocyclopropanes was seen as an interesting opportunity for the design of a novel Nazarov process. Appropriately substituted *gem*-dihalocyclopropanes may be used to access a pentadienyl cationic species capable of undergoing Nazarov cyclization. The results of this investigation, including preliminary findings and development of the methodology, will be discussed herein.

2.2.1 Introduction

In an effort to mimic the Nazarov cyclization with non-traditional substrates, the first goal of this project was to design *gem*-dihalocyclopropane compounds that were appropriately substituted for participation in a sequential 2π disrotatory ring opening and 4π electrocyclization (Figure 2.6).¹⁶ It was believed that 1,1-dihalo-2-(silyloxy)-2-

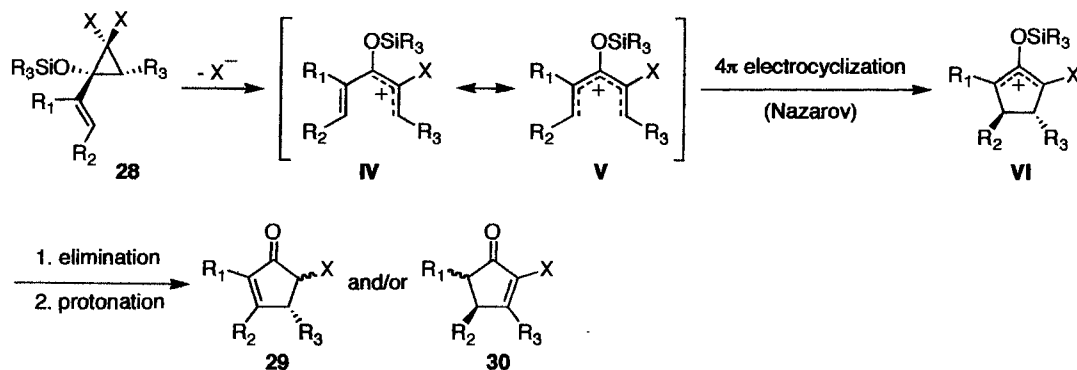
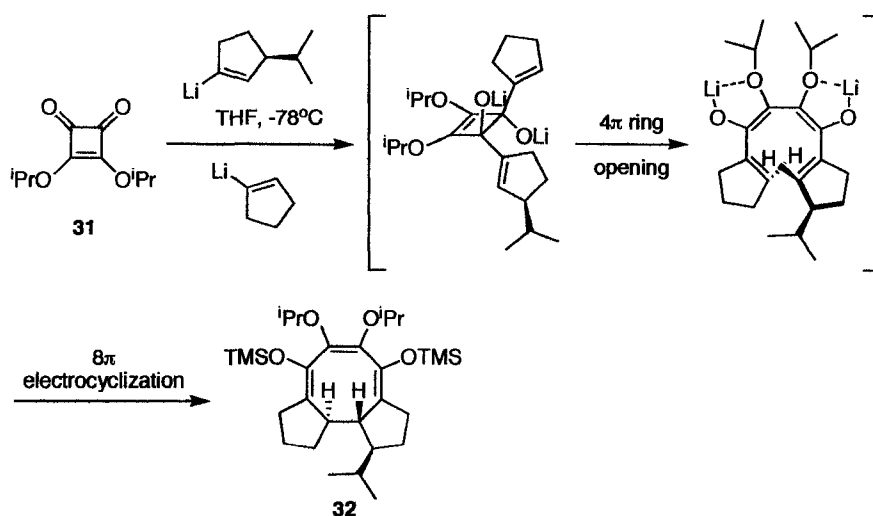


Figure 2.6. Concept behind the use of *gem*-dihalocyclopropanes in the Nazarov reaction.

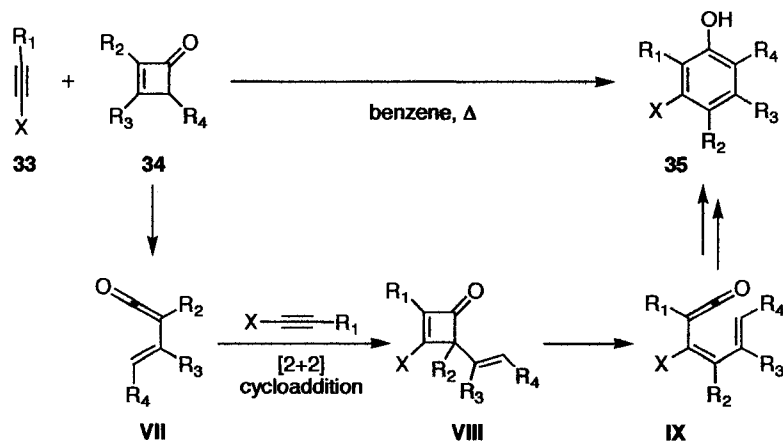
vinylcyclopropanes **28** would be ideal substrates for this investigation since computational experiments¹⁷ have shown that alkenyl substitution on *gem*-dihalocyclopropanes accelerates the ring opening process relative to hydrogen. Oxygen substitution at the same position on the cyclopropane moiety was also shown to assist in the disrotatory ring opening, which would aid in efficient generation of allyl cation **IV**. Due to the presence of the vinyl substituent, cation **IV** might also be viewed as the pentadienyl cation **V**, which is analogous to the cationic species observed during conventional Nazarov cyclizations. It was believed that the pentadienyl cation would undergo conrotatory electrocyclization to furnish a 2-silyloxycyclopentenyl cation (**VI**) that would experience conventional elimination and subsequent hydrolysis to provide α -halocyclopentenone products **29** and/or **30**. To our knowledge, this type of sequential ring opening and electrocyclization involving *gem*-dihalocyclopropanes has not been investigated, although conceptually similar protocols have been reported. For example,



Scheme 2.5. Paquette's sequential ring opening/ 8π electrocyclization process.

Paquette has reported that conrotatory ring opening of divinyl squarate esters **31** leads to the formation of tetraene intermediates that can undergo 8π electrocyclization to afford cyclooctatrienes **32** (*Scheme 2.5*).¹⁸

Similarly, Danheiser and co-workers have reported a thermally induced cascade process that involves four pericyclic reactions in sequence (*Scheme 2.6*).¹⁹ In this work, cyclobutenones **34** underwent 4π electrocyclic ring opening, followed by regioselective [2+2] cycloaddition with hetero-substituted acetylenes (**33**). The resultant vinyl cyclobutenones **VII** then provided dienyl ketenes **IX**, which underwent 6π electrocyclization and tautomerization to furnish the highly substituted phenol products **35**.



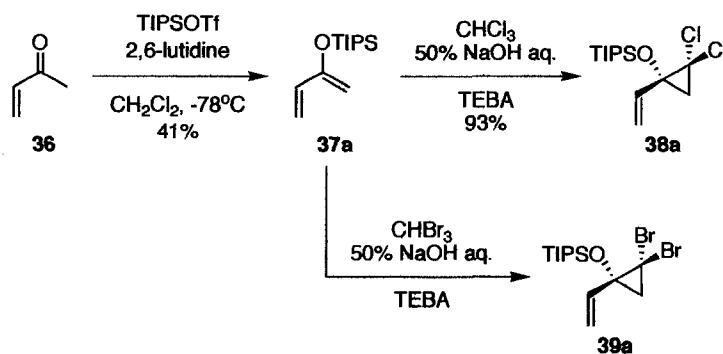
Scheme 2.6. Methodology for the synthesis of substituted aromatic rings.

In an effort to examine the viability of our proposal, a number of 1,1-dihalo-2-(silyloxy)-2-vinylcyclopropanes (**28**) were prepared and their reactivity towards heating in acetonitrile and exposure to a variety of Lewis acids was investigated.

2.2.2 Results & Discussion

Preliminary Investigation: Methyl vinyl ketone

Initial experiments to investigate the use of *gem*-dihalocyclopropanes in the Nazarov reaction were performed on methyl vinyl ketone **36**, a simple and readily available substrate. Methyl vinyl ketone was smoothly converted to 2-triisopropylsilyloxydiene **37a** in low yield after immediate purification on an alumina column (*Scheme 2.7*). The choice of silyl substituent was made based on the durability of a triisopropylsilyl (TIPS) group relative to other, less bulky silyl groups. It



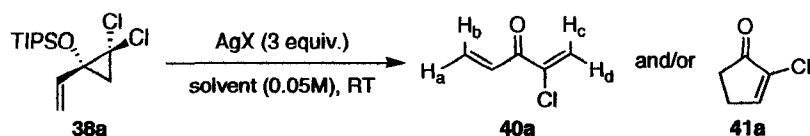
Scheme 2.7. The synthesis of 1,1-dihalo-2-(silyloxy)-2-vinylcyclopropanes.

was important to ensure that the silyl substituent would remain on the oxygen during cyclization to prevent premature termination of the reaction by desilylation to give 2-chlorodienones. Other silyl groups were investigated during optimization of the reaction conditions and will be discussed more thoroughly later in this chapter.

Preparation of both *gem*-dichlorocyclopropane compound **38a** and the *gem*-dibromocyclopropane compound **39a** was investigated (*Scheme 2.7*). Dichlorocyclopropanation of **37a** proceeded smoothly when the Makosza methodology was used, providing **38a** in 93% yield after purification on a silica column. The

analogous dibromocyclopropanation reaction was very messy and afforded a mixture of compounds, including the desired product **39a**, that could not be separated. *gem*-Dibromocyclopropanes are inherently less stable than the dichloro-species.^{1c} Additional alkenyl and silyloxy substitution on the dibromo-substrates (**39**) more than likely adds to their instability, promoting facile decomposition at room temperature as well as during attempted purification on silica or alumina-based columns. These observations prompted selection of *gem*-dichlorocyclopropane compounds (**38**) for use in development of the new Nazarov methodology.

Substrate **38a** was exposed to a variety of reaction conditions in a qualitative investigation used to assess the practicality of the proposed ring opening and 4π electrocyclization sequence (*Table 2.1*). It was found that treatment of **38a** with AgOTf in CH₂Cl₂ did not induce any reaction after 12 hours except for mild decomposition of the starting material; however, when AgBF₄ was used under the same reaction conditions the crude ¹H NMR spectrum indicated complete consumption of starting material and the presence of chlorodienone **40a** as the major product in a mixture of compounds. Dienone **40a** was implicated by the presence of two sets of terminal olefin protons: H_a and H_b appeared at 5.9 ppm and 6.5 ppm (²J_{ab} = 1.6 Hz), while H_c and H_d appeared at 6.4 ppm and 6.1 ppm (²J_{cd} = 2.0 Hz) in the NMR spectrum. *gem*-Dichlorocyclopropane **38a** was then subjected to treatment with AgBF₄ in MeCN, CH₂Cl₂, or CF₃CH₂OH. These solvents were chosen based on their historical use in cationic ring opening reactions of *gem*-dihalocyclopropane compounds. No reaction was observed when MeCN was used as the solvent, which is most likely due to the limited solubility of AgBF₄ in MeCN at room temperature. Although ring opening was induced in CF₃CH₂OH, the major product



entry	AgX	solvent	time (h)	products
1	AgOTf	CH ₂ Cl ₂	12	no reaction
2	AgBF ₄	CH ₂ Cl ₂	12	40a
3	AgBF ₄	MeCN	24	no reaction
4	AgBF ₄	CH ₂ Cl ₂	24	41a
5	AgBF ₄	CF ₃ CH ₂ OH	24	40a + 41a

Table 2.1. Preliminary results using *gem*-dichlorocyclopropane **38a**.

observed was, once again, chlorodienone **40a**; however, when the reaction in CH₂Cl₂ was allowed to stir for a prolonged period of time, peaks corresponding to α -chlorocyclopentenone **41a** appeared in the crude ¹H NMR spectrum, with concomitant disappearance of the chlorodienone. These observations suggest the formation of a long-lived pentadienyl cation (**X**) that slowly undergoes cyclization to furnish the desired α -chlorocyclopentenone products (Figure 2.7). Prematurely stopping the reaction yields a chlorodienone as the result of desilylation of the pentadienyl cation during work-up. To avoid the isolation of undesirable chlorodienones **40**, the Ag(I)-mediated Nazarov reaction must be monitored very closely by TLC analysis. Monitoring the reaction progress by TLC permits observation of the emergence and subsequent disappearance of the chlorodienone, which is representative of the formation and consumption of the long-lived pentadienyl cation.

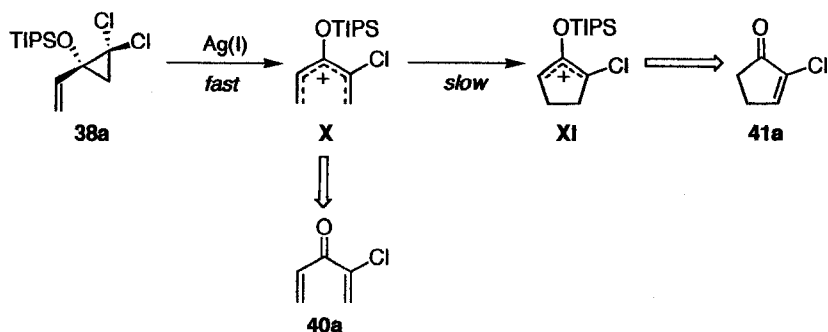
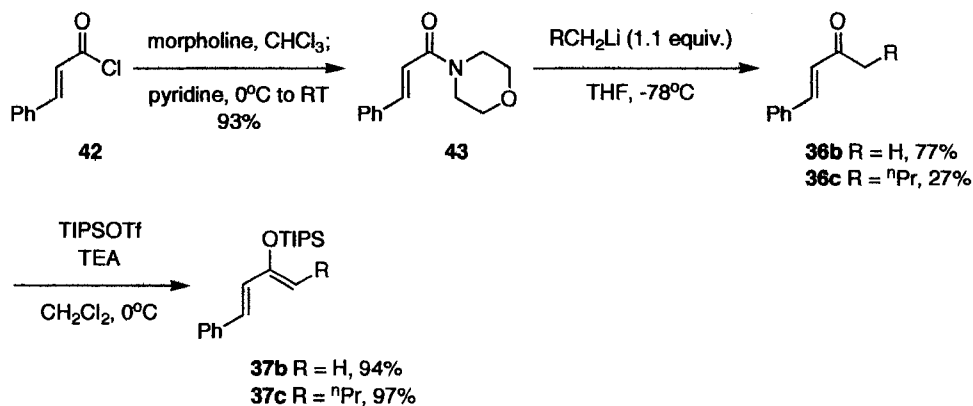


Figure 2.7. The formation of products due to treatment of **38a** with AgBF_4 .

Preparation of 2-Triisopropylsilyloxydienes

While the two products **40a** and **41a** were unstable to standard purification techniques, the observation of α -chlorocyclopentenone **41a** was very encouraging and prompted the construction of more highly substituted *gem*-dichlorocyclopropane substrates for use in the new Nazarov methodology. It was believed that substitution on the vinyl and cyclopropane moieties would increase the efficiency of the reaction and provide products that were amenable to purification. To this end, ketones **36b-i** were obtained and subsequently converted to 2-triisopropylsilyloxydienes **37** in excellent yields.

Dienes **37b** and **37c** were synthesized from cinnamoyl chloride **42** in 3 steps (Scheme 2.8). Cinnamoyl chloride was cleanly converted to morpholine amide **43** using a literature procedure,²⁰ and subsequent treatment with 1.1 equivalents of methyllithium or butyllithium furnished ketones **36b** and **36c**, respectively.²¹ Alkylolithium additions to the morpholine amide were not optimized, and the resultant ketones were subjected to TIPSOTf in the presence of triethylamine (TEA) at 0°C to provide the desired silyl enol ethers in excellent yields after purification. In the case of **37c**, the *Z*-geometry of the



Scheme 2.8. Preparation of 2-triisopropylsilyloxydienes **37b** and **37c**.

enol ether olefin was determined by analysis of a 1D TROESY experiment, wherein an nOe enhancement of H_a was observed when H_b was irradiated at 4.90 ppm (*Figure 2.8*).

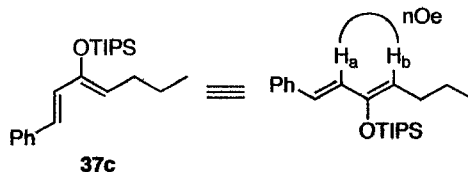
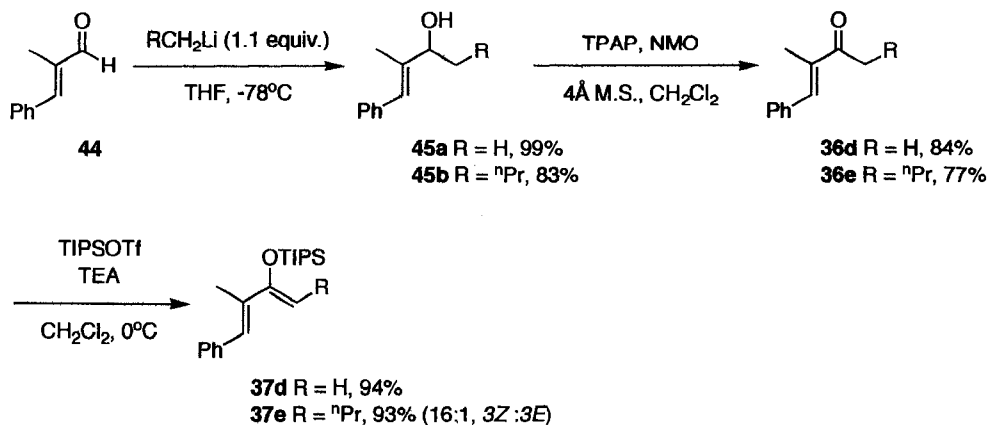


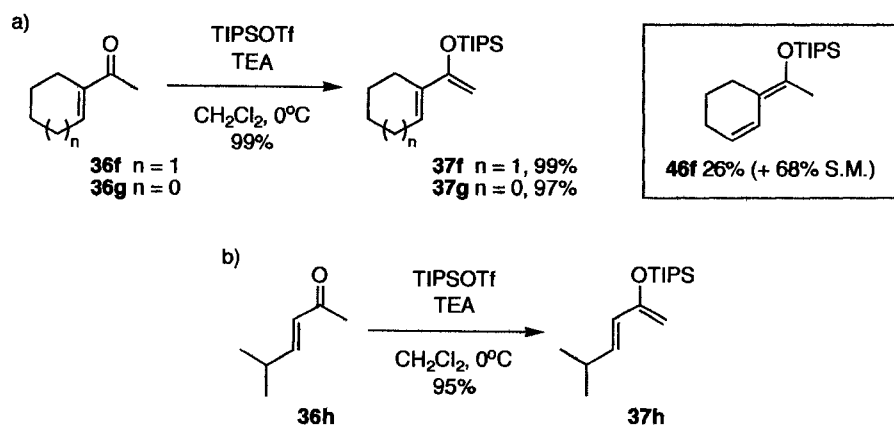
Figure 2.8. nOe enhancement illustrating the *Z*-geometry of the enol ether.

Preparation of substrates **37d** and **37e** was accomplished through the initial addition of an alkyl lithium reagent (methyl lithium or butyllithium) to α -methyl-*trans*-cinnamaldehyde **44**, followed by oxidation of the secondary alcohol using TPAP and NMO (*Scheme 2.9*). This sequence furnished ketones **36d** and **36e**, which could then be converted to the desired silyl enol ethers **37** in excellent yields. 2-Triisopropylsilyloxydiene **37e** was formed as a mixture of geometric isomers in which the major isomer was determined to exist in a *Z*-configuration. Once again, the double bond geometry was established through analysis of a 1D TROESY spectrum.



Scheme 2.9. Preparation of 2-triisopropylsilyloxydienes **37d** and **37e**.

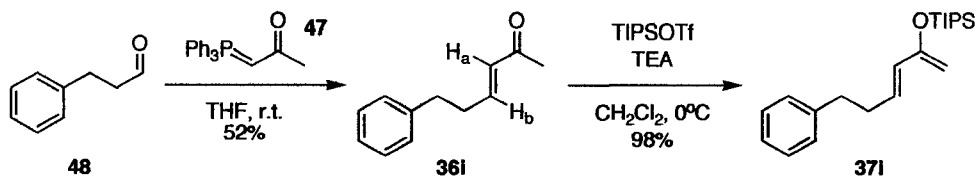
The commercial availability of 1-acetyl-1-cyclohexene **36f**, 1-acetyl-1-cyclopentene **36g**, and 5-methyl-(*3E*)-hexene-2-one **36h** allowed direct synthesis of the corresponding silyl enol ethers **37** in excellent yields (*Scheme 2.10*). Interestingly, an undesired silyl enol ether (**46a**) was observed when 2,6-lutidine was used as the base in place of triethylamine.



Scheme 2.10. Preparation of 2-triisopropylsilyloxydienes **37f-h**.

Finally, 2-triisopropylsilyloxydiene **37i** was synthesized in two steps as the result of a Wittig olefination involving 1-(triphenylphosphoranylidene)-2-propanone (**47**) and hydrocinnamaldehyde **48**, followed by conversion to **37i** using the standard reaction

conditions (*Scheme 2.11*). The Wittig olefination proceeded in moderate yield, providing exclusive generation of the *trans*-isomer of **36i**, which was confirmed by the observation of a large coupling constant ($^3J_{ab} = 16.0$ Hz) between the two vinyl protons.

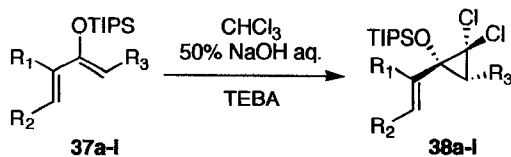


Scheme 2.11. Preparation of 2-triisopropylsilyloxydienes **37i**.

Dichlorocyclopropanation

With 2-triisopropylsilyloxydienes **37** in hand, the cyclopropanation of these substrates was investigated. It was believed that subjection of these compounds to phase transfer catalysis (the Makosza conditions) would result in selective cyclopropanation on the more electron-rich olefin, as observed in studies with methyl vinyl ketone. In most cases, monocyclopropanation occurred very quickly to provide the corresponding *gem*-dichlorocyclopropane compounds without incident and in good to excellent isolated yields (*Table 2.2*). Substrates that proved to be problematic will be discussed further in an effort to ascertain the limitations of this methodology.

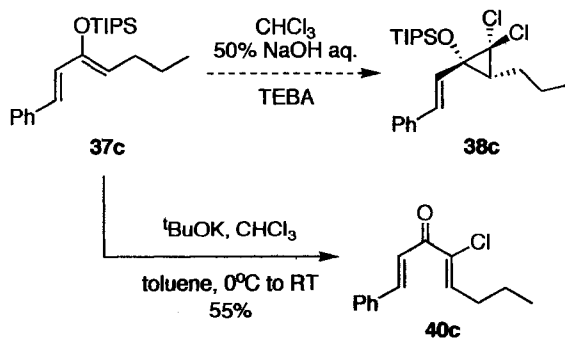
Silyl enol ether **37c** did not react well under the standard phase transfer catalysis conditions for dichlorocyclopropanation, furnishing a complex mixture of inseparable products at every attempt. In an effort to circumvent these issues, **37c** was treated with ^tBuOK and CHCl₃ in toluene instead of using the Makosza methodology. Unfortunately, these attempts at cyclopropanation were also unsuccessful, providing dienone **40c** directly in 55% yield (*Scheme 2.12*). Although formation of **40c** undoubtedly proceeds



entry	diene	R ₁	R ₂	R ₃	product	yield (%)
1	37a	H	H	H	38a	93
2	37b	H	Ph	H	38b	76
3	37c	H	Ph	Pr	-	-
4	37d	Me	Ph	H	38d	90
5	37e	Me	Ph	Pr	38e	87
6	37f	-(CH ₂) ₄ -		H	38f	91
7	37g	-(CH ₂) ₃ -		H	38g	92
8	37h	H	CH(CH ₃) ₂	H	38h	95
9	37i	H	CH ₂ CH ₂ Ph	H	38i	71

Table 2.2. Dichlorocyclopropanation of 2-trisopropylsilyloxydienes.

through the cyclopropanated product (**38c**), none of this material was isolated. An explanation for this poor reactivity is not clear since a similar substrate (**37e**) underwent smooth cyclopropanation to provide the corresponding *gem*-dichlorocyclopropane compound in 87% yield.



Scheme 2.12. Attempts to cyclopropanate silyl enol ether **37c**.

While most of the substrates proceeded to provide clean monocyclopropanated products under the phase transfer catalysis conditions, it was necessary to monitor cyclic substrates **37f** and **37g** very carefully to avoid the formation of over-cyclopropanated products (*Figure 2.9*). When reactions were left to stir for 20 minutes, compounds **38f** and **38g** were obtained as the sole products in excellent isolated yields; however, if the

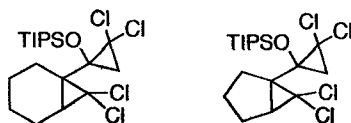
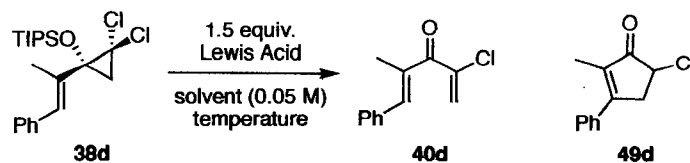


Figure 2.9. Overcyclopropanation of cyclic 2-triisopropylsilyloxydienes **37f** and **37g**.

reactions were left to stir for an extended period of time, dicyclopropanated compounds were also formed that could not be separated from the desired products. In general, the *gem*-dichlorocyclopropanation reactions proceed very quickly and should be stopped as soon as starting material is no longer observed by TLC analysis. These reactions cannot be monitored by gas chromatography, since the high injection temperatures used in this technique bring about rapid decomposition of the thermally labile *gem*-dichlorocyclopropane products.

Ag(I)-Mediated Rearrangement

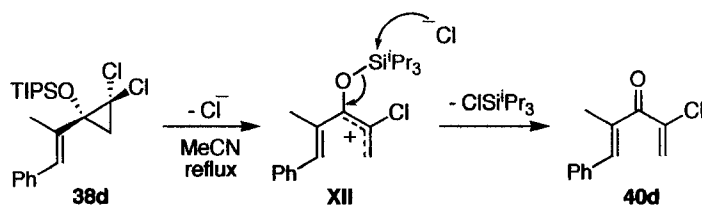
Although methyl vinyl ketone was used in preliminary studies of the sequential ring opening/Nazarov cyclization methodology, the products could not be isolated nor the yields accurately determined. In an effort to examine this reaction more thoroughly, *gem*-dichlorocyclopropane **38d** was subjected to a number of different Lewis acids in different solvent systems (*Table 2.3*) to qualitatively assess the optimal reaction conditions for generation of α -chlorocyclopentenones.



entry	Lewis acid	solvent	time (h)	temperature	products
1	-	MeCN	96	81 °C	S.M. + 40d (1.6:1)
2	AlCl ₃	CH ₂ Cl ₂	72	r.t.	no reaction
3	AlClEt ₂	CH ₂ Cl ₂	72	r.t.	no reaction
4	AgOCOCF ₃	CH ₂ Cl ₂	72	r.t.	S.M. + 40d + 49d
5	AgOTf	CH ₂ Cl ₂	72	r.t.	S.M. + 40d + 49d
6	AgBF ₄	CH ₂ Cl ₂	48	r.t.	49d
7	AgBF ₄	toluene	72	r.t.	no reaction
8	AgBF ₄	CF ₃ CH ₂ OH	72	r.t.	40d + 49d
9	AgBF ₄	CH ₂ Cl ₂ : CF ₃ CH ₂ OH (5:1)	36	r.t.	49d

Table 2.3. Optimization for sequential ring opening/Nazarov cyclization reaction.

Initially, **38d** was dissolved in refluxing MeCN to determine whether cyclization would occur in the absence of Lewis acid. Not surprisingly, these thermal conditions led to slow conversion of the starting material to chlorodienone **40d** and none of the desired α -chlorocyclopentenone was observed. This result is most likely due to chloride-assisted desilylation of the intermediate pentadienyl cation generated from ring opening of the *gem*-dichlorocyclopropane, which forces premature termination of the cationic species (*Scheme 2.13*). In order to prevent this untimely desilylation, a variety of halophilic Lewis acids were examined in order to sequester the free chloride anions present as a result of the ring opening process. All of the reactions in which Ag(I) salts were present

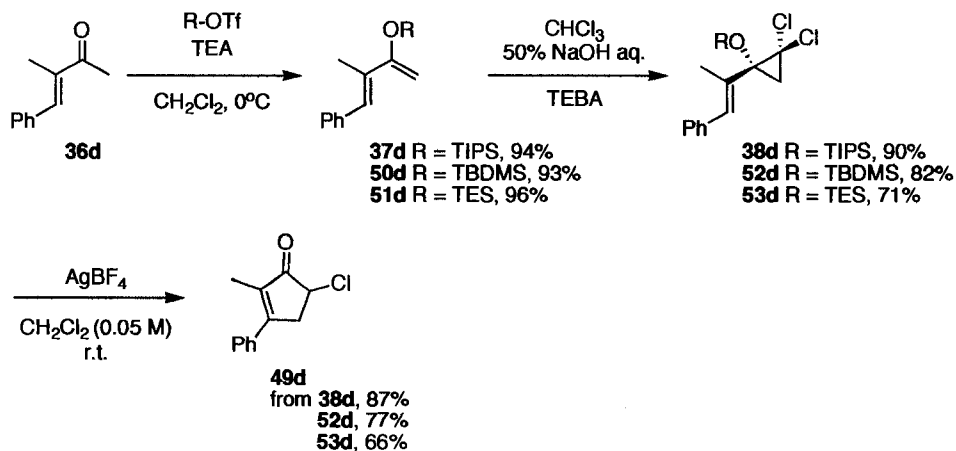


Scheme 2.13. Chloride-assisted termination of the pentadienyl cation **XII**.

promoted ring opening and subsequent Nazarov cyclization to some extent; however, we were pleased to observe very clean conversion of **38d** to α -chlorocyclopentenone **49d** in 78% yield when AgBF_4 was used in CH_2Cl_2 at room temperature. Although reactions in $\text{CF}_3\text{CH}_2\text{OH}$ proceeded to completion more quickly than in CH_2Cl_2 , the crude reaction mixtures were not as clean. A mixed solvent system of $\text{CH}_2\text{Cl}_2:\text{CF}_3\text{CH}_2\text{OH}$ (5:1) could also be used to effect the transformation in a shorter reaction time and with no apparent effect on the efficiency of the reaction. It is important to note that $\text{CH}_3\text{CH}_2\text{OH}$ can sometimes be used as the solvent for these reactions; however, its efficacy appears to be very substrate-specific.

The effect of the silyl substituent on the efficiency of this reaction sequence was also examined. To this end, 2-*tert*-butyldimethylsilyloxydiene **50d** and 2-triethylsilyloxydiene **51d** were synthesized using the previously outlined strategy (*Scheme 2.14*). All of the 2-silyloxydiene compounds were prepared in excellent yields, but the subsequent dichlorocyclopropanation reactions showed evidence of decreased yields when more labile silyl groups were involved. The same trend was observed in the Ag(I)-mediated Nazarov reactions of *gem*-dichlorocyclopropanes **38d**, **52d**, and **53d**, providing cyclopentenone **49d** in decreased yields when the labile triethylsilyl substrate

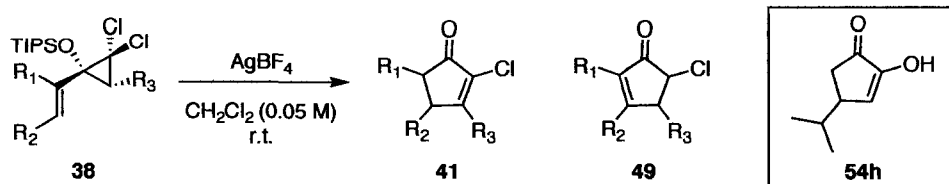
was employed. These results can be attributed to unwanted formation of the chlorodienone during purification or the ring-opening step.



Scheme 2.14. Effect of silyl substituents on sequential ring opening/ Nazarov cyclization.

With optimized reaction conditions in hand, the other *gem*-dichlorocyclopropane substrates (**38**) were cleanly converted to α -chlorocyclopentenones **41** and/or **49** in moderate to good yields (*Table 2.4*). The reactions were stirred at room temperature until the starting material had been consumed and there was no trace of chlorodienone by TLC analysis.

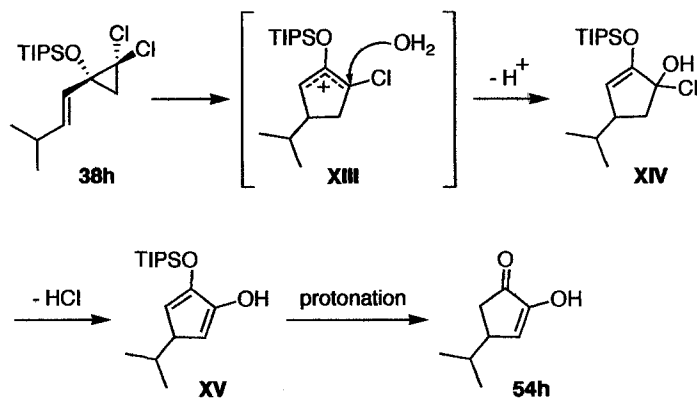
In general, those substrates lacking additional substitution on the cyclopropane moiety provided products **49** selectively as a result of regioselective elimination to deliver the more electron-rich olefin; however, this observation does not hold true for the reaction involving *gem*-dichlorocyclopropane **38h**. Subjection of **38h** to the standard reaction conditions furnished a mixture of **41h** and **49h** (1:1.7) as well as varying amounts of dione enol **54h**. Dione **54h** is most likely the result of trapping 2-silyloxycyclopentenyl cation **XIII** with adventitious water in the reaction mixture,



entry	substrate	R ₁	R ₂	R ₃	product(s)	yield (%)
1	38a	H	H	H	41a	-
2	38b	H	Ph	H	49b	(see text)
3	38d	Me	Ph	H	49d	78
4	38e	Me	Ph	Pr	41e + 49e	87
5	38f		-(CH ₂) ₄ -	H	49f	45
6	38g		-(CH ₂) ₃ -	H	49g	74
7	38h	H	CH(CH ₃) ₂	H	41h + 49h	63

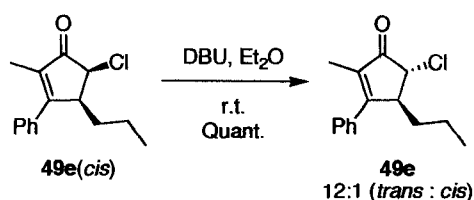
Table 2.4. AgBF₄-mediated rearrangement of *gem*-dichlorocyclopropanes **38**.

followed by dehydrochlorination and subsequent protonation of silyl enol ether **XV** (Scheme 2.15). Formation of this side-product was exclusive to substrate **38h**, and accounted for as little as trace amounts to as much as 37% of the product yield. Attempts to rigorously exclude moisture from the reaction mixture helped to minimize the production of **54h**, but did not prevent its formation.



Scheme 2.15. Mechanism for the formation of dione enol **54h**.

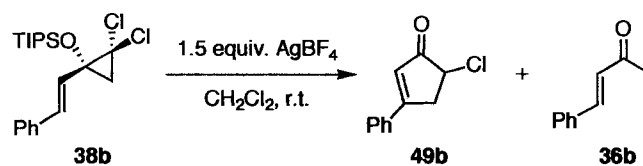
The effect of additional substitution on the cyclopropane moiety was investigated when *gem*-dichlorocyclopropane **38e** was subjected to the standard reaction conditions. This substrate was cleanly converted to a mixture of α -chlorocyclopentenone products **41e** and **49e** in 87% yield (**41e**(*trans*):**49e**(*trans*):**41e**(*cis*):**49e**(*cis*), 1:3:4.5:7.7). The stereochemistry of these isomers was assigned based on comparison of the coupling constants shared by methine protons in the five-membered ring.²² Typical coupling constants for *cis*-disubstituted cyclopentenones are in the range of 6-7 Hz, whereas the value is much smaller (2-3 Hz) for *trans*-disubstituted compounds. The stereochemical assignment was confirmed when the major product **49e**(*cis*) was converted to the more stable **49e**(*trans*) by stirring in Et₂O in the presence of DBU, providing a 12:1 mixture in favor of the *trans* diastereomer (Scheme 2.16). Notably, the *cis*-isomers of both **41e** and **49e** were the major products observed under these reaction conditions.



Scheme 2.16. Equilibration experiment: conversion of **49e**(*cis*) to **49e**(*trans*).

The majority of *gem*-dichlorocyclopropanes **38** provided the desired α -chlorocyclopentenones as a result of sequential electrocyclic ring opening and Nazarov cyclization without the occurrence of unexplained side reactions. Unfortunately, while substrate **38b** did participate in the expected reaction sequence to furnish **49b**, the cyclopentenone product was not isolated. Unanticipated formation of the methyl vinyl ketone **36b** was observed in the crude reaction mixture and could not be separated from

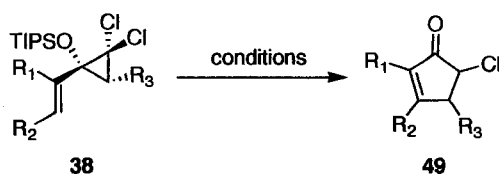
the α -chlorocyclopentenone product (*Scheme 2.17*). Originally it was believed that this impurity was due to the presence of unreacted 2-triisopropylsilyloxydiene in the Ag(I)-mediated Nazarov reaction; however, close examination of the $^1\text{H NMR}$ spectrum of



Scheme 2.17. Anomalous reactivity of *gem*-dichlorocyclopropane **38b**.

gem-dichlorocyclopropane **38b** after purification showed no evidence of contamination by the silyloxydiene. As a result of this anomaly, accurate yields for the formation of **49b** cannot be reported.

In a later examination of these substrates, it was found that yields could be significantly improved and reaction times reduced when the Ag(I)-mediated rearrangement was carried out in refluxing MeCN and in the presence of 1 equivalent of AgBF₄. A comparison of the yields obtained from these new reaction conditions is shown in Table 2.5.

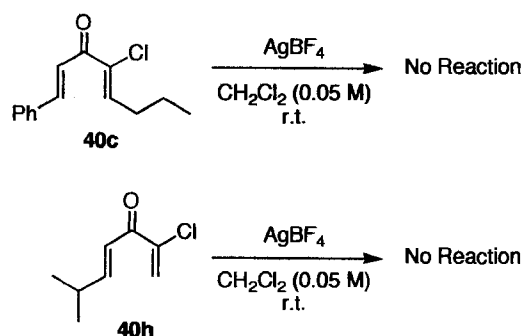


entry	substrate	R ₁	R ₂	R ₃	1.5 equiv. AgBF ₄ CH ₂ Cl ₂ / r.t.	1 equiv. AgBF ₄ MeCN / reflux
1	38d	Me	Ph	H	78%	99%
2	38f	-(CH ₂) ₄ -	H	H	45%	86%
3	38g	-(CH ₂) ₃ -	H	H	74%	85%

Table 2.5. Comparison of reaction conditions for the Ag(I)-mediated Nazarov reaction.

Support for the Mechanistic Proposal

The mechanism for the transformation of *gem*-dichlorocyclopropanes **38** to their respective cyclopentenone products is believed to occur through disrotatory ring opening followed by conrotatory 4π electrocyclization, as outlined at the beginning of this chapter (Figure 2.6). In an attempt to provide support for the proposed mechanism, dienones **40c** and **40h** were subjected to AgBF_4 in CH_2Cl_2 to ascertain whether the Ag(I) salt would promote cyclization of a dienone intermediate (Scheme 2.18). In both cases, no reaction

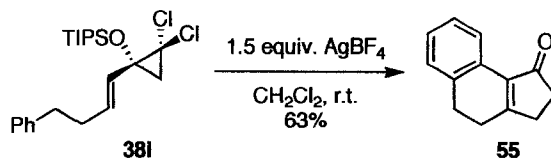


Scheme 2.18. Treatment of chlorodienones with AgBF_4 .

was observed, which suggests that the mechanism does not proceed through a discrete chlorodienone intermediate, but rather through *in situ* generation of a pentadienyl cation capable of undergoing Nazarov cyclization.

An Interrupted Nazarov Reaction

When phenethyl-substituted *gem*-dichlorocyclopropane **38i** was subjected to the established reaction conditions, none of the expected α -chlorocyclopentenone product was isolated; instead, the interesting tricyclic product **55** was isolated in 63% yield (Scheme 2.19). This product is undoubtedly the result of intramolecular trapping of the transient oxyallyl cation by the pendent phenyl group, followed by apparent loss of HCl



Scheme 2.19. A surprising interrupted Nazarov variant.

and olefin migration. Although there is precedent for arene-trapping in the traditional interrupted Nazarov reaction,²³ the major limitation of this reaction cascade was that non-substituted aromatic rings could not participate in the trapping process. Remarkable participation of the simple phenyl substituent in this reaction suggests that the cationic intermediates formed during ring opening and subsequent electrocyclization are more reactive than those generated under traditional Nazarov conditions. The 2-silyloxycyclopentenyl cation appears to possess more cationic character than the analogous Lewis acid-bound species, presenting the possibility for new modes of trapping using *gem*-dichlorocyclopropane compounds. This intramolecular trapping sequence, including a discussion of the probable mechanism for the cascade, will be presented in greater detail in chapter 3.

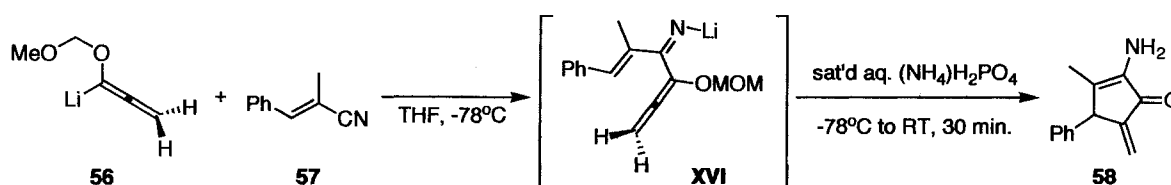
2.2.3 Conclusions

It has been established that the Nazarov cyclization can be accomplished from strategically designed *gem*-dichlorocyclopropane compounds. The process is believed to proceed through disrotatory ring opening of the *gem*-dichlorocyclopropane moiety, followed by 4π electrocyclization of the resultant pentadienyl cation. This sequence leads to the generation of α -chlorocyclopentenones analogous to those observed from traditional Nazarov cyclization. The desired *gem*-dichlorocyclopropane substrates can be

generated in two high-yielding steps from the corresponding α,β -unsaturated ketones, which are readily accessible starting materials. The Ag(I)-mediated rearrangements proceed in moderate to good yields with substitution at the α - and/or β -positions on the vinyl moiety, as well as alkyl substitution on the cyclopropane unit. In cases where a potential nucleophile is tethered to the *gem*-dichlorocyclopropane substrate, an unexpected intramolecular trapping cascade was initiated to furnish a benzohydrindenone product. The noteworthy participation of an unsubstituted phenyl ring under these conditions implicates the generation of highly reactive cationic intermediates compared to those formed during traditional Nazarov cyclization.

2.3 A General Approach to the Imino Nazarov Reaction

The evolution of the *gem*-dichlorocyclopropane variant of the Nazarov reaction has exposed a number of opportunities for new directions in Nazarov methodology. One of the areas we have become interested in is the development of a general approach to an imino Nazarov cyclization. The only example of such a process was reported by Tius and co-workers in 2001,²⁴ and involved the addition of α -lithio- α -(methoxy)methoxyallene **56** to α -methylcinnamionitrile **57** to provide an allenyl vinyl imine intermediate (**XVI**) (Scheme 2.20). During a mild acidic work-up of the reaction mixture, intermediate **XVI** was protonated and underwent spontaneous cyclopentannulation to furnish α -aminocyclopentenone **58**. Although a number of examples were presented, one limitation of this methodology is that α -substitution on the unsaturated nitrile is required for cyclization to occur.



Scheme 2.20. Tius' imino Nazarov cyclization.

The success of Tius' imino Nazarov reaction is significant because it contradicts a computational study that predicted the failure of the simplest possible imino Nazarov reaction. The calculations carried out by Smith and co-workers²⁵ predicted that nitrogen (NH_2) substitution at the 3-position of a pentadienyl cation would impede the cyclization process due to the relative stability of the acyclic cation **XVII** as compared to the cyclic cationic species **XVIII** (Figure 2.10). Tius' explanation for the success of this

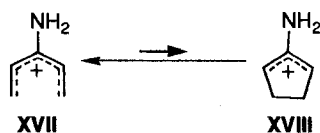


Figure 2.10. The relative stabilities of cyclic and acyclic cationic species.

imino Nazarov variant relies on the ease of his allene-based cyclopentannulation reactions compared to the classic electrocyclization of divinyl ketones, as well as facile termination of the cyclic oxyallyl intermediate through loss of the MOM protecting group under acidic conditions. These structural features (the allene functionality and MOM protecting group) are apparently necessary for efficient cyclization.

In an attempt to access an alternative and potentially more general approach to the imino Nazarov reaction, we sought a straightforward strategy for the synthesis of 2-aminobutadienes **59** as substrates for dihalocyclopropanation. Dichlorocyclopropanation of enamines has previously been reported,²⁶ and we were hoping to take advantage of the electron-rich nature of the enamine olefin to promote selective cyclopropanation of 2-aminobutadienes, providing *gem*-dihalocyclopropane compounds **60**. It was our expectation that strictly thermal conditions might promote sequential ring opening and 4π electrocyclization to provide aminocyclopentadienes **61** and/or cyclopentenones **62**, depending on conditions used to work-up the reactions (Figure 2.11). In these cases, the presence of Ag(I) may not be necessary since premature chloride-assisted termination of the reactive intermediate by desilylation is no longer an issue; however, competing nucleophilic trapping by chloride might be a problem.

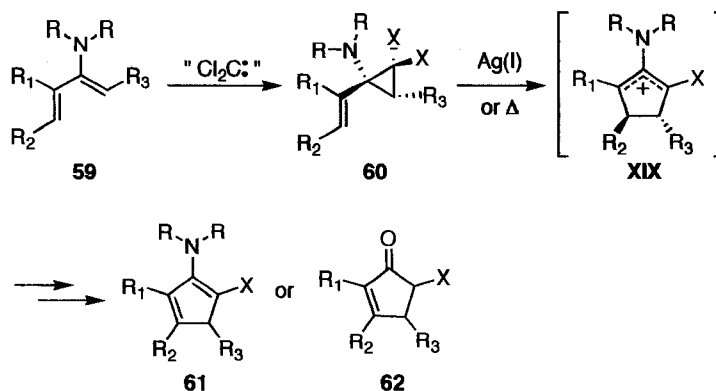
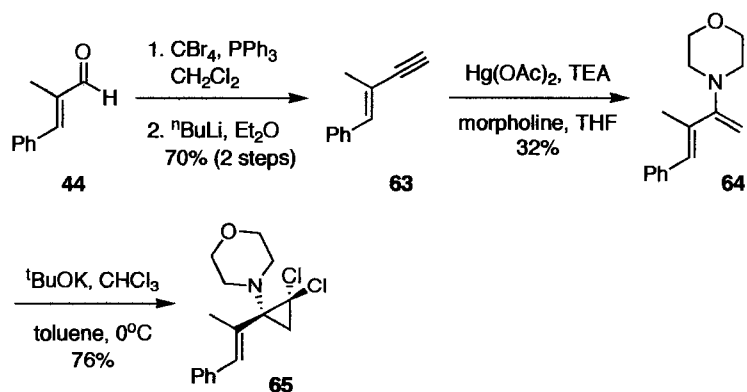


Figure 2.11. Proposed strategy for a general imino Nazarov methodology.

2.3.1 Preliminary Results and Discussion

At present, only the preliminary results of this investigation are available for discussion; however, the success of our initial attempts has encouraged our efforts in this area. We approached the synthesis of *gem*-dichlorocyclopropane compounds **60** using an aminomercuration reaction²⁷ to prepare the desired 2-amino-1,3-butadienes. Enyne **63** was synthesized from α -methyl-*trans*-cinnamaldehyde **44** in 70% yield (2 steps) using a Corey-Fuchs sequence (Scheme 2.21).²⁸ Subsequently, enyne **63** was subjected to

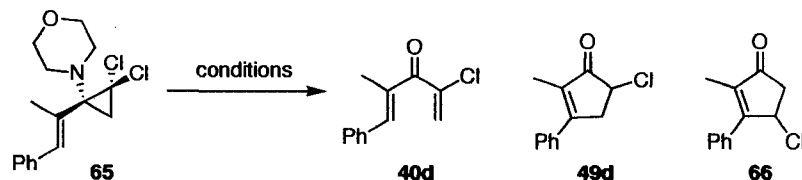


Scheme 2.21. Preparation of *gem*-dichlorocyclopropane **65**.

aminomercuration with $\text{Hg}(\text{OAc})_2$ in the presence of TEA and morpholine to provide the 2-morpholino-1,3-butadiene **64**. The low yield for these reactions is most likely due to facile hydrolysis of the dienamine when exposed to water as well as polymerization/decomposition that may occur during purification by distillation. It is our belief that the yields of these reactions can be improved, but optimization has yet to be performed. Nonetheless, pure dienamine was isolated as a pale yellow oil from this reaction and was subjected to dichlorocyclopropanation using $t\text{BuOK}$ and CHCl_3 in toluene, rather than phase transfer catalysis. The anhydrous conditions utilizing $t\text{BuOK}$ were consistently higher yielding than the phase transfer conditions, furnishing desired product **65** with very little evidence of enamine hydrolysis. The minimal amount of ketone that was present due to hydrolysis could not be separated from the *gem*-dichlorocyclopropane product; therefore, anhydrous cyclopropanation conditions proved to be the best choice for these substrates.

The *gem*-dichlorocyclopropane compound **65** was then subjected to a variety of conditions deemed likely to induce the desired ring opening/Nazarov cyclization sequence (*Table 2.6*). When **65** was treated with AgBF_4 in CH_2Cl_2 , the reaction did not proceed to completion. After 72 h stirring at room temperature, starting material was still observed by TLC analysis along with evidence of decomposition; however, signals observed in the ^1H NMR spectrum of the crude reaction mixture indicated the presence of a minor product, α -chlorocyclopentenone **49d**. These results encouraged further investigation, wherein the substrate (**65**) was subjected to 1 equivalent of AgBF_4 in refluxing MeCN. Under these conditions, we were pleased to see formation of α -

chlorocyclopentenone **49d**, which was isolated in 57% yield. Despite the fact that these reactions were not treated to an aqueous work-up, none of the aminocyclopentadiene compound (**61**) was observed. This result reflects the sensitivity of the aminocyclopentadiene intermediates towards moisture in the air as well as purification by silica gel chromatography.

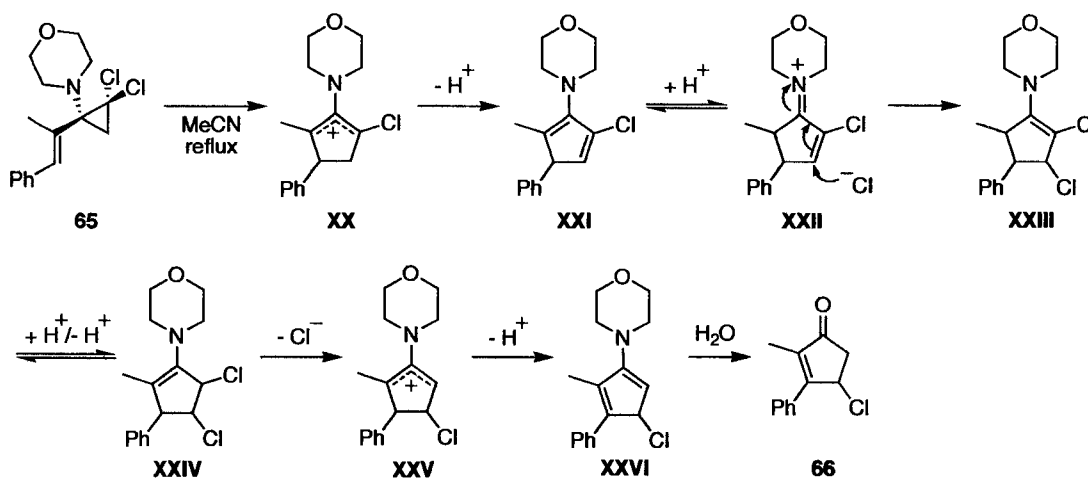


entry	conditions	temperature	time (h)	products
1	AgBF ₄ CH ₂ Cl ₂	r.t.	72	S.M. + 49d
2	AgBF ₄ MeCN	~ 81°C	12	49d
3	MeCN	~ 81°C	12	40d + 49d + 66

Table 2.6. Reactivity of aminodichlorocyclopropane **65**.

With these results in hand, we were interested to learn whether the aminodichlorocyclopropanes could undergo efficient Nazarov cyclization in the absence of the Ag(I) salt. When *gem*-dichlorocyclopropane **65** was dissolved in refluxing MeCN, complete consumption of the starting material was observed after stirring for 12 hours. The reaction provided a mixture of dienone **40d** and cyclopentenone products **49d** and **66**, with **66** appearing as the major cyclopentenone isomer as observed by ¹H NMR. The yields and ratio of products for this reaction were very inconsistent, pointing to an obvious need for further investigation; however, formation of the unusual β -chlorocyclopentenone **66** warrants some discussion. We propose that the mechanism for

its formation (*Scheme 2.22*) proceeds through disrotatory ring opening of the *gem*-dichlorocyclopropane moiety, followed by the expected 4π electrocyclization to provide a 2-aminocyclopentenyl cation **XX**. Subsequent elimination would provide a cyclopentadiene species that could experience protonation to generate the iminium intermediate **XXII**. This very reactive iminium species (**XXII**) could readily participate in a Michael addition reaction in the presence of free chloride anions. The resultant cyclopentene (**XXIII**) might then undergo tautomerization to provide **XXIV**, followed by ionization to afford a second 2-aminocyclopentenyl cation (**XXV**). Facile conversion to β -chlorocyclopentenone **66** would then result from conventional elimination and subsequent hydrolysis of the enamine functionality upon work-up. The formation of cyclopentenone **66** suggests that Ag(I) is still a requirement in these reaction mixtures to sequester free chloride anions, removing them from potential interference after the cyclization process.



Scheme 2.22. Mechanistic proposal for the formation of cyclopentenone **66**.

Although only preliminary results have been obtained thus far, it appears that *gem*-dichlorocyclopropane chemistry is a promising starting point for the development of a general approach to the imino Nazarov reaction.

2.4 Future Directions

Strategically designed *gem*-dichlorocyclopropane compounds, with alkenyl and oxygen substitution on the cyclopropane moiety, have been found to undergo efficient ring opening, followed by Nazarov cyclization to afford α -chlorocyclopentenone products. Development of this methodology has opened a number of avenues for investigation. One such avenue involves the examination of a general approach to the imino Nazarov reaction. We are very eager to investigate the reactivity of various aminodichlorocyclopropanes under established Ag(I)-mediated reaction conditions, with the ultimate intention of using the amine functionality as a traceless chiral auxiliary in an asymmetric Nazarov reaction (*Figure 2.12*).

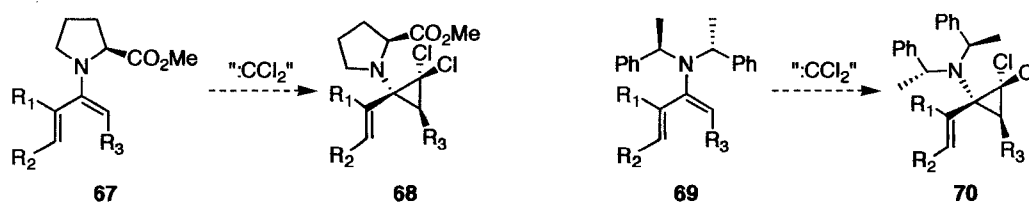


Figure 2.12. Potential chiral amine substrates for use in an asymmetric Nazarov reaction.

We are also invested in the use of alkoxy groups in place of silyloxy substitution on the *gem*-dichlorocyclopropane substrates. It is our belief that these substrates can be appended with carbon- or heteroatom-based nucleophiles that might participate in

interrupted Nazarov reactions. Such trapping processes would permit the construction of complex polycyclic frameworks, such as **73** and/or **74**, in a single operation (*Figure 2.13*). In an analogous manner the nitrogen functionality on an imino Nazarov substrate could also be equipped with tethered nucleophiles. These substrates would provide the opportunity for valuable new modes of trapping in interrupted Nazarov sequences leading to the construction of novel polycyclic compounds.

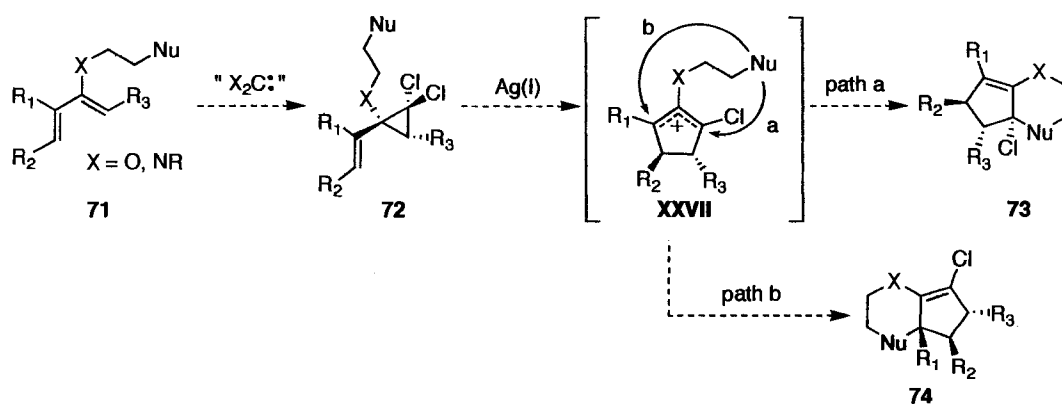


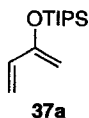
Figure 2.13. Novel modes of trapping in interrupted Nazarov reactions.

2.5 Experimental

2.5.1 General Information

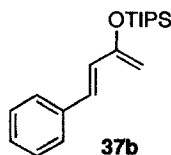
Reactions were carried out in flame-dried glassware under a positive argon atmosphere unless otherwise stated. Transfer of anhydrous solvents and reagents was accomplished with oven-dried syringes or cannulae. Solvents were distilled before use: methylene chloride from calcium hydride, tetrahydrofuran, diethyl ether and benzene from sodium/benzophenone ketyl, toluene from sodium metal. Thin layer chromatography was performed on glass plates precoated with 0.25 mm Kieselgel 60 F₂₅₄ (Merck). Flash chromatography columns were packed with 230-400 mesh silica gel (Silicycle). Proton nuclear magnetic resonance spectra (¹H NMR) were recorded at 400 MHz or 500 MHz and coupling constants (*J*) are reported in Hertz (Hz). Carbon nuclear magnetic resonance spectra (¹³C NMR) were recorded at 100 MHz or 125 MHz and are reported (ppm) relative to the center line of the triplet from chloroform-*d* (77.00 ppm). Infrared (IR) spectra were measured with a Mattson Galaxy Series FT-IR 3000 spectrophotometer. Mass spectra were determined on a PerSeptive Biosystems Mariner high-resolution electrospray positive ion mode spectrometer.

2.5.2 Characterization



2-(Triisopropylsiloxy)-1,3-butadiene (37a). Methyl vinyl ketone (0.41 mL, 5.0 mmol) was dissolved in anhydrous CH₂Cl₂ (40 mL). The solution was cooled to -78°C. Freshly distilled 2,6-lutidine (0.87 mL, 7.5 mmol) was added dropwise to the reaction mixture.

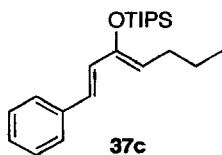
Triisopropylsilyl trifluoromethanesulfonate (1.5 mL, 5.5 mmol) was added dropwise and the solution was stirred at -78°C for 4 h. The reaction was allowed to warm to room temperature before being quenched with a mixture of triethylamine (20 mL) and H_2O (20 mL). The aqueous layer was extracted with CH_2Cl_2 (20 mL). The organic layer was washed with H_2O (2 x 20 mL) and brine (20 mL) and dried (Na_2SO_4). After filtration, the solvent was removed by rotary evaporation and the crude oil purified by flash column chromatography (silica gel, hexanes:EtOAc:TEA 25:1:1) to yield 2-(triisopropylsiloxy)-1,3-butadiene **37a** (463 mg, 2.0 mmol, 41 %) as a colorless oil: R_f 0.72 (hexanes/EtOAc 8:1); IR (thin film) 2946, 2893, 2868, 1586, 1464, 1375, 1303, 1060, 1009, 883, 684 cm^{-1} ; ^1H NMR (500 MHz, CDCl_3) δ 6.23 (dd, $J = 17.2, 10.8$ Hz, 1H) 5.63 (dd, $J = 17.2, 2.4$ Hz, 1H), 5.13 (br d, $J = 10.4$ Hz, 1H), 4.38 (s, 1H), 4.32 (s, 1H), 1.25-1.34 (m, 3H), 1.16 (d, $J = 7.0$ Hz, 18H); ^{13}C NMR (125 MHz, CDCl_3) δ 155.6, 135.2, 114.6, 95.3, 18.3, 13.1; HRMS (EI, M^+) for $\text{C}_{13}\text{H}_{26}\text{OSi}$ calcd 226.1753, found: m/z 226.1754.



(*E*)-4-Phenyl-2-(triisopropylsiloxy)-1,3-butadiene (37b). *N*-morpholino cinnamide²⁰ **43** (1.08 g, 5.0 mmol) was dissolved in freshly distilled THF (20 mL). The temperature of the reaction mixture was dropped to -78°C before adding MeLi (1.6 M, 3.4 mL, 5.5 mmol) dropwise by syringe. The reaction mixture was stirred at low temperature and allowed to warm to room temperature overnight before being quenched by the addition of saturated NH_4Cl solution. The organic layer was washed with H_2O (1 x 20 mL) and brine (1 x 20 mL). The aqueous layer was extracted with Et_2O (2 x 20 mL) and the combined organic layers were dried (MgSO_4). After filtration, the solvent was removed by rotary evaporation and the crude oil was purified by flash column chromatography

(silica gel, hexanes:EtOAc 5:1) to yield 1-phenyl-butene-3-one **36b** (0.56 g, 0.38 mmol, 77 %) as a colorless oil: IR (thin film) 3026, 1691, 1668, 1609, 1449, 1256 cm^{-1} ; ^1H NMR (500 MHz, CDCl_3) δ 2.38 (s, 3H), 6.73 (d, $J = 15.5$ Hz, 1H), 7.39-7.42 (m, 3H), 7.52 (d, $J = 15.5$ Hz, 1H), 7.53-7.57 (m, 2H); ^{13}C NMR (125 MHz, CDCl_3) δ 198.3, 143.4, 134.4, 130.5, 129.0, 128.2, 127.2, 27.5; HRMS (EI, M^+) for $\text{C}_{10}\text{H}_{10}\text{O}$ calcd 146.0731, found: 146.0728 m/z.

1-Phenyl-butene-3-one **36b** (0.30 g, 2.1 mmol) was dissolved in anhydrous THF (5.3 mL). The solution was cooled to 0°C . Freshly distilled triethylamine (0.73 mL, 5.3 mmol) was added dropwise to the reaction mixture. Triisopropylsilyl trifluoromethanesulfonate (0.62 mL, 2.3 mmol) was added dropwise and the solution was stirred at 0°C for 2 h. The reaction was quenched with a mixture of triethylamine (0.5 mL), hexanes (2.5 mL), and saturated NaHCO_3 solution (5 mL). The organic layer was washed with H_2O (2 x 5 mL) and brine (5 mL) and dried (MgSO_4). After filtration, the solvent was removed to yield 4-phenyl-2-(triisopropylsiloxy)-1,3-butadiene, **37b**, (571 mg, 1.9 mmol, 90 %) as a clear, colorless oil: IR (thin film) 3081, 2943, 2891, 2866, 1587, 1327, 1027 cm^{-1} ; ^1H NMR (500 MHz, CDCl_3) δ 1.15 (d, $J = 7.0$ Hz, 18H), 1.26-1.34 (m, 3H), 4.41 (s, 1H), 4.42 (s, 1H), 6.58 (d, $J = 15.5$ Hz, 1H), 6.95 (d, $J = 15.5$ Hz, 1H), 7.23 (t, $J = 7.5$ Hz, 1H), 7.32 (t, $J = 7.5$ Hz, 2H), 7.42 (d, $J = 7.5$ Hz, 2H); ^{13}C NMR (125 MHz, CDCl_3) δ 155.4, 136.9, 129.1, 128.5, 127.6, 126.7, 126.6, 95.8, 18.1, 12.8; HRMS (EI, M^+) for $\text{C}_{19}\text{H}_{30}\text{OSi}$ calcd 302.2066, found: 302.2062 m/z.

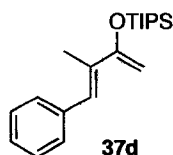


(1E,3Z)-1-Phenyl-3-(triisopropylsiloxy)-1,3-heptadiene (37c). *N*-morpholino cinnamide²⁰ **43** (0.23 g, 1.0 mmol) was dissolved in freshly distilled THF (10 mL). The

solution was cooled to -78°C before adding $^n\text{BuLi}$ (1.6 M in hexanes, 0.72 mL, 1.1 mmol) dropwise by syringe. The reaction mixture was stirred at low temperature for 3 h before being quenched by the addition of saturated NH_4Cl solution. The organic layer was washed with H_2O (10 mL) and brine (10 mL). The aqueous layer was extracted with Et_2O (2 x 10 mL) and the combined organic layers were dried (MgSO_4). After filtration, the solvent was removed and the crude oil purified by flash column chromatography (silica gel, hexanes: EtOAc 8:1) to yield 1-phenyl-(*IE*)-heptene-3-one **36c** (0.053 g, 0.28 mmol, 27 % [unoptimized]) as a white solid: m.p. $34\text{-}36^{\circ}\text{C}$; R_f 0.48 (hexanes/ EtOAc 8:1); IR (thin film) 3023, 2954, 2939, 2864, 1650, 1464, 1452, 984, 745, 688 cm^{-1} ; ^1H NMR (500 MHz, CDCl_3) δ 7.54-7.57 (m, 3H), 7.39-7.41 (m, 3H), 6.75 (d, $J = 16.5$ Hz, 1H), 2.67 (t, $J = 7.5$ Hz, 2H), 1.67 (pent, $J = 7.5$ Hz, 2H), 1.39 (sextet, $J = 7.5$ Hz, 2H), 0.95 (t, $J = 7.0$ Hz, 3H); ^{13}C NMR (125 MHz, CDCl_3) δ 200.6, 142.3, 134.6, 130.3, 128.9, 128.2, 126.3, 40.7, 26.5, 22.5, 13.9; HRMS (EI, M^+) for $\text{C}_{13}\text{H}_{16}\text{O}$ calcd 188.1201, found: m/z 188.1201; Anal. Calcd for $\text{C}_{13}\text{H}_{16}\text{O}$: C, 82.94; H, 8.57. Found: C, 82.74; H, 8.73.

1-Phenyl-(*IE*)-heptene-3-one **36c** (0.086 g, 0.49 mmol) was dissolved in anhydrous THF (1.5 mL). The solution was cooled to 0°C . Freshly distilled triethylamine (0.17 mL, 1.2 mmol) was added dropwise to the reaction mixture. Triisopropylsilyl trifluoromethanesulfonate (0.17 mL, 0.62 mmol) was added dropwise and the solution was stirred at 0°C for 2 h. The reaction was quenched with a mixture of triethylamine (0.5 mL), hexanes (2.5 mL), and saturated NaHCO_3 solution (5 mL). The organic layer was washed with H_2O (2 x 5 mL) and brine (5 mL) and dried (MgSO_4). After filtration, the solvent was removed to yield (*IE,3Z*)-1-phenyl-3-

(triisopropylsiloxy)-1,3-heptadiene **37c** (164 mg, 0.47 mmol, 97%) as a colorless oil: *R_f* 0.76 (hexanes/EtOAc 8:1); IR (thin film) 3025, 2946, 2867, 1618, 1464, 1062 cm^{-1} ; ^1H NMR (500 MHz, CDCl_3) δ 7.37 (d, $J = 7.5$ Hz, 2H), 7.31 (app. t, $J = 8.0$ Hz, 2H), 7.21 (t, $J = 7.5$ Hz, 1H), 6.71 (d, $J = 15.5$ Hz, 1H), 6.56 (d, $J = 15.5$ Hz, 1H), 4.90 (t, $J = 7.5$ Hz, 1H), 2.18 (q, $J = 7.5$ Hz, 2H), 1.42 (sextet, $J = 7.5$ Hz, 2H), 1.22-1.30 (m, 3H), 1.16 (d, $J = 7.0$ Hz, 18H), 0.95 (t, $J = 7.5$ Hz, 3H); ^{13}C NMR (125 MHz, CDCl_3) δ 149.4, 137.4, 128.6, 128.1, 127.1, 126.5, 126.3, 115.3, 28.3, 22.8, 18.1, 14.0, 13.9; HRMS (EI, M^+) for $\text{C}_{22}\text{H}_{36}\text{OSi}$ calcd, 344.2535, found: m/z 344.2535.



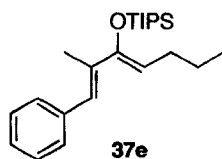
(3E)-3-Methyl-4-phenyl-2-(triisopropylsiloxy)-1,3-butadiene (37d). α -Methyl-*trans*-cinnamaldehyde **44** (1.4 mL, 10.0 mmol) was dissolved in freshly distilled THF (25 mL). The reaction mixture was cooled to -78°C before adding MeLi (1.6 M, 6.3 mL, 10 mmol) dropwise by syringe. The reaction mixture was stirred at low temperature for 3 h and then quenched by the addition of saturated NH_4Cl solution. The organic layer was washed with H_2O (20 mL) and brine (20 mL). The aqueous layer was extracted with Et_2O (2 x 20 mL) and the combined organic layers were dried (MgSO_4). After filtration, the solvent was removed and the crude oil was purified by flash column chromatography (silica gel, hexanes:EtOAc 10:1) to yield 3-methyl-4-phenyl-(3E)-butene-2-ol **45a** (1.6 g, 9.8 mmol, 98 %) as a pale yellow oil: *R_f* 0.38 (hexanes/EtOAc 2:1); IR (thin film) 3347, 2974, 1947, 1806, 1600, 1443, 1074, 698 cm^{-1} ; ^1H NMR (500 MHz, CDCl_3) δ 7.34 (app. t, $J = 7.5$ Hz, 2H), 7.28 (app. d, $J = 6.5$ Hz, 2H), 7.22 (app. t, $J = 7.0$ Hz, 1H), 6.53 (br s, 1H), 4.39 (q, 1H, $J = 6.5$ Hz), 1.89 (d, 3H, $J = 1.0$ Hz), 1.60 (br s, 1H), 1.38 (d, 3H, $J =$

6.5 Hz); ^{13}C NMR (125 MHz, CDCl_3) δ 141.6, 137.6, 128.9, 128.1, 126.4, 124.4, 73.6, 21.8, 13.4; HRMS (EI, M^+) for $\text{C}_{11}\text{H}_{14}\text{O}$ calcd 162.1045, found: m/z 162.1045.

3-Methyl-4-phenyl-(3*E*)-butene-2-ol **45a** (1.56 g, 9.6 mmol) was dissolved in freshly distilled CH_2Cl_2 (30 mL). To the solution was added powdered 4 Å molecular sieves (7 g). The reaction mixture was cooled to 0°C before adding NMO (1.7 g, 14.4 mmol) in one portion. At low temperature, tetrapropylammonium perruthenate (0.17 g, 0.48 mmol) was next added in three equal portions. The reaction was left to stir at room temperature for 3 h before being quenched by filtration through a silica gel plug. The solvent was removed and the crude material purified by flash column chromatography (silica gel, hexanes:EtOAc 10:1) to yield 3-methyl-4-phenyl-(3*E*)-butene-2-one **36d** (1.3 g, 8.1 mmol, 85 %) as a white solid: m.p. 36-37.5 °C; R_f 0.49 (hexanes/EtOAc 2:1); IR (thin film) 3056, 2999, 2961, 2925, 1956, 1666, 1626, 1245, 1006 cm^{-1} ; ^1H NMR (500 MHz, CDCl_3) δ 7.52 (s, 1H), 7.42-7.45 (m, 4H), 7.34-7.38 (m, 1H), 2.48 (s, 3H), 2.07 (s, 3H); ^{13}C NMR (125 MHz, CDCl_3) δ 200.3, 139.6, 137.8, 135.9, 129.7, 128.5, 128.4, 25.8, 12.9; HRMS (EI, M^+) for $\text{C}_{11}\text{H}_{12}\text{O}$ calcd 160.0888, found: m/z 160.0884; Anal. Calcd for $\text{C}_{11}\text{H}_{12}\text{O}$: C, 82.46; H, 7.55. Found: C, 82.50; H, 7.62.

3-Methyl-4-phenyl-(3*E*)-butene-2-one **36d** (0.20 g, 1.2 mmol) was dissolved in anhydrous THF (3.5 mL). The solution was cooled to 0°C. Freshly distilled triethylamine (0.43 mL, 3.1 mmol) was added dropwise to the reaction mixture. Triisopropylsilyl trifluoromethanesulfonate (0.40 mL, 1.5 mmol) was added dropwise and the solution was stirred at 0°C for 2 h. The reaction was quenched with a mixture of triethylamine (0.5 mL), hexanes (2.5 mL), and saturated NaHCO_3 solution (5 mL). The organic layer was washed with H_2O (2 x 5 mL) and brine (5 mL) and dried (MgSO_4).

After filtration, the solvent was removed to yield (3*E*)-3-methyl-4-phenyl-2-(triisopropylsiloxy)-1,3-butadiene, **37d**, (371 mg, 1.17 mmol, 94%) as a colorless oil: *R_f* 0.75 (hexanes/EtOAc 8:1); IR (thin film) 3022, 2944, 2866, 1600, 1589, 1463, 1124, 1021 cm^{-1} ; ^1H NMR (500 MHz, CDCl_3) δ 7.35 (t, $J = 7.5$ Hz, 2H), 7.29 (d, $J = 7.0$ Hz, 2H), 7.23 (t, $J = 7.0$ Hz, 1H), 7.18 (br s, 1H), 4.59 (d, $J = 1.5$ Hz, 1H), 4.44 (d, $J = 1.0$ Hz, 1H), 2.00 (d, $J = 1.0$ Hz, 3H), 1.26-1.34 (m, 3H), 1.15 (d, $J = 7.5$ Hz, 18H); ^{13}C NMR (125 MHz, CDCl_3) δ 157.8, 138.2, 133.0, 129.3, 128.0, 127.1, 126.4, 92.0, 18.1, 14.7, 12.9; HRMS (EI, M^+) for $\text{C}_{20}\text{H}_{32}\text{OSi}$ calcd, 316.2222, found: m/z 316.2218.



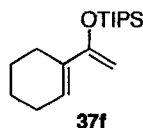
(1*E*,3*Z*)-2-Methyl-1-phenyl-3-(triisopropylsiloxy)-1,3-heptadiene (37e). α -Methyl-*trans*-cinnamaldehyde **44** (1.4 mL, 10.0 mmol) was dissolved in freshly distilled Et_2O (40 mL). The reaction mixture was cooled to -78°C before adding $^n\text{BuLi}$ (1.45 M in hexanes, 7.1 mL, 10.3 mmol) dropwise by syringe. The reaction mixture was stirred at low temperature for 4 h and then quenched by the addition of 0.5 M HCl (aq) at room temperature. The organic layer was washed with H_2O (2 x 30 mL) and brine (30 mL). The aqueous layer was extracted with Et_2O (2 x 30 mL) and the combined organic layers were dried (MgSO_4). After filtration, the solvent was removed and the crude oil was purified by flash column chromatography (silica gel, hexanes:EtOAc 10:1) to yield 2-methyl-1-phenyl-(1*E*)-heptene-3-ol **45b** (1.3 g, 6.6 mmol, 66 %) as a colorless oil: *R_f* 0.24 (hexanes/EtOAc 8:1); IR (thin film) 3349, 3024, 2956, 2860, 1446, 1011 cm^{-1} ; ^1H NMR (500 MHz, CDCl_3) δ 7.18-7.37 (m, 5H), 6.49 (br s, 1H), 4.18 (t, $J = 6.6$ Hz, 1H), 1.87 (d, $J = 1.2$ Hz, 3H), 1.65 (app. q, $J = 6.5$ Hz, 2H), 1.59 (br s, 1H), 1.24-1.44 (m, 4H),

0.93 (t, $J = 7.2$ Hz, 3H); ^{13}C NMR (125 MHz, CDCl_3) δ 140.4, 137.6, 128.9, 128.1, 126.4, 125.7, 78.2, 34.8, 28.0, 22.6, 14.0, 13.1; HRMS (EI, M^+) for $\text{C}_{14}\text{H}_{20}\text{O}$ calcd 204.1514, found: m/z 204.1510.

2-Methyl-1-phenyl-(*IE*)-heptene-3-ol **45b** (2.1 g, 10.3 mmol) was dissolved in freshly distilled CH_2Cl_2 (30 mL). To the solution was added powdered 4 Å molecular sieves (7 g). The reaction mixture was cooled to 0°C before adding NMO (1.8 g, 31 mmol) in one portion. At low temperature, tetrapropylammonium perruthenate (0.17 g, 0.50 mmol) was next added in three equal portions. The reaction was left to stir at room temperature for 5 h before being quenched by filtration through a silica gel plug. The solvent was removed and the crude material purified by gradient column chromatography (silica gel, hexanes:EtOAc 50:1, 40:1, 30:1, 20:1) to yield (*IE*)-2-methyl-1-phenylheptene-3-one **36e** (1.6 g, 7.8 mmol, 76 %) as a colorless oil: R_f 0.42 (hexanes/EtOAc 8:1); IR (thin film) 3057, 2958, 2932, 2872, 1667 cm^{-1} ; ^1H NMR (300 MHz, CDCl_3) δ 7.52 (br q, $J = 1.2$ Hz, 1H), 7.31-7.43 (m, 5H), 2.80 (t, $J = 7.5$ Hz, 2H), 2.07 (d, $J = 1.5$ Hz, 3H), 1.68 (pent, $J = 7.5$ Hz, 2H), 1.40 (sextet, $J = 7.2$ Hz, 2H), 0.96 (t, $J = 7.5$ Hz, 3H); ^{13}C NMR (125 MHz, CDCl_3) δ 202.7, 138.3, 137.5, 136.1, 129.7, 128.4, 128.4, 37.4, 27.1, 22.5, 13.9, 13.2; HRMS (EI, M^+) for $\text{C}_{14}\text{H}_{18}\text{O}$ calcd 202.1358, found: m/z 202.1363.

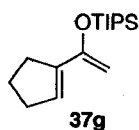
(*IE*)-2-Methyl-1-phenylheptene-3-one **36e** (0.20 g, 1.0 mmol) was dissolved in anhydrous THF (2.5 mL). The solution was cooled to 0°C . Freshly distilled triethylamine (0.35 mL, 2.5 mmol) was added dropwise to the reaction mixture. Triisopropylsilyl trifluoromethanesulfonate (0.32 mL, 1.2 mmol) was added dropwise and the solution was stirred at 0°C for 4 h. The reaction was quenched with a mixture of

triethylamine (0.5 mL), hexanes (2.5 mL), and saturated NaHCO₃ solution (5 mL). The organic layer was washed with H₂O (2 x 5 mL) and brine (5 mL) and dried (MgSO₄). After filtration, the solvent was removed to yield (*1E,3Z*)-2-methyl-1-phenyl-3-(triisopropylsiloxy)-hepta-1,3-diene, **37e**, (16:1, (*1E,3Z*):(*1E,3E*)); 0.33 g, 0.93 mmol, 93 %) as a pale yellow oil: *R*_f 0.75 (hexanes/EtOAc 8:1); IR (thin film) 3022, 2958, 2867, 1622, 1464, 1090 cm⁻¹; ¹H NMR (500 MHz, CDCl₃) δ 7.34 (t, *J* = 7.5 Hz, 2H), 7.26-7.28 (m, 2H), 7.22 (t, *J* = 7.5 Hz, 1H), 6.86 (s, 1H), 4.97 (t, *J* = 7.0 Hz, 1H), 2.19 (q, *J* = 7.0 Hz, 2H), 1.99 (s, 3H), 1.43 (sextet, *J* = 7.5 Hz, 2H), 1.22-1.30 (m, 3H), 1.14 (d, *J* = 7.0 Hz, 18H), 0.96 (t, *J* = 7.5 Hz, 3H); ¹³C NMR (125 MHz, CDCl₃) δ 152.0, 138.4, 134.9, 129.1, 128.0, 126.2, 125.3, 111.1, 28.5, 23.0, 18.1, 15.5, 14.1, 13.9; HRMS (EI, M⁺) for C₂₃H₃₈OSi calcd, 358.2692, found: *m/z* 358.2684.

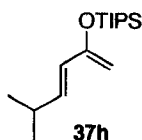


1-Triisopropylsiloxy-1-(cyclohexen-1-yl)-ethene (37f). 1-Acetyl-1-cyclohexene **36f** (0.13 mL, 1.0 mmol) was dissolved in anhydrous THF (2.5 mL). The solution was cooled to 0°C. Freshly distilled triethylamine (0.35 mL, 2.5 mmol) was added dropwise to the reaction mixture. Triisopropylsilyl trifluoromethanesulfonate (0.29 mL, 1.1 mmol) was added dropwise and the solution was stirred at 0°C for 2 h. The reaction was quenched with a mixture of triethylamine (0.5 mL), hexanes (2.5 mL), and saturated NaHCO₃ solution (5 mL). The organic layer was washed with H₂O (2 x 5 mL) and brine (5 mL) and dried (MgSO₄). After filtration, the solvent was removed to yield 1-(triisopropylsiloxy)-1-(cyclohexen-1-yl)-ethene, **37f**, (278 mg, 0.99 mmol, 99%) as a colorless oil: *R*_f 0.76 (hexanes/EtOAc 8:1); IR (thin film) 2943, 2867, 1591, 1464, 1288,

1017, 883 cm^{-1} ; ^1H NMR (500 MHz, CDCl_3) δ 6.32 (br s, 1H), 4.31 (s, 1H), 4.18 (s, 1H), 2.12-2.16 (m, 4H), 1.64-1.70 (m, 2H), 1.56-1.60 (m, 2H), 1.20-1.28 (m, 3H), 1.11 (d, $J = 7.0$ Hz, 18H); ^{13}C NMR (125 MHz, CDCl_3) δ 157.1, 133.1, 125.1, 88.6, 25.5, 25.1, 22.8, 22.1, 18.1, 12.9; HRMS (EI, M^+) for $\text{C}_{17}\text{H}_{32}\text{OSi}$ calcd 280.2222, found: m/z 280.2220.

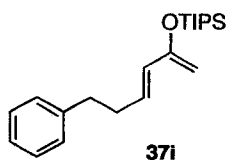


1-Triisopropylsilyloxy-1-(cyclopenten-1-yl)-ethene (37g). The above procedure was used in the synthesis of **37g** starting with 1-acetyl-1-cyclopentene **36g** (0.11 mL, 1.0 mmol). The reaction yielded 1-(triisopropylsilyloxy)-1-(cyclopenten-1-yl)-ethene, **37g**, (266 mg, 1.0 mmol, 100%) as a pale yellow oil: R_f 0.76 (hexanes/EtOAc 8:1); IR (thin film) 2945, 2867, 1586, 1464, 1363, 1014, 883 cm^{-1} ; ^1H NMR (500 MHz, CDCl_3) δ 6.06 (br s, 1H), 4.26 (s, 1H), 4.24 (s, 1H), 2.44 (app. t, $J = 7.5$ Hz, 4H), 1.94 (pent, $J = 7.5$ Hz, 2H), 1.20-1.28 (m, 3H), 1.11 (d, $J = 7.0$ Hz, 18H); ^{13}C NMR (125 MHz, CDCl_3) δ 154.3, 141.3, 128.5, 91.6, 32.9, 32.2, 23.6, 18.1, 12.8; HRMS (EI, M^+) for $\text{C}_{16}\text{H}_{30}\text{OSi}$ calcd 266.2066, found: m/z 266.2067.



(3E)-4-Isopropyl-2-(triisopropylsilyloxy)-1,3-butadiene (37h). 5-Methyl-(3E)-hexene-2-one **36h** (0.26 mL, 2.0 mmol) was dissolved in anhydrous THF (5.0 mL). The solution was cooled to 0°C . Freshly distilled triethylamine (0.70 mL, 5.0 mmol) was added dropwise to the reaction mixture. Triisopropylsilyl trifluoromethanesulfonate (0.59 mL, 2.2 mmol) was added dropwise and the solution was stirred at 0°C for 2 h. The reaction was quenched with a mixture of triethylamine (1 mL), hexanes (5 mL), and saturated

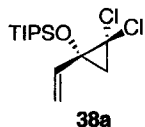
NaHCO₃ solution (5 mL). The organic layer was washed with H₂O (2 x 5 mL) and brine (5 mL) and dried (MgSO₄). After filtration, the solvent was removed to yield (3*E*)-4-isopropyl-2-(triisopropylsiloxy)-1,3-butadiene, **37h**, (535 mg, 2.0 mmol, 100 %) as a colorless oil: R_f 0.84 (hexanes/EtOAc 8:1); IR (thin film) 2960, 2868, 1589, 1464, 1306, 1026, 883, 678 cm⁻¹; ¹H NMR (500 MHz, CDCl₃) δ 6.06 (dd, *J* = 15.5, 6.5 Hz, 1H), 5.82 (dd, *J* = 15.5, 1.0 Hz, 1H), 4.23 (s, 1H), 4.19 (s, 1H), 2.36 (app. octet, *J* = 7.0 Hz, 1H), 1.20-1.28 (m, 3H), 1.11 (d, *J* = 7.5 Hz, 18H), 1.02 (d, *J* = 7.0 Hz, 6H); ¹³C NMR (125 MHz, CDCl₃) δ 155.6, 138.5, 124.9, 93.1, 30.5, 22.2, 18.0, 12.8; HRMS (EI, M⁺) for C₁₆H₃₂OSi calcd 268.2222, found: m/z 268.2219.



(3*E*)-2-(triisopropylsiloxy)-6-phenyl-1,3-hexadiene (**37i**). 1-(Triphenylphosphoranylidene)-2-propanone **47** (0.32 g, 1.0 mmol) was dissolved in freshly distilled THF (10 mL). Hydrocinnamaldehyde **48** (0.13 mL, 1.0 mmol) was added dropwise to the reaction mixture at room temperature. The colorless solution was allowed to stir at room temperature for 18 h before being quenched by the addition of hexanes (25 mL). The addition of hexanes precipitated a white solid, which was removed by filtration. The solvent was removed and the crude oil was purified by flash column chromatography (silica gel, hexanes:EtOAc 15:1) to yield 6-phenyl-(3*E*)-hexene-2-one **36i** (0.09 g, 0.52 mmol, 52 %) as a colorless oil: R_f 0.22 (hexanes/EtOAc 8:1); IR (thin film) 3028, 2928, 2858, 1697, 1675, 1627, 1360, 1255, 976, 748 cm⁻¹; ¹H NMR (400 MHz, CDCl₃) δ 7.29-7.33 (m, 2H), 7.18-7.24 (m, 3H), 6.82 (dt, *J* = 16.0, 6.8 Hz, 1H), 6.10 (dt, *J* = 16.0, 1.6 Hz, 1H), 2.80 (t, *J* = 7.6 Hz, 2H), 2.53-2.59 (m, 2H), 2.23 (s, 3H);

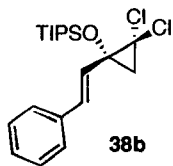
^{13}C NMR (125 MHz, CDCl_3) δ 198.5, 147.0, 140.6, 131.7, 128.5, 128.3, 126.2, 34.4, 34.1, 26.9; HRMS (EI, M^+) for $\text{C}_{12}\text{H}_{14}\text{O}$ calcd 174.1045, found: m/z 174.1043.

6-Phenyl-(3*E*)-hexene-2-one **36i** (0.15 g, 0.86 mmol) was dissolved in anhydrous THF (3.0 mL). The solution was cooled to 0°C. Freshly distilled triethylamine (0.30 mL, 2.1 mmol) was added dropwise to the reaction mixture. Triisopropylsilyl trifluoromethanesulfonate (0.24 mL, 0.95 mmol) was added dropwise and the solution was stirred at 0°C for 2.5 h. The reaction was quenched with a mixture of triethylamine (0.5 mL), hexanes (2.5 mL), and saturated NaHCO_3 solution (5 mL). The organic layer was washed with H_2O (2 x 5 mL) and brine (5 mL) and dried (MgSO_4). After filtration, the solvent was removed to yield (3*E*)-2-(triisopropylsiloxy)-6-phenyl-1,3-hexadiene, **37i**, (0.25 g, 0.84 mmol, 98%) as a clear, colorless oil: R_f 0.82 (hexanes:EtOAc 8:1); IR (thin film) 3028, 2944, 2867, 1589, 1464, 1321, 1028, 883, 697 cm^{-1} ; ^1H NMR (400 MHz, CDCl_3) δ 7.25-7.30 (m, 2H), 7.15-7.20 (m, 3H), 6.09 (dt, $J = 15.3, 6.9$ Hz, 1H), 5.90 (dt, $J = 15.3, 1.2$ Hz, 1H), 4.22 (s, 1H), 4.17 (s, 1H), 2.73 (t, $J = 7.2$ Hz, 2H), 2.42 (dt, $J = 7.5, 7.5$ Hz, 2H), 1.16-1.27 (m, 3H), 1.10 (d, $J = 6.6$ Hz, 18H); ^{13}C NMR (125 MHz, CDCl_3) δ 155.3, 141.8, 130.5, 128.5, 128.4, 128.3, 125.8, 93.2, 35.7, 33.9, 18.1, 12.8; HRMS (EI, M^+) for $\text{C}_{21}\text{H}_{34}\text{OSi}$ calcd 330.2379, found: m/z 330.2375.



1,1-Dichloro-2-(ethenyl)-2-triisopropylsilyloxycyclopropane (38a). Siloxy diene, **37a**, (0.46 g, 2.0 mmol) was dissolved in CHCl_3 (0.2 mol, 16 mL). Benzyltriethylammonium chloride (0.13 g, 0.60 mmol) was added to the reaction mixture. A solution of 50 % NaOH aq. (0.37 mol, 19.5 mL) was then added in one portion and the reaction was

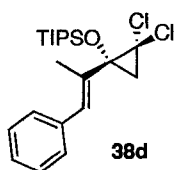
vigorously stirred at room temperature for 4 h. The reaction was quenched by dilution with CH₂Cl₂ (20 mL) and H₂O (20 mL). The organic layer was washed with H₂O (2 x 20 mL). The aqueous layer was extracted with CH₂Cl₂ (2 x 20 mL) and the combined organic layers were dried (MgSO₄). After filtration, the solvent was removed and the crude oil was purified by flash column chromatography (silica gel, hexanes:EtOAc 50:1) to yield 1,1-dichloro-2-(ethenyl)-2-triisopropylsilyloxycyclopropane **38a** (0.57 g, 1.86 mmol, 93 %) as a pale yellow oil: R_f 0.69 (hexanes/EtOAc 10:1); IR (thin film) 2946, 2893, 2868, 1464, 1228, 1070, 883, 682 cm⁻¹; ¹H NMR (500 MHz, CDCl₃) δ 6.09 (ddd, *J* = 1.0, 10.5, 17.0 Hz, 1H), 5.37 (d, *J* = 10.5 Hz, 1H), 5.32 (d, *J* = 17.0 Hz, 1H), 1.88 (d, *J* = 8.5 Hz, 1H), 1.69 (dd, *J* = 1.0, 8.5 Hz, 1H), 1.07-1.16 (m, 21H); ¹³C NMR (125 MHz, CDCl₃) δ 135.9, 118.4, 65.4, 64.6, 32.4, 18.3, 18.2, 13.0; HRMS (EI, [M-Cl]⁺) for C₁₄H₂₆OSiCl calcd 273.1441, found: *m/z* 273.1445.



1,1-Dichloro-2-(1-phenyl-*trans*-ethen-2-yl)-2-triisopropylsilyloxycyclopropane (38b).

The aforementioned method was also employed in the synthesis of **38b** starting with (*IE*)-4-phenyl-2-(triisopropylsiloxy)-1,3-butadiene **37b** (0.5 g, 1.7 mmol). The reaction was quenched after 3 h and the crude material was purified by flash column chromatography (silica gel, hexanes:EtOAc 50:1) to yield 1,1-dichloro-2-(1-phenyl-*trans*-ethen-2-yl)-2-triisopropylsilyloxycyclopropane **38b** (0.46 g, 1.2 mmol, 74 %) as a colorless oil: IR (thin film) 3028, 2945, 2867, 1496, 1213, 1082, 691 cm⁻¹; ¹H NMR (500 MHz, CDCl₃) δ 1.09-1.17 (m, 21H), 1.80 (d, *J* = 8.5 Hz, 1H), 2.02 (d, *J* = 8.5 Hz, 1H), 6.45 (d, *J* = 16.0 Hz, 1H), 6.65 (d, *J* = 16.0 Hz, 1H), 7.29 (t, *J* = 8.0 Hz, 1H), 7.36 (t, *J* = 8.0 Hz, 2H), 7.41 (d, *J* = 8.0 Hz, 2H); ¹³C NMR (125 MHz, CDCl₃) δ 136.2, 133.4,

129.0, 128.5, 127.3, 126.9, 65.9, 64.5, 33.3, 18.3, 13.1; HRMS (EI, M⁺) for C₂₀H₃₀Cl₂OSi calcd, 384.1443, found: 384.1440 m/z.



(1E)-1,1-Dichloro-2-(1-phenylpropen-2-yl)-2-triisopropylsilyloxycyclopropane (38d).

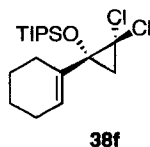
The same method was employed in the synthesis of **38d** starting with (*1E*)-2-methyl-1-phenyl-3-(triisopropylsiloxy)-1,3-butadiene **37d** (0.30 g, 0.95 mmol). The reaction was quenched after 3 h and the crude material was purified by flash column chromatography (silica gel, hexanes:EtOAc 50:1) to yield (*1E*)-1,1-dichloro-2-(1-phenylpropen-2-yl)-2-triisopropylsilyloxycyclopropane **38d** (0.30 g, 0.76 mmol, 80 %) as a colorless oil: *R_f* 0.58 (hexanes/EtOAc 20:1); IR (thin film) 3024, 2945, 2867, 1495, 1257, 1076, 700, 690 cm⁻¹; ¹H NMR (500 MHz, CDCl₃) δ 7.36 (t, *J* = 7.5 Hz, 2H), 7.24-7.28 (m, 3H), 6.49 (s, 1H), 2.13 (s, 3H), 2.14 (d, *J* = 8.5 Hz, 1H), 1.78 (d, *J* = 8.5 Hz, 1H), 1.06-1.18 (m, 21H); ¹³C NMR (125 MHz, CDCl₃) δ 136.7, 135.8, 129.4, 128.9, 128.2, 127.0, 68.7, 64.8, 32.0, 18.0, 18.0, 16.0, 12.8; HRMS (EI, M⁺) for C₂₁H₃₂Cl₂OSi calcd 398.1599, found: m/z 398.1600.



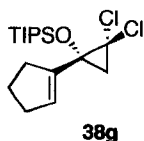
***cis*-1,1-Dichloro-2-(1-phenyl-[1E]-propen-2-yl)-3-propyl-2-**

triisopropylsilyloxycyclopropane (38e). The same method was employed in the synthesis of **38e** starting with (*1E,3Z*)-2-methyl-1-phenyl-3-(triisopropylsiloxy)-1,3-heptadiene **37e** (0.10 g, 0.28 mmol). The reaction was quenched after 1.5 h, and the crude material was purified by flash column chromatography (silica gel, hexanes:EtOAc

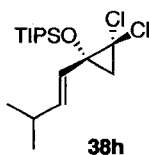
50:1) to yield (*E*)-1,1-dichloro-2-(1-phenyl-propen-2-yl)-3-propyl-2-triisopropylsilyloxycyclopropane **38e** (0.11 g, 0.24 mmol, 87 %) as a colorless oil: R_f 0.69 (hexanes/EtOAc 25:1); IR (thin film) 3027, 2947, 2868, 1630, 1464, 1257, 884, 682 cm^{-1} ; ^1H NMR (500 MHz, CDCl_3) δ 7.36 (t, $J = 7.5$ Hz, 2H), 7.25-7.29 (m, 3H), 6.61 (s, 1H), 2.11 (d, $J = 1.5$ Hz, 3H), 1.86-1.88 (m, 1H), 1.57-1.65 (m, 4H), 1.08-1.14 (m, 21H), 1.03 (t, $J = 7.0$ Hz, 3H); ^{13}C NMR (125 MHz, CDCl_3) δ 136.8, 136.2, 131.4, 128.9, 128.3, 127.0, 70.8, 69.2, 38.8, 26.8, 21.6, 18.3, 18.1, 16.8, 14.0, 13.9; HRMS (EI, M^+) for $\text{C}_{24}\text{H}_{38}\text{Cl}_2\text{OSi}$ calcd 440.2069, found: m/z 440.2078.



1,1-Dichloro-2-(1-cyclohexenyl)-2-triisopropylsilyloxycyclopropane (38f). The same method was employed in the synthesis of **38f** starting with 1-triisopropylsiloxy-1-(cyclohexen-1-yl)-ethene **37f** (0.12 g, 0.45 mmol). The reaction was quenched after 20 min. and the crude material was purified by flash column chromatography (silica gel, hexanes:EtOAc 50:1) to yield 1,1-dichloro-2-(1-cyclohexenyl)-2-triisopropylsilyloxycyclopropane **38f** (0.16 g, 0.43 mmol, 96 %) as a colorless oil: R_f 0.63 (hexanes/EtOAc 20:1); IR (thin film) 2943, 2867, 1464, 1249, 1099, 1081, 1069, 883, 682 cm^{-1} ; ^1H NMR (400 MHz, CDCl_3) δ 5.70 (app. septet, $J = 2.0$ Hz, 1H), 2.38-2.45 (m, 1H), 2.11-2.19 (m, 1H), 2.04-2.09 (m, 2H), 1.92 (d, $J = 8.0$ Hz, 1H), 1.64-1.71 (m, 2H), 1.62 (d, $J = 8.0$ Hz, 1H), 1.56-1.64 (m, 2H), 1.07-1.16 (m, 21H); ^{13}C NMR (125 MHz, CDCl_3) δ 135.8, 127.4, 67.3, 65.1, 31.5, 26.0, 25.3, 22.6, 22.3, 18.2, 18.2, 13.0; HRMS (EI, M^+) for $\text{C}_{17}\text{H}_{32}\text{OSiCl}_2$ calcd 362.1599, found: m/z 362.1599.

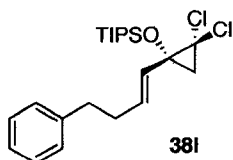


1,1-Dichloro-2-(1-cyclopentenyl)-2-triisopropylsilyloxycyclopropane (38g). The same method was employed in the synthesis of **38g** starting with 1-triisopropylsiloxy-1-(cyclopenten-1-yl)-ethene **37g** (0.15 g, 0.58 mmol). The reaction was quenched after 20 min. and the crude material was purified by flash column chromatography (silica gel, hexanes:EtOAc 50:1) to yield 1,1-dichloro-2-(1-cyclopentenyl)-2-triisopropylsilyloxycyclopropane **38g** (0.20 g, 0.57 mmol, 97 %) as a colorless oil: R_f 0.63 (hexanes/EtOAc 20:1); IR (thin film) 2946, 2868, 1464, 1265, 1243, 1099, 1068, 883, 683 cm^{-1} ; ^1H NMR (500 MHz, CDCl_3) δ 5.68 (app. pent., $J = 2.0$ Hz, 1H), 2.58-2.65 (m, 1H), 2.42-2.48 (m, 1H), 2.34-2.39 (m, 2H), 1.88-2.00 (m, 2H), 1.92 (d, $J = 8.0$ Hz, 1H), 1.70 (d, $J = 8.0$ Hz, 1H), 1.05-1.15 (m, 21H); ^{13}C NMR (125 MHz, CDCl_3) δ 142.6, 131.0, 65.3, 63.0, 33.0, 32.8, 32.4, 23.9, 18.2, 18.2, 13.0; HRMS (EI, $[\text{M}-\text{Cl}]^+$) for $\text{C}_{17}\text{H}_{30}\text{OSiCl}$ calcd 313.1754, found: m/z 313.1755.



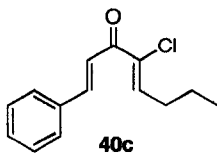
1,1-Dichloro-2-(3-methyl-[E]-buten-1-yl)-2-triisopropylsilyloxycyclopropane (38h). The aforementioned method was also employed in the synthesis of **38h** starting with (3E)-4-isopropyl-2-(triisopropylsiloxy)-1,3-butadiene **37h** (0.23 g, 0.84 mmol). The reaction was quenched after 1 h and the crude material was purified by flash column chromatography (silica gel, hexanes:EtOAc 50:1) to yield 1,1-dichloro-2-(3-methyl-*trans*-buten-1-yl)-2-triisopropylsilyloxycyclopropane **38h** (0.28 g, 0.80 mmol, 95 %) as a colorless oil: R_f 0.78 (hexanes/EtOAc 20:1); IR (thin film) 2961, 2868, 1668, 1464, 1219, 1080, 970, 883, 769, 683 cm^{-1} ; ^1H NMR (500 MHz, CDCl_3) δ 5.72 (d, $J = 15.5$ Hz, 1H),

5.66 (dd, $J = 15.5, 6.0$ Hz, 1H), 2.38 (app. octet, $J = 6.5$ Hz, 1H), 1.84 (d, $J = 8.5$ Hz, 1H), 1.61 (dd, $J = 8.5, 1.0$ Hz, 1H), 1.04-1.14 (m, 21H), 1.02 (d, $J = 7.0$ Hz, 3H), 1.01 (d, $J = 6.5$ Hz, 3H); ^{13}C NMR (125 MHz, CDCl_3) δ 141.9, 124.7, 65.8, 64.3, 32.3, 31.1, 22.2, 22.0, 18.3, 18.2, 13.0; HRMS (EI, $[\text{M}-\text{Cl}]^+$) for $\text{C}_{17}\text{H}_{32}\text{ClOSi}$ calcd 315.1911, found: m/z 315.1895.



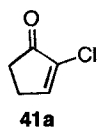
(1E)-1,1-Dichloro-2-(4-phenyl-1-butenyl)-2-triisopropylsilyloxycyclopropane (38i).

The same method was employed in the synthesis of **38i** starting with (*1E*)-2-(triisopropylsiloxy)-6-phenyl-1,3-hexadiene **37i** (0.26 g, 0.80 mmol). The reaction was quenched after 2 h and the crude material was purified by flash column chromatography (silica gel, hexanes:EtOAc 50:1) to yield (*1E*)-1,1-dichloro-2-(4-phenyl-1-butenyl)-2-triisopropylsilyloxycyclopropane **38i** (0.27 g, 0.65 mmol, 72 %) as a colorless oil: R_f 0.70 (hexanes/EtOAc 20:1); IR (thin film) 3027, 2944, 2867, 1463, 1222, 1083, 883, 697, 683 cm^{-1} ; ^1H NMR (500 MHz, CDCl_3) δ 7.27-7.30 (m, 2H), 7.17-7.21 (m, 3H), 5.82 (d, $J = 15.5$ Hz, 1H), 5.75 (dt, $J = 15.0, 6.5$ Hz, 1H), 2.73 (t, $J = 9.0$ Hz, 2H), 1.46 (dt, $J = 7.0, 7.0$ Hz, 2H), 1.81 (d, $J = 8.5$ Hz, 1H), 1.61 (d, $J = 8.5$ Hz, 1H), 1.04-1.10 (m, 21H); ^{13}C NMR (125 MHz, CDCl_3) δ 141.6, 134.3, 128.7, 128.6, 128.3, 126.2, 65.7, 64.2, 35.4, 33.9, 32.5, 18.3, 18.2, 13.0; HRMS (EI, $[\text{M}-\text{Cl}]^+$) for $\text{C}_{22}\text{H}_{34}\text{OSiCl}$ calcd 377.2068, found: m/z 377.2066.



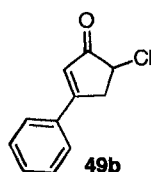
1-Phenyl-4-chloro-octa-1,4-dien-3-one (40c). The 2-siloxy-diene, **37c**, (0.12 g, 0.35 mmol) was dissolved in anhydrous toluene (0.1 M, 3.5 mL). CHCl_3 (0.11 mL, 1.43

mmol) was then added and the temperature was dropped to 0°C. Potassium *tert*-butoxide (0.16 g, 1.4 mmol) was added in portions at 0°C. The reaction was allowed to stir at low temperature for 1 h before CHCl₃ (0.057 mL, 0.71 mmol) and potassium *tert*-butoxide (0.08 g, 0.70 mmol) were added once again. The reaction was quenched by pouring into ice water after 1 h stirring at room temperature. The aqueous layer was extracted with CH₂Cl₂ (2 x 10 mL). The organic layer was washed with H₂O (2 x 10 mL) and dried (MgSO₄). After filtration, the crude material was purified by flash column chromatography (silica gel, hexanes:EtOAc 10:1) to yield 1-phenyl-4-chloro-octa-1,4-dien-3-one **40c** (0.045 g, 0.19 mmol, 55 %) as a white solid: m.p. 69-70°C; R_f 0.40 (hexanes/EtOAc 8:1); IR (thin film) 3028, 2962, 2932, 2873, 1666, 1617, 1576, 1330, 759 cm⁻¹; ¹H NMR (300 MHz, CDCl₃) δ 7.83 (d, *J* = 15.6 Hz, 1H), 7.66-7.69 (m, 2H), 7.44-7.49 (m, 4H), 7.12 (t, *J* = 7.2 Hz, 1H), 2.49 (q, *J* = 7.2 Hz, 2H), 1.65 (sextet, *J* = 7.5 Hz, 2H), 1.07 (t, *J* = 7.5 Hz, 3H); ¹³C NMR (125 MHz, CDCl₃) δ 184.1, 145.3, 141.0, 134.6, 134.0, 130.7, 128.9, 128.5, 120.5, 31.7, 21.2, 13.9; HRMS (EI, M⁺) for C₁₄H₁₅ClO calcd, 234.0811, found: *m/z* 234.0805; Anal. Calcd for C₁₄H₁₅ClO: C, 71.64; H, 6.44. Found: C, 71.31; H, 6.49.

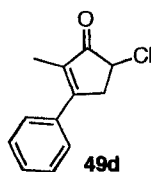


2-Chlorocyclopentenone (41a). 1,1-Dichloro-2-(ethenyl)-2-triisopropylsilyloxycyclopropane, **38a**, (0.10 g, 0.35 mmol) was dissolved in CH₂Cl₂ (0.05 M, 7.0 mL). AgBF₄ (0.10 g, 0.52 mmol) was added in one portion and the reaction mixture stirred at room temperature. The reaction was quenched after 24 h stirring by filtration through a pad of celite/silica gel. This compound was only observed as the major product in a crude reaction mixture. The product was not isolated since it readily decomposed during attempted purification by silica gel or alumina chromatography. Its

presence was implied by partial spectral data: R_f 0.12 (hexanes/EtOAc 8:1); $^1\text{H NMR}$ (500 MHz, CDCl_3) δ 7.60 (t, $J = 3.0$ Hz, 1H), 2.68-2.71 (m, 2H), 2.53-2.58 (m, 2H).



5-Chloro-3-phenyl-cyclopentenone (49b). Dissolve 1,1-dichloro-2-(1-phenyl-*trans*-ethen-2-yl)-2-triisopropylsilyloxycyclopropane **38b** (0.055 g, 0.14 mmol) in dichloromethane (0.05 M, 2.8 mL). AgBF_4 (0.042 g, 0.21 mmol) was added in one portion and the reaction mixture stirred at room temperature. The reaction was quenched after 18 h. stirring by filtration through a pad of Celite/silica gel. The product was not isolated due to the presence of a persistent contaminant (ketone **36b**) that could not be removed during attempted purification with silica gel or alumina chromatography. Its presence was implied by partial spectral data: $^1\text{H NMR}$ (500 MHz, CDCl_3) δ 2.59 (dd, 1H, $J = 2.5, 19.0$ Hz), 3.09 (dd, 1H, $J = 7.0, 18.5$ Hz), 4.17 (dd, 1H, $J = 2.5, 7.0$ Hz), 6.39 (s, 1H), 7.18 (m, 2H), 7.32 (m, 1H), 7.37 (m, 2H).

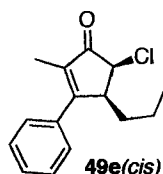


5-Chloro-2-methyl-3-phenyl-cyclopentenone (49d). The above procedure was used in the preparation of **49d** starting with (*1E*)-1,1-dichloro-2-(1-phenylpropen-2-yl)-2-triisopropylsilyloxycyclopropane, **38d**, (0.08 g, 0.20 mmol). The reaction was quenched after 6 days stirring at room temperature. The crude material was purified by gradient column chromatography (silica gel, hexanes:EtOAc 20:1, 15:1, 10:1, 8:1, 5:1) to yield 5-chloro-2-methyl-3-phenyl-cyclopentenone **49d** (0.04 g, 0.17 mmol, 87 %) as an off-white solid: m.p. 99-100 °C; R_f 0.26 (hexanes/EtOAc 8:1); IR (thin film) 3056, 2943, 1702,

1615, 1352, 762, 698 cm^{-1} ; ^1H NMR (400 MHz, CDCl_3) δ 7.47-7.55 (m, 5H), 4.43 (dd, $J = 7.2, 2.8$ Hz, 1H), 3.51 (ddq, $J = 18.0, 6.8, 2.0$ Hz, 1H), 3.14 (ddq, $J = 18.4, 2.0, 2.0$ Hz, 1H), 2.05 (t, $J = 2.0$ Hz, 3H); ^{13}C NMR (125 MHz, CDCl_3) δ 202.5, 163.8, 135.3, 134.7, 130.6, 129.1, 128.0, 53.2, 40.7, 10.6; HRMS (EI, M^+) for $\text{C}_{12}\text{H}_{11}\text{ClO}$ calcd 208.0469, found: m/z 208.0467; Anal. Calcd for $\text{C}_{12}\text{H}_{11}\text{ClO}$: C, 69.74; H, 5.36. Found: C, 69.75; H, 5.50.

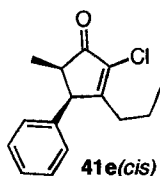
5-Chloro-2-methyl-3-phenyl-4-propyl-cyclopentenone (49e) and 2-Chloro-5-methyl-4-phenyl-3-propyl-cyclopentenone (41e). The above procedure was used in the preparation of **49e** and **41e** starting from (*IE*)-1,1-dichloro-2-(1-phenyl-propen-2-yl)-3-propyl-2-triisopropylsilyloxycyclopropane, **38e**, (0.10 g, 0.23 mmol). The reaction was quenched after 1 h stirring at room temperature. Purification by gradient column chromatography (silica gel, hexanes:EtOAc 20:1, 15:1, 10:1, 8:1, 5:1) yielded **49e(cis)** : **41e(cis)** : **49e(trans)** : **41e(trans)** (7.7 : 4.5 : 3 : 1, 87 %). Products **41e(cis)** and **49e(trans)** were inseparable by standard techniques.

Major product **49e(cis)** could be converted to the more stable **49e(trans)** by stirring in Et_2O in the presence of DBU to give a 12 : 1 mixture in favor of the *trans* diastereomer.

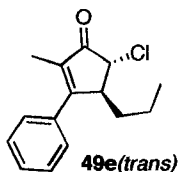


5-Chloro-2-methyl-3-phenyl-4-propyl-cyclopentenone (49e(cis)). This sample was isolated as a colorless oil: R_f 0.29 (hexanes/EtOAc 8:1); IR (thin film) 3059, 2959, 2932, 2872, 1713, 1624, 1346, 699 cm^{-1} ; ^1H NMR (500 MHz, CDCl_3) δ 7.44-7.50 (m, 3H), 7.34-7.40 (m, 2H), 4.64 (d, $J = 6.5$ Hz, 1H), 3.55-3.58 (m, 1H), 1.92 (d, $J = 2.0$ Hz, 3H), 1.56-1.62 (m, 2H), 1.19-1.26 (m, 2H), 0.80 (t, $J = 7.0$ Hz, 3H); ^{13}C NMR (125 MHz,

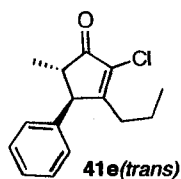
CDCl₃) δ 202.9, 168.5, 134.9, 134.5, 129.5, 128.7, 127.4, 59.9, 45.3, 32.0, 20.1, 13.8, 9.8; HRMS (EI, M⁺) for C₁₅H₁₇ClO calcd 248.0968, found: m/z 248.0968.



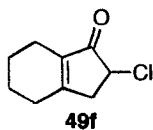
2-Chloro-5-methyl-4-phenyl-3-propyl-cyclopentenone (41e(cis)). The sample was contaminated with (**49e(trans)**), thus complete spectral data could not be reported: R_f 0.35 (hexanes/EtOAc 8:1); Partial ¹H NMR (500 MHz, CDCl₃) δ 4.20 (d, *J* = 7.0 Hz, 1H), 2.86 (pent, *J* = 7.5 Hz, 1H), 2.64 (ddd, *J* = 14.0, 9.5, 7.0 Hz), 2.13 (ddd, *J* = 14.5, 9.5, 5.5 Hz, 1H), 1.39-1.56 (m, 2H), 0.91 (t, *J* = 7.5 Hz, 3H), 0.75 (d, *J* = 7.5 Hz, 3H); ¹³C NMR (125 MHz, CDCl₃) δ 203.1, 172.4, 137.2, 132.6, 128.7, 127.8, 127.6, 51.5, 44.3, 31.6, 19.9, 14.1, 12.2.



5-Chloro-2-methyl-3-phenyl-4-propyl-cyclopentenone (49e(trans)). The sample was contaminated with (**41e(cis)**), thus complete spectral data could not be reported: R_f 0.35 (hexanes/EtOAc 8:1); ¹H NMR (500 MHz, CDCl₃) δ 7.43-7.51 (m, 3H), 7.35-7.37 (m, 2H), 4.05 (d, *J* = 2.5 Hz, 1H), 3.41 (app. d, *J* = 10.0 Hz, 1H), 1.91 (d, *J* = 2.0 Hz, 3H), 1.66 (dddd, *J* = 14.0, 10.5, 6.5, 3.0 Hz, 1H), 1.35-1.50 (m, 2H), 1.20-1.30 (m, 1H), 0.88 (t, *J* = 7.0 Hz, 3H); ¹³C NMR (125 MHz, CDCl₃) δ 201.7, 169.3, 134.8, 134.4, 129.7, 128.7, 127.8, 58.6, 51.9, 34.6, 20.0, 13.9, 9.8.

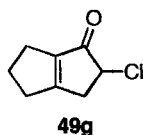


2-Chloro-5-methyl-4-phenyl-3-propyl-cyclopentenone (41e(trans)). This sample was isolated as a colorless oil: R_f 0.41 (hexanes/EtOAc 8:1); IR (thin film) 3027, 2962, 2931, 2873, 1723, 1618, 1455, 703 cm^{-1} ; ^1H NMR (500 MHz, CDCl_3) δ 7.34-7.37 (m, 2H), 7.28-7.32 (m, 1H), 7.11-7.13 (m, 2H), 3.49 (d, $J = 3.0$ Hz, 3H), 2.58 (ddd, $J = 13.5, 9.5, 7.5$ Hz, 1H), 2.44 (qd, $J = 7.5, 2.5$ Hz, 1H), 2.07 (ddd, $J = 14.5, 9.0, 5.5$ Hz, 1H), 1.49-1.56 (m, 1H), 1.38-1.44 (m, 1H), 1.29 (d, $J = 7.5$ Hz, 3H), 0.89 (t, $J = 7.0$ Hz, 3H); ^{13}C NMR (125 MHz, CDCl_3) δ 203.1, 173.0, 140.3, 131.8, 129.4, 127.9, 127.8, 56.0, 50.1, 31.3, 20.3, 15.5, 14.2; HRMS (EI, M^+) for $\text{C}_{15}\text{H}_{17}\text{ClO}$ calcd 248.0968, found: m/z 248.0973.



$\Delta^{1,6}$ -8-Chloro-bicyclo[4.3.0]nonen-7-one (49f). The above procedure was used in the preparation of **49f** starting from 1,1-dichloro-2-(1-cyclohexenyl)-2-triisopropylsilyloxycyclopropane, **38f**, (0.11 g, 0.29 mmol). The reaction was quenched after 30 h stirring at room temperature. The crude material was purified by gradient column chromatography (silica gel, hexanes:EtOAc 50:1, 30:1, 25:1, 20:1, 10:1) to yield $\Delta^{1,6}$ -8-chloro-bicyclo[4.3.0]nonen-7-one **38f** (0.022 g, 0.13 mmol, 45 %) as a colorless oil: R_f 0.13 (hexanes/EtOAc 8:1); IR (thin film) 2933, 2863, 1713, 1643, 1399, 1279, 731 cm^{-1} ; ^1H NMR (500 MHz, CDCl_3) δ 4.26 (dd, $J = 7.0, 2.5$ Hz, 1H), 3.12 (app. dd, $J = 18.5, 7.0$ Hz, 1H), 2.68 (app. d, $J = 19.0$ Hz 1H), 2.26-2.41 (m, 2H), 2.14-2.24 (m, 2H), 1.74-1.79 (m, 2H), 1.66-1.72 (m, 2H); ^{13}C NMR (125 MHz, CDCl_3) δ 203.1, 171.3,

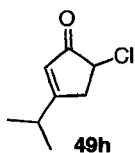
137.2, 53.6, 41.6, 28.6, 22.1, 21.7, 20.4; HRMS (EI, M⁺) for C₉H₁₁OCl calcd 172.0469, found: m/z 172.0466.



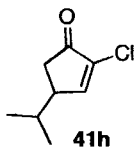
Δ^{1,5}-3-Chloro-bicyclo[3.3.0]octen-2-one (49g). The above procedure was used in the preparation of **49g** starting from 1,1-dichloro-2-(1-cyclopentenyl)-2-triisopropylsilyloxycyclopropane, **38g**, (0.12 g, 0.33 mmol). The reaction was quenched after 48 h stirring at room temperature. The crude material was purified by gradient column chromatography (silica gel, hexanes:EtOAc 50:1, 30:1, 25:1, 20:1, 10:1) to yield Δ^{1,5}-3-chloro-bicyclo[3.3.0]octen-2-one **38g** (0.038 g, 0.24 mmol, 73 %) as a colorless oil: R_f 0.11 (hexanes/EtOAc 8:1); IR (thin film) 2925, 2855, 1709, 1631, 1387, 732 cm⁻¹; ¹H NMR (400 MHz, CDCl₃) δ 5.54 (dd, *J* = 6.5, 2.5 Hz, 1H), 3.20 (app. dd, *J* = 18.5, 6.4 Hz, 1H), 2.71 (app. d, *J* = 19.0 Hz, 1H), 2.56-2.61 (m, 2H), 2.43-2.48 (m, 2H), 2.38 (app. pent, *J* = 6.4 Hz, 2H); ¹³C NMR (125 MHz, CDCl₃) δ 195.9, 184.1, 146.7, 59.3, 37.8, 32.5, 27.3, 25.2; HRMS (EI, M⁺) for C₈H₉OCl calcd 156.0342, found: m/z 156.0341.

5-Chloro-3-isopropyl-cyclopentenone (49h) and 2-Chloro-4-isopropyl-cyclopentenone (41h). 1,1-Dichloro-2-(3-methyl-*trans*-buten-1-yl)-2-triisopropylsilyloxycyclopropane, **38h**, (0.12 g, 0.33 mmol) was dissolved in CH₂Cl₂ (0.05 M, 6.6 mL). AgBF₄ (0.096 g, 0.50 mmol) was added in one portion and the reaction mixture stirred at room temperature. The reaction was quenched after 4 h stirring at room temperature, by filtration through a pad of celite/silica gel. The crude material was purified by gradient column chromatography (silica gel, hexanes:EtOAc 50:1, 30:1, 25:1, 15:1, 10:1) to yield 5-chloro-3-isopropyl-cyclopentenone, **49h**, (0.017 g,

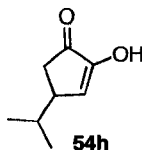
0.11 mmol, 33 %) and 2-chloro-4-isopropyl-cyclopentenone, **41h**, (0.010 g, 0.06 mmol, 19 %).



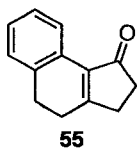
5-Chloro-3-isopropyl-cyclopentenone (49h). This compound was isolated as a pale yellow oil: R_f 0.28 (hexanes/EtOAc 8:1); IR (thin film) 2968, 2933, 2875, 1719, 1610, 1174, 878, 859, 757 cm^{-1} ; ^1H NMR (500 MHz, CDCl_3) δ 6.01 (dd, $J = 3.0, 2.0$ Hz, 1H), 4.28 (dd, $J = 7.0, 3.0$ Hz, 1H), 3.22 (dddd, $J = 19.0, 7.0, 2.0, 1.0$ Hz, 1H), 2.78 (dddd, $J = 19.0, 2.5, 2.0, 1.0$ Hz, 1H), 2.65 (sept., $J = 7.0$ Hz, 1H), 1.20 (d, $J = 7.0$ Hz, 6H); ^{13}C NMR (125 MHz, CDCl_3) δ 202.3, 185.6, 125.5, 54.2, 40.7, 32.4, 20.7; HRMS (EI, M^+) for $\text{C}_8\text{H}_{11}\text{ClO}$ calcd 158.0498, found: m/z 158.0500.



2-Chloro-4-isopropyl-cyclopentenone (41h). This compound was isolated as a colorless oil: R_f 0.39 (hexanes/EtOAc 8:1); IR (thin film) 2962, 2930, 2873, 1725, 1625, 1597, 1466, 1296, 1273, 959, 884 cm^{-1} ; ^1H NMR (500 MHz, CDCl_3) δ 7.55 (d, $J = 2.5$ Hz, 1H), 2.76 (dddd, $J = 6.5, 6.0, 2.0, 2.0$ Hz, 1H), 2.60 (dd, $J = 19.0, 6.5$ Hz, 1H), 2.24 (dd, $J = 19.0, 2.0$ Hz, 1H), 1.79 (app. octet, $J = 7.0$ Hz, 1H), 0.98 (d, $J = 7.0$ Hz, 3H), 0.96 (d, $J = 6.5$ Hz, 3H); ^{13}C NMR (125 MHz, CDCl_3) δ 200.7, 159.9, 135.8, 44.9, 37.5, 31.8, 19.8, 19.7; HRMS (EI, M^+) for $\text{C}_8\text{H}_{11}\text{ClO}$ calcd 158.0498, found: m/z 158.0494.

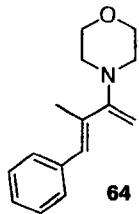


2-Hydroxy-4-isopropyl-2-cyclopentenone (54h). This compound was isolated in variable low yields under the previously mentioned reaction conditions: R_f 0.14 (hexanes/EtOAc 8:1); IR (thin film) 3351, 2960, 2931, 2873, 1699, 1652, 1396, 1240, 1199, 1105 cm^{-1} ; ^1H NMR (500 MHz, CDCl_3) δ 6.53 (d, $J = 3.5$ Hz, 1H), 5.49 (br. s, 1H), 2.63 (dddd, $J = 6.0, 6.0, 3.0, 1.5$ Hz, 1H), 2.51 (dd, $J = 19.5, 6.0$ Hz, 1H), 2.14 (dd, $J = 19.5, 1.5$ Hz, 1H), 1.70 (app. octet, $J = 6.5$ Hz, 1H), 0.95 (d, $J = 6.5$ Hz, 3H), 0.93 (d, $J = 7.0$ Hz, 3H); ^{13}C NMR (125 MHz, CDCl_3) δ 203.4, 152.6, 132.0, 41.3, 36.7, 32.2, 19.8, 19.7; HRMS (EI, M^+) for $\text{C}_8\text{H}_{12}\text{O}_2$ calcd 140.0837, found: m/z 140.0838.

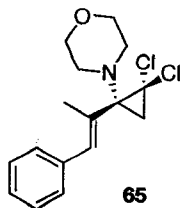


2,3,4,5-Tetrahydrocyclopenta[*a*]naphthalen-1-one (55). The above procedure was used in the preparation of **55** from (*IE*)-1,1-dichloro-2-(4-phenyl-1-buten-1-yl)-2-triisopropylsilyloxycyclopropane, **38i**, (0.09 g, 0.22 mmol). The reaction was quenched after 18 h stirring at room temperature. The crude material was purified by gradient column chromatography (silica gel, hexanes:EtOAc 20:1, 15:1, 10:1, 8:1, 5:1) to yield 2,3,4,5-tetrahydrocyclopenta[*a*]naphthalen-1-one **55** (0.028 g, 0.15 mmol, 63 %) as an off-white solid: m.p. 102-104°C; R_f 0.07 (hexanes/EtOAc 8:1); IR (thin film) 3067, 2947, 2933, 2906, 2841, 1683, 1629, 1435, 765 cm^{-1} ; ^1H NMR (500 MHz, CDCl_3) δ 8.24 (d, $J = 7.5$ Hz, 1H), 7.17-7.25 (m, 3H), 2.96 (t, $J = 8.0$ Hz, 2H), 2.68-2.70 (m, 2H), 2.66 (t, $J = 8.0$ Hz, 2H), 2.57-2.59 (m, 2H); ^{13}C NMR (125 MHz, CDCl_3) δ 206.1, 174.8, 134.9, 134.4, 129.1, 127.8, 127.5, 126.7, 123.9, 35.9, 29.2, 27.6, 27.1; HRMS (EI, M^+) for

C₁₃H₁₂O calcd 184.0888, found: m/z 184.0886. The spectral properties match those previously reported in the literature.²⁹

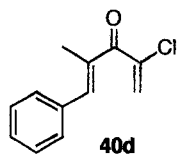


2-(N-Morpholino)-3-methyl-4-phenyl-1,3-butadiene (64). Enyne **63** (0.28 g, 2.0 mmol) and Hg(OAc)₂ (0.48 g, 1.5 mmol) were dissolved in THF (5 mL) at room temperature. To this slurry was added a solution of morpholine (0.52 mL, 6.0 mmol) in THF *via* canula. The reaction mixture was stirred vigorously for 18 h at room temperature before filtration under an argon atmosphere to remove the grey mercury(II) salts. After filtration, the solvent was removed *in vacuo* and the resultant sticky residue was washed with freshly distilled pentanes (5 x 10 mL). Once again, the solvent was removed and the crude oil subjected to Kugelrohr distillation to provide 2-morpholino-3-methyl-4-phenyl-1,3-butadiene **64** (0.15 g, 0.65 mmol, 33 %) as a pale yellow oil: IR (thin film) 2960, 2917, 2853, 1667, 1626, 1597, 1446, 1366, 1245, 1120, 987, 697 cm⁻¹; ¹H NMR (500 MHz, C₆D₆) δ 7.25 (app d, *J* = 8.0 Hz, 2H), 7.18 (app t, *J* = 7.5 Hz, 2H), 7.06 (app t, *J* = 7.5 Hz, 1H), 6.90 (br s, 1H), 4.42 (s, 1H), 4.02 (s, 1H), 3.51 (t, *J* = 5.0 Hz, 4H), 2.59 (t, *J* = 5.0 Hz, 4H), 1.96 (d, *J* = 1.2 Hz, 3H); ¹³C NMR (125 MHz, C₆D₆) δ 161.0, 138.2, 137.0, 129.5, 129.4, 128.4, 126.9, 89.6, 66.9, 50.1, 17.4; HRMS (ESI, [M+H]⁺) for C₁₅H₂₀NO calcd 230.1539, found: m/z 230.1539.

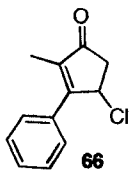


(1E)-1,1-Dichloro-2-(1-phenylpropen-2-yl)-2-(N-morpholino)cyclopropane (65). 2-Amino-1,3-butadiene **64** (0.05 g, 0.22 mmol) and CHCl_3 (0.072 mL, 0.89 mmol) were dissolved in toluene (2.5 mL). The reaction mixture was then cooled to 0°C before the addition of $^t\text{BuOK}$ (0.098 g, 0.87 mmol). The reaction was allowed to stir at low temperature with gradual warming to room temperature overnight. The reaction mixture was then transferred to a cold NaHCO_3 solution (saturated) (3 mL) and stirred for 5 min. The aqueous and organic layers were separated and the aqueous layer extracted with CH_2Cl_2 (2 x 5 mL). The combined organic layers were washed with brine solution and dried (MgSO_4). Filtration and removal of the solvent provided a brown oil that was purified by gradient column chromatography (silica gel, hexanes:EtOAc 50:1, 30:1, 20:1, 10:1, 5:1) to yield (1E)-1,1-dichloro-2-(1-phenylpropen-2-yl)-2-(N-morpholino)cyclopropane **65** (0.061 g, 0.20 mmol, 90 %) as clear, colorless oil: R_f 0.34 (hexanes/EtOAc 8:1); IR (thin film) 3024, 2957, 2854, 2828, 1666, 1448, 1266, 1116, 1073, 1026 cm^{-1} ; ^1H NMR (400 MHz, CDCl_3) δ 7.32-7.39 (m, 3H), 7.24-7.28 (m, 2H), 6.39 (br s, 1H), 3.70 (app t, $J = 4.8$ Hz, 4H), 2.86 (dt, $J = 10.8, 4.8$ Hz, 2H), 2.70 (dt, $J = 10.8, 4.8$ Hz, 2H), 2.12 (d, $J = 1.6$ Hz, 3H), 1.74 (d, $J = 6.8$ Hz, 1H), 1.64 (d, $J = 6.8$ Hz, 1H); ^{13}C NMR (100 MHz, CDCl_3) δ 136.7, 133.4, 129.7, 129.0, 128.2, 127.2, 67.4, 66.8, 61.3, 50.2, 34.8, 20.2; HRMS (EI, M^+) for $\text{C}_{16}\text{H}_{19}\text{ONCl}_2$ calcd 311.0844, found: m/z 311.0847.

(E)-4-Chloro-2-methyl-1-phenylpenta-1,4-dien-3-one (40d) and 4-chloro-2-methyl-3-phenylcyclopent-2-enone (66). *gem*-Dichlorocyclopropane **65** (0.05 g, 0.16 mmol) was dissolved in freshly distilled MeCN (3.5 mL) and the reaction mixture was brought to reflux (~ 81°C). The reaction was allowed to stir for 18 h before being cooled to room temperature. The solvent was removed *in vacuo* to provide a dark brown oil. The crude material was purified by gradient column chromatography (silica gel, hexanes:EtOAc 15:1, 10:1, 5:1, 2:1) to yield (*E*)-4-chloro-2-methyl-1-phenylpenta-1,4-dien-3-one **40d** (0.016 g, 0.077 mmol, 48 %) and an inseparable mixture of 4-chloro-2-methyl-3-phenylcyclopent-2-enone **66** and 5-chloro-2-methyl-3-phenyl-cyclopentenone **49d** (**66**:**49d**, 5:1; 0.015 g, 0.073 mmol, 46 %).



(E)-4-Chloro-2-methyl-1-phenylpenta-1,4-dien-3-one (40d). R_f 0.47 (hexanes/EtOAc 8:1); ^1H NMR (400 MHz, CDCl_3) δ 7.35-7.46 (m, 6H), 6.08 (d, $J = 2.0$ Hz, 1H), 6.02 (d, $J = 2.0$ Hz, 1H), 2.18 (d, $J = 1.2$ Hz, 3H); ^{13}C NMR (100 MHz, CDCl_3) δ 192.3, 142.3, 137.7, 135.2, 134.9, 129.8, 129.0, 128.6, 123.1, 14.1.



4-Chloro-2-methyl-3-phenylcyclopent-2-enone (66). The sample was contaminated with **49d**, thus complete spectral data could not be reported: R_f 0.26 (hexanes/EtOAc

8:1); ^1H NMR (400 MHz, CDCl_3) δ 7.45-7.55 (m, 5H), 5.43 (ddq, $J = 6.8, 1.6, 1.6$ Hz, 1H), 3.19 (dd, $J = 19.2, 6.4$ Hz, 1H), 2.85 (dd, $J = 19.2, 2.0$ Hz, 1H), 1.98 (d, $J = 1.6$ Hz, 3H); ^{13}C NMR (125 MHz, CDCl_3) δ 203.9, 164.4, 139.6, 133.3, 129.9, 128.7, 128.2, 55.2, 45.1, 10.0.

2.5 References

1. For recent reviews on this topic see: a) Kostikov, R. R.; Molchanov, A. P.; Hopf, H. *Top. Curr. Chem.* **1990**, *155* (Small Ring Compounds in Organic Synthesis), 41-80; b) Banwell, M. G.; Reum, M. E. In *Advances in Strain in Organic Chemistry*; Halton, B., Ed.; JAI Press: Greenwich, CT, 1991; Vol. 1, pp 19-64; c) Fedorynski, M. *Chem. Rev.* **2003**, *103*, 1099-1132.
2. Ogasawara, M.; Ge, Y.; Uetake, K.; Fan, L.; Takahashi, T. *J. Org. Chem.* **2005**, *70*, 3871-3876.
3. Doering, W. von E.; Hoffman, A. K. *J. Am. Chem. Soc.* **1954**, *76*, 6162-6165.
4. Seyferth, D. *Acc. Chem. Res.* **1972**, *5*, 65-74.
5. a) Léonel, E.; Lejaye, M.; Oudeyer, S.; Paugam, J. P.; Nédélec, J. -Y. *Tetrahedron Lett.* **2004**, *45*, 2635-2638; b) Chien, C.-T.; Tsai, C.-C.; Tsai, C.-H.; Chang, T.-Y.; Tsai, P.-K.; Wang, Y.-C.; Yan, T.-H. *J. Org. Chem.* **2006**, *71*, 4324-4327; c) Moss, R. A.; Tian, J.; Sauers, R. R.; Ess, D. H.; Houk, K. N.; Krogh-Jespersen, K. *J. Am. Chem. Soc.* **2007**, *129*, 5167-5174.
6. a) Makosza, M.; Wawryniewicz, M. *Tetrahedron Lett.* **1969**, *10*, 4659-4662; b) Fedorynski, M.; Makosza, M. *J. Organomet. Chem.* **1973**, *51*, 89-91.

7. For examples of intermolecular trapping see: a) Skattebøl, L.; Boulette, B. *J. Org. Chem.* **1966**, *31*, 81-85; b) Shimizu, N.; Watanabe, K.; Tsuno, Y. *Bull. Chem. Soc. Jpn.* **1984**, *57*, 1165-1166.
8. For examples of intramolecular trapping see: a) Danheiser, R. L.; Morin, J. M., Jr.; Yu, M.; Basak, A. *Tetrahedron Lett.* **1981**, *22*, 4105-4208; b) Gassman, P. G.; Tan, L.; Hoye, T. R. *Tetrahedron Lett.* **1996**, *37*, 439-442; c) Taylor, R. M. *Aust. J. Chem.* **2003**, *56*, 631; d) Banwell, M. G.; Beck, D. A. S.; Stanislawski, P. C.; Sydnes, M. O.; Taylor, R. M. *Curr. Org. Chem.* **2005**, *9*, 1589-1600; e) Stanislawski, P. C.; Willis, A. C.; Banwell, M. G. *Org. Lett.* **2006**, *8*, 2143-2146.
9. a) de Puy, C. H.; Schnack, L. G.; Hausser, J. W.; Wiedemann, W. *J. Am. Chem. Soc.* **1965**, *87*, 4006-4006; b) Woodward, R. B.; Hoffmann, R. *Conservation of Orbital Symmetry*; Academic Press: New York; 1970; c) Ito, S.; Ziffer, H.; Bax, A. *J. Org. Chem.* **1986**, *51*, 1130-1133; d) Loozen, H. J. J.; Robben, W. M. M.; Richter, T. L.; Buck, H. M. *J. Org. Chem.* **1976**, *41*, 384-385; e) Loozen, H. J. J.; de Haan, J. W.; Buck, H. M. *J. Org. Chem.* **1977**, *42*, 418-422.
10. Marvell, E. N. *Thermal Electrocyclic Reactions*; Academic Press: New York, 1980.
11. Banwell, M. G.; Sydnes, M. O. *Aust. J. Chem.* **2004**, *57*, 537-548.
12. Hart, N. K.; Johns, S. R.; Lamberton, J. A. *Aust. J. Chem.* **1968**, *21*, 2579-2581.

13. Banwell, M. G.; Ma, X.; Taylor, R. M.; Willis, A. C. *Org. Lett.* **2006**, *8*, 4959-4961.
14. Banwell, M. G.; Phillis, A. T.; Willis, A. C. *Org. Lett.* **2006**, *8*, 5341-5344.
15. a) Ketley, A. D.; Berlin, A. J.; Gorman, E.; Fisher, J. P. *J. Org. Chem.* **1966**, *31*, 305-308; b) Dolbier, W. R.; Sellers, S. F. *J. Am. Chem. Soc.* **1982**, *104*, 2494-2497; c) van Es, D. S.; Egberts, A.; Nkrumah, S.; de Nijs, H.; de Wolf, W. H.; Bickelhaupt, F. *J. Am. Chem. Soc.* **1997**, *119*, 615-616.
16. Grant, T. N.; West, F. G. *J. Am. Chem. Soc.* **2006**, *128*, 9348-9349.
17. Faza, O. N.; López, C. S.; Álvarez, R.; de Lera, Á. R. *J. Org. Chem.* **2004**, *69*, 9002-9010.
18. a) Paquette, L. A.; Hamme, A. T.; Ku, L. H.; Doyon, J.; Kreuzholz, R. *J. Am. Chem. Soc.* **1997**, *119*, 1242-1253; b) Paquette, L. A.; Liu, Z.; Ramsey, C.; Gallucci, J. C. *J. Org. Chem.* **2005**, *70*, 8154-8161.
19. a) Gee, S. K.; Danheiser, R. L. *J. Org. Chem.* **1984**, *49*, 1674-1678; b) Danheiser, R. L.; Brisbois, R. G.; Kowalczyk, J. J.; Miller, R. F. *J. Am. Chem. Soc.* **1990**, *112*, 3093-3100.
20. Badioli, M.; Ballini, R.; Bartolacci, M.; Bosica, G.; Torregiani, E.; Marcantoni, E. *J. Org. Chem.* **2002**, *67*, 8938-8942.
21. a) Sengupta, S.; Mondal, S.; Das, D. *Tetrahedron Lett.* **1999**, *40*, 4107-4110; b)

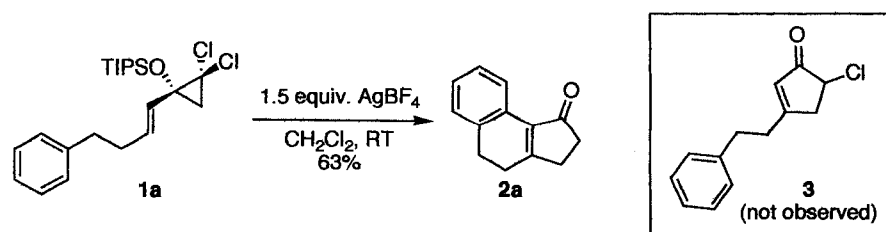
- Brown, J. D. *Tetrahedron: Asymmetry* **1992**, *3*, 1551-1552.
22. Hayakawa, Y.; Yokoyama, K.; Noyori, R. *J. Am. Chem. Soc.* **1978**, *100*, 1799–1806.
23. Browder, C. C.; Marmsäter, F. P.; West, F. G. *Org. Lett.* **2001**, *3*, 3033-3035.
24. Tius, M. A.; Chu, C. C.; Nieves-Colberg, R. *Tetrahedron Lett.* **2001**, *42*, 2419-2422.
25. Smith, D. A.; Ulmer, II, C. W. *J. Org. Chem.* **1997**, *62*, 5110-5115.
26. Ohno, M. *Tetrahedron Lett.* **1963**, *25*, 1753-1755.
27. a) Barluenga, J.; Aznar, F.; Liz, R.; Rodes, R. *J. Chem. Soc., Perkin Trans. I* **1980**, 2732-2737; b) Barluenga, J.; Aznar, F.; Liz, R.; Rodes, R. *J. Chem. Soc., Chem. Commun.* **1983**, 1087-1091; c) Barluenga, J.; Aznar, F.; Liz, R.; Cabal, M. *J. Chem. Soc., Chem. Commun.* **1985**, 1375-1376; d) Barluenga, J.; Aznar, F.; Valdes, C.; Cabal, M. *J. Org. Chem.* **1991**, *56*, 6166-6171.
28. Corey, E. J.; Fuchs, P. L. *Tetrahedron Lett.* **1972**, *36*, 3769-3772.
29. Gagnier, S.V.; Larock, R.C. *J. Am. Chem. Soc.* **2003**, *125*, 4804-4807.

Chapter 3

Interrupted Nazarov Reactions Using *gem*-Dichlorocyclopropanes

3.1 Introduction

Our investigation into the use of *gem*-dichlorocyclopropane substrates in a sequential ring opening and Nazarov cyclization led to the discovery of an intriguing “interrupted” Nazarov reaction (see Chapter 2). It was found that treatment of the phenethyl-substituted compound **1a** with 1.5 equivalents of AgBF_4 in CH_2Cl_2 provided benzohydrindenone **2a** as the sole product, with no apparent formation of the simple α -chlorocyclopentenone **3** (Scheme 3.1).¹ This result prompted our examination of



Scheme 3.1. An “interrupted” Nazarov reaction using *gem*-dichlorocyclopropanes.

appropriately substituted *gem*-dichlorocyclopropane substrates in analogous interrupted Nazarov processes to ascertain the scope of this new cascade process. The synthesis of desired *gem*-dichlorocyclopropane substrates and results from this investigation will be discussed in this chapter, along with a mechanistic rationale for the final dehydrohalogenation step.

3.2 *gem*-Dichlorocyclopropanes as Substrates for Interrupted Nazarov Reactions

Although arene-trapping has previously been demonstrated in traditional Nazarov reactions (see Chapter 1), the participation of an unactivated aromatic ring was unprecedented. This result implied that *gem*-dichlorocyclopropane substrates might proceed through highly reactive 2-silyloxycyclopentenyl cations (**I**) resulting from electrocyclization (*Figure 3.1*). Relative to traditional Nazarov intermediates, these cationic species show evidence of increased electrophilicity, which may be attributed to the presence of an electron-withdrawing chloro-substituent as well as the absence of stabilizing alkyl substitution on the cyclopentenyl cation **I**. These cationic intermediates appear to be capable of reacting with even electron-deficient nucleophiles, which presents the possibility for new modes of trapping in the interrupted Nazarov reaction. To assess

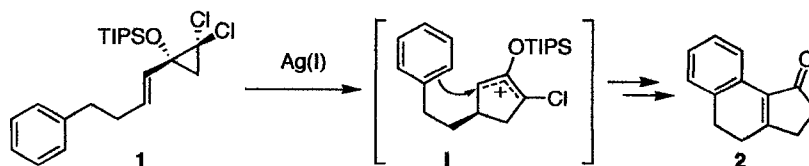


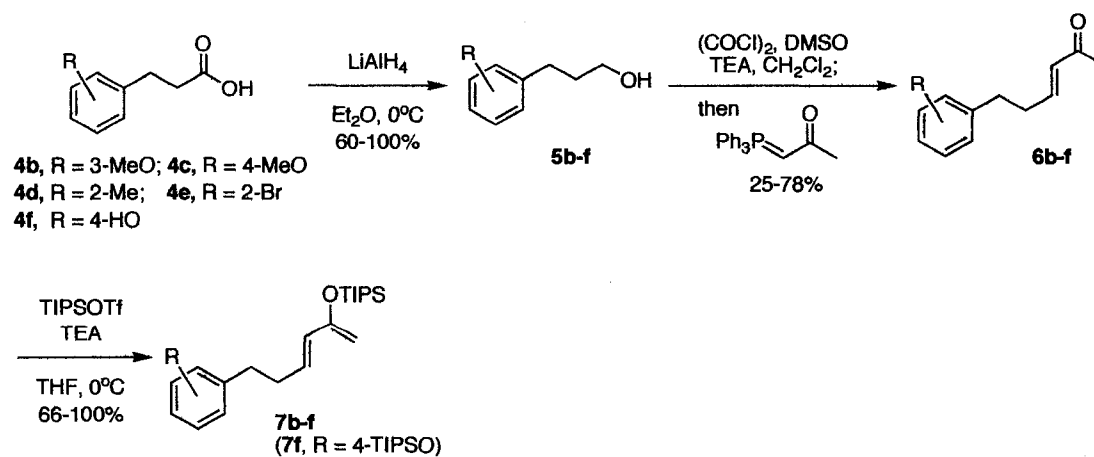
Figure 3.1. The proposed reactive oxyallyl cationic intermediate.

the generality of this reaction sequence, a number of substrates with one or more pendent arene moieties were synthesized and subjected to the standard Ag(I) reaction conditions.²

3.2.1 Traditional Arene Trapping

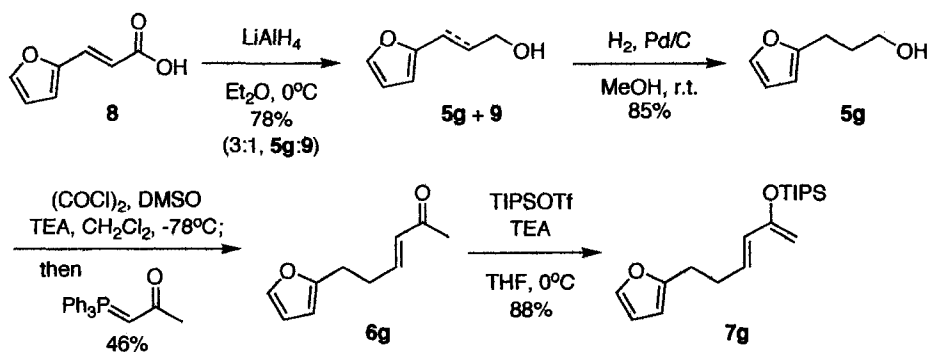
Preparation of 2-Silyloxydienes

Many of the *gem*-dichlorocyclopropane substrates prepared for this investigation were designed to examine the effects of aromatic substitution on the pendent arene nucleophile. The required 2-silyloxydiene substrates **7** were readily prepared by exhaustive reduction of the corresponding hydrocinnamic acids **4**, followed by a one-pot Swern oxidation/Wittig olefination reaction³ to provide desired α,β -unsaturated ketones **6** in moderate yields (*Scheme 3.2*). The *trans* geometry of the olefin was confirmed due to observation of a large ($^3J \sim 16$ Hz) coupling constant shared between the two vinyl protons in the corresponding ^1H NMR spectra. The ketones were cleanly converted to the 2-triisopropylsilyloxydienes **7** under standard reaction conditions using triisopropylsilyl trifluoromethanesulfonate in the presence of triethylamine, and were



Scheme 3.2. Synthesis of 2-silyloxydienes **7b-f**.

readily purified by alumina column chromatography. An analogous strategy was used to synthesize the 2-furyl-substituted compound **7g** from 3-(2-furyl)-acrylic acid **8** (Scheme 3.3). The acid was subjected to LiAlH₄ in diethyl ether to provide a mixture of two compounds, 3-(2-furyl)-propanol **5g** and 3-(2-furyl)-2-propen-1-ol **9**, in a 3:1 ratio. Prolonged reaction times did not provide complete conversion to the desired alcohol **5g**,

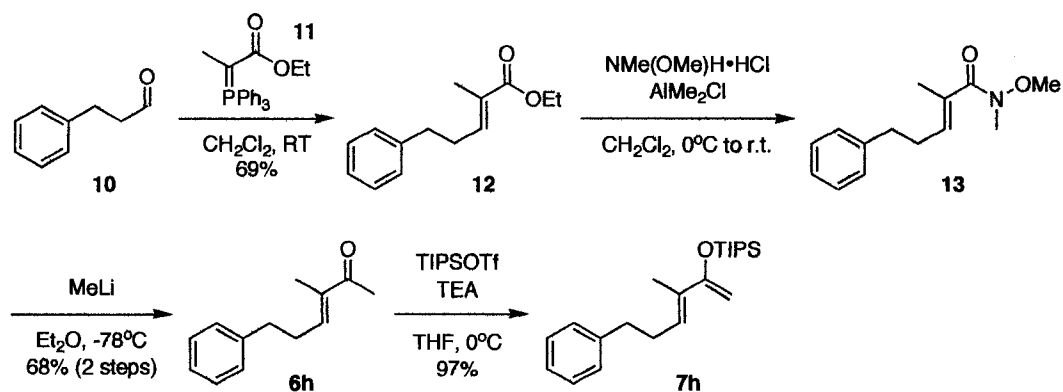


Scheme 3.3. The preparation of 2-silyloxydiene **7g**.

but resulted in generation of the same mixture of compounds in reduced yields. In order to obtain pure 3-(2-furyl)-propanol **5g**, the mixture of products **5g** and **9** was subjected to hydrogenation conditions, which furnished the desired compound in 85% yield. The alcohol was then used in a one-pot Swern oxidation/Wittig olefination reaction to provide the α,β -unsaturated ketone **6g**, followed by smooth conversion to the corresponding 2-silyloxydiene in 88% yield after purification.

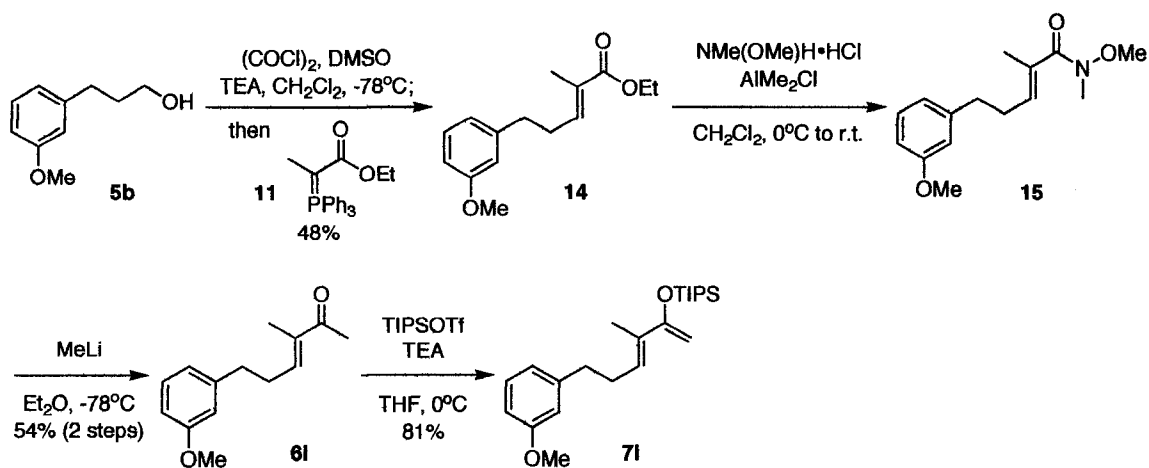
In an effort to investigate the effect of α -substitution on the vinyl moiety, ketones **6h** and **6i** were prepared and converted to the corresponding 2-silyloxydiene compounds. In the case of **6h**, the desired ketone was obtained from an initial Wittig olefination reaction between hydrocinnamaldehyde **10** and (carbethoxyethylidene)-

triphenylphosphorane **11** (*Scheme 3.4*). The resultant α,β -unsaturated ester **12** was then treated with *N,O*-dimethylhydroxylamine hydrochloride and dimethylaluminum chloride to form Weinreb amide **13**. The amide was not isolated, but used directly in the addition



Scheme 3.4. The preparation of 2-silyloxydiene **7h**.

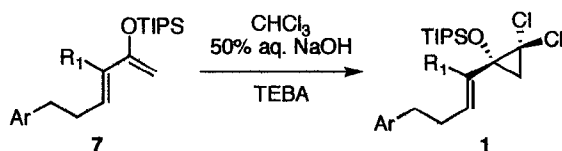
of methyllithium to provide ketone **6i** in 68% yield over two steps. Ketone **6i** was prepared in a similar fashion from 3-(3-methoxyphenyl)-propanol (**5b**) using the previously outlined one-pot procedure to furnish ester **14** (*Scheme 3.5*). This ester was also converted to the desired methyl ketone **6i** in 54% yield (two steps) through formation of a Weinreb amide and subsequent treatment with methyllithium.



Scheme 3.5. The preparation of 2-silyloxydiene **7i**.

Dichlorocyclopropanation

With the 2-triisopropylsilyloxydiene substrates **7** in hand, the dichlorocyclopropanation reaction was examined. Earlier studies had demonstrated the effectiveness of phase transfer catalysis to perform regioselective monocyclopropanation on 2-silyloxy-1,3-butadienes, hence the same reaction conditions were employed to effect cyclopropanation of substrates **7b-i** (Table 3.1). In all cases, the *gem*-dichlorocyclopropane compounds **1b-i** were isolated in good to excellent yields after treatment of the silyloxydienes with CHCl_3 and 50% NaOH solution in the presence of a phase transfer catalyst (triethylbenzylammonium chloride, TEBA). The reactions were monitored closely by TLC analysis for the consumption of starting material, which generally occurred in 20 minutes to 1 hour. Remarkably, in the case of the furyl-



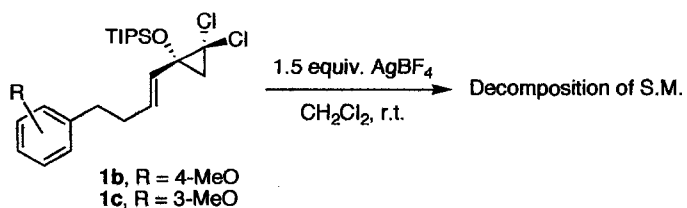
entry	substrate	Ar	R ₁	time (min)	product	yield (%)
1	7a	Ph	H	30	1a	87
2	7b	3-MeO-Ph	H	30	1b	75
3	7c	4-MeO-Ph	H	20	1c	79
4	7d	2-Me-Ph	H	30	1d	71
5	7e	2-Br-Ph	H	40	1e	85
6	7f	4-TIPSO-Ph	H	45	1f	70
7	7g	2-furyl	H	7	1g	86
8	7h	Ph	Me	45	1h	91
9	7i	3-MeO-Ph	Me	75	1i	88

Table 3.1. *gem*-Dichlorocyclopropanation of 2-silyloxydienes **7**.

substituted compound (**7g**), complete conversion to the corresponding *gem*-dichlorocyclopropane **1g** could be effected in a very short reaction time (7 minutes) and without any evidence of over-cyclopropanation of the electron-rich furyl substituent (entry 7). Although the synthesis of substrate **1a** was not presented here, the preparation of this compound was discussed in the previous chapter (see Chapter 2).

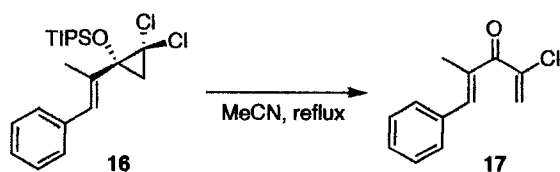
Ag(I)-Mediated Interrupted Nazarov Reactions

Once the readily available *gem*-dichlorocyclopropane substrates **1** were prepared, the ring opening/ 4π electrocyclization/electrophilic aromatic substitution (or “interrupted” Nazarov) sequence could be investigated. Preliminary investigations were carried out with substrates **1b** and **1c**. It was originally believed that these substrates would provide the intended tricyclic products more efficiently than was observed for **1a** due to the electron-rich and inherent nucleophilic character of the pendent arene functionality; however, when **1b** and **1c** were subjected to the standard reaction conditions (1.5 equiv. $\text{AgBF}_4/\text{CH}_2\text{Cl}_2/\text{r.t.}$), both substrates decomposed to form complex mixtures of inseparable and indeterminable products (*Scheme 3.6*). Since the polar solvent $\text{CF}_3\text{CH}_2\text{OH}$ had shown some success in the fundamental ring opening/Nazarov methodology, substrates **1b** and **1c** were subsequently treated with AgBF_4 in $\text{CF}_3\text{CH}_2\text{OH}$; nonetheless, the same decomposition of starting materials was observed.



Scheme 3.6. Treatment of *gem*-dichlorocyclopropanes **1b** and **1c** with AgBF_4 in CH_2Cl_2 .

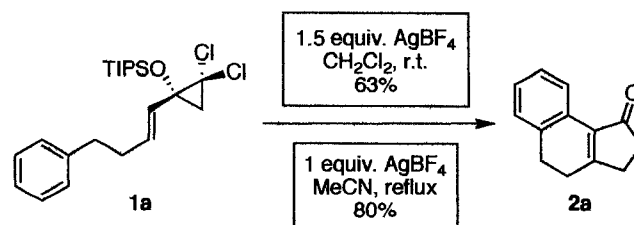
These unexpected results compelled us to re-examine the conditions for this intramolecular “interrupted” Nazarov variant. It was apparent that cationic intermediates generated from these substrates (**1**) under the standard reaction conditions were sufficiently long-lived and could therefore participate in alternate and undesirable termination and/or polymerization pathways. Since ring opening of *gem*-dichlorocyclopropanes is known to occur under strictly thermal conditions,⁴ we examined the possibility of inducing ring opening in refluxing MeCN with the expectation that higher reaction temperatures might improve the rate of ring opening and subsequent 4π electrocyclicization. Although we had previously seen facile conversion of vinyl dihalocyclopropanes to the corresponding chlorodienones under thermal conditions (*Scheme 3.7*), we believed that the addition of halophilic Ag(I) to these reactions would



Scheme 3.7. Conversion of vinyl dihalocyclopropanes to dienones in refluxing MeCN.

sequester free chloride anions generated as a result of ring opening and thereby prevent them from interfering with the desired cascade process. We were pleased to observe that *gem*-dichlorocyclopropanes **1b** and **1c** were cleanly converted to benzohydrindenones **2b** and **2c** in 53% and 76% yields, respectively, when subjected to 1 equivalent of AgBF₄ in refluxing MeCN (*Table 3.2*). The success of these reactions prompted reinvestigation of some earlier *gem*-dichlorocyclopropane substrates (*Scheme 3.8*) using the new reaction conditions. In general, it was found that reaction times were dramatically reduced and

the yields improved when the new AgBF₄/MeCN conditions were applied.



Scheme 3.8. Comparison of original reaction conditions with AgBF₄ in refluxing MeCN.

With optimized reaction conditions in hand, the remaining *gem*-dichlorocyclopropane substrates **1** were treated with AgBF₄ in refluxing MeCN to induce the “interrupted” Nazarov reaction (*Table 3.2*). In most cases, the desired product was isolated in moderate yields and as a single regioisomer due to electrophilic attack at the least hindered position of the aromatic ring (i.e. *para* to the methoxy-substituent in **2c**). Also, all of the tricyclic products (**2a-f**) had experienced dehydrochlorination and possessed a ring-fusing alkene that was conjugated to the aromatic ring and ketone functionalities. Remarkably, the deactivated aromatic ring in *gem*-dichlorocyclopropane substrate **1e** was capable of trapping the reactive 2-silyloxycyclopentenyl cation to furnish the bromo-substituted benzohydrindenone product **2e** (entry 5). This type of electron-deficient product would not be accessible from the conventional interrupted Nazarov reaction of divinyl ketone substrates, which demonstrates the value of this complementary trapping process. Another interesting observation was made when the silyl-protected phenol **1f** was subjected to AgBF₄ in refluxing MeCN (entry 6). These reaction conditions promoted deprotection of the labile phenolic protecting group to provide benzohydrindenone **2f** in 39% after an extended reaction time. The low yield of this reaction can most likely be attributed to premature desilylation, exposing a reactive

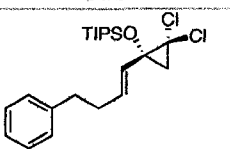
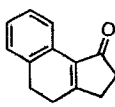
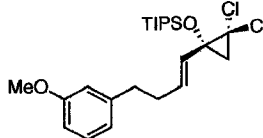
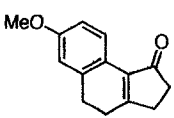
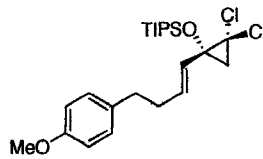
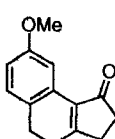
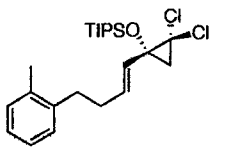
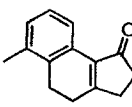
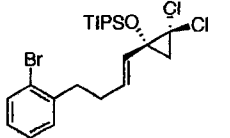
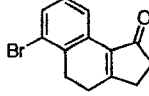
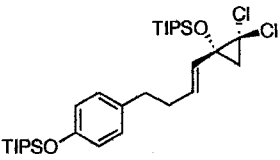
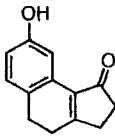
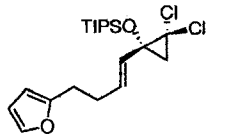
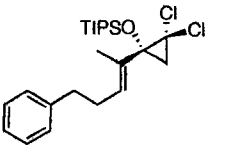
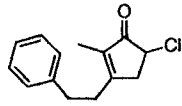
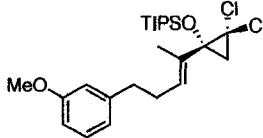
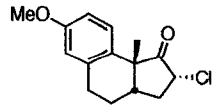
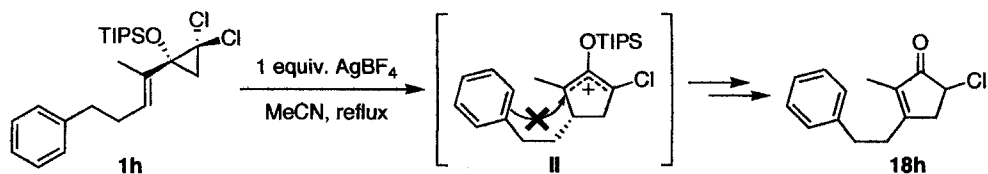
entry	substrate	product	yield (%)
1		1a 	2a 80
2		1b 	2b 53
3		1c 	2c 76
4		1d 	2d 79
5		1e 	2e 48
6		1f 	2f 39
7		1g Decomposition of S.M.	n/a
8		1h 	18h 97
9		1i 	19i 89

Table 3.2. Ag(I)-Mediated interrupted Nazarov reactions.

hydroxyl moiety that interferes with the cationic Nazarov intermediates. The presence of more robust protecting groups on phenolic substrates would most likely lead to formation of the desired tricyclic products in improved yields, as evidenced by smooth conversion of the related methoxy-substituted substrate **1c** to benzohydrindenone **2c** (entry 3).

Although tethered furan groups were found to participate in the traditional interrupted Nazarov reaction,⁵ we found that *gem*-dichlorocyclopropane **1g** was rapidly decomposed when subjected to AgBF₄ in refluxing MeCN (entry 7). Furthermore, AgBF₄ was found to promote decomposition of the same substrate in CH₂Cl₂ and CF₃CH₂OH. Decomposition was apparently initiated by the addition of AgBF₄, resulting in complete destruction of the substrate after 10 minutes regardless of the solvent or temperature of the reaction. We propose that this substrate's poor reactivity might be due to the incompatibility of the furan moiety with lingering HBF₄ generated during the reaction, since furyl-diene **7g** also underwent slow decomposition when subjected to trace amounts of HBF₄.

We also explored the effect of α -substitution on the vinyl moiety by examining the reactivity of *gem*-dichlorocyclopropane substrates **1h** and **1i** under the standard reaction conditions. When **1h** was subjected to AgBF₄, the simple α -chlorocyclopentenone **18h** was isolated as the sole product in 97% yield. None of the trapping product was observed, even after prolonged reaction time (*Scheme 3.9*). This



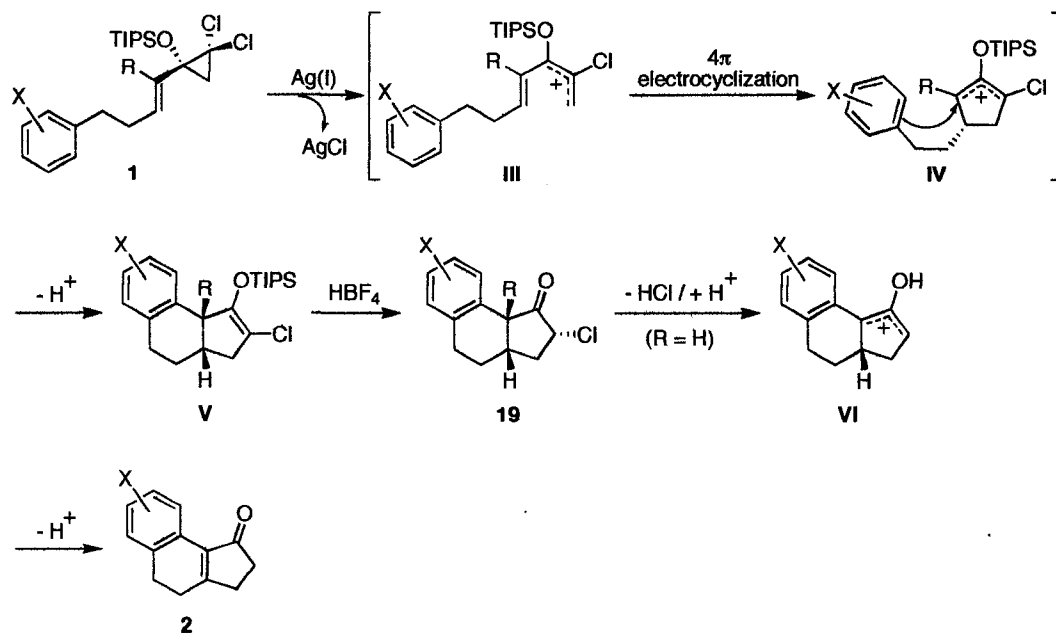
Scheme 3.9. The effect of α -substitution on the interrupted Nazarov variant.

result suggests that intramolecular trapping by a deactivated phenyl group will not occur when the 2-silyloxycyclopentenyl cation **II** is stabilized by alkyl-substitution. However, when the 3-methoxyphenyl moiety was used in place of a non-substituted phenyl, the chlorocyclopentanone **19i** was isolated in very good yield (entry 9). The *cis* relationship between the hydrogen and methyl groups at the ring fusion, as well as the relative stereochemistry of the chlorine moiety, was confirmed by single-crystal X-ray crystallography (see Appendix IV). Notably, this reaction led to the formation of a tricyclic product with retention of the chlorine substituent, which suggests that dehydrochlorination to furnish benzohydrindenones **2a-f** requires that the bridgehead position is unsubstituted.

Mechanistic Proposal

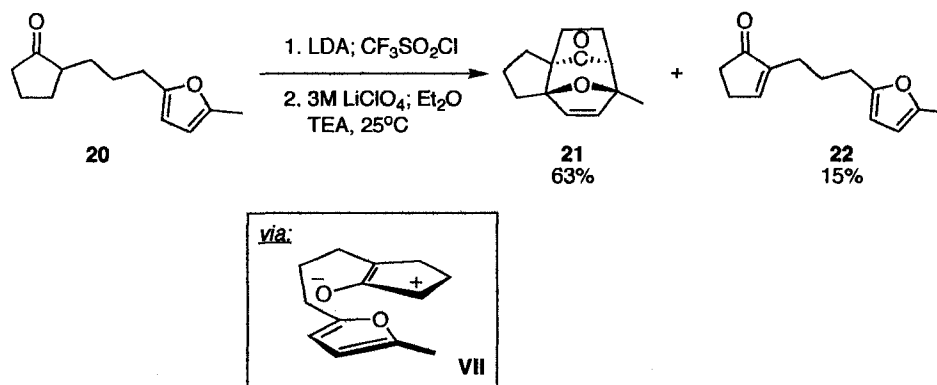
Treatment of *gem*-dichlorocyclopropanes **1a-i** with AgBF₄ led to the generation of different tricyclic products, which provided important insight into the mechanism of this cascade process (*Scheme 3.10*). We propose that the mechanism proceeds through the typical chloride-assisted disrotatory ring opening of the *gem*-dichlorocyclopropane moiety, followed by 4 π electrocyclization (Nazarov cyclization) to provide the 2-silyloxycyclopentenyl cation **IV**. This highly reactive cationic species would then be captured by a pendent arene nucleophile to afford the tricyclic intermediate **V** upon rearomatization. Protodesilylation of the silyl enol ether from the least-hindered, convex face of **V** would then result in the formation of chlorocyclopentanones **19**. In the absence of alkyl substitution at the bridgehead position, compounds **19** could experience dehydrochlorination to provide the benzohydrindenone products **2**. Since elimination of

HCl to generate an olefin is not observed when “R” is a methyl group, we propose that double-bond formation proceeds through a second oxyallyl cationic intermediate **VI**, followed by conventional Nazarov-type elimination and protonation to furnish the final products (**2**).



Scheme 3.10. Proposed mechanism for arene-trapping.

The formation of cyclic oxyallyl cations from the dehydrochlorination of chlorocyclopentanones is preceded in the literature (*Scheme 3.11*).⁶ Harmata has shown that intramolecular [4+3] cycloadditions can be accomplished by the *in situ* generation of 2-oxidocyclopentenyl cations (**VII**) resulting from chlorination and subsequent base-mediated dehydrochlorination of cyclopentanones. Under these conditions, substrates with pendent traps, such as cyclopentanone **20**, can generate complex polycyclic products **21** in good yields. The major side-product (**22**) was undoubtedly the result of a competing elimination process experienced by the cationic intermediate **VII**.

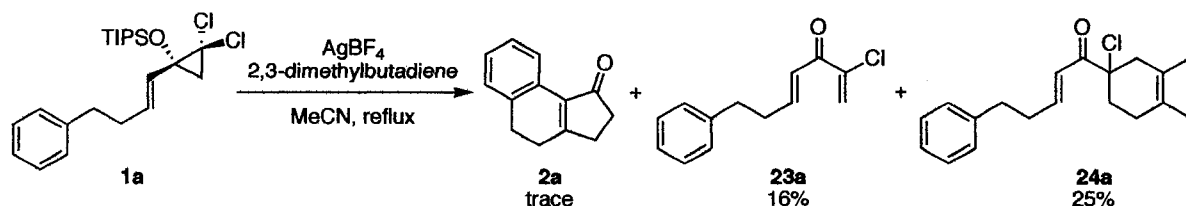


Scheme 3.11. Harmata's use of α -chlorocyclopentanones in [4+3] cycloadditions.

In order to provide experimental evidence for the formation of a second cationic intermediate, we first attempted to capture this species in an intermolecular fashion. To this end, *gem*-dichlorocyclopropane substrate **1a** was treated with AgBF_4 and 10 equivalents of diene (isoprene or 2,3-dimethylbutadiene) in CH_2Cl_2 . These components were stirred together at room temperature and the reaction progress monitored by TLC analysis. These reaction conditions prompted complete consumption of starting material, but unfortunately resulted in exclusive formation of a viscous polymeric product. Polymerization was apparently initiated by the formation of cationic intermediates from ring opening of the *gem*-dichlorocyclopropane, since the dienes themselves showed no evidence of decomposition or polymerization when treated with AgBF_4 in the absence of substrate **1a**.

In an attempt to avoid polymerization, the same reactions were carried out using refluxing MeCN instead of CH_2Cl_2 . It was our hope that the increased reaction temperatures would induce quick and facile ring opening and intramolecular arene-trapping instead of polymerization. Although polymerization was inhibited, these

reaction conditions led to the formation of trace amounts of benzohydrindenone **2a**, the chlorodienone **23a**, and a new product (**24a**) (*Scheme 3.12*). The α,β -unsaturated ketone **24a** appears to have arisen from the formal Diels-Alder cycloaddition of 2,3-dimethylbutadiene to the activated olefin resulting from disrotatory ring opening of the

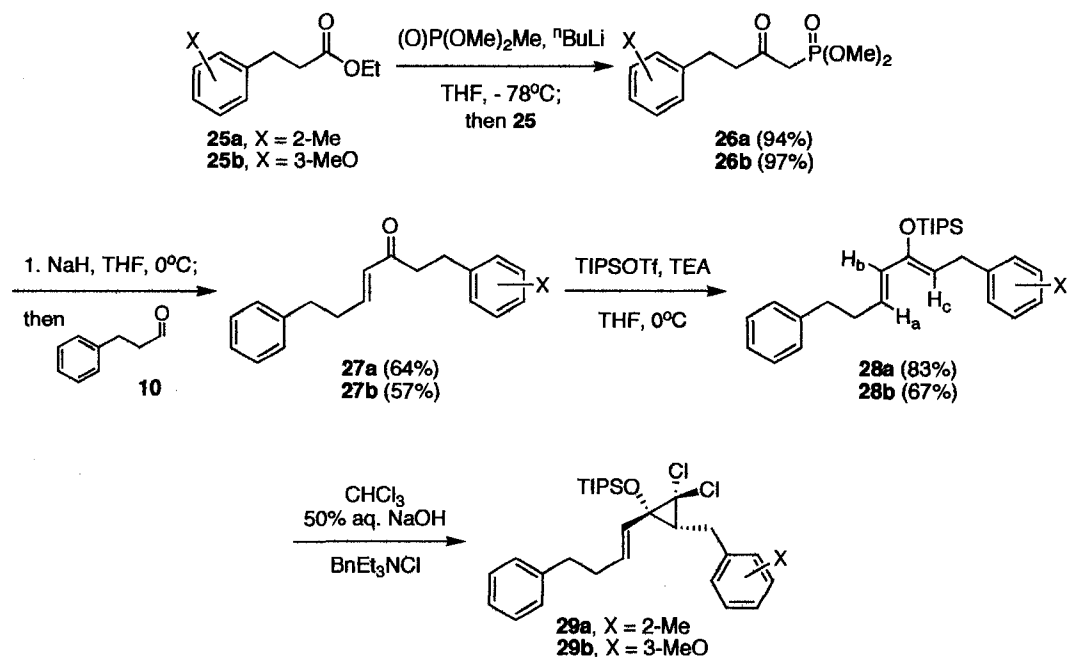


Scheme 3.12. Attempted intermolecular trapping of the second oxyallyl cation.

gem-dichlorocyclopropane moiety. Regardless of when the diene was added to the reaction mixture (i.e. before/after apparent formation of the benzohydrindenone by TLC analysis), the generation of chlorodienone **23a** and ketone **24a** was inevitable.

3.2.2 Novel Mode of Arene Trapping

In order to increase the potential for successful trapping of the putative second oxyallyl cationic intermediate, we envisioned a *gem*-dichlorocyclopropane substrate with *two* internal nucleophiles: one to participate in the initial interrupted Nazarov reaction, and the other to capture the second cationic species. The desired α,β -unsaturated ketones **27** were synthesized from a Horner-Wadsworth-Emmons olefination reaction⁷ between a dimethylphosphonate reagent **26** and hydrocinnamaldehyde **10** (*Scheme 3.13*). The ketones were cleanly converted to the silyoxydienes **28** using the previously outlined conditions of triisopropylsilyl trifluoromethanesulfonate in the presence of triethylamine.

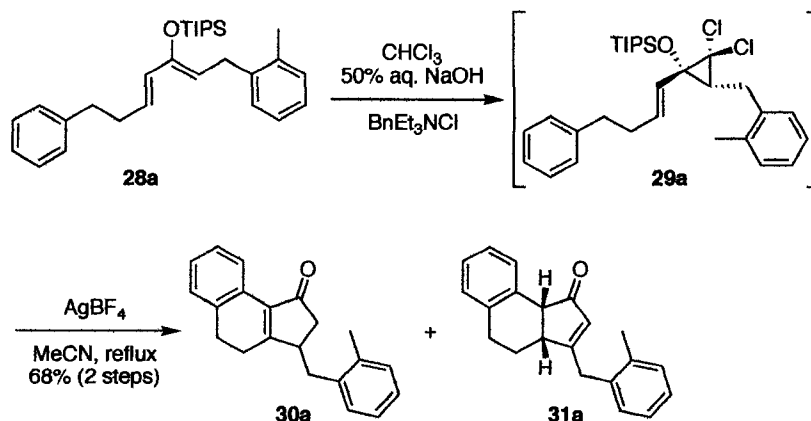


Scheme 3.13. Preparation of *gem*-dichlorocyclopropanes **29a** and **29b**.

The geometry of the silyl enol ether olefin in **28a** was confirmed by analysis of a 1D TROESY experiment, wherein nOe enhancement of H_a and H_b was observed when H_c was irradiated at 4.74 ppm. The silyloxydienes were then subjected to Makosza conditions for dichlorocyclopropanation to furnish the desired *gem*-dichlorocyclopropanes **29a** and **29b**. Although the presence of these compounds was clearly indicated by characteristic peaks in the crude ¹H NMR spectra, attempts to purify these substrates using conventional silica or alumina-based chromatography prompted rapid decomposition of these *gem*-dichlorocyclopropane substrates. Consequently, the *gem*-dichlorocyclopropanes were directly subjected to AgBF₄ in refluxing MeCN and the yields for the observed products reported over two steps.

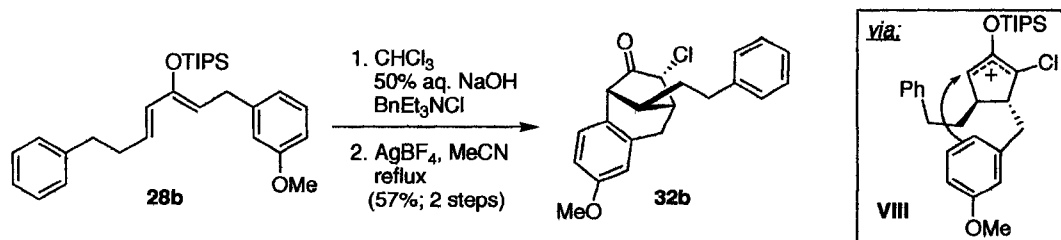
Silyloxydiene **28a** was smoothly converted to the tricyclic products **30a** and **31a** in a 2.7:1 ratio and 68% yield following cyclopropanation and direct treatment with the

standard Ag(I)-mediated reaction conditions (*Scheme 3.14*). Evidently, the 2-methylphenyl substituent was incapable of participating in a second trapping event with the intermediate oxyallyl cationic species, which is most likely due to the low nucleophilicity of the second arene trap. In an effort to overcome this obstacle *gem*-dichlorocyclopropane **29b**, bearing a more electron-rich arene moiety, was examined.



Scheme 3.14. Conversion of substrate **28a** to benzohydrindenone products.

Surprisingly, silyloxydiene **28b** was cleanly converted to a very intriguing and unexpected bridged bicyclic compound, **32b** in 57% yield over two steps (*Scheme 3.15*). This product is undoubtedly the result of nucleophilic capture by the more electron-rich arene moiety on the initial 2-silyloxy-pentadienyl cation (**VIII**). This process proceeded with complete regioselectivity in favour of 6-membered ring formation due to attack on the least hindered side of the oxyallyl cation. Dehydrochlorination to make a second cationic intermediate did not occur in this case, due to structural restrictions imposed by the bridged architecture of **32b**. To our knowledge, this type of intramolecular trapping of the cationic Nazarov intermediate is unprecedented.



Scheme 3.15. The unexpected formation of bridged bicycle **32b**.

Characterization of Bridged Bicycle 32b

Structural elucidation of the interesting bridged compound **32b** was accomplished by thorough analysis of both 1D and 2D NMR spectra and supported by characteristic infrared (IR) absorptions and electrospray mass spectrometry (MS). Initial inspection of the 1D ^1H NMR spectrum indicated the presence of only 8 aromatic protons, suggesting that electrophilic aromatic substitution had taken place. Two distinct spin systems were identified among these aromatic protons. The most revealing of these indicated the presence of a 1,3,4-trisubstituted arene moiety, as reflected by a doublet at 7.01 ppm ($^3J=8.5$ Hz), a doublet-of-doublets at 6.72 ppm ($^3J=8.5$ Hz, $^4J=3.0$ Hz), and a doublet at 6.67 ppm ($^4J=3.0$ Hz). This substitution pattern suggested that the more electron-rich (methoxy-substituted) aromatic ring had participated in capture of the cationic Nazarov intermediate.

With this information in hand, the aliphatic proton resonances were analyzed to ascertain the connectivity of the structural framework. Interestingly, three isolated spin systems were observed when coupling constants and the 2D COSY spectrum were analyzed (*Figure 3.2*). The first spin system (**A**) undoubtedly involved the chlorine-substituted position adjacent to the ketone carbonyl, since a broad doublet was observed

at a significantly high chemical shift (4.51 ppm). The presence of chlorine was also confirmed by mass spectrometric analysis. The broad doublet showed a correlation to the methine proton observed at 2.90-2.92 ppm (multiplet), which subsequently correlated to two doublet-of-doublets representative of the adjacent methylene protons. Surprisingly, the observed bridgehead proton in this spin system showed no correlation to the adjacent methine proton, a triplet at 2.32 ppm (**B**). Also, the remaining spin system contained a

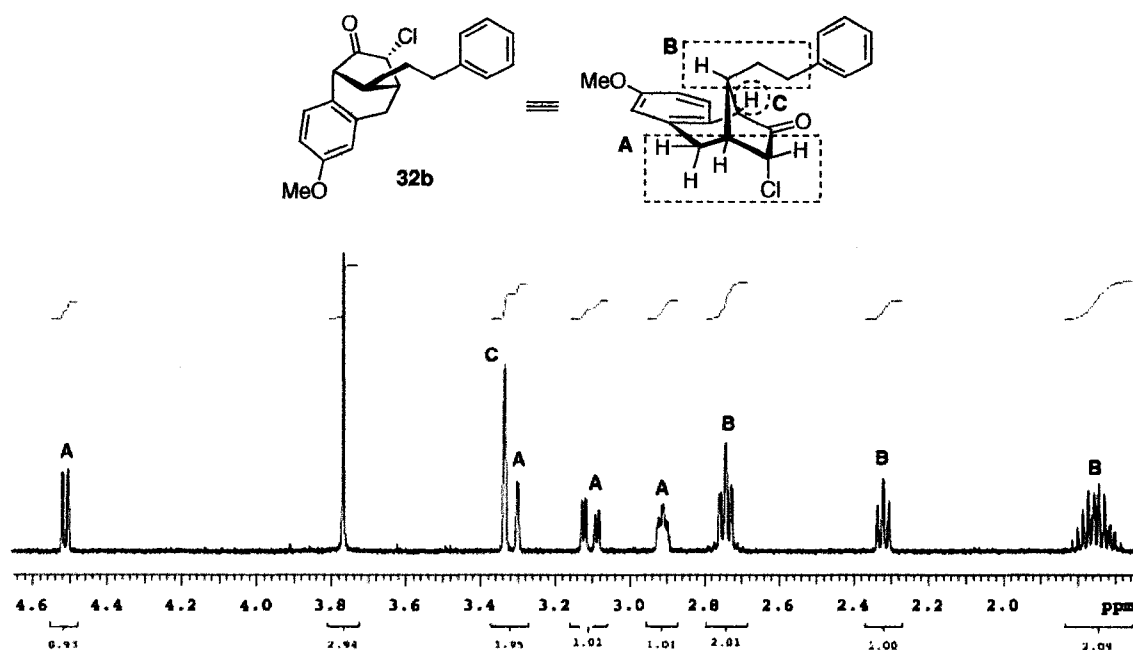


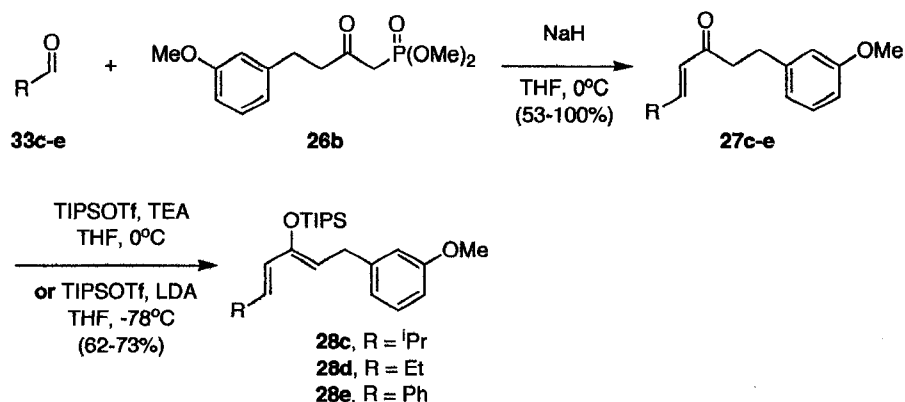
Figure 3.2. Isolated spin systems observed in the ^1H NMR spectrum.

single methine signal (**C**, singlet at 3.33 ppm) that showed no correlation to any of the other proton resonances. Undoubtedly, these observations can be explained by the bond angles inherent to these rigid frameworks and are therefore characteristic of this class of bridged bicyclic compounds.

The proposed connectivity of compound **32** was supported by the observation of distinctive correlations in 2D HMQC and HMBC spectra.

Examination of Substrate Scope

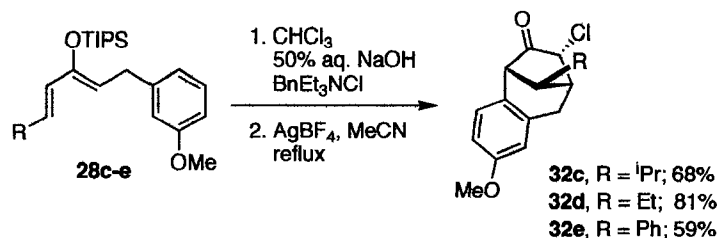
Having confirmed the intriguing architecture of bridged bicycle **32b**, we turned our attention to the investigation of β -substitution on the vinyl moiety of analogous *gem*-dichlorocyclopropane substrates **29c-e**. These compounds were prepared in the same manner as previously described utilizing Horner-Wadsworth-Emmons olefination to



Scheme 3.16. Preparation of silyl enol ethers **28c-e**.

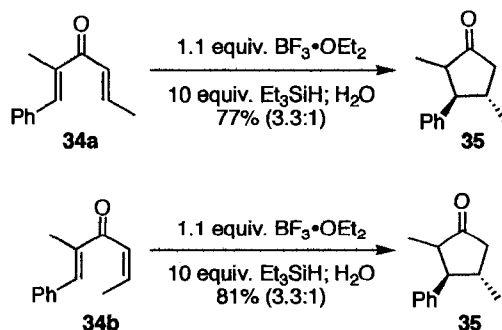
synthesize the requisite α,β -unsaturated ketones **27c-e** (*Scheme 3.16*). These compounds were smoothly transformed to the silyl enol ethers using either triethylamine or lithium diisopropylamide as the base, generating the *Z*-isomers exclusively or, in the case of substrate **28d**, as the major product in a mixture of *E/Z*-isomers (*E/Z*, 1:6.5).

The remaining silyl enol ethers (**28c-e**) were subjected to the two-step cyclopropanation/Ag(I)-mediated Nazarov cyclization and were cleanly converted to the bridged bicyclic products **32c-e** in moderate to good yields over the two-step sequence (*Scheme 3.17*). Characteristic coupling patterns observed in the 1D ^1H NMR spectra and single-crystal X-ray crystallography performed on compounds **32d** and **32e** (see Appendix IV) unambiguously confirmed the bridged architecture and relative



Scheme 3.17. The formation of bridged bicyclic products **32**.

stereochemistry of these novel trapping products. These structures reveal that the cascade sequence proceeds stereoselectively in every case to furnish a single product as the result of conrotatory 4π electrocyclicization, electrophilic aromatic substitution at the least hindered position on the arene moiety (*para* to the MeO), and desilylation with protonation from the *exo* face of the bicyclic product. A single product was even observed when the starting material existed as a mixture of *E/Z*-isomers, suggesting that double-bond isomerization occurs upon ring opening of the *gem*-dichlorocyclopropane with equilibration to the more stable *E*-isomer prior to electrocyclicization. This phenomenon has previously been observed during development of the reductive Nazarov reaction (Scheme 3.18).⁸ Dienone substrates **34a** and **34b** were individually treated with 1.1 equivalents of $\text{BF}_3 \cdot \text{OEt}_2$ in the presence of 10 equivalents of triethylsilane to afford



Scheme 3.18. *E/Z*-Isomerization of dienones in the reductive Nazarov cyclization.

the same cyclopentanone product **35** in good yields. In this case, *E/Z*-isomerization of the disubstituted olefin occurred during Lewis acid activation of the dienone substrate (**34b**) prior to electrocyclization.

The interesting carbon framework generated from this novel mode of trapping can be observed in the *Galbulimima belgraveana* family of alkaloids (Figure 3.3).⁹ Mander has approached the synthesis of these types of compounds using a rhodium (II) catalyzed C-H insertion reaction. Our interrupted Nazarov methodology offers a potentially useful and simplified approach toward advanced intermediates needed for the synthesis of these natural products.

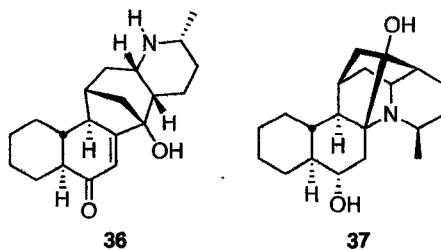


Figure 3.3. Representative *Galbulimima belgraveana* alkaloids.

3.2.3 Conclusions

We have discovered that appropriately functionalized *gem*-dichlorocyclopropane compounds can be used to participate in an efficient ring opening, 4π electrocyclization, and intramolecular electrophilic aromatic substitution sequence in the presence of AgBF_4 . This cascade process provides access to electron-deficient, neutral, and electron-rich benzohydrindenone compounds as a result of intramolecular arene-trapping and subsequent dehydrochlorination, which we believe to proceed through a second oxyallyl

cationic species. This second cationic intermediate is not formed when alkyl substitution exists at the α -position of the vinyl moiety, providing tricyclic products that retain the chlorine substituent.

We have also discovered a novel interrupted Nazarov reaction utilizing electron-rich aromatic rings tethered through the cyclopropane moiety. This new trapping pathway provides an expedient and stereoselective route to the construction of complex bridged bicyclic compounds from simple and readily accessible starting materials. The ease with which the *gem*-dichlorocyclopropanes can be prepared and the efficiency of the cascade processes makes these substrates attractive intermediates for the synthesis of natural products.

3.3 Future Directions

We have become very interested in expanding the *gem*-dichlorocyclopropane approach to both Nazarov and interrupted Nazarov reactions. As outlined in chapter 2, it is our goal to further examine the effects of substitution on these substrates to develop an imino Nazarov variant. We are also interested in the design of new modes of trapping for interrupted Nazarov reactions to generate novel carbon frameworks from simple *gem*-dichlorocyclopropane substrates.

We have observed that aromatic rings tethered through the cyclopropane unit and on the vinyl moiety can lead to the construction of benzohydrindenones and unique bridged bicyclic compounds. Aside from arene traps, we are also interested in examining the use of different trapping species, including oxygen and nitrogen-based, as well as olefin nucleophiles. These trapping processes have been observed in the context of the traditional Nazarov cyclization, and the related interrupted Nazarov reactions utilizing *gem*-dichlorocyclopropane substrates are currently under investigation in the West laboratories.

Finally, the selective functionalization of chlorine atoms on *gem*-dichlorocyclopropanes is well documented and might allow access to a variety of monochlorocyclopropanes that can participate in sequential ring opening and Nazarov cyclization (*Figure 3.4*). Similarly, we recognize that the replacement of a single chloro-substituent with a tethered nucleophile would provide another opportunity for novel intramolecular trapping processes.

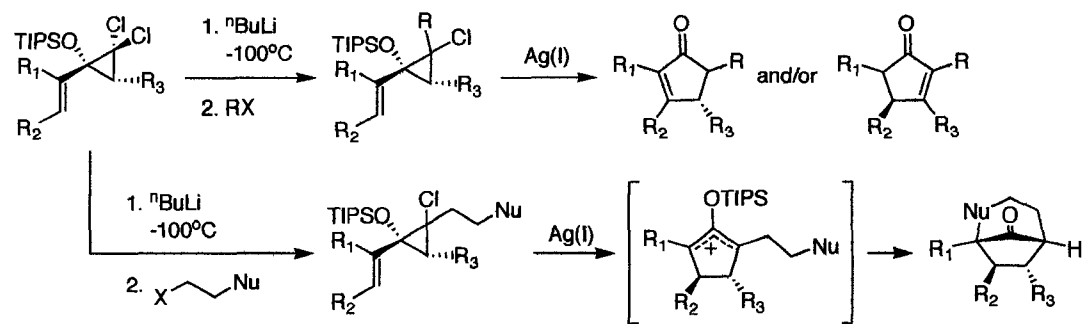


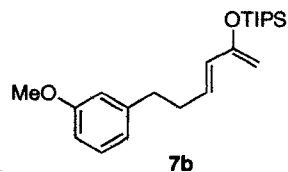
Figure 3.4. Participation of monochlorocyclopropanes in Nazarov processes.

3.4 Experimental

3.4.1 General Information

Reactions were carried out in flame-dried glassware under a positive argon atmosphere unless otherwise stated. Transfer of anhydrous solvents and reagents was accomplished with oven-dried syringes or cannulae. Solvents were distilled before use: methylene chloride (CH_2Cl_2) from calcium hydride, tetrahydrofuran (THF) and diethyl ether (Et_2O) from sodium/benzophenone ketyl, and toluene from sodium metal. Thin layer chromatography was performed on glass plates precoated with 0.25 mm Kieselgel 60 F₂₅₄ (Merck). Flash chromatography columns were packed with 230-400 mesh silica gel (Silicycle) or ~150 mesh activated, neutral, Brockmann I, standard grade aluminum oxide (Sigma-Aldrich). Proton nuclear magnetic resonance spectra (^1H NMR) were recorded at 400 MHz or 500 MHz and coupling constants (J) are reported in Hertz (Hz). Standard notation was used to describe the multiplicity of signals observed in ^1H NMR spectra: broad (br), apparent (app), multiplet (m), singlet (s), doublet (d), triplet (t), etc. Carbon nuclear magnetic resonance spectra (^{13}C NMR) were recorded at 100 MHz or 125 MHz and are reported (ppm) relative to the center line of the triplet from chloroform-*d* (77.26 ppm). Infrared (IR) spectra were measured with a Mattson Galaxy Series FT-IR 3000 spectrophotometer. Mass spectra were determined on a PerSeptive Biosystems Mariner high-resolution electrospray positive ion mode spectrometer.

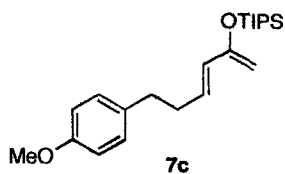
3.4.2 Characterization



(3E)-2-(Triisopropylsiloxy)-6-(3-methoxy-phenyl)-1,3-hexadiene, 7b. DMSO (0.12 mL, 1.7 mmol) was added to a solution of oxalyl chloride (0.13 mL, 1.5 mmol) in CH₂Cl₂ (8 mL) at -78°C .² The reaction mixture was stirred for 10 min before adding 3-(3-methoxyphenyl)-propanol **5b** (0.17 g, 1.0 mmol) in CH₂Cl₂ (2 mL) *via* cannula. The reaction was stirred for 15 min before adding triethylamine (0.52 mL, 3.7 mmol) dropwise *via* syringe. The reaction was then allowed to stir for another 15 min before transferring a solution of (triphenylphosphoranylidene)-2-propanone (0.60 g, 1.9 mmol) in CH₂Cl₂ (5 mL) to the stirring reaction mixture at -78°C . The reaction was allowed to warm slowly to room temperature and stirred until disappearance of starting material was observed by TLC analysis (hexanes/EtOAc 2:1). The reaction was then diluted with Et₂O (15 mL). The cloudy organic layer was then washed with H₂O (2 x 25 mL) and brine (25 mL). The organic layer was dried (MgSO₄) and filtered. The solvent was removed and the crude oil purified by flash column chromatography (silica gel, hexanes:EtOAc 10:1) to yield 6-(3-methoxy-phenyl)-(3E)-hexene-2-one **6b** (0.16 g, 0.78 mmol, 78 %) as a colorless oil: R_f 0.53 (hexanes/EtOAc 2:1); IR (thin film) 3003, 2939, 2836, 1696, 1674, 1602, 1257 cm^{-1} ; ¹H NMR (500 MHz, CDCl₃) δ 7.21 (t, $J = 8.0$ Hz, 1H), 6.82 (dt, $J = 16.0, 7.0$ Hz, 1H), 6.73-6.79 (m, 3H), 6.10 (dt, $J = 16.0, 1.5$ Hz, 1H), 3.80 (s, 3H), 2.77 (t, $J = 7.5$ Hz, 2H), 2.55 (app q, $J = 7.0$ Hz, 2H), 2.23 (s, 3H); ¹³C NMR (125 MHz, CDCl₃)

δ 198.5, 159.8, 147.0, 142.3, 131.7, 129.5, 120.7, 114.2, 111.4, 55.1, 34.4, 34.0, 26.9; HRMS (EI, M^+) for $C_{13}H_{16}O_2$ calcd 204.1150, found: m/z 204.1152.

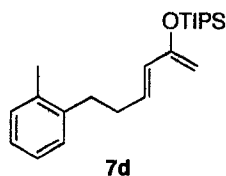
6-(3-Methoxy-phenyl)-(3*E*)-hexene-2-one **6b** (0.15 g, 0.76 mmol) was treated with triisopropylsilyl trifluoromethanesulfonate (0.23 mL, 0.84 mmol) under the previously outlined conditions to obtain (3*E*)-2-(triisopropylsiloxy)-6-(3-methoxy-phenyl)-1,3-hexadiene, **7b**, (0.27 g, 0.76 mmol, 100%) as a clear, colorless oil: R_f 0.87 (alumina, hexanes:EtOAc 4:1); IR (thin film) 2944, 2867, 1586, 1490, 1464, 1320, 1260, 1152, 1028 cm^{-1} ; 1H NMR (500 MHz, $CDCl_3$) δ 7.19 (td, $J = 7.5, 1.0$ Hz, 1H), 6.78 (d, $J = 7.5$ Hz, 1H), 6.72-6.74 (m, 2H), 6.09 (dt, $J = 15.5, 7.0$ Hz, 1H), 5.91 (dt, $J = 15.5, 1.5$ Hz, 1H), 4.22 (s, 1H), 4.17 (s, 1H), 3.80 (s, 3H), 2.71 (t, $J = 7.5$ Hz, 2H), 2.43 (app qd, $J = 7.5, 1.0$ Hz, 2H), 1.19-1.26 (m, 3H), 1.10 (d, $J = 7.5$ Hz, 18H); ^{13}C NMR (125 MHz, $CDCl_3$) δ 159.6, 155.2, 143.4, 130.5, 129.2, 128.4, 120.9, 114.2, 111.2, 83.2, 55.1, 35.7, 33.8, 18.1, 12.8; HRMS (EI, M^+) for $C_{22}H_{36}O_2Si$ calcd 360.2485, found: m/z 360.2482.



(3*E*)-2-(Triisopropylsiloxy)-6-(4-methoxy-phenyl)-1,3-hexadiene, **7c**. The previously outlined procedure was used in the synthesis of **7c** starting with 3-(4-methoxyphenyl)-propanol **5c** (0.18 g, 1.1 mmol). The reaction was diluted with Et_2O (15 mL) after 48 h stirring at room temperature. The crude material was purified by flash column chromatography (silica gel, hexanes:EtOAc 10:1) to yield 6-(4-methoxy-phenyl)-(3*E*)-hexene-2-one **6c** (0.12 g, 0.61 mmol, 56 %) as a colorless oil: R_f 0.44 (hexanes/EtOAc 2:1); IR (thin film) 3004, 2934, 2836, 1674, 1626, 1513, 1361, 1248, 1035 cm^{-1} ; 1H NMR

(500 MHz, CDCl₃) δ 7.09 (d, J = 9.0 Hz, 2H), 6.84 (d, J = 8.5 Hz, 2H), 6.81 (dt, J = 16.0, 7.0 Hz, 1H), 6.09 (dt, J = 16.0, 1.5 Hz, 1H), 3.80 (s, 3H), 2.74 (t, J = 7.5 Hz, 2H), 2.52 (app q, J = 7.0 Hz, 2H), 2.23 (s, 3H); ¹³C NMR (125 MHz, CDCl₃) δ 198.5, 158.0, 147.2, 132.7, 131.7, 129.2, 113.9, 55.2, 34.4, 33.5, 26.8; HRMS (EI, M⁺) for C₁₃H₁₆O₂ calcd 204.1150, found: m/z 204.1150.

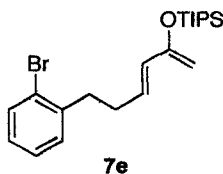
6-(4-Methoxy-phenyl)-(3*E*)-hexene-2-one **6c** (0.20 g, 1.0 mmol) was treated with triisopropylsilyl trifluoromethanesulfonate (0.30 mL, 1.1 mmol) under the previously outlined conditions to obtain (3*E*)-2-(triisopropylsiloxy)-6-(4-methoxy-phenyl)-1,3-hexadiene, **7c**, (0.36 g, 1.0 mmol, 100%) as a clear, colorless oil: R_f 0.78 (alumina, hexanes:EtOAc 8:1); IR (thin film) 2944, 2867, 1588, 1513, 1464, 1320, 1247, 1029 cm⁻¹; ¹H NMR (500 MHz, CDCl₃) δ 7.10 (app d, J = 8.5 Hz, 2H), 6.82 (app d, J = 8.5 Hz, 2H), 6.08 (dt, J = 15.0, 7.0 Hz, 1H), 5.89 (dt, J = 15.0, 1.0 Hz, 1H), 4.22 (s, 1H), 4.16 (s, 1H), 3.79 (s, 3H), 2.67 (t, J = 7.5 Hz, 2H), 2.39 (app q, J = 7.5 Hz, 2H), 1.18-1.28 (m, 3H), 1.10 (d, J = 7.0 Hz, 18H); ¹³C NMR (125 MHz, CDCl₃) δ 158.0, 155.6, 134.2, 130.9, 129.6, 128.6, 114.0, 93.4, 55.5, 35.0, 34.4, 18.3, 13.1; HRMS (EI, M⁺) for C₂₂H₃₆O₂Si calcd 360.2485, found: m/z 360.2486.



(3*E*)-2-(Triisopropylsiloxy)-6-(2-methylphenyl)-1,3-hexadiene, **7d**. The previously outlined procedure was used in the synthesis of **7d** starting with 3-(2-methylphenyl)-propanol **5d** (0.15 g, 1.0 mmol). The crude material was purified by flash column chromatography (silica gel, hexanes:EtOAc 10:1) to yield 6-(2-methyl-phenyl)-(3*E*)-

hexene-2-one **6d** (0.14 g, 0.72 mmol, 72 %) as a colorless oil: R_f 0.55 (hexanes/EtOAc 2:1); IR (thin film) 3016, 2940, 1675, 1626, 1361, 1254, 976, 744 cm^{-1} ; ^1H NMR (500 MHz, CDCl_3) δ 7.11-7.17 (m, 4H), 6.86 (dt, $J = 16.5, 6.5$ Hz, 1H), 6.12 (dt, $J = 16.0, 1.5$ Hz, 1H), 2.78 (t, $J = 7.5$ Hz, 2H), 2.52 (app q, $J = 6.5$ Hz, 2H), 2.32 (s, 3H), 2.25 (s, 3H); ^{13}C NMR (125 MHz, CDCl_3) δ 198.5, 147.2, 138.8, 135.8, 131.6, 130.3, 128.6, 126.4, 126.1, 32.9, 31.8, 26.9, 19.3; HRMS (EI, M^+) for $\text{C}_{13}\text{H}_{16}\text{O}$ calcd 188.1201, found: m/z 188.1201.

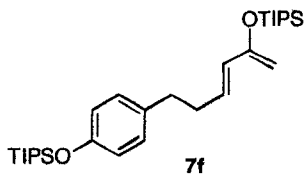
6-(2-Methyl-phenyl)-(3*E*)-hexene-2-one **6d** (0.16 g, 0.85 mmol) was treated with triisopropylsilyl trifluoromethanesulfonate (0.25 mL, 0.94 mmol) under the previously outlined conditions to obtain (3*E*)-2-(triisopropylsiloxy)-6-(2-methyl-phenyl)-1,3-hexadiene, **7d**, (0.29 g, 0.85 mmol, 100 %) as a clear, colorless oil: R_f 0.93 (alumina, hexanes:EtOAc 4:1); IR (thin film) 2945, 2867, 1589, 1463, 1321, 1027, 883, 685 cm^{-1} ; ^1H NMR (500 MHz, CDCl_3) δ 7.11-7.16 (m, 4H), 6.14 (dt, $J = 15.0, 7.0$ Hz, 1H), 5.93 (d, $J = 15.5$ Hz, 1H), 4.24 (s, 1H), 4.19 (s, 1H), 2.73 (t, $J = 7.5$ Hz, 2H), 2.40 (app q, $J = 7.5$ Hz, 2H), 2.33 (s, 3H), 1.22-1.30 (m, 3H), 1.12 (d, $J = 7.5$ Hz, 18H); ^{13}C NMR (125 MHz, CDCl_3) δ 155.3, 139.9, 135.8, 130.6, 130.1, 128.9, 128.4, 125.9, 125.9, 93.1, 32.9, 32.7, 19.3, 18.1, 12.8; HRMS (EI, M^+) for $\text{C}_{22}\text{H}_{36}\text{OSi}$ calcd 344.2535, found: m/z 344.2530.



(3*E*)-2-(Triisopropylsiloxy)-6-(2-bromophenyl)-1,3-hexadiene, **7e**. The previously outlined procedure was used in the synthesis of **7e** starting with 3-(2-bromophenyl)-propanol **5e** (0.21 g, 1.0 mmol). The crude material was purified by flash column

chromatography (silica gel, hexanes:EtOAc 5:1) to yield 6-(2-bromophenyl)-(3*E*)-hexene-2-one **6e** (0.18 g, 0.70 mmol, 70 %) as a colorless oil: R_f 0.46 (hexanes/EtOAc 2:1); IR (thin film) 3010, 2931, 2862, 1674, 1626, 1471, 1360, 1254, 1023, 752 cm^{-1} ; ^1H NMR (500 MHz, CDCl_3) δ 7.56 (d, $J = 8.0$ Hz, 1H), 7.25 (app t, $J = 7.0$ Hz, 1H), 7.20 (app d, $J = 8.0$ Hz, 1H), 7.09 (app t, $J = 7.5$ Hz, 1H), 6.84 (dt, $J = 16.0, 6.5$ Hz, 1H), 6.10 (d, $J = 16.0$ Hz, 1H), 2.92 (t, $J = 7.5$ Hz, 2H), 2.56 (app q, $J = 8.0$ Hz, 2H), 2.25 (s, 3H); ^{13}C NMR (100 MHz, CDCl_3) δ 198.5, 146.5, 139.9, 132.9, 131.9, 130.3, 128.0, 127.6, 124.3, 34.7, 32.6, 26.9; HRMS (EI, M^+) for $\text{C}_{12}\text{H}_{13}\text{OBr}$ calcd 252.0150, found: m/z 252.0143.

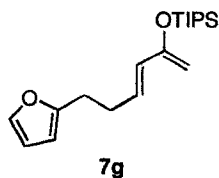
6-(2-Bromophenyl)-(3*E*)-hexene-2-one **6e** (0.42 g, 1.7 mmol) was treated with triisopropylsilyl trifluoromethanesulfonate (0.45 mL, 1.7 mmol) under the previously outlined conditions to yield (3*E*)-2-(triisopropylsiloxy)-6-(2-bromophenyl)-1,3-hexadiene, **7e**, (0.57 g, 1.4 mmol, 83 %) as a clear, colorless oil: R_f 0.79 (alumina, hexanes:EtOAc 8:1); IR (thin film) 2944, 2866, 1589, 1470, 1321, 1025, 883, 748, 685 cm^{-1} ; ^1H NMR (400 MHz, CDCl_3) δ 7.53 (app d, $J = 8.0$ Hz, 1H), 7.20-7.22 (m, 2H), 7.03-7.07 (m, 1H), 6.10 (dt, $J = 15.2, 6.8$ Hz, 1H), 5.91 (dt, $J = 15.2, 1.2$ Hz, 1H), 4.23 (s, 1H), 4.18 (s, 1H), 2.85 (t, $J = 7.6$ Hz, 2H), 2.43 (app qd, $J = 8.0, 1.2$ Hz), 1.19-1.29 (m, 3H), 1.11 (d, $J = 6.8$ Hz, 18H); ^{13}C NMR (100 MHz, CDCl_3) δ 155.1, 140.8, 132.7, 130.4, 129.8, 128.6, 127.4, 127.2, 124.3, 93.2, 35.8, 32.0, 18.0, 12.7; HRMS (EI, M^+) for $\text{C}_{21}\text{H}_{33}\text{OSiBr}$ calcd 408.1484, found: m/z 408.1494.



(3E)-2-(Triisopropylsiloxy)-6-(4-triisopropylsiloxyphenyl)-1,3-hexadiene, 7f. The previously outlined procedure was used in the synthesis of **7f** starting with 3-(4-hydroxyphenyl)-propanol **5f** (0.30 g, 2.0 mmol). The crude material was purified by gradient column chromatography (silica gel, hexanes:EtOAc 5:1) to yield 6-(4-hydroxyphenyl)-(3E)-hexene-2-one **6f** (0.095 g, 0.50 mmol, 25 %) as a colorless oil: R_f 0.28 (hexanes/EtOAc 2:1); IR (thin film) 3347, 3020, 2924, 2855, 1665, 1614, 1515, 1447, 1363, 1365, 1227, 974, 832 cm^{-1} ; ^1H NMR (500 MHz, CDCl_3) δ 7.04 (app d, $J = 8.5$ Hz, 2H), 6.83 (dt, $J = 16.0, 6.5$ Hz, 1H), 6.78 (app d, $J = 8.5$ Hz, 2H), 6.10 (d, $J = 16.5$ Hz, 1H), 5.45 (br s, 1H), 2.72 (t, $J = 7.5$ Hz, 2H), 2.51 (app q, $J = 7.5$ Hz, 2H), 2.24 (s, 3H); ^{13}C NMR (125 MHz, CDCl_3) δ 199.0, 154.1, 147.5, 132.6, 131.6, 129.4, 115.4, 34.4, 33.5, 26.9; HRMS (EI, M^+) for $\text{C}_{12}\text{H}_{14}\text{O}_2$ calcd 190.0994, found: m/z 190.0994.

6-(4-Hydroxyphenyl)-(3E)-hexene-2-one **6f** (0.089 g, 0.47 mmol) was treated with triisopropylsilyl trifluoromethanesulfonate (0.25 mL, 0.94 mmol) under the previously outlined conditions to obtain (3E)-2-(triisopropylsiloxy)-6-(4-triisopropylsiloxyphenyl)-1,3-hexadiene, **7f**, (0.15 g, 0.31 mmol, 66 %) as a clear, colorless oil: R_f 0.86 (alumina, hexanes:EtOAc 8:1); IR (thin film) 2944, 2867, 1510, 1464, 1263, 1028, 917, 883 685 cm^{-1} ; ^1H NMR (500 MHz, CDCl_3) δ 7.01 (app d, $J = 8.5$ Hz, 2H), 6.78 (app d, $J = 8.5$ Hz, 2H), 6.09 (dt, $J = 15.5, 7.0$ Hz, 1H), 5.86 (dt, $J = 15.5, 1.5$ Hz, 1H), 4.21 (s, 1H), 4.15 (s, 1H), 2.64 (t, $J = 7.5$ Hz, 2H), 2.38 (app q, $J = 8.0$ Hz, 2H), 1.18-1.28 (m, 6H), 1.10 (d, $J = 7.0$ Hz, 18H), 1.09 (d, $J = 7.0$ Hz, 18H); ^{13}C NMR

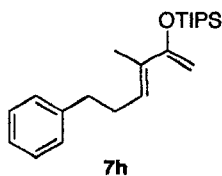
(125 MHz, CDCl₃) δ 155.3, 154.0, 134.1, 130.6, 129.2, 128.4, 119.6, 93.1, 34.9, 34.2, 18.1, 17.9, 12.8, 12.7; HRMS (EI, M⁺) for C₃₀H₅₄O₂Si₂ calcd 502.3662, found: m/z 502.3669.



(3E)-2-(Triisopropylsiloxy)-6-(2-furyl)-1,3-hexadiene, 7g. The previously outlined procedure was used in the synthesis of **7g** starting with 3-(2-furyl)-propanol **5g** (0.13 g, 1.0 mmol). The crude material was purified by gradient column chromatography (silica gel, hexanes:EtOAc 10:1) to yield 6-(2-furyl)-(3E)-hexene-2-one **6g** (0.075 g, 0.46 mmol, 46 %) as a colorless oil: R_f 0.48 (hexanes/EtOAc 2:1); IR (thin film) 2919, 1734, 1675, 1627, 1361, 1255, 1010, 734 cm⁻¹; ¹H NMR (500 MHz, CDCl₃) δ 7.32 (d, J = 2.0 Hz, 1H), 6.81 (dt, J = 16.0, 7.0 Hz, 1H), 6.29 (dd, J = 3.5, 2.0 Hz, 1H), 6.11 (dt, J = 16.5, 1.5 Hz, 1H), 6.02 (d, J = 3.0 Hz, 1H), 2.82 (t, J = 7.0 Hz, 2H), 2.59 (app q, J = 7.0 Hz, 2H), 2.24 (s, 3H); ¹³C NMR (100 MHz, CDCl₃) δ 198.4, 154.1, 146.3, 141.1, 131.7, 110.1, 105.4, 30.7, 26.8, 26.5; HRMS (EI, M⁺) for C₁₀H₁₂O₂ calcd 164.0837, found: m/z 164.0838.

6-(2-Furyl)-(3E)-hexene-2-one **6g** (0.36 g, 2.2 mmol) was treated with triisopropylsilyl trifluoromethanesulfonate (0.59 mL, 2.2 mmol) under the previously outlined conditions to obtain (3E)-2-(triisopropylsiloxy)-6-(2-furyl)-1,3-hexadiene, **7g**, (0.62 g, 1.9 mmol, 88 %) as a pale yellow oil: R_f 0.80 (alumina, hexanes:EtOAc 8:1); IR (thin film) 2944, 2867, 1591, 1464, 1321, 1027, 883, 727, 684 cm⁻¹; ¹H NMR (500 MHz, CDCl₃) δ 7.30 (dd, J = 1.5, 0.5 Hz, 1H), 6.27 (dd, J = 3.5, 2.0 Hz, 1H), 6.09 (dt, J = 15.0,

7.0 Hz, 1H), 5.99 (dd, $J = 2.0, 1.0$ Hz, 1H), 5.91 (dt, $J = 15.5, 1.5$ Hz, 1H), 4.23 (s, 1H), 4.18 (s, 1H), 2.74 (t, $J = 7.0$ Hz, 2H), 2.45 (app q, $J = 6.5$ Hz, 2H), 1.19-1.27 (m, 3H), 1.10 (d, $J = 7.0$ Hz, 18H); ^{13}C NMR (125 MHz, CDCl_3) δ 155.5, 155.2, 140.8, 130.0, 128.7, 110.0, 105.0, 93.4, 30.5, 27.8, 18.0, 12.8; HRMS (EI, M^+) for $\text{C}_{19}\text{H}_{32}\text{O}_2\text{Si}$ calcd 320.2172, found: m/z 320.2174.



(3E)-3-Methyl-6-phenyl-2-(triisopropylsiloxy)-1,3-hexadiene, 7h.

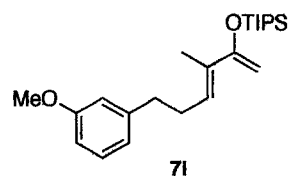
(Carbethoxyethylidene)triphenylphosphorane **11** (0.72 g, 2.0 mmol) was added to a solution of hydrocinnamaldehyde **10** (0.26 mL, 2.0 mmol) in CH_2Cl_2 (7 mL) at room temperature. After 18 h stirring, the reaction was diluted with Et_2O (15 mL). The organic layer was washed with H_2O (2 x 15 mL) and brine (15 mL) and dried (MgSO_4). After filtration and evaporation of solvent under reduced pressure, the crude material was purified by flash column chromatography (silica gel, hexanes: EtOAc 8:1) to yield ethyl 2-methyl-5-phenyl-2E-pentenoate **12** (0.30 g, 1.4 mmol, 69 %) as a colorless oil: R_f 0.64 (hexanes/ EtOAc 2:1); IR (thin film) 2981, 2930, 1709, 1650, 1266, 1116, 1081, 699 cm^{-1} ; ^1H NMR (400 MHz, CDCl_3) δ 7.27-7.32 (m, 2H), 7.17-7.23 (m, 3H), 6.81 (tq, $J = 7.2, 1.2$ Hz, 1H), 4.19 (q, $J = 7.2$ Hz, 2H), 2.76 (t, $J = 7.5$ Hz, 2H), 2.49 (app q, $J = 7.5$ Hz, 2H), 1.79 (dt, $J = 1.2, 1.2$ Hz, 3H), 1.30 (t, $J = 7.2$ Hz, 3H); ^{13}C NMR (100 MHz, CDCl_3) δ 168.0, 141.1, 140.8, 128.3, 128.2 (2 C), 126.0, 60.3, 34.6, 30.5, 14.2, 12.2; HRMS (EI, M^+) for $\text{C}_{14}\text{H}_{18}\text{O}_2$ calcd 218.1307, found: m/z 218.1306.

N,O-Dimethylhydroxylamine hydrochloride (1.18 g, 12.1 mmol) was dissolved in CH₂Cl₂ (50 mL) and the temperature lowered to 0°C. Dimethylaluminum chloride (12.10 mL, 12.1 mmol) was then added to the reaction mixture dropwise *via* syringe. The reaction mixture was stirred for 1 h during which it was slowly allowed to warm to room temperature. A solution of ethyl 2-methyl-5-phenyl-2*E*-pentenoate **12** (0.29 g, 1.3 mmol) in CH₂Cl₂ (50 mL) was then added to the reaction flask dropwise *via* cannula. The reaction was allowed to stir at room temperature for 48 h before being quenched by the addition of H₂O (50 mL). The aqueous and organic layers were separated after 10 min of vigorous stirring. The aqueous layer was extracted with Et₂O (2 x 25 mL) and the combined organic layers were then washed with brine (50 mL). The organic layer was dried (MgSO₄) and the solvent removed by rotary evaporation to yield an orange oil.

The crude material was subsequently re-dissolved in Et₂O (14 mL) and the solution was cooled to -78°C. MeLi (1.6M in Et₂O, 2.0 mmol, 1.3 mL) was added dropwise *via* syringe, during which the reaction mixture changed color from pale orange to dark red. The reaction was quenched at -78°C after stirring for 45 min. Aqueous HCl (1.0M, 10 mL) was added dropwise and the aqueous and organic layers were subsequently separated. The aqueous layer was extracted with Et₂O (2 x 15 mL) and the combined organic layers washed with brine (15 mL). The organic layer was dried (MgSO₄), filtered, and the solvent removed by rotary evaporation to yield a pale yellow oil. The crude material was purified by gradient column chromatography (hexanes/EtOAc 10:1, 9:1, 7:1, 5:1, 3:1) to provide 3-methyl-6-phenyl-3*E*-hexen-2-one **6h** (0.17 g, 0.90 mmol, 68 %) as a clear, colorless oil: R_f 0.60 (hexanes/EtOAc 2:1); IR (thin film) 3027, 2927, 2859, 1668, 1642, 1367, 1277, 700 cm⁻¹; ¹H NMR (400 MHz,

CDCl₃) δ 7.31 (app t, $J = 7.5$ Hz, 2H), 7.19-7.23 (m, 3H), 6.65 (tq, $J = 7.5, 1.5$ Hz, 1H), 2.79 (t, $J = 8.0$ Hz, 2H), 2.57 (app q, $J = 7.5$ Hz, 2H), 2.28 (s, 3H), 1.73 (d, $J = 0.5$ Hz, 3H); ¹³C NMR (125 MHz, CDCl₃) δ 199.8, 142.2, 141.0, 138.2, 128.5, 128.3, 126.2, 34.7, 30.9, 30.3, 25.4; HRMS (EI, M⁺) for C₁₃H₁₆O calcd 188.1201, found: m/z 188.1202.

3-Methyl-6-phenyl-3*E*-hexen-2-one **6h** (0.14 g, 0.73 mmol) was treated with triisopropylsilyl trifluoromethanesulfonate (0.20 mL, 0.73 mmol) under the previously outlined conditions to yield (3*E*)-3-methyl-6-phenyl-2-(triisopropylsiloxy)-1,3-hexadiene, **7h**, (0.57 g, 1.4 mmol, 83 %) as a clear, colorless oil: R_f 0.79 (alumina, hexanes:EtOAc 8:1); IR (thin film) 2945, 2867, 1590, 1463, 1299, 1021, 883, 697 cm⁻¹; ¹H NMR (400 MHz, CDCl₃) δ 7.25-7.29 (m, 2H), 7.16-7.21 (m, 3H), 6.13 (app t, $J = 7.2$ Hz, 1H), 4.36 (d, $J = 0.8$ Hz, 1H), 4.24 (d, $J = 0.8$ Hz, 1H), 2.71 (t, $J = 7.6$ Hz, 2H), 2.47 (app q, $J = 7.6$ Hz, 2H), 1.72 (s, 3H), 1.17-1.27 (m, 3H), 1.09 (d, $J = 7.2$ Hz, 18H); ¹³C NMR (100 MHz, CDCl₃) δ 157.6, 141.9, 131.5, 128.4, 128.3, 127.3, 125.7, 90.0, 35.7, 30.1, 18.1, 13.3, 12.8; HRMS (EI, M⁺) for C₂₂H₃₆OSi calcd 344.2535, found: m/z 344.2528.



(3*E*)-3-Methyl-6-(3-methoxyphenyl)-2-(triisopropylsiloxy)-1,3-hexadiene, **7i**. DMSO (0.36 mL, 5.2 mmol) was added to a solution of oxalyl chloride (0.39 mL, 4.5 mmol) in CH₂Cl₂ (24 mL) at -78 °C.³ The reaction mixture was stirred for 10 min before adding 3-(3-methoxyphenyl)-propanol **5b** (0.46 g, 2.8 mmol) in CH₂Cl₂ (6 mL) *via* cannula. The reaction was stirred for 15 min before the addition of triethylamine (1.5 mL, 11.1 mmol)

dropwise *via* syringe. The reaction was then allowed to stir for another 15 min before transferring a solution of (carboethoxyethylidene)triphenylphosphorane **11** (1.5 g, 4.2 mmol) in CH₂Cl₂ (15 mL) to the stirring reaction mixture at -78°C. The reaction was slowly allowed to warm to room temperature and stirred until the disappearance of starting material was observed by TLC analysis (hexanes/EtOAc 2:1). The reaction was then diluted with Et₂O (15 mL). The cloudy organic layer was then washed with H₂O (2 x 25 mL) and brine (25 mL). The organic layer was dried (MgSO₄) and filtered. The solvent was removed and the crude oil purified by flash column chromatography (silica gel, hexanes:EtOAc 10:1) to yield ethyl 2-methyl-5-(3-methoxyphenyl)-2*E*-pentenoate **14** (0.33 g, 1.3 mmol, 48 %) as a colorless oil: R_f 0.56 (hexanes/EtOAc 2:1); IR (thin film) 2981, 2938, 1710, 1650, 1602, 1489, 1264, 1153, 1114, 1080, 1051 cm⁻¹; ¹H NMR (500 MHz, CDCl₃) δ 7.21 (app dt, *J* = 7.5, 1.0 Hz, 1H), 6.76-6.82 (m, 3H), 6.75 (s, 1H), 4.19 (q, *J* = 7.5 Hz, 2H), 3.80 (s, 3H), 2.73 (t, *J* = 8.5 Hz, 2H), 2.49 (app q, *J* = 8.0 Hz, 2H), 1.80 (s, 3H), 1.29 (t, *J* = 7.0 Hz, 3H); ¹³C NMR (125 MHz, CDCl₃) δ 168.1, 159.7, 142.9, 140.8, 129.4, 128.5, 120.7, 114.1, 111.4, 60.4, 55.1, 34.8, 30.5, 14.3, 12.3; HRMS (EI, M⁺) for C₁₅H₂₀O₃ calcd 248.1412, found: m/z 248.1409.

N,O-Dimethylhydroxylamine hydrochloride (0.16 g, 1.6 mmol) was dissolved in CH₂Cl₂ (20 mL) and the temperature lowered to 0°C. Dimethylaluminum chloride (1.6 mL, 1.6 mmol) was then added to the reaction mixture dropwise *via* syringe. The reaction mixture was stirred for 1 h during which it was slowly warmed to room temperature. A solution of ethyl 2-methyl-5-(3-methoxyphenyl)-2*E*-pentenoate **14** (0.08 g, 0.32 mmol) in CH₂Cl₂ (12 mL) was then added to the reaction flask dropwise *via* cannula. The reaction was allowed to stir at room temperature for 48 h before being

quenched by the addition of H₂O (50 mL). The aqueous and organic layers were separated after 10 min of vigorous stirring. The aqueous layer was extracted with Et₂O (2 x 25 mL) and the combined organic layers were then washed with brine (50 mL). The organic layer was dried (MgSO₄) and the solvent removed by rotary evaporation to yield a yellow oil.

The crude material was subsequently re-dissolved in Et₂O (5 mL) and the temperature dropped to -78°C. MeLi (1.6M in Et₂O, 0.25 mL, 0.4 mmol) was added dropwise *via* syringe. The reaction was quenched after 2 h stirring at low temperature by the addition of HCl aq. (1.0M, 10 mL). The aqueous and organic layers were subsequently separated, and the aqueous layer extracted with Et₂O (2 x 15 mL). The combined organic layers were then washed with brine (15 mL). The organic layer was dried (MgSO₄), filtered, and the solvent removed by rotary evaporation to yield a pale yellow oil. The crude material was purified by flash column chromatography (hexanes/EtOAc 10:1) to isolate 3-methyl-6-(3-methoxyphenyl)-3*E*-hexen-2-one **6i** (0.038 g, 0.17 mmol, 54 %) as a clear, colorless oil: R_f 0.53 (hexanes/EtOAc 2:1); IR (thin film) 3000, 2928, 1668, 1642, 1602, 1489, 1265, 1152, 1051, 780, 696 cm⁻¹; ¹H NMR (400 MHz, CDCl₃) δ 7.22 (app td, *J* = 7.6, 0.4 Hz, 1H), 6.77-6.75-6.81 (m, 3H), 6.64 (tq, *J* = 6.8, 1.2 Hz, 1H), 3.81 (s, 3H), 2.77 (t, *J* = 7.6 Hz, 2H), 2.57 (app q, *J* = 8.0 Hz, 2H), 2.29 (s, 3H), 1.74 (d, *J* = 1.2 Hz, 3H); ¹³C NMR (100 MHz, CDCl₃) δ 199.6, 159.6, 142.5, 142.1, 138.0, 129.4, 120.6, 114.1, 111.2, 55.0, 34.6, 30.6, 25.3, 11.0; HRMS (EI, M⁺) for C₁₄H₁₈O₂ calcd 218.1307, found: m/z 218.1308.

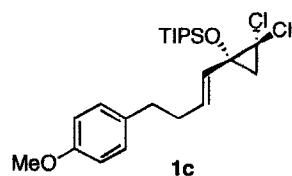
3-Methyl-6-(3-methoxyphenyl)-3*E*-hexen-2-one **6i** (0.11 g, 0.49 mmol) was treated with triisopropylsilyl trifluoromethanesulfonate (0.13 mL, 0.49 mmol) under the

previously outlined conditions to yield (3*E*)-3-methyl-6-(3-methoxyphenyl)-2-(triisopropylsiloxy)-1,3-hexadiene, **7i** (0.15 g, 0.40 mmol, 81 %) as a clear, colorless oil: R_f 0.79 (alumina, hexanes:EtOAc 8:1); IR (thin film) 2945, 2867, 1586, 1464, 1299, 1260, 1152, 1021, 883, 684 cm^{-1} ; ^1H NMR (400 MHz, CDCl_3) δ 7.19 (t, $J = 8.0$ Hz, 1H), 6.80 (d, $J = 8.0$ Hz, 1H), 6.72-6.76 (m, 2H), 6.13 (t, $J = 7.2$ Hz, 1H), 4.37 (s, 1H), 4.24 (s, 1H), 3.80 (s, 3H), 2.69 (t, $J = 8.0$ Hz, 2H), 2.47 (app q, $J = 7.6$ Hz, 2H), 1.74 (d, $J = 0.8$ Hz, 3H), 1.17-1.26 (m, 3H), 1.09 (d, $J = 6.8$ Hz, 18H); ^{13}C NMR (100 MHz, CDCl_3) δ 159.5, 157.4, 143.5, 131.3, 129.1, 127.1, 120.8, 114.1, 111.0, 89.9, 55.0, 35.6, 29.9, 18.0, 13.2, 12.7; HRMS (EI, M^+) for $\text{C}_{23}\text{H}_{38}\text{O}_2\text{Si}$ calcd 374.2641, found: m/z 374.2644.



(1*E*)-1,1-Dichloro-2-(4-(3-methoxyphenyl)-1-butenyl)-2-triisopropylsilyloxycyclopropane, 1b. Siloxy diene, **7b**, (0.26 g, 0.73 mmol) was dissolved in CHCl_3 (0.073 mol, 5.8 mL). Benzyltriethylammonium chloride (0.05 g, 0.22 mmol) was added to the reaction mixture. A solution of 50 % NaOH aq. (0.14 mol, 5.5 mL) was then added in one portion and the reaction was vigorously stirred at room temperature for 30 min. The reaction was quenched by dilution with CH_2Cl_2 (10 mL) and H_2O (10 mL). The organic layer was washed with H_2O (2 x 10 mL). The aqueous layer was extracted with CH_2Cl_2 (2 x 10 mL) and the combined organic layers were dried (MgSO_4). The solvent was removed and the crude oil was purified by flash column chromatography (silica gel, hexanes:EtOAc 50:1) to yield (1*E*)-1,1-dichloro-2-(4-(3-methoxyphenyl)-1-butenyl)-2-triisopropylsilyloxycyclopropane (0.24 g, 0.54 mmol, 75

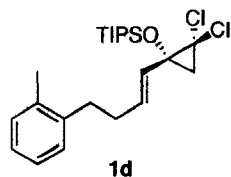
%) as a clear, colorless oil: R_f 0.40 (hexanes/EtOAc 50:1); IR (thin film) 2945, 2867, 1602, 1585, 1465, 1261, 1083, 883, 772, 685 cm^{-1} ; ^1H NMR (500 MHz, CDCl_3) δ 7.20 (t, $J = 8.0$ Hz, 1H), 6.73-6.79 (m, 3H), 5.82 (d, $J = 15.5$ Hz, 1H), 5.74 (dt, $J = 15.5, 6.5$ Hz, 1H), 3.80 (s, 3H), 2.70 (t, $J = 8.5$ Hz, 2H), 2.46 (app q, $J = 7.5$ Hz, 2H), 1.82 (d, $J = 8.5$ Hz, 1H), 1.62 (dd, $J = 8.0, 1.0$ Hz, 1H), 1.04-1.12 (m, 21H); ^{13}C NMR (125 MHz, CDCl_3) δ 159.7, 142.9, 134.0, 129.3, 128.1, 120.7, 114.2, 111.2, 65.4, 64.0, 55.1, 35.2, 33.5, 32.2, 18.0, 17.9, 12.8; HRMS (ESI, $[\text{M}+\text{H}]^+$) for $\text{C}_{23}\text{H}_{37}\text{O}_2\text{SiCl}_2$ calcd 443.1934, found: m/z 443.1937.



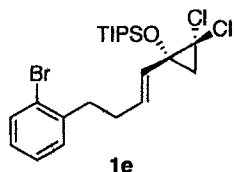
(1E)-1,1-Dichloro-2-(4-(4-methoxyphenyl)-1-butenyl)-2-

triisopropylsilyloxycyclopropane, 1c. The same method was employed in the synthesis of **1c** starting with siloxy diene **7c** (0.36 g, 1.0 mmol). The reaction mixture was diluted with $\text{H}_2\text{O}/\text{CH}_2\text{Cl}_2$ after 20 min and the crude material purified by flash column chromatography (silica gel, hexanes:EtOAc 20:1) to yield (1E)-1,1-dichloro-2-(4-(4-methoxyphenyl)-1-butenyl)-2-triisopropylsilyloxycyclopropane (0.39 g, 0.88 mmol, 88 %) as a clear, colorless oil: R_f 0.26 (hexanes/EtOAc 50:1); IR (thin film) 2945, 2867, 1613, 1513, 1464, 1247, 1040, 883 cm^{-1} ; ^1H NMR (400 MHz, CDCl_3) δ 7.09 (app d, $J = 8.4$ Hz, 2H), 6.83 (app d, $J = 8.4$ Hz, 2H), 5.81 (dd, $J = 15.2, 0.8$ Hz, 1H), 5.74 (dt, $J = 15.2, 6.4$ Hz, 1H), 3.79 (s, 3H), 2.67 (t, $J = 6.8$ Hz, 2H), 2.42 (app q, $J = 6.4$ Hz, 2H), 1.81 (d, $J = 8.4$ Hz, 1H), 1.62 (dd, $J = 8.4, 0.8$ Hz, 1H), 1.03-1.12 (m, 21H); ^{13}C NMR (125 MHz, CDCl_3) δ 157.9, 134.2, 133.4, 129.2, 127.9, 113.8, 64.0, 65.9, 55.2, 34.3,

33.9, 32.2, 18.0, 17.9, 12.8; HRMS (EI, M^+) for $C_{23}H_{36}O_2SiCl_2$ calcd 442.1862, found: m/z 442.1872.

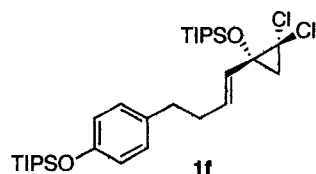


(1E)-1,1-Dichloro-2-(4-(2-methylphenyl)-1-butenyl)-2-triisopropylsilyloxycyclopropane, 1d. The same method was employed in the synthesis of **1d** starting with siloxy diene **7d** (0.29 g, 0.85 mmol). The reaction mixture was diluted with H_2O/CH_2Cl_2 after 30 min and the crude material purified by flash column chromatography (silica gel, hexanes:EtOAc 20:1) to yield (1E)-1,1-dichloro-2-(4-(2-methylphenyl)-1-butenyl)-2-triisopropylsilyloxycyclopropane (0.19 g, 0.45 mmol, 53 %) as a clear, colorless oil: R_f 0.67 (hexanes/EtOAc 50:1); IR (thin film) 2945, 2967, 1463, 1222, 1083, 883, 683 cm^{-1} ; 1H NMR (400 MHz, $CDCl_3$) δ 7.10-7.18 (m, 4H), 5.86 (dd, $J = 15.5, 0.5$ Hz, 1H), 5.80 (dt, $J = 15.5, 6.0$ Hz, 1H), 2.71 (br t, $J = 7.5$ Hz, 2H), 2.42 (app q, $J = 6.5$ Hz, 2H), 2.31 (s, 3H), 1.85 (d, $J = 8.0$ Hz, 1H), 1.64 (dd, $J = 8.0, 1.0$ Hz, 1H), 1.06-1.14 (m, 21H); ^{13}C NMR (125 MHz, $CDCl_3$) δ 139.5, 135.8, 134.3, 130.2, 128.6, 127.9, 126.1, 126.0, 65.4, 64.0, 32.5, 32.4, 32.2, 19.2, 18.0, 18.0, 12.8; HRMS (ESI, $[M+H]^+$) for $C_{23}H_{37}OSiCl_2$ calcd, 427.1985 found: m/z 427.1986.



(1E)-1,1-Dichloro-2-(4-(2-bromophenyl)-1-butenyl)-2-triisopropylsilyloxycyclopropane, 1e. The same method was employed in the synthesis

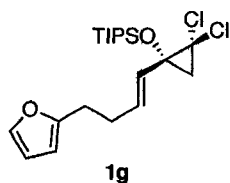
of **1e** starting with siloxy diene **7e** (0.57 g, 1.4 mmol). The reaction mixture was diluted with H₂O/CH₂Cl₂ after 45 min and the crude material purified by flash column chromatography (silica gel, hexanes:EtOAc 20:1) to yield (*IE*)-1,1-dichloro-2-(4-(2-bromophenyl)-1-butenyl)-2-triisopropylsilyloxycyclopropane (0.49 g, 1.0 mmol, 72 %) as a clear, colorless oil: R_f 0.48 (hexanes/EtOAc 50:1); IR (thin film) 2944, 2866, 1470, 1221, 1083, 1024, 882, 749, 682 cm⁻¹; ¹H NMR (400 MHz, CDCl₃) δ 7.53 (dd, *J* = 8.0, 1.5 Hz, 1H), 7.18-7.24 (m, 2H), 7.04-7.08 (m, 1H), 5.85 (dd, *J* = 15.5, 1.0 Hz, 1H), 5.77 (dt, *J* = 15.5, 6.5 Hz, 1H), 2.85 (t, *J* = 7.0 Hz, 2H), 2.46 (app q, *J* = 6.5 Hz, 2H), 1.84 (d, *J* = 8.5 Hz, 1H), 1.63 (dd, *J* = 8.0, 0.5 Hz, 1H), 1.05-1.12 (m, 21H); ¹³C NMR (125 MHz, CDCl₃) δ 140.5, 133.7, 132.9, 130.2, 128.3, 127.7, 127.4, 124.4, 65.4, 64.0, 35.4, 32.2, 32.1, 18.0, 18.0, 12.8; HRMS (ESI, [M+Na]⁺) for C₂₂H₃₃OSiBrCl₂Na calcd 513.0753, found: m/z 513.0754.



(*IE*)-1,1-Dichloro-2-(4-(4-triisopropylsilyloxyphenyl)-1-butenyl)-2-

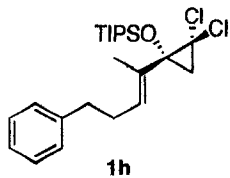
triisopropylsilyloxycyclopropane, 1f. The same method was employed in the synthesis of **1f** starting with siloxy diene **7f** (0.15 g, 0.31 mmol). The reaction mixture was diluted with H₂O/CH₂Cl₂ after 40 min and the crude material purified by flash column chromatography (silica gel, hexanes:EtOAc 20:1) to yield (*IE*)-1,1-dichloro-2-(4-(4-triisopropylsilyloxyphenyl)-1-butenyl)-2-triisopropylsilyloxycyclopropane (0.14 g, 0.24 mmol, 77 %) as a clear, colorless oil: R_f 0.40 (hexanes/EtOAc 50:1); IR (thin film) 3029, 2945, 2867, 1609, 1510, 1463, 1264, 1083, 917, 883, 684 cm⁻¹; ¹H NMR (500 MHz,

CDCl₃) δ7.01 (app d, *J* = 8.0 Hz, 2H), 6.79 (app d, *J* = 8.0 Hz, 2H), 5.81 (dd, *J* = 15.5, 0.5 Hz, 1H), 5.73 (dt, *J* = 15.5, 6.5 Hz, 1H), 2.60-2.69 (m, 2H), 2.41 (app q, *J* = 7.0 Hz, 2H), 1.80 (d, *J* = 8.5 Hz, 1H), 1.61 (dd, *J* = 8.5, 0.5 Hz, 1H), 1.21-1.30 (m, 3H), 1.10 (d, *J* = 7.5 Hz, 18H), 1.04-1.07 (m, 21H); ¹³C NMR (100 MHz, CDCl₃) δ 154.2, 134.3, 133.6, 129.1, 127.8, 119.7, 64.0, 34.4, 33.9, 32.2, 18.0, 18.0, 17.9, 12.8, 12.7; HRMS (ESI, [M+H]⁺) for C₃₁H₅₅O₂Si₂Cl₂ calcd 585.3112, found: *m/z* 585.3112.



(*1E*)-1,1-Dichloro-2-(4-(2-furyl)-1-butenyl)-2-triisopropylsilyloxycyclopropane, 1g.

The same method was employed in the synthesis of **1g** starting with siloxy diene **7g** (0.084 g, 0.26 mmol). The reaction mixture was diluted with H₂O/CH₂Cl₂ after 7 min and the crude material purified by flash column chromatography (silica gel, hexanes:EtOAc 20:1) to yield (*1E*)-1,1-dichloro-2-(4-(2-furyl)-1-butenyl)-2-triisopropylsilyloxycyclopropane (0.10 g, 0.25 mmol, 95 %) as a clear, yellow oil: *R_f* 0.53 (hexanes/EtOAc 50:1); IR (thin film) 2945, 2867, 1669, 1597, 1464, 1223, 1083, 883, 729, 683 cm⁻¹; ¹H NMR (500 MHz, CDCl₃) δ 7.29-7.30 (m, 1H), 6.27 (dd, *J* = 2.0, 3.5 Hz, 1H), 5.99 (dd, *J* = 3.0, 0.5 Hz, 1H), 5.82 (dd, *J* = 16.0, 1.0 Hz, 1H), 5.75 (dt, *J* = 15.5, 6.5 Hz, 1H), 2.69-2.79 (m, 2H), 2.48 (app q, *J* = 7.0 Hz, 2H), 1.81 (d, *J* = 8.5 Hz, 1H), 1.63 (dd, *J* = 8.5, 1.0 Hz, 1H), 1.02-1.15 (m, 21H); ¹³C NMR (125 MHz, CDCl₃) δ 155.0, 140.9, 133.5, 128.4, 110.1, 105.1, 63.9, 32.3, 30.4, 27.4, 18.0, 18.0, 12.8; HRMS (ESI, [M+H]⁺) for C₂₀H₃₃O₂SiCl₂ calcd 403.1621, found: *m/z* 403.1621.



(2E)-1,1-Dichloro-2-(5-phenyl-2-penten-2-yl)-2-triisopropylsilyloxycyclopropane, 1h.

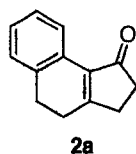
The same method was employed in the synthesis of **1h** starting with siloxy diene **7h** (0.24 g, 0.69 mmol). The reaction mixture was diluted with H₂O/CH₂Cl₂ after 45 min and the crude material purified by flash column chromatography (silica gel, hexanes:EtOAc 50:1) to yield (2E)-1,1-dichloro-2-(5-phenyl-2-penten-2-yl)-2-triisopropylsilyloxycyclopropane (0.27 g, 0.63 mmol, 91 %) as a clear, colorless oil: R_f 0.68 (hexanes/EtOAc 50:1); IR (thin film) 2945, 2868, 1464, 1256, 1087, 1071, 884, 686 cm⁻¹; ¹H NMR (500 MHz, CDCl₃) δ 7.26-7.29 (m, 2H), 7.17-7.20 (m, 3H), 5.47 (tq, *J* = 7.0, 1.0 Hz, 1H), 2.67 (t, *J* = 8.0 Hz, 2H), 2.36-2.43 (m, 2H), 1.92 (d, *J* = 8.5 Hz, 1H), 1.87 (d, *J* = 1.0 Hz, 3H), 1.62 (d, *J* = 8.5 Hz, 1H), 1.04-1.14 (m, 21H); ¹³C NMR (125 MHz, CDCl₃) δ 141.6, 133.6, 129.3, 128.3, 128.3, 125.9, 68.2, 64.7, 35.0, 31.7, 29.3, 18.0, 17.9, 14.4, 12.7; HRMS (ESI, [M+Na]⁺) for C₂₃H₃₆OSiCl₂Na calcd 449.1805, found: *m/z* 449.1799.



(2E)-1,1-Dichloro-2-(5-(3-methoxyphenyl)-2-penten-2-yl)-2-

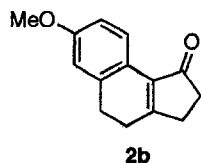
triisopropylsilyloxycyclopropane, 1i. The same method was employed in the synthesis of **1i** starting with siloxy diene **7i** (0.13 g, 0.34 mmol). The reaction mixture was diluted with H₂O/CH₂Cl₂ after 1.5 h and the crude material purified by flash column chromatography (silica gel, hexanes:EtOAc 20:1) to yield (2E)-1,1-dichloro-2-(5-(3-

methoxyphenyl)-2-penten-2-yl)-2-triisopropylsilyloxycyclopropane (0.14 g, 0.30 mmol, 88 %) as a clear, colorless oil: R_f 0.56 (hexanes/EtOAc 50:1); IR (thin film) 2945, 2867, 1602, 1585, 1464, 1257, 1084, 1046, 883, 687 cm^{-1} ; ^1H NMR (500 MHz, CDCl_3) δ 7.20 (td, $J = 7.5, 1.0$ Hz, 1H), 6.74-6.78 (m, 2H), 6.73 (s, 1H), 5.47 (tq, $J = 7.0, 1.0$ Hz, 1H), 3.80 (s, 3H), 2.65 (t, $J = 8.0$ Hz, 2H), 2.36-2.42 (m, 2H), 1.92 (d, $J = 8.5$ Hz, 1H), 1.88 (s, 3H), 1.63 (d, $J = 8.5$ Hz, 1H), 1.04-1.14 (m, 21H); ^{13}C NMR (125 MHz, CDCl_3) δ 159.7, 143.2, 133.6, 129.3 (2 C), 120.7, 114.2, 111.1, 68.2, 64.7, 55.1, 35.1, 31.7, 29.2, 18.0, 17.9, 14.4, 12.7; HRMS (ESI, $[\text{M}+\text{Na}]^+$) for $\text{C}_{24}\text{H}_{38}\text{O}_2\text{SiCl}_2\text{Na}$ calcd 479.1910, found: m/z 479.1909.

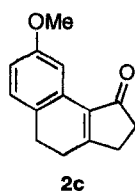


2,3,4,5-Tetrahydrocyclopenta[*a*]naphthalen-1-one, 2a. (*IE*)-1,1-dichloro-2-(4-phenyl-1-buten-1-yl)-2-triisopropylsilyloxycyclopropane, **1a**, (0.17 g, 0.42 mmol) was dissolved in acetonitrile (0.05 M, 8.3 mL). AgBF_4 (0.082 g, 0.42 mmol) was added in one portion and the reaction flask was equipped with a reflux condenser. The reaction was stirred at reflux for 12 h and was then allowed to cool to room temperature. The reaction mixture was then filtered through a short pad of Celite and silica gel. After removal of the solvent, the crude material was purified by gradient column chromatography (silica gel, hexanes:EtOAc 5:1) to yield 2,3,4,5-tetrahydrocyclopenta[*a*]naphthalen-1-one (0.062 g, 0.34 mmol, 80 %) as an off-white solid: m.p. 102-104°C; R_f 0.07 (hexanes/EtOAc 8:1); IR (thin film) 3067, 2947, 2933, 2906, 2841, 1683, 1629, 1435, 765 cm^{-1} ; ^1H NMR (500 MHz, CDCl_3) δ 8.24 (d, $J = 7.5$ Hz, 1H), 7.17-7.25 (m, 3H), 2.96 (t, $J = 8.0$ Hz, 2H), 2.68-2.70 (m, 2H), 2.66 (t, $J = 8.0$ Hz, 2H), 2.57-2.59 (m, 2H); ^{13}C NMR (125 MHz,

CDCl₃) δ 206.1, 174.8, 134.9, 134.4, 129.1, 127.8, 127.5, 126.7, 123.9, 35.9, 29.2, 27.6, 27.1; HRMS (EI, M⁺) for C₁₃H₁₂O calcd 184.0888, found: m/z 184.0886.

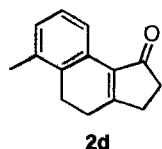


7-Methoxy-2,3,4,5-tetrahydro-cyclopenta[a]naphthalen-1-one, 2b. The previously outlined procedure was used in the preparation of **2b** from (*IE*)-1,1-dichloro-2-(4-(3-methoxyphenyl)-1-buten-1-yl)-2-triisopropylsilyloxycyclopropane, **1b**, (0.13 g, 0.29 mmol). The reaction was cooled to room temperature after 7 h stirring at reflux. The crude material was purified by column chromatography (silica gel, hexanes:EtOAc 5:1) to yield **2b** (0.033 g, 0.15 mmol, 53 %) as an off-white solid: m.p. 93-97°C; R_f 0.15 (hexanes/EtOAc 8:1); IR (thin film) 2935, 2838, 1680, 1607, 1502, 1253, 1037, 872 cm⁻¹; ¹H NMR (500 MHz, CDCl₃) δ 8.18 (d, *J* = 8.5 Hz, 1H), 6.74-6.80 (m, 2H), 3.81 (s, 3H), 2.93 (t, *J* = 8.0 Hz, 2H), 2.65-2.67 (m, 2H), 2.63 (t, *J* = 8.5 Hz, 2H), 2.55-2.57 (m, 2H); ¹³C NMR (125 MHz, CDCl₃) δ 206.2, 172.3, 159.2, 136.4, 134.7, 125.1, 122.2, 114.0, 111.0, 55.2, 35.9, 29.1, 28.0, 26.9; HRMS (EI, M⁺) for C₁₄H₁₄O₂ calcd 214.0994, found: m/z 214.0996.



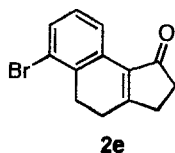
8-Methoxy-2,3,4,5-tetrahydro-cyclopenta[a]naphthalen-1-one, 2c. The previously outlined procedure was used in the preparation of **2c** from (*IE*)-1,1-dichloro-2-(4-(4-methoxyphenyl)-1-buten-1-yl)-2-triisopropylsilyloxycyclopropane, **1c**, (0.17 g, 0.38

mmol). The reaction was cooled to room temperature after 24 h stirring at reflux. The crude material was purified by column chromatography (silica gel, hexanes:EtOAc 5:1) to yield **2c** (0.043 g, 0.20 mmol, 53 %) as an off-white solid: m.p. 98-101°C; R_f 0.13 (hexanes/EtOAc 8:1); IR (thin film) 2937, 2838, 1692, 1607, 1495, 1218, 1041 cm^{-1} ; ^1H NMR (500 MHz, CDCl_3) δ 7.89 (d, $J = 2.5$ Hz, 1H), 7.08 (d, $J = 8.5$ Hz, 1H), 6.76 (dd, $J = 8.5, 3.0$ Hz, 1H), 3.83 (s, 3H), 2.89 (t, $J = 8.0$ Hz, 2H), 2.68-2.69 (m, 2H), 2.63 (t, $J = 8.5$ Hz, 2H), 2.57-2.59 (m, 2H); ^{13}C NMR (125 MHz, CDCl_3) δ 206.0, 175.5, 158.5, 134.8, 130.0, 128.2, 126.4, 113.8, 109.1, 55.4, 35.8, 29.9, 27.4, 26.8; HRMS (EI, M^+) for $\text{C}_{14}\text{H}_{14}\text{O}_2$ calcd 214.0994, found: m/z 214.0995.

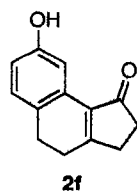


6-Methyl-2,3,4,5-tetrahydro-cyclopenta[a]naphthalen-1-one, 2d. The previously outlined procedure was used in the preparation of **2d** from (*1E*)-1,1-dichloro-2-(4-(2-methylphenyl)-1-buten-1-yl)-2-triisopropylsilyloxycyclopropane, **1d**, (0.06 g, 0.14 mmol). The reaction was cooled to room temperature after 7 h stirring at reflux. The crude material was purified by column chromatography (silica gel, hexanes:EtOAc 5:1) to yield **2d** (0.022 g, 0.11 mmol, 79 %) as an off-white solid: m.p. 95-97°C; R_f 0.18 (hexanes/EtOAc 8:1); IR (thin film) 2949, 2922, 2902, 1682, 1635, 1476, 1428, 1378, 1044, 949, 795 cm^{-1} ; ^1H NMR (500 MHz, CDCl_3) δ 8.16 (d, $J = 7.5$ Hz, 1H), 7.15 (t, $J = 7.5$ Hz, 1H), 7.08 (d, $J = 7.5$ Hz, 1H), 2.90 (t, $J = 8.0$ Hz, 2H), 2.65-2.68 (m, 4H), 2.56-2.58 (m, 2H), 2.30 (s, 3H); ^{13}C NMR (125 MHz, CDCl_3) δ 206.1, 174.2, 135.0, 134.9,

132.6, 129.9, 129.0, 126.1, 121.9, 35.9, 29.0, 26.8, 23.6, 20.0; HRMS (EI, M⁺) for C₁₄H₁₄O calcd 198.1045, found: m/z 198.1047.

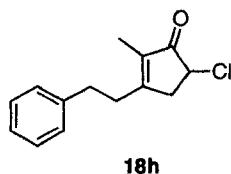


6-Bromo-2,3,4,5-tetrahydro-cyclopenta[a]naphthalen-1-one, 2e. The previously outlined procedure was used in the preparation of **2e** from (*IE*)-1,1-dichloro-2-(4-(2-bromophenyl)-1-buten-1-yl)-2-triisopropylsilyloxycyclopropane, **1e**, (0.23 g, 0.48 mmol). The reaction was cooled to room temperature after 24 h stirring at reflux. The crude material was purified by column chromatography (silica gel, hexanes:EtOAc 5:1) to yield **2e** (0.61 g, 0.23 mmol, 48 %) as a white solid: m.p. 92-95°C; R_f 0.12 (hexanes/EtOAc 8:1); IR (thin film) 2922, 1688, 1637, 1554, 1464, 1430, 1384, 1167, 1114, 941, 796, 722 cm⁻¹; ¹H NMR (400 MHz, CDCl₃) δ 8.26 (dd, *J* = 7.6, 0.8 Hz, 1H), 7.45 (dd, *J* = 8.0, 1.2 Hz, 1H), 7.11 (t, *J* = 7.6 Hz, 1H), 3.10 (t, *J* = 8.0 Hz, 2H), 2.67-2.71 (m, 4H), 2.59-2.61 (m, 2H); ¹³C NMR (100 MHz, CDCl₃) δ 205.3, 175.2, 134.2, 133.6, 131.9, 131.0, 127.9, 123.6, 123.0, 35.9, 28.8, 27.2, 26.5; HRMS (EI, M⁺) for C₁₃H₁₁OBr calcd 261.9993, found: m/z 261.9994.



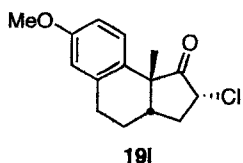
8-Hydroxy-2,3,4,5-tetrahydro-cyclopenta[a]naphthalen-1-one, 2f. The previously outlined procedure was used in the preparation of **2f** from (*IE*)-1,1-dichloro-2-(4-(4-triisopropylsiloxyphenyl)-1-buten-1-yl)-2-triisopropylsilyloxycyclopropane, **1f**, (0.13 g,

0.22 mmol). The reaction was cooled to room temperature after 48 h stirring at reflux. The crude material was purified by column chromatography (silica gel, hexanes:EtOAc 3:1) to yield **2f** (0.017 g, 0.085 mmol, 39 %) as a white solid: m.p. 197-200°C; R_f 0.21 (hexanes/EtOAc 2:1); IR (thin film) 3225, 2922, 2810, 1655, 1625, 1451, 1397, 1235, 895, 833 cm^{-1} ; ^1H NMR (500 MHz, CDCl_3) δ 7.96 (d, $J = 2.5$ Hz, 1H), 7.06 (t, $J = 8.0$ Hz, 1H), 6.73 (dd, $J = 8.0, 2.5$ Hz, 1H), 6.08 (br s, 1H), 2.89 (t, $J = 8.0$ Hz, 2H), 2.68-2.71 (m, 2H), 2.65 (t, $J = 8.5$ Hz, 2H), 2.60-2.62 (m, 2H); ^{13}C NMR (125 MHz, CDCl_3) δ 207.0, 176.6, 154.9, 134.6, 129.6, 128.4, 125.8, 114.4, 111.0, 35.8, 29.3, 27.4, 26.6; HRMS (EI, M^+) for $\text{C}_{13}\text{H}_{12}\text{O}_2$ calcd 200.0837, found: m/z 200.0837.

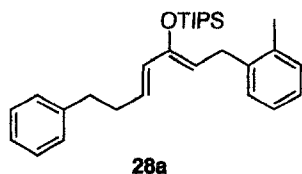


5-Chloro-2-methyl-3-(2-phenylethyl)-cyclopent-2-en-1-one, 18h. The previously outlined procedure was used in the preparation of **18h** from (*2E*)-1,1-dichloro-2-(5-phenyl-2-penten-2-yl)-2-triisopropylsilyloxycyclopropane, **1h**, (0.064 g, 0.15 mmol). The reaction was cooled to room temperature after 6 h stirring at reflux. The crude material was purified by gradient column chromatography (silica gel, hexanes:EtOAc 25:1, 20:1, 15:1, 10:1, 8:1, etc.) to yield **18h** (0.034 g, 0.14 mmol, 97 %) as a white solid: m.p. 41-43°C; R_f 0.19 (hexanes/EtOAc 8:1); IR (thin film) 3027, 2924, 1711, 1642, 1454, 1385, 751, 700 cm^{-1} ; ^1H NMR (500 MHz, CDCl_3) δ 7.30 (t, $J = 7.5$ Hz, 2H), 7.23 (t, $J = 7.0$ Hz, 1H), 7.16 (d, $J = 7.0$ Hz, 2H), 4.21 (dd, $J = 6.5, 2.5$ Hz, 1H), 3.07 (br dd, $J = 18.5, 6.5$ Hz, 1H), 2.84-2.87 (m, 2H), 2.71-2.80 (m, 2H), 2.67 (br d, $J = 18.5$ Hz, 1H), 1.63 (t, $J = 2.0$ Hz, 3H); ^{13}C NMR (125 MHz, CDCl_3) δ 202.2, 169.6, 140.1, 135.1,

128.7, 128.2, 126.6, 52.9, 40.7, 33.0, 32.8, 8.2; HRMS (EI, M^+) for $C_{14}H_{15}OCl$ calcd 234.0811, found: m/z 234.0809.



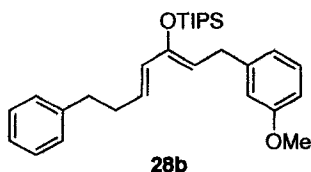
2-Chloro-7-methoxy-9b-methyl-2,3,3a,4,5,9b-hexahydro-cyclopenta[a]naphthalen-1-one, 19i. The previously outlined procedure was used in the preparation of **19i** from (2*E*)-1,1-dichloro-2-(5-(3-methoxyphenyl)-2-penten-2-yl)-2-triisopropylsilyloxycyclopropane, **1i**, (0.049 g, 0.11 mmol). The reaction was cooled to room temperature after 18 h stirring at reflux. The crude material was purified by gradient column chromatography (silica gel, hexanes:EtOAc 10:1, 9:1, 8:1, 7:1, etc.) to yield **19i** (0.026 g, 0.098 mmol, 89 %) as a white solid: m.p. 98-100°C; R_f 0.25 (hexanes/EtOAc 8:1); IR (thin film) 2928, 2863, 1750, 1608, 1499, 1453, 1260, 1244, 1037, 834 cm^{-1} ; 1H NMR (400 MHz, $CDCl_3$) δ 7.47 (d, $J = 8.8$ Hz, 1H), 6.76 (dd, $J = 8.8, 2.8$ Hz, 1H), 6.60 (d, $J = 2.8$ Hz, 1H), 4.25 (dd, $J = 10.8, 8.4$ Hz, 1H), 3.77 (s, 3H), 2.87 (ddd, $J = 18.4, 12.4, 6.4$ Hz, 1H), 2.76 (ddd, $J = 17.6, 6.0, 2.8$ Hz, 1H), 2.51 (ddd, $J = 12.8, 8.4, 5.6$ Hz, 1H), 2.25 (dddd, $J = 18.0, 5.6, 3.6, 3.6$ Hz, 1H), 1.90-2.08 (m, 3H), 1.43 (s, 3H); ^{13}C NMR (100 MHz, $CDCl_3$) δ 212.6, 158.1, 136.2, 130.1, 126.2, 113.8, 113.0, 56.9, 55.0, 49.3, 39.8, 33.7, 26.9, 24.9, 20.8; HRMS (ESI, $[M+Na]^+$) for $C_{15}H_{17}O_2ClNa$ calcd 287.0809, found: m/z 287.0809.



(2Z, 4E)-1-(2-Methylphenyl)-7-phenyl-3-(triisopropylsiloxy)-2,4-heptadiene, 28a.

Dimethyl 4-(2-methylphenyl)-2-oxobutylphosphonate⁷ (0.26 g, 0.96 mmol) was dissolved in THF (2 mL). This solution was transferred by cannula to a suspension of NaH (0.020 g, 0.88 mmol) in THF (1 mL) at 0°C. The reaction was allowed to stir for 10 min at low temperature before removal of the ice bath and subsequent stirring at room temperature for 30 min. Hydrocinnamaldehyde (0.053 mL, 0.40 mmol) in THF (2 mL) was then transferred by cannula to the reaction mixture, which was allowed to stir for another 18 h before the addition of glacial acetic acid. The crude material was then filtered through a short pad of silica gel (EtOAc) and the solvent removed under reduced pressure to provide a yellow oil. The crude material was purified by gradient column chromatography (silica gel, hexanes:EtOAc 10:1, 9:1, 8:1, 7:1, etc.) to yield 1-(2-methylphenyl)-7-phenyl-(4E)-hepten-3-one **27a** as a clear, colorless oil: R_f 0.62 (silica gel, hexanes:EtOAc 2:1); IR (thin film) 3062, 3026, 2931, 2860, 1696, 1670, 1629, 1495, 1454, 977, 747 cm^{-1} ; ^1H NMR (500 MHz, CDCl_3) δ 7.30 (pseudo t, $J = 7.0$ Hz, 2H), 7.11-7.23 (m, 7H), 6.85 (dt, $J = 16.0, 7.0$ Hz, 1H), 6.13 (dt, $J = 16.0, 1.5$ Hz, 1H), 2.90-2.93 (m, 2H), 2.76-2.81 (m, 4H), 2.54 (pseudo q, $J = 7.0$ Hz, 2H), 2.32 (s, 3H); ^{13}C NMR (125 MHz, CDCl_3) δ 199.5, 146.2, 140.7, 139.3, 135.9, 130.7, 130.3, 128.6, 128.5, 128.3, 126.2, 126.2, 126.1, 40.4, 34.4, 34.1, 27.5, 19.3; HRMS (EI, M^+) for $\text{C}_{20}\text{H}_{22}\text{O}$ calcd 278.1670, found: m/z 278.1671.

1-(2-Methylphenyl)-7-phenyl-(4*E*)-hepten-3-one **27a** (0.090 g, 0.32 mmol) was dissolved in anhydrous THF (1.0 mL). The solution was cooled to 0°C, and freshly distilled triethylamine (0.11 mL, 0.80 mmol) was added dropwise to the reaction mixture. Triisopropylsilyl trifluoromethanesulfonate (0.094 mL, 0.35 mmol) was added dropwise and the solution was stirred at 0°C for 1.5 h. The reaction was quenched with a mixture of triethylamine (0.5 mL), hexanes (2.5 mL), and saturated NaHCO₃ solution (5 mL). The organic layer was washed with H₂O (2 x 5 mL) and brine (5 mL) and dried (MgSO₄). After filtration, the solvent was removed and the crude oil purified by flash column chromatography (alumina, hexanes:EtOAc:TEA 50:1:1) to yield (2*Z*, 4*E*)-1-(2-methylphenyl)-7-phenyl-3-(triisopropylsiloxy)-2,4-heptadiene, **28a**, (0.12 g, 0.27 mmol, 86 %) as a clear, colorless oil: *R_f* 0.81 (alumina, hexanes:EtOAc 8:1); IR (thin film) 3026, 2944, 2866, 1651, 1462, 1014, 883, 742, 698, 682 cm⁻¹; ¹H NMR (500 MHz, CDCl₃) δ 7.28 (t, *J* = 8.5 Hz, 2H), 7.10-7.20 (m, 7H), 5.90 (d, *J* = 15.5 Hz, 1H), 5.85 (dd, *J* = 15.5, 6.0 Hz, 1H), 4.74 (t, *J* = 7.0 Hz, 1H), 3.45 (d, *J* = 7.0 Hz, 2H), 2.72 (t, *J* = 7.5 Hz, 2H), 2.43 (pseudo q, *J* = 7.5 Hz, 2H), 2.29 (s, 3H), 1.10-1.19 (m, 21H); ¹³C NMR (125 MHz, CDCl₃) δ 149.6, 141.7, 139.8, 136.3, 130.0, 129.6, 128.7, 128.6, 128.4, 128.3, 126.0, 126.0, 125.9, 109.5, 35.7, 34.0, 30.1, 19.5, 18.2, 13.8; HRMS (EI, M⁺) for C₂₉H₄₂OSi calcd 434.3005, found: *m/z* 434.3004.



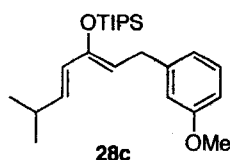
(2*Z*, 4*E*)-1-(3-Methoxyphenyl)-7-phenyl-3-(triisopropylsiloxy)-2,4-heptadiene, 28b.

The previously outlined procedure was used in the synthesis of **28b** starting with dimethyl 4-(3-methoxyphenyl)-2-oxobutylphosphonate⁷ (0.29 g, 1.0 mmol) and

hydrocinnamaldehyde (0.069 mL, 0.53 mmol). The crude material was purified by gradient column chromatography (silica gel, hexanes:EtOAc 10:1, 9:1, 8:1, 7:1, etc.) to yield 1-(3-methoxyphenyl)-7-phenyl-(4*E*)-hepten-3-one **27b** as a clear, colorless oil: R_f 0.57 (silica gel, hexanes:EtOAc 2:1); IR (thin film) 3027, 2935, 2860, 1695, 1671, 1629, 1602, 1491, 1454, 1260, 1153, 1050, 976, 781, 699 cm^{-1} ; ^1H NMR (500 MHz, CDCl_3) δ 7.31 (pseudo t, $J = 7.5$ Hz, 2H), 7.18-7.24 (m, 4H), 6.86 (dt, $J = 16.0, 7.0$ Hz, 1H), 6.80 (d, $J = 8.0$ Hz, 1H), 6.76-6.77 (m, 2H), 6.13 (dt, $J = 16.0, 1.0$ Hz, 1H), 3.81 (s, 3H), 2.91-2.94 (m, 2H), 2.84-2.88 (m, 2H), 2.79 (t, $J = 7.5$ Hz, 2H), 2.55 (pseudo q, $J = 7.0$ Hz, 2H); ^{13}C NMR (125 MHz, CDCl_3) δ 199.3, 159.7, 146.3, 142.9, 140.7, 130.7, 129.5, 128.5, 128.3, 126.2, 120.7, 114.2, 111.4, 55.2, 41.6, 34.4, 34.1, 30.1; HRMS (EI, M^+) for $\text{C}_{20}\text{H}_{22}\text{O}_2$ calcd 294.1620, found: m/z 294.1618.

1-(3-Methoxyphenyl)-7-phenyl-(4*E*)-hepten-3-one **27b** (0.40 g, 0.14 mmol) was treated with triisopropylsilyl trifluoromethanesulfonate (0.072 mL, 0.27 mmol) under the previously outlined conditions to yield (2*Z*, 4*E*)-1-(3-methoxyphenyl)-7-phenyl-3-(triisopropylsiloxy)-2,4-heptadiene, **28b**, (0.040 g, 0.09 mmol, 63 %) as a clear, colorless oil: R_f 0.63 (alumina, hexanes:EtOAc 8:1); IR (thin film) 3027, 2944, 2866, 1601, 1490, 1465, 1454, 1258, 1149, 1015, 884, 696 cm^{-1} ; ^1H NMR (400 MHz, CDCl_3) δ 7.31 (pseudo t, $J = 7.2$ Hz, 2H), 7.20-7.24 (m, 4H), 6.84 (d, $J = 7.6$ Hz, 1H), 6.80 (br s, 1H), 6.76 (dd, $J = 8.0, 2.4$ Hz, 1H), 5.95 (d, $J = 15.2$ Hz, 1H), 5.90 (dd, $J = 15.6, 5.6$ Hz, 1H), 4.86 (t, $J = 7.2$ Hz, 1H), 3.82 (s, 3H), 3.49 (d, $J = 7.2$ Hz, 2H), 2.76 (t, $J = 7.2$ Hz, 2H), 2.47 (m, 2H), 1.12-1.23 (m, 21H); ^{13}C NMR (100 MHz, CDCl_3) δ 159.7, 149.6, 143.3, 141.6, 129.5, 129.2, 128.8, 128.4, 128.3, 125.8, 120.8, 114.0, 111.2, 109.9, 55.1, 35.6,

33.9, 32.2, 18.1, 13.8; HRMS (EI, M^+) for $C_{29}H_{42}O_2Si$ calcd 450.2954, found: m/z 450.2955.

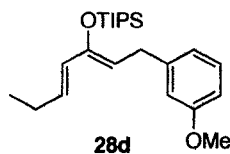


(2Z, 4E)-1-(3-Methoxyphenyl)-6-methyl-3-(triisopropylsiloxy)-2,4-heptadiene, 28c.

The previously outlined procedure was used in the synthesis of **28c** starting with dimethyl 4-(3-methoxyphenyl)-2-oxobutylphosphonate⁷ (0.46 g, 1.6 mmol) and isobutyraldehyde (0.060 mL, 0.66 mmol). The crude material was purified by gradient column chromatography (silica gel, hexanes:EtOAc 10:1, 9:1, 8:1, 7:1, etc.) to yield 1-(3-methoxyphenyl)-6-methyl-(4E)-hepten-3-one **27c** (0.087 g, 0.38 mmol, 57 %) as a pale yellow oil: R_f 0.66 (silica gel, hexanes:EtOAc 2:1); IR (thin film) 2962, 2871, 1672, 1602, 1491, 1260, 1153, 1051, 982, 780 cm^{-1} ; 1H NMR (500 MHz, $CDCl_3$) δ 7.20 (t, $J = 8.0$ Hz, 1H), 6.74-6.81 (m, 4H), 6.05 (dd, $J = 16.0, 1.5$ Hz, 1H), 3.80 (s, 3H), 2.85-2.93 (m, 4H), 2.46 (pseudo oct-of-d, $J = 7.0, 1.5$ Hz, 1H), 1.06 (d, $J = 7.0$ Hz, 6H); ^{13}C NMR (125 MHz, $CDCl_3$) δ 199.8, 159.7, 153.7, 143.0, 129.4, 127.5, 120.7, 114.2, 111.3, 55.1, 41.6, 31.1, 30.2, 21.3; HRMS (EI, M^+) for $C_{15}H_{20}O_2Si$ calcd 232.1463, found: m/z 232.1459.

1-(3-Methoxyphenyl)-6-methyl-(4E)-hepten-3-one **27c** (0.042 g, 0.18 mmol) was treated with triisopropylsilyl trifluoromethanesulfonate (0.054 mL, 0.20 mmol) under the previously outlined conditions to yield (2Z, 4E)-1-(3-methoxyphenyl)-6-methyl-3-(triisopropylsiloxy)-2,4-heptadiene, **28c**, (0.043 g, 0.11 mmol, 62 %) as a clear, colorless oil: R_f 0.75 (alumina, hexanes:EtOAc 8:1); IR (thin film) 2947, 2867, 1610, 1490, 1465, 1258, 1149, 1014, 883, 682 cm^{-1} ; 1H NMR (400 MHz, $CDCl_3$) δ 7.20 (t, $J = 7.6$ Hz, 1H),

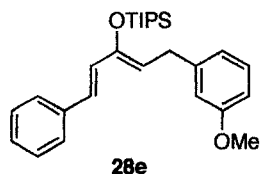
6.82 (br d, $J = 7.6$ Hz, 1H), 6.79 (br s, 1H), 6.74 (dd, $J = 8.0, 2.4$ Hz, 1H), 5.88 (dd, $J = 15.6, 6.0$ Hz, 1H), 5.82 (d, $J = 15.6$ Hz, 1H), 4.84 (t, $J = 7.2$ Hz, 1H), 3.80 (s, 3H), 3.48 (d, $J = 6.8$ Hz, 2H), 2.35 (app oct, $J = 6.4$ Hz, 1H), 1.20-1.30 (m, 3H), 1.15 (d, $J = 6.4$ Hz, 18H), 1.02 (d, $J = 6.8$ Hz, 6H); ^{13}C NMR (100 MHz, CDCl_3) δ 159.6, 149.8, 143.5, 137.0, 129.2, 125.9, 120.8, 114.1, 111.1, 109.4, 55.1, 32.2, 30.8, 22.3, 18.1, 13.7; HRMS (EI, M^+) for $\text{C}_{24}\text{H}_{40}\text{O}_2\text{Si}$ calcd 388.2797, found: m/z 388.2800.



(2Z, 4E)-1-(3-Methoxyphenyl)-3-(triisopropylsiloxy)-2,4-heptadiene, 28d. The previously outlined procedure was used in the synthesis of **28d** starting with dimethyl 4-(3-methoxyphenyl)-2-oxobutylphosphonate⁷ (0.55 g, 1.92 mmol) and propionaldehyde (0.058 mL, 0.80 mmol). The crude material was purified by gradient column chromatography (silica gel, hexanes:EtOAc 10:1, 9:1, 8:1, 7:1, etc.) to yield 1-(3-methoxyphenyl)-(4E)-hepten-3-one **27d** (0.17 g, 0.78 mmol, 97 %) as a clear, colorless oil: R_f 0.65 (silica gel, hexanes:EtOAc 2:1); IR (thin film) 2966, 2936, 1671, 1696, 1628, 1602, 1491, 1455, 1260, 1153, 1051, 978, 781 cm^{-1} ; ^1H NMR (500 MHz, CDCl_3) δ 7.20 (t, $J = 7.5$ Hz, 1H), 6.88 (dt, $J = 16.0, 6.5$ Hz, 1H), 6.80 (d, $J = 7.5$ Hz, 1H), 6.73-6.76 (m, 2H), 6.10 (dt, $J = 16.0, 1.5$ Hz, 1H), 3.80 (s, 3H), 2.85-2.94 (m, 4H), 2.21 (pseudo pent, $J = 7.5$ Hz, 2H), 1.07 (t, $J = 7.5$ Hz, 3H); ^{13}C NMR (125 MHz, CDCl_3) δ 199.6, 159.7, 149.0, 143.0, 129.4, 129.4, 120.7, 114.1, 111.3, 55.1, 41.5, 30.1, 25.6, 12.4; HRMS (EI, M^+) for $\text{C}_{14}\text{H}_{18}\text{O}_2$ calcd 218.1307, found: m/z 218.1301.

1-(3-Methoxyphenyl)-(4E)-hepten-3-one **27d** (0.11 g, 0.52 mmol) in THF (4 mL) was added by cannula to a stirring solution of LDA (0.58 mmol) in THF (4 mL) at -

78°C.¹⁰ The reaction was allowed to stir at low temperature for 40 min before the dropwise addition of triisopropylsilyl trifluoromethanesulfonate (0.15 mL, 0.58 mmol) by syringe. The reaction was slowly allowed to warm to room temperature and was quenched by the addition of triethylamine (1 mL), hexanes (5 mL), and saturated NaHCO₃ solution (10 mL). The organic layer was washed with H₂O (2 x 5 mL) and brine (5 mL) and dried (MgSO₄). After filtration, the solvent was removed and the crude oil purified by flash column chromatography (alumina, hexanes:EtOAc:TEA 50:1:1) to yield (2*Z*, 4*E*)-1-(3-methoxyphenyl)-3-(triisopropylsiloxy)-2,4-heptadiene, **28d**, as the major product in a mixture of 2*Z*:2*E* (6.5:1) isomers (0.14 g, 0.38 mmol, 73 %): R_f 0.76 (alumina, hexanes:EtOAc 8:1); IR (thin film) 2962, 2868, 1601, 1464, 1356, 1258, 1149, 1051, 884, 683 cm⁻¹; ¹H NMR (400 MHz, CDCl₃) δ 7.19 (t, *J* = 8.0 Hz, 1H), 6.71-6.82 (m, 3H), 5.92 (dt, *J* = 15.2, 6.4 Hz, 1H), 5.85 (d, *J* = 15.6 Hz, 1H), 4.82 (t, *J* = 7.2 Hz, 1H), 3.79 (s, 3H), 3.46 (d, *J* = 7.2 Hz, 2H), 2.10 (app pent, *J* = 6.8 Hz, 2H), 1.18-1.28 (m, 3H), 1.14 (d, *J* = 6.8 Hz, 18H), 1.01 (t, *J* = 7.2 Hz, 3H); ¹³C NMR (125 MHz, CDCl₃) δ 159.6, 149.7, 143.5, 131.6, 129.2, 127.9, 120.8, 114.0, 111.2, 109.2, 55.1, 32.2, 25.3, 18.1, 13.7, 13.4; HRMS (EI, M⁺) for C₂₃H₃₈O₂Si calcd 374.2641, found: m/z 374.2638.



(1*E*, 3*Z*)-5-(3-Methoxyphenyl)-1-phenyl-3-(triisopropylsiloxy)-1,3-pentadiene, 28e.

The previously outlined procedure was used in the synthesis of **28e** starting with dimethyl 4-(3-methoxyphenyl)-2-oxobutylphosphonate⁷ (0.20 g, 0.71 mmol) and benzaldehyde (0.030 mL, 0.29 mmol). The crude material was purified by gradient column chromatography (silica gel, hexanes:EtOAc 10:1, 9:1, 8:1, 7:1, etc.) to yield 5-(3-

methoxyphenyl)-1-phenyl-(*IE*)-penten-3-one **27e** (0.077 g, 0.29 mmol, 100 %) as a white solid: m.p. 41-44°C; R_f 0.53 (silica gel, hexanes:EtOAc 2:1); IR (thin film) 3027, 2937, 2835, 1690, 1662, 1611, 1493, 1450, 1260, 1153, 1051, 782 cm^{-1} ; ^1H NMR (500 MHz, CDCl_3) δ 7.56 (d, $J = 16.5$ Hz, 1H), 7.53-7.54 (m, 2H), 7.39-7.41 (m, 3H), 7.23 (t, $J = 7.5$ Hz, 1H), 6.85 (d, $J = 7.5$ Hz, 1H), 6.81 (br s, 1H), 6.77 (dd, $J = 8.0, 3.0$ Hz, 1H), 6.75 (d, $J = 16.5$ Hz, 1H), 3.81 (s, 3H), 3.01 (br s, 4H); ^{13}C NMR (125 MHz, CDCl_3) δ 199.2, 159.8, 142.9, 142.7, 134.5, 130.5, 129.5, 129.0, 128.3, 126.2, 120.7, 114.2, 111.4, 55.2, 42.3, 30.2; HRMS (EI, M^+) for $\text{C}_{18}\text{H}_{18}\text{O}_2$ calcd 266.1307, found: m/z 266.1305; Anal. Calcd for $\text{C}_{18}\text{H}_{18}\text{O}_2$: C, 81.17; H, 6.81. Found: C, 81.40; H, 6.96.

5-(3-Methoxyphenyl)-1-phenyl-(*IE*)-penten-3-one **27e** (0.11 g, 0.41 mmol) was treated with triisopropylsilyl trifluoromethanesulfonate (0.12 mL, 0.45 mmol) under the previously outlined conditions to yield (*IE*, *3Z*)-5-(3-methoxyphenyl)-1-phenyl-3-(triisopropylsiloxy)-1,3-pentadiene, **28e**, (0.13 g, 0.31 mmol, 75 %) as a clear, colorless oil: R_f 0.81 (alumina, hexanes:EtOAc 8:1); IR (thin film) 2945, 2867, 1600, 1490, 1465, 1359, 1258, 1149, 1049, 1014, 884, 692 cm^{-1} ; ^1H NMR (400 MHz, CDCl_3) δ 7.40 (pseudo d, $J = 7.2$ Hz, 2H), 7.34 (pseudo t, $J = 8.0$ Hz, 2H), 7.21-7.26 (m, 2H), 6.86 (d, $J = 7.6$ Hz, 1H), 6.82 (br s, 1H), 6.80 (d, $J = 15.6$ Hz, 1H), 6.77 (dd, $J = 9.6, 2.4$ Hz, 1H), 6.62 (d, $J = 16.0$ Hz, 1H), 5.10 (t, $J = 7.2$ Hz, 1H), 3.82 (s, 3H), 3.57 (d, $J = 7.2$ Hz, 2H), 1.28-1.38 (m, 3H), 1.21 (d, $J = 6.8$ Hz, 18H); ^{13}C NMR (100 MHz, CDCl_3) δ 159.7, 149.9, 142.9, 137.1, 129.3, 128.6, 127.7, 127.5, 127.4, 126.4, 120.9, 114.1, 112.9, 111.4, 55.1, 32.5, 18.1, 13.9; HRMS (EI, M^+) for $\text{C}_{27}\text{H}_{38}\text{O}_2\text{Si}$ calcd 422.2641, found: m/z 422.2641.

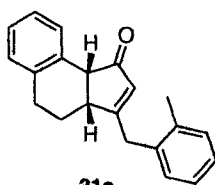
3-(2-Methylbenzyl)-2,3,4,5-tetrahydrocyclopenta[*a*]naphthalen-1-one, 30a, and 3-(2-methylbenzyl)-4,5-dihydro-3*aH*-cyclopenta[*a*]naphthalen-1(9*bH*)-one, 31a. (2*Z*, 4*E*)-1-(2-Methylphenyl)-7-phenyl-3-(triisopropylsiloxy)-2,4-heptadiene, **28a**, (0.092 g, 0.21 mmol) was dissolved in CHCl₃ (0.021 mol, 1.7 mL). The CHCl₃ does not need to be freshly distilled or pre-dried for this reaction. Benzyltriethylammonium chloride (0.014 g, 0.060 mmol) was added to the reaction mixture. A solution of 50 % aq. NaOH (0.040 mol, 1.6 mL) was then added in one portion and the reaction was vigorously stirred at room temperature for 12 min. The reaction was then diluted with H₂O (5 mL) and CH₂Cl₂ (5 mL) at 0°C. The aqueous layer was extracted with CH₂Cl₂ (2 x 10 mL). The combined organic layers were then washed with H₂O (2 x 10 mL) and dried (MgSO₄). After filtration, the solvent was removed to provide a brown-orange oil.

The crude oil was re-dissolved in acetonitrile (0.05 M, 4.2 mL). AgBF₄ (0.041 g, 0.21 mmol) was added in one portion and the reaction flask was equipped with a reflux condenser. The reaction was stirred at reflux for 20 h and was then allowed to cool to room temperature. The reaction mixture was then filtered through a short pad of Celite/silica gel. After removal of the solvent, the crude material was purified by gradient column chromatography (silica gel, 1%→2%→4%→6%→8%→10% EtOAc in hexanes) to yield **30a** (0.030 g, 0.10 mmol, 50 %) and **31a** (0.011 g, 0.040 mmol, 18 %) as an off-white solid and a yellow oil, respectively.



30a

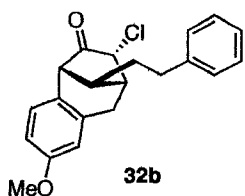
3-(2-Methylbenzyl)-2,3,4,5-tetrahydrocyclopenta[*a*]naphthalen-1-one, 30a: R_f 0.32 (hexanes/EtOAc 8:1); IR (thin film) 3060, 2928, 2693, 1490, 1385, 764, 745 cm^{-1} ; ^1H NMR (500 MHz, CDCl_3) δ 8.27 (d, $J = 7.5$ Hz, 1H), 7.17-7.28 (m, 7H), 3.23-3.27 (m, 1H), 3.19 (dd, $J = 14.0, 5.0$ Hz, 1H), 2.96 (pseudo t, $J = 7.5$ Hz, 2H), 2.73 (ddd, $J = 18.0, 8.5, 8.5$ Hz, 1H), 2.64 (dd, $J = 18.5, 6.5$ Hz, 1H), 2.55 (ddd, $J = 19.0, 7.5, 7.5$ Hz, 1H), 2.51 (dd, $J = 14.0, 10.0$ Hz, 1H), 2.38 (s, 3H), 2.35 (dd, $J = 19.0, 2.0$ Hz, 1H); ^{13}C NMR (125 MHz, CDCl_3) δ 205.0, 177.0, 137.6, 136.0, 135.0, 134.5, 130.6, 129.1, 129.0, 128.0, 127.5, 126.8, 126.7, 126.2, 124.3, 42.6, 41.1, 37.1, 27.8, 25.4, 19.6; HRMS (EI, M^+) for $\text{C}_{21}\text{H}_{20}\text{O}$ calcd 288.1514, found: m/z 288.1513.



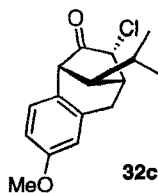
31a

3-(2-Methylbenzyl)-4,5-dihydro-3aH-cyclopenta[*a*]naphthalen-1(9bH)-one, 31a: R_f 0.27 (hexanes/EtOAc 8:1); IR (thin film) 3021, 2929, 1701, 1616, 1493, 1453, 1172, 745 cm^{-1} ; ^1H NMR (500 MHz, CDCl_3) δ 7.50 (d, $J = 7.5$ Hz, 1H), 7.14-7.25 (m, 6H), 7.08 (d, $J = 7.5$ Hz, 1H), 5.71 (app q, $J = 1.5$ Hz, 1H), 3.86 (d, $J = 17.5$ Hz, 1H), 3.65 (d, $J = 17.5$ Hz, 1H), 3.65 (d, $J = 7.0$ Hz, 1H), 3.37 (app q, $J = 6.0$ Hz, 1H), 2.68 (ddd, $J = 15.5, 6.0, 4.0$ Hz, 1H), 2.54 (ddd, $J = 15.0, 9.0, 4.5$ Hz, 1H), 2.27 (s, 3H), 1.98-2.09 (m, 2H); ^{13}C NMR (125 MHz, CDCl_3) δ 205.8, 181.6, 137.5, 136.3, 135.2, 132.5, 131.0, 130.6, 129.9,

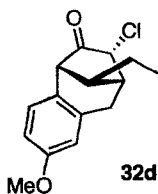
127.8, 127.3, 126.6, 126.4, 126.3, 50.5, 43.4, 35.8, 27.0, 26.5, 19.4; HRMS (EI, M⁺) for C₂₁H₂₀O calcd 288.1514, found: m/z 288.1515.



Compound 32b. The previously outlined procedure was used in the preparation of **32b** from (2*Z*, 4*E*)-1-(3-methoxyphenyl)-7-phenyl-3-(triisopropylsiloxy)-2,4-heptadiene, **28b**, (0.10 g, 0.22 mmol). The crude material was purified by gradient column chromatography (silica gel, 1%→2%→4%→6%→8%→10% EtOAc in hexanes) to yield **32b** (0.043 g, 0.12 mmol, 57 %) as a white solid: m.p. 111-114°C; R_f 0.25 (hexanes/EtOAc 8:1); IR (thin film) 3025, 2930, 2856, 1751, 1605, 1496, 1260, 1154, 1122, 1034, 700 cm⁻¹; ¹H NMR (500 MHz, CDCl₃) δ 7.29 (t, *J* = 7.5 Hz, 2H), 7.21 (pseudo t, *J* = 7.5 Hz, 1H), 7.16 (pseudo d, *J* = 7.0 Hz, 2H), 7.01 (d, *J* = 8.5 Hz, 1H), 6.72 (dd, *J* = 8.5, 3.0 Hz, 1H), 6.67 (d, *J* = 2.5 Hz, 1H), 4.51 (br d, *J* = 7.5 Hz, 1H), 3.77 (s, 3H), 3.33 (s, 1H), 3.32 (dd, *J* = 18.0, 2.0 Hz, 1H), 3.10 (dd, *J* = 17.5, 5.0 Hz, 1H), 2.90-2.92 (m, 1H), 2.74 (pseudo t, *J* = 7.5 Hz, 2H), 2.32 (t, *J* = 8.0 Hz, 1H), 1.68-1.81 (m, 2H); ¹³C NMR (125 MHz, CDCl₃) δ 205.0, 159.5, 140.8, 135.1, 128.6, 128.6, 128.3, 126.8, 126.2, 113.9, 113.3, 60.2, 55.2, 55.1, 41.9, 40.3, 33.8, 33.7, 32.1; HRMS (ESI, [M+Na]⁺) for C₂₁H₂₁O₂ClNa calcd 363.1122, found: m/z 363.1121.



Compound 32c. The previously outlined procedure was used in the preparation of **32c** from (2*Z*, 4*E*)-1-(3-methoxyphenyl)-6-methyl-3-(triisopropylsiloxy)-2,4-heptadiene, **28c**, (0.034 g, 0.10 mmol). The crude material was purified by gradient column chromatography (silica gel, 1%→2%→4%→6%→8%→10% EtOAc in hexanes) to yield **32c** (0.018 g, 0.065 mmol, 65 %) as a white solid: m.p. 102-104°C; R_f 0.30 (hexanes/EtOAc 8:1); IR (thin film) 2962, 1749, 1606, 1498, 1470, 1260, 1038, 810 cm^{-1} ; ^1H NMR (500 MHz, CDCl_3) δ 7.04 (d, $J = 8.5$ Hz, 1H), 6.73 (dd, $J = 8.5, 3.5$ Hz, 1H), 6.68 (d, $J = 3.0$ Hz, 1H), 4.44 (br d, $J = 7.0$ Hz, 1H), 3.77 (s, 3H), 3.48 (br s, 1H), 3.35 (d, $J = 17.0$ Hz, 1H), 3.05-3.12 (m, 2H), 1.88 (d, $J = 11.0$ Hz, 1H), 1.43 (dq, $J = 11.0, 6.5, 6.5$ Hz, 1H), 1.06 (d, $J = 7.0$ Hz, 3H), 1.02 (d, $J = 6.5$ Hz, 3H); ^{13}C NMR (100 MHz, CDCl_3) δ 205.1, 159.5, 135.1, 128.7, 127.1, 113.8, 113.2, 60.1, 55.2, 54.0, 50.0, 38.1, 32.3, 28.3, 21.5, 20.2; HRMS (ESI, $[\text{M}+\text{Na}]^+$) for $\text{C}_{16}\text{H}_{19}\text{O}_2\text{ClNa}$ calcd 301.0966, found: m/z 301.0968.



Compound 32d. The previously outlined procedure was used in the preparation of **32d** from (2*Z*, 4*E*)-1-(3-methoxyphenyl)-3-(triisopropylsiloxy)-2,4-heptadiene, **28d**, (0.074 g, 0.20 mmol). The crude material was purified by gradient column chromatography (silica gel, 1%→2%→4%→6%→8%→10% EtOAc in hexanes) to yield **32d** (0.044 g, 0.017

mmol, 84 %) as a white solid: m.p. 111-114°C; R_f 0.25 (hexanes/EtOAc 8:1); IR (thin film) 2960, 2933, 1755, 1606, 1497, 1463, 1258, 1122, 1036, 895 cm^{-1} ; ^1H NMR (500 MHz, CDCl_3) δ 7.03 (d, $J = 8.5$ Hz, 1H), 6.73 (dd, $J = 8.5, 3.0$ Hz, 1H), 6.68 (d, $J = 3.0$ Hz, 1H), 4.49 (d, $J = 7.0$ Hz, 1H), 3.77 (s, 3H), 3.34 (s, 1H), 3.33 (dd, $J = 17.5, 1.5$ Hz, 1H), 3.13 (dd, $J = 17.5, 4.5$ Hz, 1H), 2.89-2.91 (m, 1H), 2.20 (t, $J = 8.0$ Hz, 1H), 1.40-1.50 (m, 2H), 1.03 (t, $J = 7.5$ Hz, 3H); ^{13}C NMR (125 MHz, CDCl_3) δ 205.2, 159.5, 135.2, 128.6, 127.0, 114.0, 113.2, 60.3, 55.2, 54.9, 44.3, 40.0, 32.2, 25.0, 12.1; HRMS (ESI, $[\text{M}+\text{Na}]^+$) for $\text{C}_{15}\text{H}_{17}\text{O}_2\text{ClNa}$ calcd 287.0809, found: m/z 287.0811.



Compound 32e. The previously outlined procedure was used in the preparation of **32e** from (*1E, 3Z*)-5-(3-methoxyphenyl)-1-phenyl-3-(triisopropylsiloxy)-1,3-pentadiene, **28e**, (0.079 g, 0.19 mmol). The crude material was purified by gradient column chromatography (silica gel, 1%→2%→4%→6%→8%→10% EtOAc in hexanes) to yield **32e** (0.035 g, 0.11 mmol, 59 %) as a white solid: m.p. 109-112°C; R_f 0.25 (hexanes/EtOAc 8:1); IR (thin film) 2927, 2854, 1748, 1606, 1497, 1277, 1261, 1120, 1038, 794, 700 cm^{-1} ; ^1H NMR (500 MHz, CDCl_3) δ 7.28 (pseudo t, $J = 7.5$ Hz, 2H), 7.29 (pseudo t, $J = 7.5$ Hz, 1H), 7.25 (pseudo d, $J = 7.5$ Hz, 2H), 7.13 (d, $J = 8.5$ Hz, 1H), 6.78 (dd, $J = 8.5, 2.5$ Hz, 1H), 6.75 (d, $J = 2.5$ Hz, 1H), 4.39 (dd, $J = 7.5, 1.0$ Hz, 1H), 3.89 (br s, 1H), 3.80 (s, 3H), 3.66 (s, 1H), 3.45 (dd, $J = 18.0, 2.0$ Hz, 1H), 3.38 (dd, $J = 17.5, 4.5$ Hz, 1H), 3.17-3.19 (m, 1H); ^{13}C NMR (125 MHz, CDCl_3) δ 204.5, 159.7, 140.1, 135.0,

129.1, 129.0, 127.2, 126.6, 126.5, 114.0, 113.6, 60.0, 55.3, 53.6, 46.3, 43.5, 32.1; HRMS (ESI, $[M+Na]^+$) for $C_{19}H_{17}O_2ClNa$ calcd 335.0809, found: m/z 335.0807.

3.5 References

1. Grant, T. N.; West, F. G. *J. Am. Chem. Soc.* **2006**, *128*, 9348-9349.
2. Grant, T. N.; West, F. G. *Org. Lett.* **2007**, *9*, 3789-3792.
3. Ireland, R. E.; Norbeck, D. W. *J. Org. Chem.* **1985**, *50*, 2198-2200.
4. a) Kostikov, R. R.; Molchanov, A. P.; Hopf, H. *Top. Curr. Chem.* **1990**, *155* (Small Ring Compounds in Organic Synthesis), 41-80; b) Banwell, M. G.; Reum, M. E. In *Advances in Strain in Organic Chemistry*; Halton, B., Ed.; JAI Press: Greenwich, CT, 1991; Vol. 1, pp 19-64; c) Fedorynski, M. *Chem. Rev.* **2003**, *103*, 1099-1132.
5. Browder, C. C.; Marmsäter, F. P.; West, F. G. *Can. J. Chem.* **2004**, *82*, 375-385.
6. Harmata, M.; Elomari, S.; Barnes, C. L. *J. Am. Chem. Soc.* **1996**, *118*, 2860-2871.
7. Mitoshi, K.; Nakae, T.; Sakuyama, S.; Nishizaki, M.; Odagaki, Y.; Nakai, H.; Hamanaka, N. *Bioorg. Med. Chem.* **1997**, *5*, 1621-1647.
8. a) Giese, S.; West, F. G. *Tetrahedron Lett.* **1998**, *44*, 4043-4060; b) Giese, S.; West, F. G. *Tetrahedron* **2000**, *56*, 10221-10228.
9. Mander, L. N.; Wells, A. P. *Tetrahedron Lett.* **1997**, *38*, 5709-5712.
10. Kusama, H.; Yamabe, H.; Onizawa, Y.; Hoshino, T.; Iwasawa, N. *Angew. Chem. Int. Ed.* **2005**, *44*, 468-470.

Chapter 4

Synthesis of Functionalized Oxo- and Azacycles: A Pyridinium Acetate-Catalyzed Ring Expansion Sequence.

4.1 Synthesis of Functionalized Heterocycles

The synthesis of non-aromatic oxygen and nitrogen-containing heterocycles is an important area of organic synthesis, since these structures are frequently observed as integral parts of natural product skeletons (*Figure 4.1*).^{1,2} In recent years, synthetic approaches towards such natural products have prompted the development of many new methods to assemble heterocyclic motifs. Some of these methodologies will be outlined

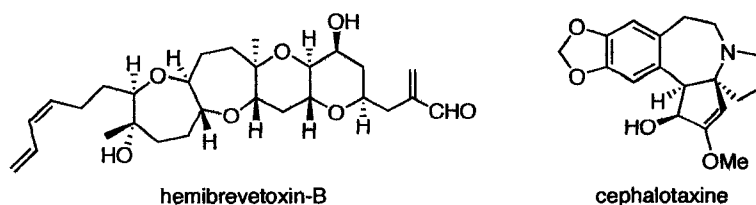


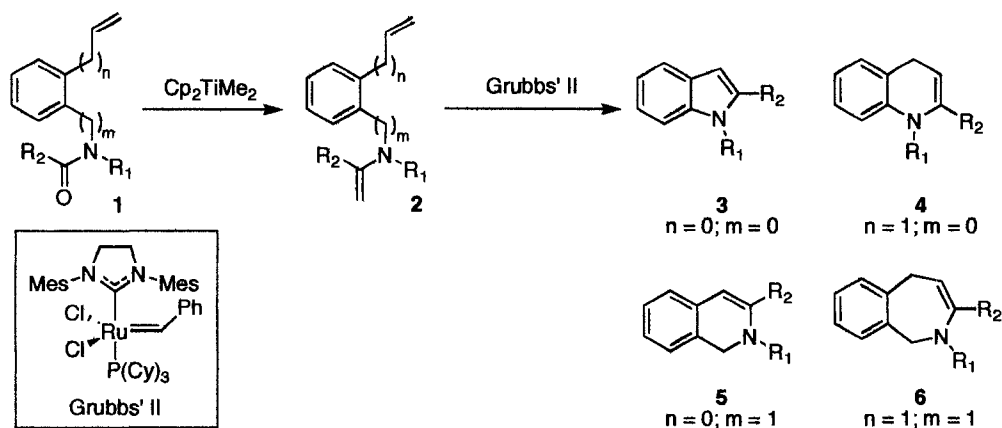
Figure 4.1. Examples of natural products containing saturated heterocyclic motifs.

in this chapter, which will also introduce a novel two-step ring expansion sequence developed in the West laboratories.

4.1.1 Recent Contributions to Heterocycle Synthesis

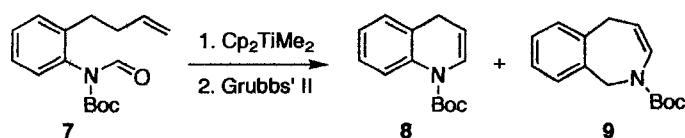
The synthesis of saturated heterocycles, particularly medium-sized heterocycles, is an important area of organic chemistry, due to the prevalence of these structures in many medicinally interesting compounds. Numerous synthetic routes towards the synthesis of these compounds have involved direct closure of linear precursors; however, the efficiency of these processes tends to decrease as ring size increases. This observation reflects an increase in enthalpic (ring strain) and entropic (likelihood of interaction between the chain termini) barriers during the formation of medium-sized rings.

Presently, one of the most common approaches towards the synthesis of small and medium-sized heterocycles utilizes transition metal-mediated ring closing metathesis (RCM). A recent example of this strategy is illustrated in Bennasar's method for the construction of benzo-fused nitrogen heterocycles (*Scheme 4.1*),³ which involves



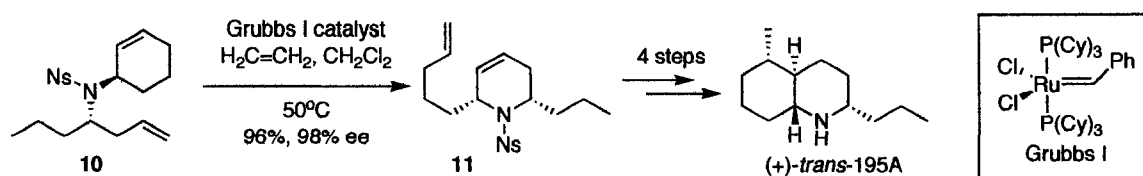
Scheme 4.1. Two-step olefination/RCM strategy for benzo-fused heterocycle synthesis.

treatment of *N*-acylamides **1** with dimethyltitanocene to provide an intermediate enamine species (**2**) that can directly participate in ring closing metathesis. In the presence of Grubbs' second-generation catalyst, enamine intermediates **2** undergo ring closure to furnish indoles **3**, 1,4-dihydroquinolines **4**, 1,2-dihydroisoquinolines **5**, and dihydrobenzoazepines **6**, depending on the length of the alkyl chains connecting both amide and olefin functionalities to the aromatic ring. In each case, the reaction conditions had to be slightly modified with regard to temperature and solvent to ensure optimal conversion of enamine intermediates to the desired heterocyclic products. For example, the generation of benzoazepine **9** was hampered by olefin isomerization in the starting material when high temperatures were applied during ring-closing metathesis. Unfavorable double bond isomerization led to isolation of 1,4-dihydroisoquinoline **8** along with the desired product, **9** (4:1, **8**:**9**); however, addition of benzoquinone and a lower reaction temperature (80 °C instead of 110 °C) provided the desired benzoazepine in 50% yield (two steps) as the major product in a 1:7 mixture of **8** and **9**, respectively (*Scheme 4.2*). This methodology provides access to numerous benzo-fused heterocycles from relatively simple starting materials; however, it necessitates the use of two transition metal-mediated transformations, which may not be attractive for use in large-scale synthesis.



Scheme 4.2. Formation of benzoazepine **9** from amide **7**.

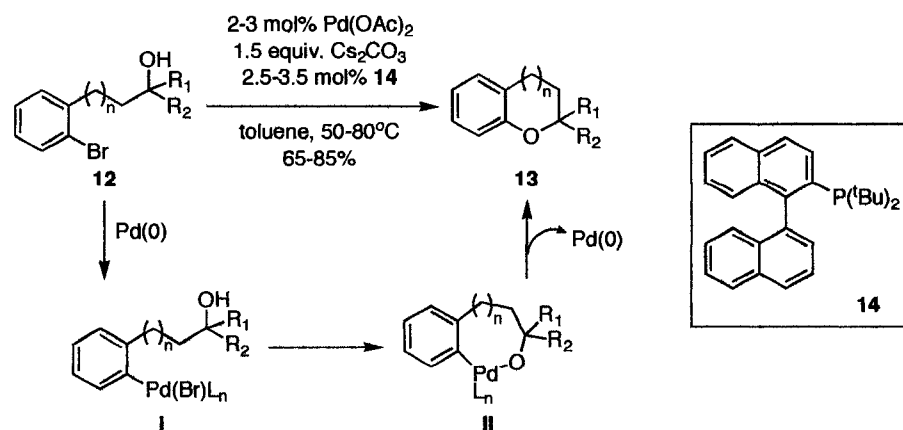
Similarly, a novel ring-rearrangement metathesis (RRM) reaction was used in the concise total synthesis of (+)-*trans*-195A, a non-toxic alkaloid isolated from the skin of numerous dendrobatid frog species (*Scheme 4.3*).⁴ During the synthesis, the authors subjected chiral sulfonamide **10** to treatment with Grubbs first-generation catalyst in the presence of ethylene gas to furnish the desired *cis*-2,6-disubstituted tetrahydropyridine **11** in 96% yield and 98% enantiomeric excess. This reaction was used in conjunction with a zirconium-mediated Negishi-coupling to assemble the decahydroquinoline core of (+)-*trans*-195A. Using this strategy, the target compound was successfully synthesized in 11 steps and in 35% overall yield.



Scheme 4.3. Key step in the synthesis of (+)-*trans*-195A.

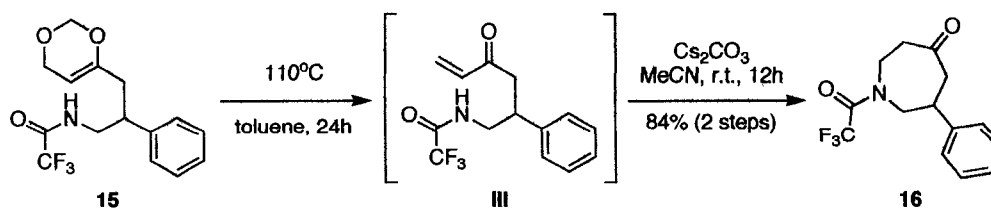
Some other interesting strategies for the synthesis of heterocyclic motifs involve intramolecular cyclization processes. Recently, Buchwald and co-workers⁵ disclosed a palladium-catalyzed synthesis of cyclic aryl ethers that allowed for the facile construction of five-, six-, and seven-membered oxygen-containing heterocycles **13** in good yields (*Scheme 4.4*). The reaction proceeds through preliminary oxidative addition of the aromatic C-Br bond in **12**, followed by coordination of the palladium(II) species to the pendent hydroxyl functionality. This coordination provides metallocycle intermediates **II** that are essential for efficient bond formation resulting from reductive elimination. This methodology was also applied to the synthesis of heterocycles containing multiple

heteroatoms and to the cyclization of chiral alcohols, providing optically active cyclic ethers.



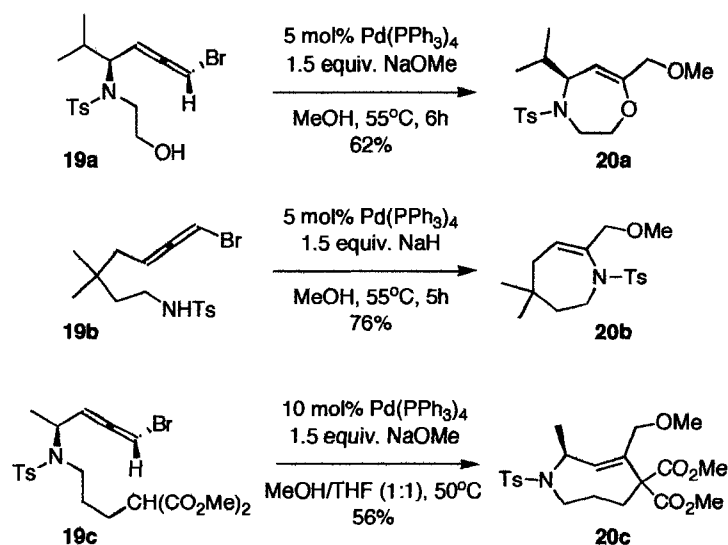
Scheme 4.4. Palladium-catalyzed construction of cyclic aryl ethers.

Greshock and Funk recently published an intramolecular cyclization approach to the formation of six-, seven-, and eight-membered nitrogen-containing heterocycles that is not reliant on transition metal catalysis.⁶ This fascinating strategy utilizes a retrocycloaddition reaction of a 1,3-dioxin moiety, seen in compound **15**, followed by Michael addition of the tethered nitrogen center onto the newly revealed α,β -unsaturated ketone to construct the desired heterocyclic structures (*Scheme 4.5*). The biggest advantage of this two-step reaction sequence is that the dioxin moiety is very robust and can be carried through multiple chemical transformations before releasing the sensitive



Scheme 4.5. The two-step assembly of a nitrogen-containing heterocycle from dioxin **15**.

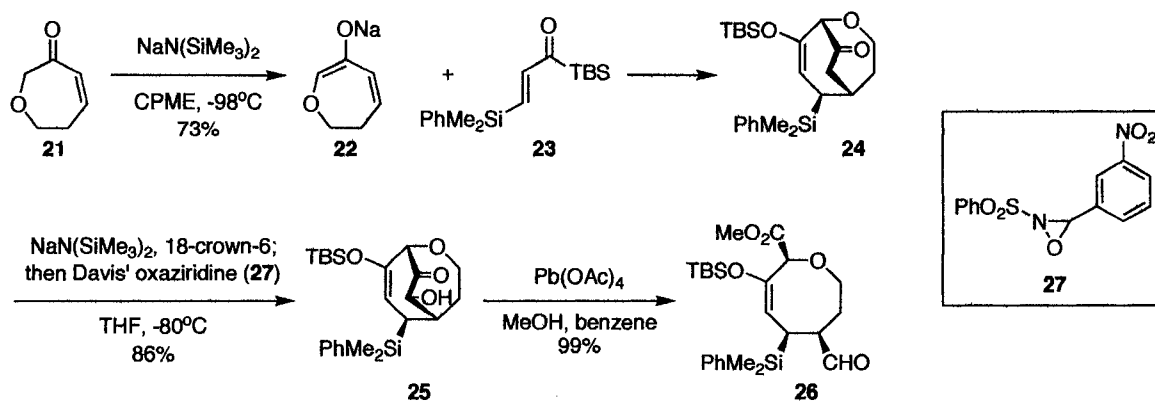
carbon nucleophiles onto the intermediate dication species. In most cases, the reactions also proceeded with high stereo- and regioselectivity due to internal nucleophilic attack at the central carbon of the dication, followed by intermolecular capture of the resultant η^3 -allylpalladium complex by methoxide.



Scheme 4.7. The synthesis of medium-sized heterocycles from bromoallene substrates.

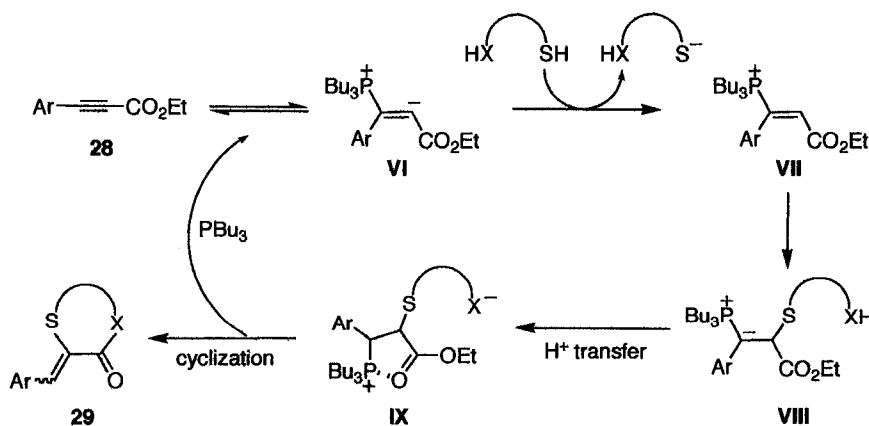
Although various intramolecular cyclization strategies have been proven effective for the synthesis of heterocyclic compounds, the preparation of non-trivial starting materials required for these processes is often a significant drawback. Intermolecular cycloadditions offer an alternative and convergent approach to the construction of heterocycles by bringing together two separately functionalized fragments. Takeda's sequential Brook rearrangement/ [3+4] annulation strategy is a good example of this type of approach to the synthesis of eight-membered oxygen heterocycles.⁹ In this investigation, it was found that the enolate (**22**) from readily available 6-oxacyclohept-2-en-1-one **21** could be coupled with β -substituted acryloylsilane **23** to form the bridged bicycle **24** (*Scheme 4.8*). Cleavage of the ketone bridge to afford the desired oxacycle **26**

was accomplished in two steps by initial α -hydroxylation using Davis' oxaziridine (**27**) to provide **25**, followed by treatment with lead tetraacetate. This protocol provides highly functionalized eight-membered heterocycles in moderate yields over three steps.



Scheme 4.8. Three-step protocol for the formation of eight-membered oxacycles.

Another recent example of heterocycle construction uses tributylphosphine as an organocatalyst that initiates a tandem umpolung addition and intramolecular cyclization reaction.¹⁰ When arylpropiolates **28** were combined with bifunctional sulfur pronucleophiles in the presence of tributylphosphine, the corresponding five- and six-membered heterocycles were obtained in moderate to excellent yields (*Scheme 4.9*). This



Scheme 4.9. Mechanism for organocatalytic preparation of sulfur heterocycles.

reaction proceeds through formation of a zwitterionic species **VI** resulting from phosphine addition to the arylpropiolate **28**. Protonation of the zwitterion would generate a polarized alkene intermediate (**VII**) susceptible to attack from the sulfur nucleophile. After sulfur addition and subsequent protonation of **VIII**, the authors propose another nucleophilic attack at the activated ester (**IX**). Finally, elimination of tributylphosphine would result in formation of the desired product **29** and regeneration of the organocatalyst (tributylphosphine). This simple and efficient method has allowed for the preparation of arylidene sulfur-containing heterocycles (*Figure 4.2*) that are commonly found in biologically active products.

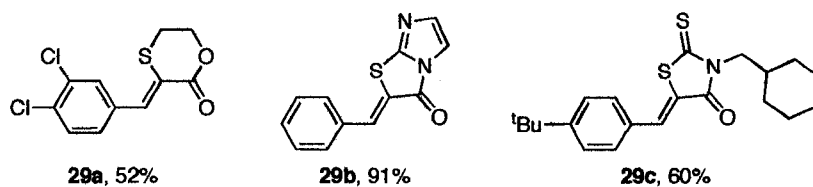


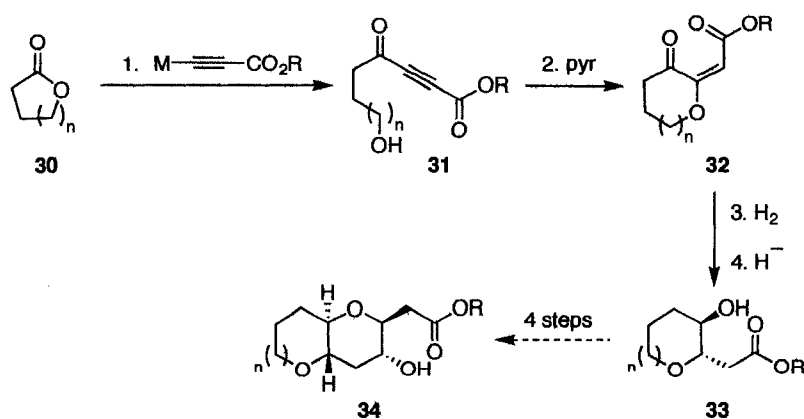
Figure 4.2. Examples of heterocycles generated from the organocatalytic process.

Organocatalysis has emerged as an important area of organic synthesis, since the reactions do not require the use of expensive transition metals and organocatalysts can often be used to effect asymmetric transformations. The development of new organocatalyzed methodologies for the synthesis of heterocyclic structures has become a recent focus in the West laboratories. In particular, a great deal of work has been done in the design of novel strategies for the assembly of saturated oxygen-heterocycles typically observed in the polyether backbones of marine ladder toxins.² During one of these investigations, a two-step ring expansion sequence was discovered that provides access to highly functionalized six- and seven-membered oxygen- and nitrogen-containing

heterocycles. The development of this methodology, including evaluation of the reaction scope and evidence to support a proposed mechanism for the transformation, will be discussed in this chapter.

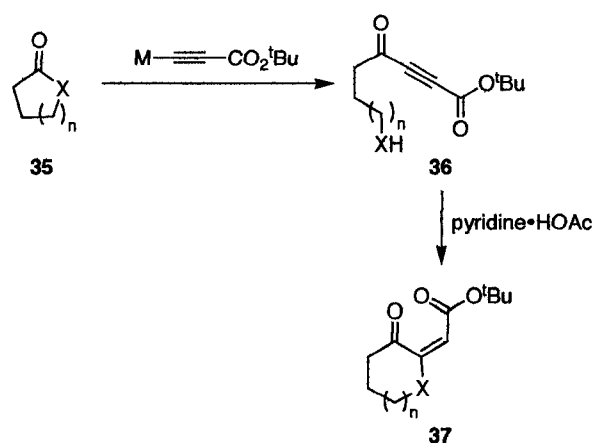
4.2 Pyridinium Acetate-Catalyzed Ring Expansions

The development of a novel two-step ring expansion sequence for the synthesis of saturated heterocycles has evolved from an initial investigation into an iterative approach towards the synthesis of polycyclic ethers.^{2b} Originally, we envisioned the addition of a propiolate anion into readily available lactone substrates **30**, followed by cyclization of the resultant ynones (**31**) to afford functionalized oxacycles **32** (Scheme 4.10). Controlled reduction of the alkene and ketone moieties would afford the requisite *trans*-substituted saturated intermediates **33**, and subsequent repetition of the simple four-step sequence was believed to provide a rapid route to the construction of polyether fragments **34**. Although our attempts to utilize this methodology to construct polyether motifs were



Scheme 4.10. Proposed strategy for the iterative assembly of polyether motifs.

unproductive, the two-step ring expansion sequence was successfully applied to the synthesis of novel oxygen- and nitrogen-containing heterocyclic structures (*Scheme 4.11*). The ring expansion strategy utilizes a BF_3 -mediated addition of *tert*-butyl propiolate to readily available lactones or lactams **35**, followed by a pyridinium acetate-catalyzed cyclization to form highly functionalized six- and seven-membered heterocycles **37**. Development of this methodology and mechanistic insights will be discussed herein.

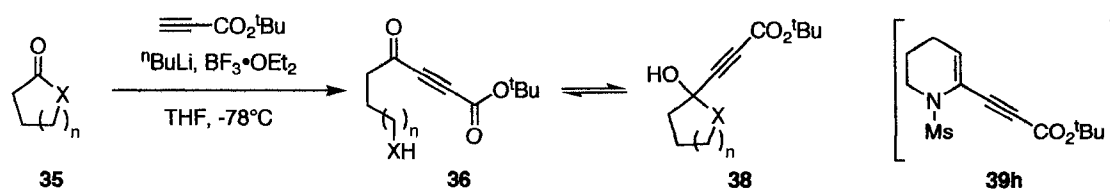


Scheme 4.11. Outline of two-step ring expansion methodology.

4.2.1 *tert*-Butyl Propiolate Addition

In order to investigate the feasibility of the proposed ring expansion sequence, the first objective was to determine optimal conditions for accessing the requisite ynone substrates **36**. Conjugated ynones can be accessed in a number of ways. The most common protocol utilizes a strong base to deprotonate a terminal alkyne, which is then added into an aldehyde and the resulting propargyl alcohol oxidized to provide the desired ketone.¹¹ Other methods have involved the addition of potentially explosive

silver acetylides¹² to acid chlorides, or the more synthetically useful Pd(II)¹³ or Cu(I)¹⁴ catalyzed addition of terminal alkynes to activated carboxylic acids. For this study, we decided that the best approach toward the synthesis of desired substrates **31** would utilize a BF₃-mediated addition of *tert*-butyl propiolate to γ -, δ -, and ϵ -lactones.¹⁵ Although the addition of *tert*-butyl propiolate to lactones was also possible through simple deprotonation by *n*-butyllithium, LDA, and the use of Ce(III)-mediated propiolate anions, the highest yields and most reproducible results were obtained when 1.1 equivalents of BF₃•OEt₂ were added to the reaction mixtures. These reactions presumably proceed through an intermediate lithium alkynyl trifluoroborate species; however, unlike



entry	substrate	X	n	product ratio [36:38] ^a	yield (%)
1	35a	O	1	4 : 1	63
2	35b	O	2	1.3 : 1	82
3	35c	O	3	1 : 0	83
4	35d	N-Boc	2	1 : 0	77
5	35e	N-Ts	1	1 : 0	60
6	35f	N-Ts	2	1 : 0	84
7	35g	N-Ms	1	1 : 0	63
8	35h	N-Ms	2	2.3 : 0 : 1 ^b	82
9	35i	N-Ns	1	1 : 0	37 (39) ^c
10	35j	N-Ns	2	1 : 0	37 (40)

^a Ratios obtained from ¹H NMR spectra; ^b The ratio displayed is for **36:38:39h**; ^c The yield in brackets corresponds to recovered starting material.

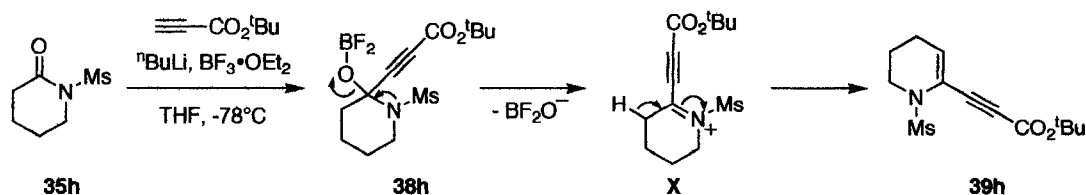
Table 4.1. ^tBu-propiolate addition to lactones/lactams.

potassium organotrifluoroborates, the lithium analogues are not air stable and have not been fully characterized.¹⁶ *tert*-Butyl propiolate was chosen for use in this methodology due to the ease with which the subsequent cyclization step occurred. Although ethyl propiolate could be effectively added to lactones using the same reaction conditions, the following cyclization step was unsuccessful.

The BF₃-mediated propiolate addition cleanly afforded the addition products in good yields; however, in the case of γ -butyrolactone, (**35a**) and δ -valerolactone (**35b**) the products were observed as an inseparable mixture of the acyclic keto-alcohols **36** and lactols **38** (*Table 4.1*). The ratio of products in these mixtures appeared to be solvent dependent, since ¹H NMR spectra taken in *d*-chloroform indicated a ratio of 1.3:1 (**36b:38b**) while spectra of the same mixture taken in a less polar solvent (*d*₆-benzene) indicated a product ratio of 1:1.8 (**36b:38b**). This observation implied that the keto-alcohol (**36**) and lactol (**38**) isomers existed in rapid equilibrium, which could be shifted upon dissolution in either polar or non-polar solvents.

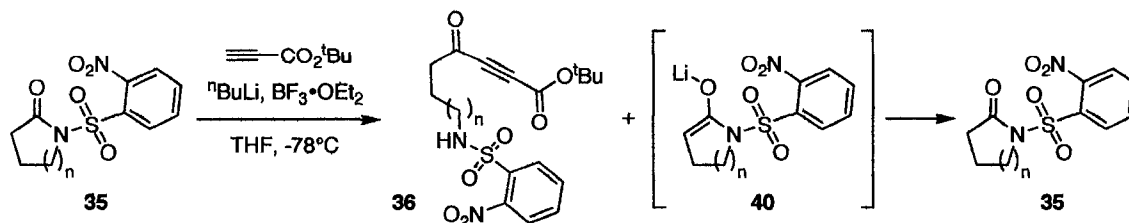
Although the addition of terminal alkynes to lactams is not prevalent in the literature, the addition of a lithium acetylide to *N*-Boc-protected lactams has been accomplished¹⁷ and the use of BF₃•OEt₂ to mediate a similar propiolate addition to Weinreb amides has also been observed.¹⁸ Given this precedent, the previously outlined conditions used for *tert*-butyl propiolate addition to lactones were utilized in the addition to lactam substrates **35d-j** (*Table 4.1*). In the case of the *N*-Boc protected (**35d**),¹⁹ *N*-tosylated (**35e-f**),²⁰ and *N*-mesylated lactams (**35g-h**),²⁰ the addition reactions proceeded smoothly to provide the corresponding addition products in good yields; however, the

reactions required 1.6 equivalents of propiolate in order to drive them to completion. Also, the addition of *tert*-butyl propiolate to *N*-mesyl lactam **35h** led to isolation of a minor product, cyclic enyne **39h**, as the result of six-membered cyclic aminal (**38h**) formation and subsequent Lewis acid-assisted dehydration under the reaction conditions (*Scheme 4.12*). Although there was some indication in crude ¹H NMR spectra that analogous side-products had been formed after propiolate addition to other 6-membered lactams, none of those enyne products were successfully isolated during purification by flash column chromatography.



Scheme 4.12. Formation of cyclic enyne side-product **39h**.

In the case of *N*-nosyl substrates (**35i-j**), the addition of *tert*-butyl propiolate did not proceed to completion even when the number of equivalents of propiolate anion was doubled. A competing proton-transfer process may be responsible for the incomplete formation of desired adducts **36i-j** (*Scheme 4.13*). The more electron-withdrawing nosyl (2-nitrophenylsulfonyl) group may sufficiently enhance the acidity of the α -protons on the starting lactams to permit enolization. The resulting unreactive enolate **40** would then furnish recovered lactam **35** upon aqueous work-up. In the presence of excess propiolate anion, the product of a second addition to the newly formed ketone of **36** was also evident in the crude ¹H NMR spectra. As a result, only 1.1 equivalents of *tert*-butyl propiolate anion were used in these particular addition reactions.



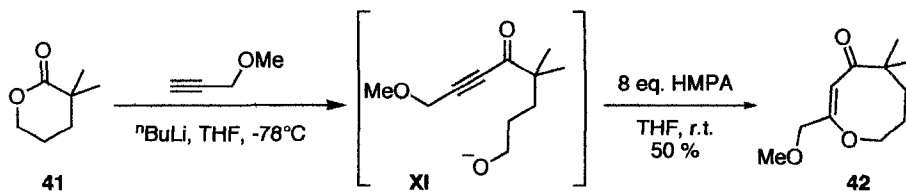
Scheme 4.13. Possible formation of lactam enolates during *tert*-butyl propiolate addition.

In general, the addition of *tert*-butyl propiolate to lactones and various lactam substrates was successful when the propiolate anion was generated by deprotonation with *n*-butyllithium, followed by treatment with $\text{BF}_3 \cdot \text{OEt}_2$. Under these conditions the desired acetylenic ketoesters could be obtained in moderate yields, with additions to five-membered lactones/lactams proceeding in slightly lower yields than additions to the six-membered analogues. Although *tert*-butyl propiolate addition to *N*-nosyl lactams could be accomplished, the yields for these substrates were significantly decreased; nonetheless, both *N*-nosyl compounds were examined in the subsequent cyclization step due to the potential ease with which *N*-nosyl protecting groups can be removed from the cyclic products compared to *N*-tosyl and *N*-mesyl functionalities.

4.2.2 Ring Expansion

With substrates **36** in hand, the second step of the ring expansion sequence was investigated. Previously, Schreiber had shown that a ring expansion reaction could occur following the addition of alkynyl lithium reagents to δ -lactones.²¹ In Schreiber's work, the alkyne addition products were allowed to warm to room temperature in the presence of 8 equivalents of HMPA, which effected oxocenone formation as a result of 1,4-addition of the pendent alkoxide to the intermediate ynone (*Scheme 4.14*). The alkyne

moieties in Schreiber's substrates were polarized to effect exclusive 1,4-addition towards the ketone functionality; however, substrates **36** present the possibility of 1,4-addition towards either the ketone or ester. We believed that a complementary ring expansion reaction could be induced using substrates **36** in the presence of an organocatalyst to access functionalized heterocycles bearing an exocyclic double bond.



Scheme 4.14. Schreiber's ring expansion reaction.

Preliminary Investigations: Oxygen Heterocycles

Initially, the keto-alcohol/lactol mixture of **36b** and **38b** was examined to establish the feasibility of the desired cyclization reaction. The mixture (**35b/38b**) was treated with numerous organic nucleophiles as well as nucleophilic and non-nucleophilic bases, including triphenylphosphine (Ph_3P), pyridine, *N,N*-dimethyl-4-aminopyridine (DMAP), 1,4-diazabicyclo[2.2.2]octane (DABCO), thiophenol (PhSH), and 2,6-lutidine in CH_2Cl_2 . As a result of this qualitative investigation, it was found that both pyridine and DMAP induced the desired ring expansion reaction, providing the highly functionalized 3-oxooxepan-2-ylidene **43a** (Figure 4.3). At the outset of this study, it was important to establish that ring expansion had occurred to form the desired product **43a** as opposed to the larger ring **44a**, which would have similar 1D ^1H and ^{13}C NMR spectra. Confirmation of the formation of this product was obtained from examination of the corresponding 1D and 2D NMR spectra, with the most important evidence observed in the form of an HMBC correlation between H_a and the quaternary carbon, C_b . This

three-bond correlation clearly distinguishes **43a** from **44a**, since it would not be observed in the HMBC spectrum of the eight-membered oxacycle.

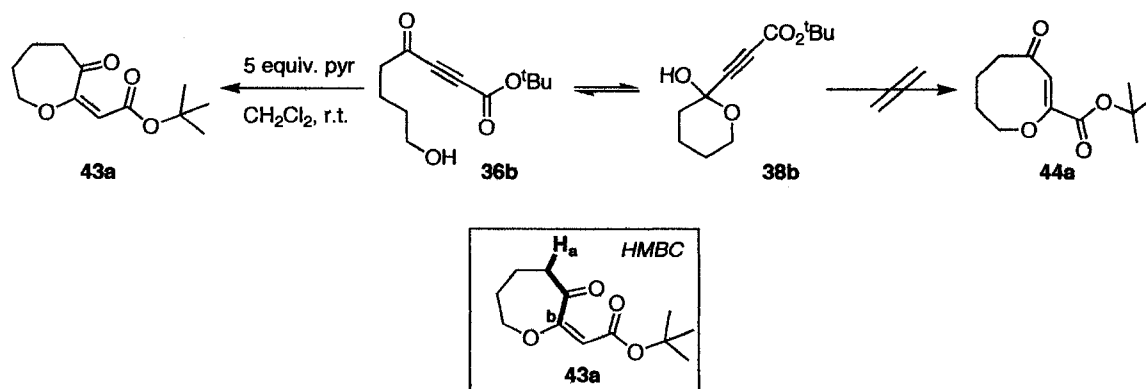
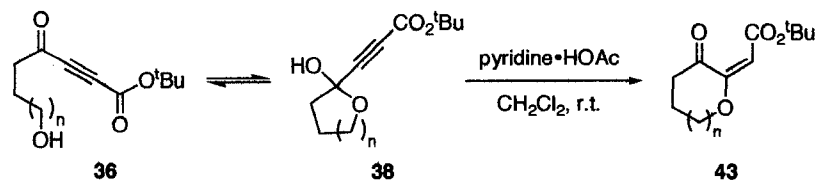


Figure 4.3. Evidence for the formation of 3-oxooxepan-2-ylidene **43a**.

Ring expansion results using pyridine catalysis were inconsistent in some cases. Given our mechanistic hypothesis (see next section), one concern was slow proton-transfer during the ring expansion. Keck has found that DMAP/DMAP•HCl mixtures were superior in the nucleophilic catalysis of lactonization reactions, so we chose to examine a series of pyridinium salts.²² Pyridinium acetate (pyr•HOAc), pyridinium chloride (pyr•HCl), and pyridinium 4-methylbenzenesulfonate (pyr•TsOH) were also examined as catalysts for this reaction, leading to the discovery of optimal reaction conditions: treatment of the **36b/38b** mixture with 1.5 equivalents of pyridinium acetate in CH_2Cl_2 at room temperature. Under these conditions the ring expansion reaction proceeded cleanly for both **36b/38b** and **36a/38a** mixtures, providing the desired products as single geometric isomers²³ in 78% and 82% respectively; however, the ring expansion was not successful in inducing formation of the eight-membered ring from **36c** (Table 4.2). This result may reflect the inability of the chain termini to interact in a constructive manner to access the larger eight-membered oxacycle. This entropic barrier is a

prevalent obstacle in the construction of medium-sized rings. Although numerous attempts were made to catalyze this reaction, including treatment of **36c** with simple bases (LiH and NaH) as well as Lewis acids, generation of the desired eight-membered oxacycle was unsuccessful. Unfortunately, no reaction or mere decomposition of starting material was observed under the various reaction conditions.

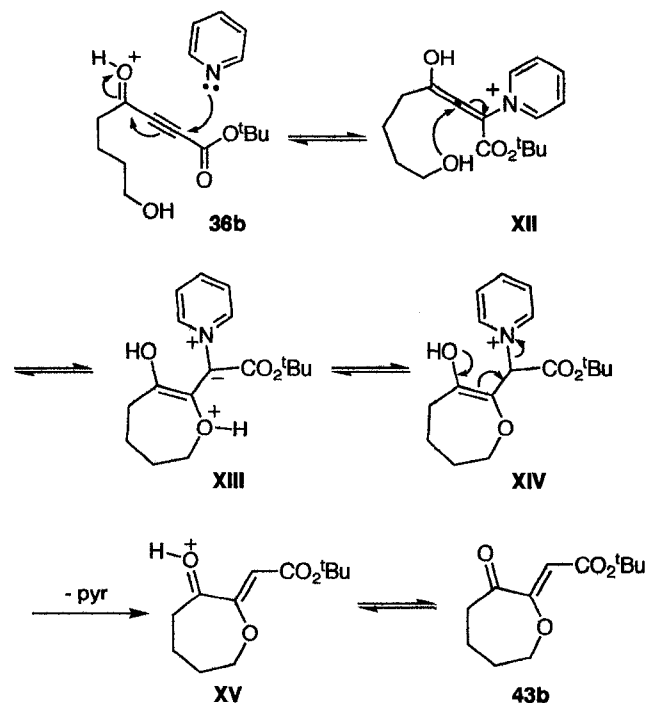


entry	substrate	n	yield (%)
1	36a/38a	1	82
2	36b/38b	2	78
3	36c	3	-

Table 4.2. Pyridinium acetate-catalyzed ring expansion.

Mechanistic Implications

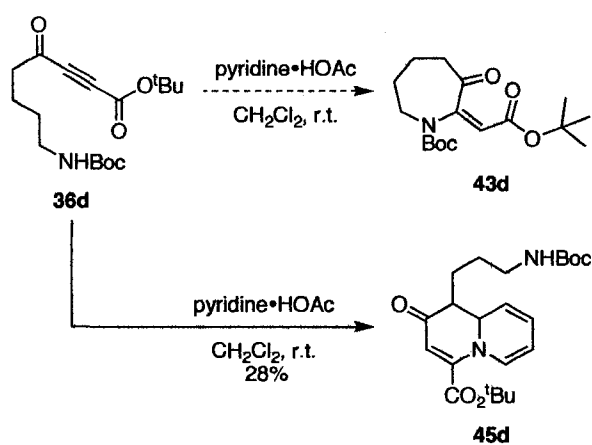
On first examination, the mechanism for this cyclization process might be presumed to proceed through simple 1,4-addition of the pendent hydroxyl moiety towards the ester functionality in **36**; however, the observation that simple, non-nucleophilic bases were unable to initiate cyclization suggests that the mechanism for the ring expansion process does, in fact, involve nucleophilic catalysis (*Scheme 4.15*). A feasible mechanism for this transformation would involve initial activation of the ketone through protonation with pyridinium acetate, followed by nucleophilic 1,4-addition of pyridine to provide intermediate **XII**. The direction of pyridine addition into the conjugated keto-ester (**36**) can be explained by the inherent electron-withdrawing ability of the ketone



Scheme 4.15. Proposed mechanism.

functionality when compared with the ester. At this point, the pendent nucleophile could add into the polarized allenyl moiety of **XII**, resulting in the formation of a cyclic zwitterionic intermediate (**XIII**). This intramolecular cyclization process occurs in a *6-exo-dig* or *7-exo-dig* manner, which is in accordance with Baldwin's rules for ring closure.²⁴ Subsequent proton transfer would result in the formation of **XIV**, which would undergo elimination of pyridine to generate the final product **43b**. This type of mechanism is not without precedent. For example, an analogous mechanism was previously outlined to describe the synthesis of sulfur heterocycles using tributylphosphine as the organocatalyst (*Scheme 4.9*).¹⁰ Furthermore, evidence of pyridine participation in the reaction mechanism was observed when this methodology was applied to the synthesis of nitrogen heterocycles (see below).

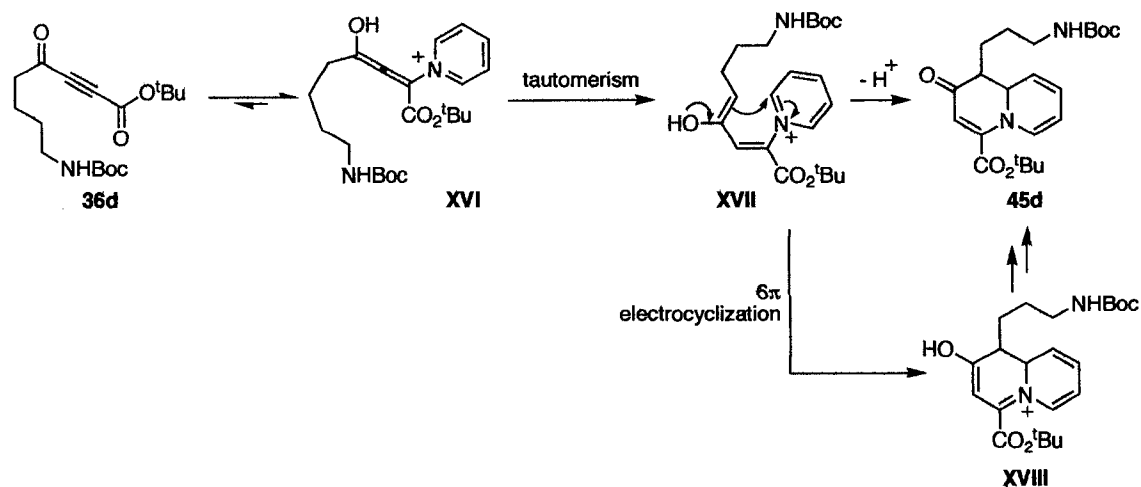
When the *N*-Boc-protected substrate **36d** was treated with pyridinium acetate under the previously outlined reaction conditions, none of the expected ring expanded product (**43d**) was observed. Instead, a novel bicyclic product, **45d**, was isolated in 28% yield as a result of pyridine incorporation into the substrate (*Scheme 4.16*). Although this type of reactivity is not unparalleled in the literature,²⁵ no evidence of these bicyclic products was observed when the analogous oxygen substrates were subjected to the same reaction conditions. The interesting reactivity of this substrate (**36d**) suggests that the



Scheme 4.16. Treatment of *N*-Boc substrate **36d** to pyridinium acetate.

nucleophilicity of the Boc-protected nitrogen is insufficient to allow its participation in the ring expansion reaction, leading to side-reactions that result in the formation of **45d** (*Scheme 4.17*). In the absence of a competent nucleophile, the cationic intermediate generated from 1,4-addition of pyridine (**XVI**) would be long-lived. Tautomerization of the enol functionality to afford intermediate **XVII** would set the stage for cyclization involving the pyridinium moiety to give **45d**. This cyclization could be interpreted as a direct nucleophilic attack by the enol, or more likely, as a 6π electrocyclization. Although the *N*-Boc-protected substrate **36d** does not furnish the desired 3-oxoazepane

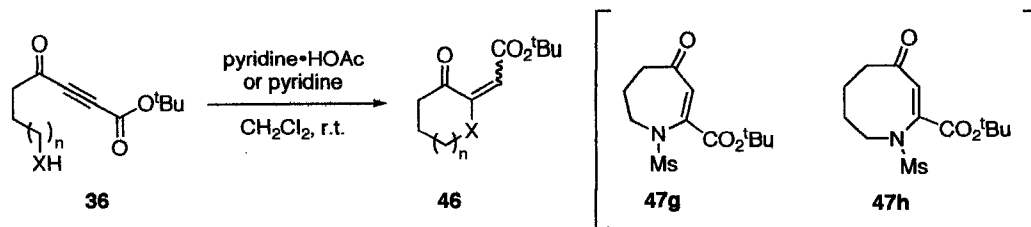
43d, formation of the bicyclic product (**45d**) provides some insight into the mechanism of this reaction by implicating the participation of pyridine as a nucleophilic organocatalyst.



Scheme 4.17. Mechanism for the formation of bicycle **45d**.

Nitrogen Heterocycles

In an effort to find a nitrogen-protecting group that was compatible with the ring expansion reaction, the *N*-tosyl, *N*-mesyl, and *N*-nosyl substrates (**36e-j**) were examined. Initially, *N*-tosyl substrate **36e** was subjected to the optimized reaction conditions using pyridinium acetate to catalyze the ring expansion. After only 1 hour, these conditions afforded an inseparable mixture of two 3-oxo-1-tosylpiperidin-2-ylidenes, **46e**, in a 1.6:1 ratio of *Z*:*E*-isomers (*Table 4.3*). Next, the ring expansion reaction of the *N*-tosyl substrate **36f** was examined and it was observed that standard pyridinium acetate catalysis did not effect cyclization to the desired product, but instead promoted rapid decomposition of the starting material. Fortunately, when **36f** was subjected to 1.5 equivalents of pyridine in CH₂Cl₂, the ring expansion reaction proceeded quickly to furnish 3-oxo-1-tosylazepan-2-ylidene **46f** in a 1:1.6 ratio of separable *Z*:*E* isomers. The

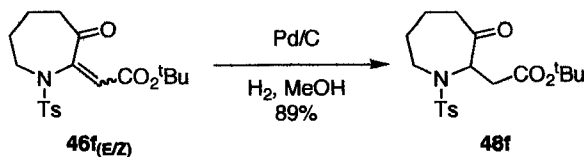


entry	substrate	X	n	catalyst	product (Z:E)	yield (%)
1	36e	N-Ts	1	pyr•HOAc	46e (1.6 : 1)	58
2	36f	N-Ts	2	pyr	46f (1 : 1.6)	74
3	36g	N-Ms	1	pyr•HOAc	46g (23 : 6 : 1) ^a	60
4	36h	N-Ms	2	pyr	46h (2 : 5 : 1) ^a	77
5	36i	N-Ns	1	pyr•HOAc	46i (1 : 1.3)	42
6	36j	N-Ns	2	pyr	46j (1 : 1.8)	55

^a The ratio displayed is for Z:E:47.

Table 4.3. Ring expansion of nitrogen-substrates **36**.

structure of **46f_E** was confirmed by single crystal X-ray crystallography (see Appendix V). The geometry of the Z-isomer, **46f_Z**, was also confirmed when the **46f_(E/Z)** mixture was subjected to hydrogenation conditions, providing a single product (**48f**) (Scheme 4.18).



Scheme 4.18. Hydrogenation of 3-oxo-1-tosylazepan-2-ylidenes **46f_(E/Z)**.

With these results in hand, the remaining *N*-mesyl and *N*-nosyl substrates (**36g-j**) were examined in the ring expansion reaction. The reactions proceeded in moderate to good yields affording a mixture of *Z/E*-isomers in each case (Table 4.3). Only the *N*-

mesyl substrates, **36g** and **36h**, showed evidence of the alternate, two-carbon ring expansion pathway described by Schreiber²¹ providing the undesired azapen-4-one **47g** and azacen-4-one **47h**, respectively, as minor products. These products were identified based on characteristic correlations observed in the HMBC spectra (*Figure 4.4*). For example, the HMBC spectrum for azacen-4-one **47h** showed a three-bond correlation

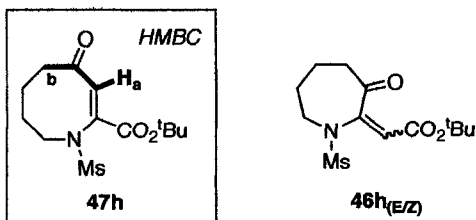


Figure 4.4. Characteristic HMBC correlations for azapen-4-one **47h**.

between the vinyl proton H_a and the methylene carbon (C_b) adjacent to the ketone functionality. This correlation was not observed in the HMBC spectrum for the seven-membered analogue **46h**. Also, it is notable that the *N*-nosyl substrates underwent ring expansion in diminished yields: isomers of **46i** were isolated in a combined yield of 42%, while isomers of **46j** were isolated in 55% yield. These results may reflect the decreased nucleophilicity of the nitrogen moiety in starting materials **36i** and **36j**, due to the inherent electron-withdrawing nature of the nosyl protecting group.

The geometry of the double bonds for all of these compounds (**46**) could be clearly assigned based on the chemical shifts of the vinyl protons in the *Z*- and *E*-isomers. In ¹H NMR spectra, vinyl protons in the *Z*-isomers were observed at higher chemical shifts than those corresponding to the *E*-isomers, due to anisotropic deshielding from the adjacent ketone carbonyl (*Figure 4.5*). Additionally, the emergence of unexpected side products after prolonged reaction times provided experimental evidence for the

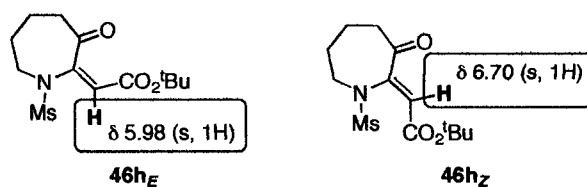
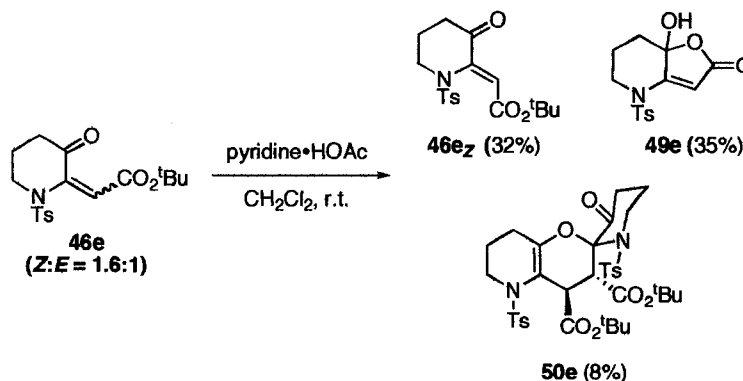


Figure 4.5. Comparison of ^1H NMR data for *E/Z*-isomers of **46h**.

geometrical assignments. When a mixture of *E/Z*-isomers (**46e**) was re-subjected to standard reaction conditions, the *Z*-isomer was recovered along with two side-products: the hemiacetal **49e** and a single diastereomer of an interesting spirocycle **50e**, which is the result of a formal Diels-Alder reaction between two molecules of the 3-oxo-1-tosylpiperidin-2-ylidene, **46e** (Scheme 4.19). The formation of spirocyclic product **50e** was implied by the presence of two distinct *N*-tosyl groups and fourteen diastereotopic protons in the ^1H NMR spectrum, a deshielded spirocyclic sp^3 -carbon (89.6 ppm) in the ^{13}C NMR spectrum, as well as the important observance of a mass peak in the mass spectrum that corresponded to two units of **46e** (m/z 753.2480 for $\text{C}_{36}\text{H}_{46}\text{N}_2\text{O}_{10}\text{S}_2\text{Na}$).



Scheme 4.19. Re-subjection of a mixture of *E/Z*-isomers to pyridinium acetate.

The structure was then confirmed by the observation of characteristic correlations in the 2D COSY, HMQC, and HMBC spectra (see Appendix III).

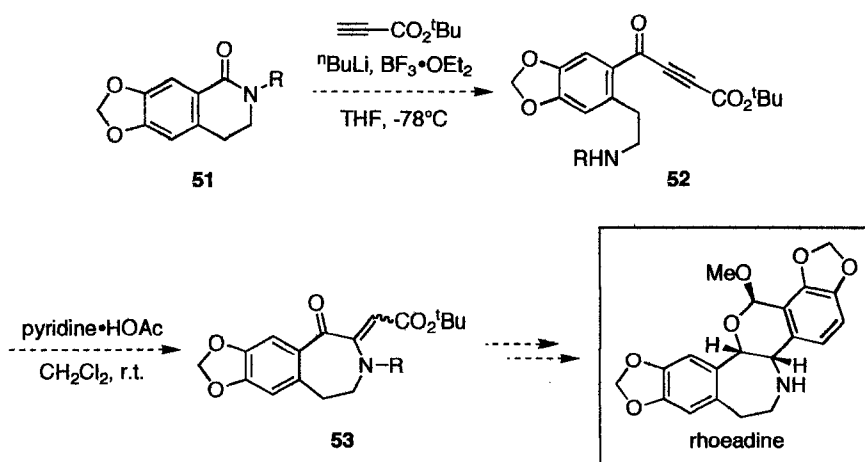
The formation of hemiacetal product **49e** presumably results from acid-promoted lactonization during prolonged exposure to pyridinium acetate and subsequent aqueous work-up. This product can only arise from the *E*-isomer, thus supporting our earlier assignment. In order to prevent the formation of these side products, the ring expansion reactions for all nitrogen substrates were monitored closely by TLC analysis and stopped as soon as the starting material was consumed. It should be noted that these side-products were not observed when the analogous oxygen substrates were subjected to the same prolonged reaction times.

4.2.3 Conclusions

The synthesis of oxygen and nitrogen-containing heterocycles has been accomplished by BF₃-mediated *tert*-butyl propiolate addition to readily available lactones and lactams, followed by ring expansion using pyridinium acetate. When pyridinium acetate led to decomposition of the intermediate acetylenic ketoesters, pyridine was successfully used to catalyze the reaction. The ring expansion reactions to generate six- and seven-membered oxacycles and azacycles proceed smoothly to provide the desired products in moderate to good yields. This method provides a short and efficient strategy to access highly functionalized heterocycles that can be further functionalized to assemble interesting heterocyclic frameworks.

4.3 Future Directions

Preliminary investigations into this ring expansion methodology have led to the development of optimized reaction conditions and provided information on the mechanism of this transformation. The general substrate scope has been established; however, the synthesis of more highly substituted heterocycles might be possible through the use of increasingly elaborate lactone or lactam starting materials. Ideally, requisite starting materials should be readily accessible through functionalization of the corresponding α,β -unsaturated lactone/lactams or simple alkylation. The two-step ring expansion sequence might then be used in synthetic strategies towards the total synthesis of numerous natural products, such as compounds in the rhoeadine class of benzazepine alkaloids (*Scheme 4.20*).^{26,27} *tert*-Butyl propiolate addition to an aromatic lactam such as **51**, followed by ring expansion under the influence of pyridinium acetate, would lead to a highly functionalized intermediate **53**. This intermediate might then be further manipulated to furnish the final product.



Scheme 4.20. Possible strategy towards the synthesis of the core of rhoeadine.

4.4 Experimental

4.4.1 General Information

Reactions were carried out in flame-dried glassware under a positive argon atmosphere unless otherwise stated. Transfer of anhydrous solvents and reagents was accomplished with oven-dried syringes or cannulae. Solvents were distilled before use: methylene chloride (CH_2Cl_2) from calcium hydride, tetrahydrofuran (THF) and diethyl ether (Et_2O) from sodium/benzophenone ketyl, and toluene from sodium metal. Thin layer chromatography was performed on glass plates precoated with 0.25 mm Kieselgel 60 F₂₅₄ (Merck). Flash chromatography columns were packed with 230-400 mesh silica gel (Silicycle) or ~150 mesh activated, neutral, Brockmann I, standard grade aluminum oxide (Sigma-Aldrich). Proton nuclear magnetic resonance spectra (^1H NMR) were recorded at 400 MHz or 500 MHz and coupling constants (J) are reported in Hertz (Hz). Standard notation was used to describe the multiplicity of signals observed in ^1H NMR spectra: broad (br), multiplet (m), singlet (s), doublet (d), triplet (t), etc. Carbon nuclear magnetic resonance spectra (^{13}C NMR) were recorded at 100 MHz or 125 MHz and are reported (ppm) relative to the center line of the triplet from chloroform-*d* (77.00 ppm). Infrared (IR) spectra were measured with a Mattson Galaxy Series FT-IR 3000 spectrophotometer. Mass spectra were determined on a PerSeptive Biosystems Mariner high-resolution electrospray positive ion mode spectrometer.

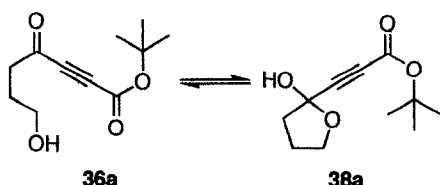
4.4.2 Characterization

^tBu-propiolate Addition to Lactones/Lactams.

Method A: ⁿBuLi (1.6 M in hexanes, 4.5 mmol, 2.8 mL) was added dropwise to a stirring solution of *tert*-butyl propiolate (1.1 equiv, 4.1 mmol, 0.56 mL) in THF (20 mL) at -78°C. The reaction mixture was allowed to stir for 30 min and the temperature gradually raised to -50°C before the dropwise addition of BF₃•OEt₂ (4.5 mmol, 0.57 mL) using a syringe. The reaction was allowed to stir for another 10 min. The temperature was then dropped to -78°C before the dropwise addition of the lactone (4.1 mmol). After 90 min stirring, with gradual warming to room temperature, saturated NH₄Cl solution (10 mL) was added. The aqueous layer was extracted with Et₂O (2 x 10 mL) and the combined organic layers washed with H₂O (10 mL) and brine solution (10 mL). The organic layer was dried (MgSO₄), filtered, and the solvent removed by rotary evaporation to provide a crude oil, which was purified by flash column chromatography (silica gel) to provide the pure addition product.

Method B: ⁿBuLi (1.47 M in hexanes, 0.85 mmol, 0.58 mL) was added dropwise to a stirring solution of *tert*-butyl propiolate (1.6 equiv, 0.80 mmol, 0.11 mL) in THF (3 mL) at -78°C. The reaction mixture was allowed to stir for 30 min and the temperature gradually raised to -50°C before the dropwise addition of BF₃•OEt₂ (0.85 mmol, 0.11 mL). The reaction was allowed to stir for 10 min. The temperature was then dropped to -78°C before the slow, dropwise addition of a solution of lactam (0.50 mmol) in THF (2 mL). After 90 min stirring, with gradual warming to room temperature, saturated NH₄Cl solution (5 mL) was added. The aqueous layer was extracted with Et₂O (2 x 5 mL) and

the combined organic layers washed with H₂O (5 mL) and brine solution (5 mL). The organic layer was dried (MgSO₄), filtered, and the solvent removed by rotary evaporation to provide a crude oil, which was purified by flash column chromatography (silica gel) to provide the pure addition product.

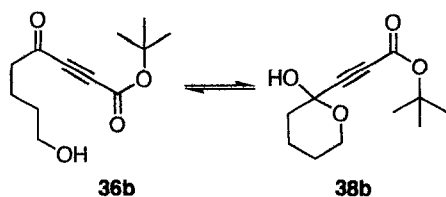


Compounds 36a/38a.

Method A was used to furnish **36a/38a** (**36b:38b** = 4:1, 63%) as a colourless oil after purification by flash column chromatography (silica gel, hexanes/EtOAc 2:1). The two isomers were observed as an inseparable mixture; therefore, the ¹H and ¹³C NMR data reported herein was extracted from spectra of the **36a/38a** mixture: *R_f* 0.26 (hexanes/EtOAc 2:1); IR (thin film) 3412, 2981, 2936, 2241, 1715, 1396, 1274, 1155, 1057, 839, 751 cm⁻¹; HRMS (ESI, [M+Na]⁺) for C₁₁H₁₆O₄Na calcd 235.0941, found: *m/z* 235.0938.

36a: ¹H NMR (500 MHz, CDCl₃) δ 3.68 (t, *J* = 6.0 Hz, 2H), 2.77 (t, *J* = 7.0 Hz, 2H), 1.94 (pent, *J* = 7.0 Hz, 2H), 1.52 (s, 9H), (OH proton not observed); ¹³C NMR (125 MHz, CDCl₃) δ 177.2, 150.8, 85.4, 79.8, 78.7, 61.5, 41.8, 27.9, 26.2.

38a: ¹H NMR (500 MHz, CDCl₃) δ 4.06-4.12 (m, 1H), 3.98-4.04 (m, 1H), 2.22-2.32 (m, 2H), 2.10-2.20 (m, 1H), 1.98-2.06 (m, 1H), 1.49 (s, 9H), (OH proton not observed); ¹³C NMR (125 MHz, CDCl₃) δ 152.1, 97.5, 83.9, 82.3, 75.2, 69.0, 39.7, 27.9, 24.4.

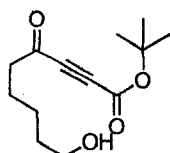


Compound 36b/38b.

Method A was used to furnish **36b/38b** (**36b:38b** = 1.3:1, 82%) as a colourless oil after purification by flash column chromatography (silica gel, hexanes/EtOAc 2:1). The two isomers were observed as an inseparable mixture; therefore, the ^1H and ^{13}C NMR data reported herein was extracted from spectra of the **36b/38b** mixture: R_f 0.33 (hexanes/EtOAc 2:1); IR (thin film) 3401, 2943, 2874, 1713, 1457, 1371, 1271, 1067, 1039, 840, 752 cm^{-1} ; HRMS (EI, M^+) for $\text{C}_{12}\text{H}_{18}\text{O}_4$ calcd 226.1205, found: m/z 226.1193.

36b: ^1H NMR (400 MHz, CDCl_3) δ 3.65 (t, $J = 6.4$ Hz, 2H), 2.68 (t, $J = 7.2$ Hz, 2H), 1.77 (pent, $J = 7.2$ Hz, 2H), 1.55-1.65 (m, 2H), 1.51 (s, 9H), (OH proton not observed); ^{13}C NMR (125 MHz, CDCl_3) δ 186.1, 151.1, 85.4, 79.6, 78.7, 63.8, 44.8, 31.6, 27.9, 19.7.

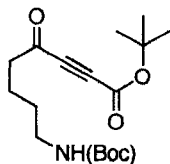
38b: ^1H NMR (400 MHz, CDCl_3) δ 3.96 (ddd, $J = 11.2, 5.2, 5.2$ Hz, 1H), 3.78 (ddd, $J = 11.6, 6.8, 4.0$ Hz, 1H), 1.94-2.00 (m, 1H), 1.70-1.90 (m, 3H), 1.55-1.65 (m, 2H), 1.49 (s, 9H), (OH proton not observed); ^{13}C NMR (125 MHz, CDCl_3) δ 152.1, 91.5, 84.0, 82.6, 75.9, 62.1, 36.0, 27.9, 24.4, 19.6.



36c

Compound 36c.

Method A was used to furnish **36c** (83%), which was generated as a single (acyclic) product. Compound **36c** was isolated as a colourless oil after purification by flash column chromatography (silica gel, hexanes/EtOAc 3:2): R_f 0.21 (hexanes/EtOAc 2:1); IR (thin film) 3368, 2981, 2937, 2867, 1716, 1605, 1476, 1459, 1396, 1371, 1258, 1154, 1071, 839 cm^{-1} ; ^1H NMR (500 MHz, CDCl_3) δ 3.65 (t, $J = 6.5$ Hz, 2H), 2.65 (t, $J = 7.0$ Hz, 2H), 1.72 (pent, $J = 7.5$ Hz, 2H), 1.59 (pent, $J = 7.0$ Hz, 2H), 1.52 (s, 9H), 1.39-1.45 (m, 2H); ^{13}C NMR (100 MHz, CDCl_3) δ 186.2, 151.1, 85.4, 79.5, 78.8, 62.5, 45.1, 32.2, 27.9, 25.0, 23.2; HRMS (EI, $[\text{M}^{-4}\text{Bu}]^+$) for $\text{C}_9\text{H}_{11}\text{O}_4$ calcd 183.0657, found: m/z 183.0652.

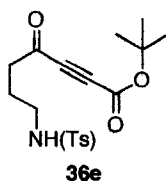


36d

Compound 36d.

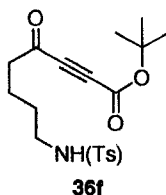
Method B was used to furnish **36d** (77%) as a yellow oil after purification by flash column chromatography (silica gel, hexanes/EtOAc 2:1): R_f 0.51 (hexanes/EtOAc 2:1); IR (thin film) 3359, 2979, 2935, 1715, 1518, 1369, 1272, 1258, 1156 cm^{-1} ; ^1H NMR (500 MHz, CDCl_3) δ 4.57 (br s, 1H), 3.12 (br q, $J = 6.0$ Hz, 2H), 2.65 (t, $J = 7.0$ Hz, 2H), 1.68 (pent, $J = 8.0$ Hz, 2H), 1.46-1.57 (m, 2H), 1.51 (s, 9H), 1.43 (br s, 9H); ^{13}C NMR (125

MHz, CDCl₃) δ 185.8, 155.9, 151.0, 85.4, 79.6, 79.2, 78.7, 44.6, 40.0, 29.2, 28.4, 28.0, 20.5; HRMS (ESI, [M+Na]⁺) for C₁₇H₂₇NO₅Na calcd 384.1781, found: m/z 348.1782.



Compound 36e.

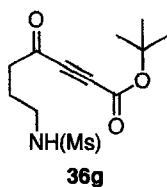
Method B was used to furnish **36e** (60%) as a white solid after purification by flash column chromatography (silica gel, hexanes/EtOAc 2:1): m.p. 78.5-80.0°C; R_f 0.38 (hexanes/EtOAc 2:1); IR (thin film) 3288, 2981, 2936, 1714, 1689, 1371, 1274, 1156, 1093, 815 cm⁻¹; ¹H NMR (500 MHz, CDCl₃) δ 7.72 (d, *J* = 8.5 Hz, 2H), 7.29 (d, *J* = 8.5 Hz, 2H), 5.00 (br t, *J* = 6.5 Hz, 1H), 2.94 (q, *J* = 6.5 Hz, 2H), 2.67 (t, *J* = 7.0 Hz, 2H), 2.41 (s, 3H), 1.80 (pent, *J* = 7.0 Hz, 2H), 1.50 (s, 9H); ¹³C NMR (125 MHz, CDCl₃) δ 185.1, 150.9, 143.5, 136.7, 129.7, 127.0, 85.5, 79.8, 78.4, 42.0, 41.9, 27.8, 23.1, 21.4; HRMS (ESI, [M+Na]⁺) for C₁₈H₂₃NO₅SNa calcd 388.1189, found: m/z 388.1192; Anal. Calcd for C₁₈H₂₃NO₅S: C, 59.16; H, 6.34; N, 3.83; S, 8.77. Found: C, 59.21; H, 6.34; N, 3.77; S, 8.76.



Compound 36f.

Method B was used to furnish **36f** (84%) as a pale yellow oil after purification by flash column chromatography (silica gel, hexanes/EtOAc 2:1): R_f 0.34 (hexanes/EtOAc 2:1); IR (thin film) 3288, 2981, 2937, 2873, 1714, 1688, 1371, 1327, 1275, 1157, 1095, 838

cm⁻¹; ¹H NMR (400 MHz, CDCl₃) δ 7.74 (d, *J* = 8.4 Hz, 2H), 7.31 (d, *J* = 8.4 Hz, 2H), 4.70 (br t, *J* = 6.4 Hz, 1H), 2.93 (q, *J* = 6.8 Hz, 2H), 2.58 (t, *J* = 7.2 Hz, 2H), 2.43 (s, 3H), 1.62-1.68 (m, 2H), 1.52 (s, 9H), 1.46-1.52 (m, 2H); ¹³C NMR (100 MHz, CDCl₃) δ 185.5, 151.0, 143.5, 136.8, 129.7, 127.0, 85.5, 79.7, 78.6, 44.3, 42.6, 28.6, 27.9, 21.5, 20.1; HRMS (ESI, [M+Na]⁺) for C₁₉H₂₅NO₅SNa calcd 402.1346, found: *m/z* 402.1345.

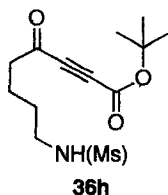


Compound 36g.

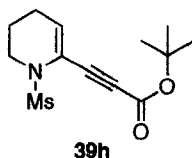
Method B was used to furnish **36g** (63%) as a white solid after purification by flash column chromatography (silica gel, hexanes/EtOAc 2:1): m.p. 84.0-85.5°C; R_f 0.24 (hexanes/EtOAc 1:1); IR (thin film) 3295, 2982, 2937, 1714, 1689, 1321, 1275, 1259, 1152 cm⁻¹; ¹H NMR (500 MHz, CDCl₃) δ 4.74 (br s, 1H), 3.15 (q, *J* = 6.5 Hz, 2H), 2.95 (s, 3H), 2.77 (t, *J* = 7.0 Hz, 2H), 1.92 (pent, *J* = 7.0 Hz, 2H), 1.51 (s, 9H); ¹³C NMR (125 MHz, CDCl₃) δ 185.2, 151.0, 85.6, 80.0, 78.5, 42.1, 42.0, 40.2, 27.9, 23.7; HRMS (ESI, [M+Na]⁺) for C₁₂H₁₉NO₅SNa calcd 312.0876, found: *m/z* 312.0874; Anal. Calcd for C₁₂H₁₉NO₅S: C, 49.81; H, 6.62; N, 4.84; S, 11.08. Found: C, 50.04; H, 6.57; N, 4.76; S, 10.85.

Compounds 36h and 39h.

Method B was used to furnish **36h** (57%) and **39h** (25%) after purification by flash column chromatography (silica gel, hexanes/EtOAc 2:1).



36h: pale orange oil; R_f 0.24 (hexanes/EtOAc 1:1); IR (thin film) 3296, 2981, 2937, 1714, 1688, 1321, 1276, 1260, 1153 cm^{-1} ; ^1H NMR (500 MHz, CDCl_3) δ 4.50 (br s, 1H), 3.14 (q, $J = 6.5$ Hz, 2H), 2.96 (s, 3H), 2.69 (t, $J = 7.0$ Hz, 2H), 1.72-1.78 (m, 2H), 1.58-1.64 (m, 2H), 1.52 (s, 9H); ^{13}C NMR (125 MHz, CDCl_3) δ 185.6, 151.0, 85.6, 79.9, 78.6, 44.4, 42.7, 40.4, 29.2, 27.9, 20.1; HRMS (ESI, $[\text{M}+\text{Na}]^+$) for $\text{C}_{13}\text{H}_{21}\text{NO}_5\text{SNa}$ calcd 326.1033, found: m/z 326.1033.



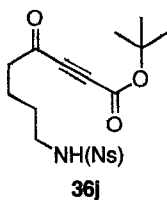
39h: yellow oil; R_f 0.57 (hexanes/EtOAc 1:1); IR (thin film) 2980, 2936, 2213, 1704, 1354, 1291, 1154, 1094, 950 cm^{-1} ; ^1H NMR (500 MHz, CDCl_3) δ 6.01 (t, $J = 4.0$ Hz, 1H), 3.62 (t, $J = 5.0$ Hz, 2H), 3.19 (s, 3H), 2.26 (td, $J = 6.5, 4.5$ Hz, 2H), 1.87-1.92 (m, 2H), 1.50 (s, 9H); ^{13}C NMR (125 MHz, CDCl_3) δ 152.5, 1287, 119.2, 83.8, 82.7, 78.9, 45.3, 42.4, 28.0, 23.6, 22.3; HRMS (ESI, $[\text{M}+\text{Na}]^+$) for $\text{C}_{13}\text{H}_{19}\text{NO}_4\text{SNa}$ calcd 308.0927, found: m/z 308.0926.



Compound 36i.²⁰

2-Pyrrolidinone (0.99 g, 0.010 mol) was dissolved in THF (25 mL) and the temperature was lowered to -78°C (dry ice/acetone bath). $n\text{-BuLi}$ (1.6 M in hexanes, 6.9 mL, 0.011 mol) was added dropwise by syringe and the reaction was allowed to stir at -78°C . After 1 hour, a solution of 2-nitrobenzenesulfonyl chloride (2.4 g, 0.011 mol) in THF (25 mL) was transferred to the stirring reaction mixture dropwise by canula. The reaction was allowed to warm to room temperature overnight before the addition of saturated NH_4Cl solution (25 mL). The aqueous layer was extracted with Et_2O (2 x 25 mL), the combined organic layers were washed with H_2O (25 mL), brine (25 mL), and dried (MgSO_4). After filtration, the solvent was removed by rotary evaporation and the crude material was purified by flash column chromatography (silica gel, hexanes:EtOAc 1:1) to provide *N*-(2-nitrobenzenesulfonyl)-2-pyrrolidinone **35i** (1.9 g, 7.0 mmol, 70%) as a white solid: m.p. $112.0\text{-}113.0^{\circ}\text{C}$; R_f 0.18 (hexanes/EtOAc 2:1); IR (thin film) 3102, 2993, 2913, 1741, 1543, 1367, 1171, 1126, 962 cm^{-1} ; $^1\text{H NMR}$ (500 MHz, CDCl_3) δ 8.45 (m, 1H), 7.73-7.79 (m, 3H), 4.07 (t, $J = 7.0\text{ Hz}$, 2H), 2.52 (t, $J = 8.0\text{ Hz}$, 2H), 2.20 (app pent, $J = 7.5\text{ Hz}$, 2H); $^{13}\text{C NMR}$ (125 MHz, CDCl_3) δ 173.6, 148.0, 134.9, 134.5, 131.9, 131.5, 124.2, 47.5, 32.1, 18.9; HRMS (ESI, $[\text{M}+\text{Na}]^+$) for $\text{C}_{10}\text{H}_{10}\text{N}_2\text{O}_5\text{SNa}$ calcd 293.0203, found: m/z 293.0199; Anal. Calcd for $\text{C}_{10}\text{H}_{10}\text{N}_2\text{O}_5\text{S}$: C, 44.44; H, 3.73; N, 10.37; S, 11.86. Found: C, 44.65; H, 3.72; N, 10.13; S, 11.67.

Method A was used to furnish **36i** (26%) as a pale yellow oil after purification by flash column chromatography (silica gel, hexanes/EtOAc 3:2): R_f 0.27 (hexanes/EtOAc 2:1); IR (thin film) 3338, 2982, 1712, 1688, 1542, 1370, 1276, 1154 cm^{-1} ; ^1H NMR (500 MHz, CDCl_3) δ 8.12-8.14 (m, 1H), 7.87-7.88 (m, 1H), 7.74-7.78 (m, 2H), 5.36 (br t, $J = 6.0$ Hz, 1H), 3.14 (app q, $J = 6.5$ Hz, 2H), 2.77 (t, $J = 7.0$ Hz, 2H), 1.91 (app pent, $J = 7.0$ Hz, 2H), 1.53 (s, 9H); ^{13}C NMR (125 MHz, CDCl_3) δ 184.9, 150.9, 148.1, 133.7, 133.52, 132.88, 131.1, 125.5, 85.6, 80.1, 78.3, 42.5, 41.7, 27.9, 23.4; HRMS (ESI, $[\text{M}+\text{Na}]^+$) for $\text{C}_{17}\text{H}_{20}\text{N}_2\text{O}_7\text{SNa}$ calcd 419.0883, found: m/z 419.0881.



Compound **36j**.²⁰

2-Piperidinone (0.99 g, 0.01 mol) was dissolved in THF (25 mL) and the temperature was lowered to -78°C (dry ice/acetone bath). $n\text{BuLi}$ (1.6 M in hexanes, 6.9 mL, 0.011 mol) was added dropwise by syringe and the reaction was allowed to stir at -78°C . After 1 hour, a solution of 2-nitrobenzenesulfonyl chloride (2.4 g, 0.011 mol) in THF (25 mL) was transferred to the stirring reaction mixture dropwise by canula. The reaction was allowed to warm to room temperature overnight before the addition of saturated NH_4Cl solution (25 mL). The aqueous layer was extracted with Et_2O (2 x 25 mL), the combined organic layers were washed with H_2O (25 mL), brine (25 mL), and dried (MgSO_4). After filtration, the solvent was removed by rotary evaporation and the crude material was purified by flash column chromatography (silica gel, hexanes:EtOAc 1:1) to provide *N*-(2-nitrobenzenesulfonyl)-2-piperidinone **35j** (2.0 g, 0.007 mol, 70%) as a white solid:

m.p. 173.5-175.0°C; R_f 0.18 (hexanes/EtOAc 2:1); IR (thin film) 3103, 2960, 1686, 1544, 1353, 1177, 1155, 1125 cm^{-1} ; ^1H NMR (500 MHz, CDCl_3) δ 8.48-8.50 (m, 1H), 7.74-7.78 (m, 3H), 3.91 (t, $J = 6.0$ Hz, 2H), 2.48 (t, $J = 7.0$ Hz, 2H), 2.00 (app pent, $J = 6.0$ Hz, 2H), 1.87 (app pent, $J = 6.5$ Hz, 2H); ^{13}C NMR (125 MHz, CDCl_3) δ 170.4, 148.0, 135.1, 134.4, 133.2, 131.8, 124.2, 46.8, 33.7, 22.8, 20.1; HRMS (ESI, $[\text{M}+\text{Na}]^+$) for $\text{C}_{11}\text{H}_{12}\text{N}_2\text{O}_5\text{SNa}$ calcd 307.0359, found: m/z 307.0356; Anal. Calcd for $\text{C}_{11}\text{H}_{12}\text{N}_2\text{O}_5\text{S}$: C, 46.47; H, 4.25; N, 9.85; S, 11.28. Found: C, 46.43; H, 4.33; N, 9.59; S, 10.98.

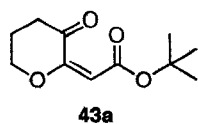
Method A was used to furnish **36j** (41%) as a pale yellow oil after purification by flash column chromatography (silica gel, hexanes/EtOAc 3:2): R_f 0.25 (hexanes/EtOAc 2:1); IR (thin film) 3342, 2982, 2938, 2241, 1711, 1541, 1370, 1276, 1154, 1080, 838, 742 cm^{-1} ; ^1H NMR (500 MHz, CDCl_3) δ 8.12-8.16 (m, 1H), 7.85-7.89 (m, 1H), 7.73-7.78 (m, 2H), 5.31 (br t, $J = 6.5$ Hz, 1H), 3.12 (app q, $J = 7.0$ Hz, 2H), 2.63 (t, $J = 7.0$ Hz, 2H), 1.70 (pent, $J = 7.0$ Hz, 2H), 1.54-1.60 (m, 2H), 1.52 (s, 9H); ^{13}C NMR (125 MHz, CDCl_3) δ 185.4, 151.0, 148.1, 133.7, 133.6, 132.8, 131.4, 125.4, 85.6, 79.9, 78.5, 44.3, 43.3, 28.8, 27.9, 20.2; HRMS (ESI, $[\text{M}+\text{Na}]^+$) for $\text{C}_{18}\text{H}_{22}\text{N}_2\text{O}_7\text{SNa}$ calcd 433.1040, found: m/z 433.1038.

Ring Expansion Reactions.

Method C: The substrate (1.5 mmol) was dissolved in CH_2Cl_2 (15 mL) at room temperature. Pyridinium acetate (2.3 mmol, 0.32 g) was added in one portion to the stirring solution. The reaction mixture was then allowed to stir at room temperature and was monitored for the disappearance of starting material by TLC analysis. The reaction was quenched by the addition of 1N HCl (15 mL). The aqueous layer was extracted with

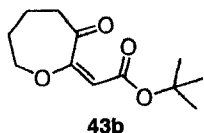
CH₂Cl₂ (2 x 10 mL), the combined organic layers washed with brine solution (10 mL) and dried (MgSO₄). After filtration, the solvent was removed by rotary evaporation to provide a crude oil, which was purified by flash column chromatography (silica gel or alumina) to provide the desired product(s).

Method D: The substrate (1.5 mmol) was dissolved in CH₂Cl₂ (15 mL) at room temperature. Pyridine (2.3 mmol, 0.19 mL) was added in one portion to the stirring solution. The reaction mixture was then allowed to stir at room temperature and was monitored for the disappearance of starting material by TLC analysis. The reaction was quenched by the addition of 1N HCl (aq.) (15 mL). The aqueous layer was extracted with CH₂Cl₂ (2 x 10 mL), the combined organic layers washed with brine solution (10 mL) and dried (MgSO₄). After filtration, the solvent was removed by rotary evaporation to provide a crude oil, which was purified by flash column chromatography (silica gel or alumina) to provide the desired product(s).



Compound 43a.

Method C was used to generate **43a** (82%) after purification by flash column chromatography (silica gel, hexanes:EtOAc 2:1): *R_f* 0.34 (hexanes/EtOAc 2:1); IR (thin film) 2978, 2934, 1704, 1619, 1477, 1456, 1254, 1148 cm⁻¹; ¹H NMR (500 MHz, CDCl₃) δ 5.81 (s, 1H), 4.29 (t, *J* = 5.0 Hz, 2H), 2.61 (t, *J* = 7.0 Hz, 2H), 2.17-2.22 (m, 2H), 1.45 (s, 9H); ¹³C NMR (125 MHz, CDCl₃) δ 192.9, 164.3, 156.6, 101.5, 80.5, 67.3, 35.9, 28.1, 22.2; HRMS (EI, M⁺) for C₁₁H₁₆O₄ calcd 212.1049, found: *m/z* 212.1053.



Compound 43b.

Method C was used to generate **43b** (78%) after purification by flash column chromatography (silica gel, hexanes:EtOAc 2:1): R_f 0.45 (hexanes/EtOAc 2:1); IR (thin film) 2976, 2937, 1699, 1630, 1455, 1392, 1367, 1240, 1147, 1031 cm^{-1} ; ^1H NMR (400 MHz, CDCl_3) δ 5.69 (s, 1H), 4.14 (t, $J = 5.2$ Hz, 2H), 2.71 (t, $J = 6.0$ Hz, 2H), 1.99 (pent, $J = 5.6$ Hz, 2H), 1.83-1.89 (m, 2H), 1.49 (s, 9H); ^{13}C NMR (125 MHz, CDCl_3) δ 201.0, 163.9, 162.0, 105.8, 80.8, 74.1, 42.0, 29.8, 28.1, 23.2; HRMS (ESI, $[\text{M}+\text{Na}]^+$) for $\text{C}_{12}\text{H}_{18}\text{O}_4\text{Na}$ calcd 249.1097, found: m/z 249.1094.



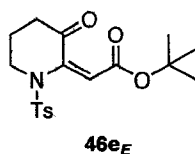
Compound 45d.

Method C was used to generate **45d** (28%) after purification by flash column chromatography (alumina, hexanes:EtOAc 2:1): R_f 0.34 (hexanes/EtOAc 2:1); IR (thin film) 3339, 2976, 2932, 2869, 1700, 1646, 1611, 1558, 1365, 1249, 1147 cm^{-1} ; ^1H NMR (500 MHz, CDCl_3) δ 6.65 (d, $J = 8.0$ Hz, 1H), 6.01-6.05 (m, 1H), 5.68 (s, 1H), 5.53 (br dd, $J = 10.0, 1.0$ Hz, 1H), 5.18 (dd, $J = 7.0, 6.5$ Hz, 1H), 4.79 (br s, 1H), 4.57 (br d, $J = 16.5$ Hz, 1H), 3.09-3.14 (m, 2H), 2.66 (ddd, $J = 16.0, 5.0, 3.5$ Hz, 1H), 1.86-1.93 (m, 1H), 1.65-1.77 (m, 1H), 1.54 (s, 9H), 1.44 (br s, 9H), 1.40-1.50 (m, 2H); ^{13}C NMR (125 MHz, CDCl_3) δ 193.0, 162.2, 156.0, 148.3, 127.8, 122.9, 118.0, 106.1, 103.1, 84.5, 79.0,

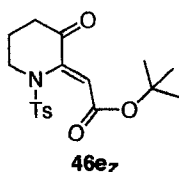
58.6, 48.0, 40.5, 28.4, 27.9, 25.9, 21.2; HRMS (ESI, $[M+Na]^+$) for $C_{22}H_{32}N_2O_5Na$ calcd 427.2203, found: m/z 427.2206.

Compound 46e.

Method C was used to furnish **46e** (58%) after purification by flash column chromatography (silica gel, hexanes:EtOAc 2:1). The *E/Z* isomers were observed as an inseparable mixture (**46e_E**:**46e_Z** = 1:1.6). The 1H and ^{13}C NMR data reported for **46e_E** were extracted from spectra of the *E/Z* mixture, while those for **46e_Z** were obtained when pure compound was isolated after **46e** was re-subjected to the reaction conditions for 72 hours (See **49e** and **50e**).



46e_E: R_f 0.30 (hexanes/EtOAc 2:1); 1H NMR (400 MHz, $CDCl_3$) δ 7.69 (d, $J = 8.4$ Hz, 2H), 7.31 (d, $J = 8.4$ Hz, 2H), 6.51 (s, 1H), 3.70 (t, $J = 6.0$ Hz, 2H), 2.42 (s, 3H), 2.21 (t, $J = 6.8$ Hz, 2H), 1.89-1.95 (m, 2H), 1.51 (s, 9H); ^{13}C NMR (100 MHz, $CDCl_3$) δ 194.6, 164.8, 144.6, 138.3, 135.6, 129.9, 127.2, 121.4, 82.1, 45.8, 36.7, 27.9, 21.6, 20.4; HRMS (ESI, $[M+Na]^+$) for $C_{18}H_{23}NO_5SNa$ calcd 388.1189, found: m/z 388.1190.

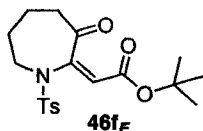


46e_Z: off-white solid; m.p. 104.0-109.0°C; R_f 0.30 (hexanes/EtOAc 2:1); IR (thin film) 2978, 2934, 1713, 1630, 1363, 1166, 1091 cm^{-1} ; 1H NMR (500 MHz, $CDCl_3$) δ 7.63 (d, $J = 8.5$ Hz, 2H), 7.29 (s, $J = 8.5$ Hz, 2H), 6.62 (s, 1H), 3.62 (t, $J = 6.5$ Hz, 2H), 2.41 (s,

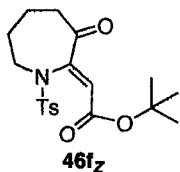
3H), 1.96 (t, $J = 6.0$ Hz, 2H), 1.78 (app pent, $J = 6.5$ Hz, 2H), 1.56 (s, 9H); ^{13}C NMR (125 MHz, CDCl_3) δ 195.9, 164.0, 144.2, 137.6, 135.9, 130.0, 127.2, 124.4, 82.1, 45.3, 36.4, 28.0, 21.5, 19.0; HRMS (ESI, $[\text{M}+\text{Na}]^+$) for $\text{C}_{18}\text{H}_{23}\text{NO}_5\text{SNa}$ calcd 388.1189, found: m/z 388.1188.

Compound 46f.

Method D was used to furnish **46f_E** (46%) and **46f_Z** (28%) after purification by flash column chromatography (silica gel, hexanes:EtOAc 2:1).



46f_E: pale yellow oil; R_f 0.39 (hexanes/EtOAc 2:1); IR (thin film) 2978, 2937, 1700, 1604, 1456, 1347, 1142, 1089, 931, 815 cm^{-1} ; ^1H NMR (400 MHz, CDCl_3) δ 7.74 (d, $J = 8.4$ Hz, 2H), 7.34 (d, $J = 8.4$ Hz, 2H), 6.02 (s, 1H), 3.66 (t, $J = 5.6$ Hz, 2H), 2.62 (t, $J = 6.4$ Hz, 2H), 2.45 (s, 3H), 1.87-1.94 (m, 2H), 1.78-1.84 (m, 2H), 1.43 (s, 9H); ^{13}C NMR (125 MHz, CDCl_3) δ 202.0, 165.5, 149.3, 144.7, 135.8, 130.0, 127.3, 110.0, 81.4, 49.1, 41.5, 28.4, 28.0, 24.1, 21.6; HRMS (ESI, $[\text{M}+\text{Na}]^+$) for $\text{C}_{19}\text{H}_{25}\text{NO}_5\text{SNa}$ calcd 402.1346, found: m/z 402.1348.

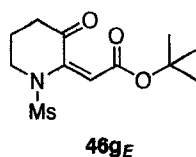


46f_Z: pale yellow oil; R_f 0.50 (hexanes/EtOAc 2:1); IR (thin film) 2978, 2936, 1703, 1631, 1455, 1355, 1242, 1163, 1092, 887 cm^{-1} ; ^1H NMR (400 MHz, CDCl_3) δ 7.68 (d, $J = 8.4$ Hz, 2H), 7.28 (d, $J = 8.4$ Hz, 2H), 6.74 (s, 1H), 3.82 (br s, 2H), 2.40 (t, $J = 8.0$ Hz,

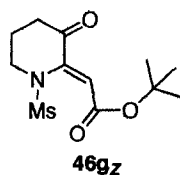
2H), 2.40 (s, 3H), 1.85 (br pent, $J = 5.6$ Hz, 2H), 1.64-1.71 (m, 2H), 1.40 (s, 9H); ^{13}C NMR (125 MHz, CDCl_3) δ 200.8, 162.8, 143.6, 142.3, 138.2, 129.8, 129.1, 127.0, 82.4, 52.5, 40.8, 29.4, 27.9, 23.2, 21.5; HRMS (ESI, $[\text{M}+\text{Na}]^+$) for $\text{C}_{19}\text{H}_{25}\text{NO}_5\text{SNa}$ calcd 402.1346, found: m/z 402.1347.

Compound 46g and 47g.

Method C was used to furnish **46g_E** (12%), **46g_Z** (46%), and **47g** (2%) after purification by flash column chromatography (silica gel, hexanes:EtOAc 2:1).

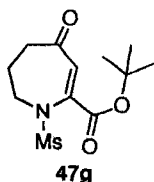


46g_E: yellow oil; R_f 0.26 (hexanes/EtOAc 1:1); IR (thin film) 2978, 2934, 1717, 1611, 1337, 1154, 1154, 977 cm^{-1} ; ^1H NMR (500 MHz, CDCl_3) δ 6.33 (s, 1H), 3.71 (t, $J = 6.0$ Hz, 2H), 3.01 (s, 3H), 2.66 (t, $J = 7.0$ Hz, 2H), 2.14 (app pent, $J = 7.0$ Hz, 2H), 1.49 (s, 9H); ^{13}C NMR (125 MHz, CDCl_3) δ 195.0, 164.9, 140.8, 116.2, 82.2, 45.6, 38.0, 37.1, 28.0, 21.3; HRMS (ESI, $[\text{M}+\text{Na}]^+$) for $\text{C}_{12}\text{H}_{19}\text{NO}_5\text{SNa}$ calcd 312.0876, found: m/z 312.8877.



46g_Z: white solid; m.p. 110.0-112.5°C; R_f 0.33 (hexanes/EtOAc 1:1); IR (thin film) 2979, 2936, 1708, 1628, 1334, 1257, 1148, 1008, 832 cm^{-1} ; ^1H NMR (400 MHz, CDCl_3) δ 6.49 (s, 1H), 3.70 (t, $J = 6.4$ Hz, 2H), 3.20 (s, 3H), 2.64 (t, $J = 7.2$ Hz, 2H), 2.18 (app pent, $J = 6.4$ Hz, 2H), 1.50 (s, 9H); ^{13}C NMR (125 MHz, CDCl_3) δ 195.0, 164.6, 138.4,

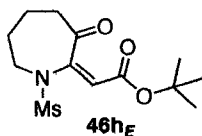
118.2, 81.8, 44.8, 39.0, 36.2, 27.9, 20.6; HRMS (ESI, $[M+Na]^+$) for $C_{12}H_{19}NO_5SNa$ calcd 312.0876, found: m/z 312.0878; Anal. Calcd for $C_{12}H_{19}NO_5S$: C, 49.81; H, 6.62; N, 4.84; S, 11.08. Found: C, 49.59; H, 6.53; N, 4.99; S, 11.26.



47g: off-white solid; R_f 0.40 (hexanes/EtOAc 1:1); IR (thin film) 2978, 2934, 1724, 1672, 1610, 1341, 1274, 1229, 1154 951, 778 cm^{-1} ; 1H NMR (400 MHz, $CDCl_3$) δ 6.17 (s, 1H), 3.66 (t, $J = 6.8$ Hz, 2H), 3.33 (s, 3H), 2.84 (t, $J = 7.2$ Hz, 2H), 2.29 (app pent, $J = 6.8$ Hz, 2H), 1.54 (s, 9H); ^{13}C NMR (125 MHz, $CDCl_3$) δ 201.0, 163.2, 146.1, 124.3, 84.1, 52.3, 41.4, 40.1, 28.3, 27.8; HRMS (ESI, $[M+Na]^+$) for $C_{12}H_{19}NO_5SNa$ calcd 312.0876, found: m/z 312.0876.

Compounds 46h and 47h.

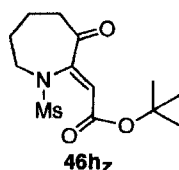
Method D was used to furnish **46h_E** (48%), **46h_Z** (19%), and **47h** (10%) after purification by flash column chromatography (silica gel, hexanes:EtOAc 2:1).



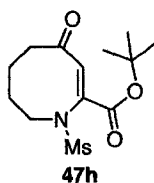
46h_E: white solid; m.p. 90.0-94.0°C; R_f 0.43 (hexanes/EtOAc 1:1); IR (thin film) 2934, 2872, 1701, 1604, 1457, 1347, 1141, 961, 931 cm^{-1} ; 1H NMR (500 MHz, $CDCl_3$) δ 5.98 (s, 1H), 3.67 (br t, $J = 4.5$ Hz, 2H), 3.09 (s, 3H), 2.79 (br t, $J = 6.0$ Hz, 2H), 1.90-1.93 (m, 4H), 1.45 (s, 9H); ^{13}C NMR (125 MHz, $CDCl_3$) δ 202.8, 165.4, 151.0, 107.7, 81.6, 48.3, 41.6, 38.8, 28.1, 28.0, 24.0; HRMS (ESI, $[M+Na]^+$) for $C_{13}H_{21}NO_5SNa$ calcd 326.1033,

found: m/z 326.1034; Anal. Calcd for C₁₃H₂₁NO₅S: C, 51.47; H, 6.98; N, 4.62; S, 10.57.

Found: C, 51.71; H, 6.92; N, 4.54; S, 10.27.



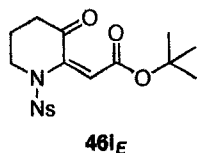
46hz: white solid; m.p. 110.0-112.0°C; R_f 0.55 (hexanes/EtOAc 1:1); IR (thin film) 2978, 2936, 1705, 1634, 1455, 1352, 1334, 1244, 1144, 888, 776 cm⁻¹; ¹H NMR (500 MHz, CDCl₃) δ 6.70 (s, 1H), 3.64 (br t, *J* = 5.5 Hz, 2H), 3.04 (s, 3H), 2.85-2.87 (m, 2H), 2.02 (pent, *J* = 5.5 Hz, 2H), 1.78-1.83 (m, 2H), 1.51 (s, 9H); ¹³C NMR (125 MHz, CDCl₃) δ 200.9, 163.2, 143.9, 126.3, 82.6, 52.5, 40.9, 40.8, 30.3, 28.0, 23.3; HRMS (ESI, [M+Na]⁺) for C₁₃H₂₁NO₅SNa calcd 326.1033, found: m/z 326.1031; Anal. Calcd for C₁₃H₂₁NO₅S: C, 51.47; H, 6.98; N, 4.62; S, 10.57. Found: C, 51.37; H, 6.94; N, 4.59; S, 10.41.



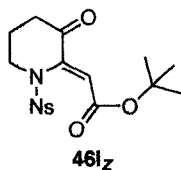
47h: off-white solid; R_f 0.48 (hexanes/EtOAc 1:1); IR (thin film) 2982, 2937, 1716, 1668, 1619, 1449, 1332, 1245, 1150, 971, 769 cm⁻¹; ¹H NMR (500 MHz, CDCl₃) δ 6.87 (s, 1H), 3.58 (t, *J* = 6.0 Hz, 2H), 3.22 (s, 3H), 3.06 (t, *J* = 7.0 Hz, 2H), 1.87 (app pent, *J* = 5.5 Hz, 2H), 1.75 (pent, *J* = 6.0 Hz, 2H), 1.54 (s, 9H); ¹³C NMR (125 MHz, CDCl₃) δ 201.8, 163.9, 136.9, 136.7, 84.1, 48.0, 39.8, 39.1, 27.9, 24.5, 22.1; HRMS (ESI, [M+Na]⁺) for C₁₃H₂₁NO₅SNa calcd 326.1033, found: m/z 326.1032.

Compound 46i.

Method C was used to furnish **46i_E** (24%) and **46i_Z** (18%) after purification by flash column chromatography (silica gel, hexanes:EtOAc 2:1).



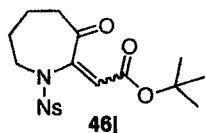
46i_E: pale yellow oil; R_f 0.39 (hexanes/EtOAc 1:1); IR (thin film) 2979, 2936, 1721, 1635, 1546, 1370, 1173, 1009, 754 cm^{-1} ; ^1H NMR (500 MHz, CDCl_3) δ 8.05 (dd, $J = 7.5$, 1.0 Hz, 1H), 7.76 (dt, $J = 7.5$, 1.5 Hz, 1H), 7.72 (dt, $J = 8.0$, 1.5 Hz, 1H), 7.68 (dd, $J = 8.0$, 1.5 Hz, 1H), 6.43 (s, 1H), 3.88 (t, $J = 6.0$ Hz, 2H), 2.49 (t, $J = 6.5$ Hz, 2H), 2.10 (app pent, $J = 6.5$ Hz, 2H), 1.49 (s, 9H); ^{13}C NMR (125 MHz, CDCl_3) δ 194.0, 164.3, 147.8, 137.1, 134.7, 132.5, 131.9, 131.3, 124.5, 121.7, 82.5, 46.0, 36.8, 27.9, 20.3; HRMS (ESI, $[\text{M}+\text{Na}]^+$) for $\text{C}_{17}\text{H}_{20}\text{N}_2\text{O}_7\text{SNa}$ calcd 419.0883, found: m/z 419.0890.



46i_Z: pale yellow oil; R_f 0.32 (hexanes/EtOAc 1:1); IR (thin film) 2980, 2936, 1726, 1678, 1546, 1369, 1273, 1167, 997, 734 cm^{-1} ; ^1H NMR (500 MHz, CDCl_3) δ 8.27-8.29 (m, 1H), 7.70-7.78 (m, 3H), 6.40 (s, 1H), 3.80 (t, $J = 7.0$ Hz, 2H), 2.66 (t, $J = 7.0$ Hz, 2H), 2.13 (pent, $J = 7.0$ Hz, 2H), 1.51 (s, 9H); ^{13}C NMR (125 MHz, CDCl_3) δ 200.8, 163.1, 148.8, 143.1, 134.3, 132.0, 131.9, 131.3, 127.9, 124.4, 84.1, 51.4, 40.6, 27.8, 25.6; HRMS (ESI, $[\text{M}+\text{Na}]^+$) for $\text{C}_{17}\text{H}_{20}\text{N}_2\text{O}_7\text{SNa}$ calcd 419.0883, found: m/z 419.0888.

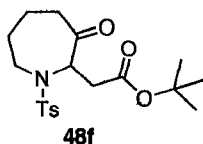
Compound 46j.

Method D was used to furnish **46j** (55%) as a pale yellow oil after purification by flash column chromatography (silica gel, hexanes:EtOAc 2:1). The two isomers were observed as an inseparable mixture (*E:Z* = 1.8:1). The ^1H and ^{13}C NMR data reported herein were extracted from spectra of the **46j** mixture: R_f 0.57 (hexanes/EtOAc 1:1); IR (thin film) 3099, 2934, 1705, 1614, 1545, 1369, 1167, 779 cm^{-1} ; HRMS (ESI, $[\text{M}+\text{Na}]^+$) for $\text{C}_{18}\text{H}_{22}\text{N}_2\text{O}_7\text{SNa}$ calcd 433.1040, found: m/z 433.1039.



46j_E: ^1H NMR (500 MHz, CDCl_3) δ 8.05 (ddd, $J = 7.5, 1.5, 1.0$ Hz, 1H), 7.73-7.81 (m, 2H), 7.64-7.71 (m, 1H), 5.83 (s, 1H), 3.78 (t, $J = 5.5$ Hz, 2H), 2.79 (t, $J = 6.5$ Hz, 2H), 1.96-2.01 (m, 2H), 1.89-1.95 (m, 2H), 1.45 (s, 9H); ^{13}C NMR (125 MHz, CDCl_3) δ 201.0, 164.5, 147.9, 146.7, 134.5, 132.2, 132.0, 131.5, 124.9, 116.6, 82.2, 51.1, 41.4, 29.3, 27.9, 23.6.

46j_Z: ^1H NMR (500 MHz, CDCl_3) δ 7.99-8.01 (m, 1H), 7.73-7.81 (m, 2H), 7.64-7.71 (m, 1H), 6.80 (s, 1H), 3.82-4.22 (br s, 2H), 2.68 (br t, $J = 5.5$ Hz, 2H), 1.89-1.95 (m, 2H), 1.71-1.81 (m, 2H), 1.33 (s, 9H); ^{13}C NMR (125 MHz, CDCl_3) δ 200.0, 162.6, 147.5, 141.6, 134.1, 133.7, 132.0, 131.2, 129.0, 124.2, 82.7, 53.3, 40.6, 29.9, 27.8, 22.9.



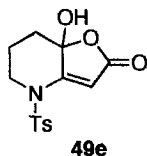
Compound 48f.

Palladium on charcoal (5% wt, 8.5 mg) was added to a solution of **46f** (*E/Z* mixture; 30 mg, 0.08 mmol) in MeOH (1 mL). The solution was allowed to stir at room temperature under an atmosphere of H₂ (1 atm) for 15 min. The reaction mixture was then filtered through a short plug of silica gel (Et₂O) and the combined organic layers dried (MgSO₄). The solvent was removed by rotary evaporation to furnish the pure product **48f** (27 mg, 0.07 mmol, 89%) as a pale yellow oil: *R_f* 0.47 (hexanes/EtOAc 2:1); IR (thin film) 2932, 2867, 1718, 1598, 1454, 1367, 1339, 1152, 1091 cm⁻¹; ¹H NMR (500 MHz, CDCl₃) δ 7.76 (d, *J* = 8.5 Hz, 2H), 7.31 (d, *J* = 8.5 Hz, 2H), 4.89 (ddd, *J* = 9.0, 3.5, 1.5 Hz, 1H), 3.96 (br d, *J* = 15.5 Hz, 1H), 2.84 (ddd, *J* = 13.5, 10.5, 3.0 Hz, 1H), 2.60 (ddd, *J* = 15.0, 11.5, 2.0 Hz, 1H), 2.54 (dd, *J* = 16.0, 9.0 Hz, 1H), 2.43 (s, 3H), 2.42-2.46 (m, 1H), 2.04 (dd, *J* = 16.0, 3.5 Hz, 1H), 1.87-1.97 (m, 2H), 1.70-1.76 (m, 1H), 1.43 (s, 9H), 1.36-1.42 (m, 1H); ¹³C NMR (125 MHz, CDCl₃) δ 209.4, 169.5, 143.7, 137.6, 129.9, 127.1, 81.0, 63.1, 46.7, 40.9, 35.5, 29.3, 27.9, 24.6, 21.5; HRMS (ESI, [M+Na]⁺) for C₁₉H₂₇NO₅SNa calcd 404.1502, found: *m/z* 404.1499.

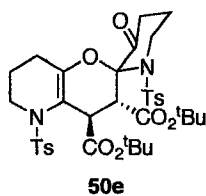
Reaction of 46e with Pyridinium Acetate.

Pyridinium acetate (0.15 g, 1.1 mmol) was added to a solution of **46e** (*E:Z* mixture; 81 mg, 0.22 mmol) in CH₂Cl₂ (2 mL) at room temperature. The reaction mixture was allowed to stir at room temperature for 72 hours before the addition of 1N HCl (2 mL). The aqueous layer was extracted with CH₂Cl₂ (2 x 5 mL), the combined organic layers

were washed with brine (5 mL) and then dried (MgSO₄). The solvent was removed by rotary evaporation and the crude material was purified by flash column chromatography (silica gel, hexanes:EtOAc 50:1) to yield **46e_z** (26 mg, 0.07 mmol, 32%), **49e** (24 mg, 0.08 mmol, 35%), and **50e** (12 mg, 0.02 mmol, 8%).



49e: pale yellow oil; *R_f* 0.15 (hexanes/EtOAc 2:1); IR (thin film) 3332, 2951, 1745, 1629, 1366, 1215, 1170, 1005, 928, 817 cm⁻¹; ¹H NMR (500 MHz, CDCl₃) δ 7.78 (d, *J* = 8.5 Hz, 2H), 7.38 (d, *J* = 8.0 Hz, 2H), 5.71 (s, 1H), 4.18 (br s, 1H), 3.71-3.82 (m, 2H), 2.46 (s, 3H), 2.33-2.39 (m, 1H), 2.00-2.08 (m, 1H), 1.71-1.82 (m, 2H); ¹³C NMR (125 MHz, CDCl₃) δ 171.0, 159.9, 145.7, 133.8, 130.3, 127.4, 101.1, 95.6, 44.6, 29.7, 21.7, 19.4; HRMS (ESI, [M+Na]⁺) for C₁₄H₁₅NO₅SNa calcd 332.0563, found: *m/z* 332.0563.



50e: yellow oil; *R_f* 0.25 (hexanes/EtOAc 2:1); IR (thin film) 2978, 2932, 1726, 1597, 1356, 1165 cm⁻¹; ¹H NMR (500 MHz, CDCl₃) δ 7.82 (d, *J* = 8.5 Hz, 2H), 7.80 (d, *J* = 8.0 Hz, 2H), 7.26 (d, *J* = 7.5 Hz, 2H), 7.21 (d, *J* = 8.5 Hz, 2H), 4.70 (d, *J* = 9.5 Hz, 1H), 4.33 (ddd, *J* = 9.5, 3.0, 2.0 Hz, 1H), 3.85 (ddd, *J* = 14.0, 5.0, 2.0 Hz, 1H), 3.66 (ddd, *J* = 13.0, 7.5, 3.5 Hz, 1H), 3.51 (ddd, *J* = 12.0, 8.5, 3.0 Hz, 1H), 2.94 (ddd, *J* = 13.5, 13.5, 4.5 Hz, 1H), 2.73 (app dt, *J* = 17.5, 6.5 Hz, 1H), 2.46 (app dt, *J* = 17.5, 7.5 Hz, 1H), 2.40 (s, 3H), 2.38 (s, 3H), 2.04-1.96 (m, 1H), 1.90 (dddd, *J* = 14.5, 7.5, 7.5, 7.5, 3.5 Hz, 1H), 1.79

(dddd, $J = 18.0, 9.0, 9.0, 2.0$ Hz, 1H), 1.57 (s, 9H), 1.47 (s, 9H), 1.31-1.39 (m, 1H), 1.21-1.27 (m, 1H), 1.11-1.19 (m, 1H); ^{13}C NMR (125 MHz, CDCl_3) δ 198.4, 170.7, 169.6, 146.9, 143.6, 143.3, 137.8, 136.5, 129.3, 129.3, 128.1, 127.9, 112.1, 89.6, 82.6, 81.2, 48.0, 47.1, 46.1, 44.7, 35.9, 28.1, 28.0, 23.1, 21.5, 21.5, 21.4, 19.6; HRMS (ESI, $[\text{M}+\text{Na}]^+$) for $\text{C}_{36}\text{H}_{46}\text{N}_2\text{O}_{10}\text{S}_2\text{Na}$ calcd 753.2486, found: m/z 753.2480.

4.5 References

1. Evans, P. A.; Holmes, A. B. *Tetrahedron* **1991**, *47*, 9131-9166.
2. a) Alvarez, E.; Candenas, M. -L.; Pérez, R.; Ravelo, J. L.; Martín, J. D. *Chem. Rev.* **1995**, *95*, 1953-1980; b) Marmsäter, F. P.; West, F. G. *Chem. Eur. J.* **2002**, *8*, 4347-4353; c) Inoue, M. *Chem. Rev.* **2005**, *105*, 4379-4405.
3. Bennasar, M. L.; Roca, T.; Monerris, M.; García-Díaz, D. *J. Org. Chem.* **2006**, *71*, 7028-2034.
4. Holub, N.; Neidhöfer, J.; Blechert, S. *Org. Lett.* **2005**, *7*, 1227-1229.
5. Torraca, K. E.; Kuwabe, S. -I.; Buchwald, S. L. *J. Am. Chem. Soc.* **2000**, *122*, 12907-12908.
6. Greshock, T. J.; Funk, R. L. *J. Am. Chem. Soc.* **2002**, *124*, 754-755.
7. Ohno, H.; Hamaguchi, H.; Ohata, M.; Kosaka, S.; Tanaka, T. *J. Am. Chem. Soc.* **2004**, *126*, 8744-8754.
8. a) Ohno, H.; Hamaguchi, H.; Tanaka, T. *Org. Lett.* **2001**, *3*, 2269-2271; b) Ohno, H.; Ando, K.; Hamaguchi, H.; Takeoka, Y.; Tanaka, T. *J. Am. Chem. Soc.* **2002**, *124*, 15255-15266.
9. Sawada, Y.; Sasaki, M.; Takeda, K. *Org. Lett.* **2004**, *6*, 2277-2279.

10. Gabillet, S.; Lecercle, D.; Loreau, O.; Carboni, M.; Dézard, S.; Gomis, J. -M.; Taran, F. *Org. Lett.* **2007**, *9*, 3925-3927.
11. a) Masquelin, T.; Obrecht, D. *Synthesis*, **1995**, 276-284; b) Palombi, L.; Arista, L.; Lattanzi, A.; Bonadies, F.; Scettri, A. *Tetrahedron Lett.* **1996**, *37*, 7849-7850; c) Larson, D. P.; Heathcock, C. D. *J. Org. Chem.* **1997**, *62*, 8407-8418; d) Hermitage, S. A.; Roberts, S. M.; Watson, D. J. *Tetrahedron Lett.* **1998**, *39*, 3567-3570; e) Serrat, X.; Cabarocas, G.; Rafel, S.; Ventura, M.; Linden, A.; Villalgorido, J. M. *Tetrahedron: Asymmetry* **1999**, *10*, 3417-3430.
12. a) Naka, T.; Koide, K. *Tetrahedron Lett.* **2003**, *44*, 443-445; b) Davis, R. B.; Scheiber, D. H. *J. Am. Chem. Soc.* **1956**, *78*, 2050-2058.
13. a) Wang, J.-X.; Wei, B.; Huang, D.; Hu, Y.; Bai, L. *Synth. Commun.* **2001**, *31*, 3337-3343; b) Yin, J.; Wang, X. -J.; Liang, Y.; Wu, X.; Chen, B.; Ma, Y. *Synthesis* **2004**, 331-333; c) Alonso, D.A.; Nájera, C.; Pacheco, M.C. *J. Org. Chem.* **2004**, *69*, 1615-1619; d) Chen, L.; Li, C.-J. *Org. Lett.* **2004**, *6*, 3151-3153.
14. a) Ramachandran, P. V.; Teodorovic, A. V.; Rangaishenvi, M. V.; Brown, H. C. *J. Org. Chem.* **1992**, *57*, 2379-2386; b) Ito, H.; Arimoto, K.; Sensui, H.; Hosomi, A. *Tetrahedron Lett.* **1997**, *38*, 3977-3980; c) Sashida, H. *Synthesis* **1998**, 745-748; d) Chowdhury, C.; Kundu, N. G. *Tetrahedron* **1999**, *55*, 7011-7016; e) Wang, J. -X.; Wei, B.; Hu, T.; Liu, Z. X.; Fu, Y. *Synth. Commun.* **2001**, *31*, 3527-3532; f) Gallagher, W. P.; Maleczka, R. E., Jr. *J. Org. Chem.* **2003**, *68*, 6775-6779.

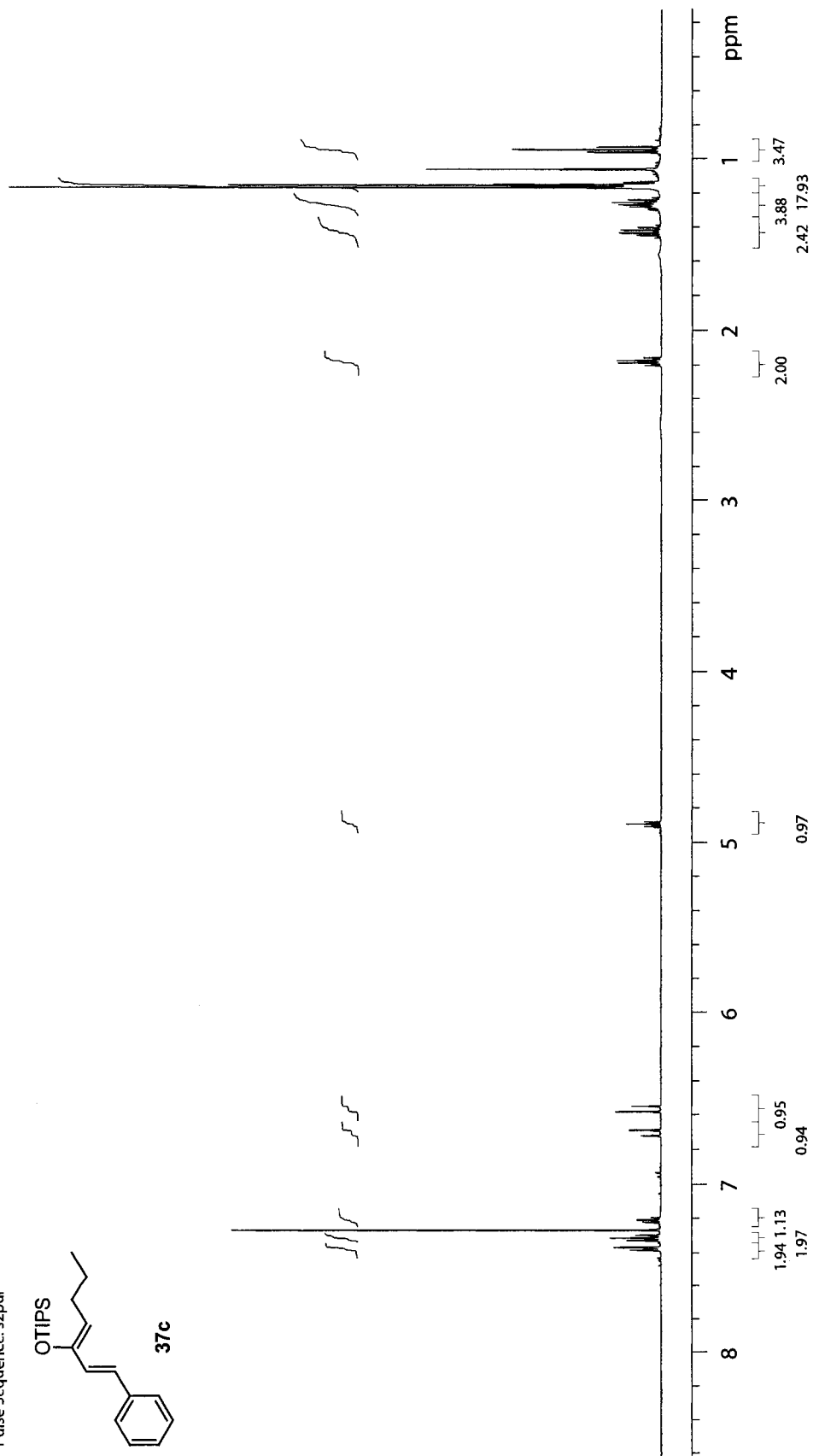
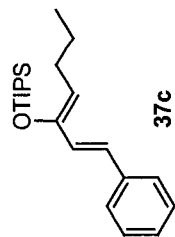
15. a) Yamaguchi, M.; Shibato, K.; Fujiwara, S.; Hirao, L. *Synthesis* **1986**, 421-422; b) Doubsky, J.; Streinz, L.; Leseticky, L.; Koutek, B. *Synlett* **2003**, 7, 937-942; c) Doubsky, J.; Streinz, L.; Saman, D.; Zednik, J.; Koutek, B. *Org. Lett.* **2004**, 6, 4909-4911.
16. a) Stefani, H. A.; Cella, R.; Vieira, A. S. *Tetrahedron* **2007**, 63, 3623-3658; b) Molander, G. A.; Rigueroa, R. *Aldrichim. Acta* **2005**, 38, 49-56.
17. a) Padwa, A.; Dean, D. C.; Fairfax, D. J.; Xu, S. L. *J. Org. Chem.* **1993**, 58, 4646-4655; b) Sun, C.; Lin, X.; Weinreb, S.M. *J. Org. Chem.* **2006**, 71, 3159-3166.
18. a) Trost, B. M.; Crawley, M. L. *Chem. Eur. J.* **2004**, 10, 2237-2252; b) Persson, T.; Nielsen, J. *Org. Lett.* **2006**, 8, 3219-3222.
19. Harrison, T. J.; Dake, G. R. *J. Org. Chem.* **2005**, 70, 10872-10874.
20. Luker, T.; Hiemstra, H.; Speckamp, W. N. *Tetrahedron Lett.* **1996**, 37, 9257-8260.
21. Schreiber, S. L.; Kelly, S. E. *Tetrahedron Lett.* **1984**, 25, 1757-1760.
22. a) Boden, E. P.; Keck, G. E. *J. Org. Chem.* **1985**, 50, 2394-2395; b) Spivey, A. C.; Arseniyadis, S. *Angew. Chem. Int. Ed.* **2004**, 43, 5436-5441.
23. The Z-geometry was assigned by comparison of the chemical shift of the vinyl proton to related literature compounds: Davies, M. J.; Moody, C. J.; Taylor, R. J. *J. Chem. Soc., Perkin Trans I*, **1991**, 1-7.

24. Baldwin, J. E. *J. Chem. Soc., Chem. Commun.* **1976**, 734-736.
25. a) Crabtree, A.; Jackman, L. M.; Johnson, A. W. *J. Chem. Soc.* **1962**, 4417-4420;
b) Acheson, R. M.; Gagan, J. M. F., Harrison, D. R. *J. Chem. Soc.* **1968**, 362-378;
c) Acheson, R. M.; Wallis, J. D.; Woollard, J. *J. Chem. Soc., Perkin Trans. I* **1979**, 584-590.
26. Shamma, M. In *The Isoquinoline Alkaloids*; Academic Press: New York, NY, 1972; pp 399.
27. Kametani, T.; Fukumoto, K. *Heterocycles*, **1975**, 3, 931-1004.

**Appendix I: Selected NMR Spectra
(Chapter 2)**

500 MHz 1D in CDCl₃ (ref. to CDCl₃ @ 7.26 ppm), temp 27.2 C-> actual temp = 27.0 C, sw5000 probe

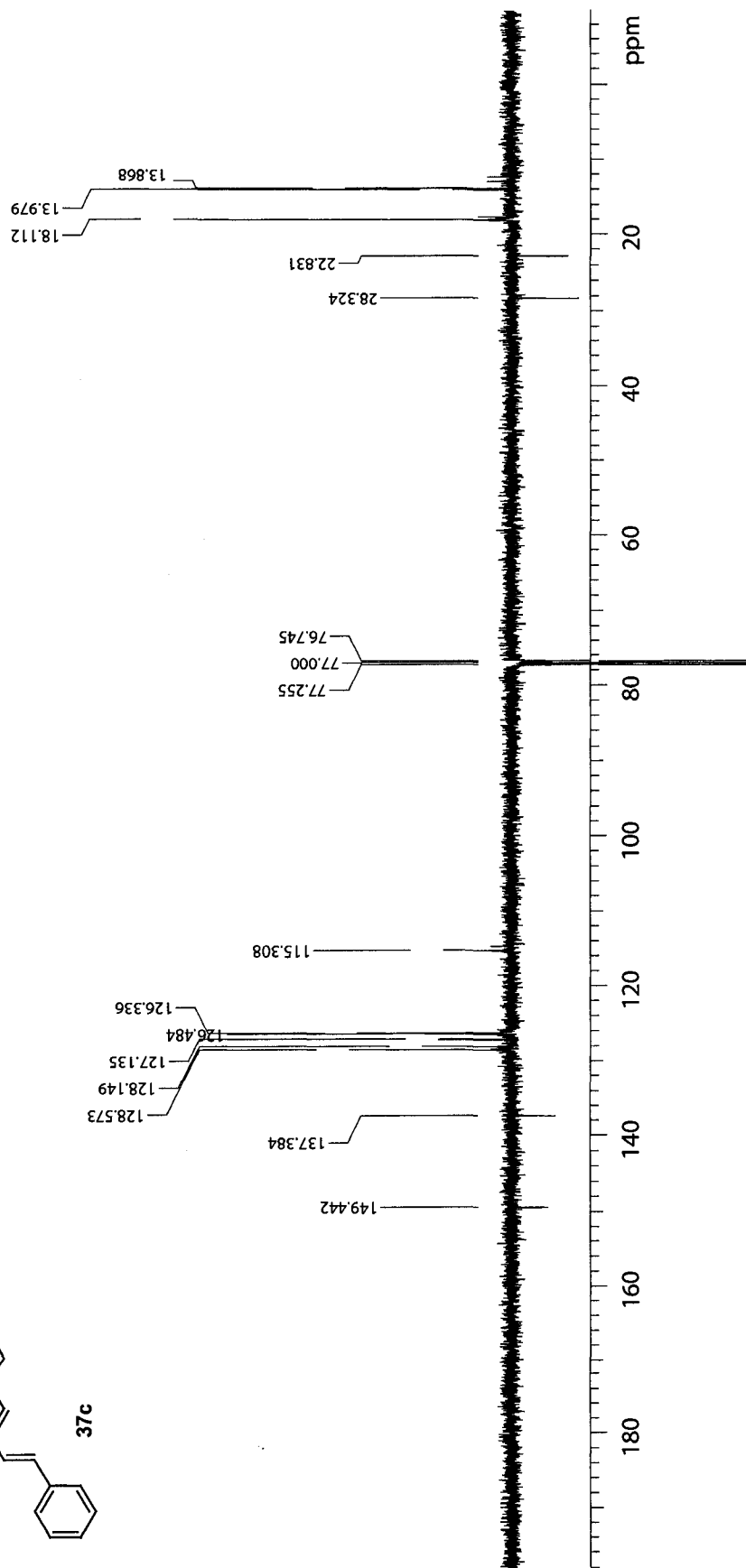
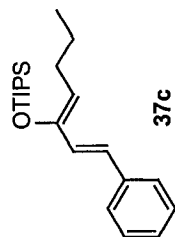
Pulse Sequence: s2pul



125 MHz APT in CDCl₃ (ref. to CDCl₃ @ 77.0 ppm), temp 27.2 C -> actual temp = 27.0 C, sw probe

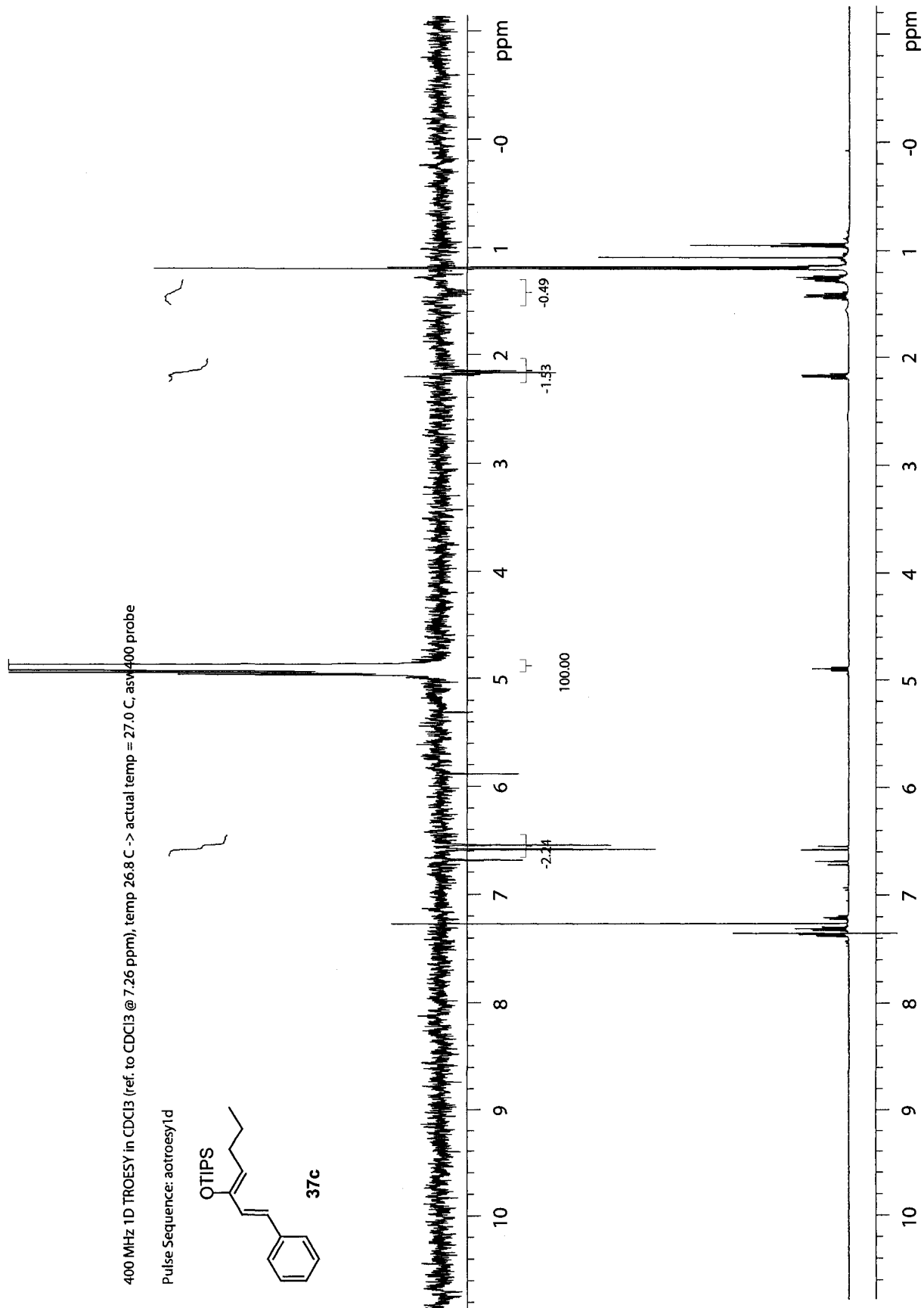
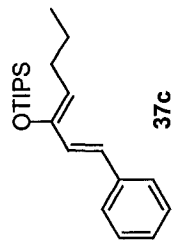
C & CH₂ same, CH & CH₃ opposite side of solvent signal

Pulse Sequence: apt

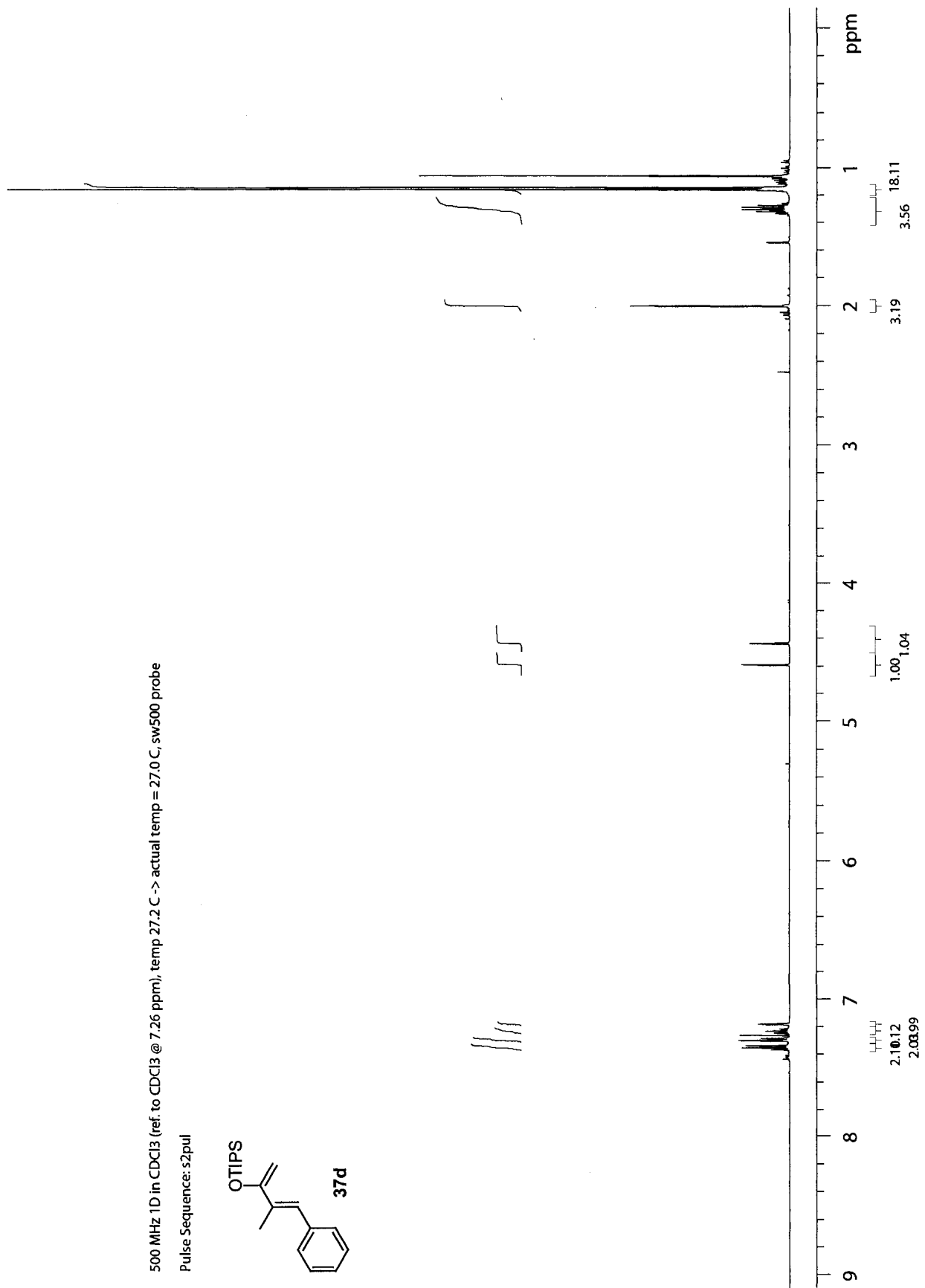
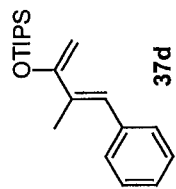


400 MHz 1D TROESY in CDCl₃ (ref. to CDCl₃ @ 7.26 ppm), temp 26.8 C -> actual temp = 27.0 C, asv400 probe

Pulse Sequence: aotroesy1d

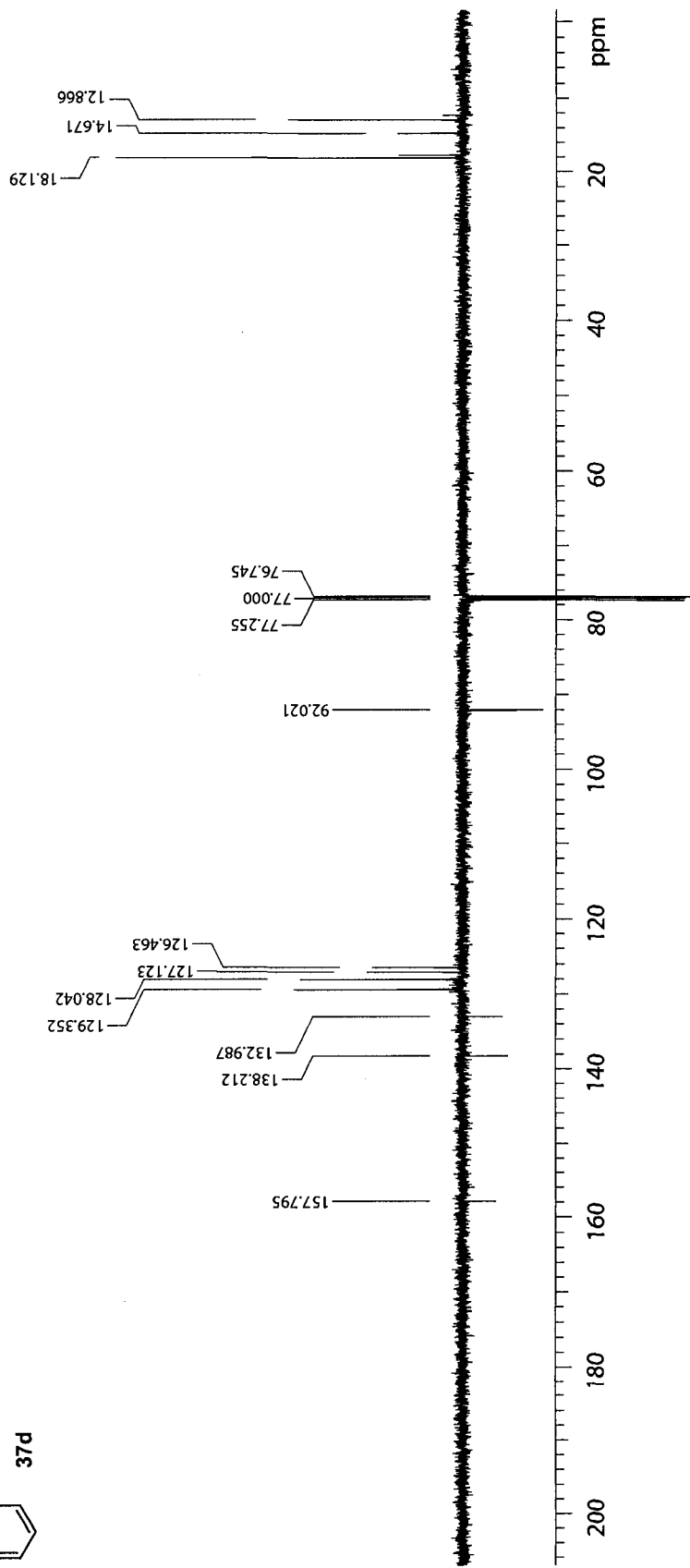
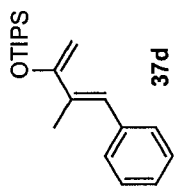


500 MHz 1D in CDCl3 (ref. to CDCl3 @ 7.26 ppm), temp 27.2 C -> actual temp = 27.0 C, sw500 probe
Pulse Sequence: s2pul



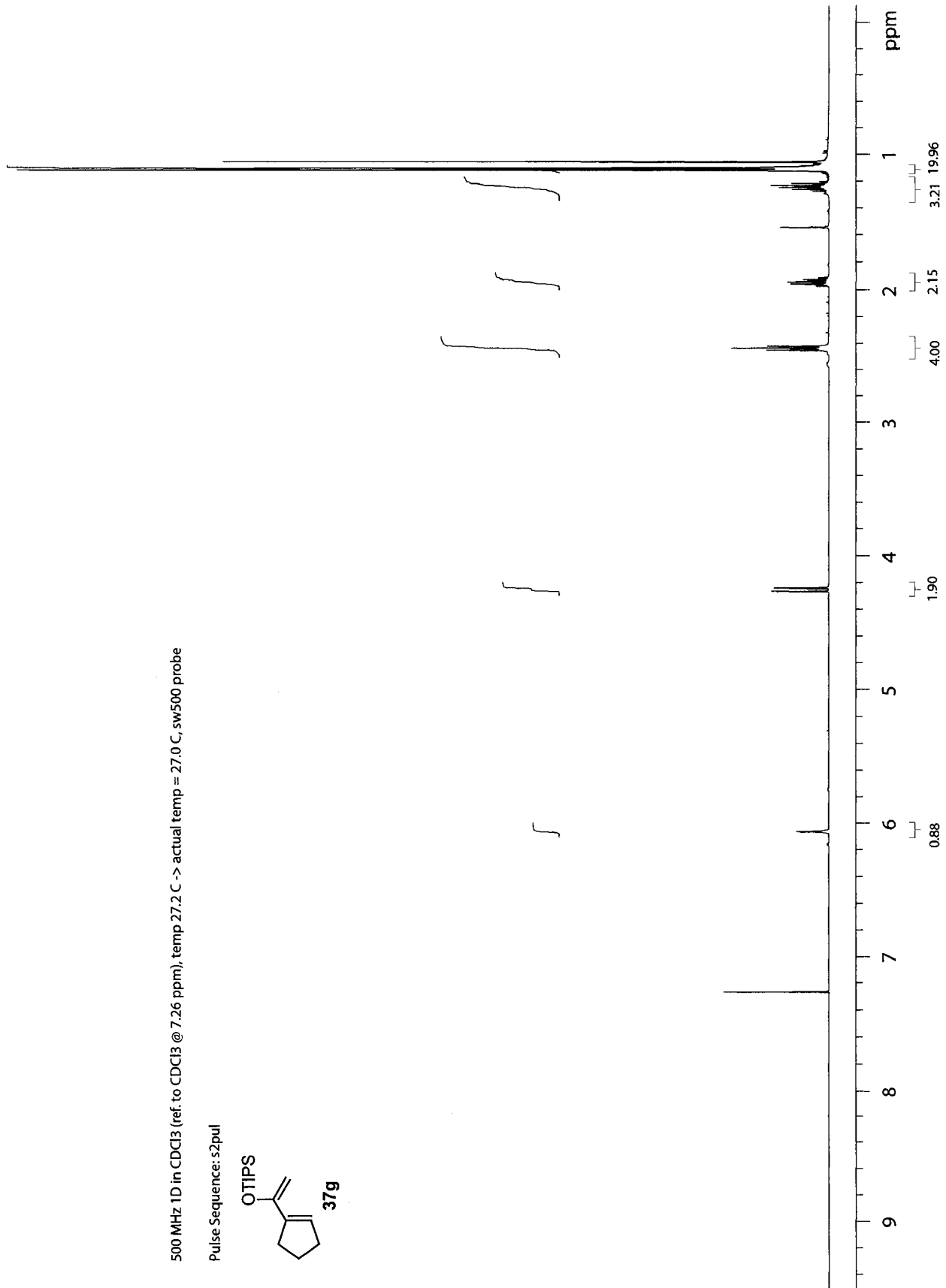
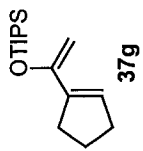
125 MHz APT in CDCl₃ (ref. to CDCl₃ @ 77.0 ppm), temp 27.2 C -> actual temp = 27.0 C, sw probe
C & CH₂ same, CH & CH₃ opposite side of solvent signal

Pulse Sequence: apt



500 MHz 1D in CDCl3 (ref. to CDCl3 @ 7.26 ppm), temp 27.2 C -> actual temp = 27.0 C, sw5000 probe

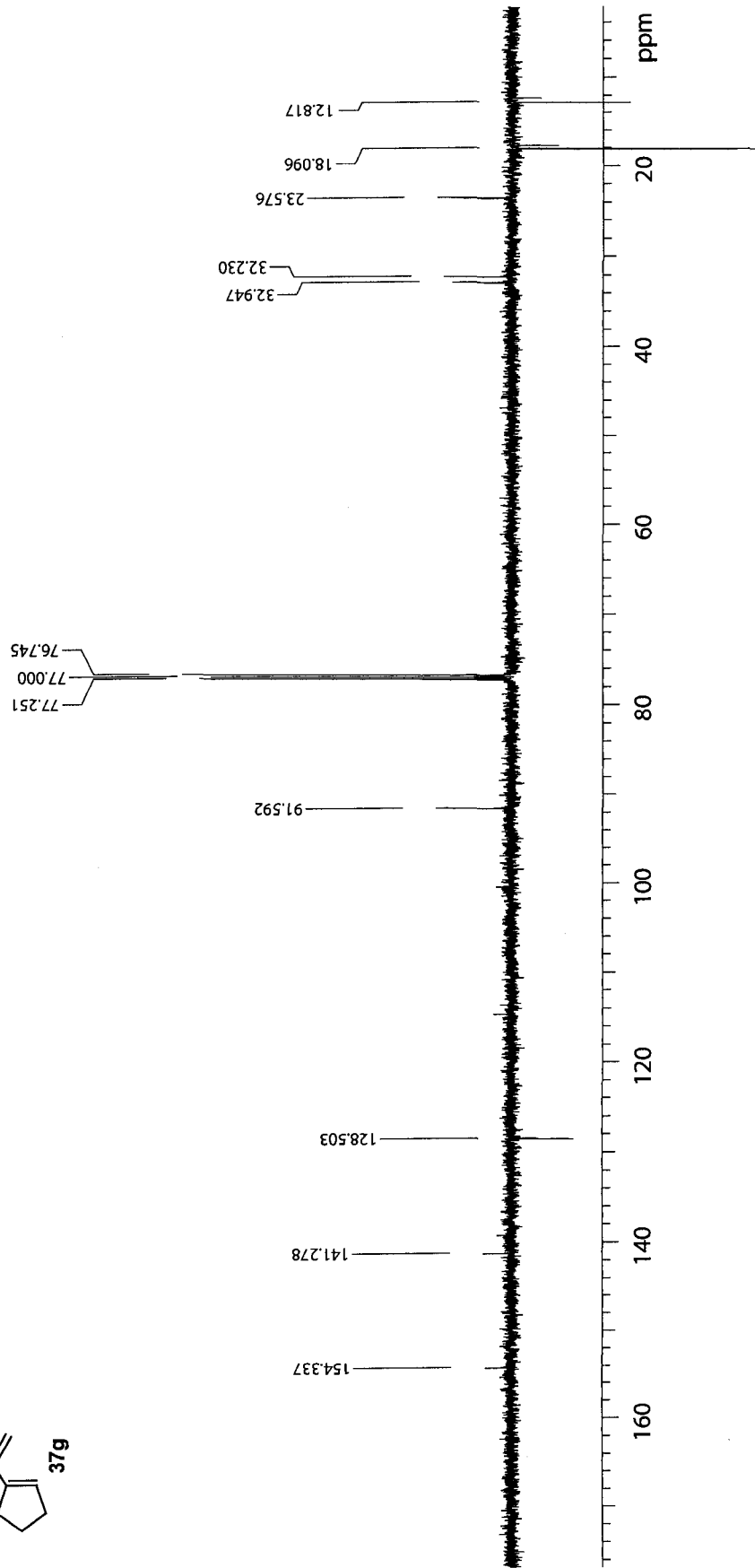
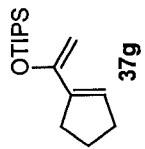
Pulse Sequence: s2pul



125 MHz APT in CDCl₃ (ref. to CDCl₃ @ 77.0 ppm), temp 27.2 C -> actual temp = 27.0 C, sw probe

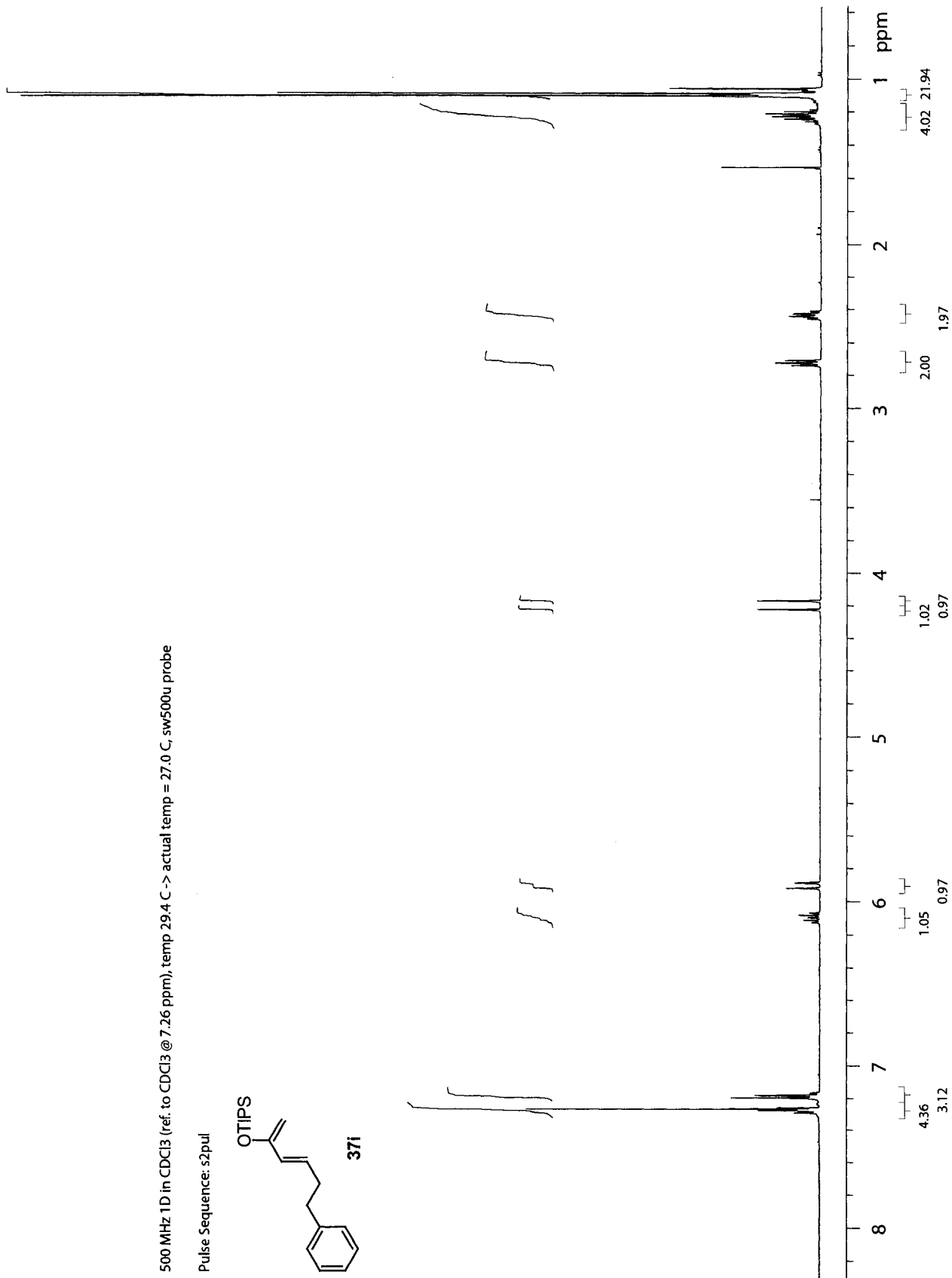
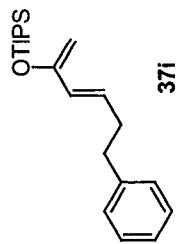
C & CH₂ same, CH & CH₃ opposite side of solvent signal

Pulse Sequence: apt



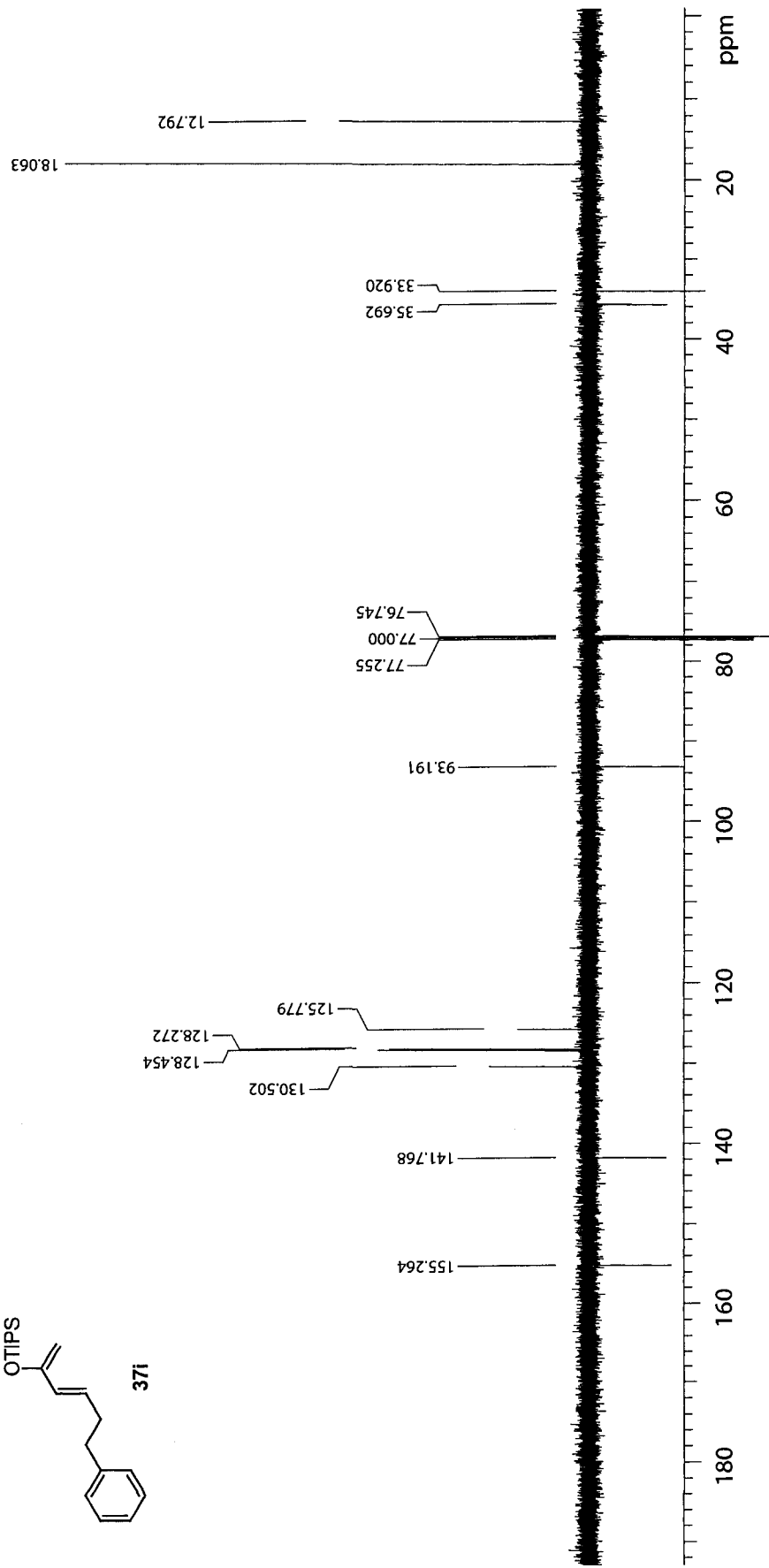
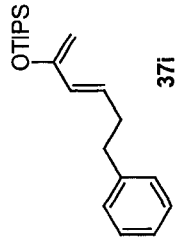
500 MHz 1D in CDCl3 (ref. to CDCl3 @ 7.26 ppm), temp 29.4 C -> actual temp = 27.0 C, sw500u probe

Pulse Sequence: s2pul



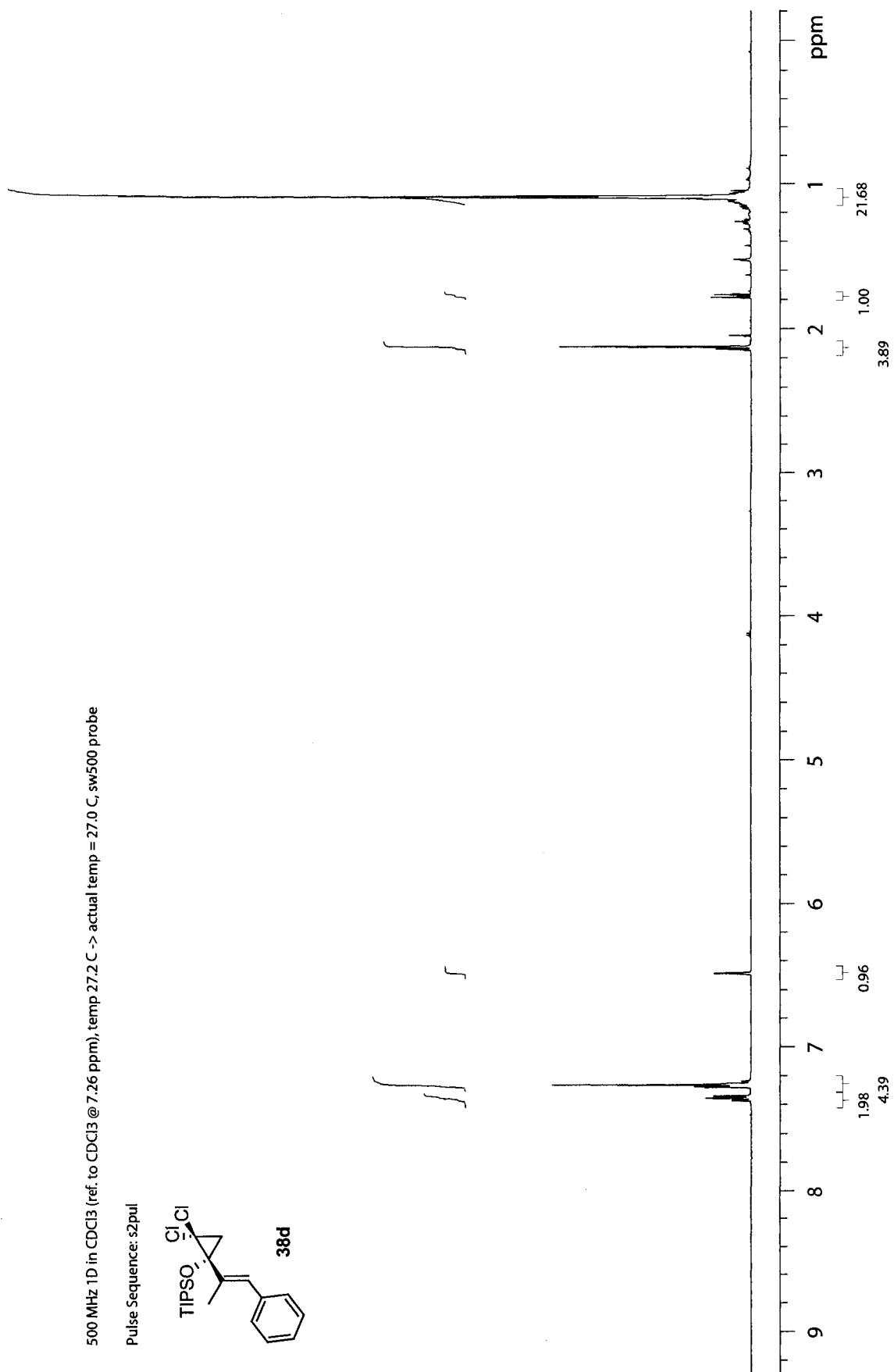
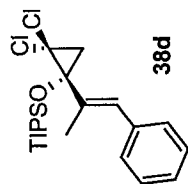
125 MHz APT in CDCl₃ (ref. to CDCl₃ @ 77.0 ppm), temp 27.2 C -> actual temp = 27.0 C, sw probe C & CH₂ same, CH & CH₃ opposite side of solvent signal

Pulse 5 sequence: apt



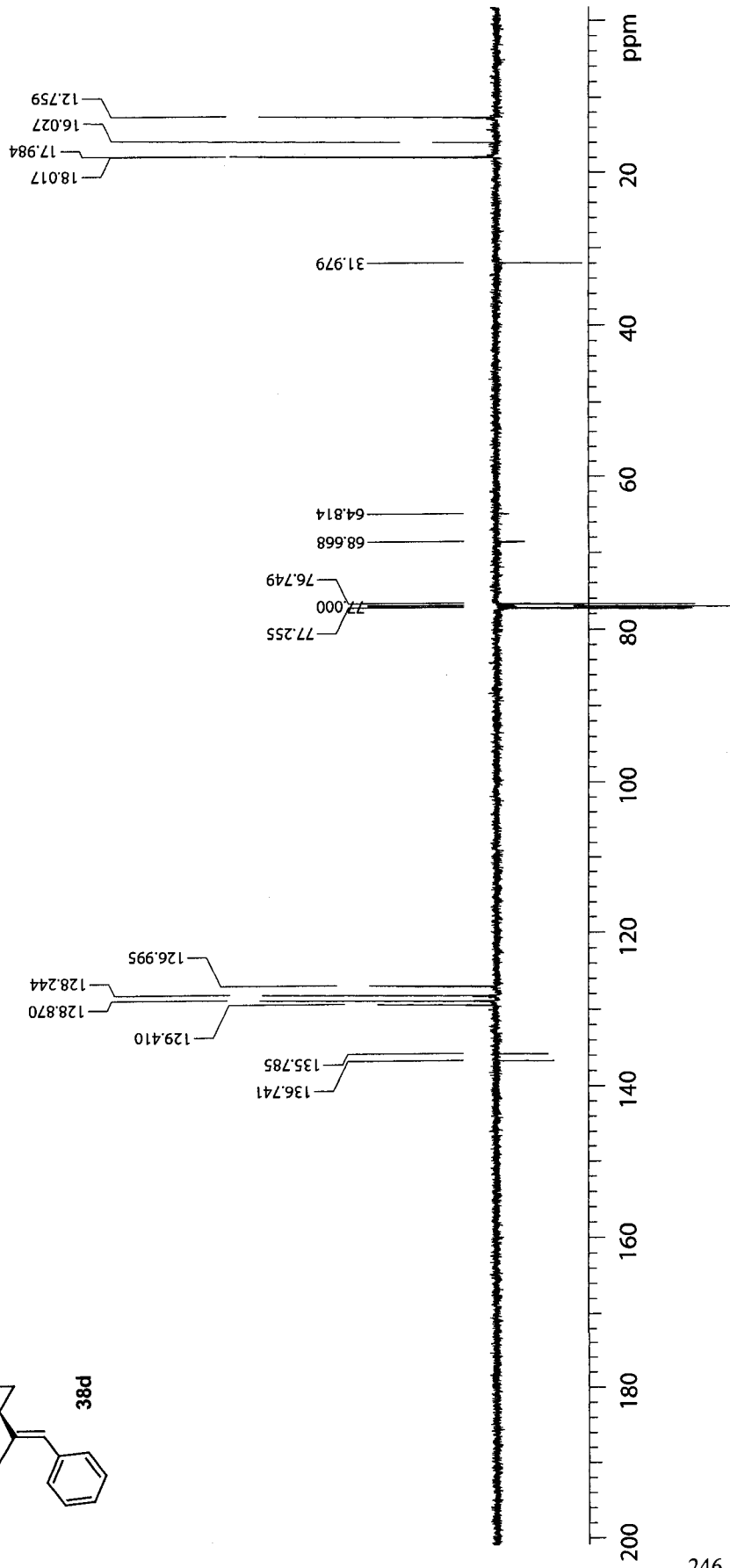
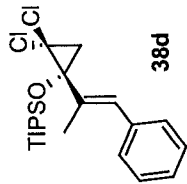
500 MHz 1D in CDCl3 (ref. to CDCl3 @ 7.26 ppm), temp 27.2 C -> actual temp = 27.0 C, sw5000 probe

Pulse Sequence: s2pul



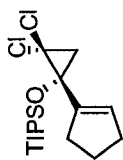
125 MHz APT in CDCl₃ (ref. to CDCl₃ @ 77.0 ppm), temp 27.2 C -> actual temp = 27.0 C, sw probe
C & CH₂ same, CH & CH₃ opposite side of solvent signal

Pulse Sequence: apt

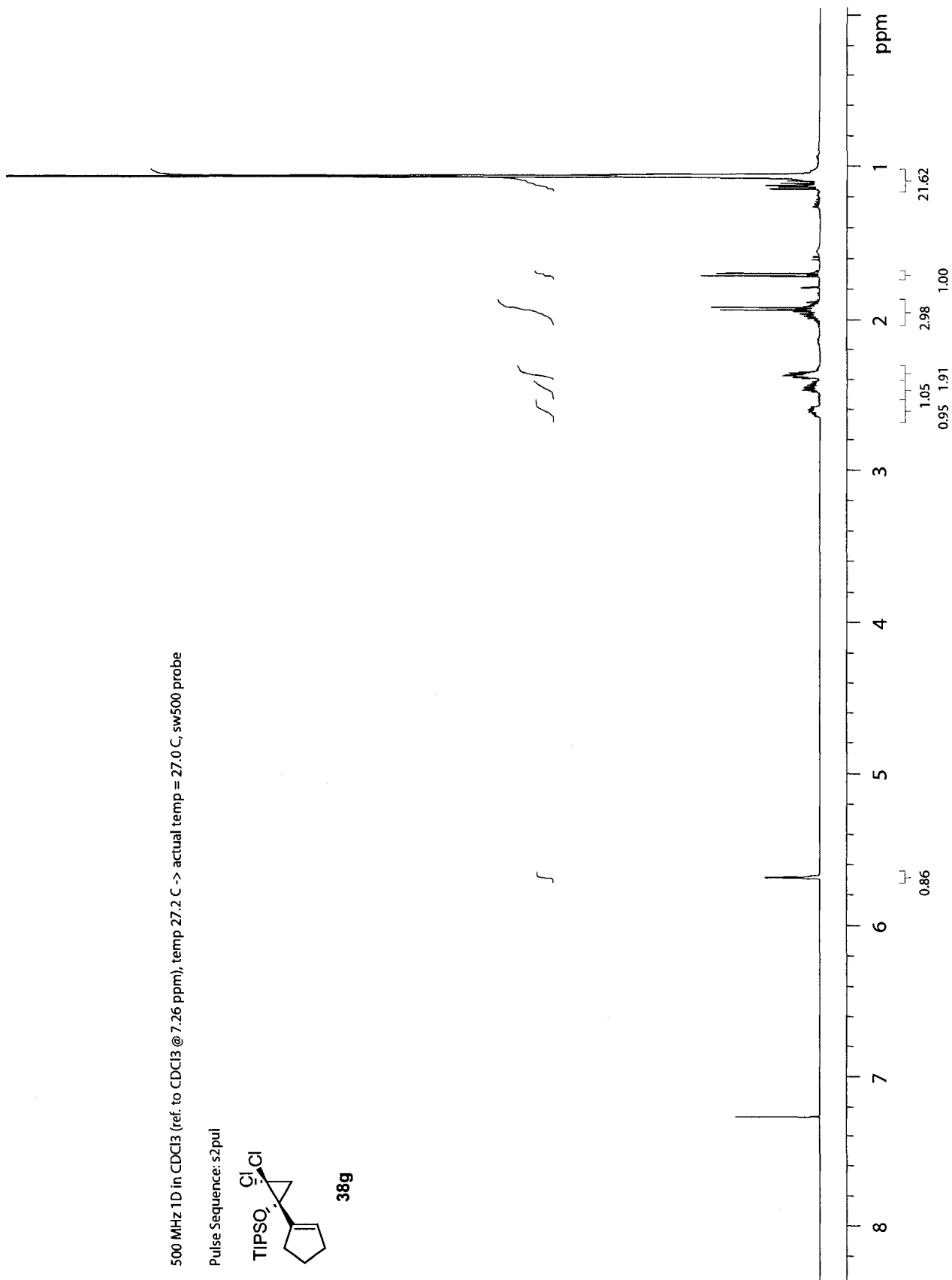


500 MHz 1D in CDCl3 (ref. to CDCl3 @ 7.26 ppm), temp 27.2 C -> actual temp = 27.0 C, sw5000 probe

Pulse Sequence: s2pul

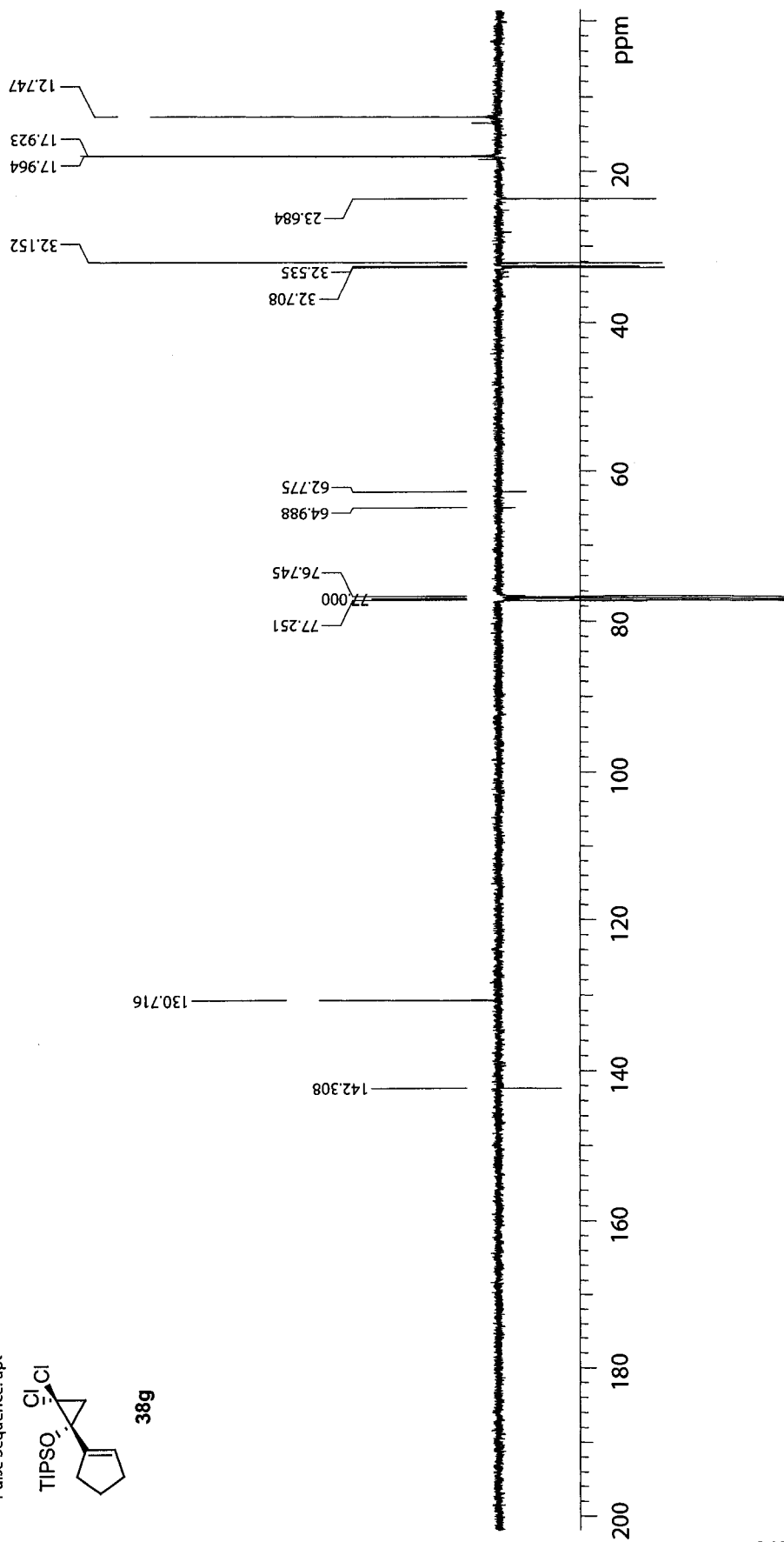
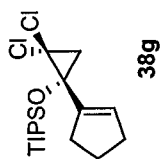


38g



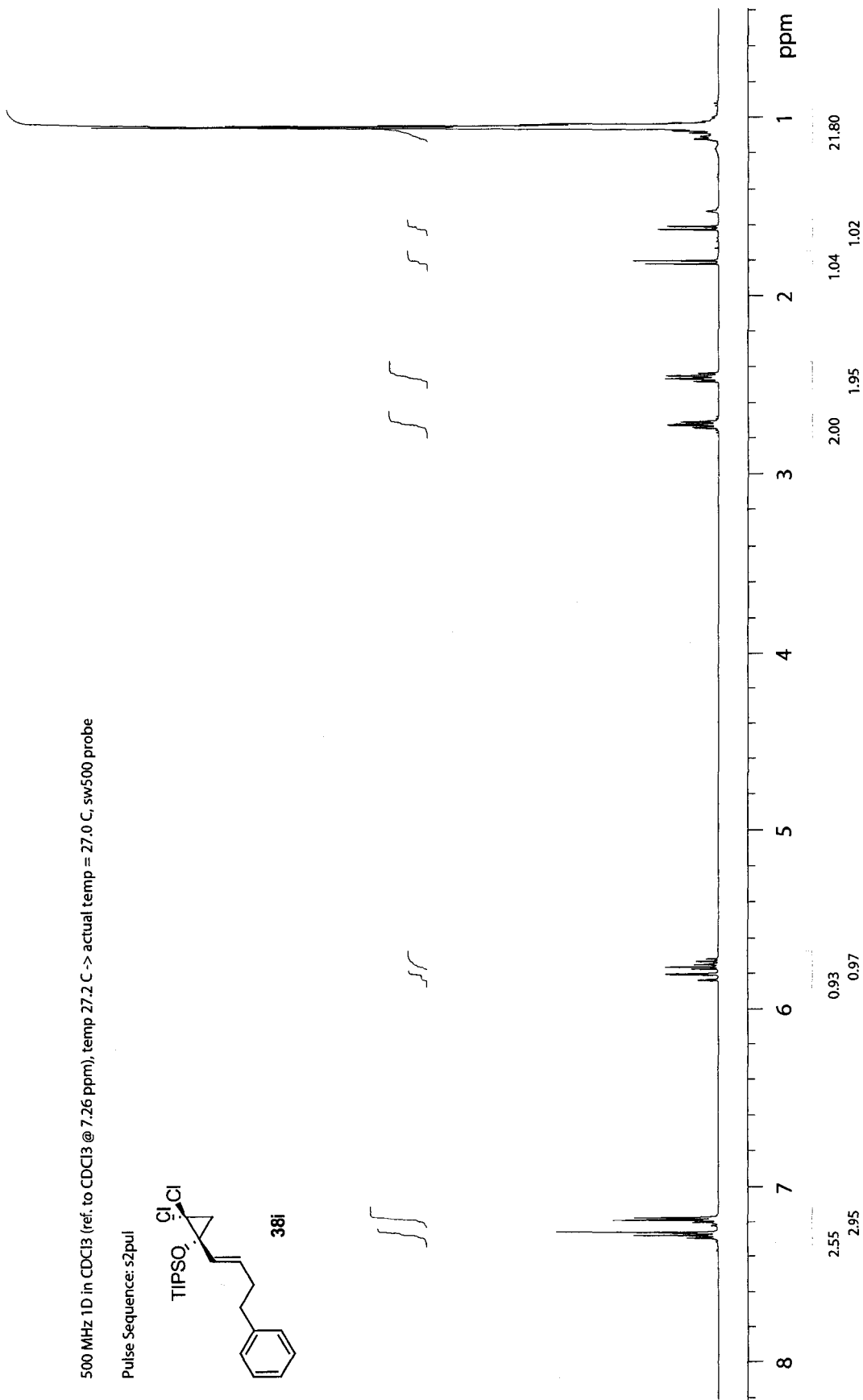
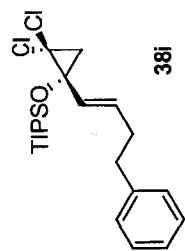
125 MHz APT in CDCl₃ (ref. to CDCl₃ @ 77.0 ppm), temp 27.2 C -> actual temp = 27.0 C, sw probe
C & CH₂ same, CH & CH₃ opposite side of solvent signal

Pulse Sequence: apt



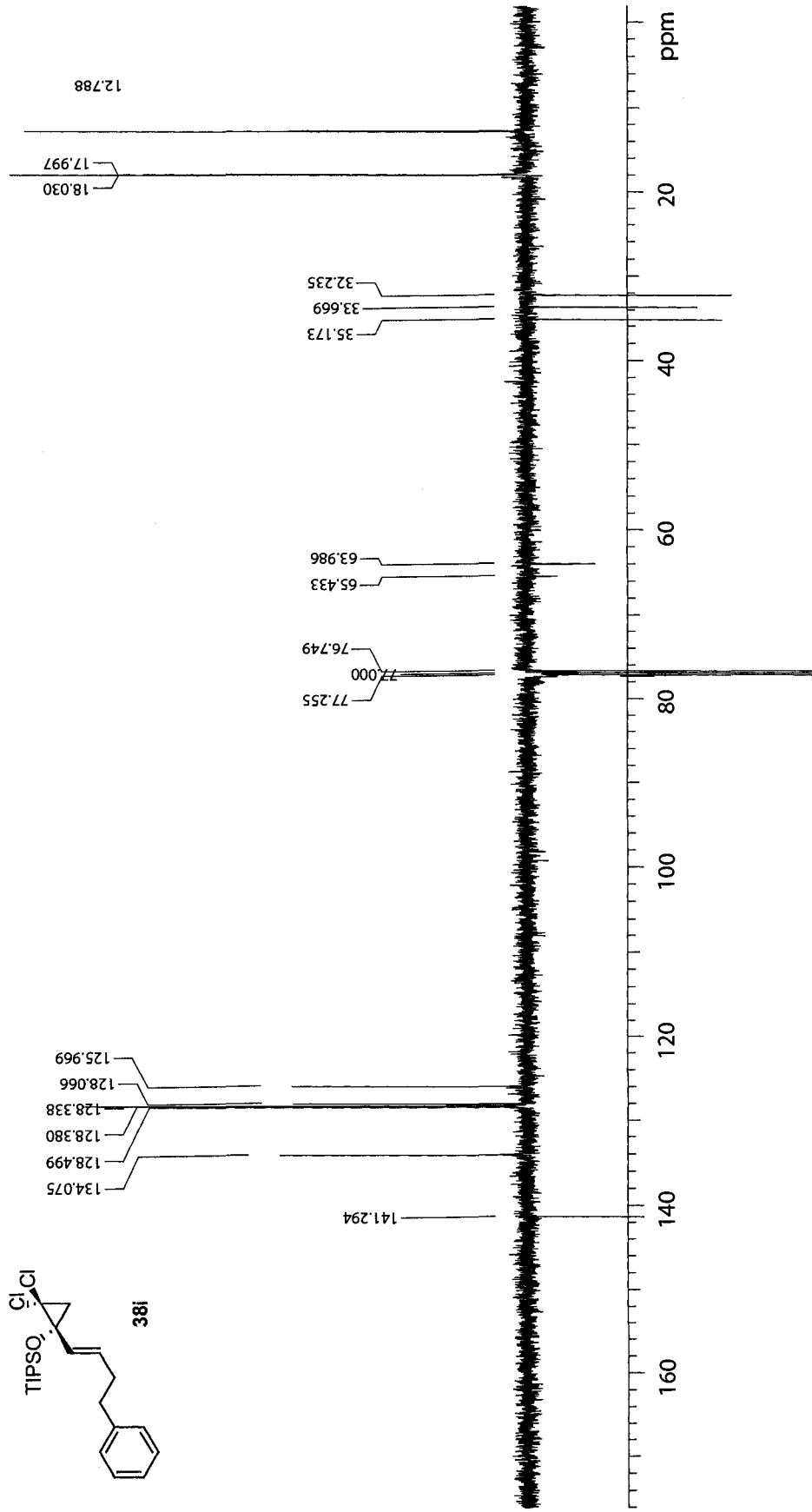
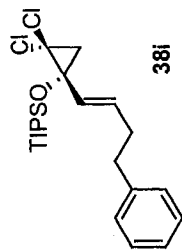
500 MHz 1D in CDCl₃ (ref. to CDCl₃ @ 7.26 ppm), temp 27.2 C -> actual temp = 27.0 C, sw5000 probe

Pulse Sequence: s2pul



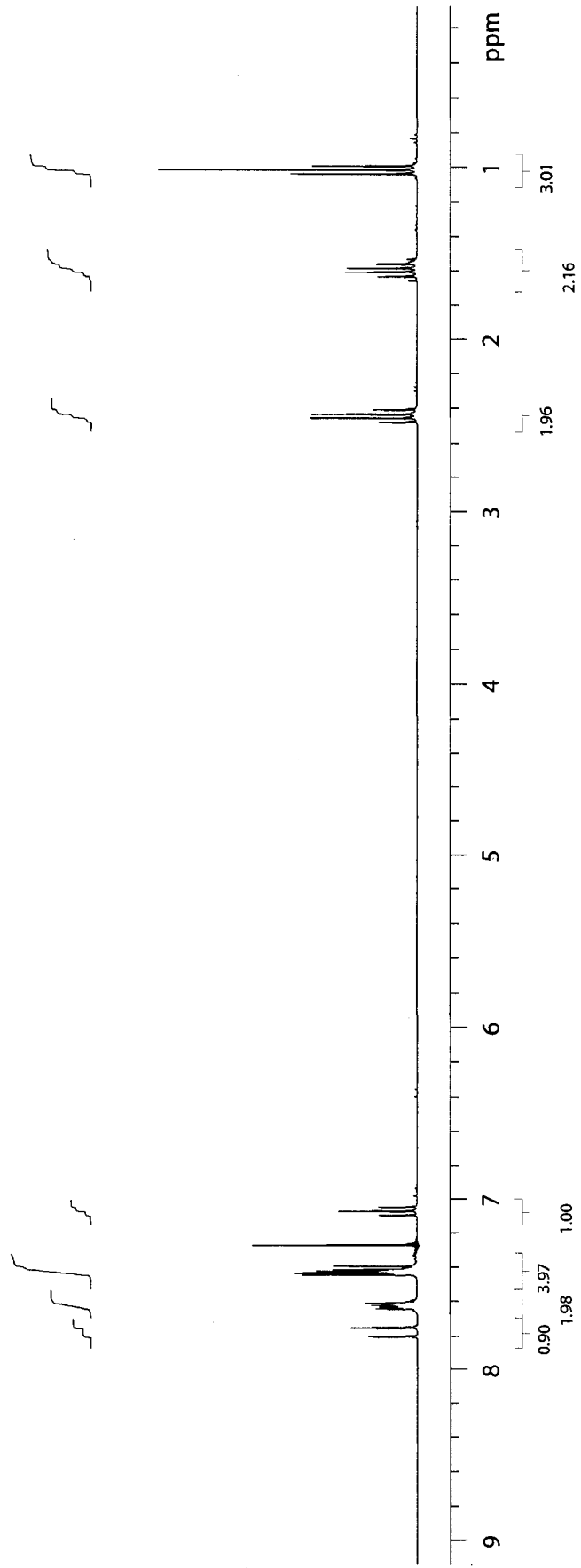
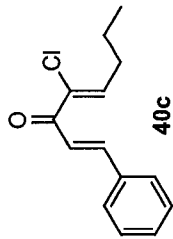
125 MHz APT in CDCl₃ (ref. to CDCl₃ @ 77.0 ppm), temp 27.2 C -> actual temp = 27.0 C, sw probe C & CH2 same, CH & CH3 opposite side of solvent signal

Pulse Sequence: apt



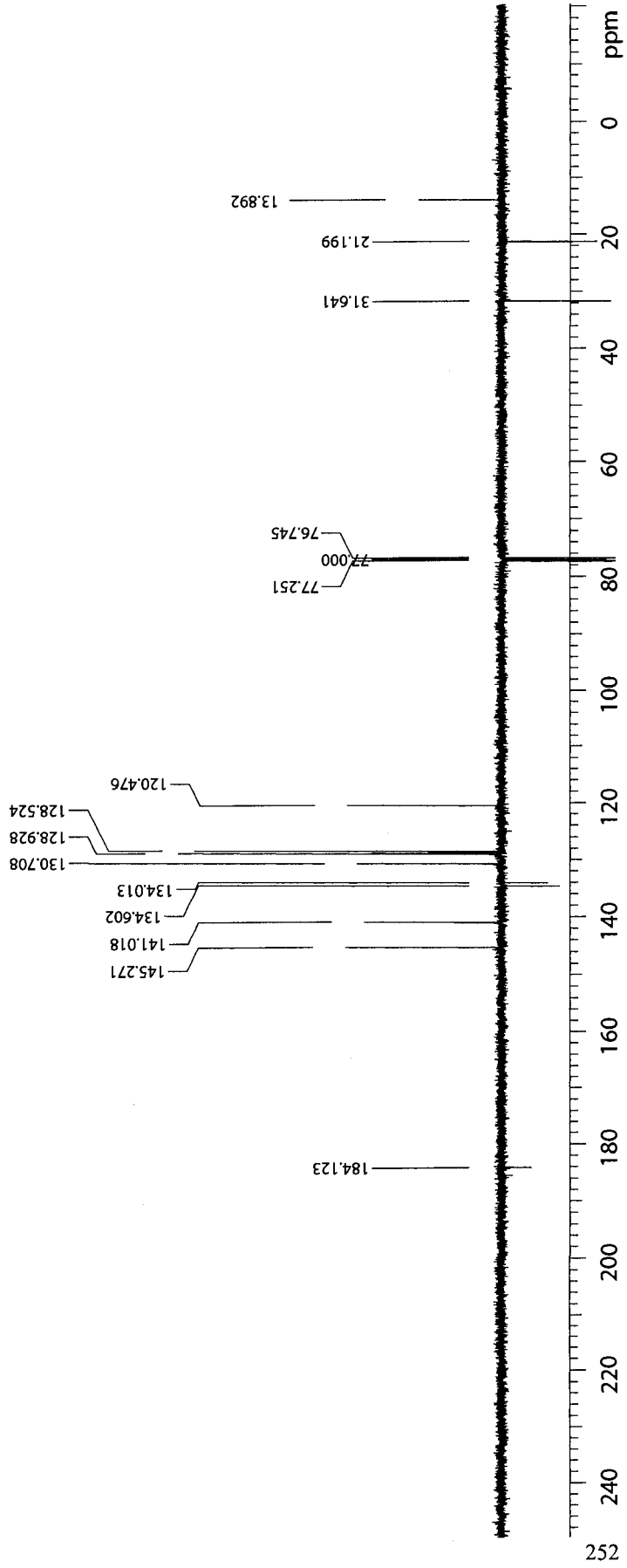
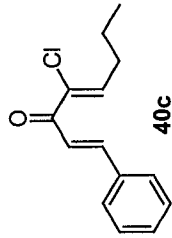
300 MHz 1D in CDCl3 (ref. to CDCl3 @ 7.26 ppm), temp 27.5 C -> actual temp = 27.0 C, id probe

Pulse Sequence: s2pul



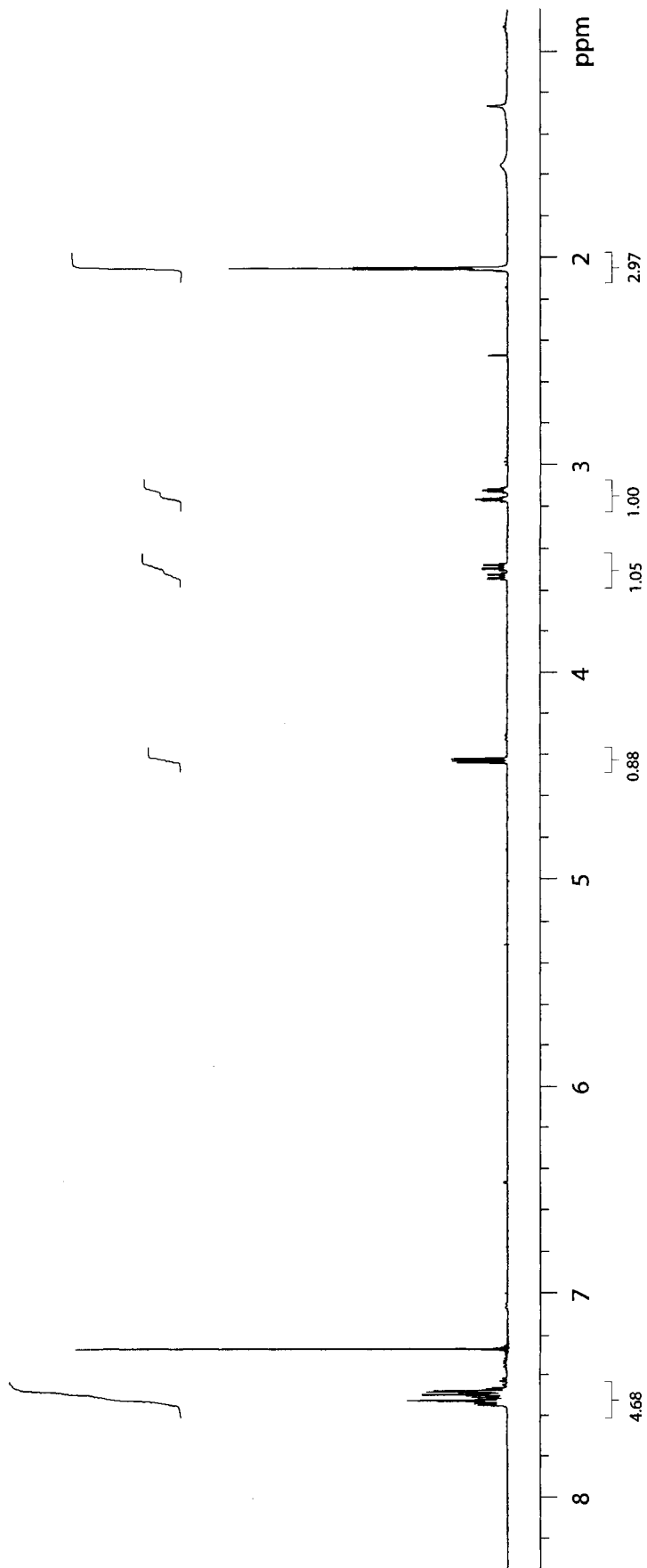
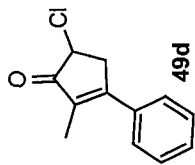
125 MHz APT in CDCl₃ (ref. to CDCl₃ @ 77.0 ppm), temp 27.2 C -> actual temp = 27.0 C, sw probe C & CH₂ same, CH & CH₃ opposite side of solvent signal

Pulse Sequence: apt



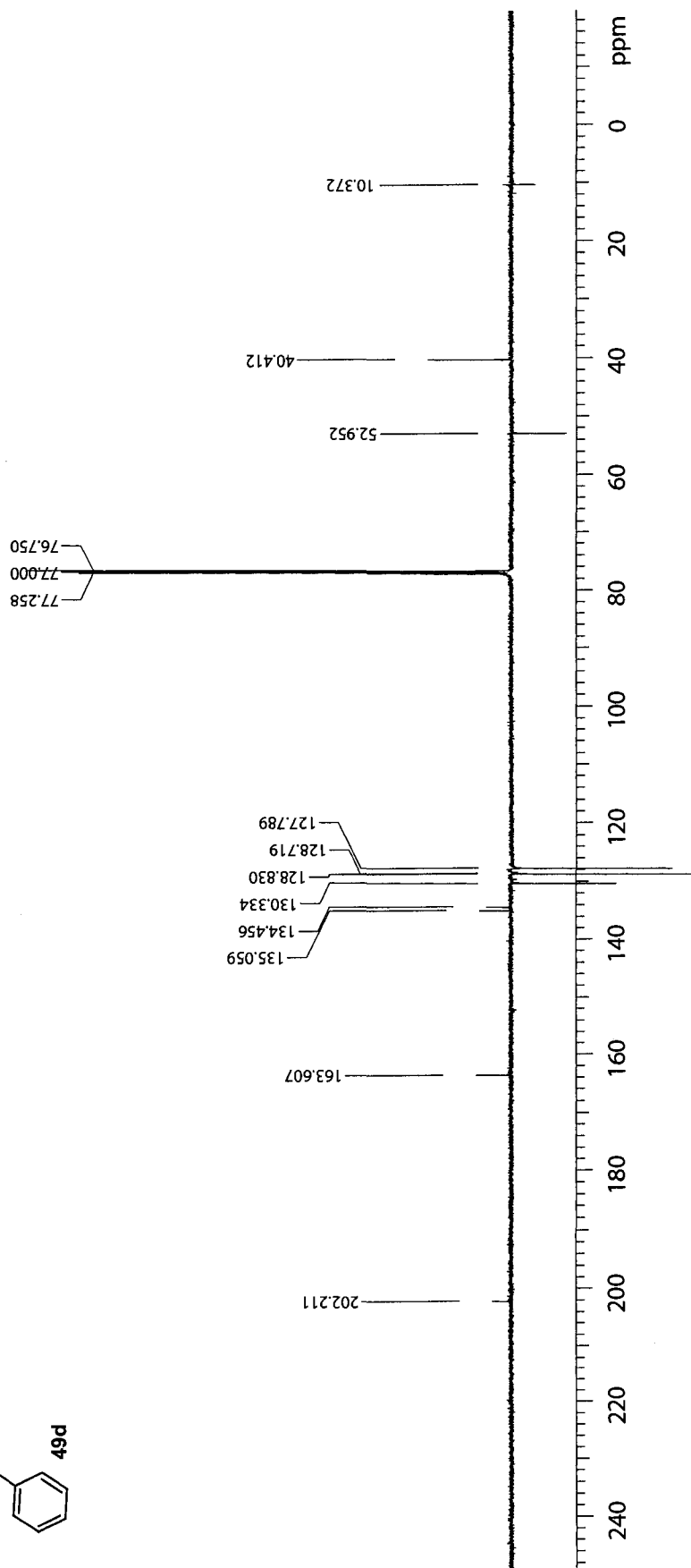
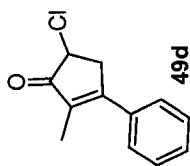
400 MHz 1D in CDCl3 (ref. to CDCl3 @ 7.26 ppm), temp 26.8 C -> actual temp = 27.0 C, asw400 probe

Pulse Sequence: s2pul



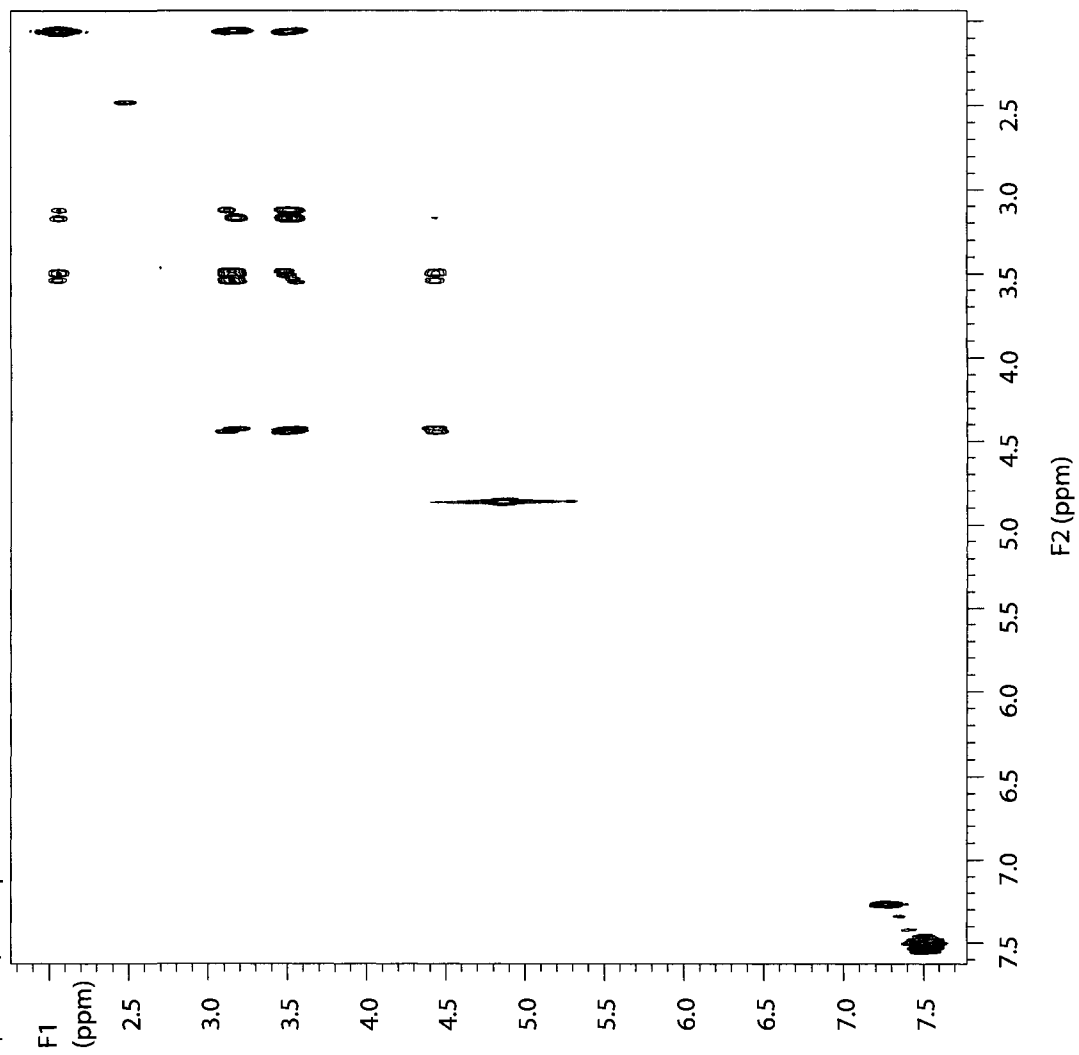
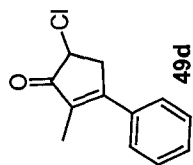
125 MHz APT in CDCl₃ (ref. to CDCl₃ @ 77.0 ppm), temp 29.4 C -> actual temp = 27.0 C, sw500u probe
C & CH₂ same, CH & CH₃ opposite side of solvent signal

Pulse Sequence: apt



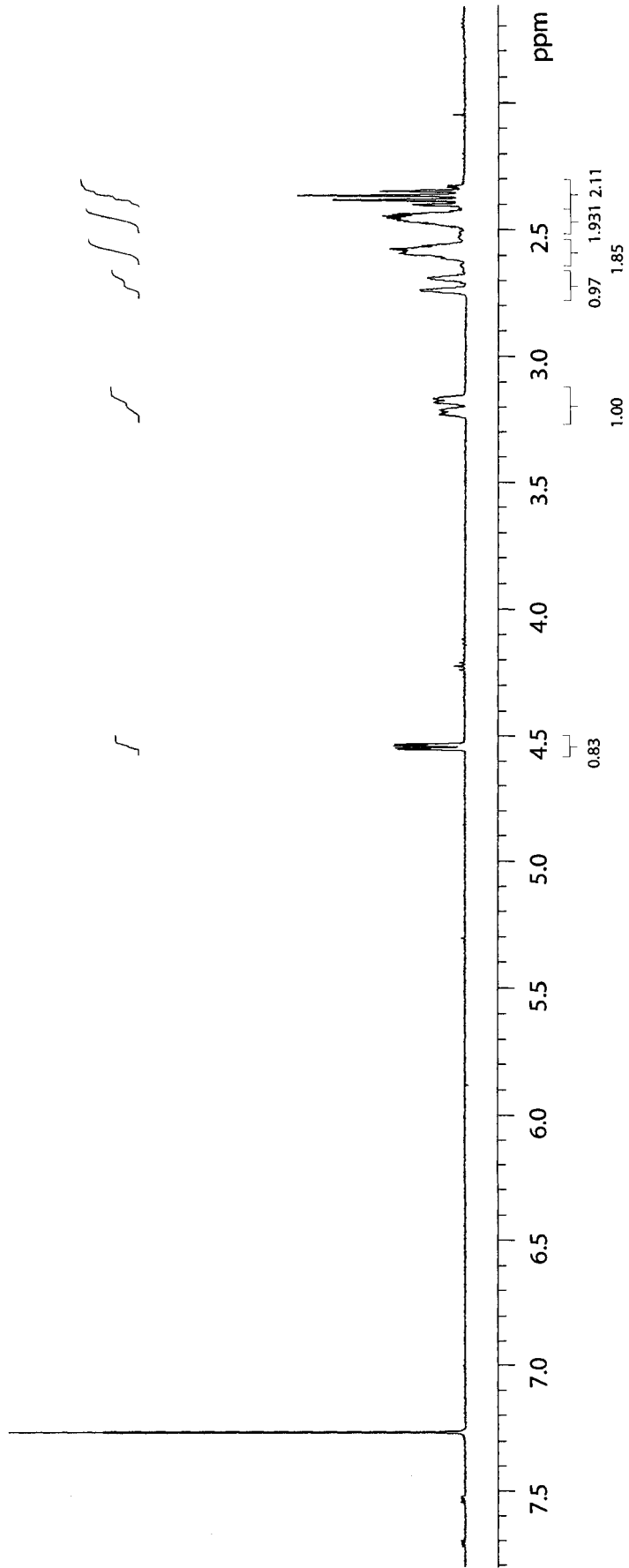
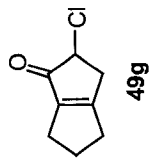
400 MHz GCOSY in CDCl₃ (ref. to CDCl₃ @ 7.26 ppm), temp 26.8 C -> actual temp = 27.0 C, asw400 probe

Pulse Sequence: aogcosy



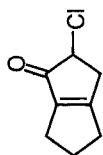
400 MHz 1D in CDCl₃ (ref. to CDCl₃ @ 7.26 ppm), temp 26.8 C -> actual temp = 27.0 C, asw400 probe

Pulse Sequence: s2pul

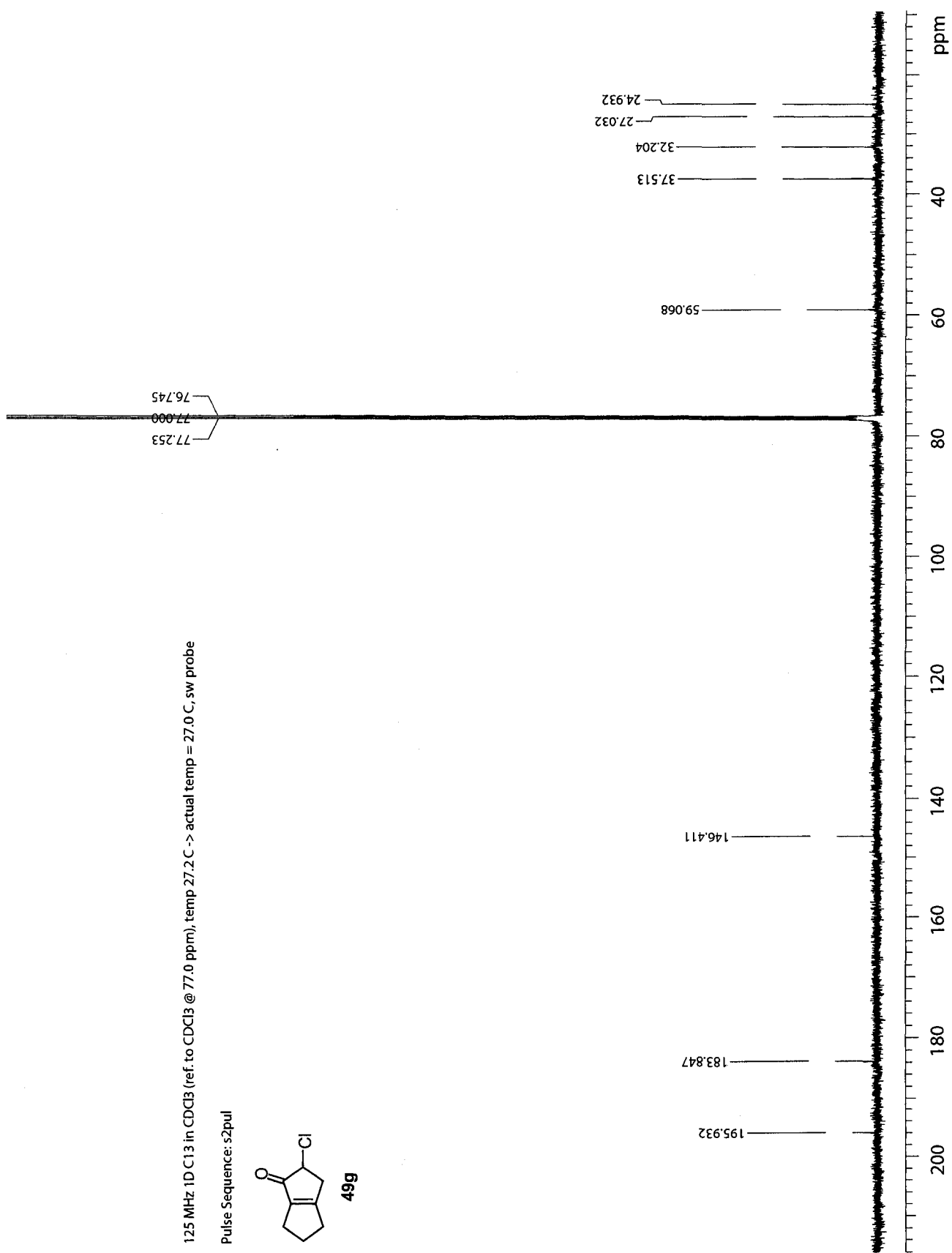


125 MHz 1D C13 in CDCl3 (ref. to CDCl3 @ 77.0 ppm), temp 27.2 C -> actual temp = 27.0 C, sw probe

Pulse Sequence: s2pul

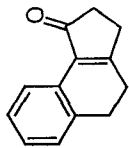


49g

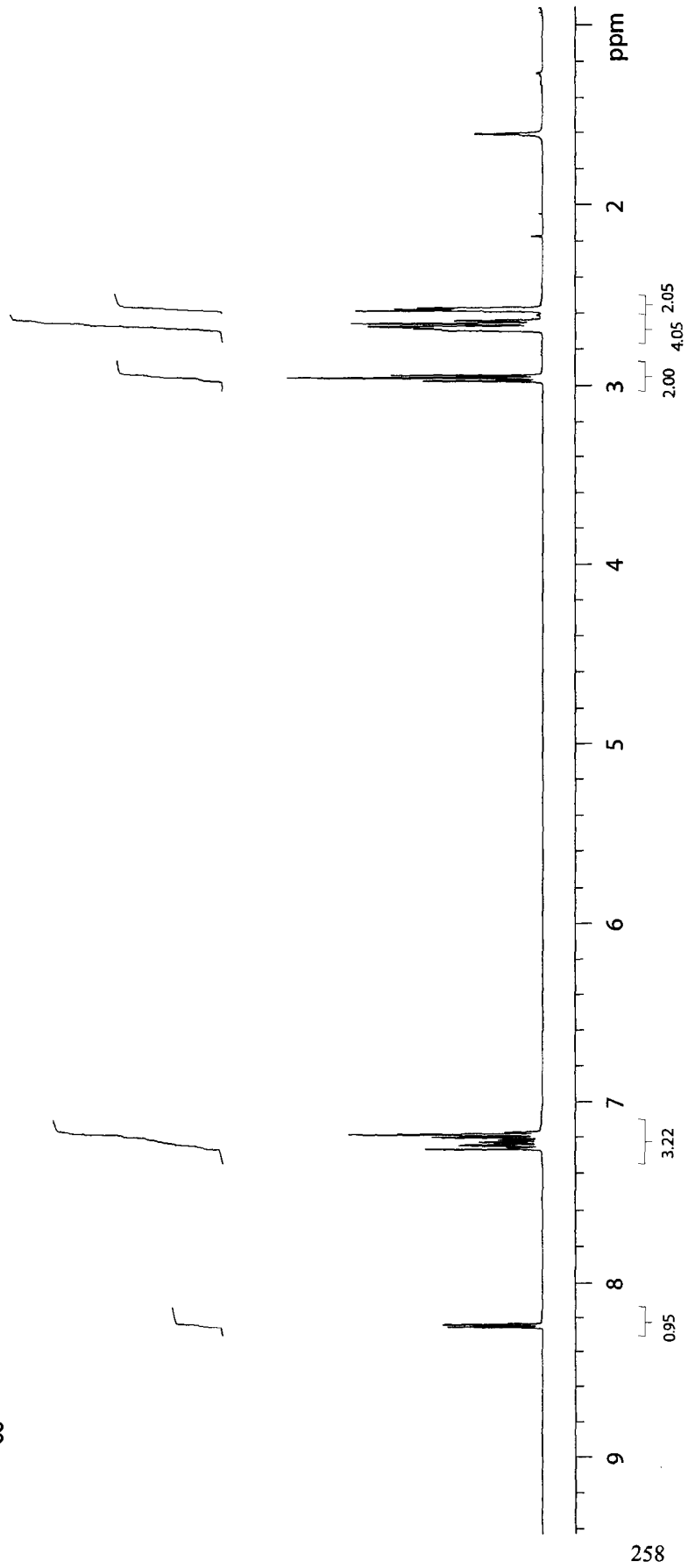


500 MHz 1D in CDCl₃ (ref. to CDCl₃ @ 7.26 ppm), temp 29.4 C -> actual temp = 27.0 C, sw500u probe

Pulse Sequence: s2pul

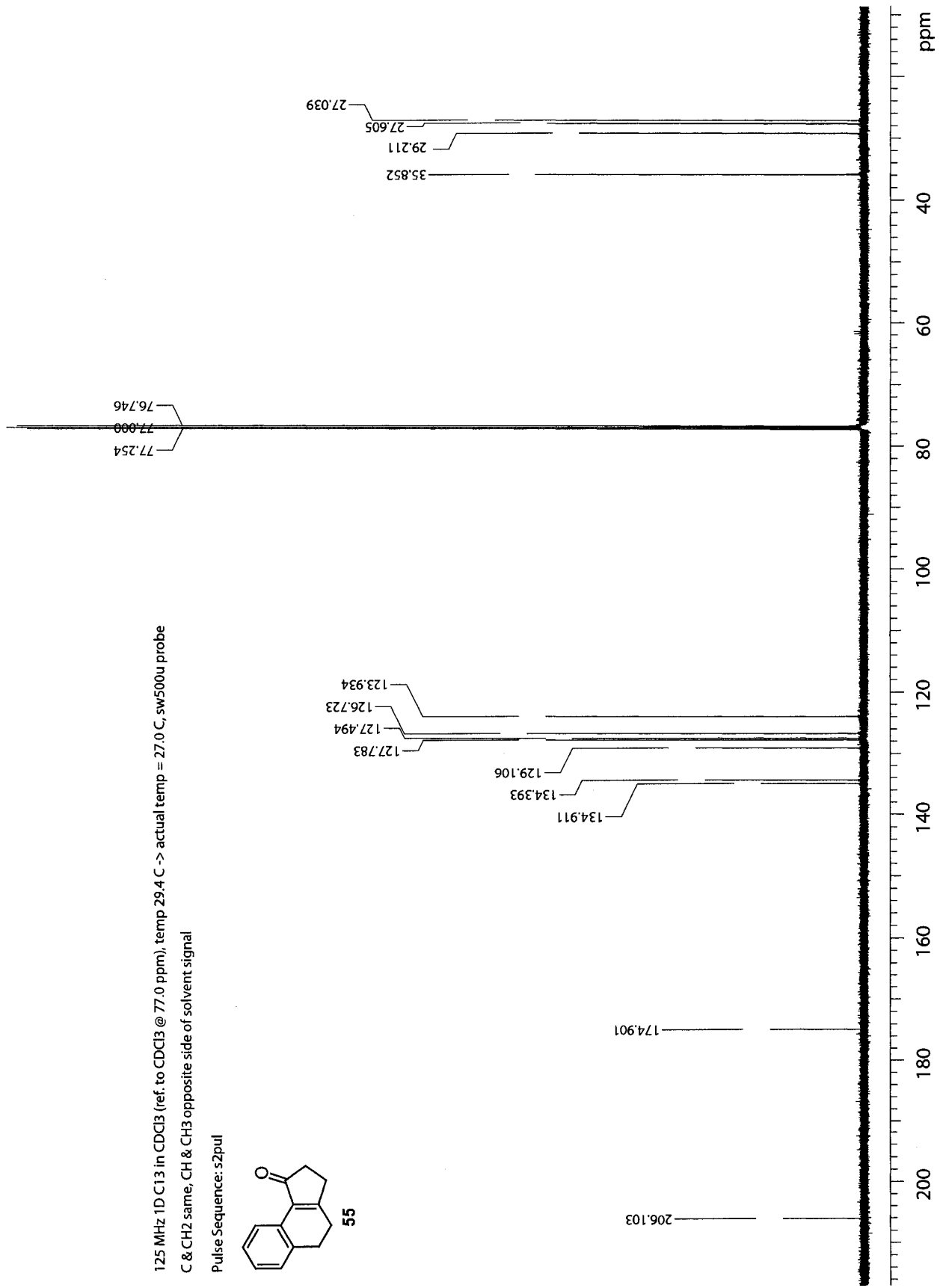
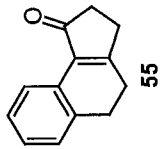


55



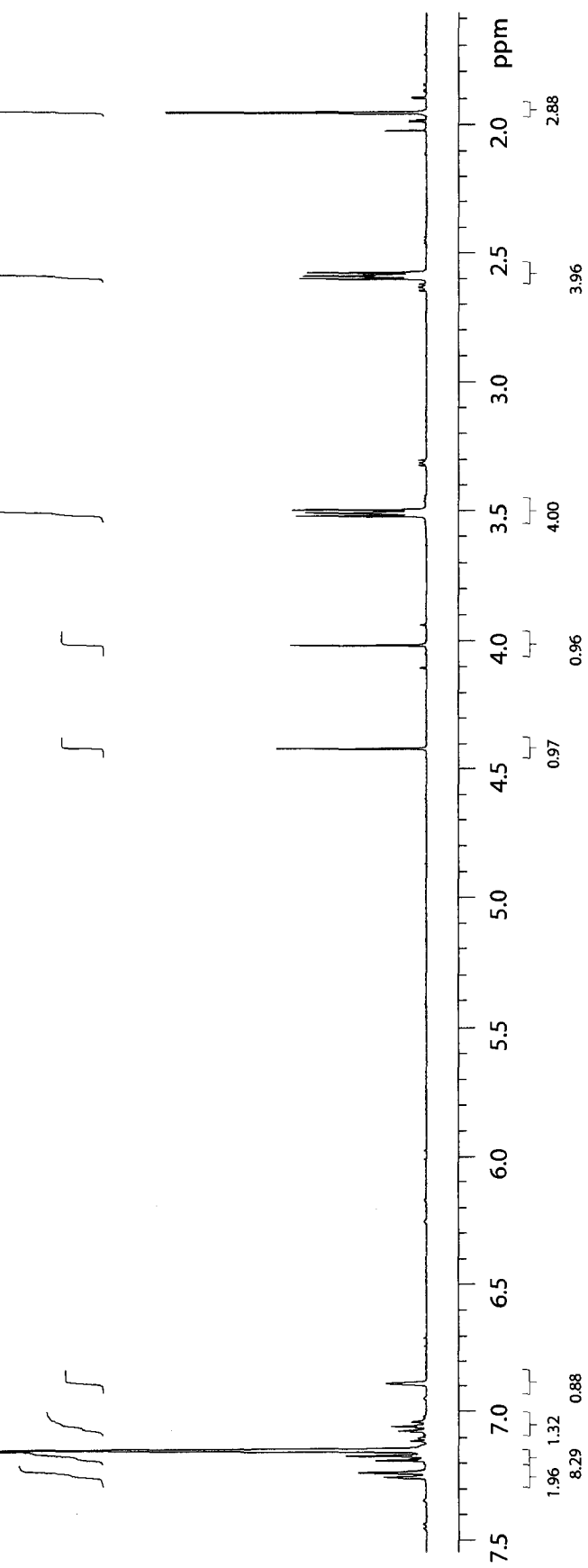
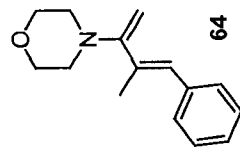
125 MHz 1D C13 in CDCl3 (ref. to CDCl3 @ 77.0 ppm), temp 29.4 C -> actual temp = 27.0 C, sw500u probe
C & CH2 same, CH & CH3 opposite side of solvent signal

Pulse Sequence: s2pul



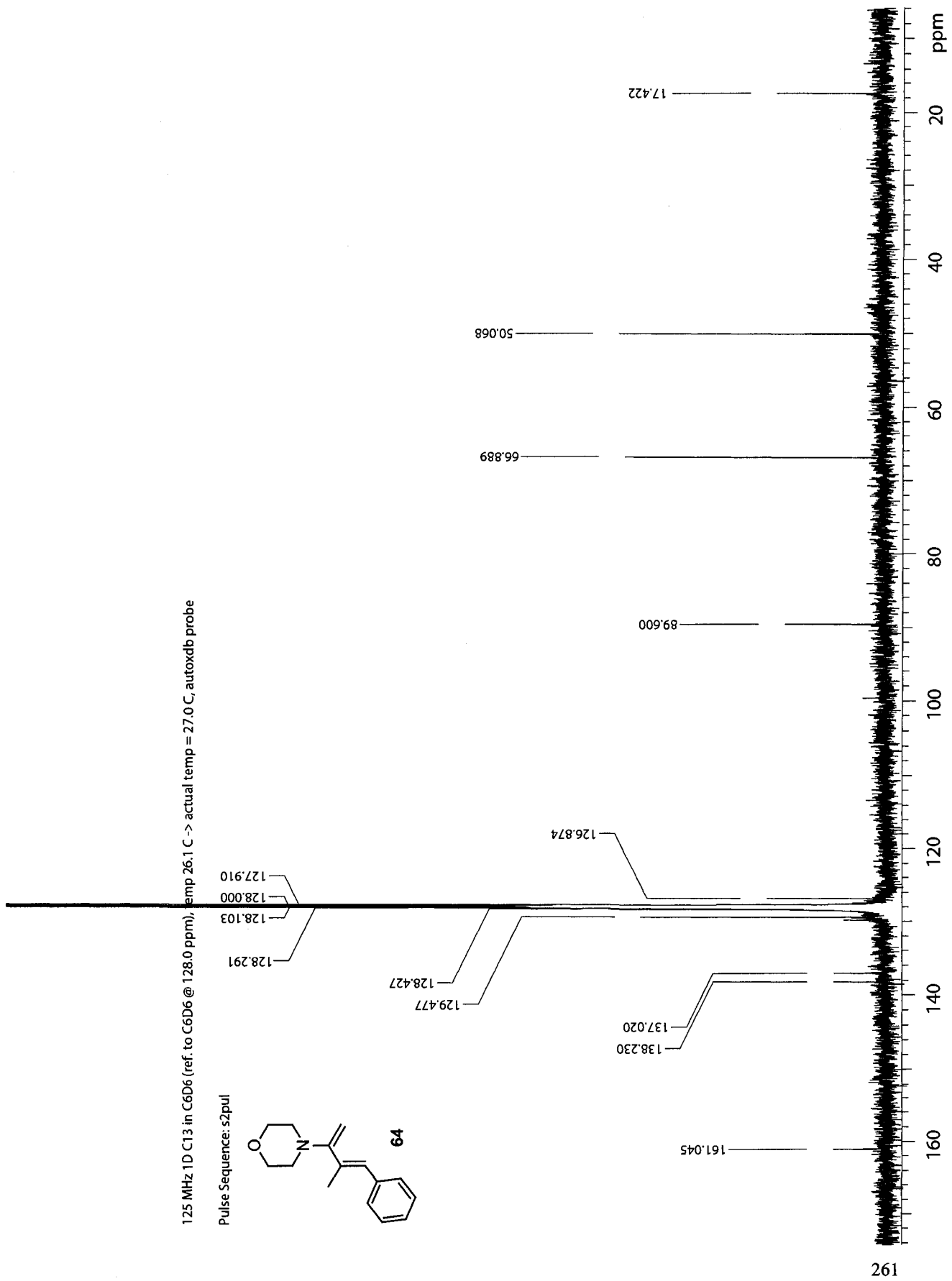
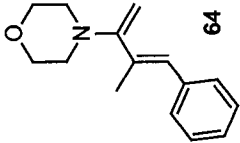
400 MHz 1D in C6D6 (ref. to C6D6 @ 7.15 ppm), temp 27.0 C -> actual temp = 27.0 C, m400gz probe

Pulse Sequence: s2pul



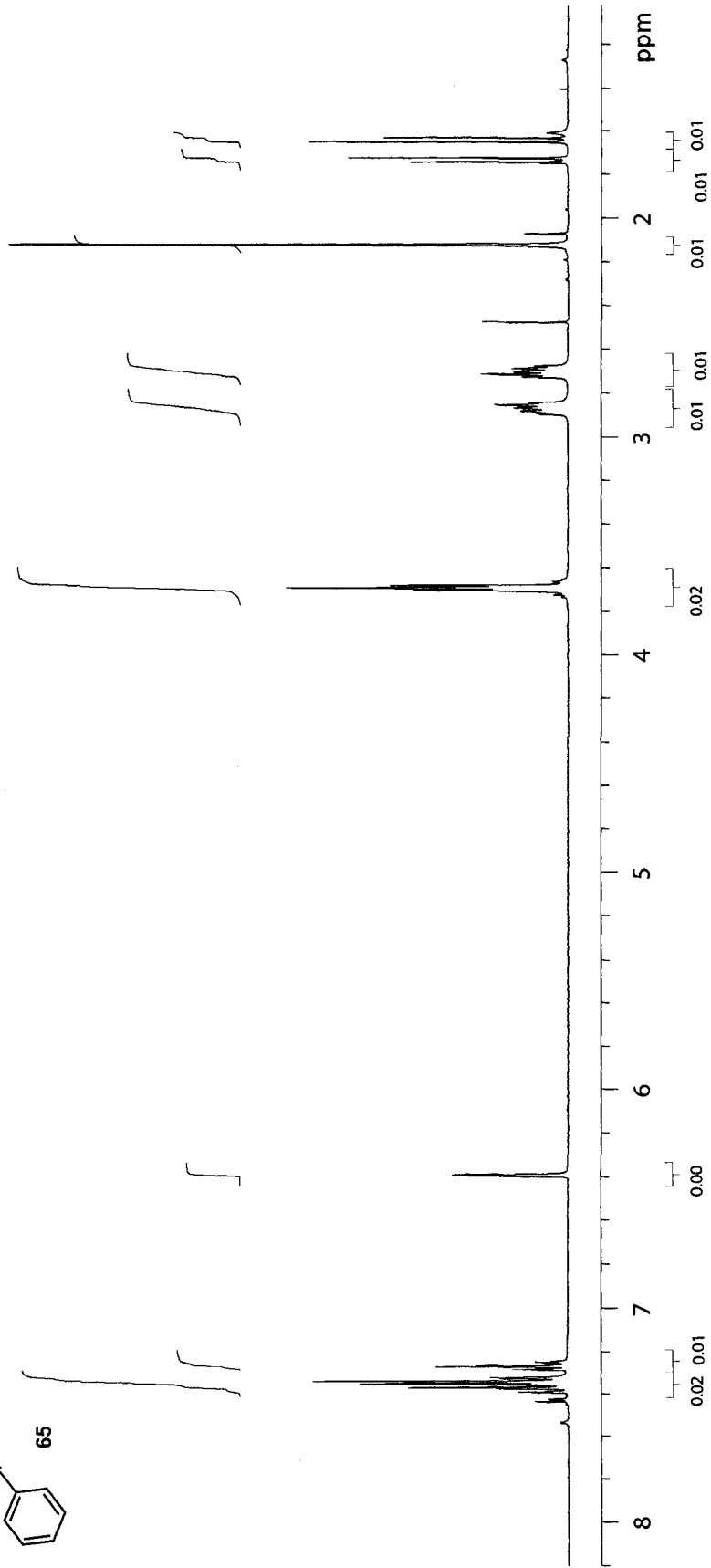
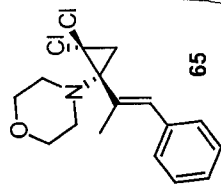
125 MHz 1D C13 in C6D6 (ref. to C6D6 @ 128.0 ppm), temp 26.1 C -> actual temp = 27.0 C, autotxdb probe

Pulse Sequence: s2pul



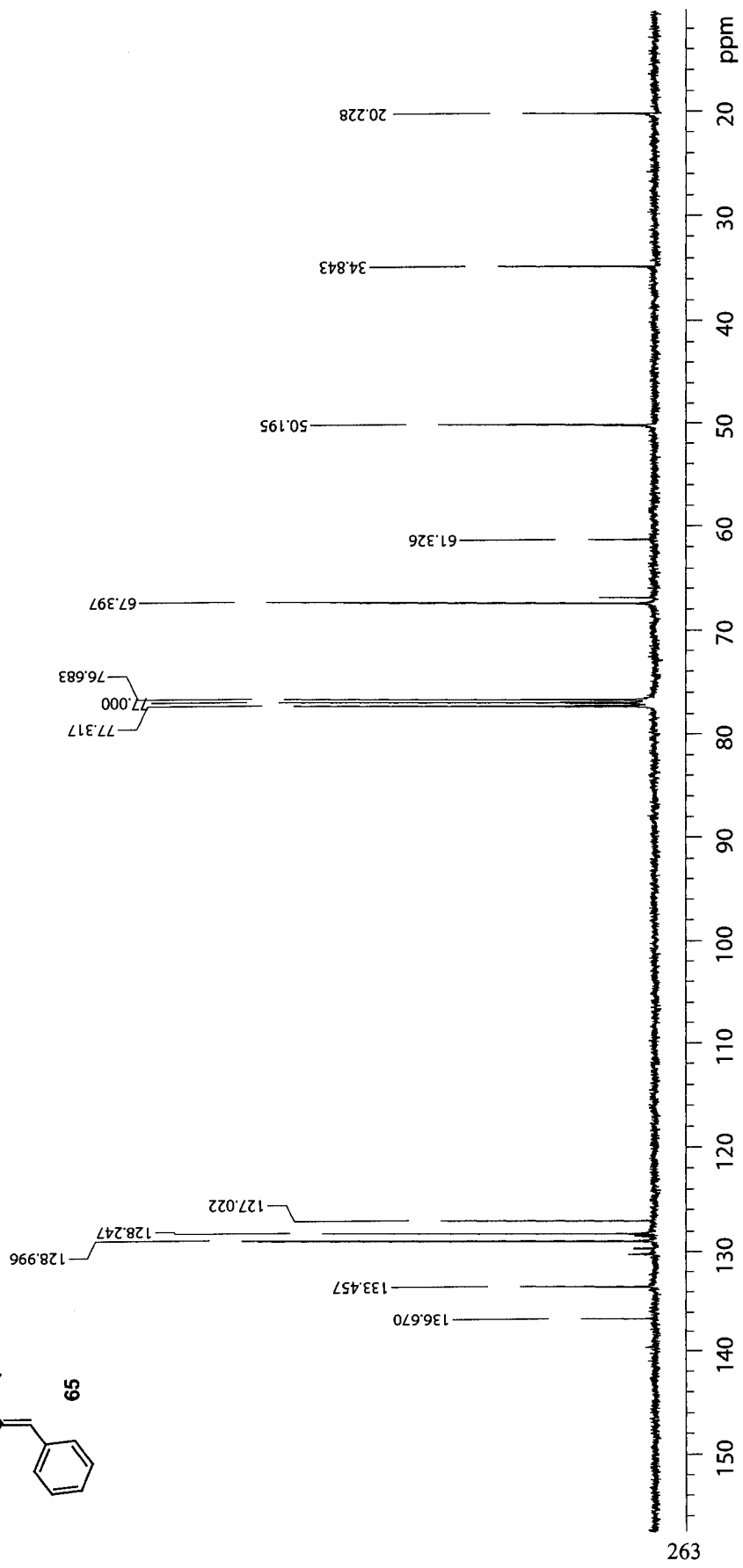
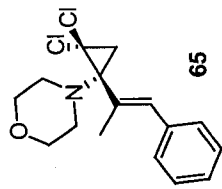
400 MHz 1D in CDCl3 (ref. to CDCl3 @ 7.26 ppm), temp 27.0 C -> actual temp = 27.0 C, m400gz probe

Pulse Sequence: s2pul



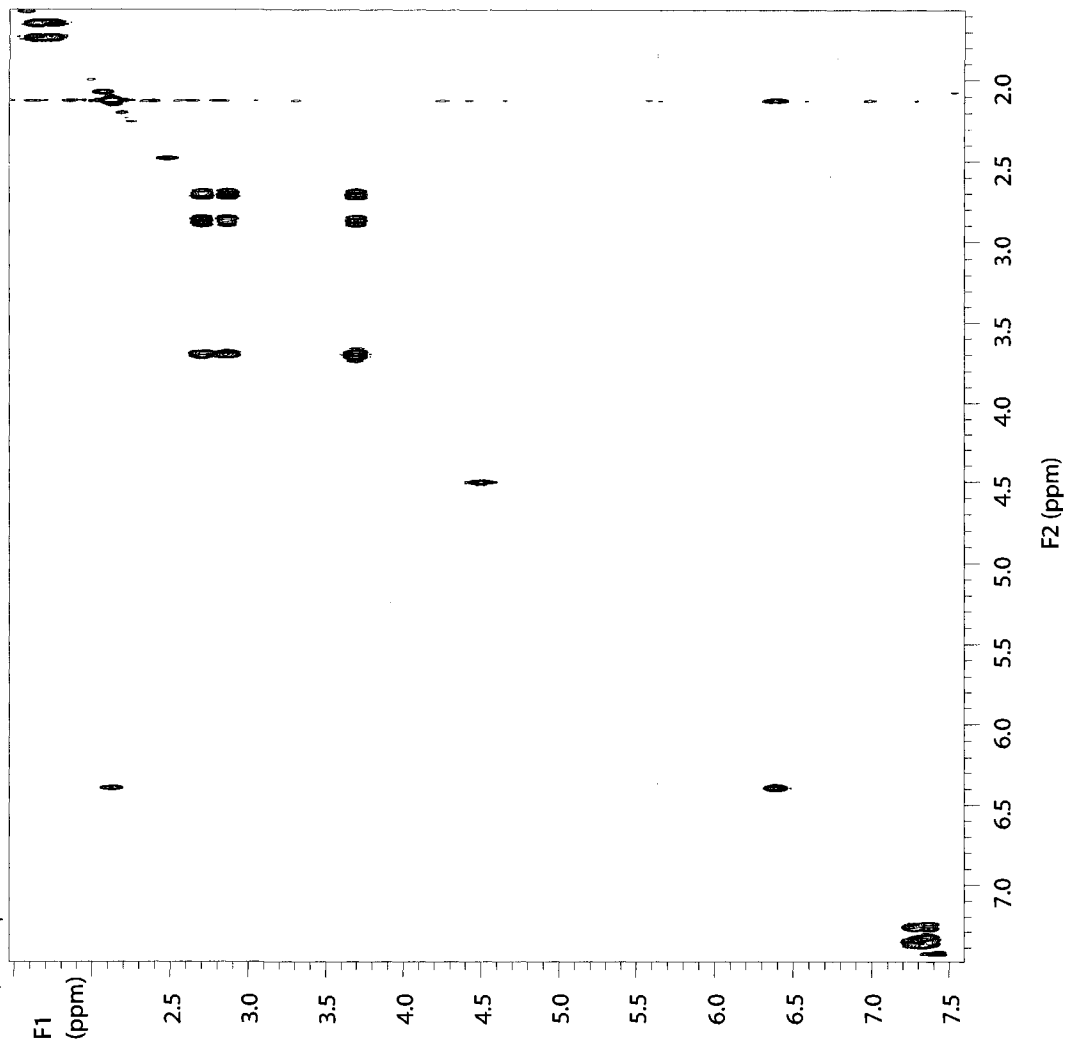
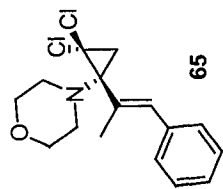
100 MHz 1D C13 in CDCl3 (ref. to CDCl3 @ 77.0 ppm), temp 27.0 C -> actual temp = 27.0 C, m400gz probe

Pulse Sequence: s2pul



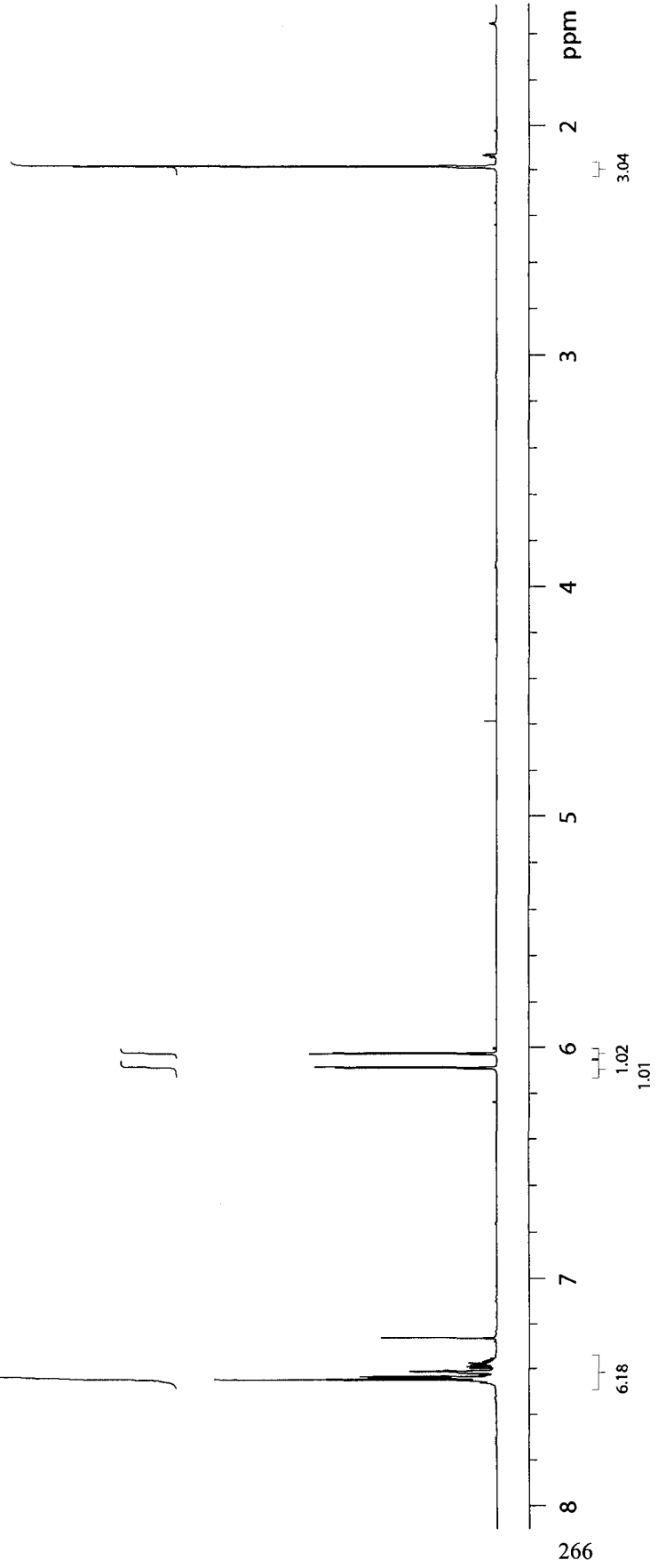
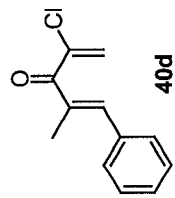
500 MHz GCOSY in CDCl₃ (ref. to CDCl₃ @ 7.26 ppm), temp 27.2 C -> actual temp = 27.0 C, sw500 probe

Pulse Sequence: aogcosy



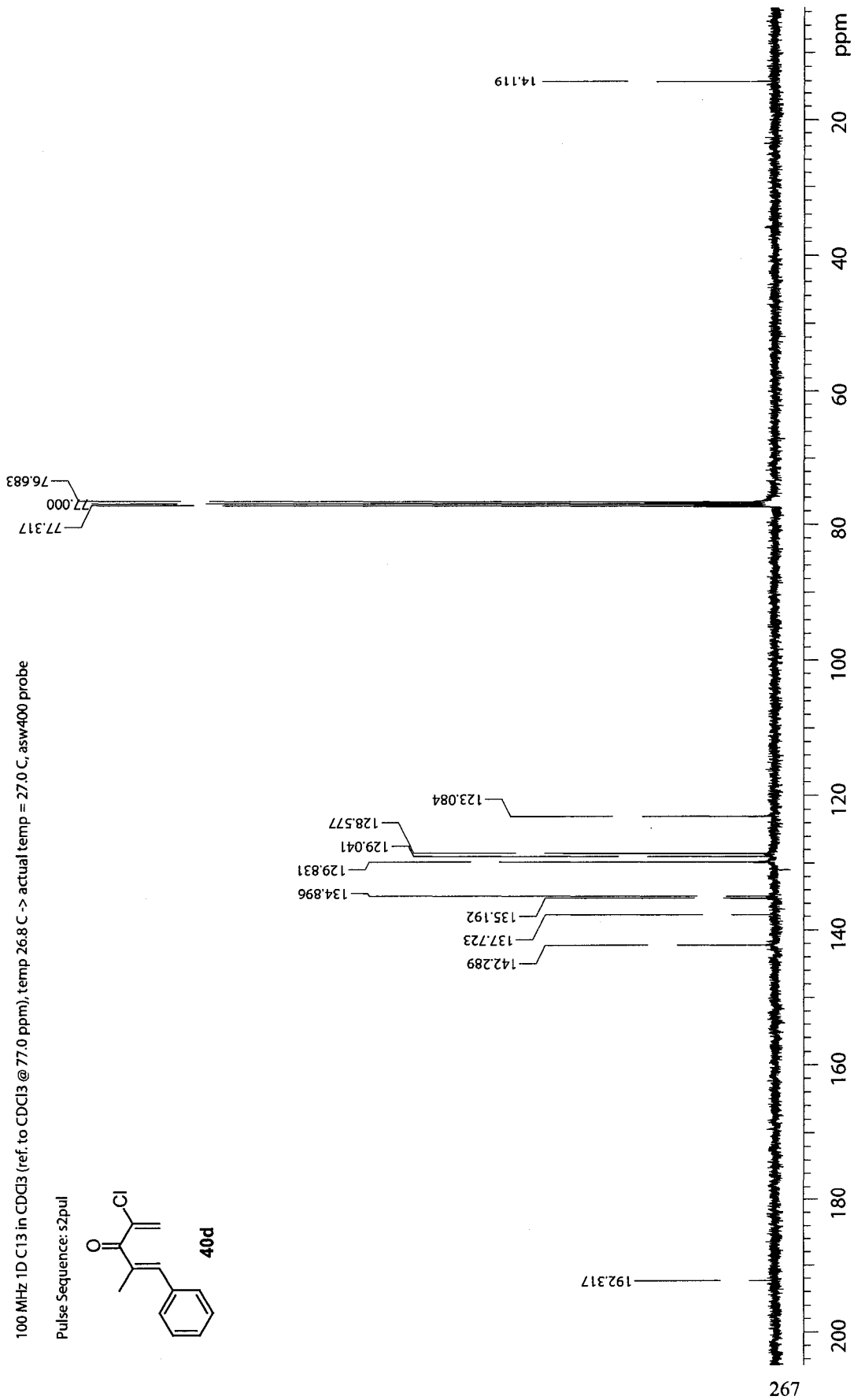
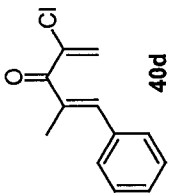
400 MHz 1D in CDCl₃ (ref. to CDCl₃ @ 7.26 ppm), temp 26.8 C -> actual temp = 27.0 C, asw400 probe

Pulse Sequence: s2pul



100 MHz ¹³C NMR in CDCl₃ (ref. to CDCl₃ @ 77.0 ppm), temp 26.8 C -> actual temp = 27.0 C, asw400 probe

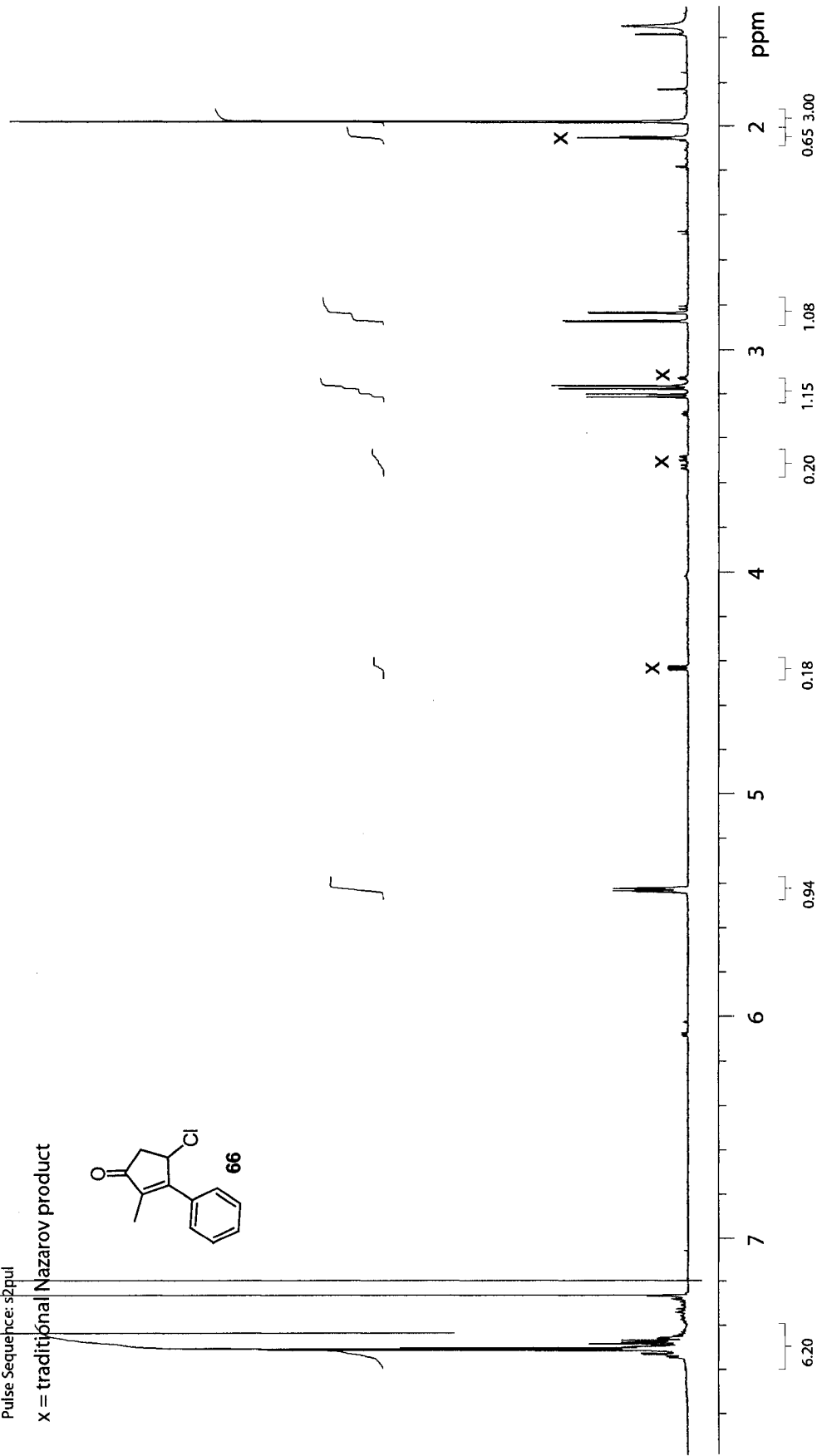
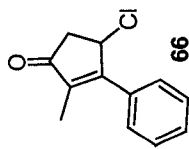
Pulse Sequence: s2pul



500 MHz ¹D in CDCl₃ (ref. to CDCl₃ @ 7.26 ppm), temp 27.2 C -> actual temp = 27.0 C, sw500 probe

Pulse Sequence: s2pul

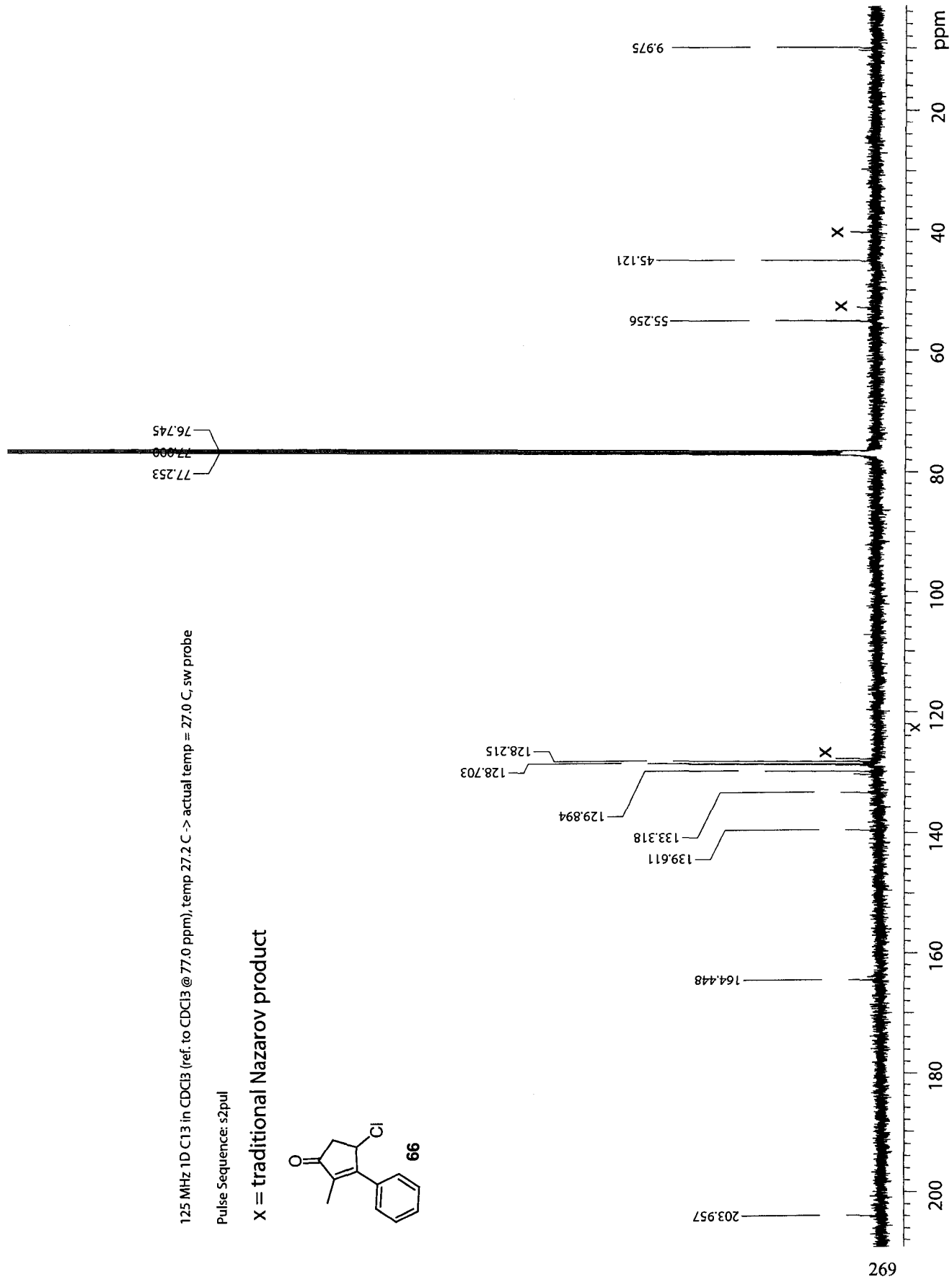
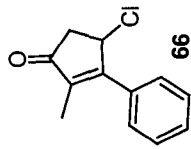
x = traditional Nazarov product



125 MHz 1D C13 in CDCl3 (ref. to CDCl3 @ 77.0 ppm), temp 27.2 C -> actual temp = 27.0 C, sw probe

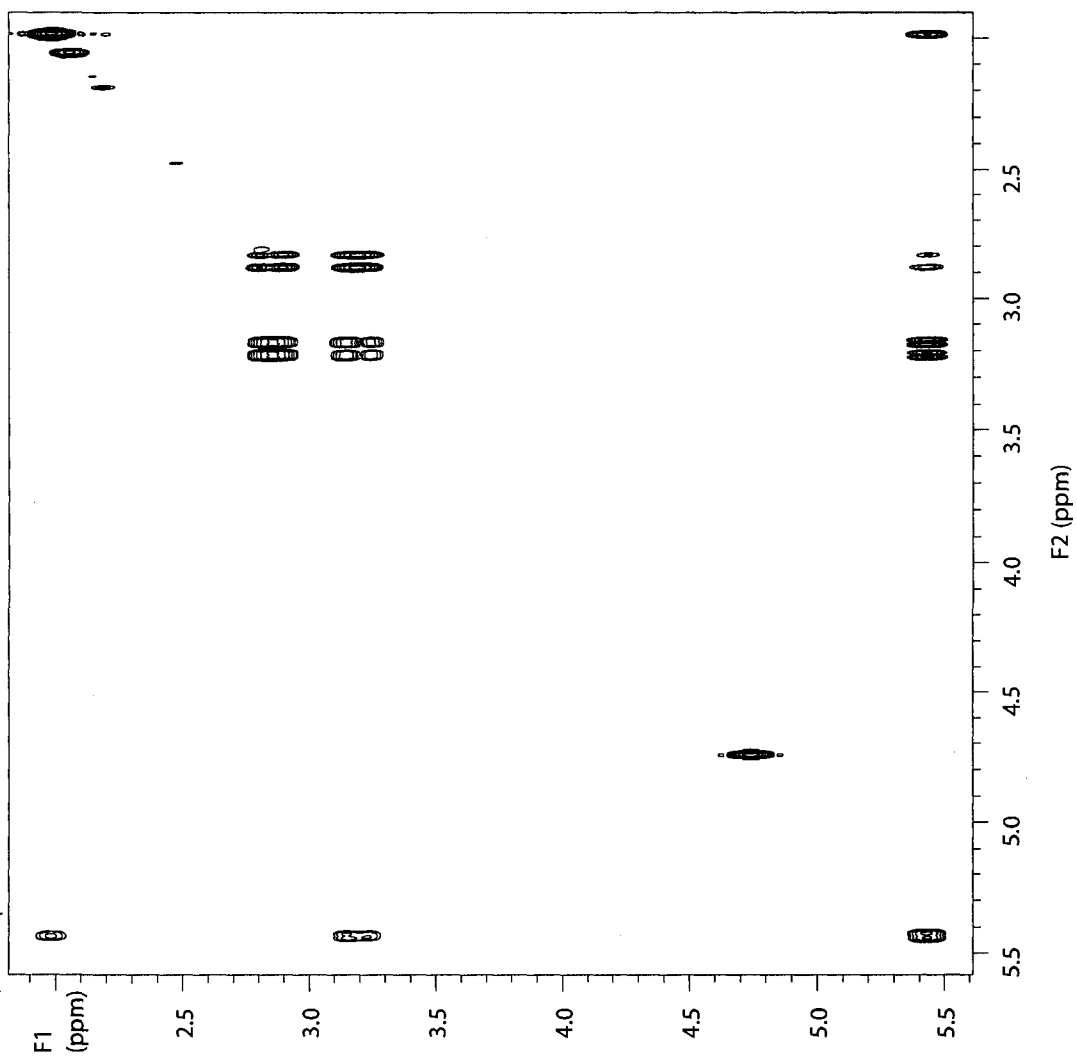
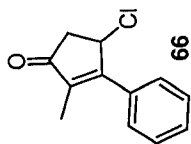
Pulse Sequence: s2pul

X = traditional Nazarov product



400 MHz GCOSY in CDCl₃ (ref. to CDCl₃ @ 7.26 ppm), temp 26.8 C -> actual temp = 27.0 C, asw400 probe

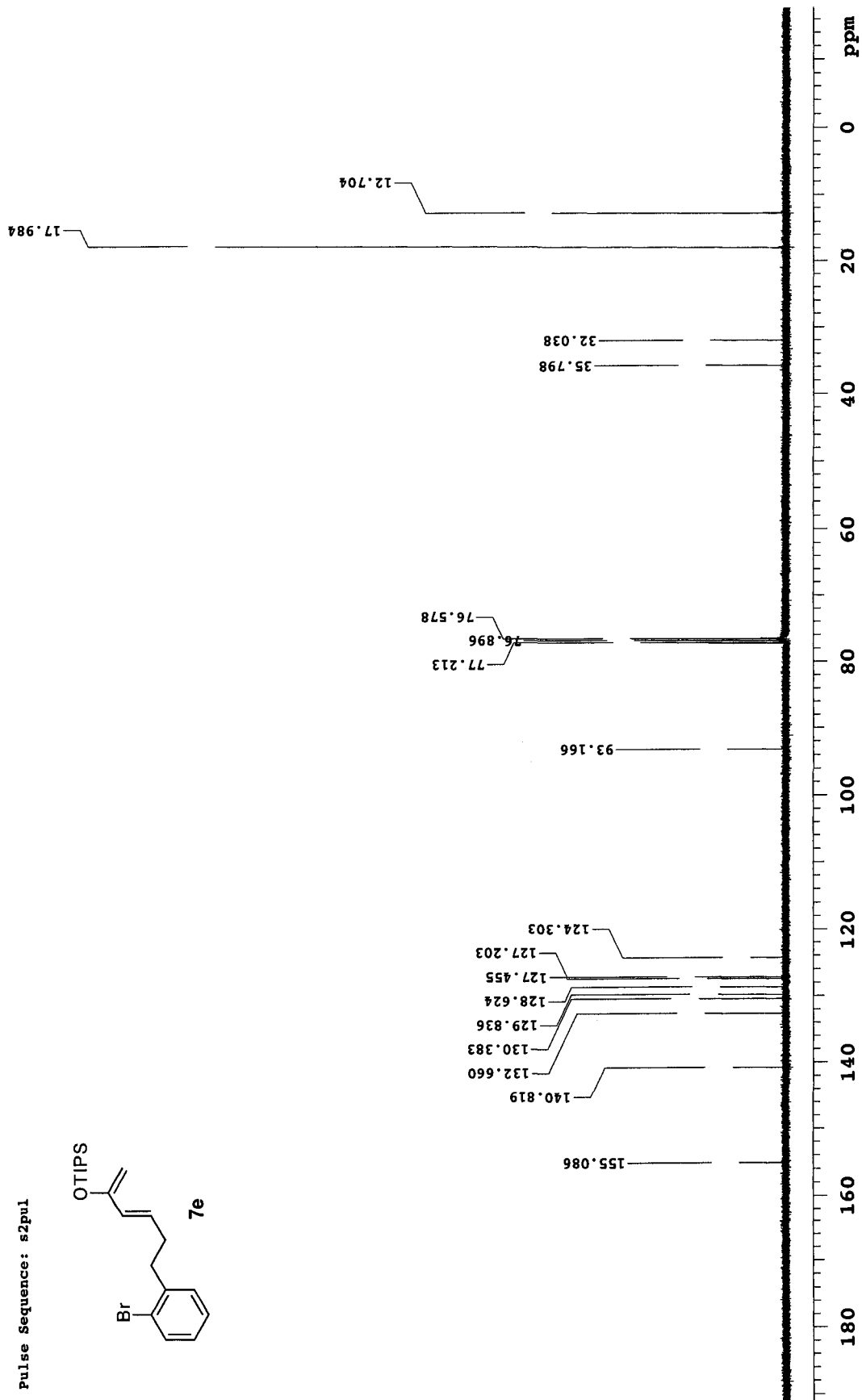
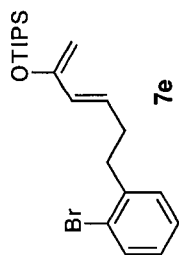
Pulse Sequence: aogcosy



**Appendix II: Selected NMR Spectra
(Chapter 3)**

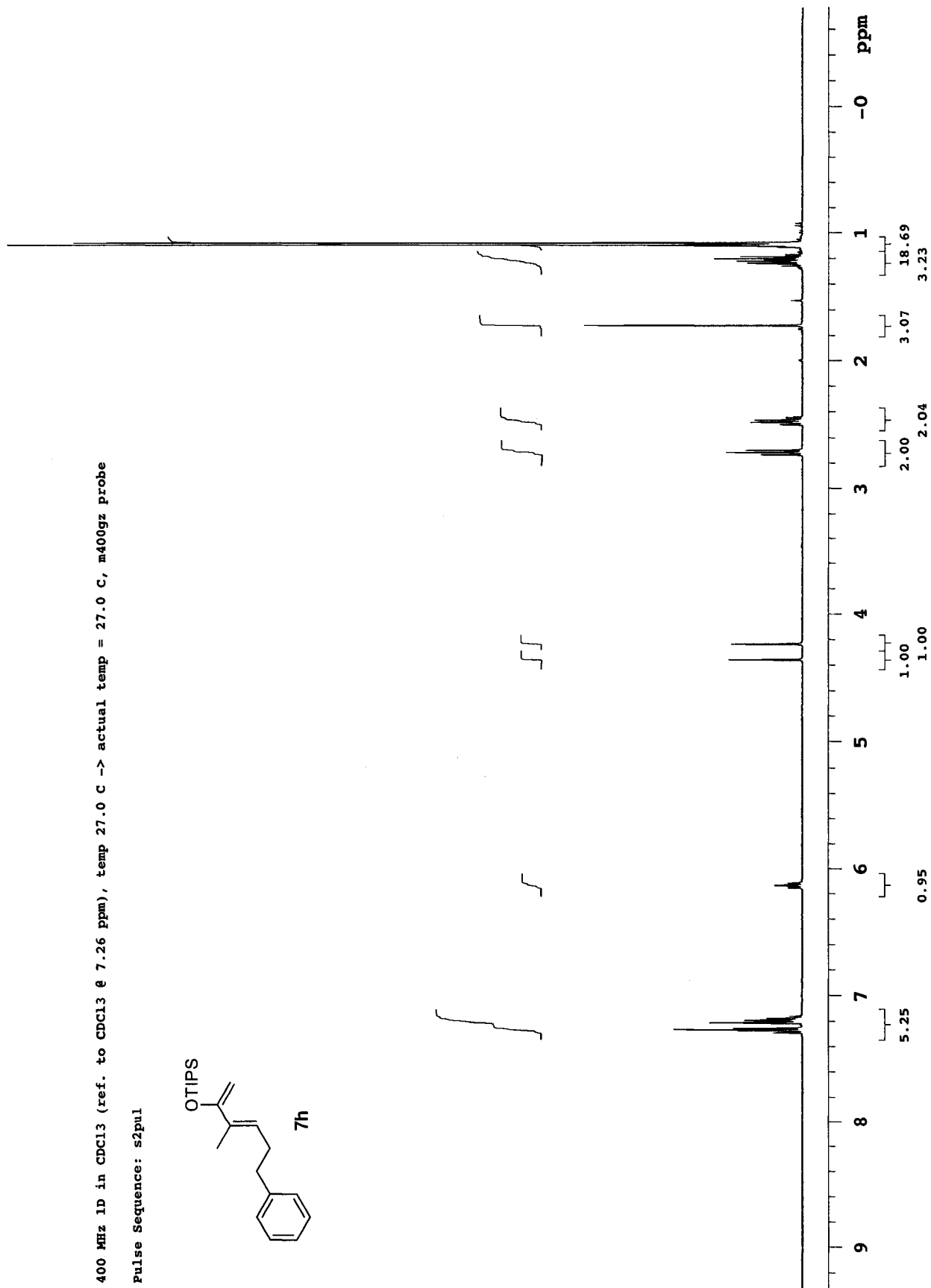
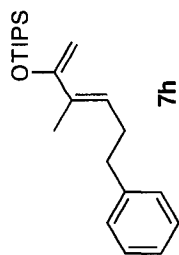
100 MHz 1D C13 in CDCl3 (ref. to CDCl3 @ 77.0 ppm), temp 27.0 C -> actual temp = 27.0 C, m400gz probe

Pulse Sequence: s2pul

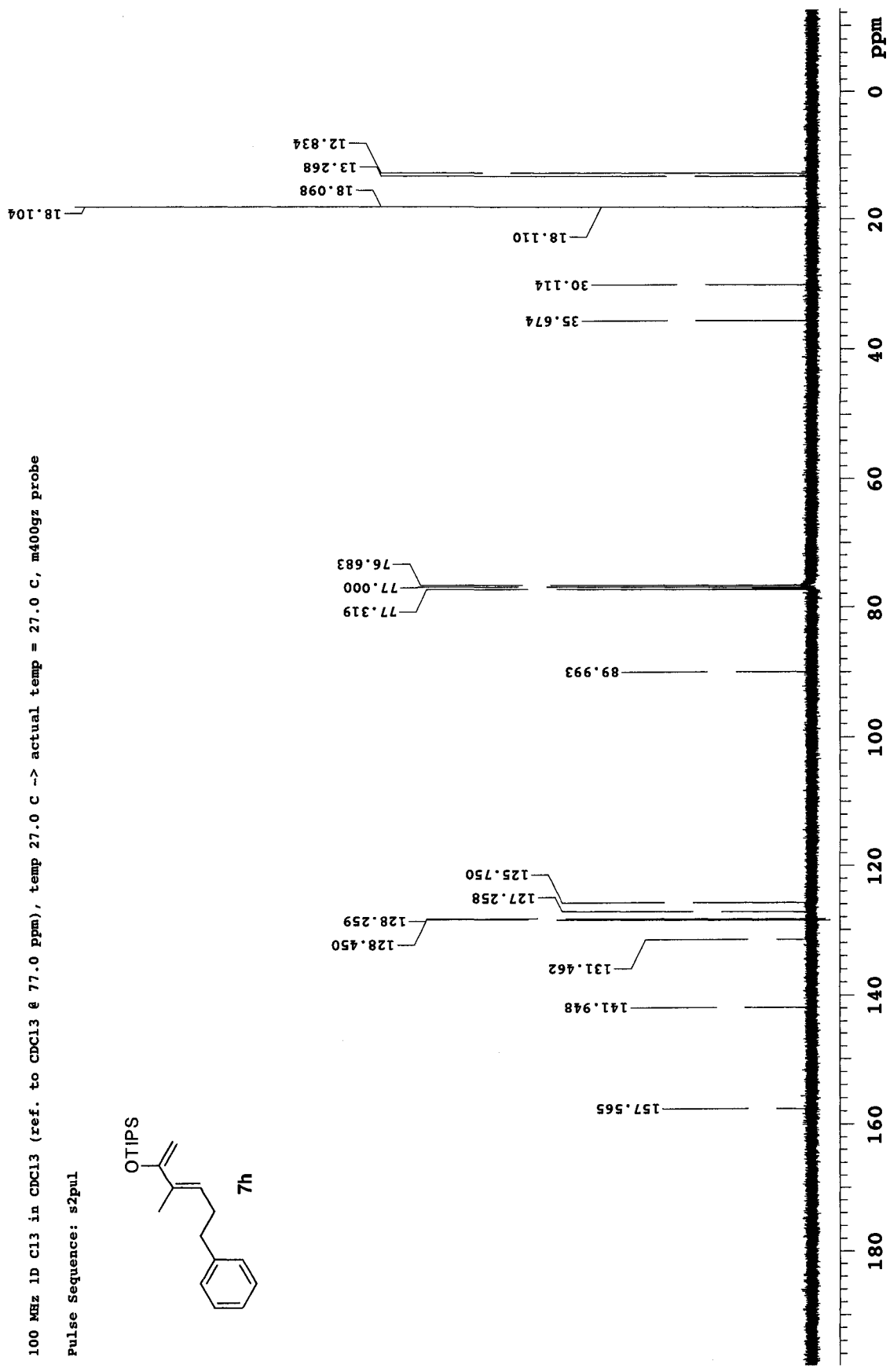
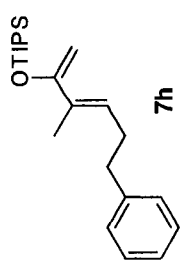


400 MHz 1D in CDCl3 (ref. to CDCl3 @ 7.26 ppm), temp 27.0 C -> actual temp = 27.0 C, m400gz probe

Pulse Sequence: s2pul

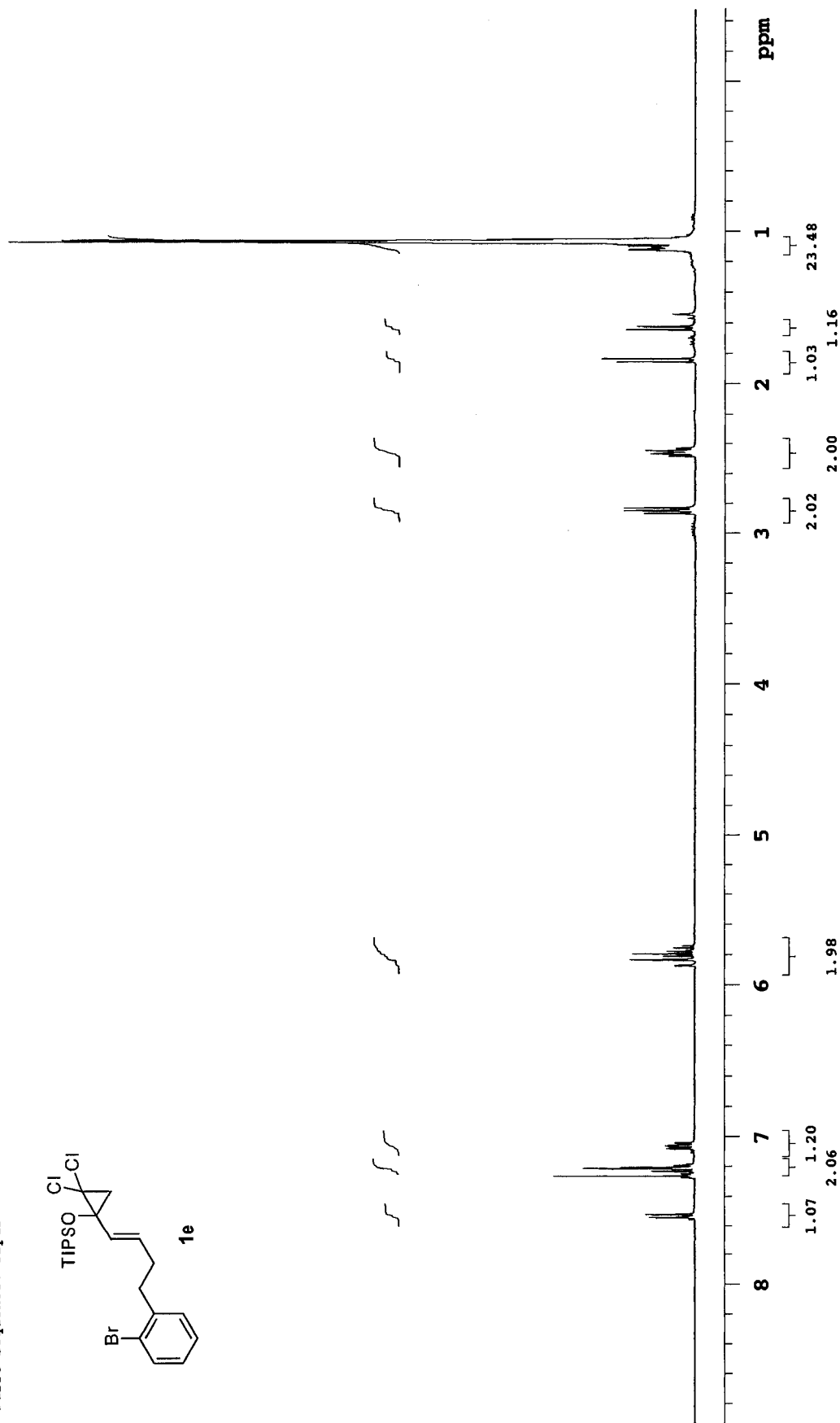
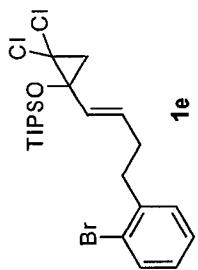


100 MHz 1D C13 in CDCl3 (ref. to CDCl3 @ 77.0 ppm), temp 27.0 C -> actual temp = 27.0 C, m400gz probe
Pulse Sequence: s2pul



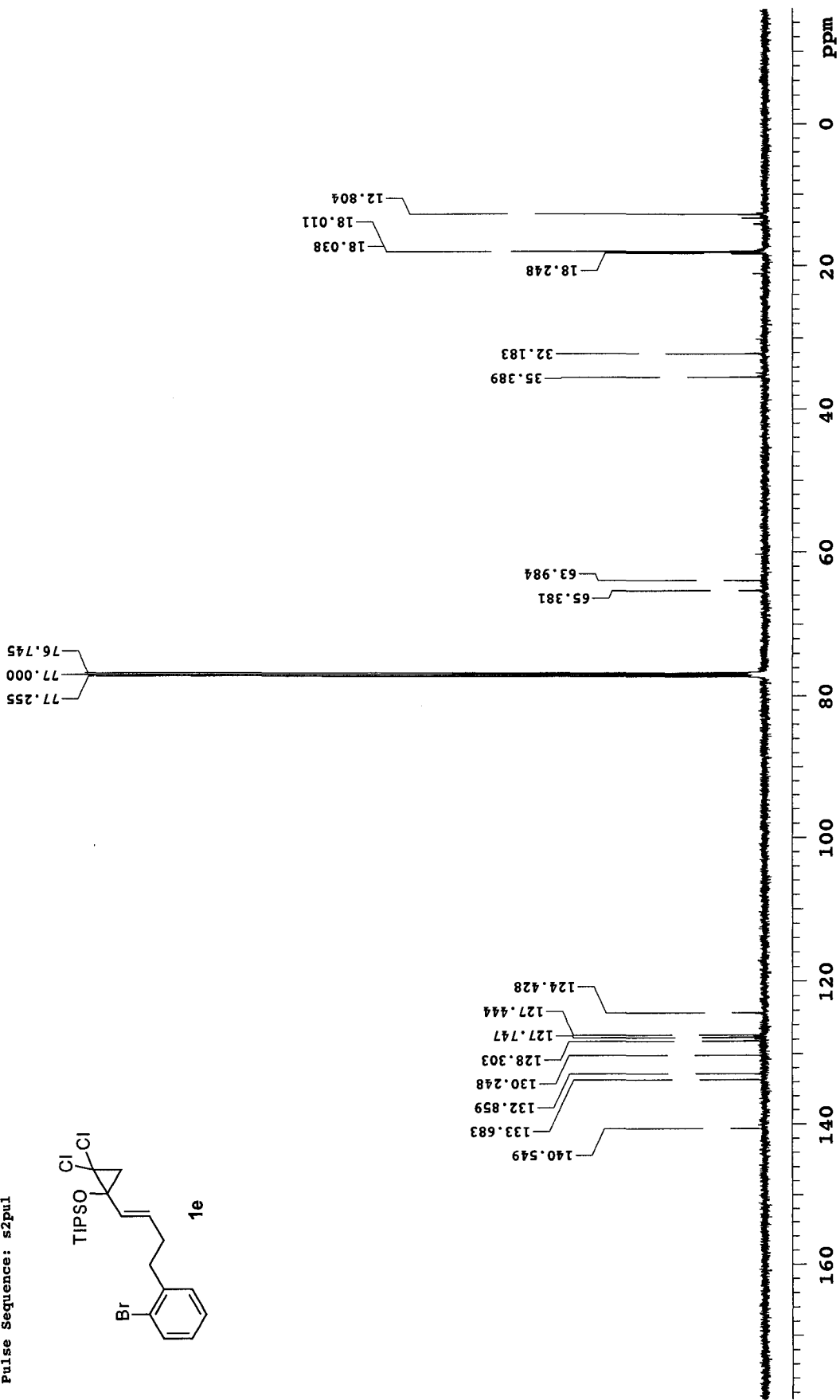
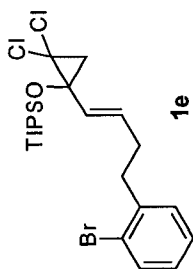
400 MHz 1D in CDCl3 (ref. to CDCl3 @ 7.26 ppm), temp 27.0 C --> actual temp = 27.0 C, m400gz probe

Pulse Sequence: s2pul



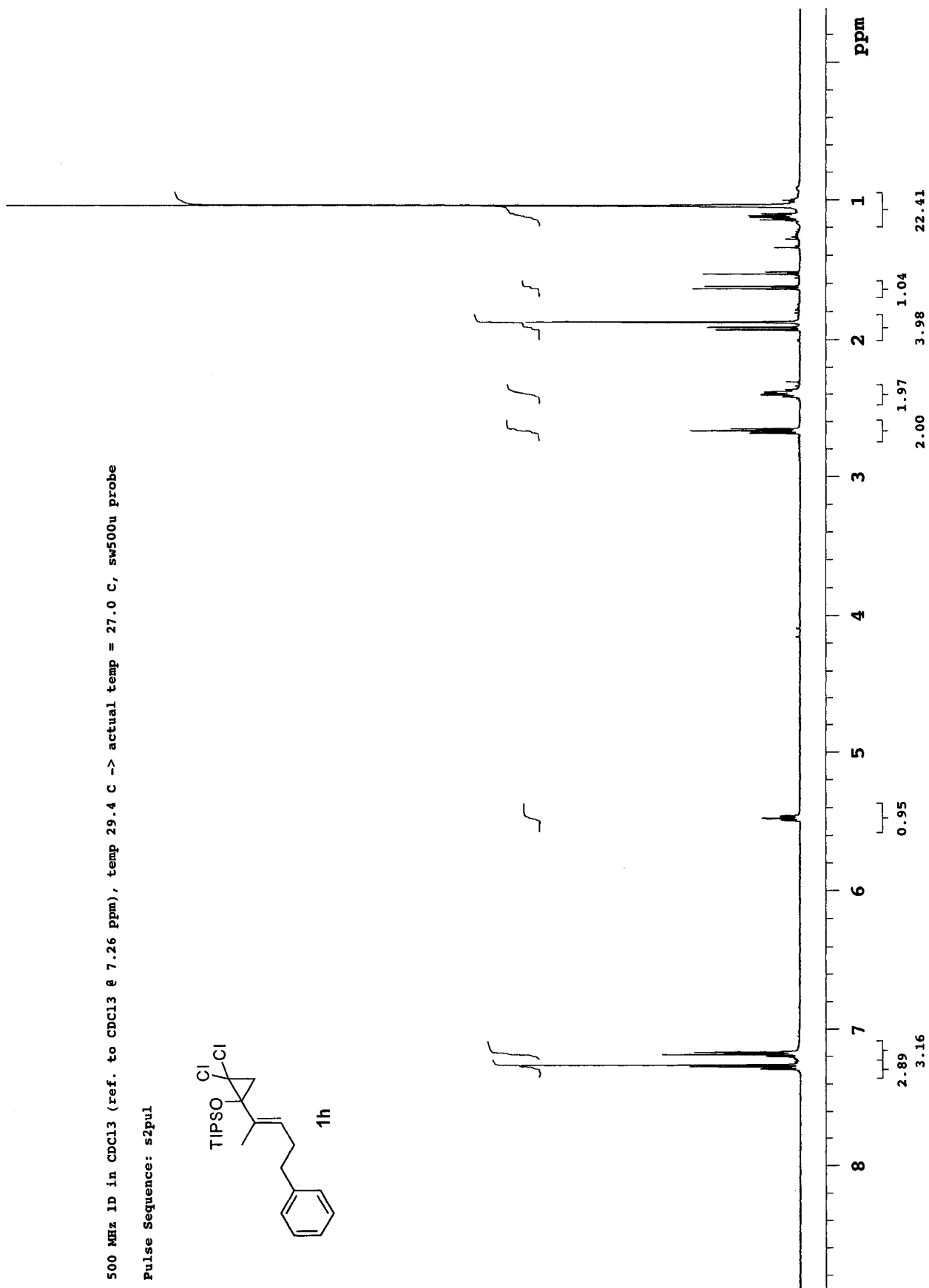
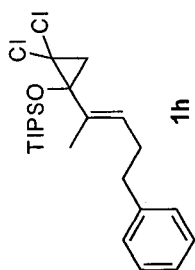
125 MHz 1D C13 in CDCl3 (ref. to CDCl3 @ 77.0 ppm), temp 26.1 C -> actual temp = 27.0 C, autordb probe

Pulse Sequence: s2pul



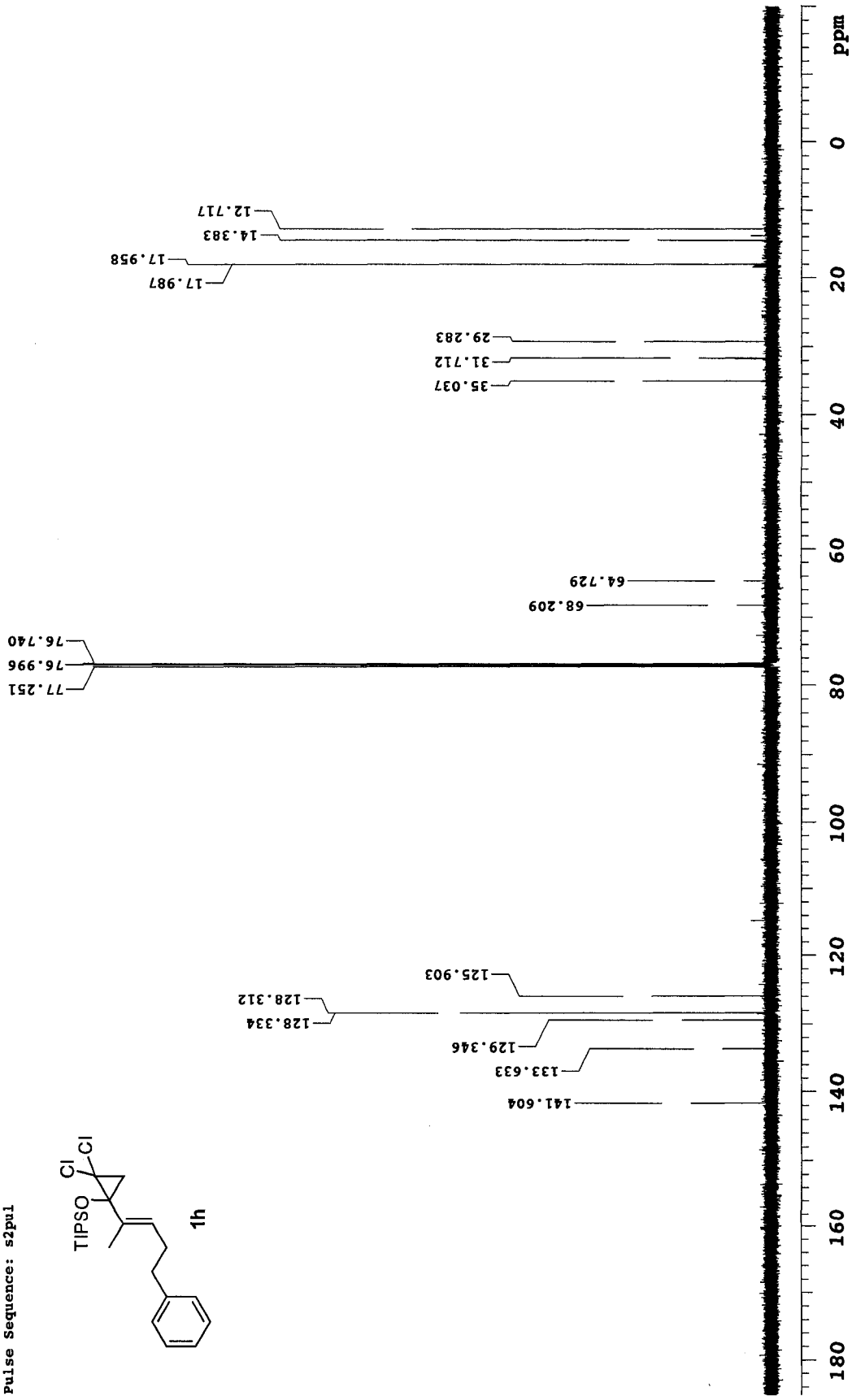
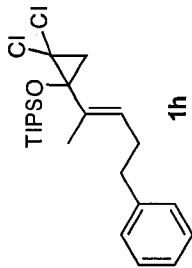
500 MHz 1D in CDCl3 (ref. to CDCl3 @ 7.26 ppm), temp 29.4 C -> actual temp = 27.0 C, sw500u probe

Pulse Sequence: s2pul



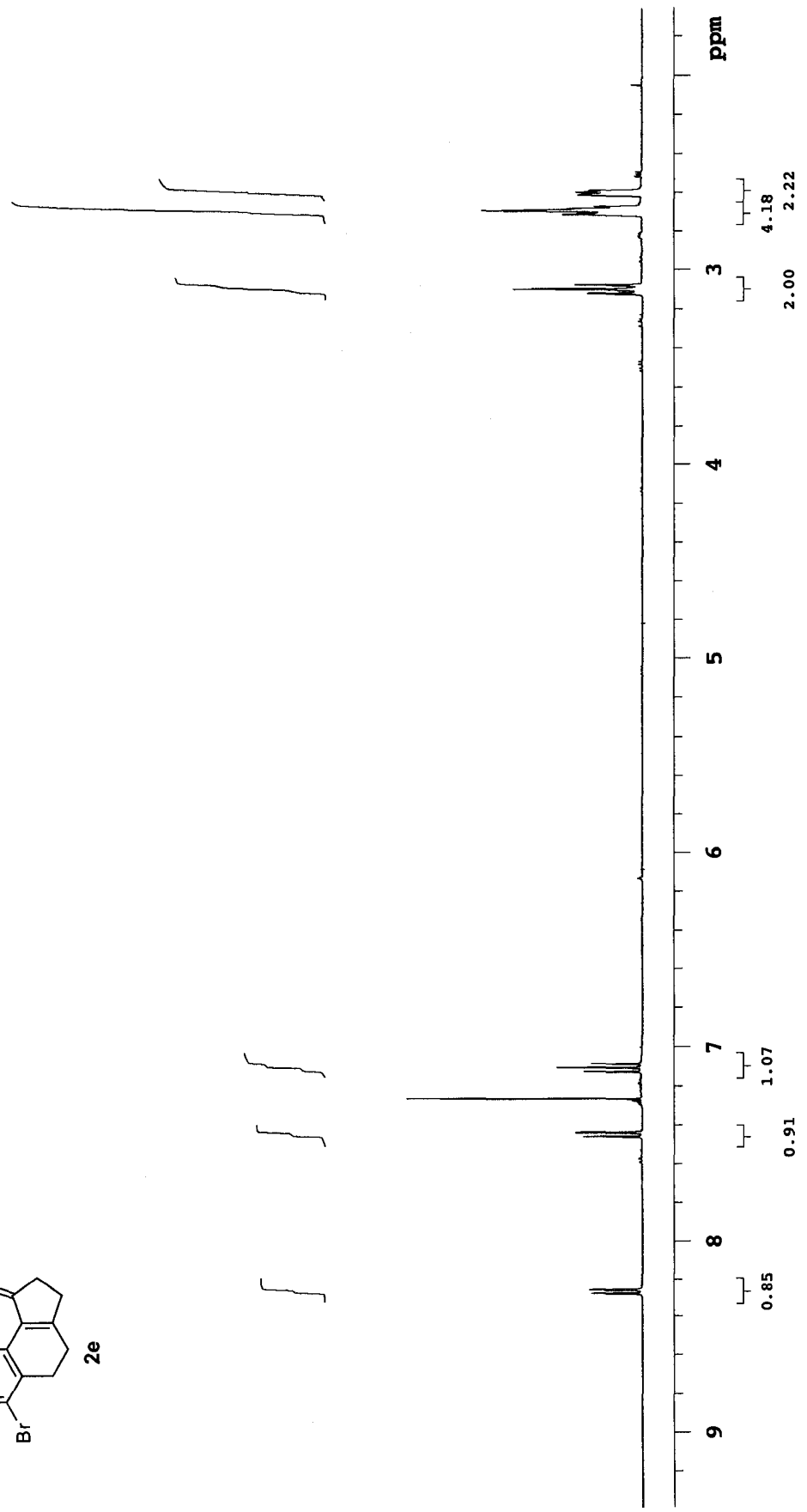
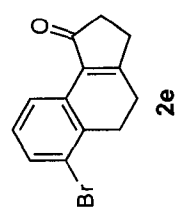
125 MHz 1D ¹³C in CDCl₃ (ref. to CDCl₃ @ 77.0 ppm), temp 26.1 C -> actual temp = 27.0 C, autordb probe

Pulse Sequence: s2pul



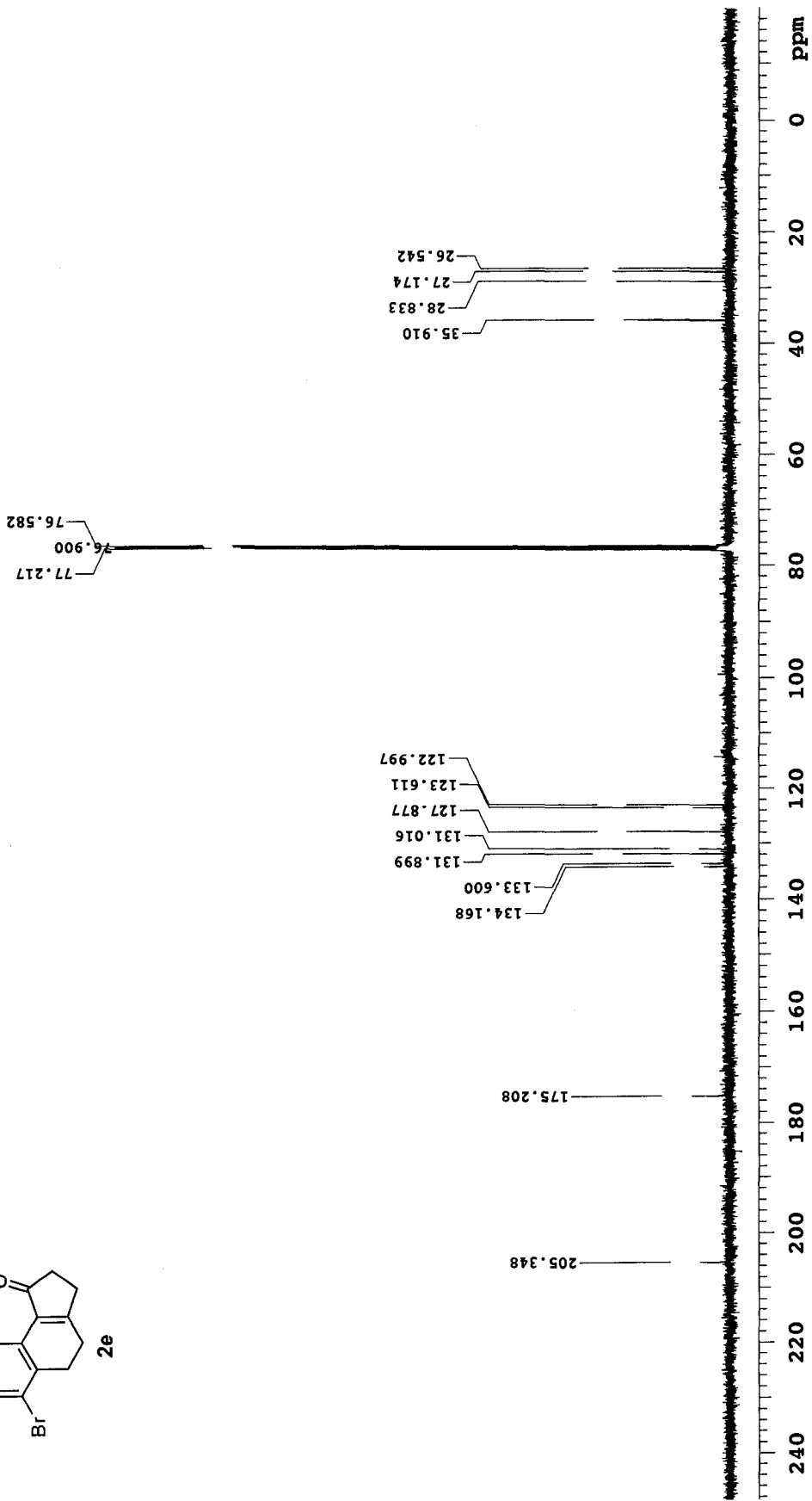
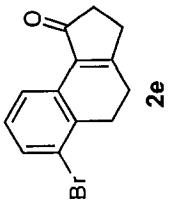
400 MHz 1D in CDCl3 (ref. to CDCl3 @ 7.26 ppm), temp 27.0 C -> actual temp = 27.0 C, m400gz probe

Pulse Sequence: s2pul



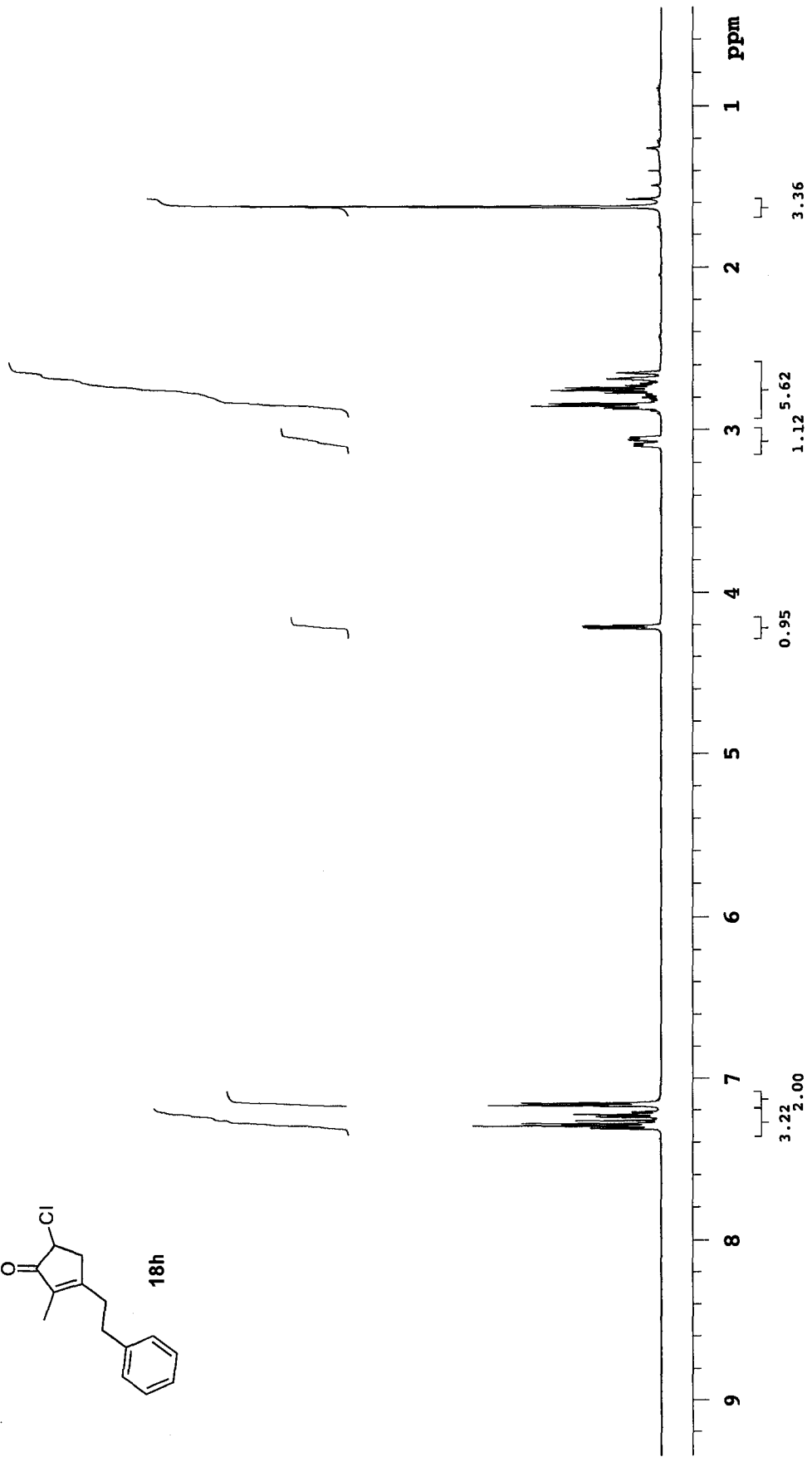
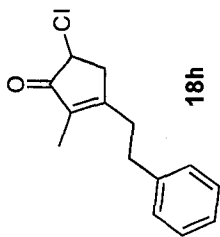
100 MHz 1D C13 in CDCl3 (ref. to CDCl3 @ 77.0 ppm), temp 27.0 C -> actual temp = 27.0 C, m400gz probe

Pulse Sequence: s2pul



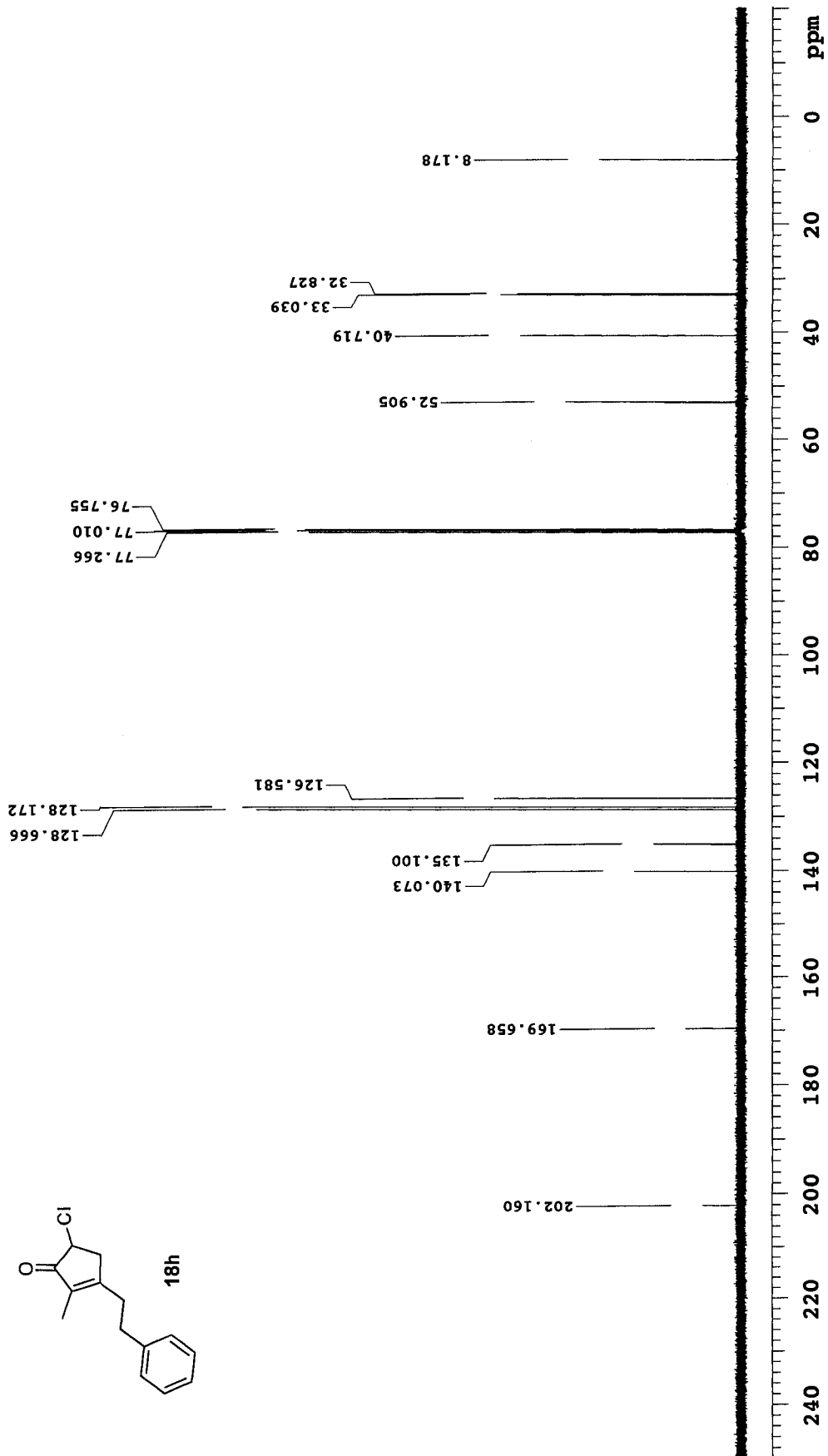
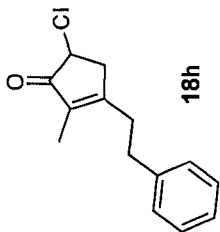
500 MHz 1D in CDCl3 (ref. to CDCl3 @ 7.26 ppm), temp 29.4 C -> actual temp = 27.0 C, sw500u probe

Pulse Sequence: s2pul



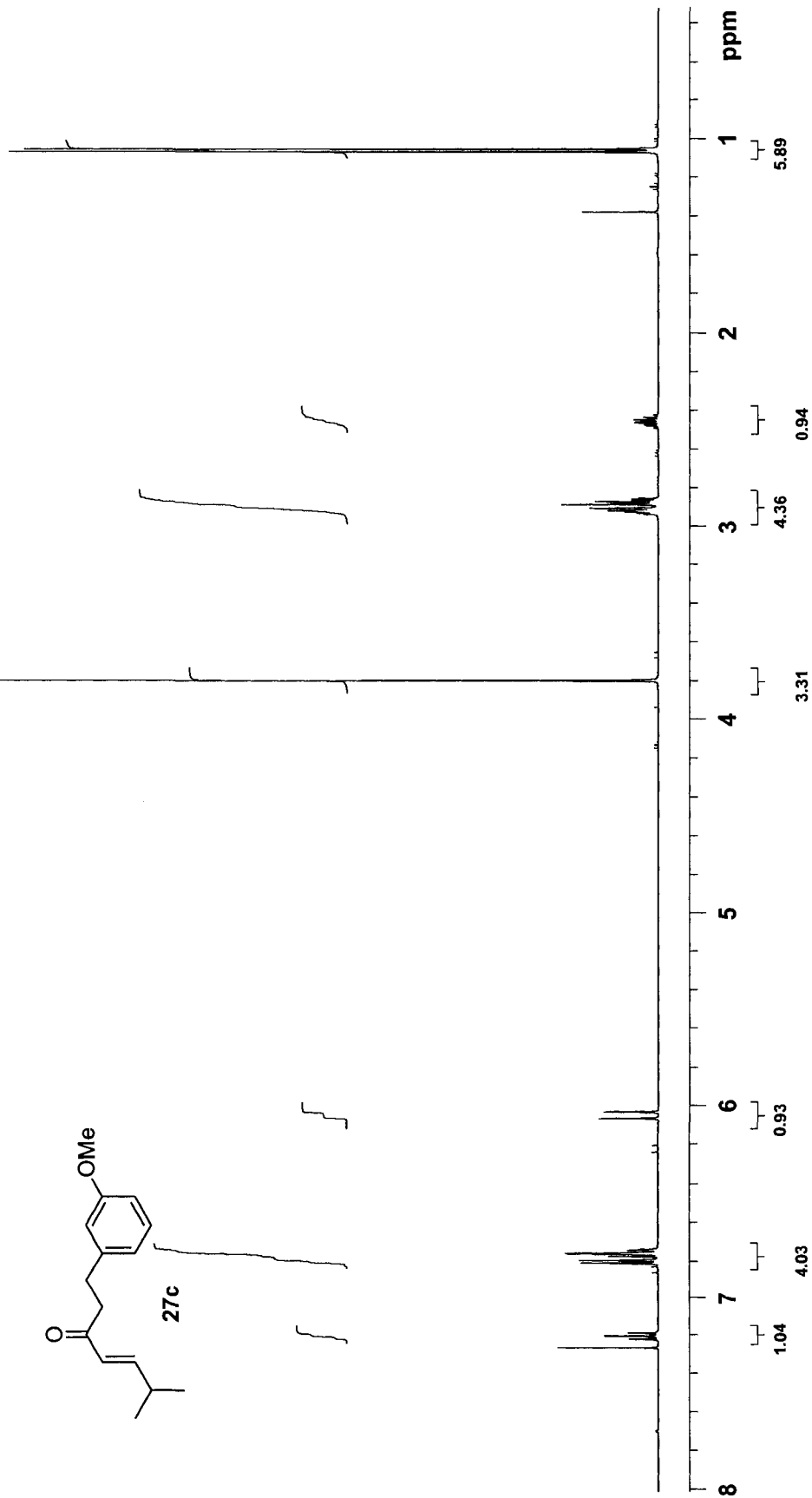
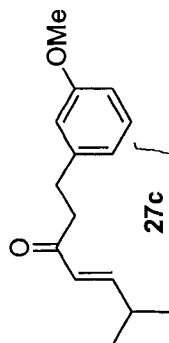
125 MHz 1D C13 in CDCl3 (ref. to CDCl3 @ 77.0 ppm), temp 26.1 C -> actual temp = 27.0 C, autotxdb probe

Pulse Sequence: s2pul



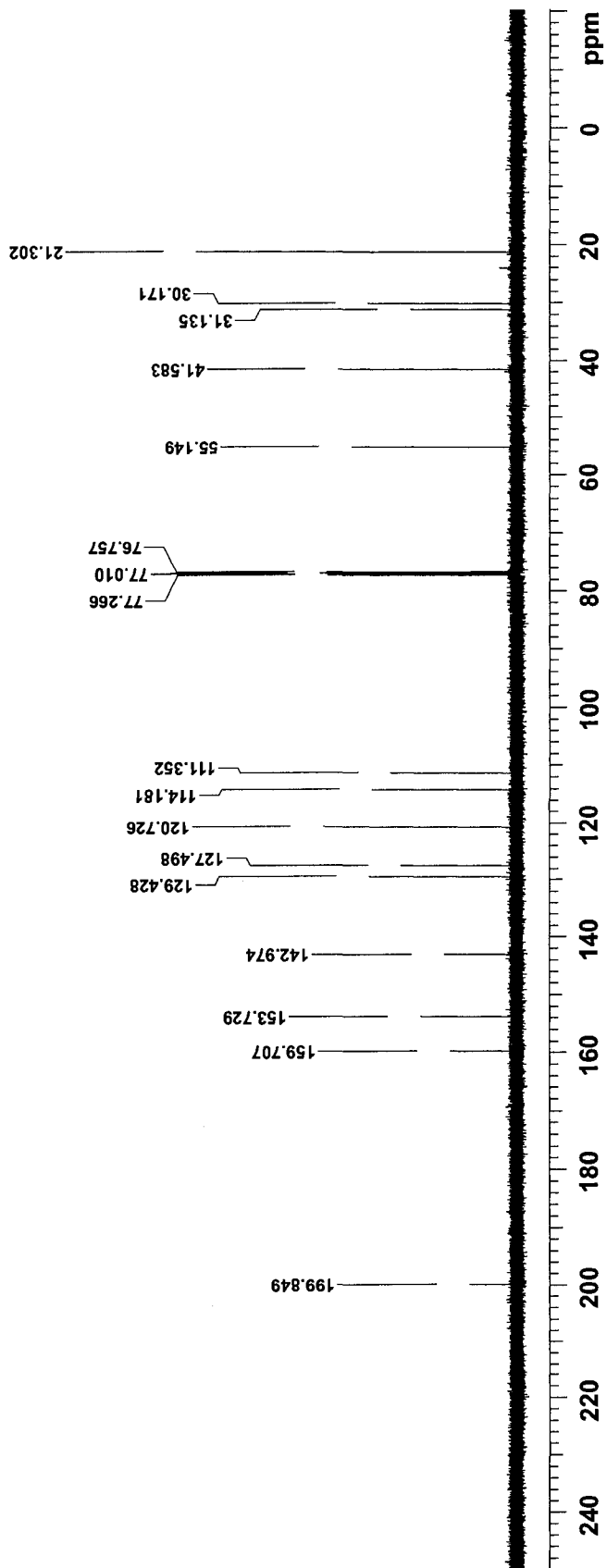
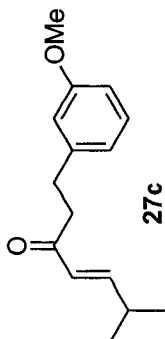
500 MHz 1D in CDCl3 (ref. to CDCl3 @ 7.26 ppm), temp 29.4 C -> actual temp = 27.0 C, sw500u probe

Pulse Sequence: s2pul



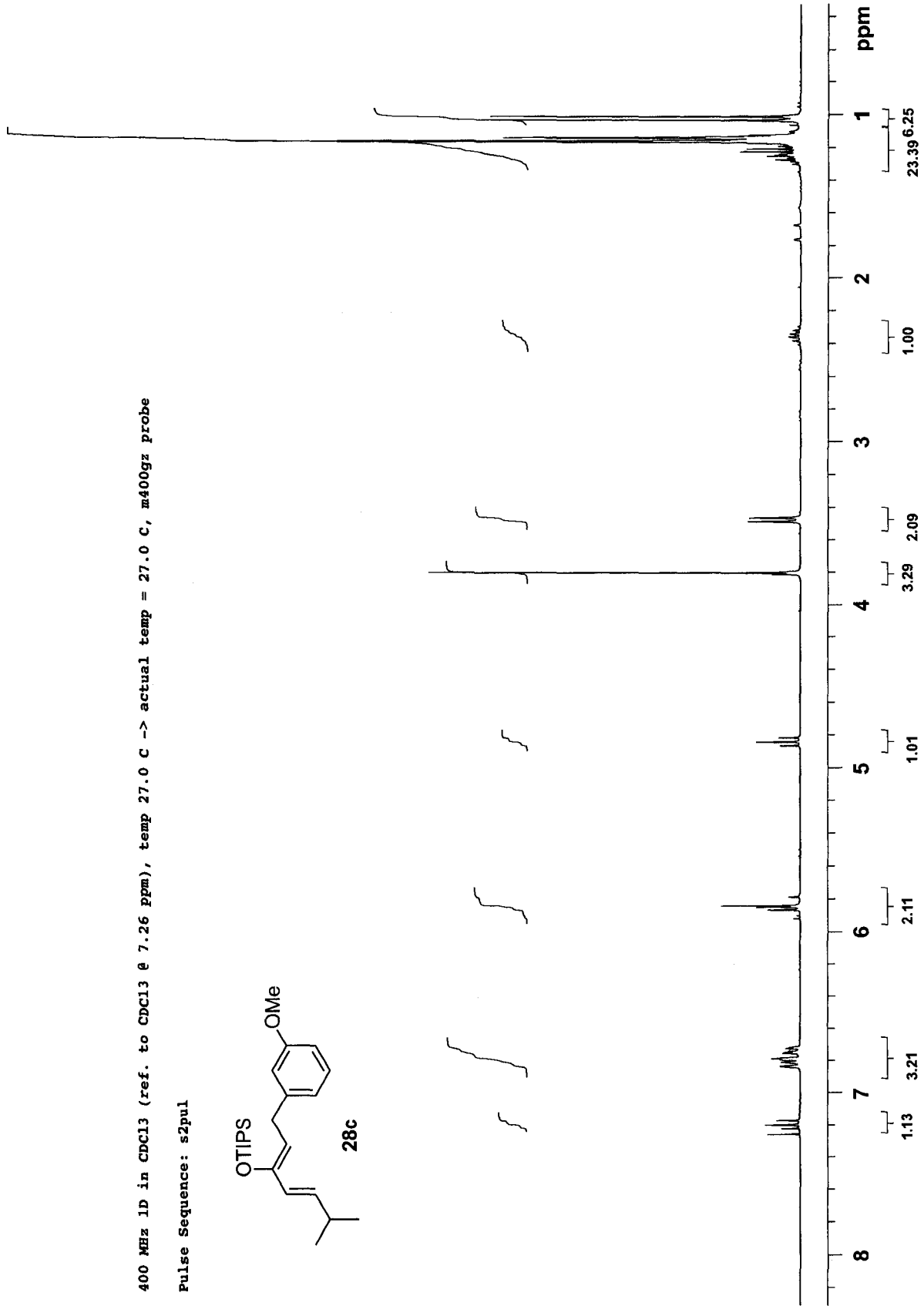
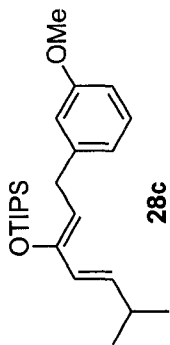
125 MHz 1D C13 in CDCl3 (ref. to CDCl3 @ 77.0 ppm), temp 26.1 C -> actual temp = 27.0 C, autoxdb probe

Pulse Sequence: s2pul

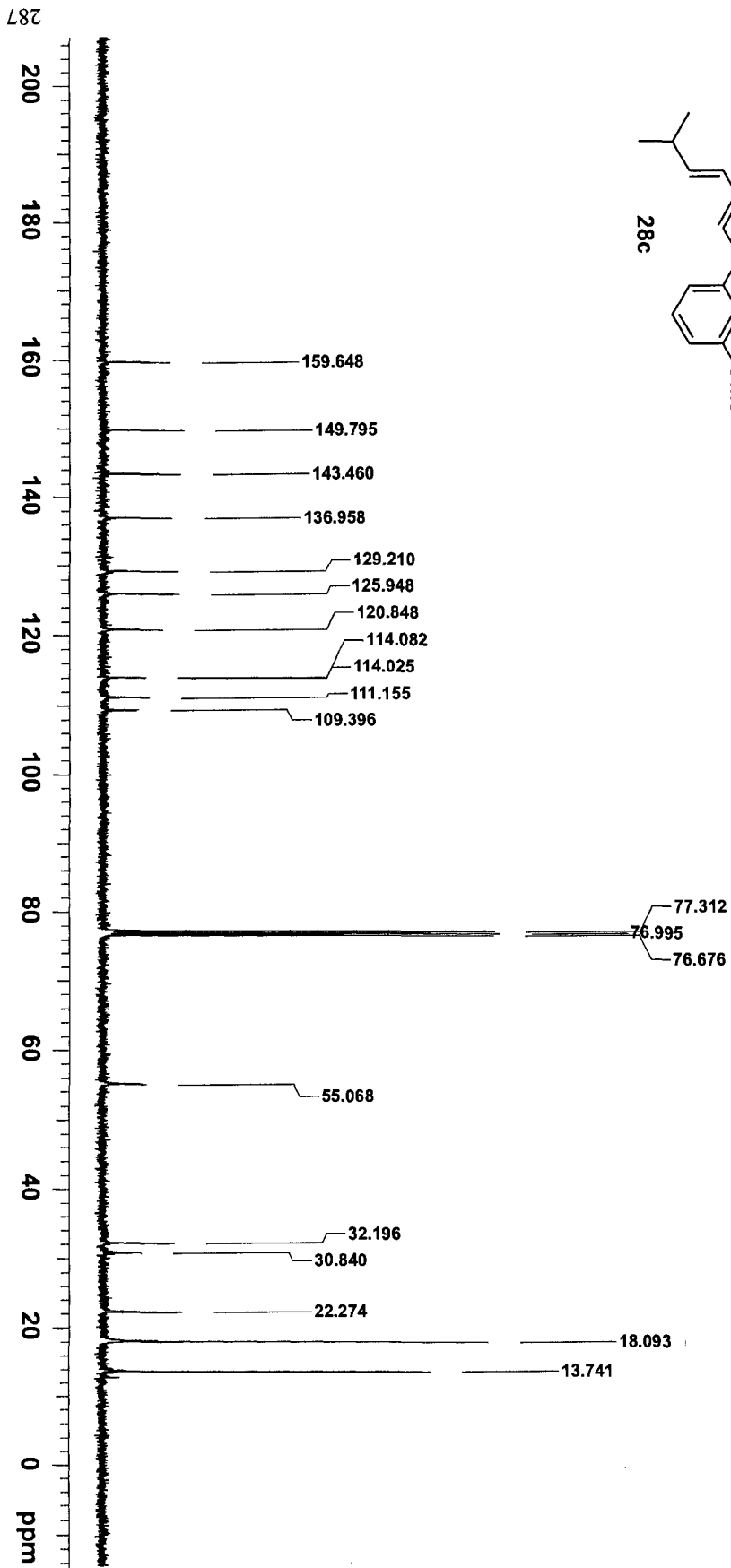
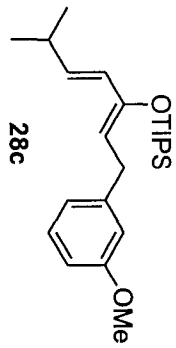


400 MHz 1D in CDCl3 (ref. to CDCl3 @ 7.26 ppm), temp 27.0 C -> actual temp = 27.0 C, m400gz probe

Pulse Sequence: s2pul

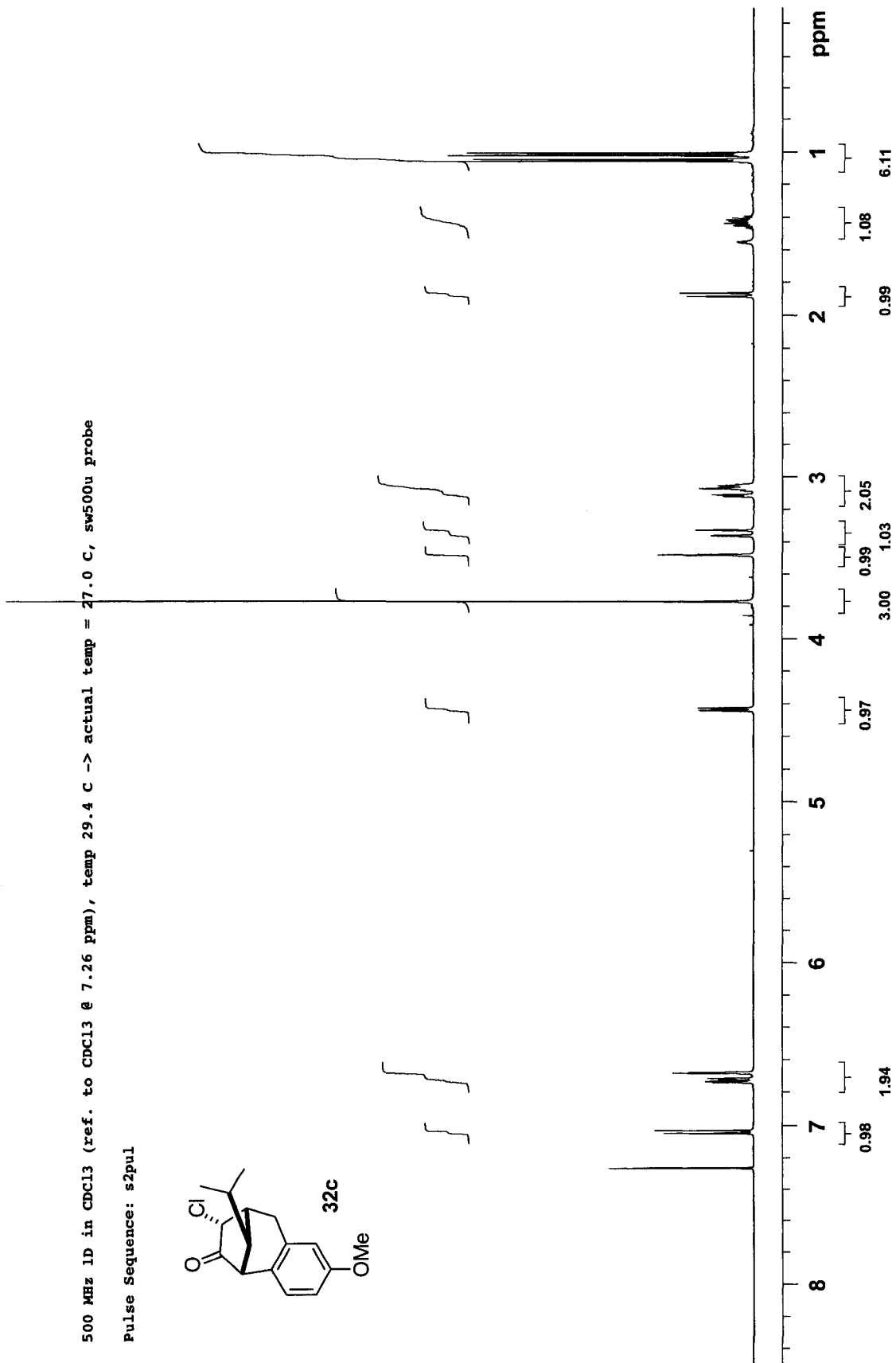
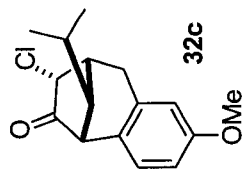


100 MHz 1D ¹³C in CDCl₃ (ref. to CDCl₃ @ 77.0 ppm), temp 27.0 C -> actual temp = 27.0 C, m400gz probe
Pulse Sequence: s2pu1



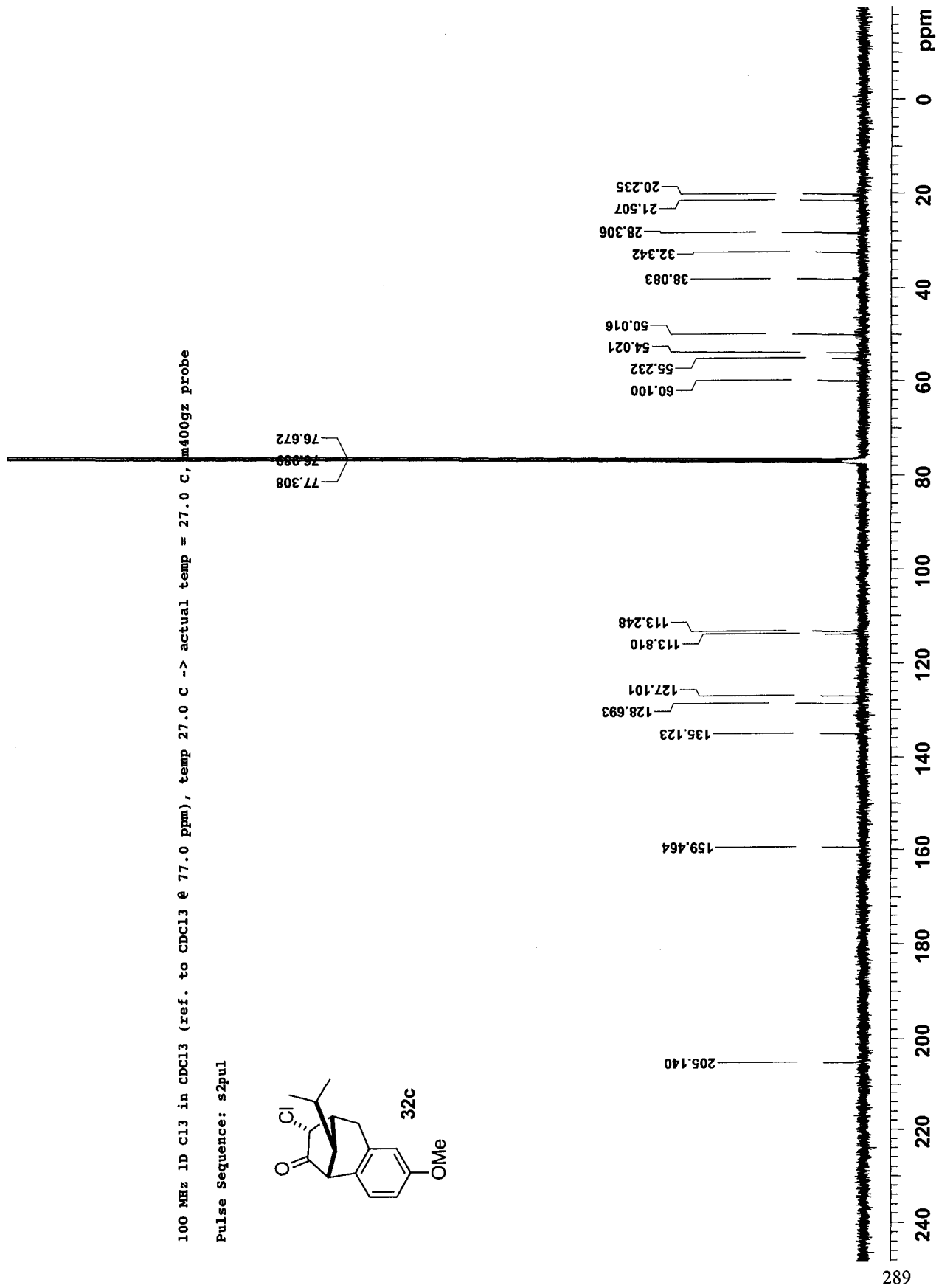
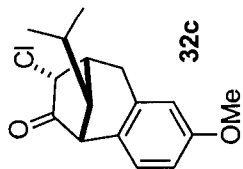
500 MHz 1D in CDCl3 (ref. to CDCl3 @ 7.26 ppm), temp 29.4 C -> actual temp = 27.0 C, sw500u probe

Pulse Sequence: s2pul



100 MHz 1D 13C in CDCl3 (ref. to CDCl3 @ 77.0 ppm), temp 27.0 C -> actual temp = 27.0 C, m400gz probe

Pulse Sequence: s2pul

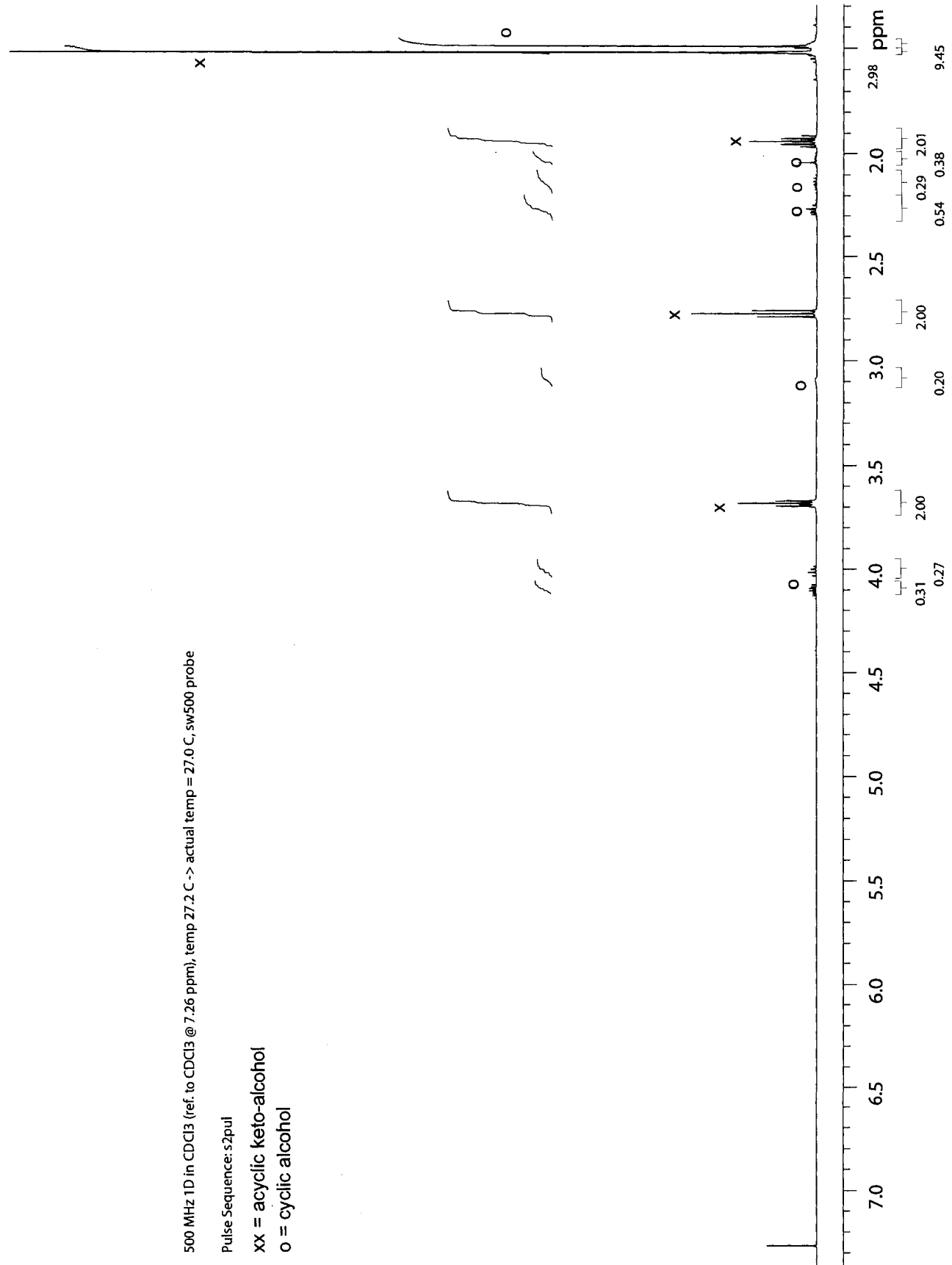


**Appendix III: Selected NMR Spectra
(Chapter 4)**

500 MHz 1D in CDCl3 (ref. to CDCl3 @ 7.26 ppm), temp 27.2 C -> actual temp = 27.0 C, sw500 probe

Pulse Sequence: s2pul

xx = acyclic keto-alcohol
o = cyclic alcohol

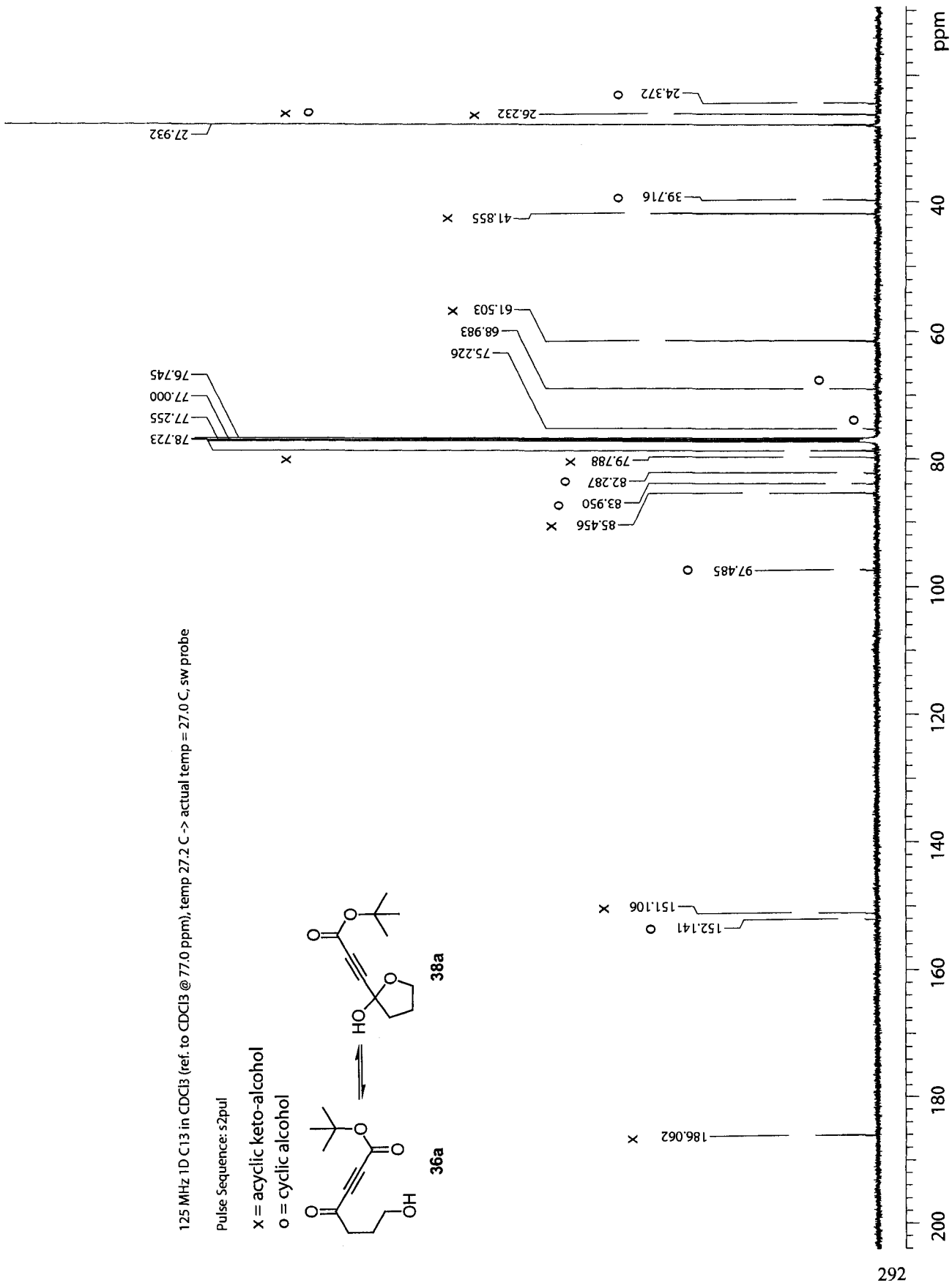
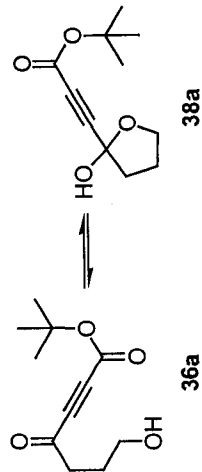


125 MHz TD C13 in CDCl3 (ref. to CDCl3 @ 77.0 ppm), temp 27.2 C -> actual temp = 27.0 C, sw probe

Pulse Sequence: s2pul

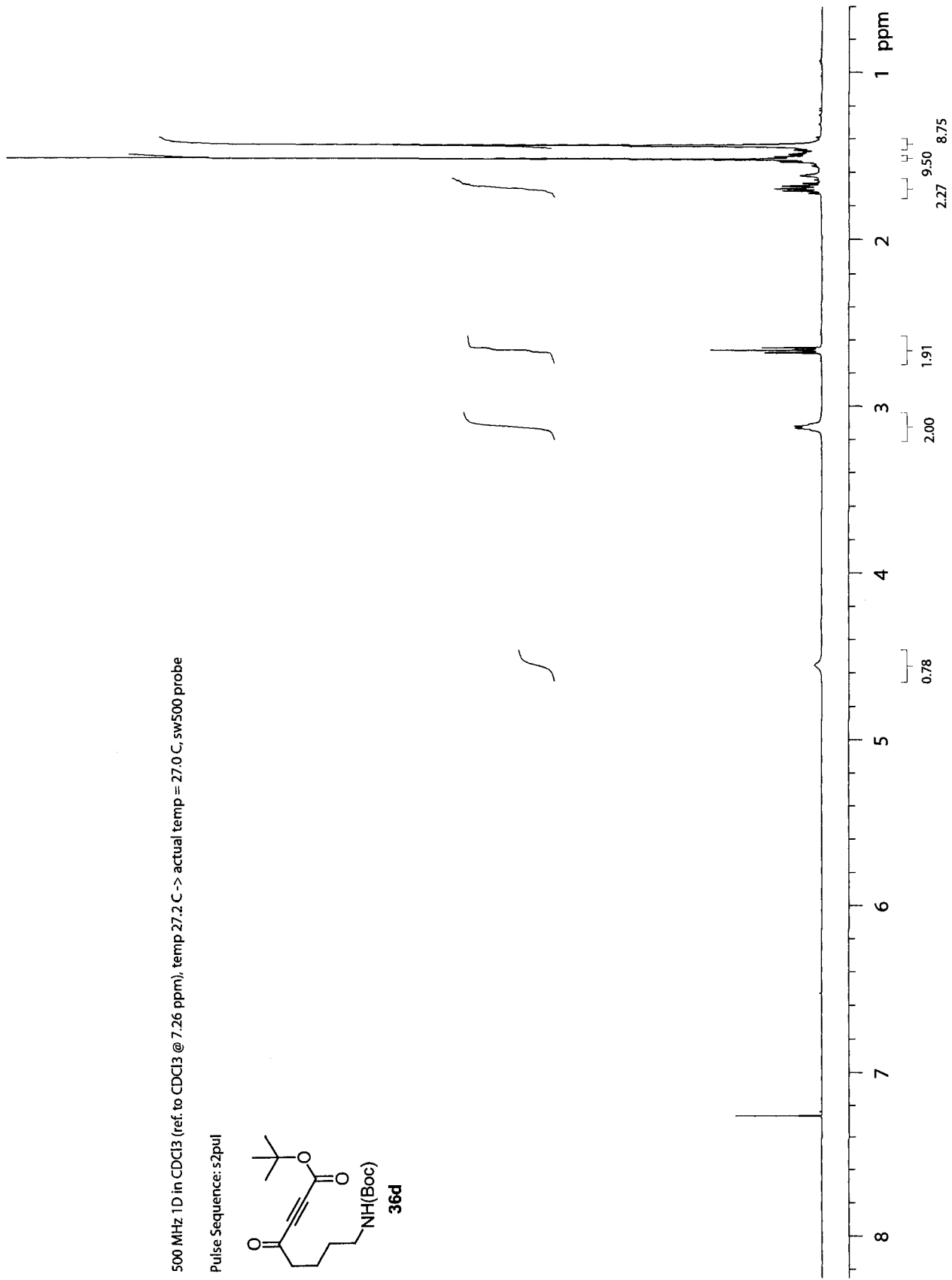
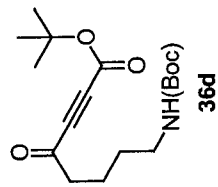
x = acyclic keto-alcohol

o = cyclic alcohol



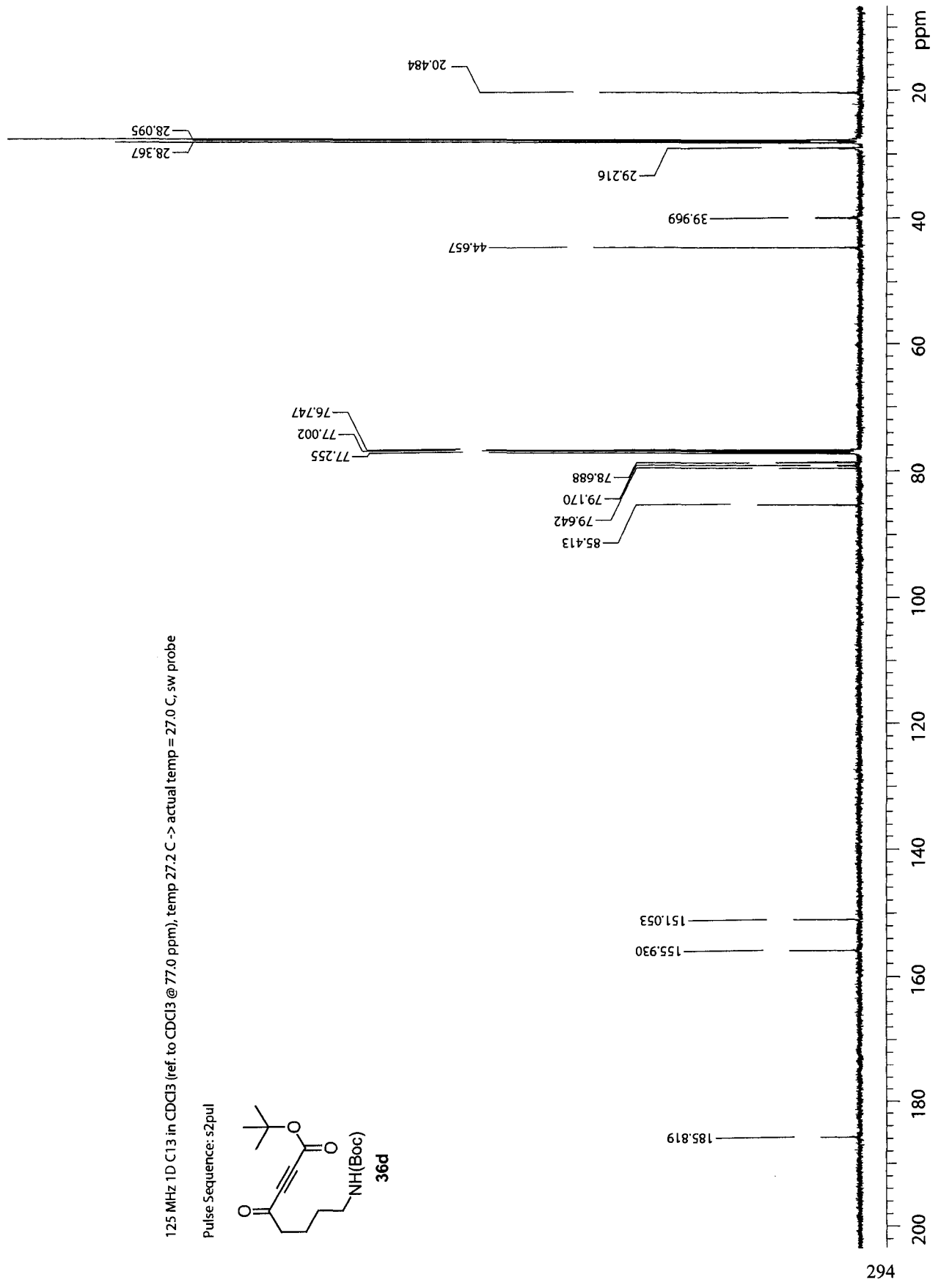
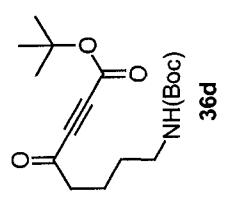
500 MHz 1D in CDCl3 (ref. to CDCl3 @ 7.26 ppm), temp 27.2 C -> actual temp = 27.0 C, sw500 probe

Pulse Sequence: s2pul



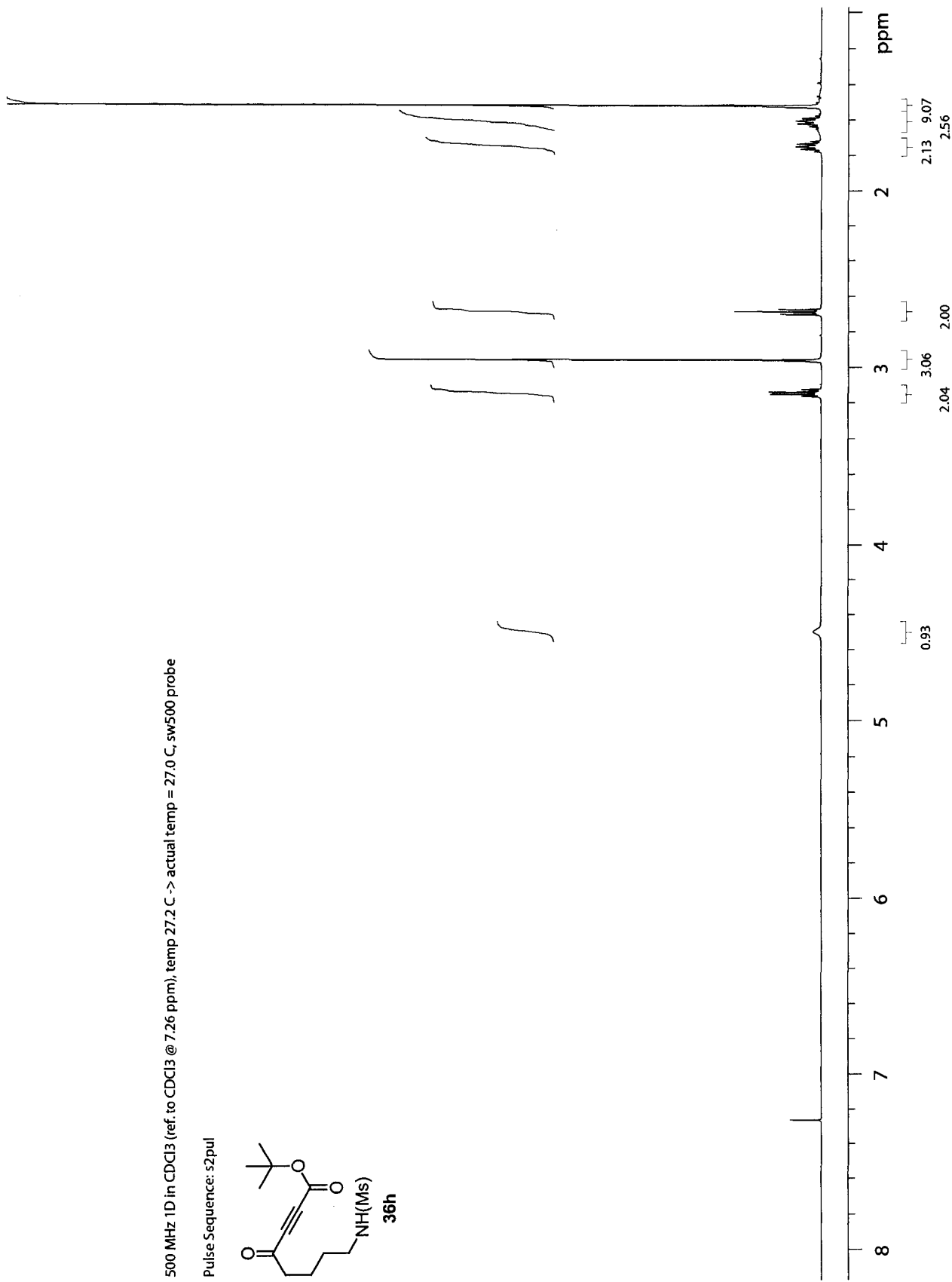
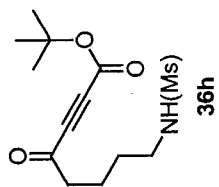
125 MHz 1D C13 in CDCl3 (ref. to CDCl3 @ 77.0 ppm), temp 27.2 C -> actual temp = 27.0 C, sw probe

Pulse Sequence: s2pul



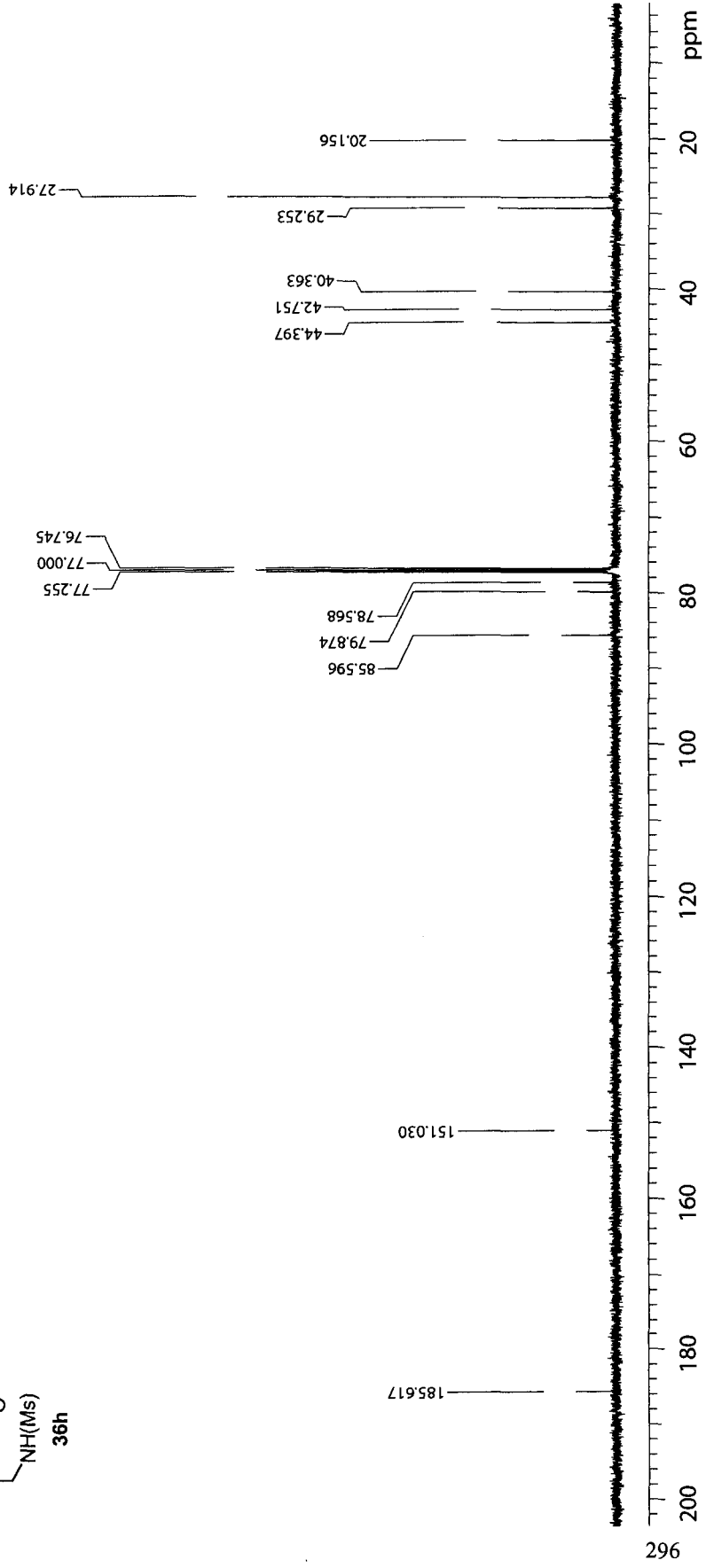
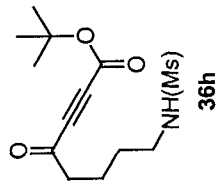
500 MHz 1D in CDCl3 (ref. to CDCl3 @ 7.26 ppm), temp 27.2 C -> actual temp = 27.0 C, sw500 probe

Pulse Sequence: s2pul



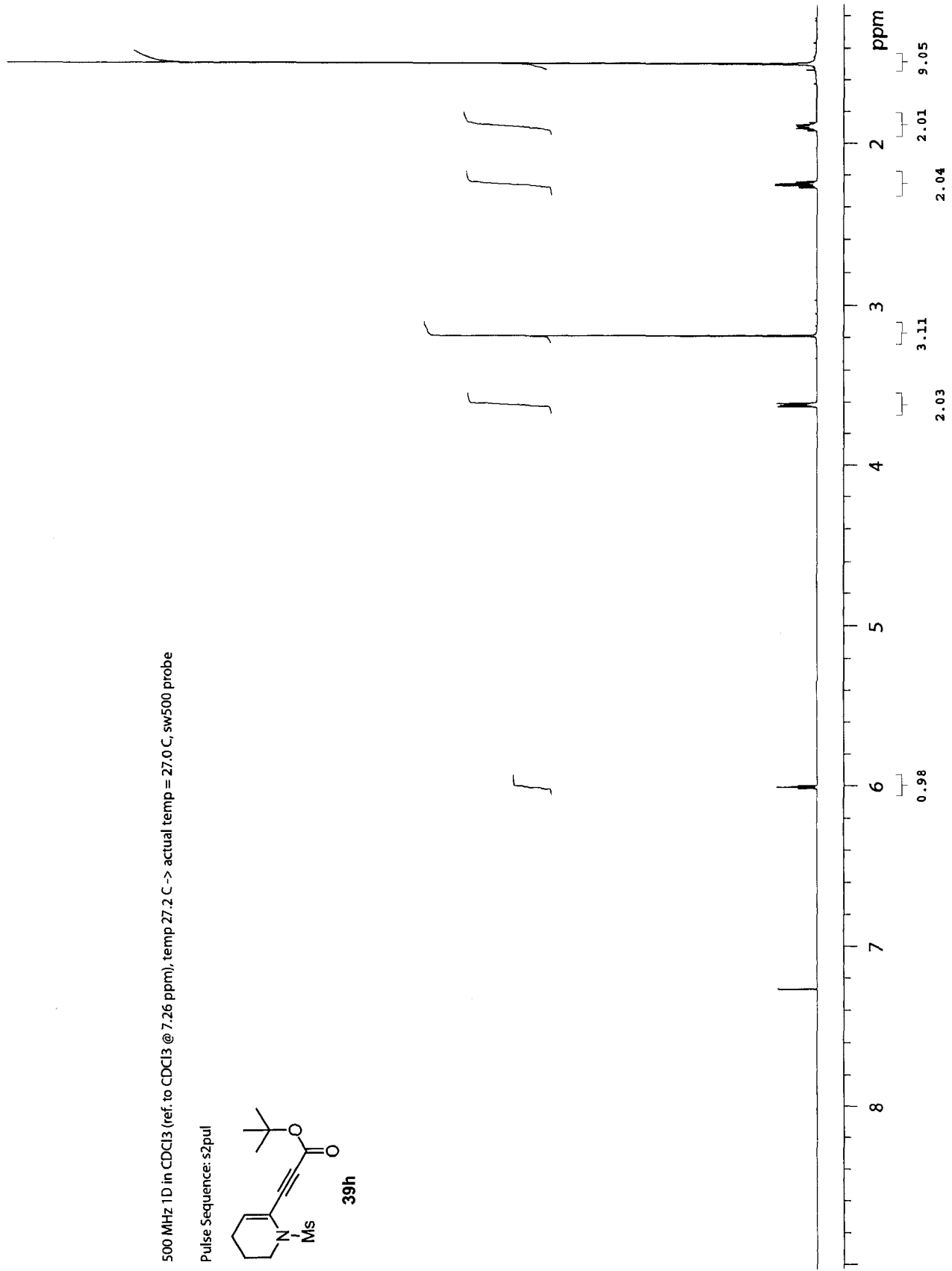
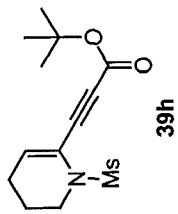
125 MHz 1D C13 in CDCl3 (ref. to CDCl3 @ 77.0 ppm), temp 27.2 C -> actual temp = 27.0 C, sw probe

Pulse Sequence: s2pul



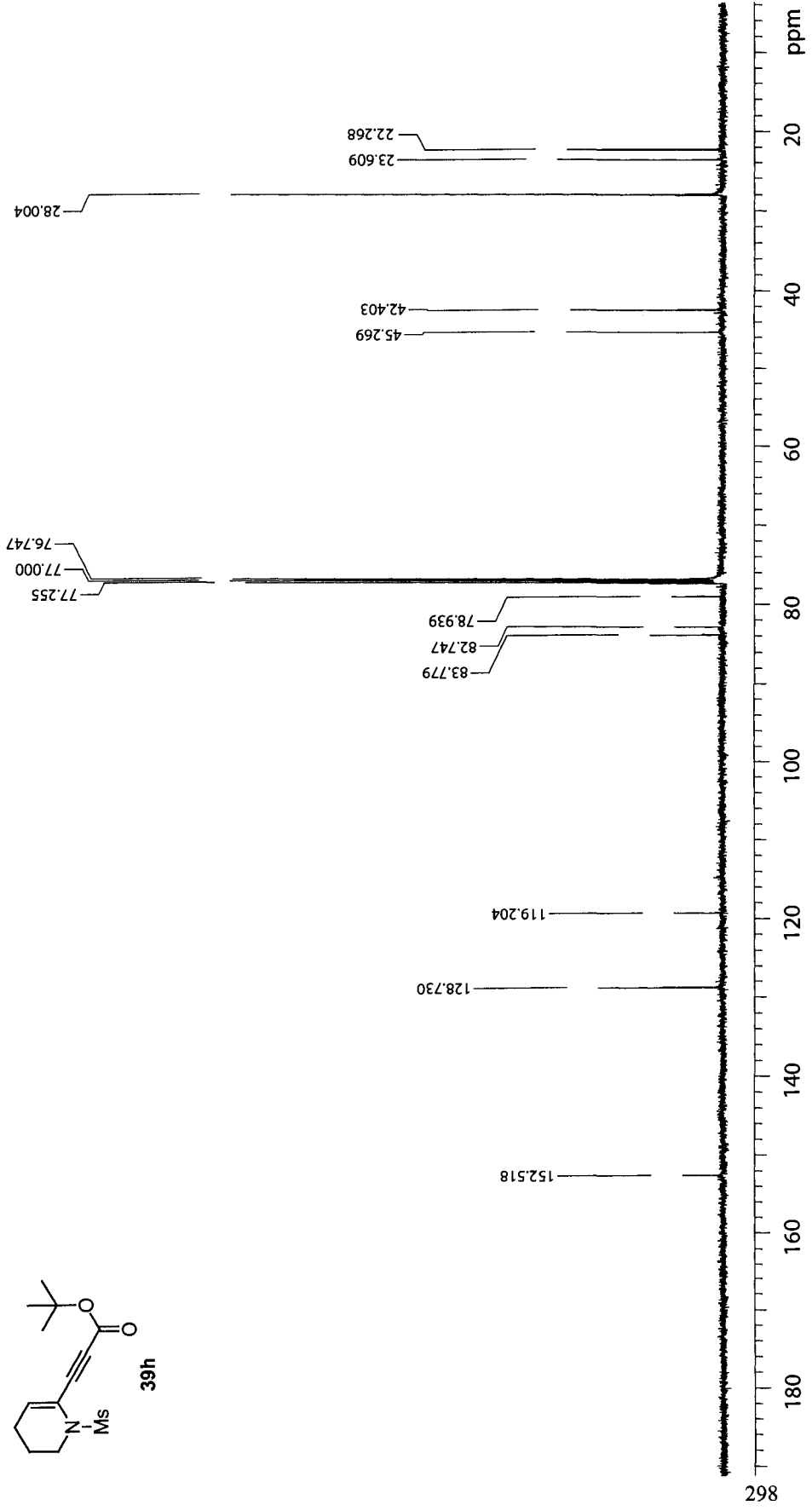
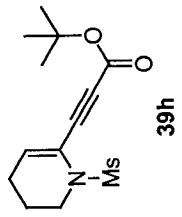
500 MHz 1D in CDCl3 (ref. to CDCl3 @ 7.26 ppm), temp 27.2 C -> actual temp = 27.0 C, sw500 probe

Pulse Sequence: s2pul



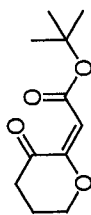
125 MHz 1D-C13 in CDCl3 (ref. to CDCl3 @ 77.0 ppm), temp 27.2 C -> actual temp = 27.0 C, sw probe

Pulse Sequence: s2pul

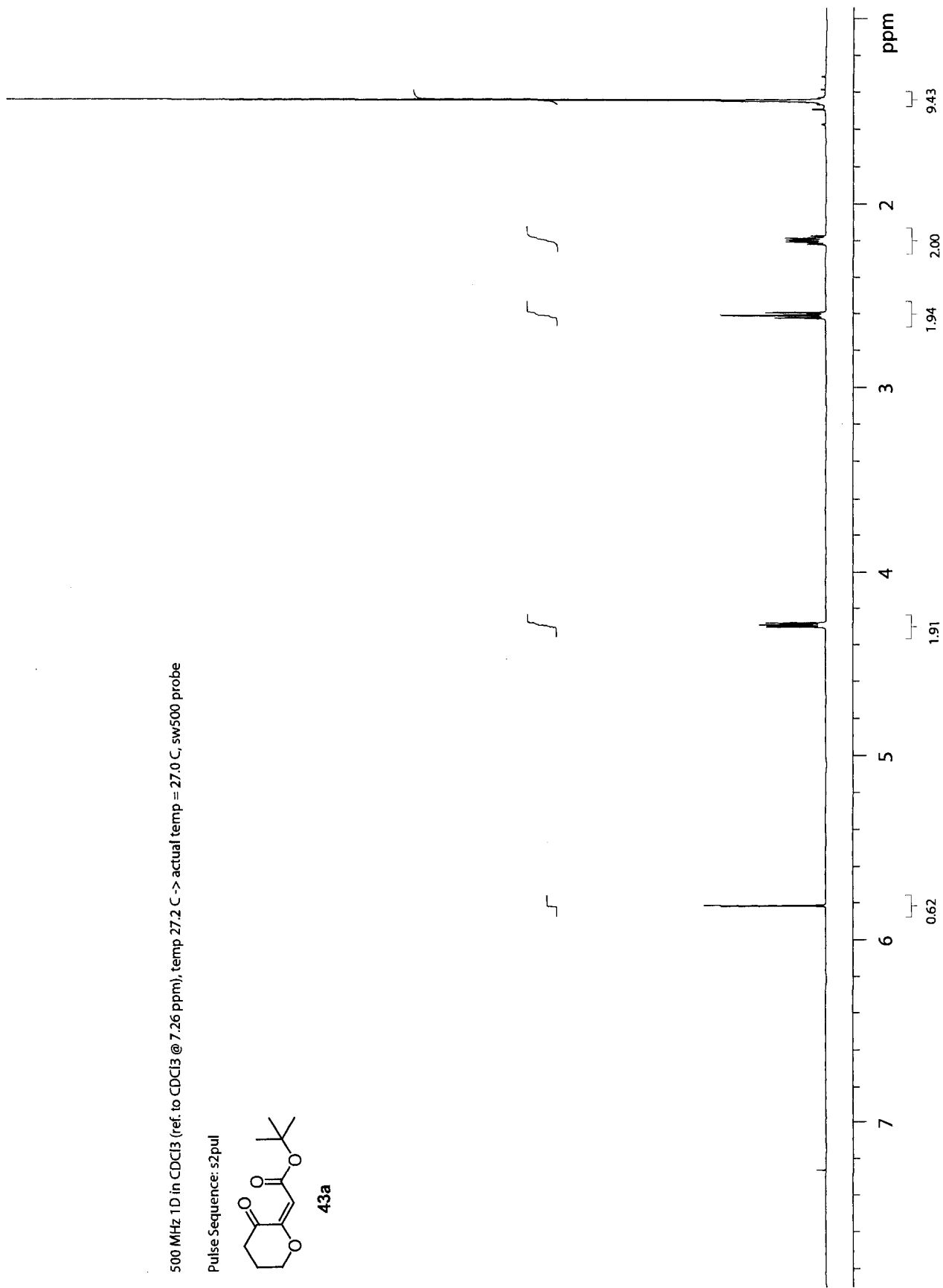


500 MHz 1D in CDCl3 (ref. to CDCl3 @ 7.26 ppm), temp 27.2 C -> actual temp = 27.0 C, sw5000 probe

Pulse Sequence: s2pul

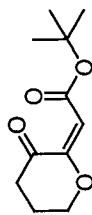


43a

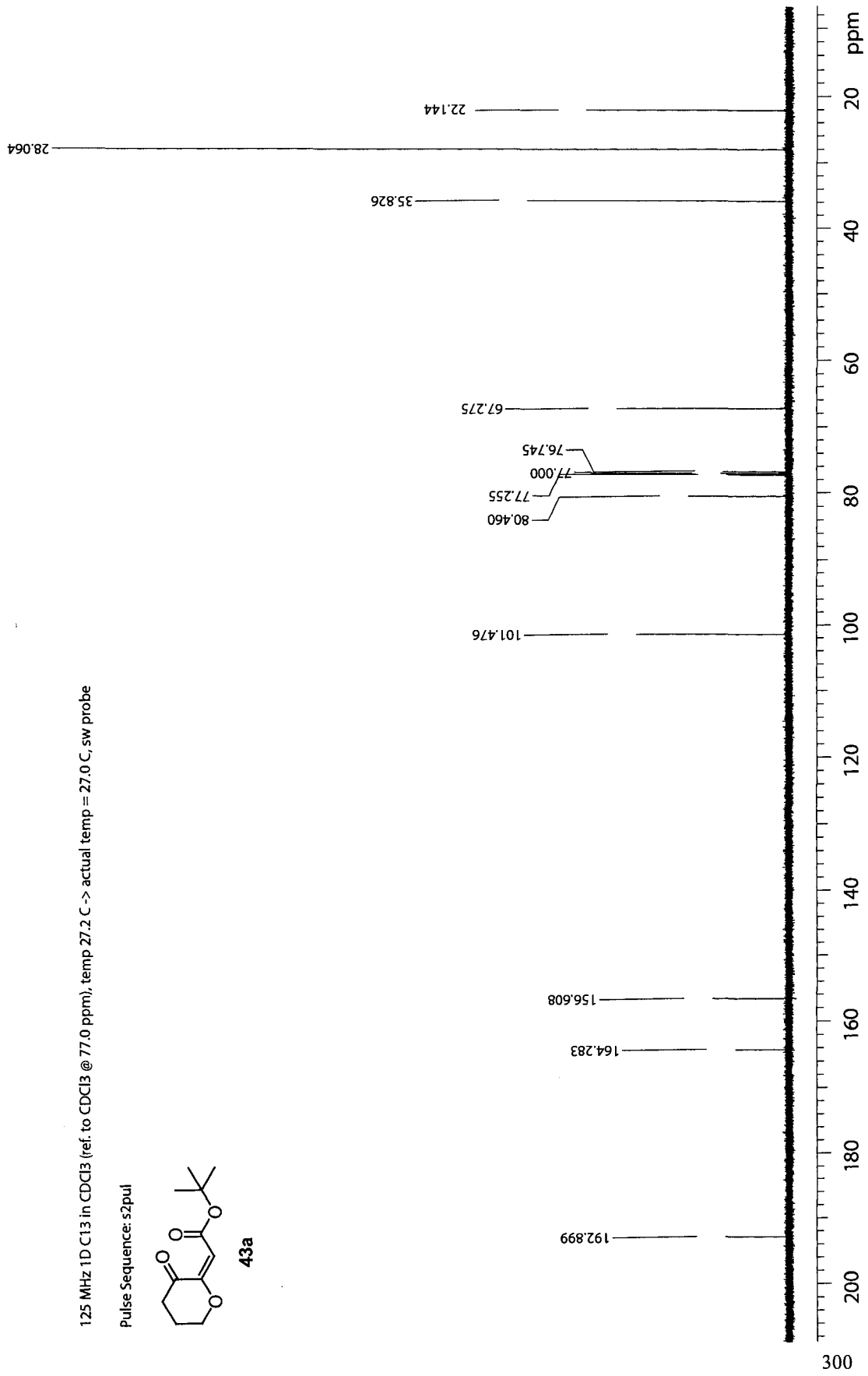


125 MHz 1D ¹³C in CDCl₃ (ref. to CDCl₃ @ 77.0 ppm), temp 27.2 C -> actual temp = 27.0 C, sw probe

Pulse Sequence: s2pul

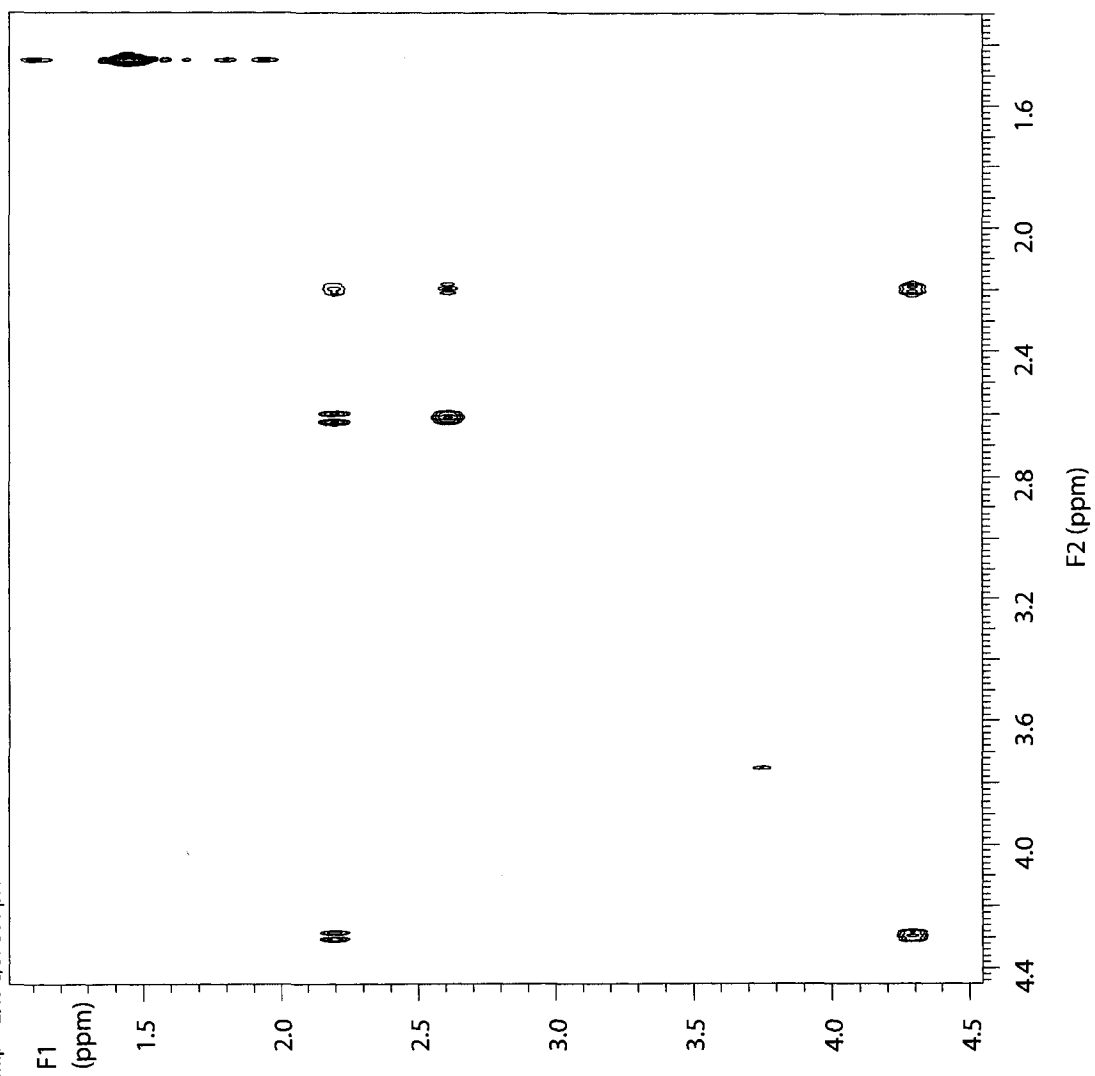
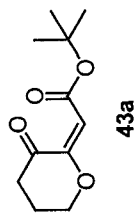


43a



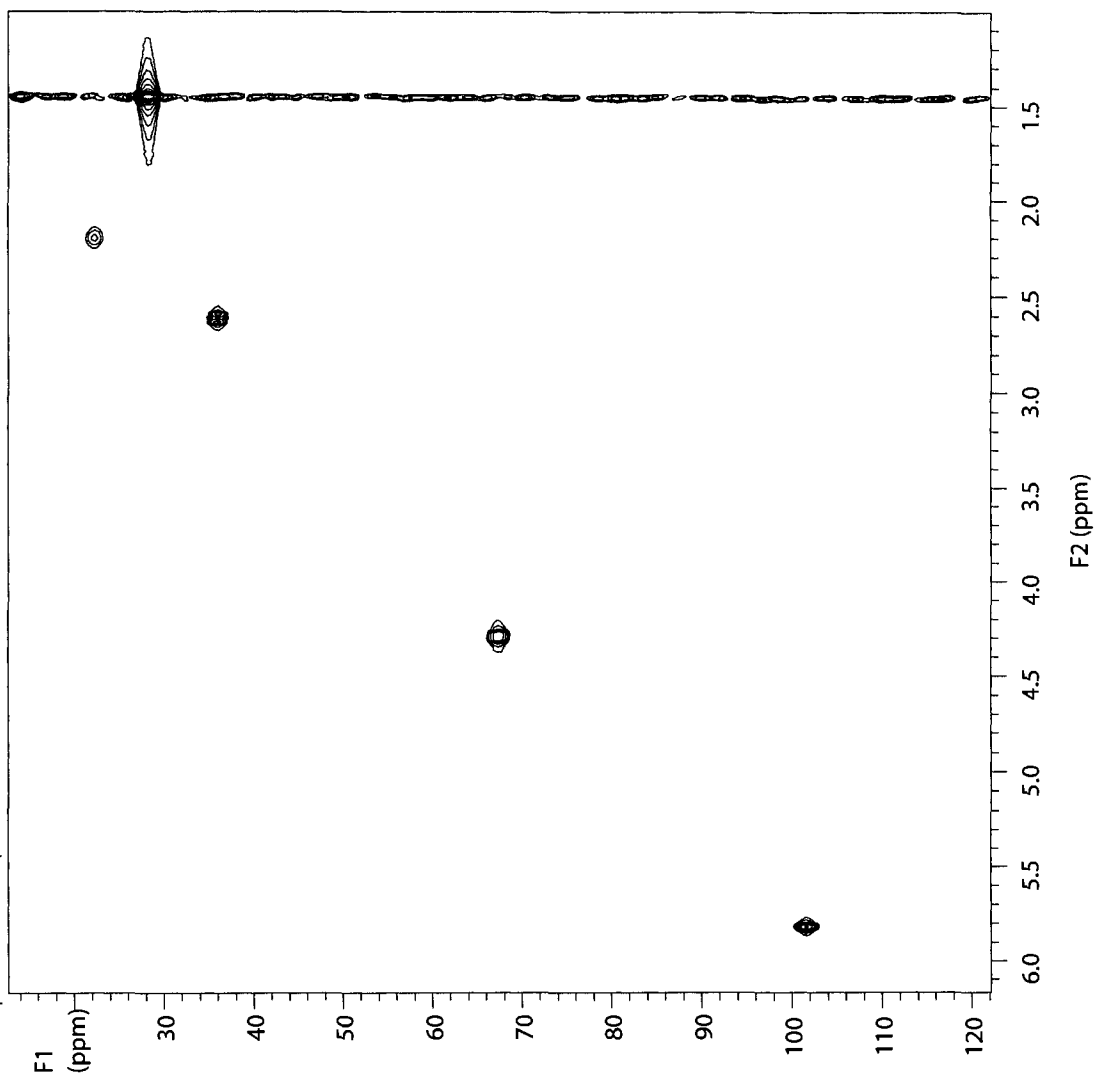
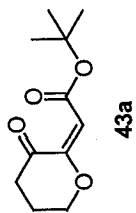
500 MHz GCOSY in CDCl₃ (ref. to CDCl₃ @ 7.26 ppm), temp 27.2 C -> actual temp = 27.0 C, sw500 probe

Pulse Sequence: aogcosy



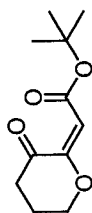
500 MHz gHMQC in CDCl₃ (ref. to CDCl₃ @ 7.26/77.0 ppm), temp 27.2 C -> actual temp = 27.0 C, sw500 probe

Pulse Sequence: gHMQC

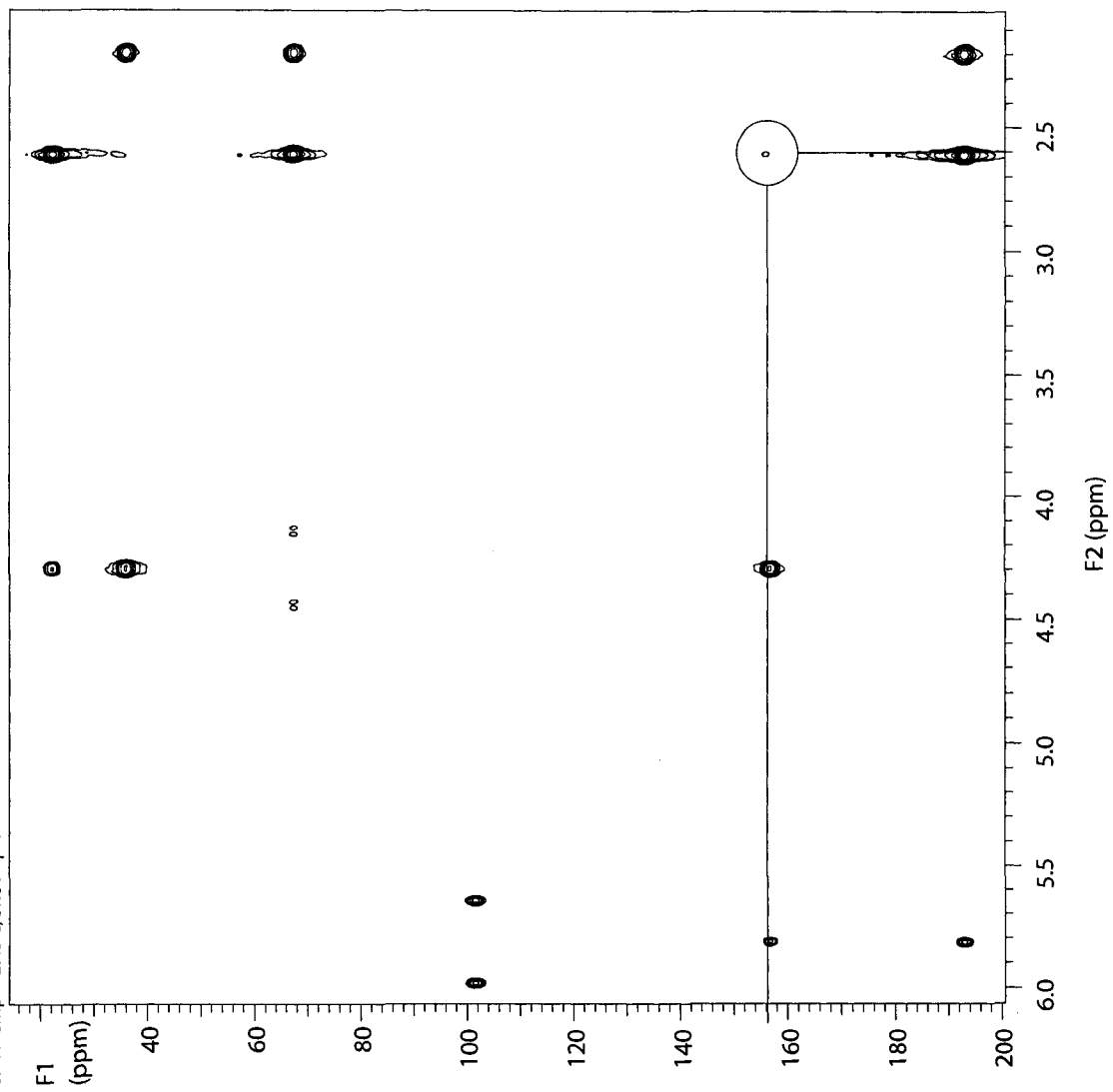


500 MHz gHMBC in CDCl₃ (ref. to CDCl₃ @ 7.26/77.0 ppm), temp 27.2 C -> actual temp = 27.0 C, sw500 probe

Pulse Sequence: gHMBC

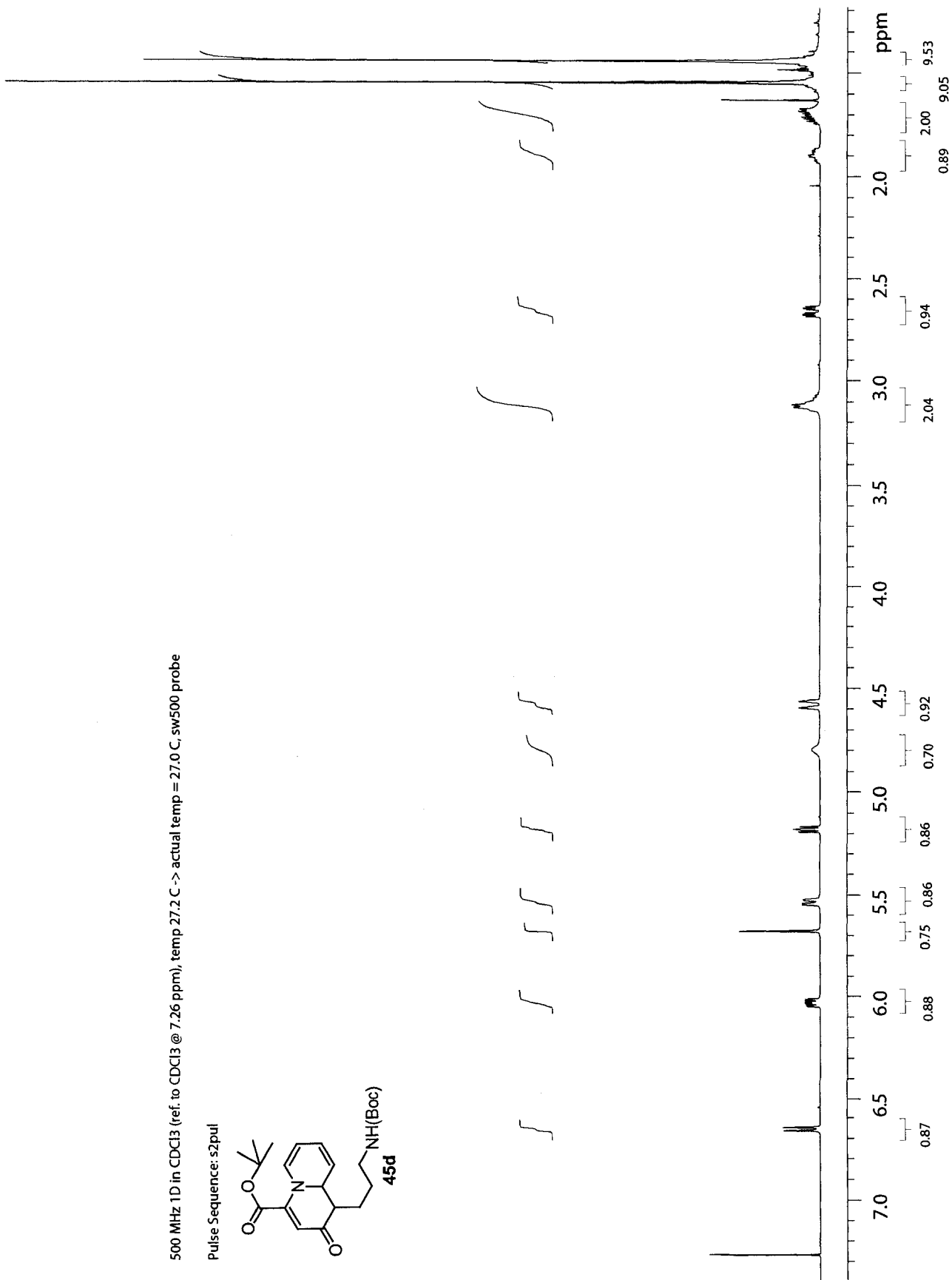
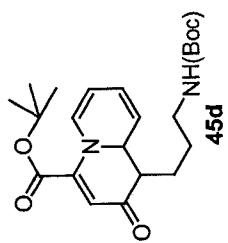


43a



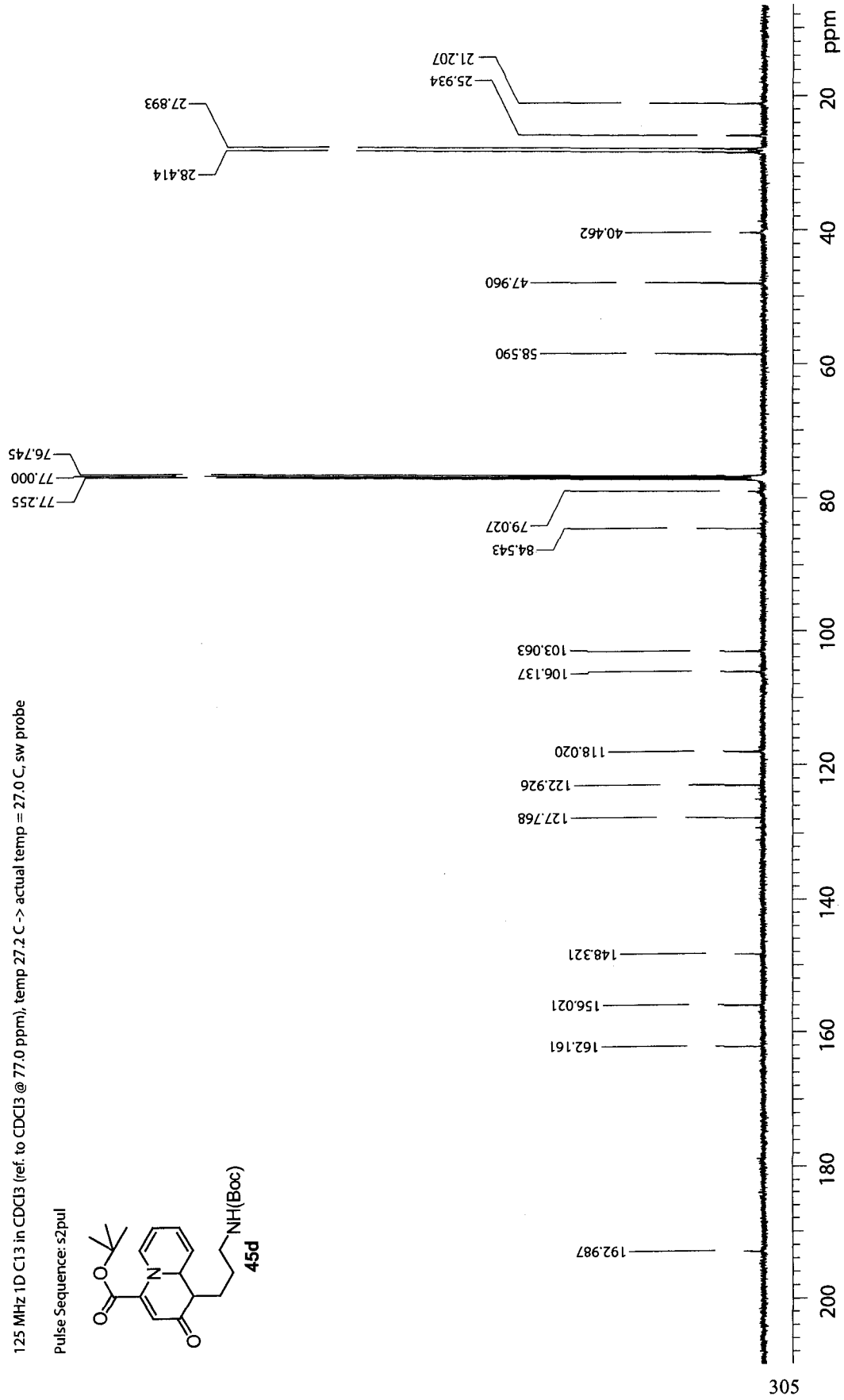
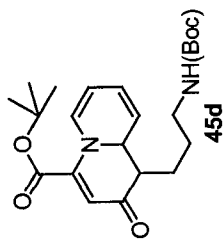
500 MHz 1D in CDCl3 (ref. to CDCl3 @ 7.26 ppm), temp 27.2 C -> actual temp = 27.0 C, sw5000 probe

Pulse Sequence: s2pul



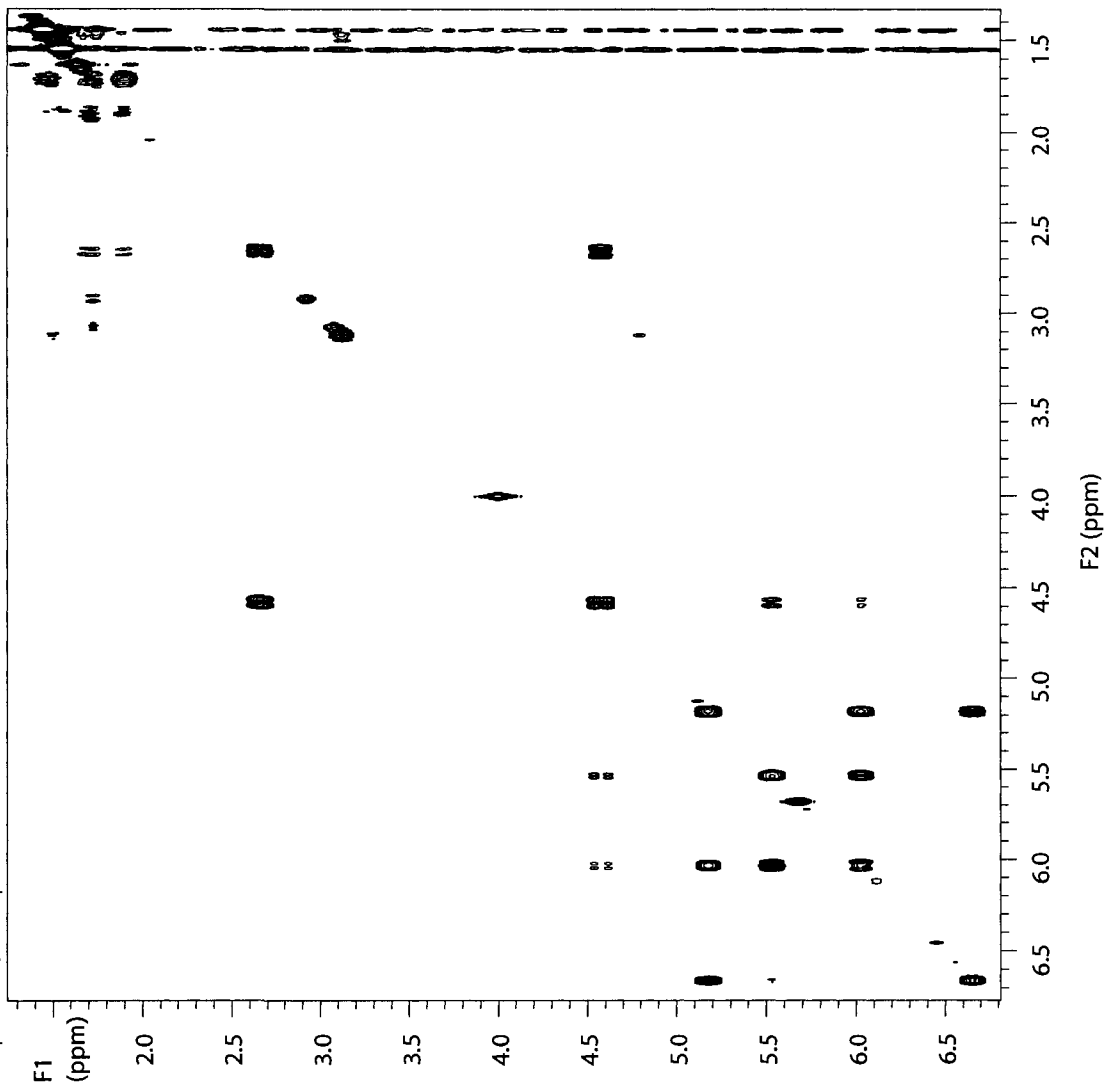
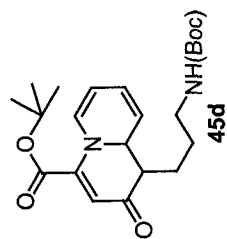
125 MHz 1D C13 in CDCl3 (ref. to CDCl3 @ 77.0 ppm), temp 27.2 C -> actual temp = 27.0 C, sw probe

Pulse Sequence: s2pul



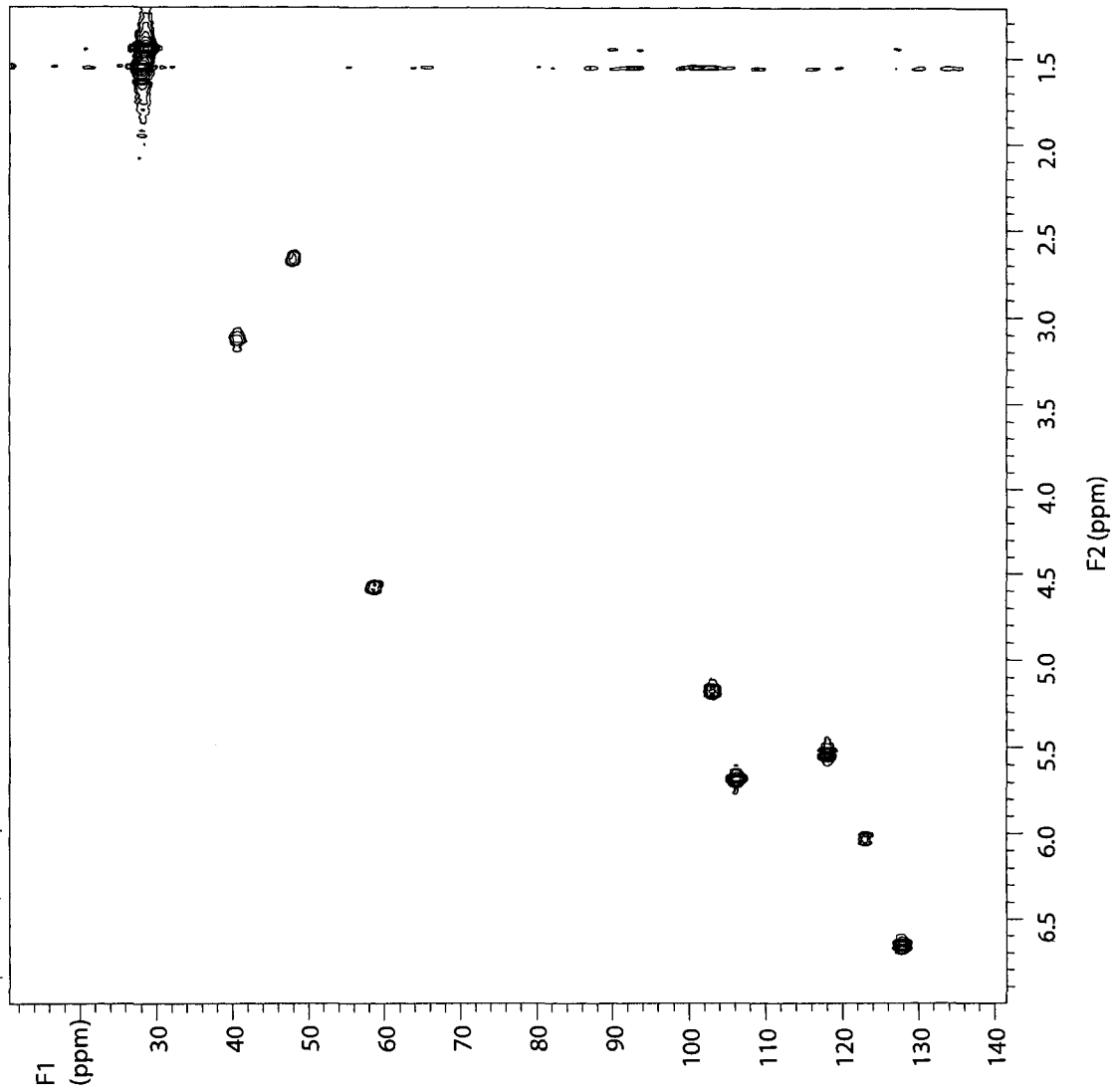
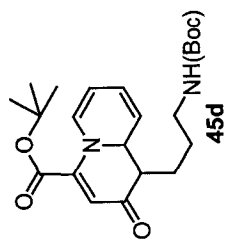
500 MHz GCOSY in CDCl₃ (ref. to CDCl₃ @ 7.26 ppm), temp 27.2 C -> actual temp = 27.0 C, sw500 probe

Pulse Sequence: aogcosy



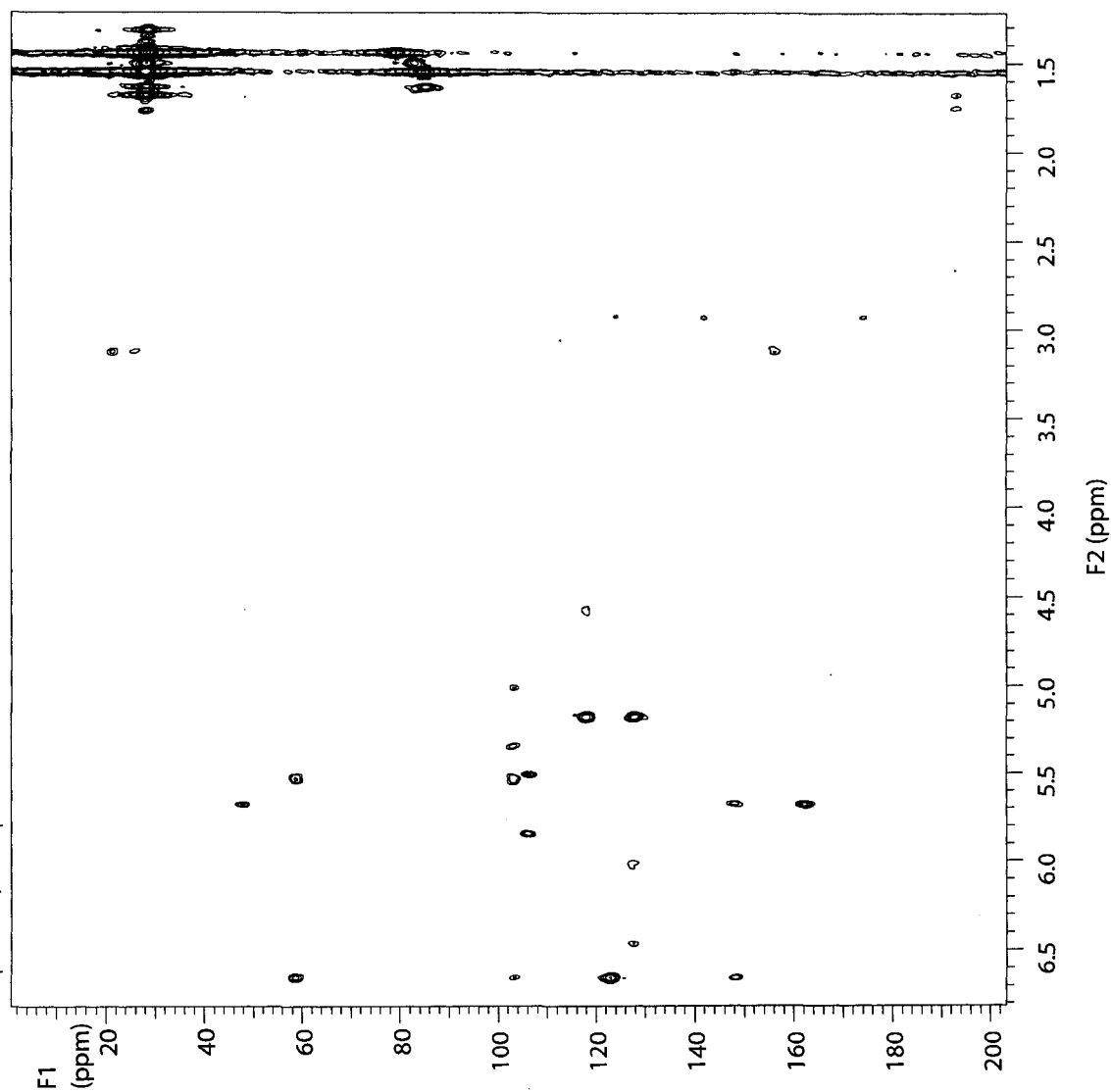
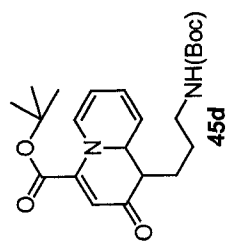
500 MHz gHMQC in CDCl₃ (ref. to CDCl₃ @ 7.26/77.0 ppm), temp 27.2 C -> actual temp = 27.0 C, sw5000 probe

Pulse Sequence: gHMQC



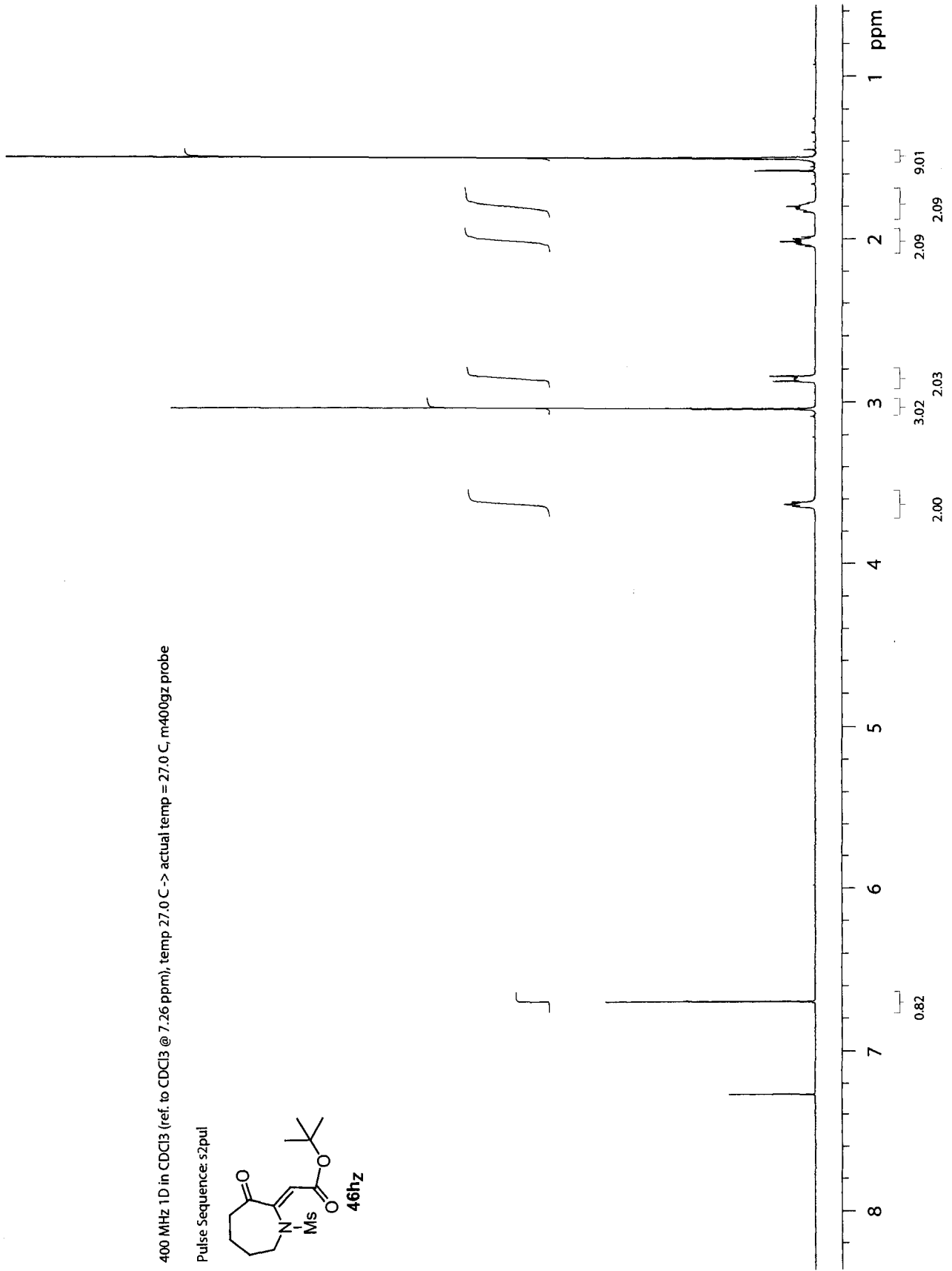
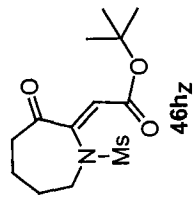
500 MHz gHMBC in CDCl₃ (ref. to CDCl₃ @ 7.26/77.0 ppm), temp 27.2 C -> actual temp = 27.0 C, sw500 probe

Pulse Sequence: gHMBC



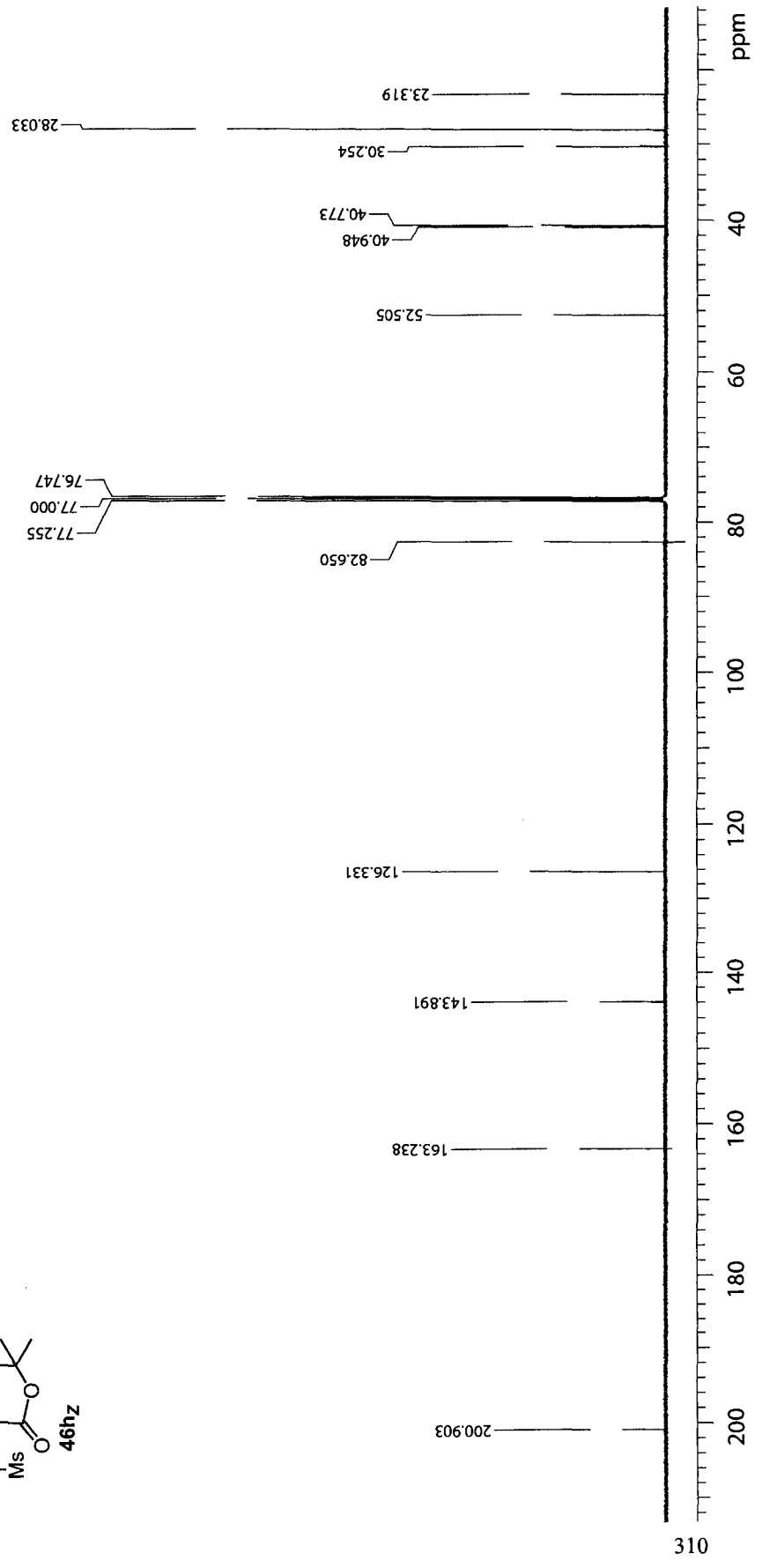
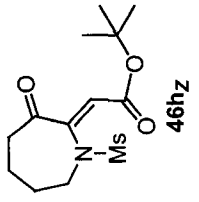
400 MHz 1D in CDCl3 (ref. to CDCl3 @ 7.26 ppm), temp 27.0 C -> actual temp = 27.0 C, m400gz probe

Pulse Sequence: s2pul



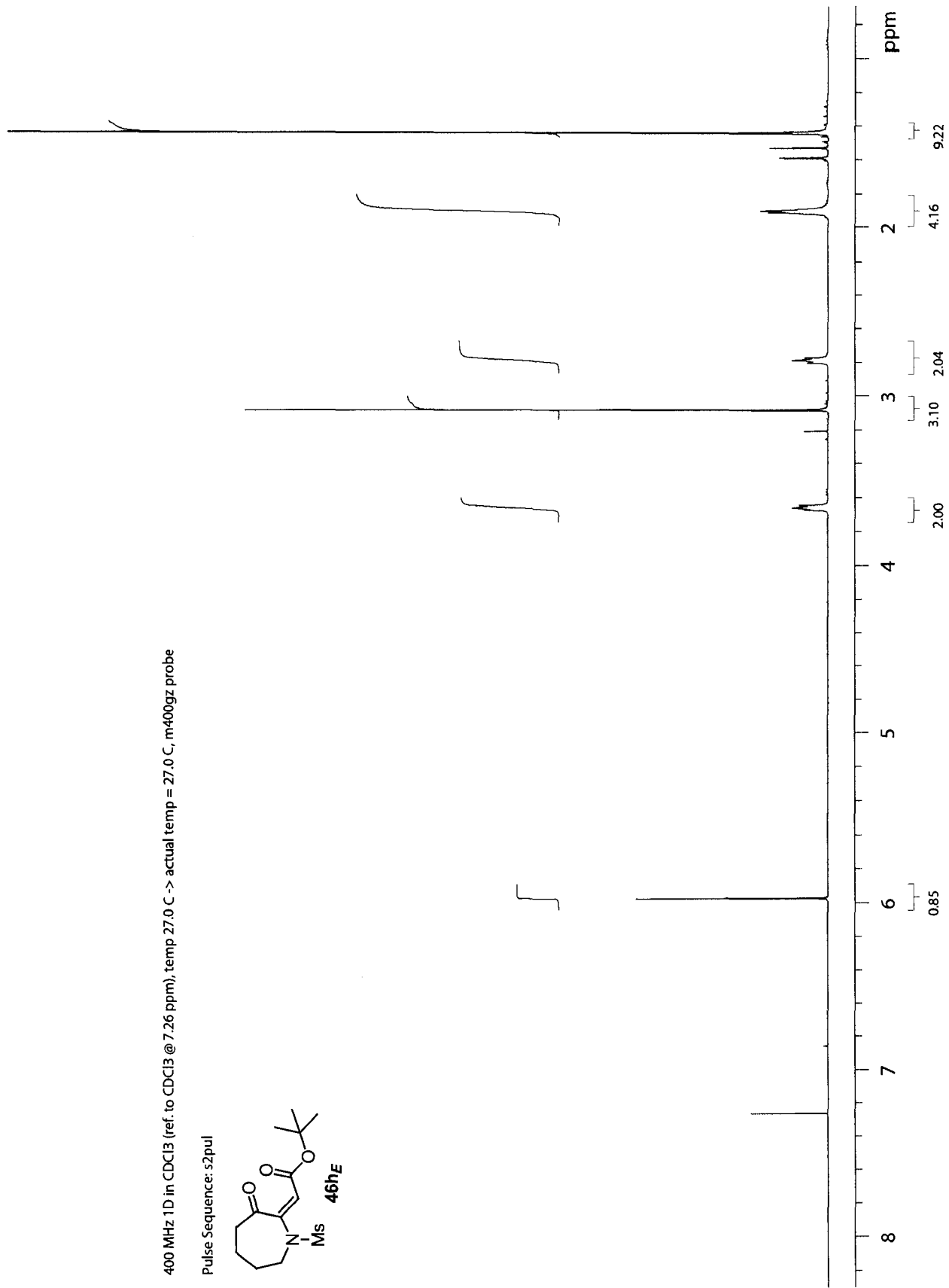
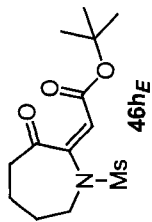
125 MHz 1D C13 in CDCl3 (ref. to CDCl3 @ 77.0 ppm), temp 27.2 C -> actual temp = 27.0 C, sw probe

Pulse Sequence: s2pul



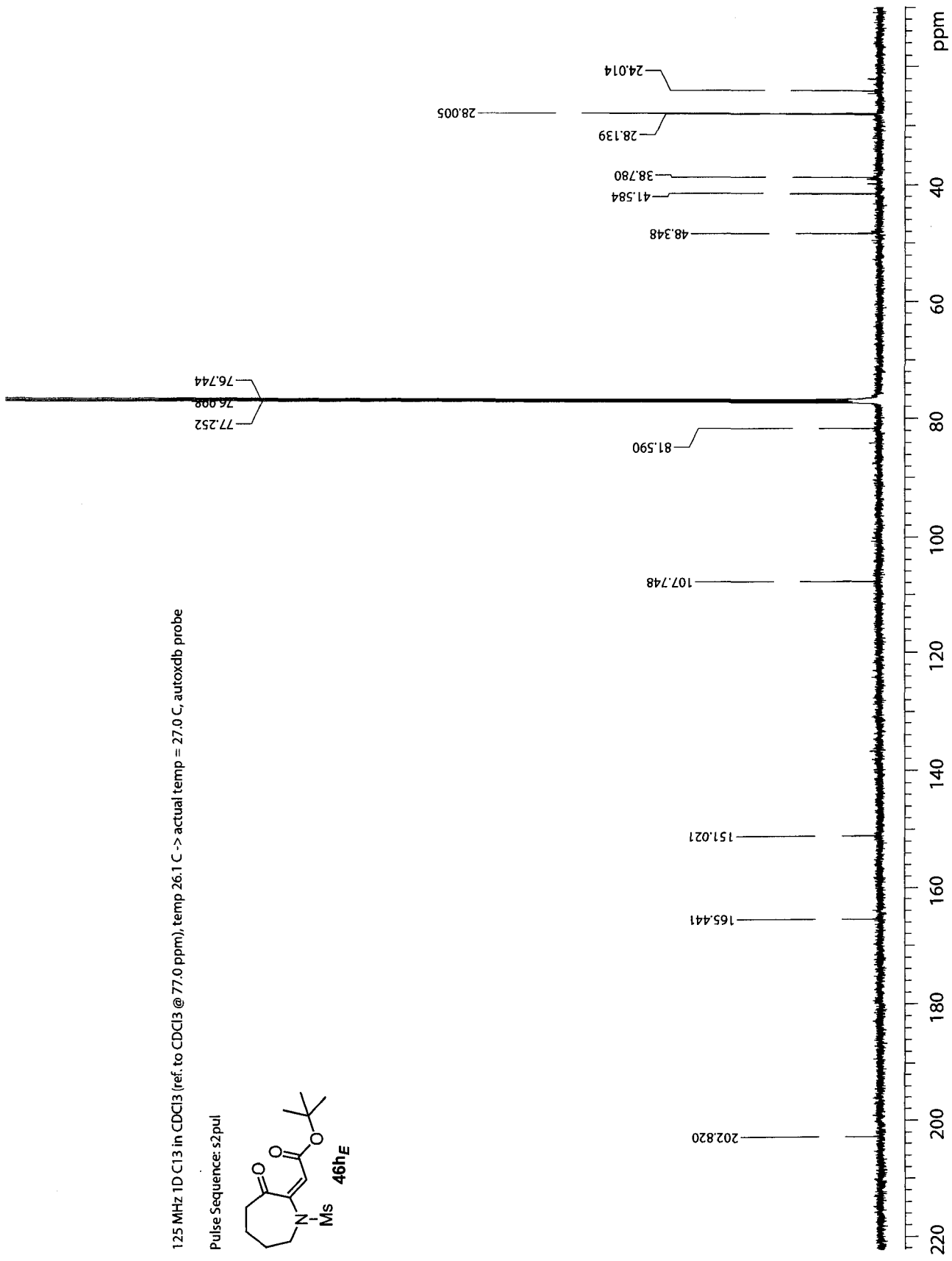
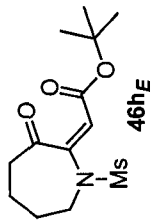
400 MHz 1D in CDCl₃ (ref. to CDCl₃ @ 7.26 ppm), temp 27.0 C -> actual temp = 27.0 C, m400grz probe

Pulse Sequence: s2pul



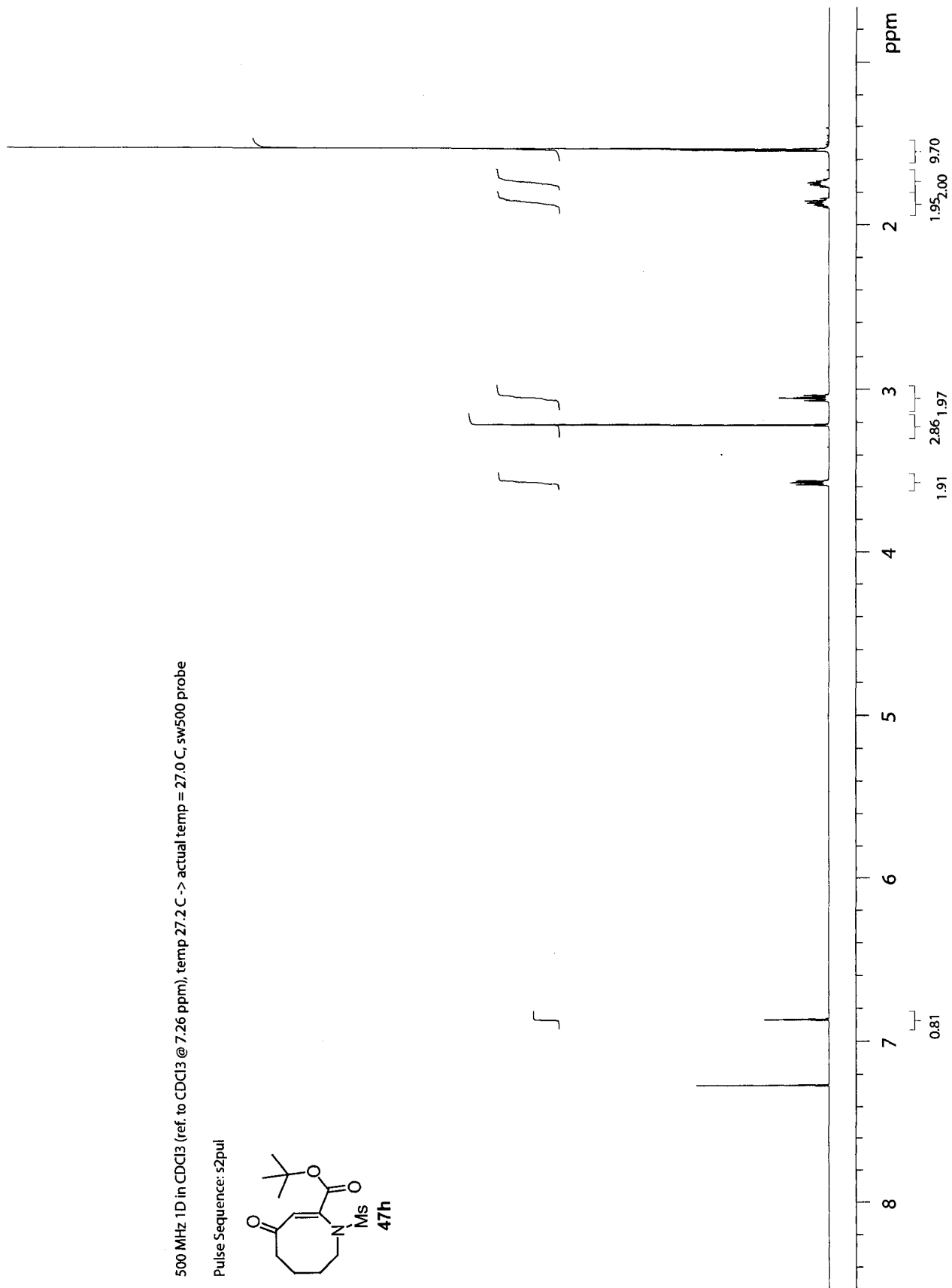
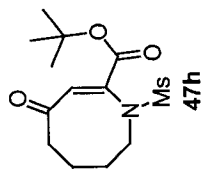
125 MHz 1D C13 in CDCl3 (ref. to CDCl3 @ 77.0 ppm), temp 26.1 C -> actual temp = 27.0 C, autoxdb probe

Pulse Sequence: s2pul



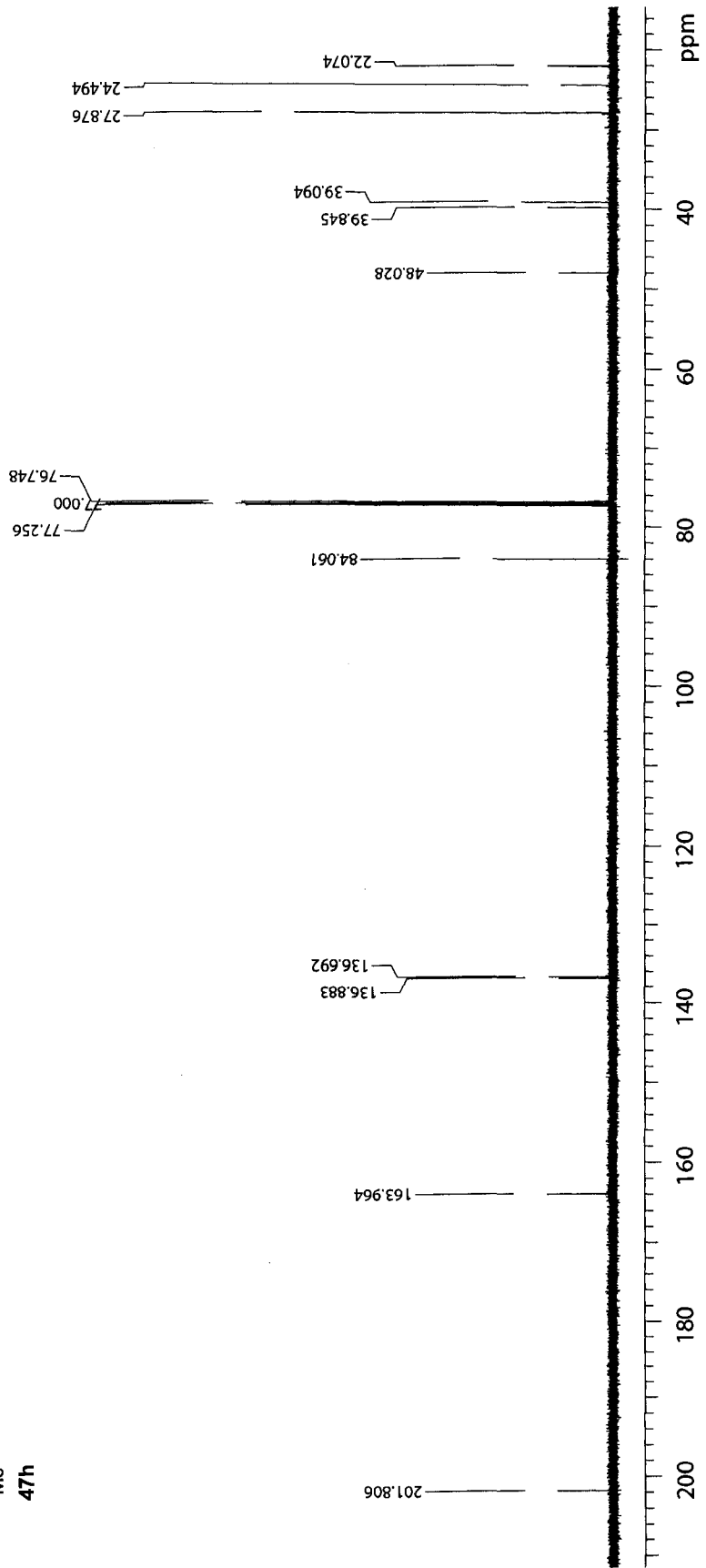
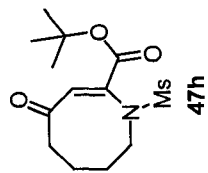
500 MHz 1D in CDCl3 (ref. to CDCl3 @ 7.26 ppm), temp 27.2 C -> actual temp = 27.0 C, sw500 probe

Pulse Sequence: s2pul



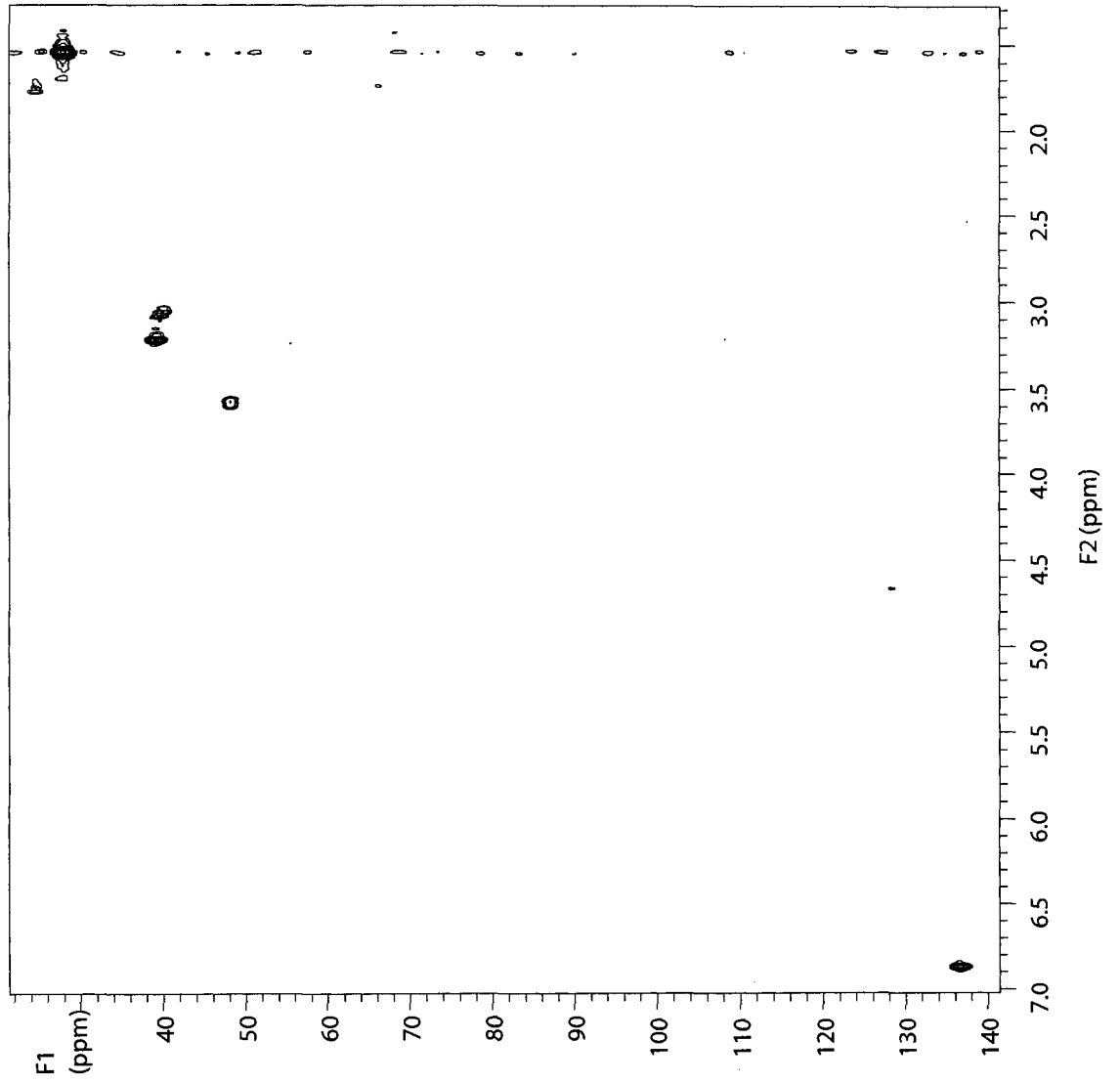
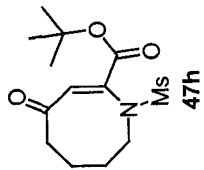
125 MHz 1D C13 in CDCl3 (ref. to CDCl3 @ 77.0 ppm), temp 26.1 C -> actual temp = 27.0 C, autoxdb probe

Pulse Sequence: s2put



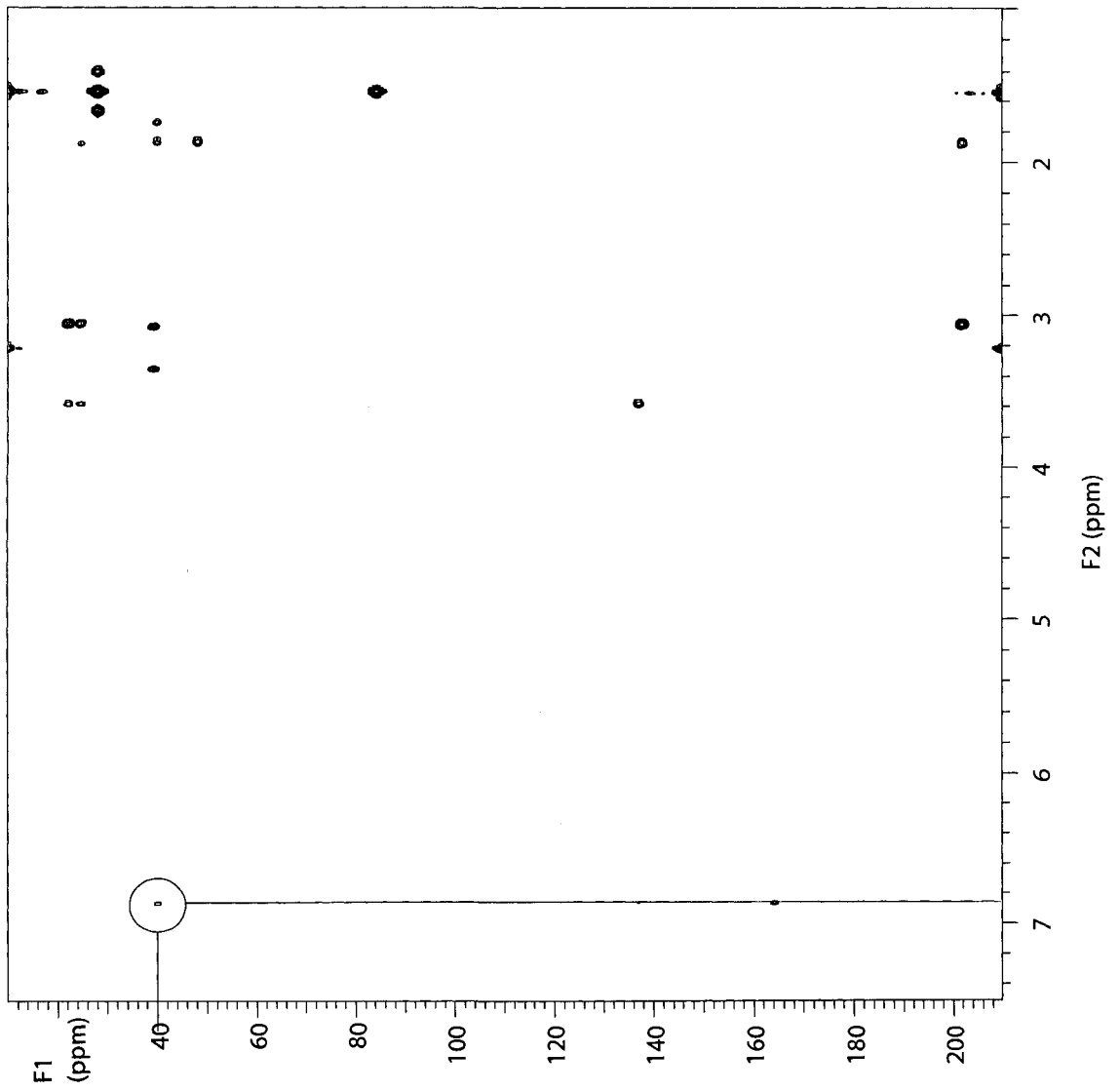
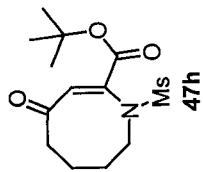
500 MHz gHMQC in CDCl₃ (ref. to CDCl₃ @ 7.26/77.0 ppm), temp 27.2 C -> actual temp = 27.0 C, sw500 probe

Pulse Sequence: gHMQC



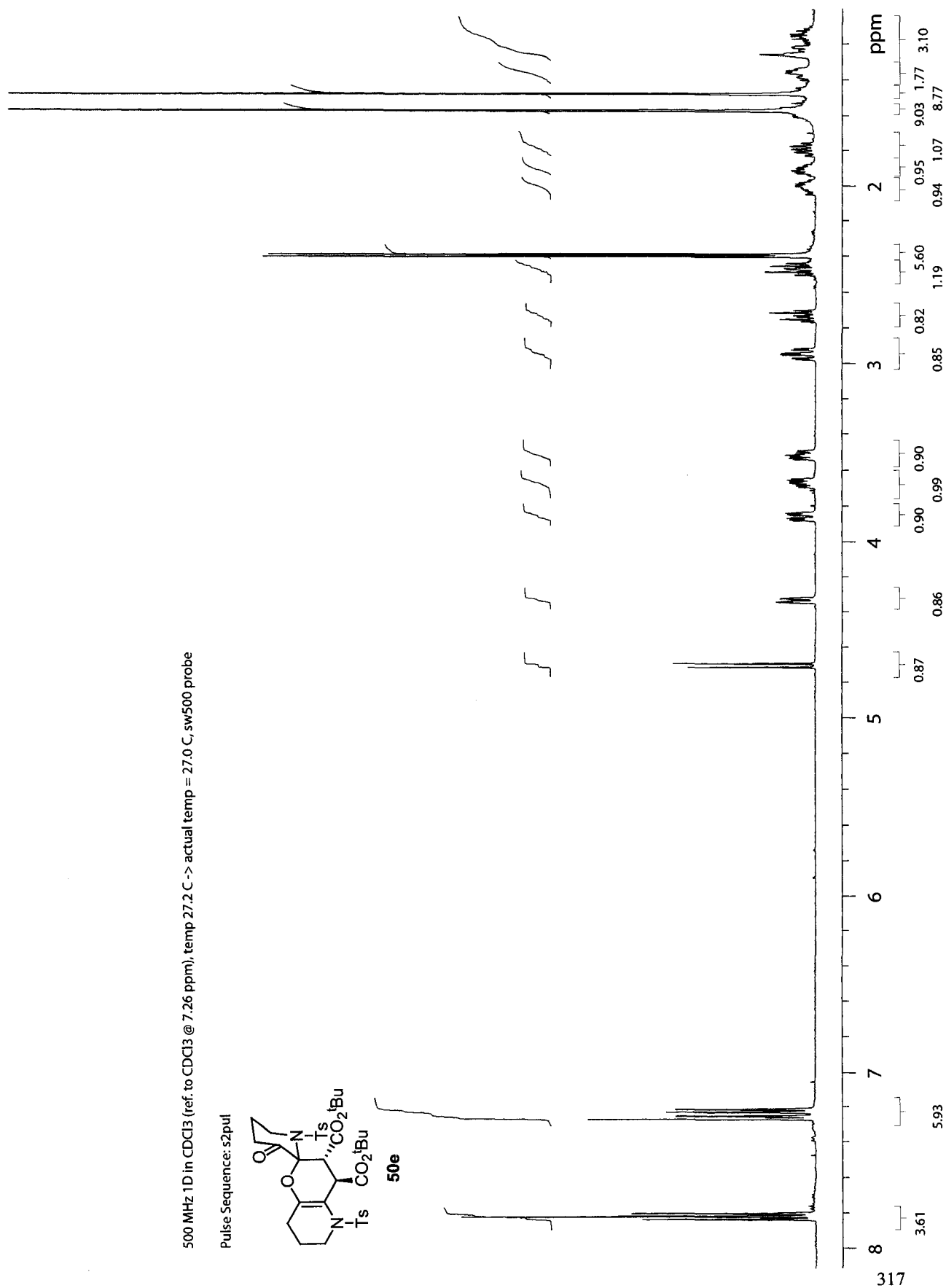
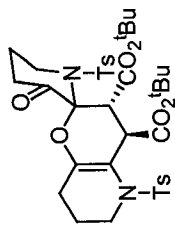
500 MHz gHMBC in CDCl₃ (ref. to CDCl₃ @ 7.26/77.0 ppm), temp 27.2 C -> actual temp = 27.0 C, sw500 probe

Pulse Sequence: gHMBC



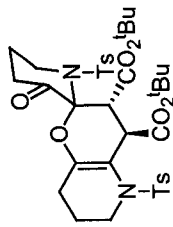
500 MHz 1D in CDCl3 (ref. to CDCl3 @ 7.26 ppm), temp 27.2 C -> actual temp = 27.0 C, sw500 probe

Pulse Sequence: s2pul

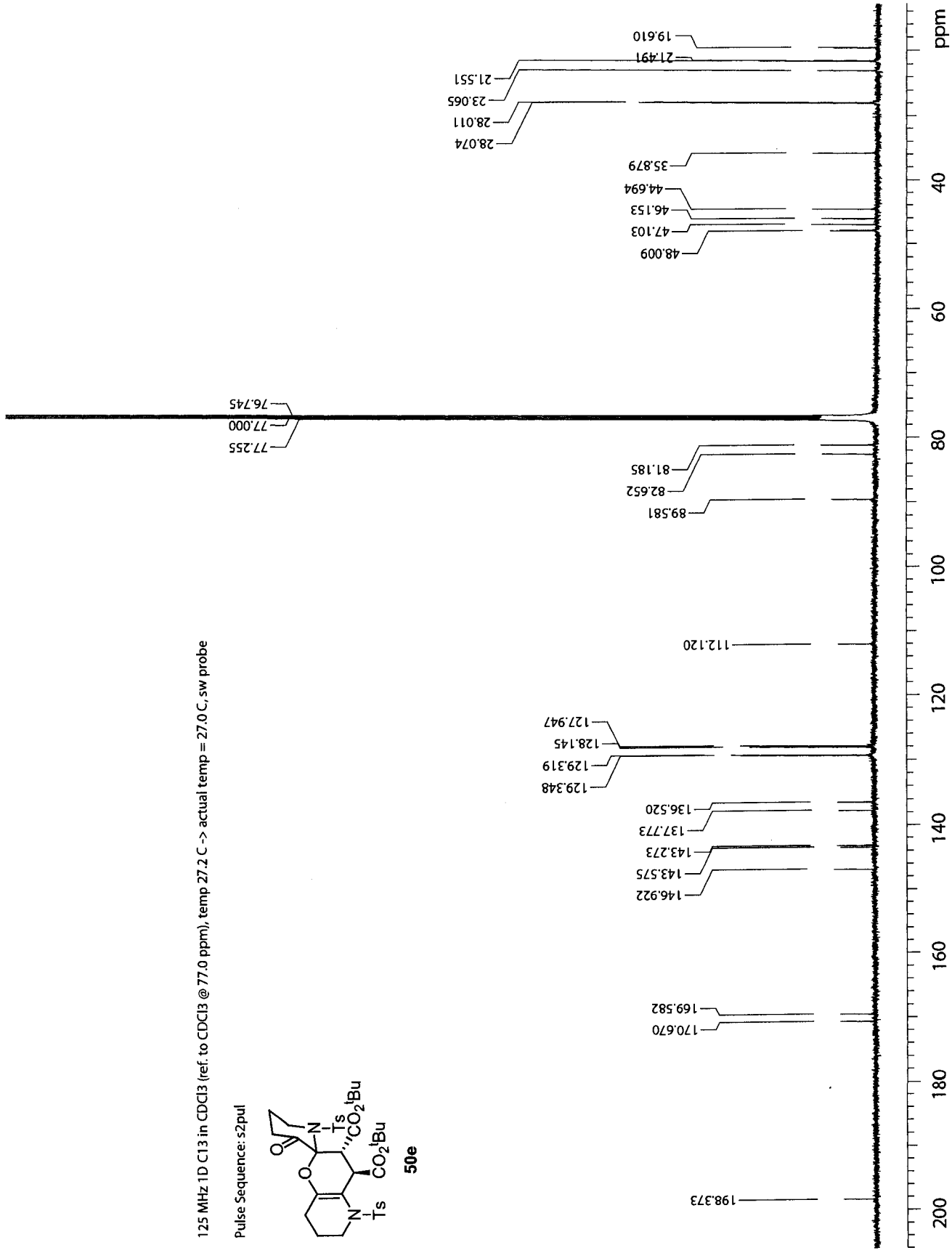


125 MHz 1D C13 in CDCl3 (ref. to CDCl3 @ 77.0 ppm), temp 27.2 C -> actual temp = 27.0 C, sw probe

Pulse Sequence: s2pul

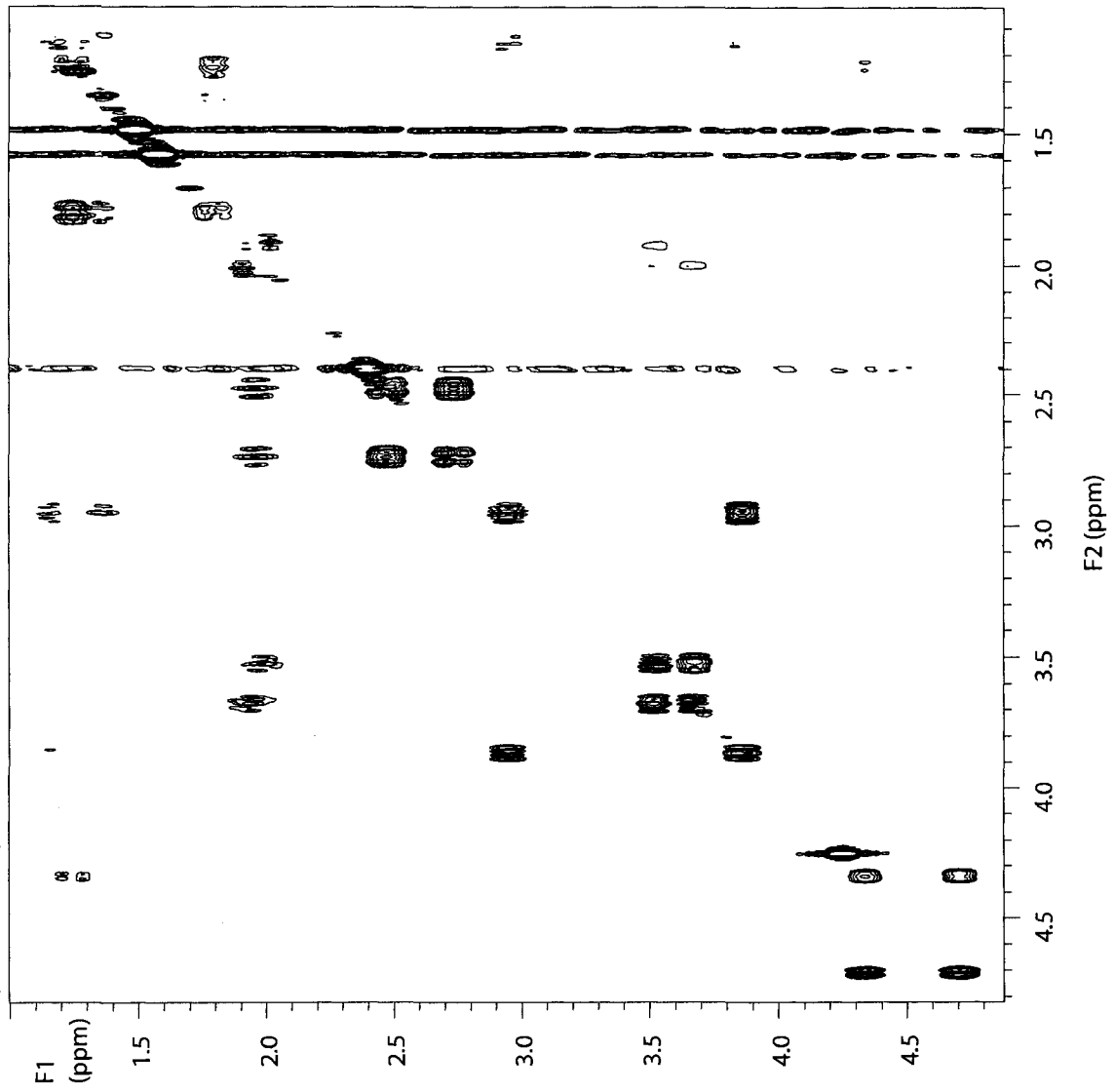
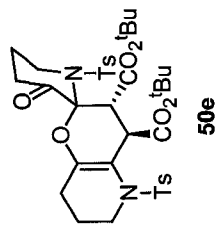


50e



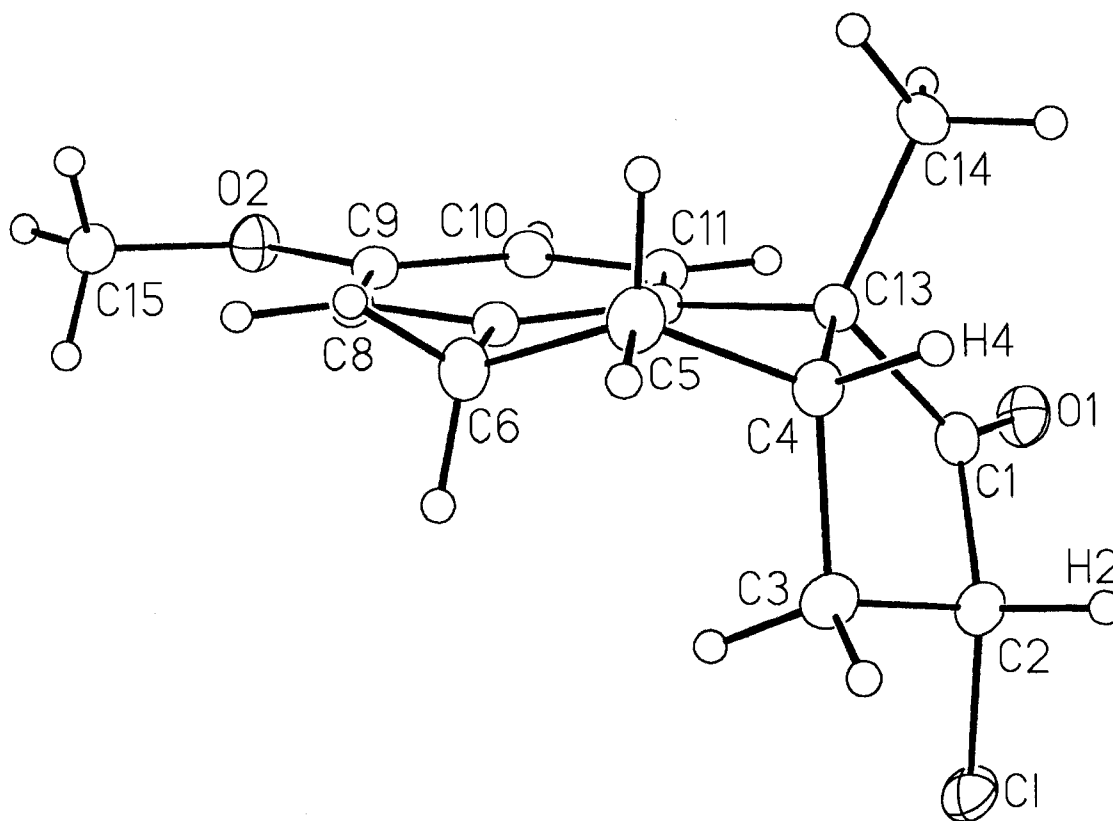
500 MHz GCOSY in CDCl₃ (ref. to CDCl₃ @ 7.26 ppm), temp 27.2 C -> actual temp = 27.0 C, sw500 probe

Pulse Sequence: aogcosy



**Appendix IV: X-ray Crystallographic Data for Compounds 19i, 32d, and 32e
(Chapter 3)**

Figure 2. Alternate view of the molecule.



List of Tables

- Table 1.** Crystallographic Experimental Details
- Table 2.** Atomic Coordinates and Equivalent Isotropic Displacement Parameters
- Table 3.** Selected Interatomic Distances
- Table 4.** Selected Interatomic Angles
- Table 5.** Torsional Angles
- Table 6.** Anisotropic Displacement Parameters
- Table 7.** Derived Atomic Coordinates and Displacement Parameters for Hydrogen Atoms

Table 1. Crystallographic Experimental Details*A. Crystal Data*

formula	C ₁₅ H ₁₇ ClO ₂
formula weight	264.74
crystal dimensions (mm)	0.66 × 0.44 × 0.40
crystal system	monoclinic
space group	<i>P</i> 2 ₁ / <i>c</i> (No. 14)
unit cell parameters ^a	
<i>a</i> (Å)	16.2372 (13)
<i>b</i> (Å)	7.5016 (6)
<i>c</i> (Å)	10.8942 (9)
β (deg)	100.0609 (11)
<i>V</i> (Å ³)	1306.56 (18)
<i>Z</i>	4
ρ _{calcd} (g cm ⁻³)	1.346
μ (mm ⁻¹)	0.284

B. Data Collection and Refinement Conditions

diffractometer	Bruker PLATFORM/SMART 1000 CCD ^b
radiation (λ [Å])	graphite-monochromated Mo Kα (0.71073)
temperature (°C)	-80
scan type	ω scans (0.3°) (15 s exposures)
data collection 2θ limit (deg)	52.80
total data collected	10062 (-20 ≤ <i>h</i> ≤ 20, -9 ≤ <i>k</i> ≤ 9, -13 ≤ <i>l</i> ≤ 13)
independent reflections	2688 (<i>R</i> _{int} = 0.0163)
number of observed reflections (<i>NO</i>)	2444 [<i>F</i> _o ² ≥ 2α(<i>F</i> _o ²)]
structure solution method	Patterson search/structure expansion (<i>DIRDIF-99</i> ^c)
refinement method	full-matrix least-squares on <i>F</i> ² (<i>SHELXL-93</i> ^d)
absorption correction method	multi-scan (<i>SADABS</i>)
range of transmission factors	0.8950–0.8350
data/restraints/parameters	2688 [<i>F</i> _o ² ≥ -3α(<i>F</i> _o ²)] / 0 / 163
goodness-of-fit (<i>S</i>) ^e	1.037 [<i>F</i> _o ² ≥ -3α(<i>F</i> _o ²)]
final <i>R</i> indices ^f	
<i>R</i> ₁ [<i>F</i> _o ² ≥ 2α(<i>F</i> _o ²)]	0.0352
<i>wR</i> ₂ [<i>F</i> _o ² ≥ -3α(<i>F</i> _o ²)]	0.1002
largest difference peak and hole	0.287 and -0.334 e Å ⁻³

^aObtained from least-squares refinement of 4478 reflections with 6.00° < 2θ < 52.78°.

^bPrograms for diffractometer operation, data collection, data reduction and absorption correction were those supplied by Bruker.

(continued)

Table 1. Crystallographic Experimental Details (continued)

^cBeurskens, P. T.; Beurskens, G.; de Gelder, R.; Garcia-Granda, S.; Israel, R.; Gould, R. O.; Smits, J. M. M. (1999). The *DIRDIF-99* program system. Crystallography Laboratory, University of Nijmegen, The Netherlands.

^dSheldrick, G. M. *SHELXL-93*. Program for crystal structure determination. University of Göttingen, Germany, 1993.

^e $S = [\sum w(F_o^2 - F_c^2)^2 / (n - p)]^{1/2}$ (n = number of data; p = number of parameters varied; $w = [\sigma^2(F_o^2) + (0.0548P)^2 + 0.4494P]^{-1}$ where $P = [\text{Max}(F_o^2, 0) + 2F_c^2]/3$).

$\int R_1 = \sum ||F_o| - |F_c|| / \sum |F_o|$; $wR_2 = [\sum w(F_o^2 - F_c^2)^2 / \sum w(F_o^4)]^{1/2}$.

Table 2. Atomic Coordinates and Equivalent Isotropic Displacement Parameters

Atom	x	y	z	$U_{eq}, \text{Å}^2$
Cl	0.47222(2)	0.33149(6)	0.07157(4)	0.05140(15)*
O1	0.35783(7)	0.38839(14)	0.26731(11)	0.0474(3)*
O2	-0.00227(6)	0.27598(15)	-0.12139(10)	0.0432(3)*
C1	0.36058(9)	0.24197(19)	0.22320(12)	0.0338(3)*
C2	0.43359(9)	0.1688(2)	0.16675(14)	0.0382(3)*
C3	0.40087(9)	0.0000(2)	0.09931(14)	0.0393(3)*
C4	0.34105(8)	-0.07199(18)	0.18285(13)	0.0336(3)*
C5	0.28264(9)	-0.21947(18)	0.12453(14)	0.0384(3)*
C6	0.22527(9)	-0.15579(18)	0.00696(14)	0.0370(3)*
C7	0.18527(8)	0.02201(16)	0.02416(12)	0.0281(3)*
C8	0.11146(8)	0.06549(18)	-0.05782(12)	0.0312(3)*
C9	0.07140(8)	0.22620(19)	-0.04734(12)	0.0321(3)*
C10	0.10569(9)	0.34801(18)	0.04399(13)	0.0351(3)*
C11	0.17783(9)	0.30459(17)	0.12530(12)	0.0318(3)*
C12	0.21871(8)	0.14124(16)	0.11812(11)	0.0267(3)*
C13	0.29437(8)	0.09428(17)	0.21839(11)	0.0292(3)*
C14	0.26674(10)	0.0780(2)	0.34581(12)	0.0399(3)*
C15	-0.04100(9)	0.1515(2)	-0.21203(14)	0.0421(4)*

Anisotropically-refined atoms are marked with an asterisk (*). The form of the anisotropic displacement parameter is: $\exp[-2\pi^2(h^2a^{*2}U_{11} + k^2b^{*2}U_{22} + l^2c^{*2}U_{33} + 2klb^{*c^{*}}U_{23} + 2hla^{*c^{*}}U_{13} + 2hka^{*b^{*}}U_{12})]$.

Table 3. Selected Interatomic Distances (Å)

Atom1	Atom2	Distance	Atom1	Atom2	Distance
C1	C2	1.7845(15)	C5	C6	1.523(2)
O1	C1	1.2029(18)	C6	C7	1.5094(17)
O2	C9	1.3726(17)	C7	C8	1.4023(18)
O2	C15	1.4230(19)	C7	C12	1.3959(18)
C1	C2	1.529(2)	C8	C9	1.3840(19)
C1	C13	1.5383(18)	C9	C10	1.393(2)
C2	C3	1.513(2)	C10	C11	1.378(2)
C3	C4	1.540(2)	C11	C12	1.4024(18)
C4	C5	1.5221(19)	C12	C13	1.5355(17)
C4	C13	1.5435(18)	C13	C14	1.5364(18)

Table 4. Selected Interatomic Angles (deg)

Atom1	Atom2	Atom3	Angle	Atom1	Atom2	Atom3	Angle
C9	O2	C15	117.61(11)	C7	C8	C9	120.78(12)
O1	C1	C2	125.01(13)	O2	C9	C8	124.22(13)
O1	C1	C13	126.64(13)	O2	C9	C10	116.09(12)
C2	C1	C13	108.31(11)	C8	C9	C10	119.68(12)
C1	C2	C1	111.36(10)	C9	C10	C11	119.51(12)
C1	C2	C3	114.79(11)	C10	C11	C12	121.87(12)
C1	C2	C3	105.33(11)	C7	C12	C11	118.26(12)
C2	C3	C4	102.17(11)	C7	C12	C13	122.35(11)
C3	C4	C5	114.81(12)	C11	C12	C13	119.24(11)
C3	C4	C13	104.64(11)	C1	C13	C4	102.69(11)
C5	C4	C13	113.24(11)	C1	C13	C12	109.06(10)
C4	C5	C6	111.59(11)	C1	C13	C14	109.81(11)
C5	C6	C7	112.70(11)	C4	C13	C12	111.95(10)
C6	C7	C8	117.70(12)	C4	C13	C14	113.34(11)
C6	C7	C12	122.45(11)	C12	C13	C14	109.72(11)
C8	C7	C12	119.85(11)				

Table 5. Torsional Angles (deg)

Atom1	Atom2	Atom3	Atom4	Angle	Atom1	Atom2	Atom3	Atom4	Angle
C15	O2	C9	C8	2.0(2)	C5	C4	C13	C14	83.48(15)
C15	O2	C9	C10	-177.29(13)	C4	C5	C6	C7	-46.92(17)
O1	C1	C2	C1	-42.79(17)	C5	C6	C7	C8	-158.18(12)
O1	C1	C2	C3	-167.82(13)	C5	C6	C7	C12	21.32(19)
C13	C1	C2	C1	139.54(9)	C6	C7	C8	C9	179.92(12)
C13	C1	C2	C3	14.50(14)	C12	C7	C8	C9	0.41(19)
O1	C1	C13	C4	-166.49(14)	C6	C7	C12	C11	178.92(12)
O1	C1	C13	C12	74.62(16)	C6	C7	C12	C13	-5.50(19)
O1	C1	C13	C14	-45.63(18)	C8	C7	C12	C11	-1.60(18)
C2	C1	C13	C4	11.14(13)	C8	C7	C12	C13	173.99(11)
C2	C1	C13	C12	-107.76(12)	C7	C8	C9	O2	-177.91(12)
C2	C1	C13	C14	131.99(12)	C7	C8	C9	C10	1.4(2)
C1	C2	C3	C4	-156.96(10)	O2	C9	C10	C11	177.40(12)
C1	C2	C3	C4	-34.10(13)	C8	C9	C10	C11	-2.0(2)
C2	C3	C4	C5	166.54(11)	C9	C10	C11	C12	0.8(2)
C2	C3	C4	C13	41.78(13)	C10	C11	C12	C7	1.03(19)
C3	C4	C5	C6	-61.32(16)	C10	C11	C12	C13	-174.70(12)
C13	C4	C5	C6	58.79(16)	C7	C12	C13	C1	128.02(13)
C3	C4	C13	C1	-32.38(13)	C7	C12	C13	C4	15.08(16)
C3	C4	C13	C12	84.47(13)	C7	C12	C13	C14	-111.67(13)
C3	C4	C13	C14	-150.78(11)	C11	C12	C13	C1	-56.44(15)
C5	C4	C13	C1	-158.13(11)	C11	C12	C13	C4	-169.38(11)
C5	C4	C13	C12	-41.28(15)	C11	C12	C13	C14	63.87(15)

Table 6. Anisotropic Displacement Parameters (U_{ij} , Å²)

Atom	U_{11}	U_{22}	U_{33}	U_{23}	U_{13}	U_{12}
C1	0.0424(2)	0.0595(3)	0.0516(3)	0.01189(18)	0.00591(17)	-0.01747(17)
O1	0.0536(7)	0.0331(5)	0.0533(6)	-0.0057(5)	0.0035(5)	-0.0088(5)
O2	0.0349(5)	0.0431(6)	0.0484(6)	0.0012(5)	-0.0016(5)	0.0109(5)
C1	0.0368(7)	0.0320(7)	0.0301(6)	0.0045(5)	-0.0016(5)	-0.0044(5)
C2	0.0317(7)	0.0412(8)	0.0398(8)	0.0089(6)	0.0007(6)	-0.0042(6)
C3	0.0332(7)	0.0385(7)	0.0465(8)	0.0004(6)	0.0077(6)	0.0041(6)
C4	0.0336(7)	0.0284(6)	0.0361(7)	0.0045(5)	-0.0010(5)	0.0030(5)
C5	0.0413(8)	0.0239(6)	0.0475(8)	0.0015(6)	0.0008(6)	0.0040(6)
C6	0.0396(7)	0.0259(6)	0.0427(8)	-0.0075(5)	-0.0008(6)	0.0039(5)
C7	0.0304(6)	0.0239(6)	0.0306(6)	-0.0003(5)	0.0068(5)	0.0007(5)
C8	0.0324(6)	0.0292(6)	0.0313(6)	-0.0024(5)	0.0038(5)	-0.0006(5)
C9	0.0297(6)	0.0337(7)	0.0334(7)	0.0042(5)	0.0066(5)	0.0045(5)
C10	0.0374(7)	0.0279(6)	0.0414(7)	-0.0007(5)	0.0111(6)	0.0080(5)
C11	0.0371(7)	0.0274(6)	0.0317(6)	-0.0046(5)	0.0084(5)	0.0005(5)
C12	0.0289(6)	0.0253(6)	0.0267(6)	0.0014(5)	0.0066(5)	0.0001(5)
C13	0.0329(6)	0.0265(6)	0.0271(6)	0.0013(5)	0.0025(5)	-0.0025(5)
C14	0.0486(8)	0.0424(8)	0.0286(7)	0.0028(6)	0.0064(6)	-0.0065(6)
C15	0.0328(7)	0.0525(9)	0.0384(8)	0.0068(6)	-0.0006(6)	0.0001(6)

The form of the anisotropic displacement parameter is:

$$\exp[-2\pi^2(h^2a^{*2}U_{11} + k^2b^{*2}U_{22} + l^2c^{*2}U_{33} + 2klb^*c^*U_{23} + 2hla^*c^*U_{13} + 2hka^*b^*U_{12})]$$

Table 7. Derived Atomic Coordinates and Displacement Parameters for Hydrogen Atoms

Atom	x	y	z	U_{eq} , Å ²
H2	0.4798	0.1360	0.2363	0.046
H3A	0.4467	-0.0852	0.0943	0.047
H3B	0.3707	0.0261	0.0141	0.047
H4	0.3757	-0.1202	0.2607	0.040
H5A	0.2483	-0.2609	0.1856	0.046
H5B	0.3162	-0.3217	0.1037	0.046
H6A	0.2580	-0.1459	-0.0614	0.044
H6B	0.1808	-0.2456	-0.0179	0.044
H8	0.0887	-0.0163	-0.1213	0.037
H10	0.0795	0.4602	0.0502	0.042
H11	0.2005	0.3877	0.1880	0.038
H14A	0.2355	0.1850	0.3614	0.048
H14B	0.3162	0.0659	0.4112	0.048
H14C	0.2310	-0.0271	0.3461	0.048
H15A	-0.0932	0.2023	-0.2574	0.050
H15B	-0.0533	0.0413	-0.1704	0.050
H15C	-0.0032	0.1253	-0.2707	0.050

Compound 32d

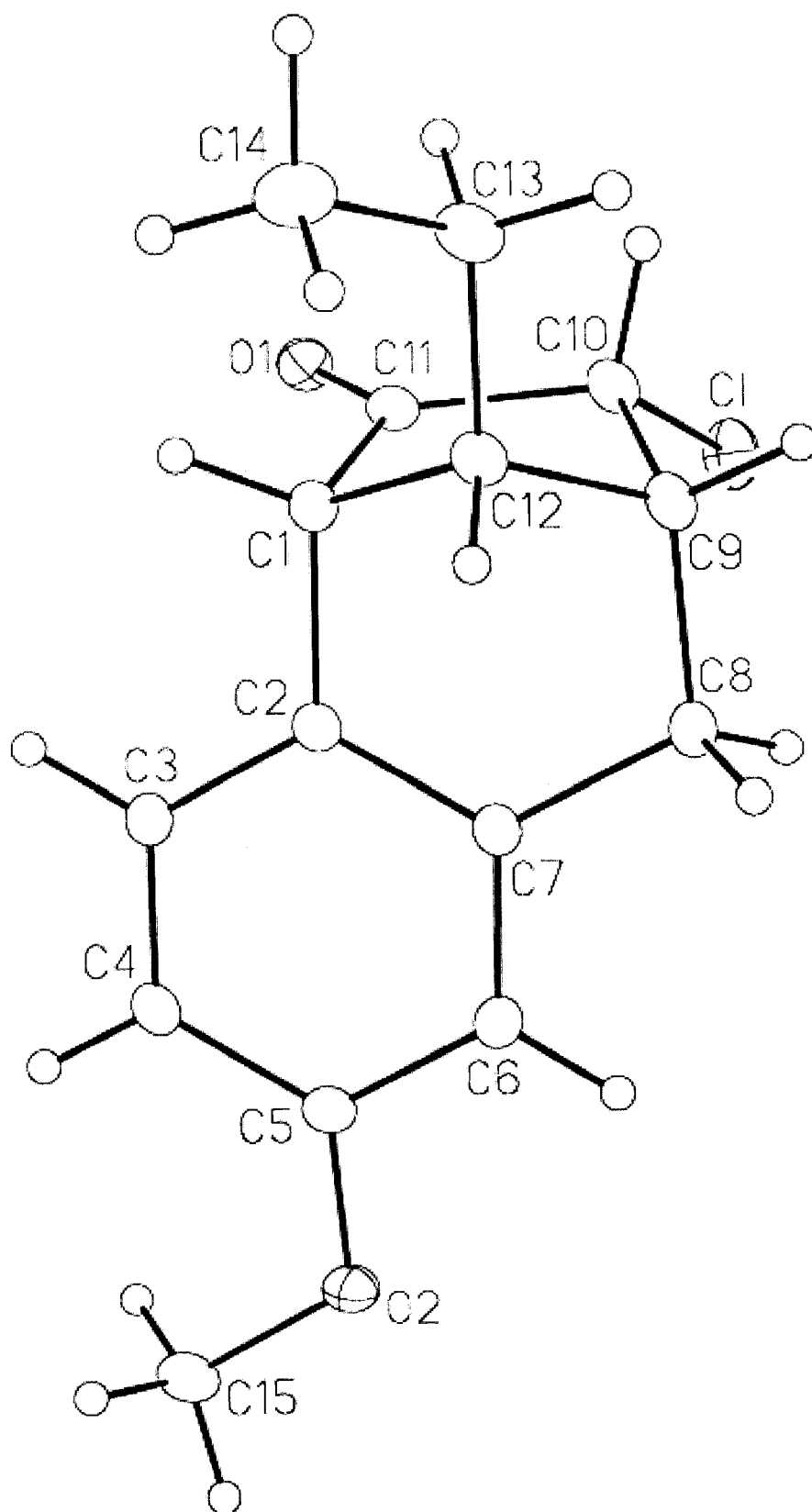
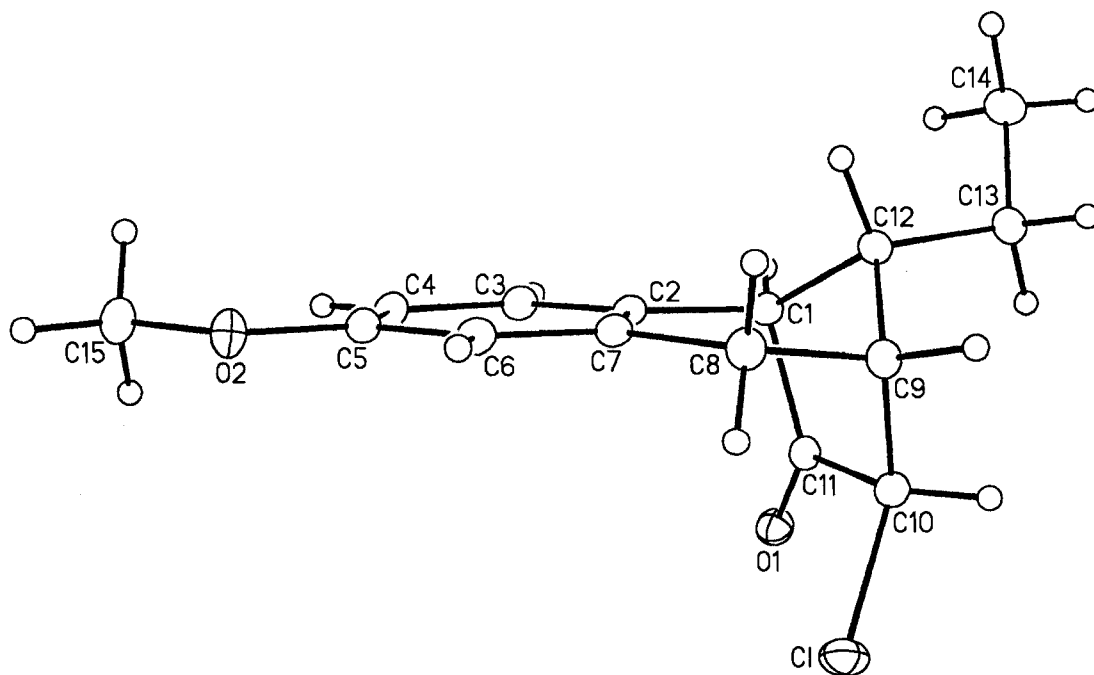


Figure 2. Alternate view of the molecule.



List of Tables

- Table 1.** Crystallographic Experimental Details
- Table 2.** Atomic Coordinates and Equivalent Isotropic Displacement Parameters
- Table 3.** Selected Interatomic Distances
- Table 4.** Selected Interatomic Angles
- Table 5.** Torsional Angles
- Table 6.** Anisotropic Displacement Parameters
- Table 7.** Derived Atomic Coordinates and Displacement Parameters for Hydrogen Atoms

Table 1. Crystallographic Experimental Details

<i>A. Crystal Data</i>	
formula	C ₁₅ H ₁₇ ClO ₂
formula weight	264.74
crystal dimensions (mm)	0.50 × 0.40 × 0.36
crystal system	orthorhombic
space group	<i>Pbca</i> (No. 61)
unit cell parameters ^a	
<i>a</i> (Å)	15.9739 (17)
<i>b</i> (Å)	8.8900 (10)
<i>c</i> (Å)	18.522 (2)
<i>V</i> (Å ³)	2630.3 (5)
<i>Z</i>	8
ρ_{calcd} (g cm ⁻³)	1.337
μ (mm ⁻¹)	0.282
<i>B. Data Collection and Refinement Conditions</i>	
diffractometer	Bruker PLATFORM/SMART 1000 CCD ^b
radiation (λ [Å])	graphite-monochromated Mo K α (0.71073)
temperature (°C)	-80
scan type	ω scans (0.3°) (15 s exposures)
data collection 2θ limit (deg)	55.04
total data collected	20945 ($-20 \leq h \leq 20, -11 \leq k \leq 11, -23 \leq l \leq 23$)
independent reflections	3017 ($R_{\text{int}} = 0.0183$)
number of observed reflections (<i>NO</i>)	2669 [$F_o^2 \geq 2\sigma(F_o^2)$]
structure solution method	direct methods (<i>SIR97</i> ^c)
refinement method	full-matrix least-squares on F^2 (<i>SHELXL-97</i> ^d)
absorption correction method	multi-scan (<i>SADABS</i>)
range of transmission factors	0.9054–0.8720
data/restraints/parameters	3017 [$F_o^2 \geq -3\sigma(F_o^2)$] / 0 / 164
goodness-of-fit (<i>S</i>) ^e	1.027 [$F_o^2 \geq -3\sigma(F_o^2)$]
final <i>R</i> indices ^f	
<i>R</i> ₁ [$F_o^2 \geq 2\sigma(F_o^2)$]	0.0333
<i>wR</i> ₂ [$F_o^2 \geq -3\sigma(F_o^2)$]	0.0943
largest difference peak and hole	0.264 and -0.226 e Å ⁻³

^aObtained from least-squares refinement of 6030 reflections with $5.08^\circ < 2\theta < 54.94^\circ$.

^bPrograms for diffractometer operation, data collection, data reduction and absorption correction were those supplied by Bruker.

(continued)

Table 1. Crystallographic Experimental Details (continued)

^cAltomare, A.; Burla, M. C.; Camalli, M.; Cascarano, G. L.; Giacovazzo, C.; Guagliardi, A.; Moliterni, A. G. G.; Polidori, G.; Spagna, R. *J. Appl. Cryst.* **1999**, *32*, 115–119.

^dSheldrick, G. M. *SHELXL-97*. Program for crystal structure determination. University of Göttingen, Germany, 1997.

^e $S = [\sum w(F_o^2 - F_c^2)^2 / (n - p)]^{1/2}$ (n = number of data; p = number of parameters varied; $w = [\sigma^2(F_o^2) + (0.0506P)^2 + 0.8602P]^{-1}$ where $P = [\text{Max}(F_o^2, 0) + 2F_c^2]/3$).

^f $R_1 = \sum ||F_o| - |F_c|| / \sum |F_o|$; $wR_2 = [\sum w(F_o^2 - F_c^2)^2 / \sum w(F_o^4)]^{1/2}$.

Table 2. Atomic Coordinates and Equivalent Isotropic Displacement Parameters

Atom	<i>x</i>	<i>y</i>	<i>z</i>	$U_{eq}, \text{Å}^2$
C1	-0.01963(2)	0.57127(4)	0.60397(2)	0.04571(12)*
O1	-0.02679(5)	0.32811(10)	0.72566(5)	0.0357(2)*
O2	0.11804(6)	-0.03833(10)	0.44685(5)	0.0394(2)*
C1	0.12394(7)	0.29080(12)	0.70926(6)	0.0276(2)*
C2	0.12419(7)	0.19811(12)	0.64020(6)	0.0265(2)*
C3	0.10250(7)	0.04637(13)	0.64100(6)	0.0296(2)*
C4	0.09912(8)	-0.03742(13)	0.57760(7)	0.0315(3)*
C5	0.11803(7)	0.03207(13)	0.51231(6)	0.0300(2)*
C6	0.13903(7)	0.18466(13)	0.51106(6)	0.0299(2)*
C7	0.14083(7)	0.26889(12)	0.57419(6)	0.0274(2)*
C8	0.16025(8)	0.43589(13)	0.57090(7)	0.0325(3)*
C9	0.14877(8)	0.51575(13)	0.64341(6)	0.0319(3)*
C10	0.05752(8)	0.52522(13)	0.67005(7)	0.0319(3)*
C11	0.04063(7)	0.37308(13)	0.70585(6)	0.0287(2)*
C12	0.18839(7)	0.41908(13)	0.70404(6)	0.0305(2)*
C13	0.20107(8)	0.50443(15)	0.77503(7)	0.0388(3)*
C14	0.25736(9)	0.42147(18)	0.82812(7)	0.0456(3)*
C15	0.09851(9)	-0.19449(15)	0.44548(8)	0.0428(3)*

Anisotropically-refined atoms are marked with an asterisk (*). The form of the anisotropic displacement parameter is: $\exp[-2\pi^2(h^2a^{*2}U_{11} + k^2b^{*2}U_{22} + l^2c^{*2}U_{33} + 2klb^*c^*U_{23} + 2hla^*c^*U_{13} + 2hka^*b^*U_{12})]$.

Table 3. Selected Interatomic Distances (Å)

Atom1	Atom2	Distance	Atom1	Atom2	Distance
Cl	C10	1.7845(12)	C4	C5	1.3911(17)
O1	C11	1.2060(14)	C5	C6	1.3976(16)
O2	C5	1.3644(14)	C6	C7	1.3888(16)
O2	C15	1.4231(16)	C7	C8	1.5179(15)
C1	C2	1.5215(15)	C8	C9	1.5302(17)
C1	C11	1.5198(15)	C9	C10	1.5412(17)
C1	C12	1.5394(16)	C9	C12	1.5493(16)
C2	C3	1.3928(16)	C10	C11	1.5303(16)
C2	C7	1.4006(15)	C12	C13	1.5316(16)
C3	C4	1.3917(17)	C13	C14	1.5228(19)

Table 4. Selected Interatomic Angles (deg)

Atom1	Atom2	Atom3	Angle	Atom1	Atom2	Atom3	Angle
C5	O2	C15	117.60(10)	C6	C7	C8	119.86(10)
C2	C1	C11	103.19(9)	C7	C8	C9	113.21(10)
C2	C1	C12	110.28(9)	C8	C9	C10	114.82(10)
C11	C1	C12	103.09(9)	C8	C9	C12	109.26(9)
C1	C2	C3	121.00(10)	C10	C9	C12	100.64(9)
C1	C2	C7	119.41(10)	C1	C10	C9	116.49(9)
C3	C2	C7	119.44(10)	C1	C10	C11	112.22(8)
C2	C3	C4	121.28(11)	C9	C10	C11	104.90(9)
C3	C4	C5	119.17(10)	O1	C11	C1	127.57(11)
O2	C5	C4	124.66(11)	O1	C11	C10	125.61(11)
O2	C5	C6	115.50(10)	C1	C11	C10	106.80(9)
C4	C5	C6	119.83(11)	C1	C12	C9	100.56(9)
C5	C6	C7	120.96(10)	C1	C12	C13	113.67(10)
C2	C7	C6	119.26(10)	C9	C12	C13	113.68(10)
C2	C7	C8	120.88(10)	C12	C13	C14	113.11(11)

Table 5. Torsional Angles (deg)

Atom1	Atom2	Atom3	Atom4	Angle	Atom1	Atom2	Atom3	Atom4	Angle
C15	O2	C5	C4	-0.97(18)	O2	C5	C6	C7	179.69(11)
C15	O2	C5	C6	178.90(11)	C4	C5	C6	C7	-0.43(18)
C11	C1	C2	C3	-99.05(12)	C5	C6	C7	C2	2.27(17)
C11	C1	C2	C7	76.48(12)	C5	C6	C7	C8	-177.42(11)
C12	C1	C2	C3	151.40(10)	C2	C7	C8	C9	-7.08(16)
C12	C1	C2	C7	-33.07(14)	C6	C7	C8	C9	172.60(10)
C2	C1	C11	O1	85.50(14)	C7	C8	C9	C10	-67.58(13)
C2	C1	C11	C10	-92.95(10)	C7	C8	C9	C12	44.57(13)
C12	C1	C11	O1	-159.66(12)	C8	C9	C10	C1	-42.39(13)
C12	C1	C11	C10	21.88(11)	C8	C9	C10	C11	82.36(12)
C2	C1	C12	C9	66.25(11)	C12	C9	C10	C1	-159.56(8)
C2	C1	C12	C13	-171.89(9)	C12	C9	C10	C11	-34.81(11)
C11	C1	C12	C9	-43.36(11)	C8	C9	C12	C1	-73.16(11)
C11	C1	C12	C13	78.50(11)	C8	C9	C12	C13	164.99(10)
C1	C2	C3	C4	177.20(10)	C10	C9	C12	C1	48.04(10)
C7	C2	C3	C4	1.68(17)	C10	C9	C12	C13	-73.81(12)
C1	C2	C7	C6	-178.46(10)	C1	C10	C11	O1	-42.79(15)
C1	C2	C7	C8	1.22(16)	C1	C10	C11	C1	135.70(8)
C3	C2	C7	C6	-2.86(16)	C9	C10	C11	O1	-170.20(11)
C3	C2	C7	C8	176.82(10)	C9	C10	C11	C1	8.30(12)
C2	C3	C4	C5	0.17(17)	C1	C12	C13	C14	78.91(14)
C3	C4	C5	O2	179.07(11)	C9	C12	C13	C14	-166.84(11)
C3	C4	C5	C6	-0.80(17)					

Table 6. Anisotropic Displacement Parameters (U_{ij} , Å²)

Atom	U_{11}	U_{22}	U_{33}	U_{23}	U_{13}	U_{12}
C1	0.0383(2)	0.0441(2)	0.0548(2)	0.01132(14)	-0.01092(14)	0.00290(13)
O1	0.0294(4)	0.0366(5)	0.0411(5)	-0.0014(4)	0.0062(3)	0.0001(3)
O2	0.0491(6)	0.0352(5)	0.0341(4)	-0.0070(4)	0.0043(4)	-0.0034(4)
C1	0.0273(5)	0.0266(5)	0.0290(5)	0.0000(4)	0.0000(4)	0.0008(4)
C2	0.0235(5)	0.0253(5)	0.0308(5)	-0.0002(4)	0.0012(4)	0.0014(4)
C3	0.0291(6)	0.0275(5)	0.0322(6)	0.0033(4)	0.0028(4)	0.0004(4)
C4	0.0320(6)	0.0234(5)	0.0392(6)	-0.0006(5)	0.0022(5)	-0.0005(4)
C5	0.0269(5)	0.0311(6)	0.0320(6)	-0.0043(4)	0.0013(4)	0.0016(4)
C6	0.0285(5)	0.0307(6)	0.0303(5)	0.0028(4)	0.0029(4)	0.0009(4)
C7	0.0234(5)	0.0262(5)	0.0326(5)	0.0014(4)	0.0014(4)	0.0007(4)
C8	0.0347(6)	0.0272(6)	0.0355(6)	0.0037(4)	0.0030(5)	-0.0037(5)
C9	0.0319(6)	0.0245(5)	0.0393(6)	-0.0001(5)	-0.0015(5)	-0.0032(4)
C10	0.0301(6)	0.0264(5)	0.0390(6)	-0.0009(5)	-0.0045(5)	0.0022(4)
C11	0.0291(6)	0.0287(5)	0.0282(5)	-0.0054(4)	-0.0002(4)	0.0009(4)
C12	0.0264(5)	0.0292(5)	0.0360(6)	-0.0032(4)	-0.0014(4)	-0.0006(4)
C13	0.0354(6)	0.0373(7)	0.0436(7)	-0.0101(5)	-0.0053(5)	-0.0008(5)
C14	0.0374(7)	0.0595(9)	0.0400(7)	-0.0107(6)	-0.0064(6)	0.0063(6)
C15	0.0470(8)	0.0359(7)	0.0453(7)	-0.0122(6)	0.0043(6)	-0.0028(6)

The form of the anisotropic displacement parameter is:

$$\exp[-2\pi^2(h^2a^2U_{11} + k^2b^2U_{22} + l^2c^2U_{33} + 2klb^*c^*U_{23} + 2hla^*c^*U_{13} + 2hka^*b^*U_{12})]$$

Table 7. Derived Atomic Coordinates and Displacement Parameters for Hydrogen Atoms

Atom	x	y	z	U_{eq} , Å ²
H1	0.1305	0.2284	0.7538	0.033
H3	0.0898	-0.0008	0.6857	0.036
H4	0.0841	-0.1408	0.5789	0.038
H6	0.1523	0.2314	0.4664	0.036
H8A	0.1232	0.4836	0.5347	0.039
H8B	0.2188	0.4495	0.5546	0.039
H9	0.1748	0.6180	0.6421	0.038
H10	0.0551	0.6039	0.7086	0.038
H12	0.2432	0.3779	0.6871	0.037
H13A	0.2259	0.6040	0.7644	0.047
H13B	0.1458	0.5215	0.7979	0.047
H14A	0.2628	0.4807	0.8725	0.055
H14B	0.3128	0.4070	0.8065	0.055
H14C	0.2327	0.3233	0.8395	0.055
H15A	0.0991	-0.2305	0.3955	0.051
H15B	0.0428	-0.2105	0.4663	0.051
H15C	0.1402	-0.2501	0.4737	0.051

Compound 32e

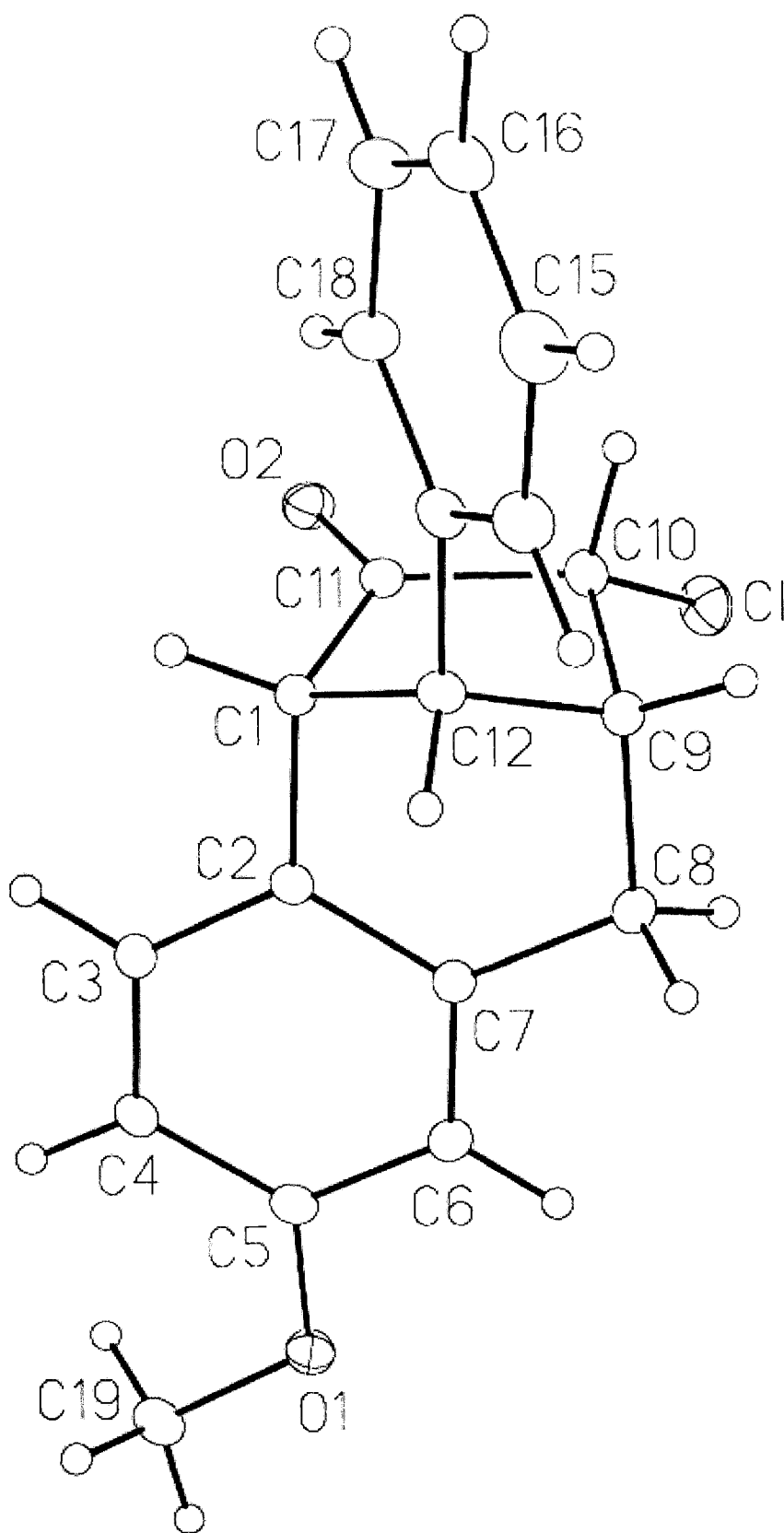
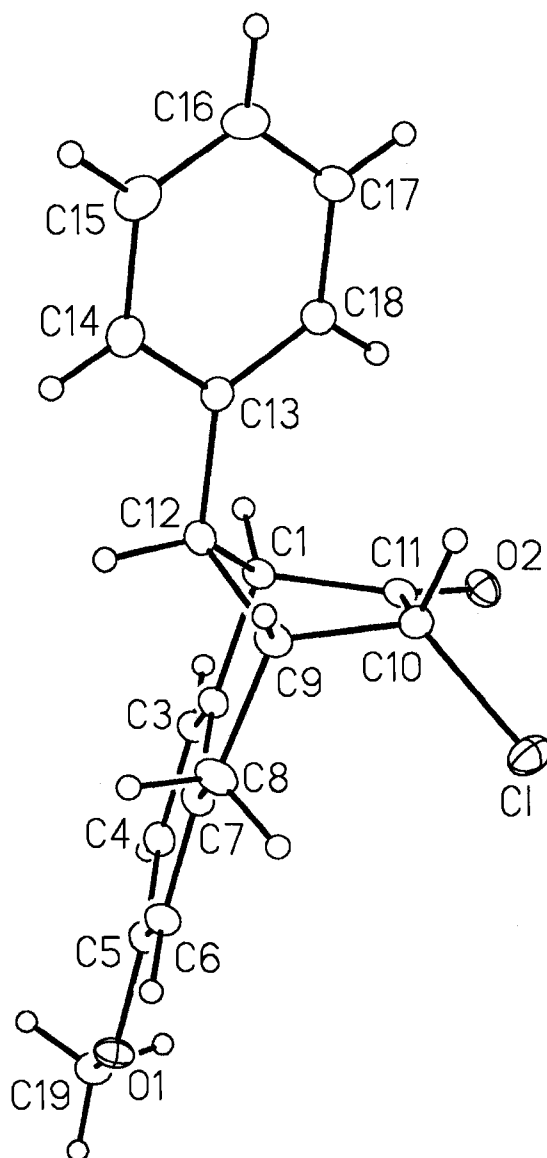


Figure 2. Alternate view of the molecule.



List of Tables

Table 1. Crystallographic Experimental Details

Table 2. Atomic Coordinates and Equivalent Isotropic Displacement Parameters

Table 3. Selected Interatomic Distances

Table 4. Selected Interatomic Angles

Table 5. Torsional Angles

Table 6. Anisotropic Displacement Parameters

Table 7. Derived Atomic Coordinates and Displacement Parameters for Hydrogen Atoms

Table 1. Crystallographic Experimental Details

<i>A. Crystal Data</i>	
formula	C ₁₉ H ₁₇ ClO ₂
formula weight	312.78
crystal dimensions (mm)	0.42 × 0.38 × 0.32
crystal system	triclinic
space group	$P\bar{1}$ (No. 2)
unit cell parameters ^a	
<i>a</i> (Å)	6.7178 (5)
<i>b</i> (Å)	10.7213 (7)
<i>c</i> (Å)	10.9182 (7)
α (deg)	102.0721 (9)
β (deg)	90.4764 (9)
γ (deg)	91.3604 (10)
<i>V</i> (Å ³)	768.69 (9)
<i>Z</i>	2
ρ _{calcd} (g cm ⁻³)	1.351
μ (mm ⁻¹)	0.253
<i>B. Data Collection and Refinement Conditions</i>	
diffractometer	Bruker PLATFORM/SMART 1000 CCD ^b
radiation (λ [Å])	graphite-monochromated Mo Kα (0.71073)
temperature (°C)	-80
scan type	ω scans (0.3°) (20 s exposures)
data collection 2θ limit (deg)	55.04
total data collected	6743 (-8 ≤ <i>h</i> ≤ 8, -13 ≤ <i>k</i> ≤ 13, -14 ≤ <i>l</i> ≤ 14)
independent reflections	3497 (<i>R</i> _{int} = 0.0081)
number of observed reflections (<i>NO</i>)	3177 [<i>F</i> _o ² ≥ 2σ(<i>F</i> _o ²)]
structure solution method	direct methods (<i>SHELXS-97</i> ^c)
refinement method	full-matrix least-squares on <i>F</i> ² (<i>SHELXL-97</i> ^d)
absorption correction method	Gaussian integration (face-indexed)
range of transmission factors	0.9234–0.9012
data/restraints/parameters	3497 [<i>F</i> _o ² ≥ -3σ(<i>F</i> _o ²)] / 0 / 199
goodness-of-fit (<i>S</i>) ^e	1.096 [<i>F</i> _o ² ≥ -3σ(<i>F</i> _o ²)]
final <i>R</i> indices ^f	
<i>R</i> ₁ [<i>F</i> _o ² ≥ 2σ(<i>F</i> _o ²)]	0.0344
<i>wR</i> ₂ [<i>F</i> _o ² ≥ -3σ(<i>F</i> _o ²)]	0.0961
largest difference peak and hole	0.286 and -0.326 e Å ⁻³

^aObtained from least-squares refinement of 6278 reflections with 4.84° < 2θ < 54.98°.

(continued)

Table 1. Crystallographic Experimental Details (continued)

^bPrograms for diffractometer operation, data collection, data reduction and absorption correction were those supplied by Bruker.

^cSheldrick, G. M. *Acta Crystallogr.* **1990**, *A46*, 467–473.

^dSheldrick, G. M. *SHELXL-97*. Program for crystal structure determination. University of Göttingen, Germany, 1997.

^e $S = [\sum w(F_o^2 - F_c^2)^2 / (n - p)]^{1/2}$ (n = number of data; p = number of parameters varied; $w = [\sigma^2(F_o^2) + (0.0464P)^2 + 0.2310P]^{-1}$ where $P = [\text{Max}(F_o^2, 0) + 2F_c^2]/3$).

^f $R_1 = \sum ||F_o| - |F_c|| / \sum |F_o|$; $wR_2 = [\sum w(F_o^2 - F_c^2)^2 / \sum w(F_o^4)]^{1/2}$.

Table 2. Atomic Coordinates and Equivalent Isotropic Displacement Parameters

Atom	<i>x</i>	<i>y</i>	<i>z</i>	<i>U</i> _{eq} , Å ²
Cl1	0.31963(6)	0.45369(3)	0.30522(3)	0.04376(12)*
O1	0.23852(14)	-0.13390(9)	-0.01690(8)	0.0360(2)*
O2	-0.07968(13)	0.35081(9)	0.39923(9)	0.0352(2)*
C1	0.11123(16)	0.18137(11)	0.46151(11)	0.0257(2)*
C2	0.14225(17)	0.09105(10)	0.33595(11)	0.0256(2)*
C3	-0.00556(17)	0.00441(11)	0.27962(11)	0.0282(2)*
C4	0.01959(18)	-0.07387(11)	0.16237(12)	0.0295(2)*
C5	0.19664(18)	-0.06382(11)	0.09936(11)	0.0291(2)*
C6	0.34653(18)	0.02198(12)	0.15509(11)	0.0302(3)*
C7	0.32143(17)	0.09955(11)	0.27260(11)	0.0274(2)*
C8	0.48883(18)	0.18990(12)	0.33164(12)	0.0333(3)*
C9	0.43070(17)	0.27987(11)	0.45305(11)	0.0284(2)*
C10	0.27935(17)	0.37942(11)	0.43476(11)	0.0274(2)*
C11	0.07561(17)	0.31031(11)	0.42736(10)	0.0260(2)*
C12	0.30973(17)	0.20265(11)	0.53500(11)	0.0277(2)*
C13	0.29718(18)	0.27047(11)	0.67084(11)	0.0284(2)*
C14	0.4476(2)	0.25237(13)	0.75379(13)	0.0379(3)*
C15	0.4459(2)	0.31474(16)	0.87824(14)	0.0464(3)*
C16	0.2953(2)	0.39757(14)	0.92263(13)	0.0437(3)*
C17	0.1454(2)	0.41604(13)	0.84190(13)	0.0387(3)*
C18	0.1449(2)	0.35244(12)	0.71716(12)	0.0338(3)*
C19	0.0920(2)	-0.22621(13)	-0.07594(12)	0.0377(3)*

Anisotropically-refined atoms are marked with an asterisk (*). The form of the anisotropic displacement parameter is: $\exp[-2\pi^2(h^2a^{*2}U_{11} + k^2b^{*2}U_{22} + l^2c^{*2}U_{33} + 2klb^{*c^{*}}U_{23} + 2hla^{*c^{*}}U_{13} + 2hka^{*b^{*}}U_{12})]$.

Table 3. Selected Interatomic Distances (Å)

Atom1	Atom2	Distance	Atom1	Atom2	Distance
Cl	C10	1.7818(12)	C7	C8	1.5144(16)
O1	C5	1.3682(14)	C8	C9	1.5270(16)
O1	C19	1.4284(15)	C9	C10	1.5329(17)
O2	C11	1.2013(14)	C9	C12	1.5609(17)
C1	C2	1.5230(15)	C10	C11	1.5342(16)
C1	C11	1.5288(16)	C12	C13	1.5130(16)
C1	C12	1.5379(16)	C13	C14	1.3950(17)
C2	C3	1.3907(16)	C13	C18	1.3928(17)
C2	C7	1.4038(16)	C14	C15	1.384(2)
C3	C4	1.3901(16)	C15	C16	1.385(2)
C4	C5	1.3921(17)	C16	C17	1.378(2)
C5	C6	1.3936(17)	C17	C18	1.3897(18)
C6	C7	1.3893(16)			

Table 4. Selected Interatomic Angles (deg)

Atom1	Atom2	Atom3	Angle	Atom1	Atom2	Atom3	Angle
C5	O1	C19	117.46(10)	C10	C9	C12	101.17(9)
C2	C1	C11	104.19(9)	Cl	C10	C9	116.22(8)
C2	C1	C12	109.24(9)	Cl	C10	C11	112.29(8)
C11	C1	C12	103.62(9)	C9	C10	C11	105.23(9)
C1	C2	C3	121.81(10)	O2	C11	C1	127.57(11)
C1	C2	C7	119.07(10)	O2	C11	C10	125.97(11)
C3	C2	C7	119.05(10)	C1	C11	C10	106.46(9)
C2	C3	C4	121.73(11)	C1	C12	C9	100.37(9)
C3	C4	C5	118.93(11)	C1	C12	C13	115.79(10)
O1	C5	C4	124.62(11)	C9	C12	C13	113.38(9)
O1	C5	C6	115.45(11)	C12	C13	C14	118.58(11)
C4	C5	C6	119.93(11)	C12	C13	C18	123.34(11)
C5	C6	C7	121.00(11)	C14	C13	C18	118.06(12)
C2	C7	C6	119.35(11)	C13	C14	C15	120.88(13)
C2	C7	C8	120.97(10)	C14	C15	C16	120.47(13)
C6	C7	C8	119.67(10)	C15	C16	C17	119.30(13)
C7	C8	C9	113.55(10)	C16	C17	C18	120.50(13)
C8	C9	C10	113.95(10)	C13	C18	C17	120.77(12)
C8	C9	C12	109.02(10)				

Table 5. Torsional Angles (deg)

Atom1	Atom2	Atom3	Atom4	Angle	Atom1	Atom2	Atom3	Atom4	Angle
C19	O1	C5	C4	-1.80(18)	C6	C7	C8	C9	173.06(11)
C19	O1	C5	C6	177.93(11)	C7	C8	C9	C10	-68.40(14)
C11	C1	C2	C3	-103.67(12)	C7	C8	C9	C12	43.76(14)
C11	C1	C2	C7	73.32(12)	C8	C9	C10	C1	-42.60(12)
C12	C1	C2	C3	146.11(11)	C8	C9	C10	C11	82.32(12)
C12	C1	C2	C7	-36.90(14)	C12	C9	C10	C1	-159.41(8)
C2	C1	C11	O2	86.67(14)	C12	C9	C10	C11	-34.50(11)
C2	C1	C11	C10	-92.87(10)	C8	C9	C12	C1	-73.09(11)
C12	C1	C11	O2	-159.06(12)	C8	C9	C12	C13	162.78(10)
C12	C1	C11	C10	21.40(11)	C10	C9	C12	C1	47.28(10)
C2	C1	C12	C9	68.29(11)	C10	C9	C12	C13	-76.84(11)
C2	C1	C12	C13	-169.27(10)	C1	C10	C11	O2	-43.67(15)
C11	C1	C12	C9	-42.31(10)	C1	C10	C11	C1	135.88(8)
C11	C1	C12	C13	80.13(12)	C9	C10	C11	O2	-171.01(11)
C1	C2	C3	C4	176.99(11)	C9	C10	C11	C1	8.54(12)
C7	C2	C3	C4	0.01(18)	C1	C12	C13	C14	156.55(11)
C1	C2	C7	C6	-176.70(11)	C1	C12	C13	C18	-24.81(16)
C1	C2	C7	C8	4.59(17)	C9	C12	C13	C14	-88.19(13)
C3	C2	C7	C6	0.37(18)	C9	C12	C13	C18	90.45(14)
C3	C2	C7	C8	-178.34(11)	C12	C13	C14	C15	178.31(13)
C2	C3	C4	C5	-0.81(18)	C18	C13	C14	C15	-0.4(2)
C3	C4	C5	O1	-179.05(11)	C12	C13	C18	C17	-177.43(12)
C3	C4	C5	C6	1.23(18)	C14	C13	C18	C17	1.22(19)
O1	C5	C6	C7	179.38(11)	C13	C14	C15	C16	-0.6(2)
C4	C5	C6	C7	-0.87(19)	C14	C15	C16	C17	0.9(2)
C5	C6	C7	C2	0.06(18)	C15	C16	C17	C18	0.0(2)
C5	C6	C7	C8	178.79(11)	C16	C17	C18	C13	-1.0(2)
C2	C7	C8	C9	-8.23(17)					

Table 6. Anisotropic Displacement Parameters (U_{ij} , Å²)

Atom	U_{11}	U_{22}	U_{33}	U_{23}	U_{13}	U_{12}
C1	0.0520(2)	0.0444(2)	0.03832(19)	0.01726(15)	0.00304(14)	-0.00652(15)
O1	0.0394(5)	0.0355(5)	0.0282(4)	-0.0040(4)	0.0034(4)	-0.0032(4)
O2	0.0294(4)	0.0351(5)	0.0388(5)	0.0023(4)	-0.0043(4)	0.0057(3)
C1	0.0242(5)	0.0248(5)	0.0267(5)	0.0023(4)	0.0024(4)	-0.0013(4)
C2	0.0263(5)	0.0221(5)	0.0273(5)	0.0030(4)	0.0012(4)	0.0010(4)
C3	0.0271(5)	0.0245(5)	0.0322(6)	0.0041(4)	0.0036(4)	-0.0015(4)
C4	0.0314(6)	0.0229(5)	0.0326(6)	0.0026(4)	-0.0010(5)	-0.0029(4)
C5	0.0345(6)	0.0247(5)	0.0268(6)	0.0021(4)	0.0009(4)	0.0023(4)
C6	0.0278(6)	0.0309(6)	0.0304(6)	0.0024(5)	0.0044(4)	0.0003(4)
C7	0.0252(5)	0.0257(5)	0.0298(6)	0.0024(4)	0.0012(4)	0.0004(4)
C8	0.0234(5)	0.0355(6)	0.0361(7)	-0.0033(5)	0.0037(5)	-0.0021(5)
C9	0.0229(5)	0.0301(6)	0.0298(6)	0.0009(4)	-0.0003(4)	-0.0020(4)
C10	0.0295(6)	0.0264(5)	0.0259(5)	0.0049(4)	0.0005(4)	-0.0033(4)
C11	0.0261(5)	0.0260(5)	0.0235(5)	-0.0003(4)	0.0010(4)	0.0006(4)
C12	0.0278(5)	0.0253(5)	0.0291(6)	0.0032(4)	-0.0012(4)	0.0030(4)
C13	0.0334(6)	0.0242(5)	0.0277(6)	0.0059(4)	-0.0026(4)	-0.0019(4)
C14	0.0395(7)	0.0375(7)	0.0371(7)	0.0087(5)	-0.0071(5)	0.0022(5)
C15	0.0489(8)	0.0537(9)	0.0365(7)	0.0101(6)	-0.0149(6)	-0.0045(7)
C16	0.0573(9)	0.0424(8)	0.0279(6)	0.0006(5)	-0.0040(6)	-0.0103(6)
C17	0.0500(8)	0.0325(6)	0.0315(7)	0.0020(5)	0.0044(6)	0.0008(6)
C18	0.0397(7)	0.0323(6)	0.0289(6)	0.0052(5)	-0.0011(5)	0.0039(5)
C19	0.0474(7)	0.0315(6)	0.0302(6)	-0.0018(5)	-0.0012(5)	-0.0049(5)

The form of the anisotropic displacement parameter is:

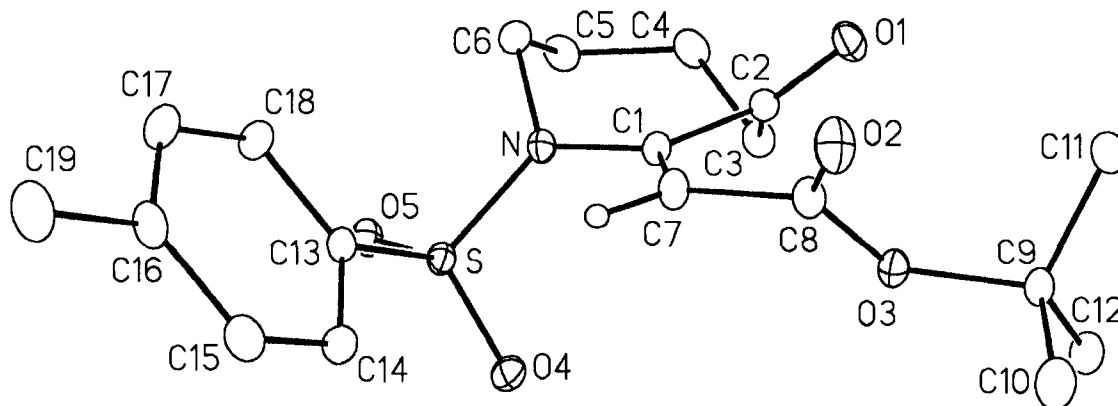
$$\exp[-2\pi^2(h^2a^2U_{11} + k^2b^2U_{22} + l^2c^2U_{33} + 2klb^*c^*U_{23} + 2hla^*c^*U_{13} + 2hka^*b^*U_{12})]$$

Table 7. Derived Atomic Coordinates and Displacement Parameters for Hydrogen Atoms

Atom	<i>x</i>	<i>y</i>	<i>z</i>	$U_{\text{eq}}, \text{\AA}^2$
H1	-0.0001	0.1529	0.5103	0.031
H3	-0.1269	-0.0014	0.3224	0.034
H4	-0.0824	-0.1333	0.1258	0.035
H6	0.4677	0.0275	0.1121	0.036
H8A	0.5331	0.2414	0.2710	0.040
H8B	0.6030	0.1392	0.3491	0.040
H9	0.5515	0.3220	0.4995	0.034
H10	0.2823	0.4481	0.5124	0.033
H12	0.3730	0.1184	0.5306	0.033
H14	0.5525	0.1965	0.7244	0.046
H15	0.5487	0.3006	0.9336	0.056
H16	0.2954	0.4412	1.0078	0.052
H17	0.0416	0.4727	0.8717	0.046
H18	0.0395	0.3650	0.6628	0.041
H19A	0.1364	-0.2664	-0.1599	0.045
H19B	-0.0344	-0.1841	-0.0825	0.045
H19C	0.0734	-0.2915	-0.0259	0.045

Appendix V: X-ray Crystallographic Data for Compound 46f_E
(Chapter 4)

Figure 2. Alternate view of the molecule illustrating the relative orientations of the carbonyl and olefin units.



List of Tables

- Table 1.** Crystallographic Experimental Details
- Table 2.** Atomic Coordinates and Equivalent Isotropic Displacement Parameters
- Table 3.** Selected Interatomic Distances
- Table 4.** Selected Interatomic Angles
- Table 5.** Torsional Angles
- Table 6.** Anisotropic Displacement Parameters
- Table 7.** Derived Atomic Coordinates and Displacement Parameters for Hydrogen Atoms

Table 1. Crystallographic Experimental Details

<i>A. Crystal Data</i>	
formula	C ₁₉ H ₂₅ NO ₅ S
formula weight	379.46
crystal dimensions (mm)	0.52 × 0.50 × 0.37
crystal system	triclinic
space group	$P\bar{1}$ (No. 2)
unit cell parameters ^a	
<i>a</i> (Å)	8.0444 (6)
<i>b</i> (Å)	10.8324 (7)
<i>c</i> (Å)	11.7001 (8)
α (deg)	86.0553 (9)
β (deg)	78.3360 (9)
γ (deg)	73.0379 (9)
<i>V</i> (Å ³)	955.01 (11)
<i>Z</i>	2
ρ _{calcd} (g cm ⁻³)	1.320
μ (mm ⁻¹)	0.199
<i>B. Data Collection and Refinement Conditions</i>	
diffractometer	Bruker PLATFORM/SMART 1000 CCD ^b
radiation (λ [Å])	graphite-monochromated Mo Kα (0.71073)
temperature (°C)	-80
scan type	ω scans (0.3°) (15 s exposures)
data collection 2θ limit (deg)	54.94
total data collected	7952 (-10 ≤ <i>h</i> ≤ 10, -14 ≤ <i>k</i> ≤ 14, -15 ≤ <i>l</i> ≤ 15)
independent reflections	4305 (<i>R</i> _{int} = 0.0106)
number of observed reflections (<i>NO</i>)	3941 [<i>F</i> _o ² ≥ 2σ(<i>F</i> _o ²)]
structure solution method	direct methods (<i>SHELXS-97</i> ^c)
refinement method	full-matrix least-squares on <i>F</i> ² (<i>SHELXL-97</i> ^d)
absorption correction method	Gaussian integration (face-indexed)
range of transmission factors	0.9302–0.9038
data/restraints/parameters	4305 [<i>F</i> _o ² ≥ -3σ(<i>F</i> _o ²)] / 0 / 236
goodness-of-fit (<i>S</i>) ^e	1.065 [<i>F</i> _o ² ≥ -3σ(<i>F</i> _o ²)]
final <i>R</i> indices ^f	
<i>R</i> ₁ [<i>F</i> _o ² ≥ 2σ(<i>F</i> _o ²)]	0.0378
<i>wR</i> ₂ [<i>F</i> _o ² ≥ -3σ(<i>F</i> _o ²)]	0.1048
largest difference peak and hole	0.415 and -0.230 e Å ⁻³

^aObtained from least-squares refinement of 7059 reflections with 5.28° < 2θ < 54.94°.

(continued)

Table 1. Crystallographic Experimental Details (continued)

^bPrograms for diffractometer operation, data collection, data reduction and absorption correction were those supplied by Bruker.

^cSheldrick, G. M. *Acta Crystallogr.* **1990**, *A46*, 467–473.

^dSheldrick, G. M. *SHELXL-97*. Program for crystal structure determination. University of Göttingen, Germany, 1997.

^e $S = [\sum w(F_o^2 - F_c^2)^2 / (n - p)]^{1/2}$ (n = number of data; p = number of parameters varied; $w = [\sigma^2(F_o^2) + (0.0585P)^2 + 0.2759P]^{-1}$ where $P = [\text{Max}(F_o^2, 0) + 2F_c^2]/3$).

^f $R_1 = \sum ||F_o| - |F_c|| / \sum |F_o|$; $wR_2 = [\sum w(F_o^2 - F_c^2)^2 / \sum w(F_o^4)]^{1/2}$.

Table 2. Atomic Coordinates and Equivalent Isotropic Displacement Parameters

Atom	<i>x</i>	<i>y</i>	<i>z</i>	<i>U</i> _{eq} , Å ²
S	0.29703(4)	0.07469(3)	0.32154(3)	0.02828(10)*
O1	-0.17183(14)	0.47710(9)	0.45698(9)	0.0390(2)*
O2	0.00165(14)	0.56991(10)	0.17223(10)	0.0452(3)*
O3	-0.19285(12)	0.45109(9)	0.21909(8)	0.0325(2)*
O4	0.18482(13)	0.05735(10)	0.24700(9)	0.0382(2)*
O5	0.36197(13)	-0.02612(9)	0.40110(9)	0.0364(2)*
N	0.18808(14)	0.20124(10)	0.40349(9)	0.0287(2)*
C1	0.06721(16)	0.30995(11)	0.36238(11)	0.0269(2)*
C2	-0.10292(16)	0.36187(12)	0.44926(11)	0.0288(3)*
C3	-0.17839(18)	0.26573(14)	0.52481(12)	0.0362(3)*
C4	-0.1004(2)	0.23460(14)	0.63613(13)	0.0401(3)*
C5	0.0910(2)	0.14998(13)	0.61496(12)	0.0385(3)*
C6	0.21772(18)	0.20380(13)	0.52490(12)	0.0330(3)*
C7	0.09382(17)	0.36336(13)	0.25702(12)	0.0323(3)*
C8	-0.03752(17)	0.47477(13)	0.21273(11)	0.0318(3)*
C9	-0.34552(18)	0.55096(14)	0.18391(12)	0.0357(3)*
C10	-0.3047(3)	0.57000(19)	0.05224(14)	0.0563(5)*
C11	-0.3841(2)	0.67552(15)	0.24928(15)	0.0440(3)*
C12	-0.4951(2)	0.48968(17)	0.22037(17)	0.0498(4)*
C13	0.48211(16)	0.10949(11)	0.23087(11)	0.0281(3)*
C14	0.49506(19)	0.11517(14)	0.11100(13)	0.0372(3)*
C15	0.6458(2)	0.13614(15)	0.04061(13)	0.0412(3)*
C16	0.78252(18)	0.15257(13)	0.08844(13)	0.0368(3)*
C17	0.76626(18)	0.14655(15)	0.20902(14)	0.0392(3)*
C18	0.61786(17)	0.12438(14)	0.28104(13)	0.0350(3)*
C19	0.9448(2)	0.17713(17)	0.01168(17)	0.0517(4)*

Anisotropically-refined atoms are marked with an asterisk (*). The form of the anisotropic displacement parameter is: $\exp[-2\pi^2(h^2a^{*2}U_{11} + k^2b^{*2}U_{22} + l^2c^{*2}U_{33} + 2klb^{*c^{*}}U_{23} + 2hla^{*c^{*}}U_{13} + 2hka^{*b^{*}}U_{12})]$.

Table 3. Selected Interatomic Distances (Å)

Atom1	Atom2	Distance	Atom1	Atom2	Distance
S	O4	1.4319(10)	C4	C5	1.525(2)
S	O5	1.4338(10)	C5	C6	1.523(2)
S	N	1.6452(11)	C7	C8	1.4942(17)
S	C13	1.7658(13)	C9	C10	1.522(2)
O1	C2	1.2104(16)	C9	C11	1.518(2)
O2	C8	1.2033(17)	C9	C12	1.513(2)
O3	C8	1.3340(16)	C13	C14	1.3837(19)
O3	C9	1.4886(15)	C13	C18	1.3922(18)
N	C1	1.4166(15)	C14	C15	1.390(2)
N	C6	1.4905(17)	C15	C16	1.390(2)
C1	C2	1.5131(17)	C16	C17	1.389(2)
C1	C7	1.3296(18)	C16	C19	1.509(2)
C2	C3	1.5033(18)	C17	C18	1.3876(19)
C3	C4	1.533(2)			

Table 4. Selected Interatomic Angles (deg)

Atom1	Atom2	Atom3	Angle	Atom1	Atom2	Atom3	Angle
O4	S	O5	120.04(6)	C1	C7	C8	124.52(12)
O4	S	N	108.07(6)	O2	C8	O3	126.49(12)
O4	S	C13	107.21(6)	O2	C8	C7	121.59(12)
O5	S	N	105.30(6)	O3	C8	C7	111.84(11)
O5	S	C13	107.61(6)	O3	C9	C10	108.49(11)
N	S	C13	108.15(6)	O3	C9	C11	110.71(11)
C8	O3	C9	120.99(11)	O3	C9	C12	102.48(12)
S	N	C1	122.28(9)	C10	C9	C11	112.29(14)
S	N	C6	119.56(8)	C10	C9	C12	111.56(14)
C1	N	C6	118.16(10)	C11	C9	C12	110.86(13)
N	C1	C2	113.99(10)	S	C13	C14	119.93(10)
N	C1	C7	124.92(12)	S	C13	C18	119.22(10)
C2	C1	C7	121.08(11)	C14	C13	C18	120.76(12)
O1	C2	C1	119.98(12)	C13	C14	C15	119.19(13)
O1	C2	C3	122.47(12)	C14	C15	C16	121.24(14)
C1	C2	C3	117.54(11)	C15	C16	C17	118.46(13)
C2	C3	C4	111.09(12)	C15	C16	C19	121.03(15)
C3	C4	C5	113.46(12)	C17	C16	C19	120.51(14)
C4	C5	C6	114.51(11)	C16	C17	C18	121.34(13)
N	C6	C5	113.13(11)	C13	C18	C17	119.00(13)

Table 5. Torsional Angles (deg)

Atom1	Atom2	Atom3	Atom4	Angle	Atom1	Atom2	Atom3	Atom4	Angle
O4	S	N	C1	-34.12(11)	N	C1	C2	O1	142.38(12)
O4	S	N	C6	146.66(10)	N	C1	C2	C3	-36.68(16)
O5	S	N	C1	-163.55(10)	C7	C1	C2	O1	-38.72(19)
O5	S	N	C6	17.23(11)	C7	C1	C2	C3	142.22(13)
C13	S	N	C1	81.63(11)	N	C1	C7	C8	177.43(12)
C13	S	N	C6	-97.59(10)	C2	C1	C7	C8	-1.3(2)
O4	S	C13	C14	-0.02(13)	O1	C2	C3	C4	-91.34(16)
O4	S	C13	C18	-176.76(10)	C1	C2	C3	C4	87.69(14)
O5	S	C13	C14	130.38(11)	C2	C3	C4	C5	-73.26(15)
O5	S	C13	C18	-46.35(12)	C3	C4	C5	C6	55.73(17)
N	S	C13	C14	-116.33(11)	C4	C5	C6	N	-70.04(15)
N	S	C13	C18	66.93(11)	C1	C7	C8	O2	127.60(16)
C9	O3	C8	O2	-5.7(2)	C1	C7	C8	O3	-55.45(18)
C9	O3	C8	C7	177.59(11)	S	C13	C14	C15	-176.75(11)
C8	O3	C9	C10	69.16(16)	C18	C13	C14	C15	-0.1(2)
C8	O3	C9	C11	-54.48(16)	S	C13	C18	C17	177.42(11)
C8	O3	C9	C12	-172.75(12)	C14	C13	C18	C17	0.7(2)
S	N	C1	C2	136.77(10)	C13	C14	C15	C16	-0.6(2)
S	N	C1	C7	-42.08(17)	C14	C15	C16	C17	0.5(2)
C6	N	C1	C2	-44.00(15)	C14	C15	C16	C19	-179.16(14)
C6	N	C1	C7	137.16(14)	C15	C16	C17	C18	0.2(2)
S	N	C6	C5	-91.06(12)	C19	C16	C17	C18	179.84(14)
C1	N	C6	C5	89.68(13)	C16	C17	C18	C13	-0.8(2)

Table 6. Anisotropic Displacement Parameters (U_{ij} , Å²)

Atom	U_{11}	U_{22}	U_{33}	U_{23}	U_{13}	U_{12}
S	0.02291(16)	0.02423(16)	0.03820(18)	0.00004(12)	-0.00734(12)	-0.00654(11)
O1	0.0421(5)	0.0277(5)	0.0406(5)	-0.0015(4)	-0.0073(4)	0.0003(4)
O2	0.0368(5)	0.0389(5)	0.0538(6)	0.0168(5)	-0.0035(5)	-0.0086(4)
O3	0.0274(4)	0.0319(5)	0.0359(5)	0.0025(4)	-0.0096(4)	-0.0028(4)
O4	0.0305(5)	0.0375(5)	0.0509(6)	-0.0055(4)	-0.0122(4)	-0.0123(4)
O5	0.0330(5)	0.0252(4)	0.0485(6)	0.0049(4)	-0.0075(4)	-0.0056(4)
N	0.0254(5)	0.0257(5)	0.0326(5)	0.0017(4)	-0.0072(4)	-0.0029(4)
C1	0.0222(5)	0.0238(5)	0.0348(6)	0.0017(5)	-0.0068(5)	-0.0061(4)
C2	0.0271(6)	0.0285(6)	0.0295(6)	0.0000(5)	-0.0071(5)	-0.0047(5)
C3	0.0296(6)	0.0363(7)	0.0398(7)	0.0010(5)	0.0007(5)	-0.0101(5)
C4	0.0465(8)	0.0345(7)	0.0337(7)	0.0027(5)	0.0006(6)	-0.0090(6)
C5	0.0495(8)	0.0301(6)	0.0329(7)	0.0042(5)	-0.0093(6)	-0.0067(6)
C6	0.0351(7)	0.0288(6)	0.0372(7)	0.0014(5)	-0.0151(5)	-0.0071(5)
C7	0.0233(6)	0.0326(6)	0.0371(7)	0.0047(5)	-0.0029(5)	-0.0050(5)
C8	0.0277(6)	0.0331(6)	0.0297(6)	0.0041(5)	-0.0024(5)	-0.0039(5)
C9	0.0295(6)	0.0364(7)	0.0357(7)	-0.0045(5)	-0.0123(5)	0.0038(5)
C10	0.0571(10)	0.0614(11)	0.0373(8)	-0.0008(7)	-0.0179(7)	0.0095(8)
C11	0.0361(7)	0.0394(8)	0.0517(9)	-0.0111(6)	-0.0103(6)	0.0006(6)
C12	0.0320(7)	0.0467(9)	0.0706(11)	-0.0113(8)	-0.0179(7)	-0.0032(6)
C13	0.0227(5)	0.0244(6)	0.0358(6)	0.0001(5)	-0.0061(5)	-0.0042(4)
C14	0.0310(7)	0.0414(7)	0.0380(7)	-0.0055(6)	-0.0083(5)	-0.0063(6)
C15	0.0390(7)	0.0425(8)	0.0355(7)	-0.0009(6)	-0.0017(6)	-0.0050(6)
C16	0.0294(6)	0.0249(6)	0.0488(8)	0.0033(5)	0.0000(6)	-0.0024(5)
C17	0.0278(6)	0.0407(7)	0.0513(8)	0.0066(6)	-0.0107(6)	-0.0125(6)
C18	0.0286(6)	0.0398(7)	0.0385(7)	0.0043(6)	-0.0102(5)	-0.0113(5)
C19	0.0387(8)	0.0430(8)	0.0631(10)	0.0069(7)	0.0084(7)	-0.0099(7)

The form of the anisotropic displacement parameter is:

$$\exp[-2\pi^2(h^2a^2U_{11} + k^2b^2U_{22} + l^2c^2U_{33} + 2klb^*c^*U_{23} + 2hla^*c^*U_{13} + 2hka^*b^*U_{12})]$$

Table 7. Derived Atomic Coordinates and Displacement Parameters for Hydrogen Atoms

Atom	<i>x</i>	<i>y</i>	<i>z</i>	$U_{\text{eq}}, \text{\AA}^2$
H3A	-0.1521	0.1854	0.4805	0.043
H3B	-0.3086	0.3011	0.5461	0.043
H4A	-0.1065	0.3164	0.6718	0.048
H4B	-0.1739	0.1902	0.6925	0.048
H5A	0.1334	0.1377	0.6898	0.046
H5B	0.0942	0.0641	0.5890	0.046
H6A	0.2039	0.2940	0.5451	0.040
H6B	0.3408	0.1529	0.5283	0.040
H7	0.2039	0.3283	0.2064	0.039
H10A	-0.2067	0.6089	0.0315	0.068
H10B	-0.4097	0.6271	0.0264	0.068
H10C	-0.2713	0.4863	0.0139	0.068
H11A	-0.2857	0.7135	0.2244	0.053
H11B	-0.3981	0.6573	0.3333	0.053
H11C	-0.4934	0.7363	0.2323	0.053
H12A	-0.4681	0.4101	0.1765	0.060
H12B	-0.6053	0.5498	0.2041	0.060
H12C	-0.5087	0.4695	0.3041	0.060
H14	0.4021	0.1049	0.0772	0.045
H15	0.6555	0.1393	-0.0418	0.049
H17	0.8586	0.1578	0.2429	0.047
H18	0.6090	0.1194	0.3633	0.042
H19A	0.9595	0.1436	-0.0665	0.062
H19B	1.0494	0.1336	0.0452	0.062
H19C	0.9310	0.2702	0.0065	0.062